



# **Neurons containing calcitonin gene-related peptide without substance P in nociception**

Garreth Kestell

Bachelor of Medical Science,  
Bachelor of Science (Hons)

Autonomic and Sensory Neurotransmission Laboratory  
Anatomy and Histology  
School of Medicine

Flinders University  
Adelaide, South Australia

-----

A thesis submitted to Flinders University in fulfilment of the requirements for the  
degree of Doctor of Philosophy

December 2014



# Table of Contents

---

List of Figures.....	v
List of Tables.....	xiii
<b>Preface</b> .....	<b>xv</b>
Thesis Summary .....	xvii
Declaration .....	xix
Acknowledgements .....	xxi
Publications from this thesis.....	xxiii
<i>Journal Publications</i> .....	xxiii
<i>Conference Proceedings</i> .....	xxiii
Awards attained during this thesis.....	xxv
Abbreviations .....	xxvii
<b>Chapter 1: Introduction.....</b>	<b>1</b>
1.1 Pain.....	3
<i>Acute nociception</i> .....	4
<i>Nociception after inflammation</i> .....	4
<i>Chronic and neuropathic pain</i> .....	5
<i>The problem with pain</i> .....	6
<i>Summary</i> .....	7
1.2 Nociceptors.....	9
<i>Conduction velocity of nociceptors: A<math>\delta</math> and C-fibre nociceptors</i> .....	9
<i>Molecular content of nociceptors: peptidergic and nonpeptidergic nociceptors</i> .....	11
<i>Preferred stimulus of nociceptors: the channels of nociceptors</i> .....	13
<i>Peripheral projections: cutaneous, muscular and visceral nociceptors</i> .....	18
<i>Central projections of nociceptors: nociceptive superficial and deep dorsal horn neurons</i> .....	21
<i>Pathways of nociceptors</i> .....	24
<i>Summary</i> .....	27
1.3 Altered pain states .....	29
<i>Pain after inflammation</i> .....	29
<i>Neuropathic pain</i> .....	32
<i>Summary</i> .....	34
1.4 Calcitonin gene-related peptide.....	35
<i>CGRP and the CGRP receptors</i> .....	35
<i>Distribution of CGRP in neural tissue</i> .....	36
<i>Role of CGRP in acute nociception</i> .....	37
<i>Role of CGRP in inflammatory pain</i> .....	38
<i>Role of CGRP in neuropathic pain</i> .....	39
<i>Summary</i> .....	40
1.5 Scope of Thesis .....	43
<i>Aims and experimental approach</i> .....	44
1.6 Figures .....	47
<b>Chapter 2: Materials and Methods.....</b>	<b>61</b>
2.1 Animals and Tissue Preparation.....	63
2.2 Tissue Processing and Sectioning .....	63
<i>Cryostat sectioning</i> .....	64
<i>Microtome sectioning</i> .....	64
2.3 Immunohistochemistry .....	64
2.4 Microscopy .....	65
<i>Fluorescence Microscopy</i> .....	65
<i>Confocal Microscopy</i> .....	66
2.5 Image Analysis and Preparation.....	66
<i>Analysis of DRG</i> .....	66
<i>Analysis of spinal cord</i> .....	67

<i>Statistical Analysis</i> .....	67
<b>Chapter 3: Prevalence and distribution of CGRP<sup>+</sup>SP<sup>-</sup> neurons</b> .....	<b>69</b>
3.1 Background .....	71
3.2 Materials and Methods .....	73
3.3 Results .....	75
<i>CGRP<sup>+</sup>SP<sup>-</sup> neurons were prominent in DRG of all spinal levels</i> .....	75
<i>CGRP<sup>+</sup>SP<sup>-</sup> terminals were prominent in the lamina I and IV/V of spinal dorsal horn</i> ...	77
<i>CGRP<sup>+</sup>SP<sup>-</sup> fibres were prominent in both glabrous and hairy paw skin</i> .....	82
3.4 Discussion .....	85
<i>CGRP<sup>+</sup>SP<sup>-</sup> neurons were prominent at all spinal levels and just as prominent as</i>	
<i>CGRP<sup>+</sup>SP<sup>+</sup> neurons</i> .....	85
<i>CGRP<sup>+</sup>SP<sup>-</sup> neurons were most likely myelinated</i> .....	86
<i>CGRP<sup>+</sup>SP<sup>-</sup> neurons most likely convey different sensory modalities</i> .....	87
3.5 Figures.....	91
<b>Chapter 4: Neurochemical profile of CGRP<sup>+</sup>SP<sup>-</sup> neurons</b> .....	<b>141</b>
4.1 Background .....	143
4.2 Materials and Methods .....	147
4.3 Results .....	149
<i>Most CGRP<sup>+</sup>SP<sup>-</sup> neurons lacked TRPV1</i> .....	149
<i>Most CGRP<sup>+</sup>SP<sup>-</sup> neurons expressed NF200</i> .....	151
<i>Most CGRP<sup>+</sup>SP<sup>-</sup> neurons lacked Galanin</i> .....	154
<i>Most CGRP<sup>+</sup>SP<sup>-</sup> expressed VIP</i> .....	157
4.4 Discussion .....	161
<i>Larger CGRP<sup>+</sup>SP<sup>-</sup> neurons are not capsaicin sensitive nociceptors</i> .....	161
<i>CGRP<sup>+</sup>SP<sup>-</sup> neurons are most likely myelinated</i> .....	162
<i>CGRP<sup>+</sup>SP<sup>-</sup> neurons do not co-express GAL under normal conditions</i> .....	163
<i>Some CGRP<sup>+</sup>SP<sup>-</sup> neurons co-express VIP</i> .....	164
4.5 Figures.....	167
<b>Chapter 5: Retrograde tracing of CGRP<sup>+</sup>SP<sup>-</sup> muscle afferents</b> .....	<b>217</b>
5.1 Background .....	219
5.2 Materials and Methods .....	221
5.3 Results .....	223
5.4 Discussion .....	225
5.5 Figures.....	227
<b>Chapter 6: Anterograde tracing of CGRP<sup>+</sup>SP<sup>-</sup> spinal afferents</b> .....	<b>239</b>
6.1 Background .....	241
6.2 Materials and Methods .....	243
6.3 Results .....	247
<i>NB labelled fibres in C7 dorsal horn</i> .....	247
<i>NB labelled more fibres in L4 dorsal horn compared to C7 dorsal horn</i> .....	248
<i>NB labelled more VGluT1-IR fibres than CGRP-IR fibres in lamina IV/V</i> .....	250
6.4 Discussion .....	251
<i>NB labelled more afferents in L4 dorsal horn compared to C7 dorsal horn</i> .....	251
<i>CGRP<sup>+</sup>SP<sup>-</sup> fibres of lamina IV/V are primary afferent and most likely larger myelinated</i>	
<i>afferents</i> .....	252
<i>CGRP<sup>+</sup>SP<sup>-</sup> fibres of lamina IV/V are most likely lightly myelinated mechanoreceptors</i>	
<i>projecting to wide-dynamic range neurons</i> .....	253
6.5 Figures.....	255
<b>Chapter 7: Relationship of CGRP<sup>+</sup>SP<sup>-</sup> terminals with nociceptive dorsal horn</b>	
<b>neurons</b> .....	<b>299</b>
7.1 Background .....	301
7.2 Materials and Methods .....	305
7.3 Results .....	309

<i>pERK and pCREB levels were increased after stimulation of afferents with capsaicin.....</i>	309
<i>Capsaicin stimulated afferents activated dorsal horn neurons that received contacts from CGRP<sup>+</sup>SP<sup>-</sup> afferents .....</i>	310
<i>pERK and pCREB levels increased after electrical stimulation of afferents.....</i>	311
<i>Electrical stimulated afferents activated cells that received contacts from CGRP<sup>+</sup>SP<sup>-</sup> afferents .....</i>	311
<b>7.4 Discussion .....</b>	<b>313</b>
<i>Capsaicin stimulation induced pERK and pCREB expression in dorsal horn neurons</i>	313
<i>Electrical stimulation of dorsal roots induced pERK and pCREB expression in dorsal horn neurons .....</i>	314
<i>pERK expressing dorsal horn cells activated by capsaicin sensitive nociceptors received convergent contacts from CGRP<sup>+</sup>SP<sup>-</sup> afferents in lamina I.....</i>	315
<i>pCREB expressing dorsal horn cells activated by electrically stimulated afferents nociceptors received contacts from CGRP<sup>+</sup>SP<sup>-</sup> afferents in lamina I .....</i>	317
<i>CGRP<sup>+</sup>SP<sup>-</sup> afferents in lamina IV/V must have a different function to lamina I .....</i>	318
<b>7.5 Figures .....</b>	<b>321</b>
<b>Chapter 8: Discussion and Conclusions .....</b>	<b>355</b>
<i>CGRP<sup>+</sup>SP<sup>-</sup> neurons are a prominent population of neurons .....</i>	359
<i>CGRP<sup>+</sup>SP<sup>-</sup> neurons are most likely myelinated .....</i>	360
<i>Larger CGRP<sup>+</sup>SP<sup>-</sup> neurons are not capsaicin sensitive nociceptors .....</i>	363
<i>Larger CGRP<sup>+</sup>SP<sup>-</sup> neurons are not classical mechanoreceptors .....</i>	364
<i>How do CGRP<sup>+</sup>SP<sup>-</sup> neurons function without SP? .....</i>	366
<i>What is the possible role of CGRP<sup>+</sup>SP<sup>-</sup> neurons? .....</i>	369
<i>Future directions.....</i>	372
<i>Summary .....</i>	372
<b>Reference List .....</b>	<b>375</b>



# List of Figures

---

Figure 1.1: A diagrammatic representation of the three different pain states. ....	48
Figure 1.2: Changes in pain sensation induced by injury.....	48
Figure 1.3: Myelination of sensory neurons.....	50
Figure 1.4: First and second pain .....	50
Figure 1.5: Schematic representation of the thermal response of TRP receptors .....	52
Figure 1.6: Schematic representation of the sensory innervation of human skin.....	54
Figure 1.7: Rexed laminae of the spinal cord.....	56
Figure 1.8: Central terminations of nociceptors.....	58
Figure 3.1: CGRP-IR and SP-IR in neuronal somata of the C7 DRG .....	92
Figure 3.2: Intensity of CGRP-IR and soma size in DRG neurons.....	94
Figure 3.3: Intensity of SP-IR and soma size in DRG neurons.....	94
Figure 3.4: Proportion of neuronal somata expressing CGRP-IR in DRG of all spinal levels.....	96
Figure 3.5: Proportion of CGRP-IR expressing neuronal somata that lacked SP-IR in DRG of all spinal levels .....	96
Figure 3.6: Soma size of neurons in DRG of all spinal levels .....	98
Figure 3.7: Soma size of neurons expressing CGRP-IR without SP-IR in DRG of all spinal levels .....	98
Figure 3.8: Intensity of CGRP-IR in DRG of all spinal levels .....	100
Figure 3.9: Proportion and size of neuronal somata expressing CGRP-IR in C7 DRG .....	102
Figure 3.10: Proportion and size of neuronal somata expressing CGRP-IR in T5 DRG .....	102
Figure 3.11: Proportion and size of neuronal somata expressing CGRP-IR in L4 DRG .....	104
Figure 3.12: Proportion and size of neuronal somata expressing CGRP-IR in S3 DRG .....	104

Figure 3.13: CGRP-IR and SP-IR in the C7, T5, L4 and S3 dorsal horn .....	106
Figure 3.14: Volume of CGRP-IR boutons in the dorsal horn of all spinal levels..	108
Figure 3.15: Proportion of CGRP-IR boutons lacking SP-IR in the dorsal horn of all spinal levels.....	110
Figure 3.16: Volume of CGRP-IR boutons containing or lacking SP-IR in the dorsal horn of all spinal levels .....	112
Figure 3.17: CGRP-IR and SP-IR in the C7 dorsal horn.....	114
Figure 3.18: Volume of CGRP-IR terminals in the C7 dorsal horn .....	116
Figure 3.19: Percentage of CGRP-IR terminals that lack SP-IR in the C7 dorsal horn .....	116
Figure 3.20: Volume of CGRP-IR terminals lacking SP-IR in the C7 dorsal horn.	116
Figure 3.21: CGRP-IR and SP-IR in the T5 dorsal horn .....	118
Figure 3.22: Volume of CGRP-IR terminals in the T5 dorsal horn.....	120
Figure 3.23: Percentage of CGRP-IR terminals that lack SP-IR in the T5 dorsal horn .....	120
Figure 3.24: Volume of CGRP-IR terminals lacking SP-IR in the T5 dorsal horn .	120
Figure 3.25: CGRP-IR and SP-IR in the L4 dorsal horn .....	122
Figure 3.26: Volume of CGRP-IR terminals in the L4 dorsal horn.....	124
Figure 3.27: Percentage of CGRP-IR terminals that lack SP-IR in the L4 dorsal horn .....	124
Figure 3.28: Volume of CGRP-IR terminals lacking SP-IR in the L4 dorsal horn .	124
Figure 3.29: CGRP-IR and SP-IR in the S3 dorsal horn .....	126
Figure 3.30: Volume of CGRP-IR terminals in the S3 dorsal horn.....	128
Figure 3.31: Percentage of CGRP-IR terminals that lack SP-IR in the S3 dorsal horn .....	128
Figure 3.32: Volume of CGRP-IR terminals lacking SP-IR in the S3 dorsal horn .	128
Figure 3.33: CGRP-IR in dermal papillae of glabrous paw skin .....	130
Figure 3.34: CGRP-IR fibres penetrating the epidermis of glabrous paw skin .....	132

Figure 3.35: CGRP-IR in Meissner's corpuscles of glabrous paw skin.....	134
Figure 3.36: CGRP-IR in hairy paw skin.....	136
Figure 3.37: CGRP-IR in hair follicle afferents of hairy paw skin.....	138
Figure 4.1: TRPV1, CGRP and SP-IR in neuronal soma of the C7 DRG .....	168
Figure 4.2: Intensity of TRPV1-IR and soma size in DRG neurons.....	170
Figure 4.3: Proportion of neuronal somata expressing TRPV1-IR in DRG of all spinal levels.....	172
Figure 4.4: Soma size of neurons expressing TPRV1-IR in DRG of all spinal levels .....	172
Figure 4.5: Proportion of CGRP <sup>+</sup> SP <sup>-</sup> TRPV1 <sup>-</sup> neurons in DRG of all spinal levels .	174
Figure 4.6: Soma size of CGRP <sup>+</sup> SP <sup>-</sup> TRPV1 <sup>-</sup> neurons in DRG of all spinal levels..	174
Figure 4.7: Proportion of CGRP <sup>+</sup> SP <sup>-</sup> TRPV1 <sup>-</sup> neurons in individual DRG .....	176
Figure 4.8: Soma size of CGRP <sup>+</sup> SP <sup>-</sup> TRPV1 <sup>-</sup> neurons in individual DRG.....	178
Figure 4.9: NF200, CGRP and SP-IR in neuronal soma of the C7 DRG .....	180
Figure 4.10: Intensity of NF200-IR and soma size in DRG neurons.....	182
Figure 4.11: Proportion of neuronal somata expressing NF200-IR in DRG of all spinal levels.....	184
Figure 4.12: Soma size of neurons expressing NF200-IR in DRG of all spinal levels .....	184
Figure 4.13: Proportion of CGRP <sup>+</sup> SP <sup>-</sup> NF200 <sup>+</sup> neurons in DRG of all spinal levels	186
Figure 4.14: Soma size of CGRP <sup>+</sup> SP <sup>-</sup> NF200 <sup>+</sup> neurons in DRG of all spinal levels	186
Figure 4.15: Proportion of CGRP <sup>+</sup> SP <sup>-</sup> NF200 <sup>+</sup> neurons in individual DRG.....	188
Figure 4.16: Soma size of CGRP <sup>+</sup> SP <sup>-</sup> NF200 <sup>+</sup> neurons in individual DRG .....	190
Figure 4.17: GAL, CGRP and SP-IR in neuronal soma of the L4 DRG.....	192
Figure 4.18: Intensity of GAL-IR and soma size in DRG neurons.....	194
Figure 4.19: Proportion of neuronal somata expressing GAL-IR in DRG of all spinal levels.....	196

Figure 4.20: Size of neuronal somata expressing GAL-IR in DRG of all spinal levels .....	196
Figure 4.21: Proportion of CGRP <sup>+</sup> SP <sup>-</sup> GAL <sup>-</sup> neurons in DRG of all spinal levels...	198
Figure 4.22: Soma size of CGRP <sup>+</sup> SP <sup>-</sup> GAL <sup>-</sup> neurons in DRG of all spinal levels....	198
Figure 4.23: Proportion of CGRP <sup>+</sup> SP <sup>-</sup> GAL <sup>-</sup> neurons in individual DRG.....	200
Figure 4.24: Proportion and soma size of CGRP <sup>+</sup> SP <sup>-</sup> GAL <sup>-</sup> neurons in DRG of all spinal levels.....	202
Figure 4.25: VIP, CGRP and SP-IR in neuronal soma of the S3 DRG .....	204
Figure 4.26: Intensity of VIP-IR and soma size in DRG neurons .....	206
Figure 4.27: Proportion of neuronal somata expressing VIP-IR in DRG of all spinal levels .....	208
Figure 4.28: Soma size of neurons expressing VIP-IR in DRG of all spinal levels	208
Figure 4.29: Proportion of CGRP <sup>+</sup> SP <sup>-</sup> VIP <sup>-</sup> neurons in DRG of all spinal levels....	210
Figure 4.30: Soma size of CGRP <sup>+</sup> SP <sup>-</sup> TRPV1 <sup>-</sup> neurons in DRG of all spinal levels	210
Figure 4.31: Proportion of CGRP <sup>+</sup> SP <sup>-</sup> VIP <sup>-</sup> neurons in individual DRG.....	212
Figure 4.32: Soma size of CGRP <sup>+</sup> SP <sup>-</sup> VIP <sup>-</sup> neurons in individual DRG .....	214
Figure 5.1: CTXb labelled neuronal somata in L4 DRG .....	228
Figure 5.2: CTXb labelled neuronal somata of various sizes in L4 DRG .....	230
Figure 5.3: CTXb labelled neurons expressing CGRP-IR in L4 DRG.....	232
Figure 5.4: Proportion of CTXb labelled neurons expressing CGRP-IR -IR in L4 DRG .....	234
Figure 5.5: The somata size of CTXb labelled neurons in L4 DRG.....	236
Figure 5.6: Proportion CGRP-IR labelled with CTXb in L4 DRG .....	236
Figure 6.1: C7 anterograde tracing set up .....	256
Figure 6.2: NB labelled neuronal somata in the C7 DRG .....	258
Figure 6.4: Volume of NB labelled fibres in the C7 dorsal horn.....	262
Figure 6.5: NB labelled neuronal somata in C7 DRG .....	264

Figure 6.6: NB labelled fibres in the C7 dorsal horn in association with CGRP-IR terminals .....	266
Figure 6.7: Volume of NB labelled fibres that contained CGRP-IR in the C7 dorsal horn.....	268
Figure 6.8: Proportion of NB labelled fibres that contained CGRP-IR in the C7 dorsal horn.....	270
Figure 6.9: Proportion of CGRP-IR within NB labelled fibres in the C7 dorsal horn .....	272
Figure 6.10: NB labelled fibres in the L4 dorsal horn.....	274
Figure 6.11: Volume of NB labelled fibres in the L4 dorsal horn .....	276
Figure 6.12: Volume of NB labelled fibres in the C7 dorsal horn compared to the L4 dorsal horn.....	276
Figure 6.13: NB labelled fibres in the L4 dorsal horn in association with CGRP-IR terminals .....	278
Figure 6.14: Volume of NB labelled fibres that contained CGRP-IR in the L4 dorsal horn.....	280
Figure 6.15: Volume of NB labelled fibres that contained CGRP-IR in the C7 dorsal horn compared to the L4 dorsal horn .....	282
Figure 6.16: Proportion of NB labelled fibres that contained CGRP-IR in the L4 dorsal horn.....	284
Figure 6.17: Proportion of NB labelled fibres that contained CGRP-IR in the C7 dorsal horn compared to the L4 dorsal horn.....	286
Figure 6.18: Proportion of CGRP-IR within NB labelled fibres in the L4 dorsal horn .....	288
Figure 6.19: Proportion of CGRP-IR within NB labelled fibres in the C7 dorsal horn compared to the L4 dorsal horn.....	290
Figure 6.20: NB labelled fibres in the L4 dorsal horn in association with CGRP-IR and VGluT1-IR terminals.....	292
Figure 6.21: Proportion of NB-labelled fibres containing VGluT-IR compared to CGRP-IR in C7 dorsal horn .....	294

Figure 6.22: Proportion of NB-labelled fibres containing VGluT-IR compared to CGRP-IR in L4 dorsal horn .....	294
Figure 6.23: Proportion of NB-labelled fibres containing VGluT-IR or CGRP-IR in C7 dorsal horn compared to L4 dorsal horn .....	296
Figure 7.1: MAPK/ERK signal transduction pathways .....	322
Figure 7.2: pERK levels in lumbar dorsal horn after stimulation with capsaicin....	324
Figure 7.3: Number of pERK-IR cells in the dorsal horn after stimulation with capsaicin.....	326
Figure 7.4: Proportion of pERK-IR cells in the dorsal horn after stimulation with capsaicin.....	326
Figure 7.5: pCREB-IR levels in lumbar dorsal horn after stimulation with capsaicin .....	328
Figure 7.6: Number of pCREB-IR cells in the dorsal horn after stimulation with capsaicin.....	330
Figure 7.7: Proportion of pCREB-IR cells in the dorsal horn after stimulation with capsaicin.....	330
Figure 7.8: Number of pERK-IR cells compared to the number of pCREB-IR cells in the dorsal horn after stimulation with capsaicin .....	332
Figure 7.9: Proportion of pERK-IR cells compared to the proportion of pCREB-IR cells in the dorsal horn after stimulation with capsaicin.....	332
Figure 7.10: CGRP-IR terminals and pERK-IR cells in lumbar dorsal horn stimulated with capsaicin.....	334
Figure 7.11: Peptidergic contacts onto pERK-IR cells in lumbar dorsal horn after stimulation with capsaicin.....	336
Figure 7.12: Multiple peptidergic contacts onto pERK-IR cells in lumbar dorsal horn after stimulation with capsaicin .....	338
Figure 7.13: pERK levels in lumbar dorsal horn after electrical stimulation of afferent fibres .....	340
Figure 7.14: pCREB levels in lumbar dorsal horn after electrical stimulation of afferent fibres .....	342

Figure 7.15: Number of pCREB-IR cells in the dorsal horn after electrical stimulation of afferent fibres .....	344
Figure 7.16: Proportion of pCREB-IR cells in the dorsal horn after electrical stimulation of afferent fibres .....	344
Figure 7.17: Number of pCREB-IR cells in the dorsal horn after electrical stimulation of afferent fibres compared to the number of pCREB-IR cells after capsaicin stimulation .....	346
Figure 7.18: Proportion of pCREB-IR cells in the dorsal horn after electrical stimulation of afferent fibres compared to the number of pCREB-IR cells after capsaicin stimulation .....	346
Figure 7.19: CGRP-IR terminals and pCREB-IR cells in lumbar dorsal horn electrical stimulation of afferent fibres .....	348
Figure 7.20: Peptidergic contacts onto pCREB-IR cells in the dorsal horn after electrical stimulation of afferent fibres .....	350
Figure 7.21: Multiple peptidergic contacts onto electrically induced pCREB-IR neurons in the dorsal horn .....	352



## List of Tables

---

Table 2.1: Primary and secondary antisera .....	65
Table 2.2: Filter cube specifications for the Olympus BX50 Microscope.....	66
Table 4.1: Primary and secondary antisera .....	147
Table 4.2: Summary of the subpopulations of CGRP expressing neurons .....	166



---

# Preface

---



## Thesis Summary

---

The neural processing of pain is not entirely understood. One of the largest problems limiting the current understanding of nociception is the widespread use of oversimplified classification schemes. Nociceptors are classified as either peptidergic or nonpeptidergic. Peptidergic nociceptors usually co-express the peptides calcitonin gene-related peptide (CGRP) and substance P (SP; CGRP<sup>+</sup>SP<sup>+</sup>). CGRP enhances the nociceptive effects of SP, but has very little effect by itself. Yet, in mice dorsal root ganglia (DRG), some neurons express CGRP without SP (CGRP<sup>+</sup>SP<sup>-</sup>) and these neurons are not yet characterised.

The prevalence and distribution of CGRP<sup>+</sup>SP<sup>-</sup> neurons and their neurochemical profile was determined using multiple labelling immunohistochemistry. In DRG CGRP<sup>+</sup>SP<sup>-</sup> neurons accounted for half of the CGRP-immunoreactive (IR) DRG neurons. Cutaneous CGRP<sup>+</sup>SP<sup>-</sup> fibres were numerous within dermal papillae and around hair shafts, and CGRP<sup>+</sup>SP<sup>-</sup> boutons were prevalent in lateral laminae I/II and in lamina IV/V of the spinal dorsal horn. CGRP<sup>+</sup>SP<sup>-</sup> neurons were distinguished from CGRP<sup>+</sup>SP<sup>+</sup> neurons by their much larger soma size in DRG, and by their expression of the myelinated marker NF200 and lack of expression of the capsaicin sensitive TRPV1 receptor, which is possessed by most peptidergic nociceptors. Overall, there were two subpopulations of CGRP<sup>+</sup>SP<sup>-</sup> neurons: medium myelinated A $\delta$ -fibre CGRP<sup>+</sup>SP<sup>-</sup>TRPV1<sup>+</sup> neurons and medium-large sized myelinated A $\delta$ /A $\beta$ -fibre CGRP<sup>+</sup>SP<sup>-</sup>TRPV1<sup>-</sup> neurons.

To determine the central and peripheral projections of the CGRP<sup>+</sup>SP<sup>-</sup> neurons axonal tracing was coupled with multiple-labelling immunohistochemistry. Retrograde tracing from muscle tissue revealed that muscular CGRP<sup>+</sup>SP<sup>-</sup> afferents originated from the larger CGRP<sup>+</sup>SP<sup>-</sup> somata. Anterograde tracing revealed dual central projections of CGRP<sup>+</sup>SP<sup>-</sup> neurons in the laminae I/II and laminae IV/V of the spinal dorsal horn. The finer, most likely A $\delta$ -fibre, CGRP<sup>+</sup>SP<sup>-</sup> neurons terminated in lamina I/II, whereas the larger, most likely A $\beta$ -fibre, CGRP<sup>+</sup>SP<sup>-</sup> neurons terminated in lamina IV/V. The laminae IV/V CGRP<sup>+</sup>SP<sup>-</sup> fibres were not classical VGlut1-IR mechanoreceptors.

The central targets of these neurons were identified using the activated extracellular signal-regulated kinase (ERK) and cAMP response element-binding protein (CREB) as markers for neuronal activation. Viable spinal cord slices were stimulated both electrically and with capsaicin. Noxiously activated neurons received contacts from CGRP<sup>+</sup>SP<sup>-</sup> afferents in lamina I. In contrast, no cells were activated in lamina IV/V. Therefore, it is likely that the CGRP<sup>+</sup>SP<sup>-</sup> afferents of lamina IV/V were not nociceptive.

Overall, this research has led to an improved understanding of the properties of an uncharacterised population of presumed nociceptors. CGRP-IR neurons could be subdivided based on their SP expression. CGRP<sup>+</sup>SP<sup>-</sup> neurons could be further subdivided based on their TRPV1 expression: A $\delta$ -fibre CGRP<sup>+</sup>SP<sup>-</sup>TRPV1<sup>+</sup> neurons and A $\delta$ /A $\beta$ -fibre CGRP<sup>+</sup>SP<sup>-</sup>TRPV1<sup>-</sup> neurons. CGRP<sup>+</sup>SP<sup>-</sup>TRPV1<sup>+</sup> and CGRP<sup>+</sup>SP<sup>-</sup>TRPV1<sup>-</sup> neurons are unlikely to be involved in acute nociception. The CGRP<sup>+</sup>SP<sup>-</sup>TRPV1<sup>+</sup> neurons had central terminations in laminae I/II and likely had a modulatory role in nociception that may contribute to the central sensitisation resulting in hyperalgesia associated with inflammatory and chronic pain states. The CGRP<sup>+</sup>SP<sup>-</sup>TRPV1<sup>-</sup> neurons are likely an uncharacterized population of mechanoreceptors. While these neurons may not be involved in nociception, they may synapse on wide dynamic range neurons and could contribute to mechanical allodynia.

## Declaration

---

I certify that this thesis does not incorporate, without acknowledgement, any material previously submitted for a degree or diploma in any university; and that to the best of my knowledge and belief it does not contain any material previously written or published by another person except where due reference is made in the text. Furthermore, I have carried out all of the experimental work reported in this thesis.

Signed

A handwritten signature in black ink, appearing to read 'Gareth Kestell', written in a cursive style.

Garreth Kestell



## Acknowledgements

---

I would like to thank the members of the Autonomic (& Sensory) Neurotransmission Laboratory for allowing me to become apart of their lab for the last 5 years. I would also like to specifically thank:

- My supervisor, **Prof. Ian Gibbins**, for everything. Your seemingly endless wisdom still amazes me. I cannot thank you enough for this experience; I have learnt so much from you.
- My co-supervisor, **Assoc. Prof. Rainer Haberberger**, for your continual help and support, especially in time management. You were very accessible and managed to keep work enjoyable.
- My advisor, **Prof. Simon Brookes**, for your help, especially in the final stages of my thesis.
- My current employer, **Assoc. Prof. Nick Spencer**, for understanding the demanding nature of juggling a full-time workload with finishing a thesis
- Other laboratory members including: **Mrs. Pat Vilimas, Dr. Jen Clarke, Ms. Yvette DeGraaf and Dr. Christine Barry**, for their limitless experimental expertise, assistance in experiments when required and any additional help throughout the years.
- **Past and present students**: for keeping me relatively sane
- **Centre for Neuroscience**; for their generous financial support for conferences, and helpful feedback and awards in seminars.
- Finally, my **Mum and Dad**, for everything. You guys helped me out more than I would like to admit. I could not have finished this without you two.



## Publications from this thesis

---

### Journal Publications

**Kestell, G.R.**, Anderson, R.L., Clarke, J.N., Haberberger, R.V. and Gibbins, I.L. (2015) 'Primary afferent neurons containing calcitonin gene-related peptide but not substance P in forepaw skin, dorsal root ganglia and spinal cord of mice' *Journal of Comparative Neurology*, [Epub ahead of print] 23 May 2015

Barry, C.M., **Kestell, G.**, Gillan, M., Haberberger, R.V. and Gibbins, I.L. (2015) 'Sensory nerve fibres containing calcitonin gene-related peptide in gastrocnemius, latissimus dorsi and erector spinae muscles and thoracolumbar fascia in mice' *Neuroscience*, 291: 106-117

### Conference Proceedings

**Kestell G.R.**, Haberberger R.V. and Gibbins I.L. (2014) Nociceptive dorsal horn neurons receive convergent contacts from primary afferent terminals expressing calcitonin gene-related peptide but not substance P. *Proceedings of the Australian Neuroscience Society, 34<sup>th</sup> Annual Meeting*, Adelaide

Barry, C., Gillan M.E., Vilimas, P.V., **Kestell G.R.**, Haberberger R.V and Gibbins I.L. (2013) Sensory innervation of the thoracolumbar fascia, erector spinae and transversospinales muscles. *The Australian Physiotherapy Association Conference: 'New Moves'*, Melbourne

**Kestell G.R.**, Haberberger R.V. and Gibbins I.L. (2013) Segmental dependent differences in neurochemical profile of calcitonin gene-related peptide containing sensory neurons. *Proceedings of the Australian Neuroscience Society, 33<sup>rd</sup> Annual Meeting*, Melbourne

Gillan M.E., **Kestell G.R.**, Haberberger R.V. and Gibbins I.L. (2013) Distribution of sensory fibres containing CGRP but not substance P in skeletal muscles of mice. *Proceedings of the Australian Neuroscience Society, 33<sup>rd</sup> Annual Meeting*, Melbourne

**Kestell G.R.**, Clarke J.N., Haberberger R.V. and Gibbins I.L. (2012) Primary afferent neuron terminals containing calcitonin gene-related peptide (CGRP) but not substance P contact noxiously activated murine dorsal horn neurons. *Proceedings of the Australian Neuroscience Society, 32<sup>nd</sup> Annual Meeting*, Gold Coast

**Kestell G.R.**, Anderson, R.L., Clarke J.N., Haberberger R.V. and Gibbins I.L. (2011) Spinal projections of mid-sized sensory neurons expressing calcitonin gene-related peptide (CGRP) without substance P in mice. *Proceedings of the Australian Neuroscience Society, 31<sup>st</sup> Annual Meeting*, Auckland

**Kestell G.R.**, Anderson, R.L., Clarke J.N., Haberberger R.V. and Gibbins I.L. (2010) Peripheral and central projections of mid-size sensory neurons containing calcitonin gene-related peptide but not substance P in mice. *Proceedings of the Australian Neuroscience Society, 30<sup>th</sup> Annual Meeting*, Sydney

**Kestell G.R.**, Anderson, R.L., Clarke J.N., Haberberger R.V. and Gibbins I.L. (2010)  
Spinal projections of mid-sized sensory neurons expressing calcitonin gene-related peptide (CGRP) without substance P in mice. *Proceedings of the Australian Physiological Society* **41**, Adelaide

## **Awards attained during this thesis**

---

- 2013      **Kathleen V. Russell Prize in Neurobiology**  
*Awarded to the Honours, Masters by Research or Postgraduate student showing most promise in their field of research*  
Flinders Medical Centre Foundation  
Flinders University
- 2010      **Kathleen V. Russell Prize in Neurobiology**  
*Awarded to the Honours, Masters by Research or Postgraduate student showing most promise in their field of research*  
Flinders Medical Centre Foundation  
Flinders University
- GlaxoSmithKline Victor MacFarlane Graduate Student Prize**  
*Awarded for the best seminar given by a Postgraduate or Masters by Research student member*  
Centre for Neuroscience  
Flinders University
- Australian Postgraduate Award**  
*Awarded to students of exceptional research potential undertaking a Higher Degree by Research in Australia*  
Australian Federal Government



## Abbreviations

---

2D	two-dimensional
3D	three-dimensional
AIS	artificial intracellular solution
ANOVA	analysis of variance
ANT Lab	Autonomic and Sensory Neurotransmission Laboratory
ASIC	acid sensing ion channel
ATP	adenosine triphosphate
BMC	Bonferroni's multiple comparisons
C	cervical
cAMP	cyclic adenosine monophosphate
CBS	caudally biting and scratching
CFA	complete Freund's adjuvant
CGRP	calcitonin gene-related peptide
CGRP <sup>+</sup> SP <sup>+</sup>	CGRP with SP
CGRP <sup>+</sup> SP <sup>-</sup>	CGRP without SP
CLR	calcitonin-like receptor
CMH	c-fibre mechano-heat nociceptor
CNS	central nervous system
CREB	cAMP response element binding protein
CTXb	cholera toxin subunit B
Cy	cyanine
DC	dorsal column
DF	dorsal funiculus
DMEM	Dulbecco's modified eagle media
DMSO	dimethyl sulfoxide
DRG	dorsal root ganglia
DTAF	dichlorotriazinylaminofluorescein
ERK	extracellular regulated kinase
FITC	fluorescein isothiocyanate
FCS	foetal calf serum
G	gauge
GFAP	glial fibrillary acidic protein
h	hour

## Preface

HBSS	HEPES buffered balanced salt solution
HEPES	4-(2-hydroxyethyl)-1-piperazineethanesulfonic acid
HFA	hair follicle afferent
IASP	International Association for the Study of Pain
IB4	isolectin from <i>Bandeiraea (Griffonia) simplicifolia</i>
IBA <sub>1</sub>	ionized calcium-binding adapter molecule 1
IENF	intraepidermal nerve fibres
IgG	immunoglobulin
IL	interleukin
IR	immunoreactive/immunoreactivity
kDA	kilodaltons
L	lamina
L	lumbar
M	molar or moles per litre
MAPK	mitogen-activated protein kinase
Mg <sup>2+</sup>	magnesium ions
MIA	mechanically insensitive afferents
μ	micro
N.A.	numerical aperture
n/a	not applicable
Na <sup>2+</sup>	sodium ion
NB	Neurobiotin
NDS	normal donkey serum
NIH	National Institute of Health
NF200	neurofilament 200kDA
NK	neurokinin
ns	not statistically significant
OCT	optimal cutting temperature compound
P2X	purinoreceptor
PAN	primary afferent neuron/nerve
PBS	phosphate buffered saline
PC	personal computer
pCREB	phosphorylated CREB
PEG	polyethylene glycol
PEI	polyethyleneimine

pERK	phosphorylated ERK
RA	rapidly adapting
RMANVOA	repeated measures ANOVA
S	sacral
SA	slowly adapting
SA-	streptavidin
SC	spinal cord
SD	standard deviation
SEM	standard error of the mean
SOM	somatostatin
SP	substance P
T	thoracic
TRPA	transient receptor potential ankyrin receptor
TRPM	transient receptor potential melastatin receptor
TRPV	transient receptor potential vanilloid receptor
UV	ultra violet
VGluT	vesicular glutamate transporter
VIP	vasoactive intestinal peptide
WDR	wide dynamic range



---

# **Chapter 1: Introduction**

---



## 1.1 Pain

---

Pain describes a wide range of highly unpleasant experiences, but is defined by the International Association for the Study of Pain (IASP) as “*an unpleasant sensory and emotional experience associated with actual or potential tissue damage*” (Merskey & Bogduk, 1994). As this definition suggests, it is a perceptual experience that is composed of both sensory and emotional components.

This thesis focuses on the sensory component also known as nociception, which is the neural processing of the actual and potential tissue damage from an injury. However, the emotional aspect of pain, that includes the subjective behavioural and affective responses to an injury, means that objectively determining the underlying neural mechanisms of painful experiences is challenging (Cervero & Laird, 1991).

Therefore, the classification of pain perception usually relies on a verbal description of its location, intensity and quality rather than by an objectively determined comparable parameter. Unfortunately, there is a substantial mismatch between these descriptive aspects of pain and the underlying physiological mechanism. Recognising this, Cervero and Laird (1991) have defined three main underlying neural mechanisms that contribute to different pain states and it has been adopted by many in the field (Price *et al.*, 2001; Brooks & Tracey, 2005; Cervero, 2007; Treede *et al.*, 2008). These are:

1. Nociceptive (hence referred to in this thesis as acute nociception, to distinguish it from the following two mechanisms);
2. Inflammatory (which includes nociception after inflammation) and
3. Neuropathic pain (a form of chronic pain resulting from neurological damage)

These three underlying neural mechanisms that contribute to different pain conditions are elaborated upon in the following sections and summarised in Figure 1.1.

## **Acute nociception**

In the context of this thesis, acute nociception (or nociceptive pain) refers to the neural processing of pain under normal conditions. Acute nociception is protective, fast acting and enables us to prevent and minimise any tissue damage (Cervero & Laird, 1991). This process begins when the threshold of a specific type of neuron, known as a nociceptor, is exceeded either by an aggravating stimulus that has the potential to cause tissue damage, or by products of present tissue damage (collectively referred to as noxious stimuli). These noxious stimuli can include extremes of temperature; intense mechanical pressure, tissue damage; or irritant chemicals (Julius & Basbaum, 2001; Basbaum *et al.*, 2009).

The cell bodies of nociceptors are located outside of the spinal cord in dorsal root ganglia (DRG) and trigeminal ganglia with peripheral axons that innervate superficial and deep tissues, and central axons that enter the spinal cord and communicate with dorsal horn neurons. Once activated, an action potential is generated that propagates along the axon of the nociceptor towards the spinal cord. At the spinal cord the nociceptor either synapses with interneurons to elicit a rapid protective withdrawal reflex, or synapses with projection neurons. Projection neurons terminate in the thalamus and neurons from the thalamus then project to the primary and secondary somatosensory cortex for the descriptive aspects of pain (i.e. sensation, location, and quality of pain), and the anterior cingulate gyrus and rostral insula for the emotional aspects of pain.

## **Nociception after inflammation**

Injury and tissue damage results in inflammation that causes hyperalgesia, which is an increase in pain sensitivity from noxious stimuli, provoking an increased sensation of pain (Figure 1.2; Merskey & Bogduk, 1994). Inflammation also causes allodynia, in which normally harmless stimuli can also elicit the sensation of pain (Figure 1.2; Merskey & Bogduk, 1994)

Primary hyperalgesia is the sensitisation of the peripheral nociceptor at the site of injury, sending enhanced signals to the Central Nervous System (CNS) leading to increased pain sensitivity at the injured area (Cervero & Laird, 1991). These enhanced signals eventually cause central sensitisation, which further enhances the

signal and also leads to the recruitment of other neurons that are not usually involved in nociception (secondary hyperalgesia; Cervero & Laird, 1991).

While nociception after inflammation is still a protective mechanism, it can last for several days or weeks after an injury, in contrast to acute nociception that is fast acting and transient. This discourages the use of an injured area and allows time to heal. Once the area has healed, the pain threshold usually reverts to normal (Cervero & Laird, 1991).

## **Chronic and neuropathic pain**

Chronic pain is defined as pain that persists past the normal time of healing (Merskey & Bogduk, 1994), usually lasting in excess 3-6 months (Turk & Okifuji, 2001). While allodynia and hyperalgesia are also features of chronic pain (similar to nociception after inflammation), the prolonged response from nociceptors remains and the pain threshold does not revert to normal (Cervero & Laird, 1991). Chronic pain can present in two states, either as chronic nociceptive pain that is due to excessive activation of the nociceptors, or chronic neuropathic pain that involves damage to the nervous system (either peripherally or centrally).

Chronic nociceptive pain often accompanies chronic diseases, such as cancers and arthritis, during which the nociceptors continue to function and correctly respond to stimuli. However as mentioned, the persistent nature of such diseases and the ongoing nature of the stimuli and subsequent inflammation, result in prolonged periods of pain (Cervero & Laird, 1991).

Damage to the peripheral or central nervous system (chronic neuropathic pain), can also result in the persistent sensation of pain even without an ongoing stimulus and can occur spontaneously with no apparent stimulus to display the same reduced pain thresholds that are characteristic of inflammatory pain (hyperalgesia and allodynia) but without any injury (Cervero & Laird, 1991).

Unlike acute nociception and nociception after inflammation, chronic pain does not have an obvious and important protective function. Instead, it adversely limits the everyday function and quality of life of the afflicted individual.

## The problem with pain

It can therefore be seen that normal reactions to painful stimuli are clearly protective sensations that are needed for the survival and wellbeing of the individual, as is the case for acute nociception and nociception after inflammation. However, chronic pain becomes maladaptive, serves no protective role and instead severely limits everyday life and general well being. It is among the most debilitating and costly afflictions in America (Debono *et al.*, 2013), Europe (Breivik *et al.*, 2012), Australia (Blyth *et al.*, 2001), and perhaps even across the globe (Ospina & Harstall, 2003). Nationally, it was estimated that 3.2 million Australians (1.4 million males and 1.7 million females) experienced chronic pain in 2007 and that as many as 5 million Australians will suffer chronic pain by 2050 (Access Economics Pty Ltd, 2007 using epidemiological data from the University of Sydney Pain Management Research Institute). Chronic pain has had a substantial financial impact on society, costing Australia around \$34.3 billion in 2007. The largest components of chronic pain costs were productivity loss, burden of disease (a measure of loss due to disease and injury that remains after treatment or rehabilitation), and healthcare costs (Access Economics Pty Ltd, 2007). There is also a substantial direct financial impact on individuals that are suffering from chronic pain which was estimated to be approximately \$11,000 per person in 2007 (Access Economics Pty Ltd, 2007).

Chronic pain impacts upon a large proportion of the Australian working age population with an obvious correlation to the aged and those that are socially disadvantaged (Cervero & Laird, 1991; Blyth *et al.*, 2001). The prevalence of chronic pain is comparable with other health priority areas including cardiovascular disease, cancer and diabetes (Access Economics Pty Ltd, 2007). Chronic pain is often associated with other health priority areas and as such it is difficult to distinguish its true prevalence (Access Economics Pty Ltd, 2007). It is also associated with higher rates of depression and anxiety (Access Economics Pty Ltd, 2007). However, despite the current range of therapies for chronic pain across these broad socio-economic and health spectrums, there are a large proportion of patients for whom treatment does not offer any significant relief (Micó *et al.*, 2006; Finnerup *et al.*, 2010)

Many aspects of nociception are still not yet understood, particularly with respect to the properties of the primary afferent nociceptors that initially respond to noxious stimuli, and their projections into the spinal cord (which remain only partially characterised). These properties are unknown, both in regard to the normal functions of these nociceptors and to their contributions to chronic pain. Therefore, in order to mitigate this lack of understanding, there is an apparent need for more detailed nociception research.

## **Summary**

To summarise so far, this section has presented the concept of pain, the different pain states (acute, inflammatory and chronic) and the current prevalence and problems associated with chronic pain. As a consequence nociception has been introduced as the neural processing of a painful stimulus in which there are three differing mechanisms for acute nociception, inflammation and neuropathic pain. While normal reactions to pain are on the whole protective, chronic pain can be debilitating and costly, with an incomplete understanding of nociception causing major problems in determining the most appropriate pain therapies. In the following section, the recent advances and the remaining limitations in the understanding of nociception will be presented and discussed.



## 1.2 Nociceptors

---

This section therefore articulates the current understanding of nociceptors in regards to their normal functions. There are many different classes of nociceptors, with each specific for the neural processing of a particular noxious stimulus or combination of noxious stimuli. These different classes of nociceptors are characterised by several qualities that include:

1. The conduction velocity or myelination of their axons (e.g. A $\delta$  and C-fibre nociceptors);
2. Their molecular content or preferred neurotransmitter (e.g. peptidergic and nonpeptidergic nociceptors);
3. The tissue they innervate (e.g. cutaneous, muscular and visceral nociceptors);
4. Their preferred stimulus (e.g. mechanical, thermal and chemical nociceptors);
5. Their central projections into the spinal cord (e.g. nociceptors of superficial and deep dorsal horn) and
6. Their pathways and targets in supraspinal areas (e.g. medial and lateral spinothalamic neurons).

### **Conduction velocity of nociceptors: A $\delta$ and C-fibre nociceptors**

Nociceptors can be characterised by their conduction velocities (CV), which is the speed at which an action potential propagates along its axon. This speed is largely dependent on the diameter and level of myelination of the axon, with sensory neurons either myelinated (A-fibres) or unmyelinated (C-fibres; see Figure 1.3) The myelinated A-fibres are divided into three subtypes: A $\alpha$ , A $\beta$  and A $\delta$  fibres, among which A $\alpha$  fibres are the most myelinated, have largest diameter axons (13 – 20  $\mu\text{m}$ ) and the fastest CV (80 – 120  $\text{ms}^{-1}$ ). A $\beta$  fibres are the second most myelinated, with the second largest diameter axon (6 – 12  $\mu\text{m}$ ) and are the second fastest CV (35 – 75  $\text{ms}^{-1}$ ), while the A $\delta$  fibres are the least myelinated, with the smallest diameter axons (1 – 5  $\mu\text{m}$ ) and are the slowest CV (5 – 30  $\text{ms}^{-1}$ ) of the A-fibres. However, the unmyelinated C-fibres are even smaller with axon diameters of 0.2 – 1.5  $\mu\text{m}$  and

have the slowest CV ( $0.5 - 2 \text{ ms}^{-1}$ ) of all the sensory fibre types (Bear *et al.*, 2011 for summary see Figure 1.3)

Generally there is an inverse relationship between the CV and the mechanical threshold (Burgess & Perl, 1967), and nociceptors are distinguished from other sensory fibres by their relatively high threshold for activation. Hence, nociceptors are generally small diameter afferents with slow CV ( $< 30 \text{ ms}^{-1}$ ) and comprise myelinated A $\delta$ -fibre and unmyelinated C-fibre neurons. It is believed that A $\delta$ -fibre nociceptors mediate the acute well-localised “first” or fast pain, and C-fibres nociceptors convey the poorly localised “second” or slow pain (Bear *et al.*, 2011 for summary see Figure 1.4).

### ***Myelinated A $\delta$ fibre nociceptors***

A $\delta$  fibres are mainly low-threshold mechanoreceptors (LTM; Hathway & Fitzgerald, 2007). However, there are some A $\delta$ -fibres that are nociceptive, and these can be divided into two subclasses (type I and type II). Both of these classes respond to intense mechanical stimuli, but are distinguished by their differential responsiveness to intense heat (Treede *et al.*, 1998).

Type I A-fibre mechano-heat (AMH) nociceptors respond to both mechanical and chemical stimuli but have relatively high heat thresholds. Some of these fibres have conduction velocities in the A $\delta$ -range (around  $25 \text{ ms}^{-1}$ ). However, some have conduction velocities as high as the A $\beta$  range ( $55 \text{ ms}^{-1}$ ) and are often referred to as high-threshold mechanoreceptors (Djoughri *et al.*, 1998; Djoughri & Lawson, 2004), yet these are often overlooked.

Type II AMH nociceptors respond to heat stimuli with much lower thresholds than type I AMH and are characterised by a rapidly-adapting fast response. Most have very high mechanical thresholds or do not respond to mechanical stimuli, and are often referred to as mechanically insensitive afferents (MIAs; Lynn & Carpenter, 1982). MIAs can become sensitised after tissue damage and become mechanically sensitive (Reeh *et al.*, 1987). These CV of these II A-fibre nociceptors is in the A $\delta$ -fibre range ( $15 \text{ ms}^{-1}$ ; Ringkamp & Meyer, 2007)

### ***Unmyelinated C-fibre nociceptors***

Most C-fibres are nociceptors and the majority of nociceptors have C-fibre axons. The most common are C-fibre mechano-heat nociceptors (CMHs) and polymodal nociceptors. CMHs respond to heat and mechanical stimuli and are capable of adaptation (Ringkamp & Meyer, 2007). The adaptation to heat stimuli can also be provoked by mechanical stimuli suggesting that the responsiveness to one stimulus can be decreased by a stimulus of different modality (Peng *et al.*, 2003).

Although the majority of C fibres are nociceptors, there are some that are not. C-fibre low threshold mechanoceptors (LTMs) have been identified in hairy skin of rodents, monkeys and humans (Nordin, 1990). They respond to light stroking of the skin but not to heat and play a role in pleasant touch sensations (Löken *et al.*, 2009). Other C-fibre afferents with extremely low thresholds to heat have been identified in many species (Darian-Smith *et al.*, 1979). These afferents do not respond to mechanical stimuli yet they have ongoing activity at room temperature and respond to gentle warming.

## **Molecular content of nociceptors: peptidergic and nonpeptidergic nociceptors**

Nociceptors can also be characterised based on their molecular content and while glutamate is believed to be the predominant excitatory neurotransmitter in all sensory neurons, (Julius & Basbaum, 2001; Priestley, 2009) many nociceptors also co-express neuropeptides. Neuropeptides were originally believed to act as neuromodulators and potentiate the excitatory effects of glutamate (Hökfelt *et al.*, 1980; Kow & Pfaff, 1988). However, there is increasing evidence to suggest that certain peptides are able to act as neurotransmitters independent of glutamate. Many of these peptidergic neurons do not contain glutamate and even lack the protein machinery to utilise glutamate as a neurotransmitter (Morris *et al.*, 2005). Not all nociceptors express peptides and hence can be neurochemically subdivided into peptidergic or non-peptidergic sub-types.

The peptidergic nociceptors usually express the peptides substance P (SP) and calcitonin gene-related peptide (CGRP). They also express tyrosine kinase receptor (TrkA) for nerve growth factor (NGF), and mostly possess slowly conducting unmyelinated C-fibres that project mainly to lamina I and IIo of the spinal dorsal

horn. They are capsaicin-sensitive, respond to a wide range of noxious stimuli and are heavily involved in inflammation (Julius & Basbaum, 2001; Woolf & Ma, 2007; Belmonte & Viana, 2008; Dubin & Patapoutian, 2010).

Nonpeptidergic nociceptors lack neuropeptide and TrkA expression, but express fluoride-resistant acid phosphatase (FRAP) and can be visualized by the binding of the *Griffonia simplicifolia* lectin IB4. They also express c-Ret neurotrophin receptor for glial-derived neurotrophic factor (GDNF), purinergic P2X<sub>3</sub> receptors, mostly possess faster conducting thinly myelinated fibres (A $\delta$ -fibres) that project mainly to lamina III of the dorsal horn. They mostly are insensitive to capsaicin and respond to noxious mechanical stimuli (Julius & Basbaum, 2001; Woolf & Ma, 2007; Belmonte & Viana, 2008; Dubin & Patapoutian, 2010).

Unfortunately, the division of nociceptors into these two subclasses is imperfect and there is a degree of overlap and misrepresentation in the literature. For example: some groups (Julius & Basbaum, 2001; Basbaum *et al.*, 2009) claim that the C-fibre nociceptors are either peptidergic or nonpeptidergic and the larger A $\delta$ -fibres do not fit these categories. Yet it has been shown that SP is present in A $\delta$ - and C-fibre neurons (McCarthy & Lawson, 1989) and CGRP is even present in A $\alpha$ -, A $\beta$ -, A $\delta$ - and C-fibre neurons (McCarthy & Lawson, 1990). Therefore peptidergic nociceptors are not limited to C-fibre nociceptors. There is also an overlap of marker expression between peptidergic and nonpeptidergic neurons (Ringkamp & Meyer, 2007). For example: some IB4 neurons express TRPV1 or CGRP (Priestley, 2009). The expression of these markers also changes during development and after injury. For example: peripheral inflammation up-regulates the expression neuropeptides, whereas nerve injury down-regulates expression of neuropeptides (Ringkamp & Meyer, 2007).

Furthermore, there is increasing evidence that some nociceptors do not fit into neat peptidergic or nonpeptidergic categories. Several DRG nociceptor subpopulations neither express neuropeptides nor bind IB4. Examples include presumptive nociceptors that: express high levels of vesicular glutamate transporter 2 (VGluT2; Morris *et al.*, 2005; Clarke *et al.*, 2011); express transient receptor potential (TRP) cation channel subfamily M8 (TRPM8; Peier, Reeve, *et al.*, 2002; Dhaka *et al.*, 2008); a population that express the capsaicin receptor, TRP subfamily vanilloid 1

(Bráz & Basbaum, 2010); and small groups that express Mas-related G-protein coupled receptor member D (*Mrgprd*) and TRPA1 (Cavanaugh *et al.*, 2009).

## **Preferred stimulus of nociceptors: the channels of nociceptors**

Nociceptors are either dedicated to a particular type of noxious stimulus, or are able to respond to a variety of noxious stimuli. Those that respond to extremes of temperature (both hot and cold) are thermo-nociceptors, mechano-nociceptors respond to intense mechanical pressure, chemo-nociceptors to irritant chemicals, while those that are able to respond to a variety of noxious stimuli and are referred to as polymodal nociceptors.

To respond to a noxious stimulus, a nociceptor must first convert the stimulus into neuronal activity. This is done through a process called transduction, during which a stimulus causes a conformational change in the structure of specific receptors within nociceptor terminals. This structural change triggers the opening or closing of ion channels and produces a change in ionic flow across the plasma membrane that changes the membrane potential. If the change in membrane potential is large enough it will evoke an action potential (Gold & Caterina, 2007). The specific stimulus to which a nociceptor responds to is dependent on the type or combination of receptor-channel complexes it expresses. There is an immense breadth and diversity of receptor-channel complexes that have been identified to have roles in the transduction of a noxious stimulus into neuronal activity. Therefore, in the context of this thesis we focus on those that are important for the peptidergic nociceptor populations, which include the Transient Receptor Potential (TRP) channels; purinergic receptors; Acid-Sensing Ion Channels (ASICs) and voltage gated sodium channels ( $\text{Na}_v$ ).

### ***TRP channels***

TRP channels are a large family of ligand-gated ion channels that display unusually high diversities of cation permeability. This family currently includes seven subfamilies (TRPA, TRPC, TRPM, TRPML, TRPP, and TRPV). A number of these TRP channels are activated by noxious thermal stimuli, namely: TRPV1, TRPV2, TRPV3, TRPV4, TRPM8, and TRPA1 (see Figure 1.5 summary).

## Introduction

TRP vanilloid sub-family, member 1 (TRPV1; previously referred to as VR1: vanilloid receptor) is the best-characterised TRP channel. TRPV1 is expressed in small diameter DRG neurons (Caterina *et al.*, 1997; Tominaga *et al.*, 1998). TRPV1 is most notably activated by the vanilloid compound capsaicin (the spicy component of chilli peppers) and noxious heat ( $\geq 43^{\circ}\text{C}$ ; Caterina *et al.*, 1997), but is also activated by other chemical stimuli, including: resiniferotoxin (RTX), jelly fish and spider venoms and low pH (Szallasi *et al.*, 2007). While TRPV1 has a clear role in detecting noxious heat (Caterina *et al.*, 1997) and in thermal hyperalgesia after inflammation and injury (Caterina *et al.*, 2000; Davis *et al.*, 2000; Levine & Alessandri-Haber, 2007), it has also been shown to have a clear mechanical role in models of deep tissue pain (Jones *et al.*, 2005; Miranda *et al.*, 2007; Fujii *et al.*, 2008; Ravnfjord *et al.*, 2009) and joint pain (Fernihough *et al.*, 2005; Honore *et al.*, 2005; Keeble *et al.*, 2005; Cho & Valtschanoff, 2008), while the direct mechanism is not yet known.

TRP vanilloid sub-family, member 2 (TRPV2; previously referred to as VRL-1: vanilloid-receptor-like protein) is also activated by noxious heat ( $\geq 52^{\circ}\text{C}$ ), but unlike TRPV1, it is not chemically activated by capsaicin (Caterina *et al.*, 1999), it is expressed in a broader tissue distribution than TRPV1, and in medium to large diameter neurons that are mostly distinct from neurons expressing other TRP channels (Lewinter *et al.*, 2004; 2008). TRPV2 however, is chemically activated and has also been demonstrated to be activated by mechanical stimuli (Caterina *et al.*, 1999), suggesting a possible role in the transduction of noxious mechanical stimuli.

TRP vanilloid sub-family, member 3 (TRPV3) is activated by warm temperature in the range of  $33\text{-}39^{\circ}\text{C}$ , has a strong expression in keratinocytes and has also been demonstrated to be involved in the transduction of noxious heat stimuli (Moqrich *et al.*, 2005). TRPV3 knockout mice show deficits in response to noxious heat ( $>50^{\circ}\text{C}$ ), but unlike TRPV1, showed no deficit in inflammatory pain models (Moqrich *et al.*, 2005). TRPV3 is also chemically activated (Hu *et al.*, 2004; Xu *et al.*, 2006; Vogt-Eisele *et al.*, 2009).

TRP vanilloid sub-family, member 4 (TRPV4) is also activated by warm temperatures, but in the lower range of  $27\text{-}34^{\circ}\text{C}$ , while its role in the transduction of noxious heat is so far unclear. Unlike TRPV1-3, TRPV4 desensitises to prolonged

noxious heat (Güler *et al.*, 2002), and TRPV4 knockout mice show no deficits in response to noxious heat (Todaka, 2004). However, others studies have shown deficits in response to noxious heat (Lee, 2005) and in thermal hyperalgesia following inflammation (Todaka, 2004). TRPV4 knockout mice have also been shown to have deficits in response to intense mechanical stimulation (Liedtke *et al.*, 2003; Suzuki *et al.*, 2003) suggesting a role in the transduction of noxious mechanical stimuli.

TRP melastatin sub-family, member 8 (TRPM8; also referred to as the cold and menthol receptor: CMR1) is activated by menthol (McKemy *et al.*, 2002; chemical in mint; Peier, Moqrich, *et al.*, 2002) and cold temperatures greater or equal to ( $\geq 25^{\circ}\text{C}$ ; Tominaga & Caterina, 2004) and is mostly expressed in small-diameter DRG neurons. However, unlike TRPV1, the expression of TRPM8 does not overlap with that of other common nociceptive markers, except for a 10-20% overlap with TRPV1 (McKemy *et al.*, 2002; Peier, Moqrich, *et al.*, 2002). TRPM8 knockout mice have been shown to have deficits in detecting cold temperature levels including those in the noxious range (Bautista *et al.* 2007; Dhaka *et al.* 2007). While this indicates a clear role of TRPM8 in the transduction of noxious cold, the role of TRPM8 in cold allodynia and hyperalgesia is unknown.

TRP ankyrin sub-family, member 1 (TRPA1; previously referred to as ANKTM1) was initially found to be activated by noxious cold temperatures below or equal to  $17^{\circ}\text{C}$  (Story *et al.*, 2003), but also responds to a wide variety of compounds associated with tissue damage. These compounds include those that directly induce tissue damage, such as formalin (McNamara *et al.*, 2007), and also endogenous substances that are released from the site of tissue damage and inflammation (Patapoutian *et al.*, 2009). Upon inflammation TRPA1 has additionally been shown to be involved in cold allodynia and hyperalgesia

### ***P2X receptors***

Purinergic receptors (or purinoceptors) are a family of membrane receptors that are subdivided into two main groups: the purinergic subtype 1 (P1) receptor, which is activated by adenosine, and the purinergic subtype 2 (P2) receptor, which is activated by adenosine triphosphate (ATP). The P2 receptors are further divided into the ligand-gated ion channels (ionotropic receptors) P2X and P2Z receptors, and the G-

protein-coupled receptors (metabotropic receptors) P2Y, P2U and P2T receptors. The P2X receptors can be further subdivided based on the seven P2X subunits (P2X<sub>1-7</sub>). Of these subunits, six (P2X<sub>1-6</sub>) are expressed by DRG neurons, with P2X<sub>7</sub> expressed by cells of the immune system (Dunn *et al.*, 2001), while only P2X<sub>3</sub> is expressed by nociceptors (Dunn *et al.*, 2001).

These P2X<sub>3</sub> receptors are most notably activated by the ATP that is released into extracellular space when cells are damaged through injury (Ding *et al.*, 2000; Dunn *et al.*, 2001). They are expressed in small to medium diameter nonpeptidergic neurons (Bradbury *et al.*, 1998) which are activated after mechanical stimulation during peripheral inflammation (Dai *et al.*, 2004). Under inflammatory conditions damaged cells release ATP and this release is thought to be increased by mechanical pressure (Dai *et al.*, 2004). Therefore it has also been suggested that noxious mechanical pressure promotes the release of ATP from cells under normal conditions. However, noxious mechanical pressure does not activate P2X<sub>3</sub> expressing nociceptors and the nocifensive response to noxious mechanical pressure is unaffected in P2X<sub>3</sub> knockout mice (Souslova *et al.*, 2000; Dai *et al.*, 2004). Some P2X<sub>3</sub> expressing neurons have also been demonstrated to co-express the capsaicin sensitive TRPV1 channel and hence have a role encoding noxious heat (Tsuda *et al.*, 1999; Ueno *et al.*, 1999) and innocuous heat (Souslova *et al.*, 2000).

### **ASICs**

Acid-sensing ion channels (ASICs) are proton-gated ion channels that are activated by extracellular protons (changes in pH) with five different subtypes (ASIC1a, 1b, 2a, 2b and 3), of which four (ASIC 1-4) are expressed by sensory neurons; one of which (ASIC3) is associated with nociception (Gold & Caterina, 2007).

It is well known that acid can elicit pain (Steen *et al.*, 1995; Issberner *et al.*, 1996), with plausible evidence that acidosis contributes to the pain associated with inflammation and ischaemia. ASIC3 (also called DRASIC) channels are specifically expressed by nociceptors that mostly innervate heart, gut and muscle tissue (Gold & Caterina, 2007). In all of these tissues, anaerobic respiration leads to the build up of lactic acid and protons, which activate the ASIC3 expressing nociceptors (Immke & McCleskey, 2001). ASIC3 knockout mice have also been shown to have deficits in

the mechanical hyperalgesia that is typically induced with the build up of acid in muscle (Price *et al.*, 2001).

### ***Na<sub>v</sub> channels***

Unlike the previous channels that have been discussed, voltage-gated sodium channels (VGSCs or Na<sub>v</sub> channels) are not activated by a specific nociceptive stimulus (as they are not ligand-gated), but instead are responsible for the inward flux of sodium ions (Na<sup>+</sup>) that generates the action potential. Na<sub>v</sub> channels are activated by changes in membrane potential and are permeable to only Na<sup>+</sup> ions. Na<sub>v</sub> channels are further divided into nine different subclasses (Na<sub>v</sub>1.1-1.9), three of which (Na<sub>v</sub>1.3, 1.7 and 1.8) have a demonstrated roles in nociception (Gold & Caterina, 2007).

While most Na<sub>v</sub> channels are blocked by the puffer fish toxin, tetrodotoxin (TTX), Na<sub>v</sub>1.8 channel is one of three Na<sub>v</sub> channels (Na<sub>v</sub>1.8, Na<sub>v</sub>1.5 and Na<sub>v</sub>1.9) that are resistant to TTX (Wood, 2007). Na<sub>v</sub>1.8 has a demonstrated role in nociceptive pain (Wood, 2007), is restricted to small diameter nociceptive neurons (Ogata & Tatebayashi, 1993; Gold *et al.*, 1996) and up-regulation contributes to hyperalgesia and inflammation (England *et al.*, 1996; Cardenas *et al.*, 1997). However, its role in neuropathic pain remains unclear (McCleskey & Gold, 1999; Wood, 2007).

Up-regulation of Na<sub>v</sub>1.7 also contributes to hyperalgesia and inflammation (Black *et al.*, 2004) and while its expression has been demonstrated in all classes of DRG neurons, it is predominately expressed in small-diameter nociceptive neurons (McCleskey & Gold, 1999; Black *et al.*, 2004; Wood, 2007).

Na<sub>v</sub>1.3 has a demonstrated role in neuropathic pain. It is an embryonic channel that is down-regulated at birth, and re-expressed in sensory neurons after nerve damage (Waxman *et al.*, 1994). This re-expression causes hyperexcitability of nociceptive neurons and an increase in pain behaviours in spinal cord injury models. Knockdown of Na<sub>v</sub>1.3 reduces the hyperexcitability and decreases pain behavioural responses (Hains *et al.*, 2003).

## **Peripheral projections: cutaneous, muscular and visceral nociceptors**

The classification of neurons that project to peripheral tissues (including skin, muscle and viscera) is based on the conduction velocity of their axon, the associated specialised ending of the neuron's peripheral terminal and their preferred stimuli. Most of our understanding of nociception comes from studying cutaneous nociceptors, but there is still a lot to be understood about muscular and visceral nociceptors. In the peripheral tissues A $\delta$  and C-fibre nociceptors usually terminate as "free" nerve endings that are un-encapsulated and not associated with specialised receptors. Typically these free nerve endings consist of several terminal branches with bead-like varicosities. Their projection into the skin, muscles and viscera is elaborated in the following sections.

### ***Nociceptive projections in the skin***

The innervation of the skin is well characterised (for summary see Figure 1.6). Functionally, there are three main classes of sensory neurons innervating the skin: mechanoreceptors, thermoreceptors and nociceptors. Skin can be divided into two morphologically different categories that are either hairless (glabrous) or hairy. While an obvious factor is that hairy skin contains hair follicles and glabrous skin does not, glabrous and hairy skins also receive slightly different innervation.

In glabrous skin, most mechanoreceptors possess myelinated A $\beta$  fibres, are associated with specialised capsulated endings and are situated in the dermis. The LTM can be further subdivided based their adaptation to a stimulus: slowly adapting types I and II (SAI and SAII) and rapidly adapting types I and II (RAI and RAI). The RAI and RAI are associated with Meissner's and Pacinian corpuscles, respectively, whereas the SAI and SAII are associated with multiple Merkel's disks, and Ruffini's endings, respectively (Guinard *et al.*, 1998; Rice & Rasmusson, 2000; Paré *et al.*, 2002).

Hairy skin lacks Meissner's corpuscles, but instead contains hair follicle afferents (HFAs), which are not present in glabrous skin. These possess either A $\beta$  or A $\delta$ -fibre axons and form palisade endings composed of longitudinal (A $\beta$ -fibre) and circumferential (A $\delta$ -fibre) lanceolate endings that encircle hair follicles (Willis, 2007).

Cutaneous nociceptors and thermoreceptors terminals comprise of A-fibre nociceptors (type I and II AMH) and C-fibre nociceptors (CMH, cold and polymodal). While the mechanoreceptors are situated in the dermis, nociceptors and thermoreceptors penetrate the epidermis as free nerve endings in both glabrous and hairy skin. While not all of these free endings are nociceptive, some C-fibre LTMs have been identified (Nordin, 1990). Many cutaneous nociceptors are peptidergic (Gibbins *et al.*, 1985; Kruger *et al.*, 1989).

### ***Nociceptive projections in muscles***

Muscle pain is different from cutaneous pain in number of ways. While cutaneous pain is described as sharp and piercing and highly localised, muscle pain is described as aching and cramping and more broadly localised (Mense, 2008). These differences are believed to be because skin is more highly innervated by nociceptors than muscle, although this is yet to be quantitatively confirmed (Mense, 2007).

Muscle nociceptors are classified differently from nociceptors of the skin and viscera. In the muscle A $\alpha$ -fibres are termed group Ia and Ib fibres, A $\beta$ -fibres group II, A $\delta$ -fibre group III and C-fibre group IV fibres. Group I and II fibres are mainly proprioceptors, which include the muscle spindles (or stretch receptors) that are innervated by both group Ia and II fibres, and Golgi tendon organs that are innervated by group Ib fibres. Nociceptors are restricted to the slowly conducting group III (corresponding to cutaneous A $\delta$ -fibres) and group IV (corresponding to cutaneous C-fibres) in muscle. Group III and IV fibres are free nerve endings, but unlike cutaneous afferents there is no definitive correlation between the morphology and function of free nerve endings of muscular afferents (Jankowski *et al.*, 2013).

While most group III afferents are mechanically sensitive (Kaufman & Rybicki, 1987; Jankowski *et al.*, 2013), not all are nociceptive with many responding to non-noxious tendon stretch and probing of their receptive fields (Kaufman *et al.*, 1983; Mense & Meyer, 1985). These group III afferents have an increasing response to tetanic contractions (maximum contraction possible) that decreases as the contraction is released (Kaufman *et al.*, 1983; Mense & Meyer, 1985) and appear to protect the muscle from damage due to prolonged contraction.

The majority of group IV neurons in muscle are chemosensitive and are either metaboreceptors or metabo-nociceptors (Light *et al.*, 2008; Jankowski *et al.*, 2013).

The “metabo” refers to the fact they are activated by metabolites generated within the muscle. Metaboreceptors (also termed ergoreceptors) respond to metabolites (such as low levels as lactic acid and ATP, and normal pH) found in the muscle during work-related activity, and are thought to contribute to the activation of the exercise-pressor reflex or possibly the sensation of fatigue (Light *et al.*, 2008; Jankowski *et al.*, 2013). Whereas metabo-nociceptors respond to metabolites (such as high levels of lactic and ATP, as well as moderate pH) found in muscles during ischemic contractions and serve a more nociceptive function (Light *et al.*, 2008; Jankowski *et al.*, 2013). Many metabo-nociceptors express TRPV1 (Light *et al.*, 2008; Jankowski *et al.*, 2013), which is commonly expressed by peptidergic nociceptors, and many metaboreceptors expressed the purinergic P2X<sub>3</sub> receptor (Jankowski *et al.*, 2013), which is commonly expressed by nonpeptidergic neurons.

### ***Nociceptive projections in viscera***

Like muscle pain, visceral pain is very different from cutaneous pain. It is often dull, poorly localised and may be referred to multiple somatic structures where it is felt as cutaneous or muscular pain (Gebhart & Bielefeldt, 2007). Adjacent visceral organs also refer pain to overlapping somatic areas, making it even more difficult to determine the origin of the pain (Gebhart & Bielefeldt, 2007). Visceral nociceptors are also unresponsive to noxious stimuli that would elicit a response from cutaneous nociceptors. For example: while a small cut in the gut is not painful, spasm or ischemia is (Mense, 2007).

Visceral nociception has been mostly studied in the gastrointestinal tract, yet there is still a lot to be understood. Unlike cutaneous and muscular afferents, visceral afferents originate from both spinal (either from thoracolumbar or lumbosacral) and vagal nerves. Brookes and colleagues (2013) have recently tried to simplify the sensory innervation of the gut into five main classes: intraganglionic laminar endings (IGLEs), mucosal afferents, muscular-mucosal afferents, intramuscular endings, and vascular afferents.

IGLEs are low-threshold, tension-sensitive mechanoreceptors that are activated by distension and contraction (Iggo, 1955; Tassicker *et al.*, 1999; Zagorodnyuk & Brookes, 2000; Brookes *et al.*, 2013), whereas mucosal afferents are distinct from IGLEs by their unresponsiveness to distension or contraction. Instead mucosal

afferents respond to light mechanical distortion of the mucosa (Paintal, 1957; Hicks *et al.*, 2002; Brookes *et al.*, 2013). Muscular-mucosal afferents are responsive to both distension and light mechanical distortion of the mucosa (Page & Blackshaw, 1998).

IGLEs have also been demonstrated to respond to stretch in the noxious range (Zagorodnyuk *et al.*, 2011), however they appear to be mostly unresponsive to capsaicin (Brookes *et al.*, 2013). Intramuscular endings (or intramuscular arrays; IMAs) are another ending that responds to mechanical stimuli but with higher thresholds and lower net firing rates than IGLES (Berthoud & Powley, 1992; Brookes *et al.*, 2013). IMAs have a wide dynamic range and graded firing into the noxious range of intraluminal pressures. Importantly, many of the axons contain the TRPV1 channel, and are frequently peptidergic (Yu, Udem, *et al.*, 2005). Vascular afferents also contain peptides and the TRPV1 receptor (Malin *et al.*, 2009; Brookes *et al.*, 2013), and are believed to be the major type of nociceptor in the gut and other viscera (Floyd & Morrison, 1974; Brookes *et al.*, 2013). Vagal afferents have high thresholds to distension and slow firing rates (Malin *et al.*, 2009; Brookes *et al.*, 2013), and are modulated by a wide range of chemical mediators of damage and inflammation (Brookes *et al.*, 2013).

## **Central projections of nociceptors: nociceptive superficial and deep dorsal horn neurons**

The central projections of the primary afferent nociceptors terminate in the dorsal horn of the spinal cord. Here, the primary afferents synapse onto intrinsic dorsal horn neurons that have two different classes: interneurons and projection neurons. Interneurons have axons that completely remain within the spinal cord that can either be relatively short and involved in local circuits; or long, travelling between spinal segments (propriospinal neurons). Projection neurons have long axons that travel to the brain and are involved in most of the output from the dorsal horn (Ribeiro-da-Silva & De Koninck, 2007). Dorsal horn neurons also receive input from descending axons originating from the brain that in modulate sensory transmission (Ribeiro-da-Silva & De Koninck, 2007).

The dorsal horn is divided into six parallel laminae (I-VI; see Figure 1.7), based on variations in the size of dorsal horn neurons and their packing density (Rexed, 1954). While originally determined in the cat dorsal horn (Rexed, 1954), these divisions

have since been applied to several other species; including the monkey (Ralston, 1979), rat (Steiner & Turner, 1972; Molander *et al.*, 1984; 1989), mouse (Ma *et al.*, 1995) and human (Harmann *et al.*, 1988). Lamina I (also called the substantia spongiosa or the marginal zone; Waldeyer, 1889; Ramon & Cajal, 1909) is the most superficial lamina in the dorsal horn. Lamina I caps lamina II (also called the substantia gelatinosa; Rexed, 1954), which is divided into an outer (IIo) and inner (Ii) region based on functional differences. These laminae are clearly distinguished from deeper lamina due to their transparent appearance, which is due to the high concentration of small neurons and absence of myelinated axons (Ranson, 1913; 1914). This absence of myelinated axons has led to early associations of these laminae to likely termination sites of unmyelinated primary afferent neurons and hence a key interest in regards to nociception (Ranson, 1913; 1914). Lamina I and II have since been definitively shown to contain neurons that specifically respond to noxious stimuli (Christensen & Perl, 1970).

### ***Functional classes of dorsal horn neurons associated with nociception***

In lamina I there are dorsal horn neurons that respond to noxious stimuli, innocuous heating or cooling, innocuous mechanical stimuli and itch (Andrew & Craig, 2001; 2002a). The majority of these dorsal horn neurons are nociceptive (Andrew & Craig, 2002b) with three main functional types that have been identified based on their responsiveness to cutaneous sensory inputs: nociceptive specific neurons, polymodal neurons and innocuous thermoreceptive neurons (Andrew & Craig, 2002b). While less than half of the nociceptive lamina I dorsal horn neurons are nociceptive specific (Andrew & Craig, 2002b), those that are, are polymodal and responsive to noxious heat, cold and mechanical stimuli, with a few nociceptive specific neurons responsive to only mechanical stimuli (Andrew & Craig, 2002b).

Lamina IIo contains mainly dorsal horn neurons that respond to noxious stimuli (Light, 1992; Light & Willcockson, 1999). However, by contrast, the majority of lamina Ii neurons receive input from mainly innocuous mechanically sensitive afferents (Light, 1992; Light & Willcockson, 1999). The majority of the nociceptive lamina IIo neurons are polymodal, responding to noxious mechanical, thermal and chemical stimuli, while others are only responsive to noxious mechanical stimuli (Light, 1992). The remainder of lamina IIo neurons are wide-dynamic range (WDR)

neurons responding to both noxious and innocuous mechanical stimuli, while few neurons responded to only innocuous thermal or mechanical stimuli (Light, 1992).

Lamina V contains many WDR neurons, as well as nociceptive specific neurons and innocuous mechanoceptive neurons (Mendell & Wall, 1965; Hillman & Wall, 1969; Light & Durkovic, 1984). While lamina III and IV are dominated by innocuous mechanoceptive neurons, some WDR neurons do exist in these laminae (Pomeranz *et al.*, 1968; Price & Mayer, 1974; Light & Durkovic, 1984). WDR neurons receive information from A $\beta$ - A $\delta$ - and C-fibre afferents (Wagman & Price, 1969; Men trety *et al.*, 1977). Like nociceptive specific neurons, the rate and duration of activity in WDR neurons increases with increasing intensity of mechanical and thermal stimuli but is inclusive of innocuous stimuli (Le Bars & Cadden, 2007).

#### ***Neurochemical classes of dorsal horn neurons associated with nociception***

Unfortunately, the morphological and neurochemical properties of nociceptive dorsal horn neurons are either incomplete or simply lacking. In most cases, only the size and the location of the neurochemically characterized cell bodies are known (Ribeiro-da-Silva & De Koninck, 2007). This is mostly limited because either the staining is inadequate to allow a proper characterization of the cell or the number of labeled cells is so high that it is impossible to characterize individual cells. (Ribeiro-da-Silva & De Koninck, 2007). The largest exception to this inadequate characterisation is the characterisation of dorsal horn neurons that contain the NK-1r.

The majority of lamina I projection neurons contain NK-1r (Marshall *et al.*, 1996; Yu, da Silva, *et al.*, 2005), but only a subset of NK-1r-IR neurons are projection neurons (Yu, da Silva, *et al.*, 2005). NK-1r immunoreactivity is also found in neurons of laminae IIo and III–IV (Liu, H. *et al.*, 1994a; Nakaya, Y. *et al.*, 1994; McLeod, A.L. *et al.*, 1998; Ribeiro-da-Silva, A. *et al.*, 2000). Most of the NK-1r-IR neurons project to higher levels, such as the thalamus, the parabrachial and the periaqueductal gray (Todd *et al.*, 2000). These NK-1r neurons are also selectively innervated by substance P containing peptidergic afferent nociceptors (Todd *et al.*, 2002).

### ***Central projections of nociceptors to the dorsal horn***

The central projections of cutaneous nociceptors are well characterised (refer Figure 1.8 for summary). The A $\delta$ -fibre nociceptors terminate predominately in laminae I and V (Light & Perl, 1979), whereas the C-fibre nociceptors terminate mostly in laminae I and II (Sugiura *et al.*, 1989). Peptidergic nociceptors terminate in lamina I, lamina IIo and lamina V, whereas nonpeptidergic nociceptors terminate in lamina III (Bradbury *et al.*, 1998; Ribeiro-da-Silva & De Koninck, 2007).

The central projections of visceral nociceptors are more widely distributed in the dorsal horn than cutaneous nociceptors, terminating in laminae I, II, IV-V and X and are often branching to other spinal levels and even the contralateral dorsal horn (Sugiura *et al.*, 1989).

## **Pathways of nociceptors**

### ***Ascending nociceptive pathways***

Intrinsic dorsal horn neurons play a large role in the processing of the nociceptive information. Interneurons remain within the spinal cord and are involved in local spinal circuits while projection neurons are the main output from the dorsal horn. Projection neurons have much longer axons that travel to specific regions of the brain through a number of different ascending pathways, including the:

- Spinothalamic;
- Spinocervical;
- Spinoreticular;
- Spinohypothalamic;
- Spinoannular and
- Postsynaptic dorsal column pathways

**The spinothalamic tract (STT)** is the best-characterised ascending nociceptive pathway. As the name suggests the STT is a direct pathway from the dorsal horn of the spinal cord to the contralateral thalamus. The majority of STT projection neurons are found in lamina I and lamina IV/V of the dorsal horn (Willis *et al.*, 1979; Apkarian & Hodge, 1989; Willis *et al.*, 2001). The lamina I STT neurons are innervated predominantly by C-fibres, with some input from A $\delta$ -fibres and are thought to be nociceptive specific cells. The lamina IV/V STT neurons, on the other

hand, are innervated predominately by A $\delta$ -fibres and also receive convergent input from A $\beta$ -fibres and are hence mainly WDR neurons. Axons from both lamina I STT neurons and lamina IV/V STT neurons decussate and enter the ventrolateral quadrant of the spinal cord. The STT pathway is divided into two distinct pathways: the medial (paleospinothalamic) and lateral (neospinothalamic) spinothalamic pathways. The lamina I neurons enter the lateral STT tract and the lamina IV/V neurons enter the medial STT tract and connect with STT neurons of the thalamus. The lateral STT neurons of the thalamus terminate in the primary and secondary somatosensory cortex for discriminative aspects of pain (Bowsher, 1957; Lima, 2007). The medial STT neurons of the thalamus terminate in the anterior cingulate gyrus and rostral insula for the affective punishing aspects of pain (Bowsher, 1957; Lima, 2007).

**The spinothalamic tract (STT)** connects the dorsal horn to the lateral cervical nucleus (LCN), which is located in the upper cervical spinal cord. The LCN is thought to be a continuation of the lateral spinal nucleus, which has been shown to be involved in nociceptive ascending pathways. Neurons of the LCN then connect with neurons of the ventral posterolateral thalamic nucleus (Lima, 2007). Most STT neurons are located in lamina IV (Lima, 2007) of the dorsal horn and most are low-threshold neurons, and are activated by tactile hair movement (Brown & Franz, 1969). However, some are high-threshold nociceptive specific and WDR (Cervero *et al.*, 1977). The STT neurons are innervated by A $\beta$ -, A $\delta$ - and C-fibre primary afferents, most receiving convergent input from C-fibre afferents (Willis, 2007).

**The spinothalamic tract (STT)** connects the dorsal horn to the medullary and pontine reticular formation of the brainstem. SRT neurons from the reticular formation connect to the intralaminar thalamic nucleus. These neurons are found in lamina V-VIII of the dorsal horn and are more concentrated in cervical levels (Kvetter & Willis, 1982). They are excited by cutaneous and deep somatic noxious stimuli (Willis, 2007).

**The spinothalamic tract (SHT)** is a direct pathway from the dorsal horn to the hypothalamus (Burstein *et al.*, 1990; Katter *et al.*, 1991). SHT neurons are predominately located in the deep dorsal horn with some in lamina I. Most of these neurons are high-threshold or WDR neurons (Burstein *et al.*, 1991), while SHT

neurons of the hypothalamus connect to the periaqueductal grey (PAG) and are thought to be involved in the neuroendocrine and autonomic responses to pain.

**The spinoannular (SAT) tract** connects the dorsal horn to the PAG (Bernard *et al.*, 1989; Bernard & Besson, 1990; Bernard *et al.*, 1992). SAT neurons are located in lamina I and deeper layers of the dorsal horn and connect to a multitude of areas including the hypothalamus, amygdala and thalamus (Bernard *et al.*, 1989; Bernard & Besson, 1990; Bernard *et al.*, 1992). These neurons are believed to be involved in escape and avoidance motor responses, negative and positive reinforcement and the neuroendocrine and autonomic responses to pain (Lovick, 1993).

**The postsynaptic dorsal column tract (PDCT)** connects the dorsal horn to the ipsilateral dorsal column nuclei (DCN) of the brainstem. PDCT neurons of the DCN connect to the contralateral VPL thalamic nucleus and are located predominately in lamina III-VII (Rustioni *et al.*, 1979; Bennett *et al.*, 1983). These neurons respond to both noxious and tactile mechanical stimuli, noxious heat and noxious visceral stimuli (Kamogawa & Bennett, 1986; Al-Chaer, Lawand, Westlund, & Willis, 1996a; 1996b).

### ***Descending pathways***

Dorsal horn neurons also receive input from descending neurons via pathways originating from the brain that regulate the output of the dorsal horn neurons. While the majority of descending neurons are inhibitory and function as an endogenous analgesic system, some facilitate pain transmission (Millan, 2002; Gebhart, 2004; Ren & Dubner, 2007). Direct descending corticospinal projections that connect the sensorimotor areas of the cerebral cortex with the dorsal horn of the spinal cord can inhibit or excite neurons in spinal dorsal horn. There are also indirect descending pathways from the cortex, hypothalamus and amygdala that connect to the dorsal horn through the PAG (Millan, 2002; Gebhart, 2004; Ren & Dubner, 2007). The indirect pathways through the PAG are the best-established pathways ((Ren & Dubner, 2007). PAG neurons integrate behavioural responses to noxious stimuli (Cameron, Khan, Westlund, & Willis, 1995; Cameron, Khan, Westlund, Cliffer, *et al.*, 1995; Bandler, 2007) and ascending nociceptive projections from nociceptive dorsal horn neurons terminate in the PAG (Menétrey *et al.*, 1982; Hylden *et al.*, 1986; Azkue *et al.*, 1998). The descending projections follow two main pathways.

Projections from the PAG either connect to the dorsal horn through the rostral ventromedial medulla (RVM; the PAG-RVM-spinal pathway) or through the locus coeruleus/subcoeruleus (LC/SC) in the dorsal pons (PAG-LC/SC-spinal pathway).

In the PAG-RVM-spinal pathway, descending projections from the RVM pass through the dorsolateral funiculus (DLF) to nociceptive neurons of the superficial and deep dorsal horn (Basbaum & Fields, 1979; 1984). The RVM contains ON and OFF cells (Fields & Heinricher, 1985; Neubert *et al.*, 2004), in which OFF cells are tonically active and pause in firing immediately before a withdrawal response from a noxious thermal stimulus, whereas ON cells accelerate firing immediately before the nociceptive reflex occurs (Fields & Heinricher, 1985; Neubert *et al.*, 2004). While the OFF cells inhibit nociceptive inputs and behavioural nocifensive responses to nociception (Fields & Heinricher, 1985; Neubert *et al.*, 2004), the ON cells contrastingly serve as the source of descending facilitation from the RVM (Fields & Heinricher, 1985; Neubert *et al.*, 2004).

Unlike the PAG-RVM-spinal pathway, projections of the PAG-LC/SC-spinal pathway are not mediated through the RVM (Jones, 1991). LC/SC projections terminate predominately in laminae VII, VIII, and IX of the ventral horn, with some terminations in the deep dorsal horn but relatively few in the superficial dorsal horn (Clark & Proudfit, 1991). The LC/SC neurons of the PAG-LC/SC-spinal pathway are the major noradrenergic input to the dorsal horn (Jones, 1991). LC/SC projections can both inhibit or facilitate nociceptive dorsal horn neurons, depending on the receptors that noradrenaline activates. The inhibition of nociceptive processing is through activation of the  $\alpha_2A$ -adrenoceptors of nociceptive dorsal horn neurons (Hunter *et al.*, 1997; Holden *et al.*, 1999; Holden & Naleway, 2001), while facilitation of nociceptive processing is through activation of the  $\alpha_1$ -adrenoceptor (Holden *et al.*, 1999; Holden & Naleway, 2001).

## Summary

In summary, the concept of acute, inflammatory and chronic pain has been introduced; as well as nociception, which is the neural processing of a painful stimulus. Consequently, the present (albeit limited) understanding of the normal function of nociceptors has been discussed in this section, detailing the current acceptance that there are many types of nociceptors, with each responsible for the

## Introduction

processing specific noxious stimulus or combination of noxious stimuli. The various attributes of each type include particular conduction velocities, molecular content, tissue innervation, responsive stimulus, projections into the spinal cord and pathways.

A particularly limiting factor in the current understanding of the properties of nociceptors has been the widespread use of over simplified classification schemes. While many nociceptors conform to the conventional peptidergic and non-peptidergic classification, there is accumulating evidence that many do not. There is also an overlap of marker expression between peptidergic and nonpeptidergic neurons. Hence, there are subpopulations of neurons involved in pain that are not entirely characterised, and there are possibly neurons associated with pain that have no involvement.

However, due consideration here has only been given to the nociceptors in their normal function and so the following section considers the function of nociception in (abnormal) altered pain states.

## 1.3 Altered pain states

---

Having examined specific nociceptors and their function during normal conditions, the contributions and changes that occur to these neurons during altered pain states will now be reviewed. The altered pain states were introduced in the first section as: nociception after inflammation and chronic neuropathic pain.

### **Pain after inflammation**

Inflammation is our natural and protective response to injury or infection and a means of removing any infectious agents and debris in preparation for the process of repair. Tissue damage and injury cause inflammation in a number of different ways, all of which involves the release of inflammatory mediators which can be released by infection, traumatic stimulation of mast cells, as a result of haemostatic mechanisms stimulated by bleeding, or by cell death (Rock & Kono, 2008). These inflammatory mediators include cytokines, chemokines, neurotrophic factors (such as nerve growth factor; NGF) prostaglandins, histamine and bradykinin (Rittner *et al.*, 2007).

Inflammatory mediators can directly activate innervating nociceptors, leading to the perception of pain; or these mediators can sensitise innervating nociceptors leading to an increased sensation of pain (hyperalgesia). The activation of these nociceptors can also lead to neurogenic inflammation, which further increases the inflammatory response. This neurogenic inflammation occurs due to the axon reflex, whereby the activation of the nociceptor leads to both orthodromic and antidromic action potentials (Szolcsányi, 1996). The orthodromic action potential propagates toward the spinal cord and leads to the perception of pain, while the antidromic action potential propagates away from the spinal cord and into the periphery through the other peripheral branches of the nociceptor. This antidromic action potential causes the release of neuropeptides (CGRP and SP) from the peripheral terminals of the activated nociceptor and increases the inflammatory response (Holzer, 1998). The increase in inflammatory response sensitises the peripheral branches of the innervating nociceptor and other nociceptors innervating the tissue, increasing the hyperalgesia.

### ***Peripheral sensitisation and primary hyperalgesia***

Primary hyperalgesia is characterised by a hypersensitivity to thermal and mechanical stimuli. This hypersensitivity is largely driven by the peripheral sensitisation of the nociceptors (Meyer & Campbell, 1981; Torebjork *et al.*, 1984), in which sensitisation refers to “an increased responsiveness of nociceptive neurons to their normal input, and/or recruitment of a response to normally subthreshold inputs” (Merskey & Bogduk, 1994).

Peripheral sensitisation occurs in both A $\delta$  and C-fibre nociceptors (Beitel & Dubner, 1976; Fitzgerald & Lynn, 1977) through the change in ion conductance of the ion channels and lowers the threshold that is usually required for activation. For example: prostaglandins (PGE<sub>2</sub>), bradykinin and serotonin drive the cAMP-dependent phosphorylation of the TTX-resistant Na<sub>v</sub>1.8 and Na<sub>v</sub>1.9 channel. The phosphorylation of Na<sub>v</sub>1.8/9 increases the inward current of Na<sup>+</sup> ions, and in doing so lowers the threshold of activation required for an action potential (Basbaum & Woolf, 1999). Another example is NGF, which acts directly on the TrkA receptor expressed by peptidergic nociceptors (Snider & McMahon, 1998; Chao, 2003). Activation of TrkA activates downstream signalling pathways that leads to an increased sensitivity of TRPV1 (Chuang *et al.*, 2001). The sensitisation of the peripheral nociceptors leads to an increased sensation of pain (hyperalgesia) in the injured area.

NGF can also cause phenotypic changes. NGF is also retrogradely transported to the nucleus of the nociceptor, where it promotes increased expression of TRPV1, the Na<sub>v</sub>1.8 channel and neuropeptides (Ji, Samad, *et al.*, 2002; Chao, 2003). Together, these changes in gene expression enhance excitability of the nociceptor and amplify the neurogenic inflammatory response. Phenotypic changes can also occur in neurons not typically associated with nociception. Low-threshold A $\beta$  neurons have been shown to express the peptide substance P (which is usually found in nociceptors) after inflammation (Neumann *et al.*, 1996). These phenotypic changes to mechanoreceptors lead to previously innocuous stimuli causing pain (allodynia).

### ***Secondary hyperalgesia and central sensitisation***

Primary hyperalgesia leads to secondary hyperalgesia due to the increased nociceptor sensitivity and recruitment of neurons that are not usually involved in nociception,

causing an increase in activity of neurons in the dorsal horn. This increased activity of dorsal horn neurons leads to central sensitisation, which refers to activity- or injury-dependent changes in the excitability of central nervous system neurons (Coderre, 2007). Central sensitisation is characterised by increased spontaneous activity, reduced thresholds or increased responsiveness to afferent inputs, prolonged after-discharges to repeated stimulation, and the expansion of the peripheral receptive fields of central neurons (Woolf *et al.*, 1988; Coderre *et al.*, 1993).

Similar to peripheral sensitisation, central sensitisation involves an increase in sensitivity of ion channels and increased expression of receptors but on dorsal horn neurons. For example: central sensitisation has been demonstrated to induce an up-regulation of Na<sub>v</sub>1.3 (Hains *et al.*, 2003) and the neurokinin 1 (NK1) receptor (Aanonsen *et al.*, 1992) in dorsal horn neurons. Up-regulation of Na<sub>v</sub>1.3 would increase the inward current of Na<sup>+</sup> ions, and lower the threshold of activation required for an action potential (Basbaum & Woolf, 1999). This not only increases the sensitivity of the dorsal horn neuron but can also result in an increase in spontaneous activity (Hains, 2004). The NK1 receptor is the receptor for the peptide substance P and is known to be associated with dorsal horn neurons that respond to noxious stimuli (Salter & Henry, 1991). The up-regulation of this receptor increases the sensitivity of the dorsal horn neuron to substance P.

Studies have suggested that the mitogen activated-protein kinase (MAPK) pathway is involved in central sensitisation (Ji & Woolf, 2001), which is an intracellular messenger pathway that involves the phosphorylation of extracellular regulated kinase (ERK also known as MAPK). Phosphorylated ERK (pERK) is increased in dorsal horn neurons after noxious thermal stimulation or C-fibre electrical nerve stimulation (Ji *et al.*, 1999), in response to hind paw injections of capsaicin (Ji *et al.*, 1999), and inflammatory agents such as carrageenan (Galan *et al.*, 2002), CFA (Ji, Befort, *et al.*, 2002; Obata *et al.*, 2003) and formalin (Ji *et al.*, 1999; Karim *et al.*, 2001). ERK inhibitors reduce nociception induced by formalin (Ji *et al.*, 1999; Karim *et al.*, 2001), and the hyperalgesia or allodynia after hind paw injection of carrageenan (Sammons *et al.*, 2000), CFA (Ji, Befort, *et al.*, 2002) or capsaicin (Kawasaki *et al.*, 2004).

As part of the MAPK pathway, pERK activates several transcriptional factors including CREB (Ji & Rupp, 1997). Phosphorylated CREB (pCREB) is also increased in neurons of the spinal dorsal horn after similar noxious stimuli to pERK (Kawasaki *et al.*, 2004; Fang *et al.*, 2005) and has been shown to be dependent on the activation of ERK and other protein kinases (Kawasaki *et al.*, 2004; Miletic *et al.*, 2004; Fang *et al.*, 2005; Miyabe & Miletic, 2005). pCREB translocates into the nucleus and regulates gene transcription, which can change the expression of proteins. Hence, the increase in expression of pERK and pCREB can be linked to the up-regulation of ion channels and receptors, which drive central sensitisation.

The central sensitisation during inflammatory pain is initiated by the sensitisation of the peripheral nociceptor. When the inflammatory response is complete the peripheral nociceptor is no longer sensitised and returns to normal activity levels. This leads to a decrease in activity of primary afferent input to the neurons of the dorsal horn and so the dorsal horn neurons also return to normal activity levels. So that once the injured area is healed, pain returns to normal.

## Neuropathic pain

Neuropathic pain is caused by damage to the peripheral or central nervous system, resulting in the persistent sensation of pain without an ongoing stimulus. Central neuropathic pain is often a result of spinal cord injury where peripheral neuropathic pain is a result of injury to the peripheral nociceptors. While neuropathic pain shares the peripheral and central sensitisation of inflammatory pain, neuropathic pain differs in that these sensitised neurons do not return to normal activity levels.

Nerve injury causes sensitisation of the peripheral nerve. Peripheral nerve injury blocks TTX-resistant sodium channels at the site of damage and increases the expression of TTX-sensitive sodium channels in the injured neuron (Basbaum & Woolf, 1999). The degeneration of peripheral nerves also release pro-inflammatory cytokines and neurotrophic factors, such as NGF. NGF sensitises peptidergic nociceptors by sensitising the TRPV1 receptor and causing up-regulation of ion channels and neuropeptides (Boucher & McMahon, 2001; Ossipov & Porreca, 2007). These pro-inflammatory factors can also sensitise adjacent nerve terminals of uninjured fibres (Li *et al.*, 2000).

Much like inflammatory pain, this increased neural activity to the spinal cord causes central sensitisation. pERK is increased neurons of the spinal dorsal horn after nerve injury models, including: sciatic nerve transection (Obata *et al.*, 2003), chronic constriction injury (Obata *et al.*, 2004) partial sciatic nerve ligation (Ma & Quirion, 2002) or spinal nerve ligation (Obata, 2004). Inhibitors of ERK have been found to reduce nociception induced in rats with chronic constriction injury of the sciatic nerve (Ciruela *et al.*, 2003) or spinal nerve ligation (Obata, 2004). pCREB is also increased in neurons of the spinal dorsal horn following partial ligation or chronic constriction injury of the sciatic nerve (Ma & Quirion, 2001; Miletic & Miletic, 2002; Miletic *et al.*, 2004). Spinal cord injury also results in a central sensitisation. Following spinal cord injury, dorsal horn neurons display the characteristics of central sensitisation including: increased spontaneous activity, increased evoked responses to mechanical stimuli, and increased duration of after-discharges and enhanced windup (Yeziarski & Park, 1993; Christensen & Hulsebosch, 1997; Wang *et al.*, 2005; Zhang *et al.*, 2005). pERK, pCREB (Crown *et al.*, 2005; Yu & Yeziarski, 2005) and cFos (Yakovlev & Faden, 1994; Siddall *et al.*, 1999; Abraham & Brewer, 2001) is also increased in dorsal horn neurons after spinal cord injury. The central sensitisation in peripheral neuropathic pain shares many qualities of the central sensitisation caused during inflammatory pain. However, the behavioural signs of neuropathic pain are persistent, indicating that the mechanisms that sustain neuropathic pain differ from those of inflammatory pain (Liu *et al.*, 2001; Sun *et al.*, 2005; Ossipov & Porreca, 2007).

The persistent nature of neuropathic pain is due to changes in the descending PAG-RVM-spinal pathway (Ossipov & Porreca, 2007). As mentioned previously, the PAG-RVM-spinal pathway modulates the nociceptive output of the spinal cord by either inhibiting or exciting nociceptive processing. One such change is an increase in cholecystokinin (CCK) in the RVM (Kovelowski *et al.*, 2000). During neuropathic pain there is an increase in availability of CCK in the RVM (Kovelowski *et al.*, 2000). In the RVM CCK activates ON cells and inhibits OFF cells (Heinricher, 2004; Neubert *et al.*, 2004), which leads to descending facilitation of nociceptive processing in the dorsal horn. Another change is an up-regulation of dynorphin in the dorsal horn (Lai *et al.*, 2001). Dynorphin is up-regulated in sensitised dorsal horn neurons (Kawasaki *et al.*, 2004). The elevated levels of dynorphin enhance the

release of CGRP and SP from primary afferent terminals, leading to an increase in dorsal horn neuron activity (Gardell *et al.*, 2003). Dynorphin also causes a release of the prostaglandin PGE<sub>2</sub>, which further enhances neurotransmitter release (Koetzner, 2004) and further increases neuronal activity. Together, this causes an increase in nociceptive processing and further perpetuates the descending facilitation. This enhancement of descending facilitation leads to changes in the spinal cord that favour a sensitised state and enhanced nociceptive inputs, thereby maintaining neuropathic pain.

## Summary

This section has reviewed existing research that demonstrates how altered pain states affect nociceptors, through sensitisation and lead to hyperalgesia and allodynia, and that these modified behaviours contribute to inflammatory and chronic pain.

While inflammation is a natural protective response to injury, this inflammation can activate nociceptors and directly cause pain, with increased responsiveness leading to a hypersensitivity to thermal and mechanical stimuli. This is ultimately protective. In contrast, similar increases in nociceptor sensitivity are caused by damage to the nervous system however this pain becomes persistent develops into neuropathic pain. The persistent nature of neuropathic pain is in part potentiated by descending control mechanisms and no longer serves a protective role.

As shown, during these altered pain states the enhanced release of calcitonin gene-related peptide (CGRP) and other neuropeptides such as substance P increases the inflammatory response, further sensitising the nociceptor and other nociceptors innervating the tissue, and increasing the inflammatory pain. Therefore the following section addresses the current understanding of the role of CGRP in the different pain states.

## 1.4 Calcitonin gene-related peptide

---

So far the concept of pain has been introduction and the three different pain states (acute nociception, nociception after inflammation, and chronic neuropathic pain). The current understanding of the normal function of nociceptors has been discussed. It was noticed that the widespread use of oversimplified classification schemes was a limiting aspect of our current understanding, in particular, the classification of nociceptors into peptidergic and non-peptidergic categories. Calcitonin gene-peptide (CGRP) is the standard marker for peptidergic nociceptors, however it does not appear to be restricted to C-fibres.

The release of CGRP was also established to have a clear role in neurogenic inflammation, which can lead to the increased sensitivity of nociceptors in the altered pain states. Therefore, this section focuses on CGRP and the role of CGRP in different pain states.

### CGRP and the CGRP receptors

CGRP exists in two isoforms; CGRP $\alpha$  and CGRP $\beta$ . The first of these isoforms (CGRP $\alpha$ ) was identified through the structural analysis of the rat calcitonin gene (*Calca* gene) when it was proposed that the alternate splicing of the calcitonin gene would result the production of a 37 amino acid peptide, rather than the 32 amino acid peptide calcitonin (Amara *et al.*, 1982). This 37 amino acid peptide was dubbed CGRP and by use of immunohistochemistry was shown to exist predominately in neural and endocrine tissue in rats (Rosenfeld *et al.*, 1983; Mason *et al.*, 1984), and in humans (Tschopp *et al.*, 1985).

The second isoform (CGRP $\beta$ ) was subsequently characterized from a gene highly homologous to the calcitonin gene (Amara *et al.*, 1985). The rat CGRP $\beta$  differed from rat CGRP $\alpha$  by a single amino acid (Amara *et al.*, 1985) while the mouse and human CGRP $\beta$  differed from the mouse (Thomas *et al.*, 2001) and human (Tschopp *et al.*, 1985) CGRP $\alpha$  by three amino acids. CGRP $\alpha$  and CGRP $\beta$  possess similar biological activities (Poyner *et al.*, 2002), but the two CGRP isoforms are differentially expressed and independently regulated in different neuronal systems and endocrine structures (Russo *et al.*, 1988). The CGRP $\beta$  is preferentially expressed

in enteric neurons, whereas the CGRP $\alpha$  is preferentially expressed by sensory neurons outside the gut (Mulderry *et al.*, 1988).

CGRP binds to dedicated CGRP receptors, which are unique type II G protein-coupled receptors. The CGRP receptors consist of the seven trans-membrane domain protein called the calcitonin receptor-like receptor (CLR), and accessory proteins, which include: the receptor-activity-modifying proteins (RAMPs) and the receptor component protein (RCP). The RAMPs function to determine the receptor specificity (McLatchie *et al.*, 1998) and chaperone CLR to the cell surface. RAMP1 enables CLR to form the functional CGRP type 1 receptor (Kuwasako *et al.*, 2004). RCP facilitates signal transduction (Luebke *et al.*, 1996).

## **Distribution of CGRP in neural tissue**

CGRP is abundantly expressed in primary sensory neurons in trigeminal and dorsal root ganglia and has a marked overlap in expression with the tachykinin SP. CGRP and SP are found in medium A $\delta$ -fibre neurons and small C-fibre neurons. While often overlooked CGRP occurs in all sizes of sensory neuronal somata in DRG including A $\alpha$ - and A- $\beta$  fibre neurons (McCarthy & Lawson, 1990).

CGRP and SP coexist in cutaneous sensory neurons in many different species (Gibbins *et al.*, 1985; Gibbins, Furness, *et al.*, 1987; Gibbins, Wattchow, *et al.*, 1987). In glabrous skin, CGRP fibres innervate blood vessels, sweat glands and run parallel to the epidermis at the dermo-epidermal junction. The CGRP fibres of the dermo-epidermal junction branch and exhibit axons surrounding Meissner's corpuscles and axons entering the epidermis, called intraepidermal nerve fibres (IENF). A similar pattern is observed in hairy skin, with the addition of CGRP fibres innervating the base and encircling hair follicles (Kruger *et al.*, 1989).

CGRP and SP also coexist in primary afferent terminals in lamina I of the spinal dorsal horn (Carlton *et al.*, 1988; Merighi *et al.*, 1988; Fried *et al.*, 1989; Plenderleith *et al.*, 1990). However unlike SP, which is expressed by some intrinsic dorsal horn neurons, CGRP terminals in the dorsal horn appear to be primarily of primary afferent origin. This has been shown by dorsal rhizotomy (Gibson, Polak, Bloom, *et al.*, 1984; Chung *et al.*, 1988; Traub *et al.*, 1989; Tie-Jun *et al.*, 2001) and neonatal capsaicin treatment (which destroys a large proportion of primary afferents) that

significantly reduces the level of CGRP in the spinal cord (Franco-Cereceda *et al.*, 1987; Hammond & Ruda, 1989). CGRP is also present in lamina III-V of the dorsal horn (Gibson, Polak, Bloom, *et al.*, 1984). CGRP receptor binding sites and the receptor components (CLR, RAMP1 and RCP) are also found in high levels in lamina I and lamina III-V (van Rossum *et al.*, 1997; Ma *et al.*, 2003).

## **Role of CGRP in acute nociception**

CGRP is widely distributed in neurons of the peripheral and central nervous systems and has hence been suggested to have a role in a myriad of biological activities, including vasodilation, cardiovascular protection, muscular motility, learning and memory, the regulation of food and water intake, and nociception and inflammation (Brain & Grant, 2004).

As mentioned previously, many CGRP-containing sensory neurons also express substance P (SP). SP is an 11 amino acid neuropeptide belonging to the tachykinin family first identified by Euler and Gaddum as an unknown depressor substance (1931). All SP containing primary afferents are nociceptors (Lawson *et al.*, 1997). SP binds to neurokinin-1 receptors (NK1r), which, in the dorsal horn, are only known to be associated with dorsal horn neurons that respond to noxious stimuli (Salter & Henry, 1991). NK1r antagonists block the slow-excitatory postsynaptic potentials evoked by noxious stimuli (De Koninck & Henry, 1991). Selective ablation of the NK1r expressing neurons in the superficial dorsal horn leads to dramatic reduction in hyperalgesia in both inflammatory and neuropathic pain models (Mantyh, 1997; Nichols, 1999).

Functionally, CGRP enhances the nociceptive behavioural responses induced by SP (Wiesenfeld-Hallin *et al.*, 1984). Concentrations of CGRP that have little or no consistent effect, markedly potentiate the excitatory effect of either SP or noxious stimulation on rat dorsal horn neurons in vivo (Biella *et al.*, 1991). Co-administration of SP and CGRP significantly increases the excitability of a nociceptive flexion reflex in the rat (Woolf & Wiesenfeld-Hallin, 1986). CGRP enhances the nociceptive effects induced by SP by potentiating the release of SP (Oku *et al.*, 1987), inhibiting its degradation (Le Greves *et al.*, 1985) and enhancing the excitability of neurons receiving noxious inputs (Biella *et al.*, 1991; Seybold *et al.*, 2003; Sun *et al.*, 2004; Bird *et al.*, 2006). CGRP and SP also have cooperative peripheral actions, in that

CGRP can potentiate the effects of SP (Brain & Williams, 1985; Gamse & Saria, 1985).

Without SP, CGRP alone has minimal effects on nociceptive inputs to the spinal cord (Miletic & Tan, 1988) but has been shown to enhance the release of other excitatory neurotransmitters such as glutamate (Kangrga & Randic, 1990). CGRP was also found to increase the responses of nociceptive specific neurons and wide dynamic range neurons in the dorsal horn upon the application of NMDA or AMPA (Ebersberger *et al.*, 2000). However it has previously been demonstrated that CGRP neurons lack vesicular glutamate transporters VGLuT1 (Oliveira *et al.*, 2003; Morris *et al.*, 2005; Brumovsky *et al.*, 2011) and VGLuT2 (Clarke *et al.*, 2011), and many even lack the required protein machinery to utilise glutamate as a neurotransmitter (Morris *et al.*, 2005).

Although CGRP causes no acute behavioural effect when injected by itself (Wiesenfeld-Hallin *et al.*, 1984; Gamse & Saria, 1986), intrathecal administration of CGRP causes hyperalgesia to mechanical stimuli (Oku *et al.*, 1987), and intrathecal injection of CGRP antiserum decreases thermal and mechanical hyperalgesia during peripheral inflammation (Kawamura *et al.*, 1989; Kuraishi *et al.*, 1991). In the spinal cord, noxious thermal, mechanical, or electrical stimulation evoke the release of CGRP within the superficial dorsal horn (Morton & Hutchison, 1989; 1990). However, these effects could be mediated in part by CGRP receptors on terminals of primary afferent neurons that facilitate the release of SP (Oku *et al.*, 1987; Ryu *et al.*, 1988).

## **Role of CGRP in inflammatory pain**

The role of CGRP in inflammatory pain is reasonably well understood. CGRP is involved in inflammatory pain in two ways. Firstly, CGRP has a large role in driving the neurogenic inflammatory response, thereby increasing inflammation. Secondly, CGRP has a role in the nociceptive processing of inflammatory pain through acting on primary nociceptors of the spinal cord (Ma *et al.*, 2009).

CGRP also has an established role in neurogenic inflammation. CGRP expression is increased in DRG neurons after inflammation induced by the inflammatory agent complete Freund's adjuvant (CFA; Nahin & Byers, 1994; Hanesch & Schaible, 1995;

Ambalavanar, Dessem, *et al.*, 2006; Ambalavanar, Moritani, *et al.*, 2006; Staton *et al.*, 2012). This inflammation causes both the central release of CGRP in the spinal dorsal horn (Seybold *et al.*, 1995) and the peripheral release of CGRP in the inflamed tissue (Flores *et al.*, 2001). In the periphery CGRP release increases blood flow and increases the influx of inflammatory and immune cells into inflamed tissues. CGRP also stimulates inflammatory and immune cells to produce and release pain inducing inflammatory mediators (Brain & Grant, 2004). Several inflammatory mediators have been shown to up-regulate CGRP in primary sensory neurons (Lindsay & Harmor, 1989).

It is also known that CGRP is involved in the sensitisation of mechanical nociceptive dorsal horn neurons (Sun *et al.*, 2004) and in the generation and maintenance of tactile allodynia (Sun *et al.*, 2003). The CGRP antagonist CGRP8-37 attenuates thermal hyperalgesia caused by intradermal injection of carrageenan (Yu, Hansson, Brodda-Jansen, *et al.*, 1996), tactile allodynia caused by intradermal capsaicin (Sun *et al.*, 2003) and intramuscular CFA (Ambalavanar, Dessem, *et al.*, 2006), suggesting that CGRP and its receptors are involved in inflammatory pain at the spinal dorsal horn level.

## **Role of CGRP in neuropathic pain**

The role of CGRP in the neuropathic pain is not well understood. However, evidence suggests that CGRP may contribute to the development of neuropathic pain through its action in the dorsal horn and neurogenic action that stimulates damaged peripheral nerves (Ma *et al.*, 2009).

In DRG neurons, CGRP is down-regulated after complete transection of peripheral nerves (Verge *et al.*, 1995) and in partial sciatic nerve injury (Ma & Bisby, 1998; Miki *et al.*, 1998; Ma *et al.*, 1999). In partial sciatic nerve injury, CGRP was down-regulated in the injured DRG neurons but up-regulated in adjacent spared neurons projecting to lamina III-V of dorsal horn (Ma & Bisby, 1998; Miki *et al.*, 1998; Ma *et al.*, 1999), suggesting a role in mediating the tactile allodynia caused by nerve injury (Sun *et al.*, 2001; Ossipov *et al.*, 2002). The CGRP antagonist CGRP8-37 significantly attenuates both tactile allodynia and heat hyperalgesia caused by chronic constriction injury of sciatic nerves (Yu, Hansson, & Lundeberg, 1996). CGRP8-37 also delays the onset of tactile allodynia as well as to attenuates tactile

allodynia caused by spinal nerve ligation, suggesting a role for CGRP in the dorsal horn in the development of neuropathic pain (Lee & Kim, 2007). CGRP8-37 was effective in abolishing mechanical allodynia and heat hyperalgesia produced by spinal hemisection, a central neuropathic pain model, suggesting that CGRP and its receptors may play a role in chronic central neuropathic pain (Bennett *et al.*, 2000).

Peripherally derived CGRP possibly contributes to neuropathic pain. Intraplantar injection of CGRP8-37 delayed or reversed tactile allodynia in a spinal nerve ligation model (Jang, 2004). Partial sciatic nerve ligation increased the accumulation of CGRP in neuroma and up-regulated the synthesis of CGRP in macrophages (Ma & Quirion, 2006), while CGRP also facilitates the up-regulation of the pro-inflammatory cytokine interleukin 6 (IL-6) in invading macrophages (Ma & Quirion, 2006). Perineural injection of CGRP8-37 and the CGRP antagonist BIBN4096BS significantly attenuates heat hyperalgesia (Ma & Quirion, 2006). These findings suggest that injured nerve derived CGRP plays an important role in the beginning of neuropathic pain.

## Summary

While it has been noted that there are two forms of CGRP isoforms there is little need to differentiate between the two in the context of this thesis, since this research will focus outside of the gut where CGRP $\alpha$  is the predominate isoform.

CGRP appears to be an important neuropeptide in the increases of neuronal sensitivity in the different pain states. CGRP has an established role in inflammation. It drives neurogenic inflammation, thereby increasing the inflammatory response, and it is also involved in the central sensitisation of dorsal horn neurons in the spinal cord. This central sensitisation is important to both nociception after inflammation and chronic neuropathic pain states.

CGRP has cooperative actions with SP and they are frequently co-expressed in peptidergic nociceptors. While the role of these neurons is established in nociception, it is often overlooked that many CGRP neurons do not express SP. The CGRP neurons that lack SP appear to be A $\alpha$ - and A- $\beta$  fibre neurons, which are not typically associated with nociception. These neurons are yet to be characterised and appear to be an example of a neuronal population that has remained uncharacterised because of

oversimplified classification schemes. Therefore CGRP neurons that lack SP are the focus of this thesis.



## 1.5 Scope of Thesis

---

The previous sections have shown that while there is a solid foundational understanding of the neural processing of pain, there remain many opportunities for resolving the research questions that are not yet answered. In particular, the properties of the neurons that initially respond to potentially painful stimuli, the primary afferent nociceptors, and their projections into the spinal cord remain partially characterised, in regard to both their normal functions and their contributions to chronic pain. The focus of this thesis is therefore to address properties of an individual neurochemical class of primary afferent neurons and characterise their projections to the spinal cord, their functional properties and their role they play in the processing of pain.

A significant barrier to understanding the properties of nociceptors has been the widespread use of over simplified schemes to classify them. While it is commonly accepted that nociceptors can be subdivided into two main subclasses, it is only presumed that nociceptors are restricted to either small diameter lightly myelinated A $\delta$ -fibre or unmyelinated C-fibre afferent neurons. However, it has been shown numerous times that larger myelinated A $\alpha$ / $\beta$ -fibre afferent neurons can also be nociceptive (Djouhri *et al.*, 1998; Djouhri & Lawson, 2004). The small unmyelinated C-fibre nociceptors are capsaicin-sensitive, express neuropeptides, project to lamina I of the dorsal horn and respond to a wide range of noxious stimuli, whereas the lightly myelinated A $\delta$ -fibre nociceptors are insensitive to capsaicin, lack peptides, bind IB4, project to lamina II of the dorsal horn and respond to mainly mechanical stimuli (Julius & Basbaum, 2001; Woolf & Ma, 2007; Belmonte & Viana, 2008; Dubin & Patapoutian, 2010). Furthermore, there are numerous examples of nociceptive neurons that are neither peptidergic or fit the classification scheme of nonpeptidergic (Peier, Moqrich, *et al.*, 2002; Morris *et al.*, 2005; Dhaka *et al.*, 2008; Cavanaugh *et al.*, 2009; Bráz & Basbaum, 2010; Clarke *et al.*, 2011). Additionally, CGRP, which is the standard marker of peptidergic nociceptors, is not restricted to small diameter, capsaicin-sensitive peptidergic nociceptors: CGRP is expressed by some DRG neurons that lack SP and have cell bodies considerably larger than those of most nociceptors (McCarthy & Lawson, 1990; Morris *et al.*, 2005), yet they have not been properly characterised.

## **Aims and experimental approach**

The objective of this research was therefore to characterise neurons that contain CGRP but do not contain SP, to establish an improved understanding of their role in nociception. This involved determining: the prevalence and distribution of these neurons; their neurochemical profile; their peripheral and central projections; and their relationship with nociceptive dorsal horn neurons. Consequently, this objective comprised of the following five aims:

### ***Aim 1: To determine the prevalence and distribution of neurons containing CGRP but not SP***

The method used to establish this aim involved the use of double labelling immunohistochemistry to detect neurons containing CGRP but not SP in the dorsal horn of the spinal cord, DRG and paw skin of mice. Dorsal horn and DRG were quantitatively assessed to determine the distribution and frequency of CGRP neurons that lacked SP and how they compared to CGRP neurons that contained SP. The distribution of CGRP neurons in paw skin was qualitatively assessed.

### ***Aim 2: To determine the neurochemical profile of neurons containing CGRP but not SP***

This aim required triple labelling immunohistochemistry to firstly detect neurons containing CGRP but not SP in mice DRG and secondly to determine whether these neurons possessed any other neurochemical characteristics that may lead to a better understanding of their possible function. These neurochemical markers included the capsaicin receptor TRPV1 and the marker for larger myelinated neurons neurofilament-200 (NF200), and also included the peptides vasoactive intestinal peptide (VIP) and galanin (GAL).

### ***Aim 3: To determine the peripheral projections of neurons containing CGRP but not SP***

An axonal tracing technique coupled with multiple labelling immunohistochemistry was implemented in which the peripheral projections of afferents were retrogradely traced by injection of cholera toxin subunit B (CTXb) into mouse gastrocnemius tissue *in vivo* and detected immunohistochemically in DRG. Retrograde tracing of the peripheral projections allowed the determination of the origin of CGRP neurons that lacked SP from muscle tissue in DRG.

***Aim 4: To determine the central projections of neurons containing CGRP but not SP***

Similarly, an axonal tracing technique coupled with multiple labelling immunohistochemistry was implemented in which the central projections of afferents were anterogradely traced by application of Neurobiotin (NB) onto an isolated dorsal root *in vitro* and detected immunohistochemically in the spinal dorsal horn. Anterograde tracing of the central projections allowed the determination of the central projections from a single spinal nerve, confirmation that the deep lamina IV/V terminals containing CGRP but not SP were of primary afferent origin, and how these deep lamina IV/V terminals containing CGRP but not SP compared to primary afferent mechanoreceptor terminals.

***Aim 5: To determine the relationship of CGRP neurons lacking SP with nociceptive dorsal horn neurons***

This aim was addressed by use of two techniques to stimulate primary afferent neurons of viable spinal cord slices coupled with multiple labelling immunohistochemistry. Primary afferent neurons were stimulated with capsaicin to activate the capsaicin sensitive afferents or electrically stimulated to activate all primary afferent neurons. The resulting activated dorsal horn cells were visualised via the phosphorylation of intracellular messengers (such as pERK and pCREB), which were detected using immunohistochemistry.



## **1.6 Figures**

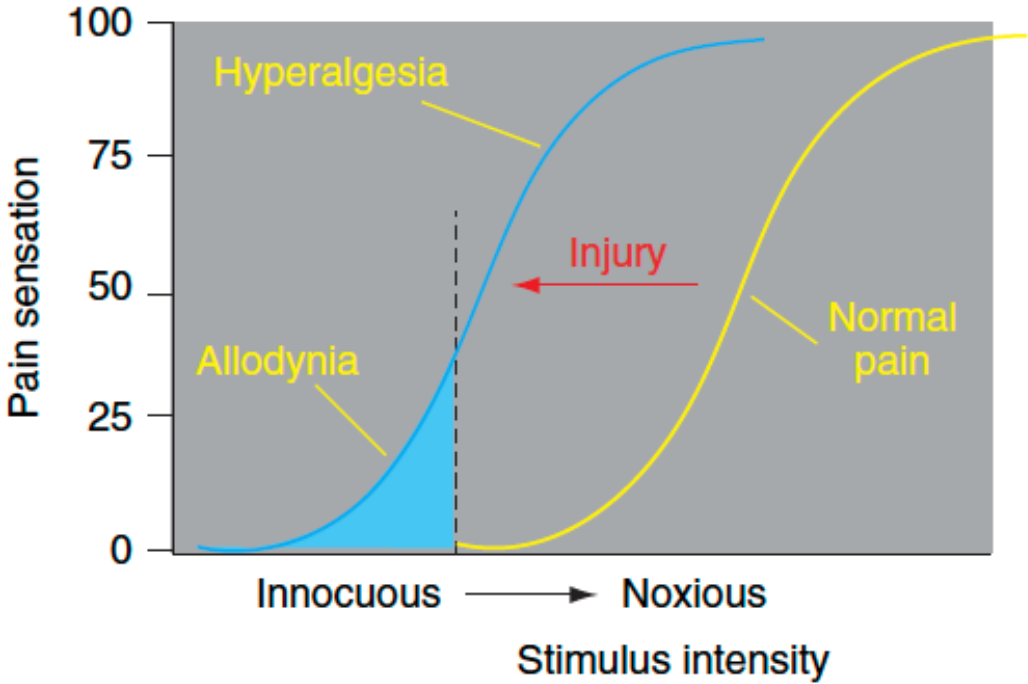
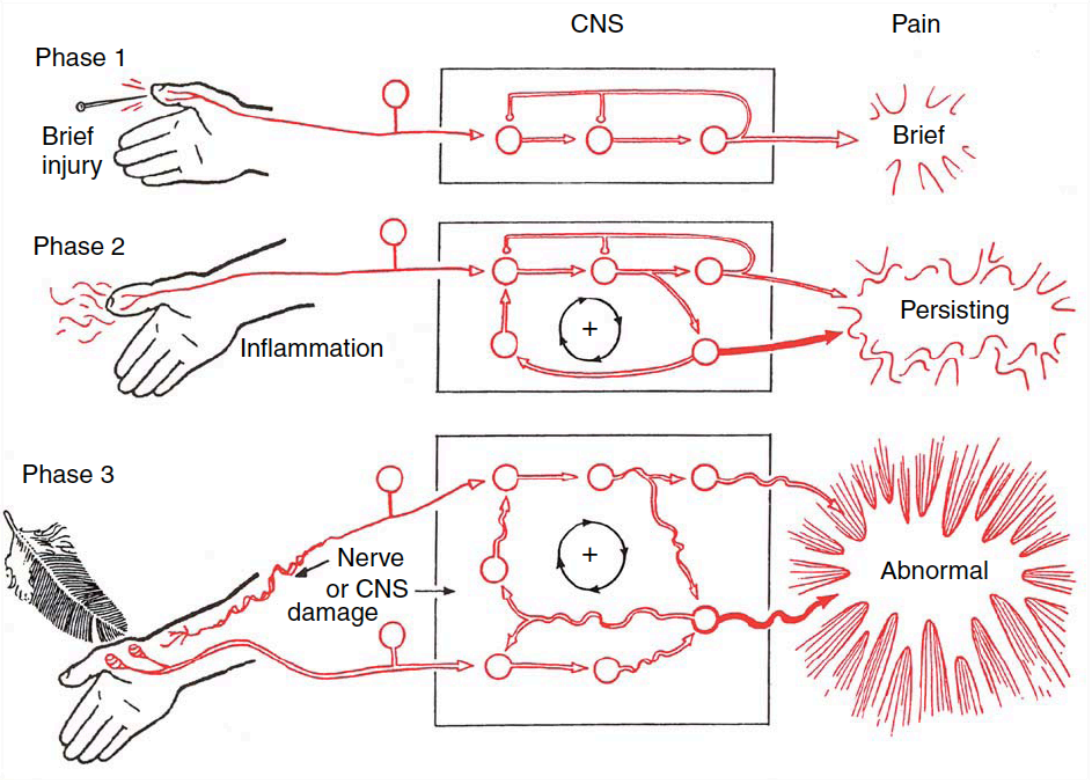
---

**Figure 1.1: A diagrammatic representation of the three different pain states.**

Nociceptive (Phase 1) is the normal processing of a brief noxious stimulus resulting in a brief sensation of pain. Inflammatory pain (Phase 2) is the consequence of prolonged noxious stimulation leading to tissue damage and resulting in a persisting sensation of pain. Neuropathic pain (Phase 3) is the consequence of neurologic damage to the peripheral or central nociceptors resulting in an abnormal painful sensation to otherwise innocuous stimuli (Cervero and Laird 1991)

**Figure 1.2: Changes in pain sensation induced by injury**

The normal relationship between stimulus intensity and the magnitude is represented by the yellow curve at the right-hand side of the figure. Pain sensation is only evoked by stimulus intensities in the noxious range (the black vertical dotted line indicates the pain threshold). Injury provokes a leftward shift in the curve relating stimulus to pain sensation. Under these conditions innocuous stimuli provoke pain (allodynia) and noxious stimuli provoke an increased pain sensation (hyperalgesia; Cervero and Laird 1996)

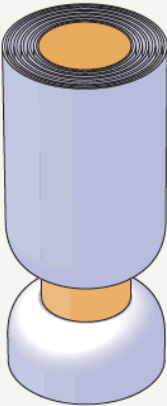


**Figure 1.3: Myelination of sensory neurons**

The axons are drawn to scale, but they are shown 2000 times larger than life size. The diameter of an axon (in  $\mu\text{m}$ ) is correlated with its conduction velocity (in m/sec) and with the type of sensory receptor to which it is connected. The A $\delta$ - and C-fibres are most associated with nociception (Bear *et al.*, 2011).

**Figure 1.4: First and second pain**

A $\delta$ -fibre nociceptors mediate the acute well-localised “first” or fast pain, and C-fibres nociceptors convey the poorly localised “second” or slow pain (Bear *et al.*, 2011).

Axons from skin	A $\alpha$	A $\beta$	A $\delta$	C
Axons from muscles	Group I	II	III	IV
				
Diameter ( $\mu\text{m}$ )	13–20	6–12	1–5	0.2–1.5
Speed (m/sec)	80–120	35–75	5–30	0.5–2
Sensory receptors	Proprioceptors of skeletal muscle	Mechanoreceptors of skin	Pain, temperature	Temperature, pain, itch

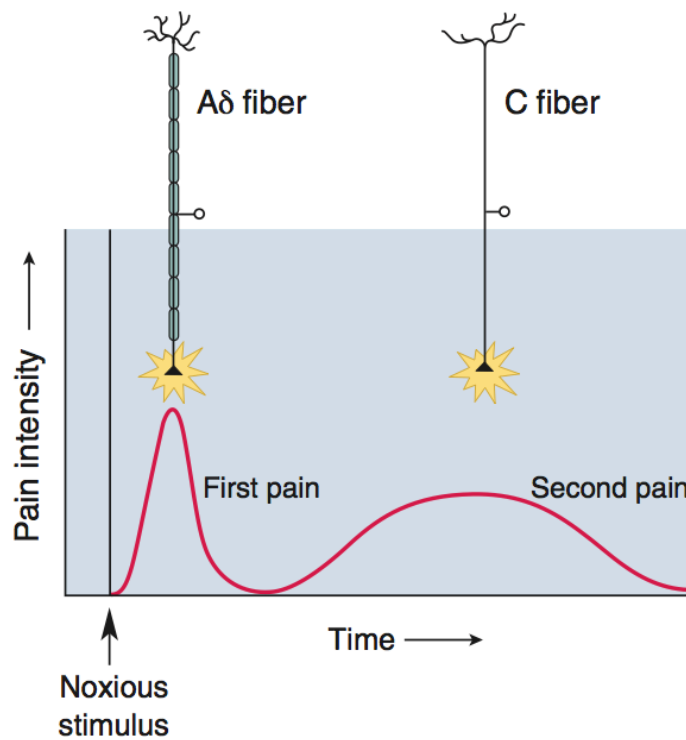


**Figure 1.5: Schematic representation of the thermal response of TRP receptors**

The TRP channels are activated by both noxious and innocuous changes in temperature. The upper segment of the schematic representation displays the thermal activation profile of various TRP channels. The middle segment of the schematic representation displays the activity in various cutaneous sensory receptors during application to their receptive fields of temperatures indicated in the thermal scale. The lower segment of the schematic representation displays the quality of sensations evoked in humans by application to the skin of different temperature values (Belmonte & Viana, 2008)

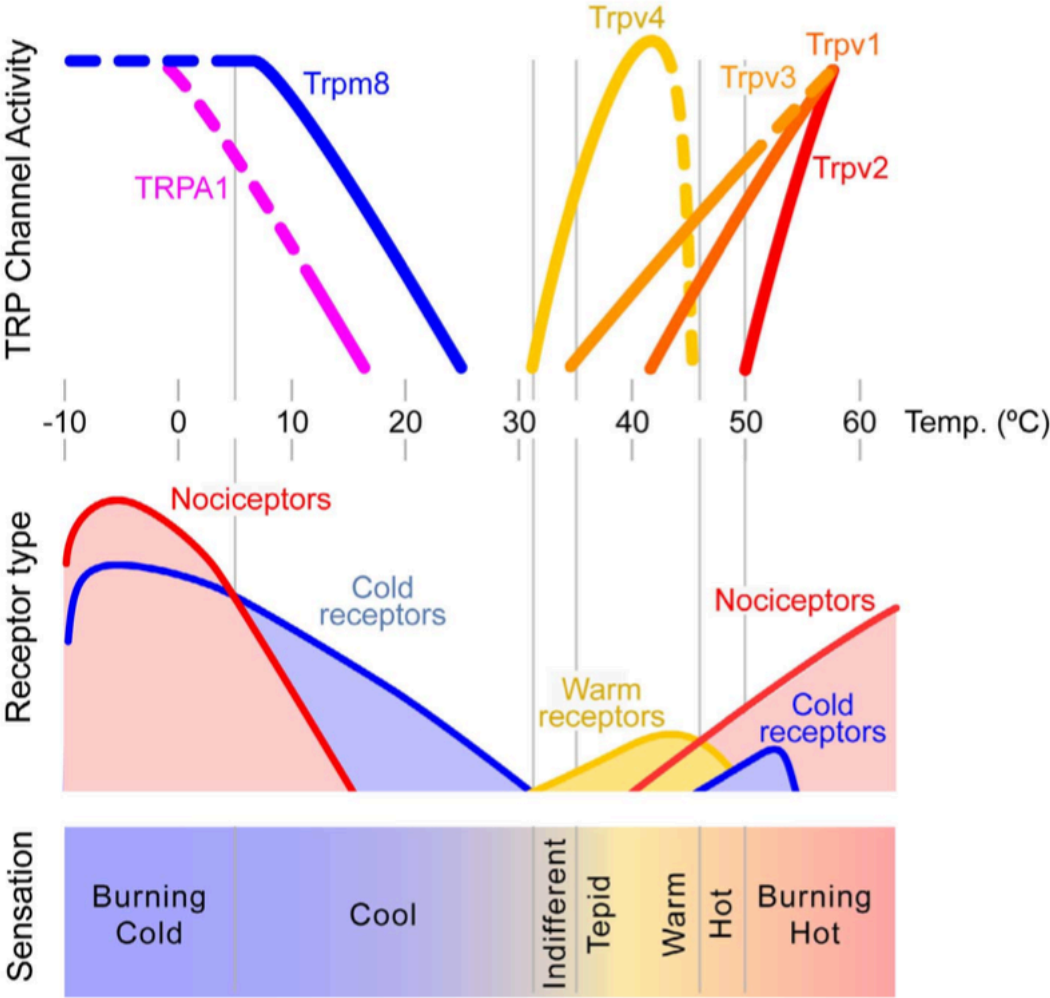


**Figure 1.6: Schematic representation of the sensory innervation of human skin**

The schematic representation displays the different sensory endings in both hairy and glabrous skin. There are three main classes of sensory neurons innervating the skin: mechanoreceptors, thermoreceptors and nociceptors. Thermoreceptors and nociceptors terminate as free nerve endings, while mechanoreceptors have specialised sensory endings, including: Pacinian corpuscles, Meissner's corpuscles, Merkel's disk, Ruffini's endings and hair follicle receptors (Bear *et al.*, 2011).

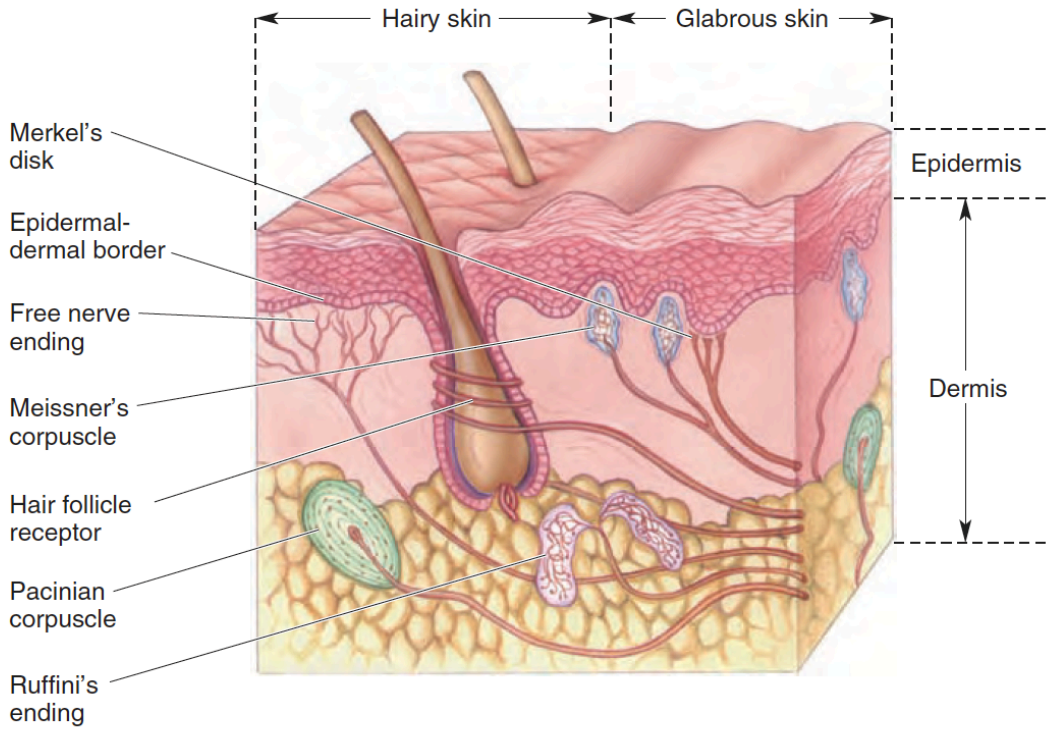


**Figure 1.7: Rexed laminae of the spinal cord**

A schematic drawing of the seventh lumbar segment of spinal cord displaying Rexed laminae. Laminae I-VI represent the dorsal horn and VII-XI the ventral horn of the spinal cord. The superficial laminae (I/II) are most heavily involved in nociception however wide dynamic range neurons exist in laminae IV/V (Rexed, 1954)

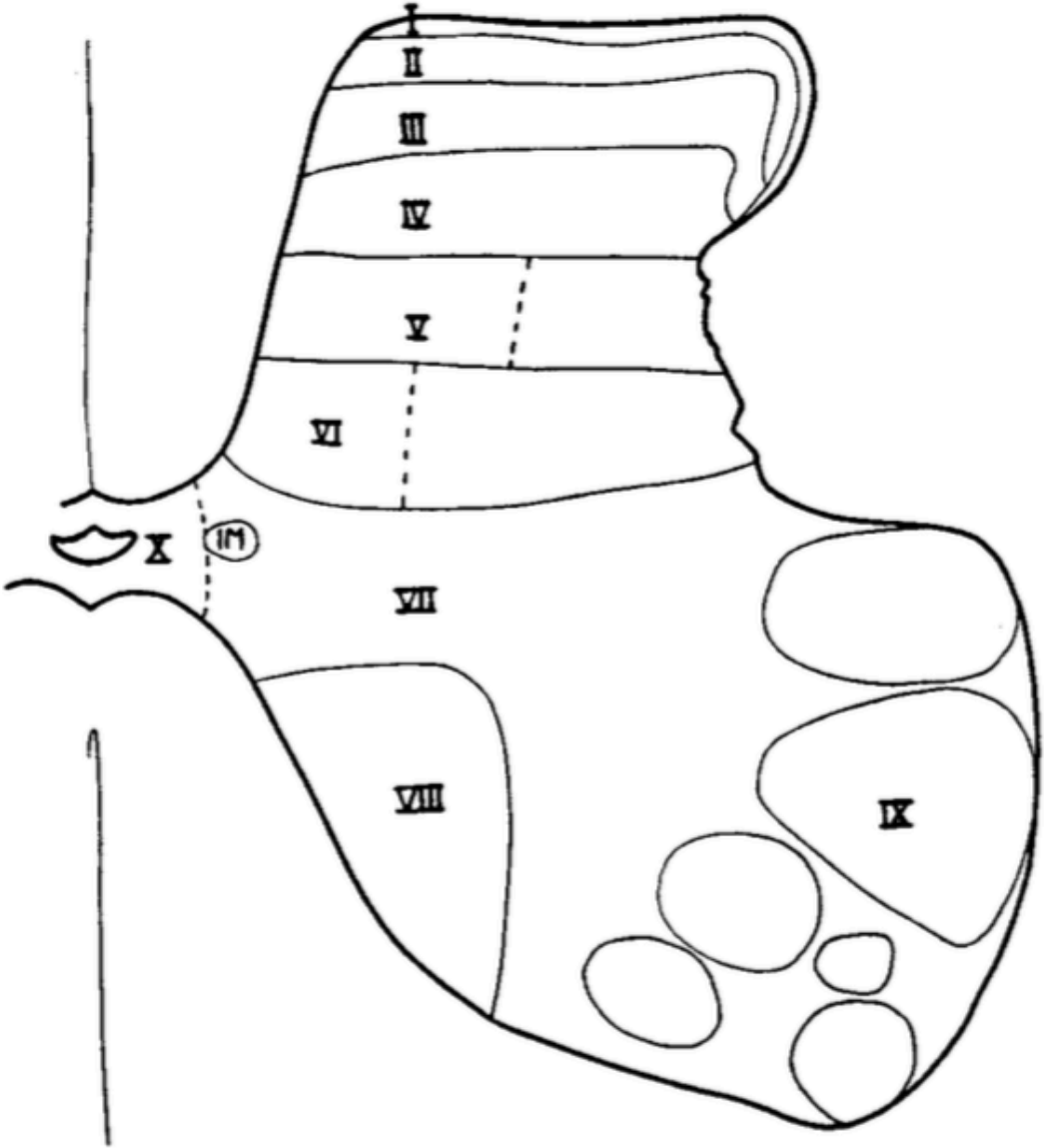
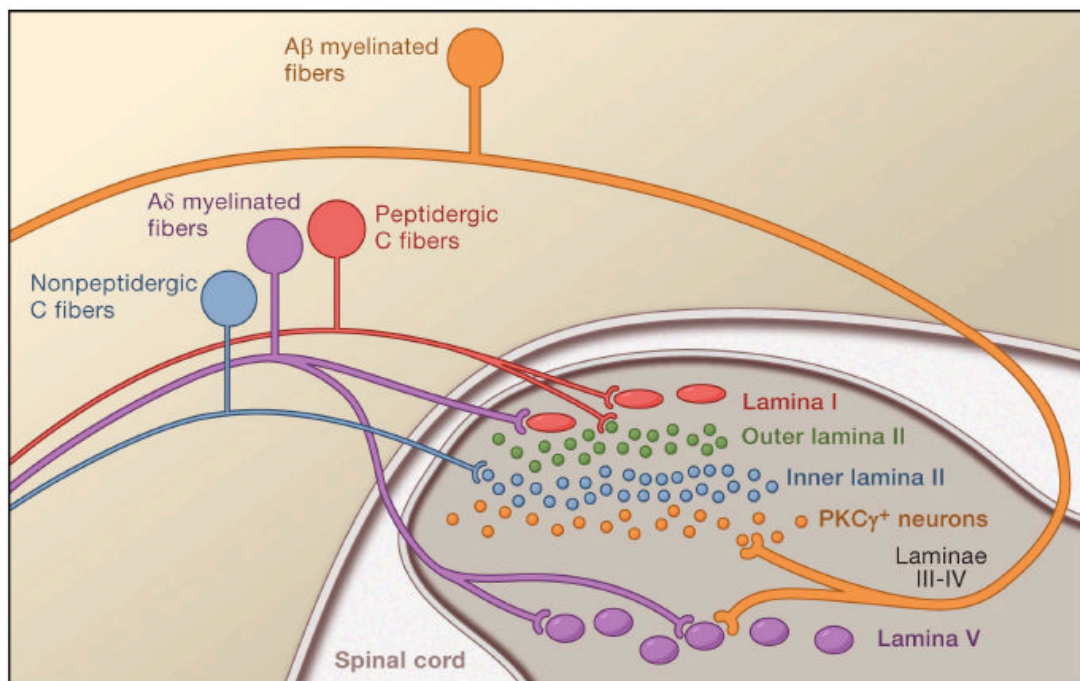


**Figure 1.8: Central terminations of nociceptors**

The central projections of cutaneous nociceptors are well characterised and subsets of primary afferent fibres target spinal neurons within distinct laminae. The peptidergic C-fibres (red) and myelinated A  $\delta$  nociceptors (purple), terminate most superficially in lamina I. The non-peptidergic C-fibre nociceptors (blue) synapse in the inner part of lamina II. By contrast, innocuous A  $\beta$  fibres mechanoreceptors (orange) terminate in lamina III-V. Lamina V receives convergent input from A  $\delta$  and A  $\beta$  fibres (Basbaum *et al.*, 2009).





---

# **Chapter 2: Materials and Methods**

---

## Materials and Methods

## 2.1 Animals and Tissue Preparation

---

Female C57Bl/6 mice (6-8 week-old, unless otherwise stated) were housed in the Flinders Medical Centre Animal House in a 12-hour light/dark cycle with unrestricted access to food and water. Female mice were chosen because this work coincided with the funded investigation of the innervation of the female genital tract. Oestrus cycle was not monitored.

All procedures involving animals followed the strict and established guidelines of the Animal Welfare Act, and were approved by the Animal Welfare Committee of Flinders University. Furthermore, these were in accordance with the National Health and Medical Research Council (NHMRC) code for the care and use of animals for scientific purposes (2013). The NHMRC Project codes for the experiments of this thesis include codes 463/06i, 695/09 and 892/12.

For experiments animals were deeply anaesthetised through inhalation of isoflurane (Veterinary Companies Australia NSW, Australia). Deep anaesthesia was confirmed by the loss of corneal and hind limb reflexes. Animals were then euthanised by exsanguination following removal of the heart. The vertebral column was removed and further dissected in phosphate buffered saline (PBS: 137 mM sodium chloride, 10 mM sodium phosphate, pH 7.0) at room temperature unless otherwise stated. Tissue was either fixed immediately in Zamboni's fixative (2% formaldehyde; 0.5% picric acid; 0.1 M sodium phosphate buffer, pH 7.0) for 24-48 hours, or prepared further for different experimental approaches. This type of immersion fixation with Zamboni's fixative has been long established within our laboratory (as far back Gibbins *et al.*, 1985) as an effective means of producing clear immuno-staining.

## 2.2 Tissue Processing and Sectioning

---

Fixative was removed from tissue through a graded series of ethanol washes and cleared with either dimethyl sulfoxide (DMSO) or xylene. DMSO processing involved a series of the following washes: 3×10 minutes in 80% ethanol; 2×15 minutes in 100% ethanol; 3×10 minutes in DMSO; and 2×15 minutes in 100% ethanol. Xylene processing involved a series of the following washes: 4×15 minutes in 80% ethanol, and a series of 30 minutes in 90% ethanol; two in 100% ethanol; two

in xylene; two in 100%; and one in each of 90%, 80% and 50% ethanol; distilled water; and finally PBS.

### **Cryostat sectioning**

Muscle and skin samples were processed through xylene and then stored in PBS/Sucrose (30% sucrose, 0.01% sodium azide) for at least 24 hours. The tissue was then placed in Cryomolds (ProSciTech, Queensland, Australia) and covered in the tissue-freezing medium: Optimal Cutting Temperature compound (OCT; Tissue-Tek, Indiana, USA). The OCT was then frozen with isopentane chilled with liquid nitrogen. Using a Cryostat the frozen sections were cut at 12  $\mu\text{m}$  (unless otherwise stated) at  $-20^{\circ}\text{C}$  and thawed onto polyethyleneimine (PEI) coated slides. They were dried using phosphorous pentoxide ( $\text{P}_2\text{O}_5$ ) under vacuum at room temperature for 30 minutes. Slides were then either stored in a sealed box at  $4^{\circ}\text{C}$  or washed twice with excess PBS to remove any OCT and prepared for immunohistochemistry.

### **Microtome sectioning**

Spinal cord and dorsal root ganglia (DRG) samples were processed through DMSO and immediately infiltrated with 1000 molecular weight polyethylene glycol (PEG<sub>1000</sub>: Sigma-Aldrich, Missouri, USA) for 30 minutes under vacuum at  $55^{\circ}\text{C}$ . Excess PEG<sub>1000</sub> was removed with filter paper and the tissue was embedded in a cryomold with 1450 molecular weight PEG (PEG<sub>1450</sub>: Sigma-Aldrich). Embedded tissue was then mounted with PEG<sub>1450</sub> onto metal chucks for sectioning. Using a rotary microtome, spinal cord was transversely sectioned at 20  $\mu\text{m}$  and DRGs at 12  $\mu\text{m}$ . Free floating sections were either stored in PBS with 0.01% sodium azide (PBS Azide) at  $4^{\circ}\text{C}$  or prepared for immunohistochemistry.

## **2.3 Immunohistochemistry**

---

To reduce non-specific antibody binding, free floating sections and sections adhered to slides were first incubated with 10% normal donkey serum (NDS, diluted in PBS) for 30 min. Sections were then incubated with a mixture of primary antisera, diluted in antibody diluent containing 10% NDS. Primary antisera incubations (see Table 2.1) were performed in a humid box at room temperature for 48 h. The specifics of the primary antisera used will be discussed in the experimental chapters.

After washing in PBS, sections were incubated for 2 hours in a mixture of species-specific secondary antisera raised in donkeys (see Table 2.1) and conjugated to Cyanine 3 (Cy3), Cyanine 5 (Cy5), fluorescein isothiocyanate (FITC), or dichlorotriazinylaminofluorescein (DTAF; all Jackson ImmunoResearch, Pennsylvania, USA). After a final PBS wash, the sections were mounted on microscope slides with carbonate-buffered glycerol (pH 8.6) and sealed with a cover slip and nail varnish.

The specificity of antibodies has been tested and verified from our group (Morris *et al.* 2005). For this project controls included incubations with the primary antibody with the secondary antisera incubation omitted to determine background fluorescence levels.

**Table 2.1: Primary and secondary antisera**

<b>Primary antisera</b>			
<b>Antigen</b>	<b>Host</b>	<b>Dilution</b>	<b>Source</b>
CGRP	goat	1:1000	code1780, Arnel, New York, USA
SP	rabbit	1:2000	Incstar (now Immunostar), Wisconsin, USA
SP	rat	1:600	clone NC1/34HL, Sera-Lab, West Sussex, UK
TRPV1	rabbit	1:500	Alomone Labs, Jerusalem, ISR
NF200	mouse	1:2000	Sigma-Aldrich, Missouri, USA
VGluT1	rabbit	1:4000	Synaptic Systems, Goettingen, GER
VIP	rabbit	1:1000	Incstar
Galanin	rabbit	1:3000	Peninsula Lab, California, USA
pERK1/2	rabbit	1:500	Cell Signalling, Massachusetts, USA
pCREB	rabbit	1:500	Cell Signalling
<b>Secondary antisera and streptavidin conjugates</b>			
Cy5 anti sheep IgG	donkey	1:50	Jackson ImmunoResearch, Pennsylvania, USA
FITC anti rabbit IgG	donkey	1:100	Jackson ImmunoResearch
FITC anti rat IgG	donkey	1:50	Jackson ImmunoResearch
Cy3 anti rabbit IgG	donkey	1:100	Jackson ImmunoResearch
Cy3 anti mouse IgG	donkey	1:100	Jackson ImmunoResearch
Cy3-Streptavidin	n/a	1:300	Jackson ImmunoResearch
DTAF-Streptavidin	n/a	1:200	Jackson ImmunoResearch

## 2.4 Microscopy

### Fluorescence Microscopy

Sections were analysed using an Olympus BX50 fluorescence microscope (Olympus, Tokyo, Japan) fitted with highly discriminating filters (detailed in Table 2.2; Chroma

Optical, Vermont, USA). Images were collected using a CoolSNAP fx CCD Camera (Photometrics, Arizona, USA) connected to a PC running AnalySIS FIVE software (v5.0, Olympus Soft Imaging System GmbH, Münster, Germany).

**Table 2.2: Filter cube specifications for the Olympus BX50 Microscope**

Filter	Excitation	Dichroic	Emission	Used for:
Olympus U-MNUA	360 – 370	400	420 - 460	UV-excitabile blue dyes
Chroma 31001	465 – 495	505	515 - 555	blue-excitabile green dyes
Chroma 31002	515 – 550	565	575 - 615	green-excitabile red dyes
Chroma 41008	590 - 650	660	665 - 740	red-excitabile far-red dyes

## Confocal Microscopy

Confocal imaging was done on a Leica TCS SP5 laser scanning confocal microscope running Leica Application Suite Advanced Fluorescence Software (Leica Microsystems GmbH, Wetzlar, Germany) in sequential scanning mode. Z-stacks were taken at designated regions of interest in the medial and lateral areas of lamina I, and deep lamina IV/V of the dorsal horn. Confocal Z-stacks were taken with a 63× N.A. 1.4 oil immersion objective with a 2-3× digital zoom. The Z-stacks were imported to Avizo Fire software for 3D reconstruction, image analysis and quantification.

## 2.5 Image Analysis and Preparation

Images were prepared for publication using Adobe Photoshop CS5 (Adobe Systems Inc., California, USA). Grey-scale images were false-coloured and adjusted for contrast and brightness before generation of merged images.

### Analysis of DRG

Widefield images of triple-labelled DRG sections were acquired with a 20x objective as TIFF files and imported into ImageJ (NIH, Maryland, USA) for analysis. Each channel was overlaid as stacks and each soma with a nuclear profile was scored for the presence or absence of immunoreactivity (IR) for each label. Soma IR was defined as “positive” when it was at least 2 standard deviations above the mean background fluorescence of unlabelled somata. Soma cross-sectional area was

determined by manual outlining of the circumference of each cell. Soma cross sectional area and grey value intensities for each neuron were exported into Microsoft Office Excel (Microsoft Corporation, Washington, USA) for further analysis.

## **Analysis of spinal cord**

Confocal Z-stacks were imported to Avizo Fire software (version 5.1.0; Mercury Computer Systems Inc., Merignac, France) for 3D reconstruction, image analysis and quantification. For 3D analysis, IR boutons were expressed as a volume (voxels or pixels<sup>3</sup>), with the assumption that each bouton was of comparable size. Each detection channel was first 3D-median filtered (kernel size 3) to reduce single pixel noise and 3D thresholds were optimised to select specific labelling of axonal boutons above background labelling and intervaricose axons. Identical thresholds were used for each of the analysed regions within a spinal cord section and the respective thresholds for each channel were set to be consistent between sections and between experiments. For each Z-stack, the exclusive AND operator (A&B) was used to determine colocalisation between the three fluorescence data channels in x-y-z coordinates. The volume of each 3D data set was calculated and exported into Microsoft Excel for further analysis.

## **Statistical Analysis**

All statistics were done using SPSS (version 19.0; IBM Company, New York, USA) and graphs were created using Prism (version 5.0d; GraphPad Software Inc., California, USA). Data are displayed as the mean  $\pm$  standard error of the mean. Statistical analyses included: one-way analysis of variance (ANOVA), multivariate analysis of variance (M-ANOVA) or repeated measures analysis of variance (RM-ANOVA) with post hoc Bonferroni's multiple comparisons (BMC) correction with 95% confidence intervals.



---

**Chapter 3:  
Prevalence and  
distribution of CGRP<sup>+</sup>SP<sup>-</sup>  
neurons**

---



## 3.1 Background

---

CGRP is expressed by small A $\delta$  and C-fibre DRG neurons (McCarthy & Lawson, 1990), many of which are capsaicin-sensitive nociceptors (Lawson *et al.*, 1997). The majority of these neurons also contain the tachykinin, substance P (SP; Wiesenfeld-Hallin *et al.*, 1984; Merighi *et al.*, 1988; Hökfelt *et al.*, 1993) and there is a high co-expression of CGRP and SP in terminals within the superficial dorsal horn (Gibson *et al.*, 1981; 1988) and in cutaneous afferents (Gibbins *et al.*, 1985; Gibbins, Wattchow, *et al.*, 1987). Functionally, CGRP enhances the nociceptive behavioural responses induced by SP (Wiesenfeld-Hallin *et al.*, 1984) by potentiating the capsaicin-induced release of SP (Oku *et al.*, 1987) and by inhibiting SP degradation (Le Greves *et al.*, 1985).

CGRP expression is not restricted to DRG neurons co-expressing SP and is also present in DRG neurons with considerably larger cell bodies (McCarthy & Lawson, 1990; Morris *et al.*, 2005), probably corresponding to neurons with fast conducting A $\beta$  fibres (McCarthy & Lawson, 1990). Furthermore, a prominent population of CGRP terminals project to lamina IV/V of the spinal dorsal horn (Gibson, Polak, Bloom, *et al.*, 1984). Despite these early observations, little is known about the functions and detailed projections of these larger CGRP primary afferent neurons that lack detectable SP expression.

In order to better characterise these CGRP<sup>+</sup>SP<sup>-</sup> neurons, we have used multiple labelling immunohistochemistry to further characterise the CGRP<sup>+</sup>SP<sup>-</sup> neurons detected in the cervical (C7) DRG and dorsal horn, and extended our analysis to other spinal cord levels. We investigated DRG and dorsal horn at representative thoracic (T5), lumbar (L4) and sacral (S3) spinal cord levels. We also further characterised these neurons in forepaw and hindpaw skin using confocal microscopy.



## 3.2 Materials and Methods

---

Spinal cord and DRG samples were taken from representative cervical (C7), thoracic (T5), lumbar (L4) and sacral (S3) levels. Samples were fixed, processed through DMSO, embedded in PEG, and sectioned using a microtome. Skin samples from the plantar and dorsal surfaces of the forepaws and hindpaws were fixed, processed through xylene and sectioned using a cryostat.

Spinal cord and DRG sections were double labelled with anti-CGRP raised in a goat (1:1000; code 1780, Arnel, New York, USA) and anti-SP raised in a rabbit (1:2000; Incstar [now Immunostar], Wisconsin, USA). Skin sections were triple labelled with anti-neuron specific enolase (NSE) raised in a rabbit (1:1000; Dako, Victoria, Australia), anti-CGRP raised in a goat (Arnel) and monoclonal anti-SP raised in a rat (1:600; clone NC1/34HL, Sera-Lab, West Sussex, UK).

Widefield images of DRG and spinal cord sections were taken with the Olympus BX50 with a 20x objective. Confocal Z-stacks of spinal cord sections, consisting of 21 optical sections 0.5  $\mu\text{m}$  apart (total depth 10.5  $\mu\text{m}$ ), were taken with the Leica confocal microscope with a 63x N.A. 1.4 oil immersion objective with 2x digital zoom.

Widefield images of skin sections were taken with a 40x objective, and confocal Z-stacks consisting of 21-33 optical sections 0.5  $\mu\text{m}$  apart (total depth 10.5-16.5  $\mu\text{m}$ ) were taken with a 63x N.A. 1.4 oil immersion objective with 2x digital zoom. Skin sections were only qualitatively analysed.

Widefield images of DRG were imported to ImageJ to determine the presence of CGRP-IR or SP-IR and soma cross-sectional area of sensory neurons. Confocal Z-stacks of spinal cord were imported to Avizo for 3D reconstruction and analysis. The volume of CGRP-IR boutons that either contained or lacked SP-IR was calculated using the AND (A&B) operator and the NOT (A-B) operator between the CGRP and SP data sets. Data were then displayed as mean $\pm$ SEM and RM-ANOVA with post hoc BMC correction with 95% confidence limits was used to determine the statistical significance.



### 3.3 Results

---

#### **CGRP<sup>+</sup>SP<sup>-</sup> neurons were prominent in DRG of all spinal levels**

CGRP-IR was detected in neuronal somata and fibres in dorsal root ganglia (DRG) of all spinal levels (C7, T5, L4 and S3). Cytoplasmic CGRP-IR was uniformly intense in small to medium sized neurons (50-500  $\mu\text{m}^2$ ), but sometimes less intense and more granular in larger neurons ( $> 500 \mu\text{m}^2$ ; Figure 3.1A). There was no correlation between the intensity of CGRP-IR and the soma size of the neurons (linear correlation:  $r < 0.01$ ,  $p = 0.08$ ;  $N = 4$  animals;  $n = 1720$  neurons; Figure 3.2). SP-IR was intense in small to medium sized neurons (50-500  $\mu\text{m}^2$ ); no cells larger than 500  $\mu\text{m}^2$  contained SP-IR (Figure 3.1B). There was no correlation between the intensity of SP-IR and the soma size of the neuron (linear correlation:  $r < 0.01$ ,  $p = 0.3$ ;  $N = 4$  animals;  $n = 873$  neurons; Figure 3.3). Immunoreactivity for CGRP occurred in two DRG neuron subpopulations based on the presence or absence of SP-IR and soma size (Figure 3.1C and 1D).

Overall, CGRP-IR was present 55% (1720/3230 neurons) of DRG neurons. At most levels there was no difference between the proportion of neurons expressing or lacking CGRP-IR (Chi-Square:  $\chi^2_3 = 6$ ,  $p = 0.1$ ;  $N = 4$  animals;  $n = 3230$  neurons; Figure 3.4). CGRP-IR neurons existed as either CGRP<sup>+</sup>SP<sup>-</sup> (54%, 953/1772) or CGRP<sup>+</sup>SP<sup>+</sup> (46%, 819/1772) in equal proportions (Chi-Square:  $\chi^2_3 = 5$ ,  $p = 0.2$ ;  $N = 4$  animals;  $n = 1720$  neurons; Figure 3.5) in DRG of all spinal levels. The CGRP-IR neurons that were CGRP<sup>+</sup>SP<sup>+</sup> had a much higher intensity of CGRP-IR than compared to the CGRP<sup>+</sup>SP<sup>-</sup> in DRG of all spinal levels (51 $\pm$ 1 and 19 $\pm$ 1 grey values above background fluorescence, respectively; RM-ANOVA:  $F_{(1,1764)} = 359$ ,  $p < 0.001$ ;  $N = 4$  animals;  $n = 1720$  neurons; Figure 3.8).

The soma sizes of neurons were larger in C7, and at L4 the neurons were larger than the neurons of T5 and S3 (RM-ANOVA:  $F_{(3,3226)} = 38$ ,  $p < 0.001$  Figure 3.6). This was also true for CGRP<sup>+</sup>SP<sup>-</sup> neurons (RM-ANOVA;  $F_{(3,1764)} = 33$ ,  $p < 0.001$ ;  $N = 4$  animals;  $n = 1720$  neurons; Figure 3.7). There was no significant difference between the soma sizes of CGRP<sup>+</sup>SP<sup>+</sup> neurons throughout the spinal levels. The soma size of CGRP<sup>+</sup>SP<sup>-</sup> neurons was greater than CGRP<sup>+</sup>SP<sup>+</sup> neurons in DRG of all spinal levels

(RM-ANOVA:  $F_{(1,1764)} = 315$ ,  $p < 0.001$ ;  $N = 4$  animals;  $n = 1720$  neurons; Figure 3.7).

### ***CGRP<sup>+</sup>SP<sup>-</sup> neurons in C7 DRG***

In C7 DRG ( $N = 4$  animals,  $n = 898$  neurons), CGRP-IR was detected in half (47%, 418/898) of the DRG neurons (Figure 3.9A) and SP-IR was detected in a third 32% (248/898) of the neurons (Figure 3.9A). Of the CGRP-IR neurons there were equal proportions of CGRP<sup>+</sup>SP<sup>-</sup> neurons (46%; 192/418) and CGRP<sup>+</sup>SP<sup>+</sup> neurons (54%; 226/418; Chi-Square:  $\chi_1^2 = 3$ ,  $p = 0.1$ ;  $N = 4$  animals,  $n = 418$  neurons; Figure 3.9A). The CGRP<sup>+</sup>SP<sup>+</sup> neurons had an average soma size of  $233 \pm 8 \mu\text{m}^2$  (Figure 3.9B), whereas the CGRP<sup>+</sup>SP<sup>-</sup> neurons had a larger soma size of  $473 \pm 14 \mu\text{m}^2$  (ANOVA:  $F_{(1,416)} = 244$ ,  $p < 0.0001$ ;  $N = 4$  animals,  $n = 418$  neurons; Figure 3.9B). Very few SP-IR neurons lacked CGRP-IR (CGRP<sup>-</sup>SP<sup>+</sup>; 9%, 22/248).

### ***CGRP<sup>+</sup>SP<sup>-</sup> neurons in T5 DRG***

In T5 DRG ( $N = 4$  animals,  $n = 865$  neurons), CGRP-IR was detected in just over half of the neurons (54%, 464/865 neurons; Figure 3.10A) and SP-IR was detected in 23% (197/865) of the neurons. Of the CGRP-IR neurons there were more CGRP<sup>+</sup>SP<sup>-</sup> neurons (65%; 282/464) than CGRP<sup>+</sup>SP<sup>+</sup> neurons (39%; 182/464; Chi-Square:  $\chi_1^2 = 22$ ,  $p < 0.001$ ;  $N = 4$  animals,  $n = 464$  neurons Figure 3.10A). The CGRP<sup>+</sup>SP<sup>+</sup> neurons had an average soma size of  $292 \pm 12 \mu\text{m}^2$  (Figure 3.10B), whereas the CGRP<sup>+</sup>SP<sup>-</sup> neurons had a larger soma size of  $324 \pm 11 \mu\text{m}^2$ ; ANOVA:  $F_{(1,462)} = 4$ ,  $p < 0.05$ ;  $N = 4$  animals,  $n = 464$  neurons; Figure 3.10B). Very few SP-IR neurons lacked CGRP-IR (CGRP<sup>-</sup>SP<sup>+</sup>; 8%, 15/197).

### ***CGRP<sup>+</sup>SP<sup>-</sup> neurons in L4 DRG***

In L4 DRG ( $N = 4$  animals,  $n = 850$  neurons), CGRP-IR was detected in just over half of the neurons (60%, 508/850 neurons; Figure 3.11A) and SP-IR was detected in 29% (244/850) of the neurons. Of the CGRP-IR neurons there were equal proportions of CGRP<sup>+</sup>SP<sup>-</sup> neurons (53%; 271/508) and CGRP<sup>+</sup>SP<sup>+</sup> neurons (47%; 237/508; Chi-Square:  $\chi_1^2 = 2$ ,  $p = 0.1$ ;  $N = 4$  animals,  $n = 508$  neurons; Figure 3.11A). The CGRP<sup>+</sup>SP<sup>+</sup> neurons had an average soma size of  $220 \pm 5 \mu\text{m}^2$  (Figure 3.11B), whereas the CGRP<sup>+</sup>SP<sup>-</sup> neurons had a larger soma size of  $416 \pm 13 \mu\text{m}^2$ ; ANOVA:  $F_{(1,506)} = 166$ ,  $p < 0.0001$ ;  $N = 4$  animals,  $n = 508$  neurons; Figure 3.11B). Very few SP-IR neurons lacked CGRP-IR (CGRP<sup>-</sup>SP<sup>+</sup>; 1%, 7/244).

***CGRP<sup>+</sup>SP<sup>-</sup> neurons in S3 DRG***

In S3 DRG (N = 4 animals, n = 617 neurons), CGRP-IR was detected in more than half of the neurons (62%, 382/617 neurons; Figure 3.12A) and SP-IR was detected in 30% (184/617) of the neurons. Of the CGRP-IR neurons there were equal proportions of CGRP<sup>+</sup>SP<sup>-</sup> neurons (54%; 208/382) and CGRP<sup>+</sup>SP<sup>+</sup> neurons (46%; 174/382; Chi-Square:  $\chi_1^2 = 3$ ,  $p = 0.08$ ; N = 4 animals, n = 382 neurons; Figure 3.12A). The CGRP<sup>+</sup>SP<sup>+</sup> neurons had an average soma size of  $236 \pm 10 \mu\text{m}^2$  (Figure 3.12B), whereas the CGRP<sup>+</sup>SP<sup>-</sup> neurons had a larger soma size of  $341 \pm 14 \mu\text{m}^2$ ; ANOVA:  $F_{(1,381)} = 36$ ,  $p < 0.0001$ ; N = 4 animals, n = 382 neurons; Figure 3.12B). Very few SP-IR neurons lacked CGRP-IR (CGRP<sup>-</sup>SP<sup>+</sup>; 5%, 10/184).

**CGRP<sup>+</sup>SP<sup>-</sup> terminals were prominent in the lamina I and IV/V of spinal dorsal horn**

All spinal levels contained high levels of CGRP-IR and SP-IR in the superficial dorsal horn (see Figure 3.13). CGRP-IR terminals were detected throughout the full length of lamina I, and also in deeper lamina (presumed IV/V) forming variably sized network (Figure 3.13). Some CGRP-IR terminals were also detected connecting between lamina I and lamina IV/V. SP-IR terminals were also detected throughout the full length of lamina I, but unlike CGRP-IR, were also prominent in the lateral spinal nucleus, and in lamina II .

All spinal levels had prominent CGRP-IR in the superficial dorsal, but each level had some unique features (see Figure 3.13). The C7 and L4 dorsal horns were both of similar size and morphology. Both dorsal horns had prominent levels of CGRP-IR in the superficial lamina (Figure 3.13). Unlike other spinal levels, the C7 and L4 dorsal horns had CGRP-IR terminals that projected deeper into the medial superficial dorsal horn (possibly entering lamina II). In L4 dorsal horn this deeper superficial projection extended more laterally than the C7 dorsal horn. In C7 dorsal horn the deeper medial superficial projection was interrupted by a lack of CGRP-IR terminals in mediolateral lamina I (Figure 3.13). Both dorsal horns had a prominent network of CGRP-IR terminals in the deeper lamina (lamina IV/V, Figure 3.13). This deep CGRP-IR network was more prominent in the L4 dorsal horn and covered more lamina (III-V) and extended further medially and laterally than the network of CGRP-IR terminals in the C7 dorsal horn (covering lamina IV-V, Figure 3.13).

The T5 dorsal horn had a similar morphology to the C7 and L4 dorsal horns, but considerably smaller in size (Figure 3.13). Much like C7 and L4 dorsal horns, the T5 dorsal horn had prominent CGRP-IR terminals in the superficial lamina. However, in the T5 dorsal horn the CGRP-IR terminals of the medial superficial lamina did not appear to penetrate into lamina II and remained confined to lamina I. T5 also had the deep CGRP-IR network of lamina IV/V, but was less prominent, more lateral and covered a smaller area than the C7 and L4 dorsal horns (Figure 3.13).

The S3 dorsal horn morphology was distinct from the other spinal levels (Figure 3.13). The dorsal horns appeared more externally rotated and the dorsal funiculus was considerably shallower than the other dorsal horn levels. CGRP-IR terminals were still prominent in the superficial lamina, but they were extended beneath the dorsal funiculus, connecting the two dorsal horns. In the midline of the spinal cord deeper to the CGRP-IR terminals beneath the dorsal funiculus were CGRP-IR terminals projecting to the central canal. These CGRP-IR fibres had branches that extended laterally into the dorsal horn and sometimes connected to the lateral curve of lamina I. The S3 dorsal horn lacked the deeper CGRP-IR network that was seen at other spinal levels (Figure 3.13).

Quantitatively, in all spinal levels the volume of CGRP-IR voxels was highest in medial lamina I and lowest lamina IV/V (RM-ANOVA:  $F_{(1,4)} = 15$ ,  $p = 0.019$ ; Figure 3.14). When analysing the spinal levels within each of the three dorsal horn regions, Figure 3.14 demonstrates that there was no significant difference in the volume of CGRP-IR voxels within medial lamina I (RM-ANOVA:  $F_{(1,4)} = 0.4$ ,  $p = 0.6$ ). This was also evident in lateral lamina I (RM-ANOVA:  $F_{(1,3)} = 0.02$ ,  $p = 0.9$ ) and lamina IV/V (RM-ANOVA:  $F_{(1,4)} = 5$ ,  $p = 0.1$ ).

As in the DRG, CGRP-IR terminals in the dorsal horn could be subdivided into two distinct subpopulations based on the presence or absence of SP-IR. There was a higher proportion of CGRP-IR voxels that were CGRP<sup>+</sup>SP<sup>-</sup> voxels compared to CGRP<sup>+</sup>SP<sup>+</sup> voxels in all spinal levels (RM-ANOVA:  $F_{(1,4)} = 22$ ,  $p = 0.009$ ; Figure 3.15). There was no difference in the proportion of CGRP-IR voxels that were either CGRP<sup>+</sup>SP<sup>+</sup> or CGRP<sup>+</sup>SP<sup>-</sup> voxels between the different spinal levels in medial lamina I or lamina IV/V (RM-ANOVA:  $F_{(1,4)} = 0.2$ ,  $p = 0.7$  and  $F_{(1,4)} = 2$ ,  $p = 0.25$ , respectively; Figure 3.15). Lateral lamina I had a higher proportion of CGRP<sup>+</sup>SP<sup>-</sup> in

the C7 dorsal horn than the L4 and S3 dorsal horns (RM-ANOVA:  $F_{(1,4)} = 20$ ,  $p = 0.01$ ; Figure 3.15).

There was a higher volume of CGRP-IR voxels that were CGRP<sup>+</sup>SP<sup>-</sup> voxels compared to CGRP<sup>+</sup>SP<sup>+</sup> voxels in all spinal levels (RM-ANOVA:  $F_{(1,4)} = 26$ ,  $p = 0.007$ ; Figure 3.15). There was no difference in the volume of CGRP<sup>+</sup>SP<sup>-</sup> voxels between the different spinal levels in medial lamina I, lateral lamina I or lamina IV/V (RM-ANOVA:  $F_{(1,4)} = 0$ ,  $p = 1$ ;  $F_{(1,4)} = 0.04$ ,  $p = 0.9$ ; and  $F_{(1,4)} = 0.02$ ,  $p = 1$ , respectively; Figure 3.15).

### ***CGRP<sup>+</sup>SP<sup>-</sup> terminals in C7 dorsal horn***

In C7 dorsal horn, the CGRP-IR and SP-IR terminals were prominent throughout lamina I. Medial lamina I appeared to have mainly CGRP<sup>+</sup>SP<sup>+</sup> terminals that projected deeper into the dorsal horn, possibly entering lamina II (Figure 3.17A, box 1; Figure 3.17B<sub>1</sub> & C<sub>1</sub>). Lateral lamina I appeared to have more CGRP<sup>+</sup>SP<sup>-</sup> terminals than CGRP<sup>+</sup>SP<sup>+</sup> terminals (Figure 3.17A, box 3, (Figure 3.17B<sub>3</sub> & C<sub>3</sub>). The region between medial and lateral lamina I (mediolateral lamina I) had fewer CGRP-IR terminals and appeared to completely separate the medial and lateral regions (Figure 3.17A). The deeper CGRP-IR network was prominent; it was situated in mediolateral lamina III/V and consisted of mainly CGRP<sup>+</sup>SP<sup>-</sup> terminals (Figure 3.17A, box 2; Figure 3.17B<sub>2</sub> & C<sub>2</sub>).

Quantitatively, the volume of CGRP-IR voxels in the C7 dorsal horn was highest in medial lamina I compared to lateral lamina I and lamina IV/V, and lowest in lamina IV/V compared to lateral lamina I (RM-ANOVA:  $F_{(1,4)} = 102$ ,  $p = 0.001$ ;  $N = 5$  animals, Figure 3.18). There was a higher proportion of CGRP-IR voxels that were CGRP<sup>+</sup>SP<sup>-</sup> compared to CGRP<sup>+</sup>SP<sup>+</sup> (RM-ANOVA:  $F_{(1,4)} = 17$ ,  $p = 0.02$ ;  $n = 5$  animals; Figure 3.19). This was evident in both lateral lamina I and lamina IV/V but not in medial lamina I. The proportion of CGRP-IR voxels that were CGRP<sup>+</sup>SP<sup>-</sup> was highest in lamina IV/V and lowest was in medial lamina I (RM-ANOVA:  $F_{(1,4)} = 33$ ,  $p = 0.005$ ;  $n = 5$  animals; Figure 3.19). There was a higher volume of CGRP<sup>+</sup>SP<sup>-</sup> voxels compared to CGRP<sup>+</sup>SP<sup>+</sup> voxels (RM-ANOVA:  $F_{(1,4)} = 13$ ,  $p = 0.002$ ;  $n = 5$  animals; Figure 3.20). This was evident in lamina IV/V, but not in lateral or medial lamina I (RM-ANOVA:  $F_{(1,4)} = 320$ ,  $p > 0.001$ ;  $n = 5$  animals; Figure 3.20). The volume of CGRP<sup>+</sup>SP<sup>-</sup> voxels was higher in medial and lateral lamina I compared to lamina IV/V (RM-ANOVA:  $F_{(1,4)} = 8$ ,  $p = 0.05$ ; Figure 3.20) and the volume of

CGRP<sup>+</sup>SP<sup>+</sup> voxels was highest in medial lamina I and lowest in lamina IV/V (RM-ANOVA:  $F_{(1,4)} = 114$ ,  $p < 0.001$ ; Figure 3.20).

### ***CGRP<sup>+</sup>SP<sup>-</sup> terminals in T5 dorsal horn***

In T5 dorsal horn, the CGRP-IR and SP-IR terminals were prominent throughout lamina I. Medial lamina I appeared to have mainly CGRP<sup>+</sup>SP<sup>+</sup> terminals (Figure 3.21A, box 1; Figure 3.21B<sub>1</sub> & C<sub>1</sub>). Lateral lamina I appeared to have more CGRP<sup>+</sup>SP<sup>-</sup> terminals than CGRP<sup>+</sup>SP<sup>+</sup> terminals (Figure 3.21A, box 3, (Figure 3.21B<sub>3</sub> & C<sub>3</sub>). The deeper CGRP-IR network was not as prominent as other spinal levels; it was situated in lamina V/VI, and consisted of mainly CGRP<sup>+</sup>SP<sup>-</sup> terminals (Figure 3.21A, box 2; Figure 3.21B<sub>2</sub> & C<sub>2</sub>).

Quantitatively, the volume of CGRP-IR voxels in the T5 dorsal horn was higher in medial and lateral lamina I compared to lamina IV/V (RM-ANOVA:  $F_{(1,4)} = 58$ ,  $p = 0.002$ ;  $N = 5$  animals, Figure 3.22). There was a higher proportion of CGRP-IR voxels that were CGRP<sup>+</sup>SP<sup>-</sup> compared to CGRP<sup>+</sup>SP<sup>+</sup> (RM-ANOVA:  $F_{(1,4)} = 49$ ,  $p = 0.002$ ;  $n = 5$  animals; Figure 3.23). This was evident in lamina IV/V, but not in medial or lateral lamina I. The proportion of CGRP-IR voxels that were CGRP<sup>+</sup>SP<sup>-</sup> was highest in lamina IV/V compared to medial and lateral lamina I (RM-ANOVA:  $F_{(1,4)} = 24$ ,  $p < 0.001$ ;  $n = 5$  animals; Figure 3.23). There was a higher volume of CGRP<sup>+</sup>SP<sup>-</sup> voxels compared to CGRP<sup>+</sup>SP<sup>+</sup> voxels (RM-ANOVA:  $F_{(1,4)} = 35$ ,  $p = 0.004$ ;  $n = 5$  animals; Figure 3.24). This was evident in lamina IV/V, but not in lateral or medial lamina I (RM-ANOVA:  $F_{(1,4)} = 24$ ,  $p < 0.008$ ;  $N = 5$  animals; Figure 3.24). The volume of CGRP<sup>+</sup>SP<sup>-</sup> voxels was higher in medial and lateral lamina I compared to lamina IV/V (RM-ANOVA:  $F_{(1,4)} = 30$ ,  $p = 0.005$ ; Figure 3.24) and the volume of CGRP<sup>+</sup>SP<sup>+</sup> voxels was highest in medial lamina I and lowest in lamina IV/V (RM-ANOVA:  $F_{(1,4)} = 371$ ,  $p < 0.001$ ; Figure 3.24).

### ***CGRP<sup>+</sup>SP<sup>-</sup> terminals in L4 dorsal horn***

In L4 dorsal horn, the CGRP-IR and SP-IR terminals were prominent throughout lamina I. Medial lamina I appeared to have mainly CGRP<sup>+</sup>SP<sup>+</sup> terminals (Figure 3.25A, box 1; Figure 3.25B<sub>1</sub> & C<sub>1</sub>). Lateral lamina I appeared to be more CGRP<sup>+</sup>SP<sup>-</sup> terminals than CGRP<sup>+</sup>SP<sup>+</sup> terminals (Figure 3.25A, box 3, Figure 3.25B<sub>3</sub> & C<sub>3</sub>). The deeper CGRP-IR network was quite prominent, situated in the middle (mediolateral) of the dorsal horn, extended as far as lamina III-V, and consisted of mainly CGRP<sup>+</sup>SP<sup>-</sup> terminals (Figure 3.25A, box 2; Figure 3.25B<sub>2</sub> & C<sub>2</sub>).

Quantitatively, the volume of CGRP-IR voxels in the L4 dorsal horn was higher in medial and lateral lamina I compared to lamina IV/V (RM-ANOVA:  $F_{(1,4)} = 29$ ,  $p = 0.006$ ;  $N = 5$  animals, Figure 3.26). There was a higher proportion of CGRP-IR voxels that were CGRP<sup>+</sup>SP<sup>-</sup> compared to CGRP<sup>+</sup>SP<sup>+</sup> (RM-ANOVA:  $F_{(1,4)} = 49$ ,  $p = 0.002$ ;  $n = 5$  animals; Figure 3.27). This was evident in lamina IV/V, but not in medial or lateral lamina I. The proportion of CGRP-IR voxels that were CGRP<sup>+</sup>SP<sup>-</sup> was highest in lamina IV/V compared to medial and lateral lamina I (RM-ANOVA:  $F_{(1,4)} = 29$ ,  $p < 0.001$ ;  $n = 5$  animals; Figure 3.27). There was a higher volume of CGRP<sup>+</sup>SP<sup>-</sup> voxels compared to CGRP<sup>+</sup>SP<sup>+</sup> voxels (RM-ANOVA:  $F_{(1,4)} = 41$ ,  $p = 0.003$ ;  $n = 5$  animals; Figure 3.28). This was evident in lamina IV/V, but not in lateral or medial lamina I (RM-ANOVA:  $F_{(1,4)} = 42$ ,  $p < 0.003$ ;  $n = 5$  animals; Figure 3.28). The volume of CGRP<sup>+</sup>SP<sup>-</sup> voxels was higher in medial and lateral lamina I compared to lamina IV/V (RM-ANOVA:  $F_{(1,4)} = 11$ ,  $p = 0.03$ ; Figure 3.28) and the volume of CGRP<sup>+</sup>SP<sup>+</sup> voxels was highest in medial lamina I and lowest in lamina IV/V (RM-ANOVA:  $F_{(1,4)} = 69$ ,  $p = 0.001$ ; Figure 3.28).

### ***CGRP<sup>+</sup>SP<sup>-</sup> terminals in S3 dorsal horn***

In S3 dorsal horn, the CGRP-IR and SP-IR terminals were prominent throughout lamina I. Medial lamina I appeared to have mainly CGRP<sup>+</sup>SP<sup>+</sup> terminals (Figure 3.29, box 1; Figure 3.29B<sub>1</sub> & C<sub>1</sub>). Lateral lamina I appeared to be more CGRP<sup>+</sup>SP<sup>+</sup> terminals than CGRP<sup>+</sup>SP<sup>-</sup> terminals (Figure 3.29A, box 3, Figure 3.29B<sub>3</sub> & C<sub>3</sub>). The deeper CGRP-IR network was non-existent. However, CGRP-IR terminals were prominent in the midline of the two dorsal horn situated directly below the dorsal funiculus and extended to the central canal. These CGRP-IR terminals extended laterally into the dorsal horn and sometimes connected to the lateral curve of lamina I.

Quantitatively, the volume of CGRP-IR in the S3 dorsal horn was the same in medial and lateral lamina I (Paired t-test:  $t_{(4)} = 1$ ,  $p = 0.3$ ;  $N = 5$  animals, Figure 3.30). Overall there was a higher proportion of CGRP-IR voxels that were CGRP<sup>+</sup>SP<sup>+</sup> compared to CGRP<sup>+</sup>SP<sup>-</sup> (RM-ANOVA:  $F_{(1,4)} = 26$ ,  $p = 0.007$ ;  $n = 5$  animals; Figure 3.31). This was evident in both medial or lateral lamina I, and there was no difference between the proportion of CGRP-IR voxels that were CGRP<sup>+</sup>SP<sup>-</sup> between these regions (Paired t-test:  $t_{(4)} = 1$ ,  $p = 0.5$ ;  $n = 5$  animals; Figure 3.31). There was a higher volume of CGRP<sup>+</sup>SP<sup>-</sup> voxels compared to CGRP<sup>+</sup>SP<sup>+</sup> voxels (RM-ANOVA:  $F_{(1,4)} = 24$ ,  $p = 0.008$ ;  $n = 5$  animals; Figure 3.32). However, there was no difference

between the volume of CGRP<sup>+</sup>SP<sup>-</sup> voxels compared to CGRP<sup>+</sup>SP<sup>+</sup> voxels in medial or lateral lamina I (RM-ANOVA:  $F_{(1,4)} = 1$ ,  $p = 0.5$ ;  $n = 5$  animals; Figure 3.32). Nor was there any difference between the volume of CGRP<sup>+</sup>SP<sup>-</sup> voxels or CGRP<sup>+</sup>SP<sup>+</sup> voxels in lateral lamina I compared to medial lamina I (RM-ANOVA:  $F_{(1,4)} = 1$ ,  $p = 0.4$  and  $F_{(1,4)} = 1$ ,  $p = 0.5$ , respectively; Figure 3.32).

## **CGRP<sup>+</sup>SP<sup>-</sup> fibres were prominent in both glabrous and hairy paw skin**

### ***CGRP<sup>+</sup>SP<sup>-</sup> fibres in glabrous forepaw and hindpaw skin***

Immunoreactivity to the pan-neuronal marker, NSE-IR, was used to visualise all nerve fibres in forepaw and hindpaw skin. In glabrous skin ( $N = 4$  animals), NSE-IR was detected in fibre bundles deep within the dermis, and in single fibres that ran parallel to the epidermis at the dermo-epidermal junction. Many of these single fibres were associated with capillaries. Other NSE-IR fibres penetrated the epidermis as complex free nerve endings or formed Meissner's corpuscles within dermal papillae.

CGRP<sup>+</sup>SP<sup>+</sup> and CGRP<sup>+</sup>SP<sup>-</sup> fibres occurred together in bundles within the deep dermis. Both CGRP<sup>+</sup>SP<sup>+</sup> and CGRP<sup>+</sup>SP<sup>-</sup> fibres were present in the dermo-epidermal junction and were associated with capillaries (Figure 3.33). Some CGRP<sup>+</sup>SP<sup>-</sup> and CGRP<sup>+</sup>SP<sup>+</sup> fibres penetrated the epidermis (Figure 3.34) and both fibre types also were associated with Meissner's corpuscles (Figure 3.35). CGRP<sup>+</sup>SP<sup>-</sup> fibres were most prominent in the dermal papillae, where there were few CGRP<sup>+</sup>SP<sup>+</sup> fibres. All fibres with SP-IR also contained CGRP-IR. There were no obvious differences between forepaw and hindpaw skin.

### ***CGRP<sup>+</sup>SP<sup>-</sup> fibres in hairy forepaw and hindpaw skin***

NSE-IR fibres were less common at the dermo-epidermal junction of hairy skin ( $N = 4$  animals) compared with glabrous skin. Single NSE-IR fibres and nerve bundles of the dermis were interspersed between hair follicles with no obvious spatial pattern. NSE-IR fibres were associated with hair follicles in two distinct patterns: as palisade fibres parallel to the hair shaft and thinner fibres that encircled the hair shaft (Figure 3.36 and Figure 3.37). NSE-IR fibres were associated with capillaries, but no NSE-IR fibres penetrated the epidermis.

As in glabrous skin, CGRP<sup>+</sup>SP<sup>+</sup> and CGRP<sup>+</sup>SP<sup>-</sup> fibres occurred together in bundles within the deep dermis. Both CGRP<sup>+</sup>SP<sup>+</sup> and CGRP<sup>+</sup>SP<sup>-</sup> fibres were present in the

Chapter 3: Prevalence and distribution of CGRP<sup>+</sup>SP<sup>-</sup> neurons dermo-epidermal junction, and associated with capillaries. Both CGRP<sup>+</sup>SP<sup>-</sup> and CGRP<sup>+</sup>SP<sup>+</sup> fibres were interspersed between the hair follicles, and also associated with hair follicles. Fine varicose CGRP<sup>+</sup>SP<sup>-</sup> fibres encircled the hair follicle at the level of the palisade nerve endings and a single CGRP<sup>+</sup>SP<sup>+</sup> fibre encircled the hair follicle deep to CGRP<sup>+</sup>SP<sup>-</sup> fibres (Figure 3.36 and Figure 3.37). Palisade nerve endings lacked CGRP-IR. There were no obvious differences between forepaw and hindpaw skin.



### 3.4 Discussion

---

We have demonstrated a distinct subpopulation of primary afferent neurons with easily demonstrable CGRP-IR but no detectable SP-IR. This population of neurons makes up a significant proportion of CGRP-IR neurons with peripheral terminations in the skin and central terminations in the dorsal horn of the spinal cord.

#### **CGRP<sup>+</sup>SP<sup>-</sup> neurons were prominent at all spinal levels and just as prominent as CGRP<sup>+</sup>SP<sup>+</sup> neurons**

CGRP-IR neuronal somata were frequently detected in DRG, as were CGRP-IR terminals in the dorsal horn of the spinal cord, and CGRP-IR fibres in both glabrous and hairy forepaw and hindpaw skin. These CGRP-IR neurons could be subdivided based on their expression of SP-IR.

It is important to note, that the lack of SP-IR detected in this study was not due to technical issues regarding the antibodies. CGRP-IR and SP-IR were detected using well-characterised antibodies (Morris *et al.*, 2005). The CGRP-IR and SP-IR expression patterns in DRG (McCarthy & Lawson, 1989; 1990; Morris *et al.*, 2005), spinal cord (Gibson, Polak, Bloom, *et al.*, 1984; Wiesenfeld-Hallin *et al.*, 1984; Morris *et al.*, 2005) and skin (Gibbins *et al.*, 1985; Gibbins, Wattchow, *et al.*, 1987) match previous descriptions in the literature. Specific and consistent features of SP-IR were used throughout this study to ensure correct antibody function. In DRG, SP-IR was easily detectable in small to medium sized neuronal somata, but not detectable in larger somata. In dorsal horn, SP-IR was easily detectable in terminals of lamina I/II and in the lateral spinal nucleus, but not in terminals of lamina IV/V. In skin, SP-IR was easily detectable in numerous cutaneous fibres but not detectable in all. Together, this suggests that the lack of detectable SP-IR in this study is true and not an antibody artefact.

CGRP<sup>+</sup>SP<sup>-</sup> neurons were equally as prominent as CGRP<sup>+</sup>SP<sup>+</sup> neurons in DRG at all spinal levels, and in T5 DRG CGRP<sup>+</sup>SP<sup>-</sup> neurons were more numerous than CGRP<sup>+</sup>SP<sup>+</sup> neurons. The size of CGRP<sup>+</sup>SP<sup>-</sup> cells in C7 and L4 were considerably larger than T5 and S3 DRG. The soma size of a neuron is related to its volume and the volume of the neuron is dependent on its axonal length, diameter and the degree of axonal branching (Pannese, 1994). Hence, the larger size of CGRP<sup>+</sup>SP<sup>-</sup> cells in C7

and L4 may be because DRG neurons of C7 and L4 innervate the limbs and hence, their axons were longer. However, S3 neurons also have relatively long axons and hence this may be because C7 and L4 DRG just has a higher proportion of larger neurons or a higher proportion of myelinated neurons (which will be discussed in the next section).

At all levels, the central and peripheral endings of CGRP<sup>+</sup>SP<sup>-</sup> neurons were consistent with observations from the DRG. The prominence of CGRP<sup>+</sup>SP<sup>-</sup> neurons in C7 DRG was consistent with the high prominence of CGRP<sup>+</sup>SP<sup>-</sup> fibres in the C7 dorsal horns and fibres in the forepaw that matched our previous descriptions (Kestell, 2009). The CGRP<sup>+</sup>SP<sup>-</sup> neurons of the L4 DRG was consistent with CGRP<sup>+</sup>SP<sup>-</sup> fibres in the L4 dorsal horns and fibres in the hindpaw skin, as well as previous observation of these fibres in gastrocnemius muscle (Gillan, 2012). The same can be said for the CGRP<sup>+</sup>SP<sup>-</sup> neurons in the T5 and S3 DRG that were consistent with fibres in the T5 and S3 dorsal horn, respectively, as well as fibres previously observed in erector spinae muscle (Gillan, 2012), and the female genital tract (Vilimas *et al.*, 2011), respectively.

While there are long-standing reports of sensory neurons that contain CGRP but not SP (Gibbins, Wattchow, *et al.*, 1987; Tamatani *et al.*, 1989; McCarthy & Lawson, 1990; Morris *et al.*, 2005), no attempts have been made to characterise their distribution or demonstrate their prominence. Here we have demonstrated the CGRP<sup>+</sup>SP<sup>-</sup> neurons were just as prominent (if not more prominent) as the well-characterised CGRP<sup>+</sup>SP<sup>+</sup> in DRG and dorsal horn of all spinal levels, and in the forepaw skin.

### **CGRP<sup>+</sup>SP<sup>-</sup> neurons were most likely myelinated**

The cross sectional area of CGRP<sup>+</sup>SP<sup>-</sup> neuronal soma were more than twice the cross sectional area of CGRP<sup>+</sup>SP<sup>+</sup> neuronal soma in the DRG at all spinal levels. Their central fibres were present in lamina IV/V of the dorsal horn of the spinal cord, and peripheral fibres were found closely associated with Meissner's corpuscles and encircled hair follicles in the skin. Taken together, these results are highly suggestive of CGRP<sup>+</sup>SP<sup>-</sup> neurons belonging to a myelinated fibre class.

McCarthy and Lawson (1990) demonstrated CGRP-IR in both small and large somata of the DRG and established that the smaller somata had C-fibre conduction

velocities whereas, the larger somata had A-fibre conduction velocities. McCarthy and Lawson (1989) also demonstrated that SP-IR was only present in small somata of the DRG with C-fibre conduction velocities. These larger CGRP-IR neurons demonstrated by McCarthy and Lawson (1990) were comparable in size to the CGRP<sup>+</sup>SP<sup>-</sup> neurons demonstrated in this current study, suggesting they may be the same population of neurons. Hence, CGRP<sup>+</sup>SP<sup>-</sup> neurons are most likely A-fibre neurons.

The notion of CGRP<sup>+</sup>SP<sup>-</sup> neurons being myelinated is further supported by their central terminations. In the dorsal horn, CGRP<sup>+</sup>SP<sup>-</sup> terminals were prominent in lamina I and lamina IV/V. Lamina IV/V neurons receive inputs from A $\beta$ - and A $\delta$ -fibres (Willis & Coggeshall, 1991). Taken together, these results are highly suggestive of CGRP<sup>+</sup>SP<sup>-</sup> neurons belonging to a myelinated fibre class.

The existence of large CGRP<sup>+</sup>SP<sup>-</sup> neurons could be interpreted in two ways: either CGRP expression is not limited to nociceptive neurons; or nociceptive neurons are not limited to A  $\delta$  and C-fibre classes. Although often overlooked, some of the earliest descriptions of nociceptors included A $\alpha$ /  $\beta$  fibre classes which almost certainly originate from large diameter DRG neurons (Burgess & Perl, 1967; Ritter & Mendell, 1992; Djouhri *et al.*, 1998; Djouhri & Lawson, 2001). Indeed, a more recent study has shown that some DRG neurons with myelinated fibres in the A $\alpha$ /  $\beta$  range both contain CGRP and possess nociceptive properties (Lawson *et al.*, 2002).

## **CGRP<sup>+</sup>SP<sup>-</sup> neurons most likely convey different sensory modalities**

CGRP<sup>+</sup>SP<sup>-</sup> fibres were observed encircling hair follicles, as intraepithelial nerve fibres and closely associated with Meissner's corpuscles. Previously, we have observed similar fibres closely associated with large, presumably mechanosensitive endings, in genital skin (Vilimas *et al.*, 2011) and as free nerve endings in erector spinae and gastrocnemius muscle (Gillan, 2012). These observations imply that CGRP<sup>+</sup>SP<sup>-</sup> afferents transduce information at different peripheral sites. Their dual projections to superficial and deeper laminae of the dorsal horn further implies they may well convey different sensory modalities and contribute to different perceptions of pain from the skin.

CGRP-IR fibres were observed penetrating the epidermis with no specialised endings in a manner that has been previously described (Gibbins *et al.*, 1985; Kruger *et al.*, 1989). Both CGRP<sup>+</sup>SP<sup>-</sup> and CGRP<sup>+</sup>SP<sup>+</sup> fibres were seen penetrating the epidermis. Given the position in the epidermis it is likely that both CGRP-IR neurons are thermally or mechanically activated nociceptive afferents (Lawson *et al.*, 2002).

CGRP-IR fibres encircled hair follicles in a distinct pattern, corresponding to previous descriptions of fine hair follicle afferents (e.g. Kruger *et al.*, 1981; Munger, 1982; Millard & Woolf, 1988). Hair follicle afferents form a pilo-neural complex: a combination of sensory endings that form an ensemble around hair follicles at the mid-level of the hair shaft, which consists of a palisade of blade-like lanceolate endings of A $\beta$ -fibre neurons, and circumferentially oriented endings supplied by C-fibres (Rice & Albrecht, 2007). While it has been previously documented that both CGRP and SP fibres encircle hair follicles (Kruger *et al.*, 1989; Fundin *et al.*, 1997; Rice *et al.*, 1997), we have demonstrated here that both CGRP<sup>+</sup>SP<sup>+</sup> and CGRP<sup>+</sup>SP<sup>-</sup> fibres encircled hair follicles. CGRP<sup>+</sup>SP<sup>-</sup> fibres encircled the hair follicle at the level of the palisade nerve endings and a single CGRP<sup>+</sup>SP<sup>+</sup> fibre encircled the hair follicle inferior to CGRP<sup>+</sup>SP<sup>-</sup> fibres. While they did not explicitly characterise their endings, Lawson and colleagues (2002) have also demonstrated CGRP<sup>+</sup>SP<sup>-</sup> fibres associated with hair follicles and determined that these fibres were non-nociceptive moderately rapidly adapting mechanoreceptors that responded to hair movement. As all SP containing primary afferent fibres are presumed nociceptive (Lawson *et al.*, 1997), it is likely that the single CGRP<sup>+</sup>SP<sup>+</sup> fibre is associated with noxious distortion of the hair follicle..

CGRP<sup>+</sup>SP<sup>-</sup> and CGRP<sup>+</sup>SP<sup>+</sup> fibres were also closely associated with Meissner's corpuscles. Like the piloneural complexes, Meissner's corpuscles are supplied by both A  $\beta$  -fibre and C-fibre neurons (Rice & Albrecht, 2007). Meissner's corpuscles contain a coiled arrangement of endings from at least three types of separate fibres: A $\alpha$ / $\beta$  fibres and peptidergic and non-peptidergic C-fibres (Paré *et al.*, 2001). CGRP and SP are associated with some Meissner's corpuscles (Ishida-Yamamoto *et al.*, 1988; Kruger *et al.*, 1989; Paré *et al.*, 2001), however we have demonstrated here that both CGRP<sup>+</sup>SP<sup>+</sup> and CGRP<sup>+</sup>SP<sup>-</sup> fibres are associated with the Meissner's corpuscles. The A $\alpha$ / $\beta$  fibres of the Meissner's corpuscle described by Paré and colleagues (2001) expressed CGRP, and are hence likely the CGRP<sup>+</sup>SP<sup>-</sup> fibres we

have demonstrated. These A $\alpha$ / $\beta$  fibres are believed to be the low-threshold mechanoreceptive endings of the Meissner's corpuscle. These A $\alpha$ / $\beta$  fibres are closely intertwined with endings from peptidergic C-fibers, which expressed both CGRP and SP (Paré *et al.*, 2001), and are hence likely the CGRP<sup>+</sup>SP<sup>+</sup> fibres we have demonstrated. While Meissner's corpuscles are activated by innocuous light touch, it is now believed that they can also be nociceptive (Paré *et al.*, 2001). Again, as all SP containing primary afferent fibres are presumed nociceptive (Lawson *et al.*, 1997), it is likely that the CGRP<sup>+</sup>SP<sup>+</sup> fibres are nociceptive.

It is not yet clear whether CGRP<sup>+</sup>SP<sup>-</sup> neurons have a role in nociception. The existence of large CGRP<sup>+</sup>SP<sup>-</sup> neurons could suggest that CGRP expression is not limited to nociceptive neurons. Yet it could also suggest that nociceptive neurons are not limited to A $\delta$  and C-fibre classes. Based on the peripheral targets of CGRP<sup>+</sup>SP<sup>-</sup> neurons and their projections to the spinal cord they may have a polymodal mechanoreceptor function.



## **3.5 Figures**

---

**Figure 3.1: CGRP-IR and SP-IR in neuronal somata of the C7 DRG**

Widefield fluorescence microscopy of mouse C7 dorsal root ganglia (DRG) double labelled for calcitonin gene-related peptide (CGRP; A), substance P (SP; B). The overlay of A and B (C), and the thresholded image (D) shows two subpopulations of neurons positive for CGRP-immunoreactivity (IR): neurons containing CGRP-IR with SP-IR (CGRP<sup>+</sup>SP<sup>+</sup>; white arrows; yellow in C and D), neurons containing CGRP-IR with no detectable SP-IR (CGRP<sup>+</sup>SP<sup>-</sup>; black arrows; red in C and D). Scale bar = 60  $\mu$ m in D (applies to A-D).

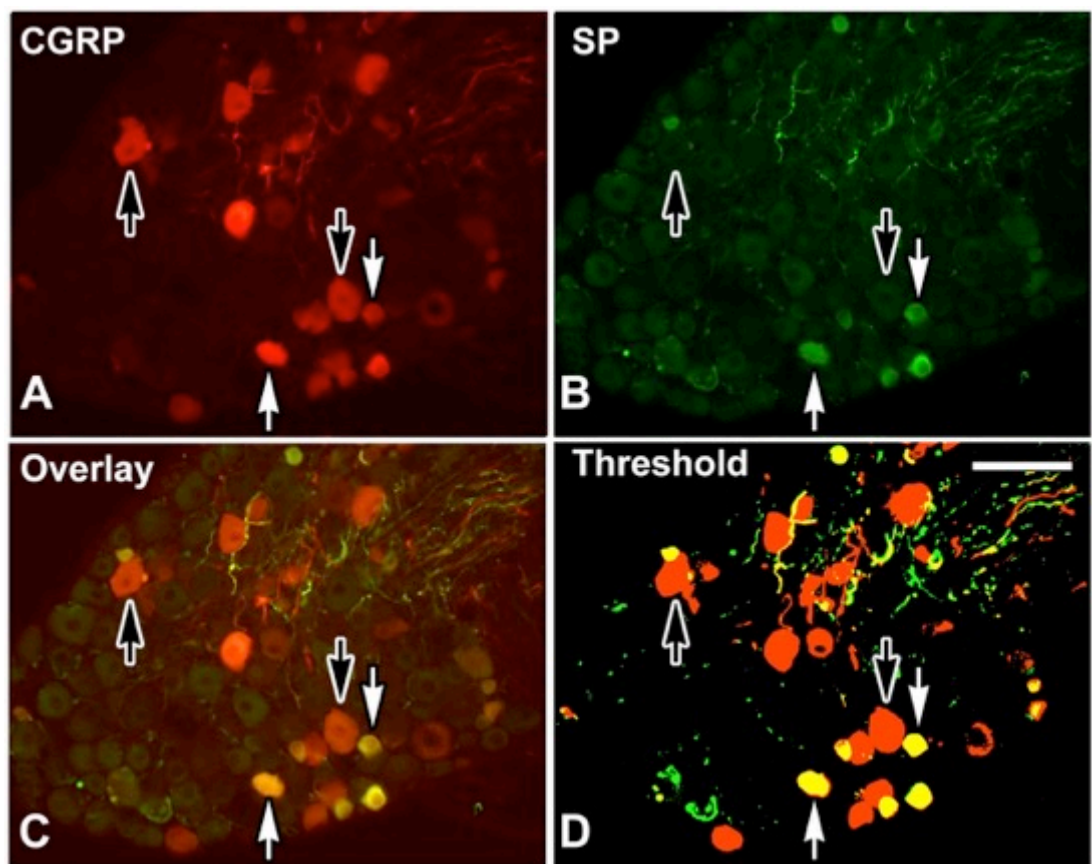


**Figure 3.2: Intensity of CGRP-IR and soma size in DRG neurons**

Scatter dot plot (dots = cells; line = linear regression with 95% confidence limits) depicting the size of neuronal somata and their intensity of calcitonin gene-related peptide-immunoreactivity (CGRP-IR) more than 2 standard deviations above background fluorescence in dorsal root ganglia (DRG) of all spinal levels. There was no correlation between the intensity of CGRP-IR and the soma size of the neurons (linear correlation:  $r < 0.01$ ,  $p = 0.08$ ;  $N = 4$  animals,  $n = 1720$  neurons).

**Figure 3.3: Intensity of SP-IR and soma size in DRG neurons**

Scatter dot plot (dots = cells; line = linear regression with 95% confidence limits) depicting the size of neuronal somata and their intensity of substance P-immunoreactivity (SP-IR) more than 2 standard deviations above background fluorescence in dorsal root ganglia (DRG) of all spinal levels. There was no correlation between the intensity of SP-IR and the soma size of the neuron (linear correlation:  $r < 0.01$ ,  $p = 0.3$   $N = 4$  animals,  $n = 873$  neurons).

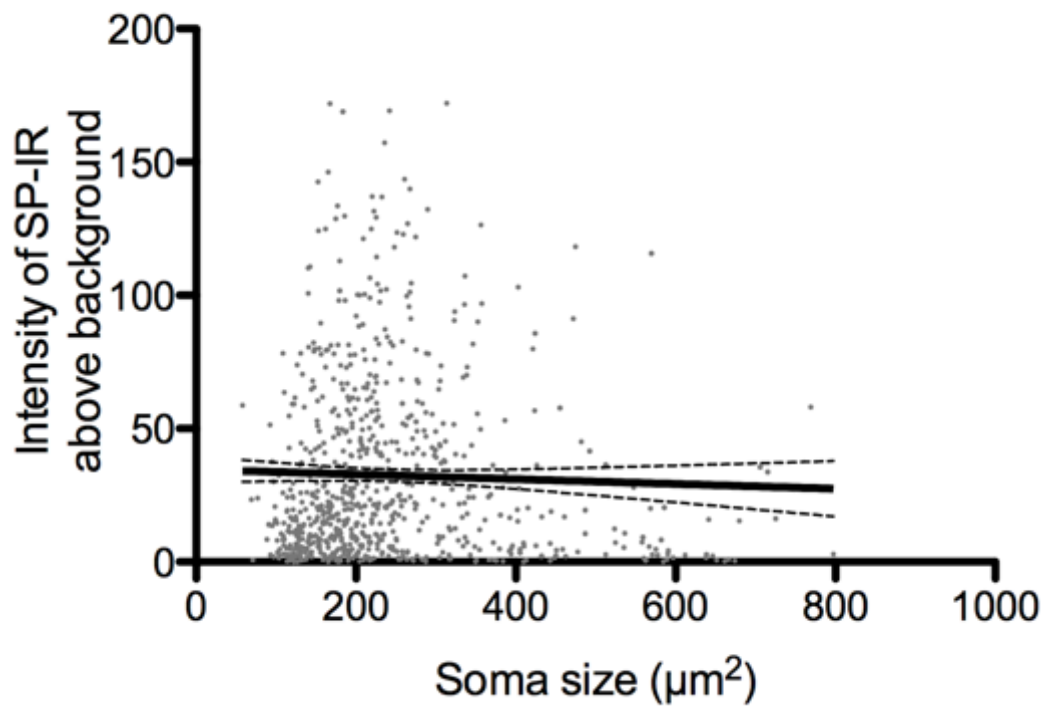
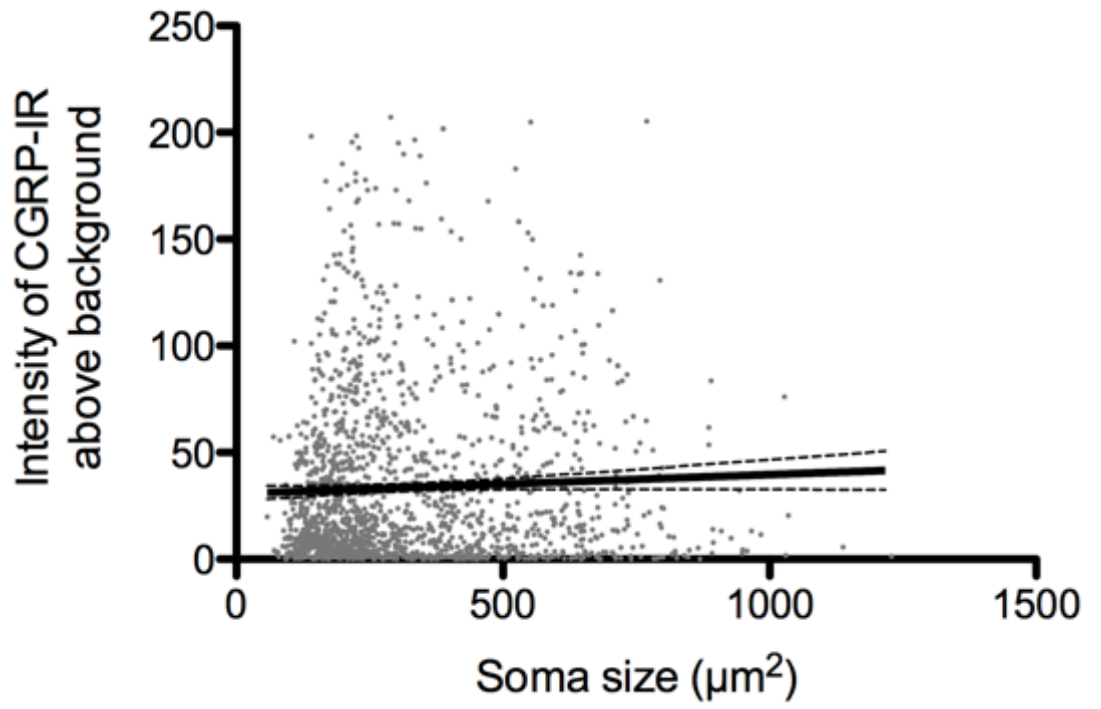


**Figure 3.4: Proportion of neuronal somata expressing CGRP-IR in DRG of all spinal levels**

Histogram depicting the proportion of neuronal somata that either expressed calcitonin gene-related peptide-immunoreactivity (CGRP-IR; CGRP<sup>+</sup>; red bars) or lacked CGRP-IR (CGRP<sup>-</sup>; black bars) in cervical (C7), thoracic (T5), lumbar (L5), and sacral (S3) dorsal root ganglia (DRG). At all spinal levels, there were equal proportions of neurons that either expressed or lacked CGRP-IR (Chi-Square:  $\chi^2_3 = 6$ ,  $p = 0.1$ ; N = 4 animals, n = 1720 neurons)

**Figure 3.5: Proportion of CGRP-IR expressing neuronal somata that lacked SP-IR in DRG of all spinal levels**

Histogram depicting the proportion of neuronal somata that expressed calcitonin gene-related peptide-immunoreactivity (CGRP-IR) with substance P-IR (SP-IR; CGRP<sup>+</sup>SP<sup>+</sup>; yellow bars) or without SP-IR (CGRP<sup>+</sup>SP<sup>-</sup>; red bars) in cervical (C7), thoracic (T5), lumbar (L5), and sacral (S3) dorsal root ganglia (DRG). At all spinal levels, there were equal proportions of CGRP<sup>+</sup>SP<sup>-</sup> and CGRP<sup>+</sup>SP<sup>+</sup> neurons (Chi-Square:  $\chi^2_3 = 5$ ,  $p = 0.2$ ; N = 4 animals, n = 1720 neurons).

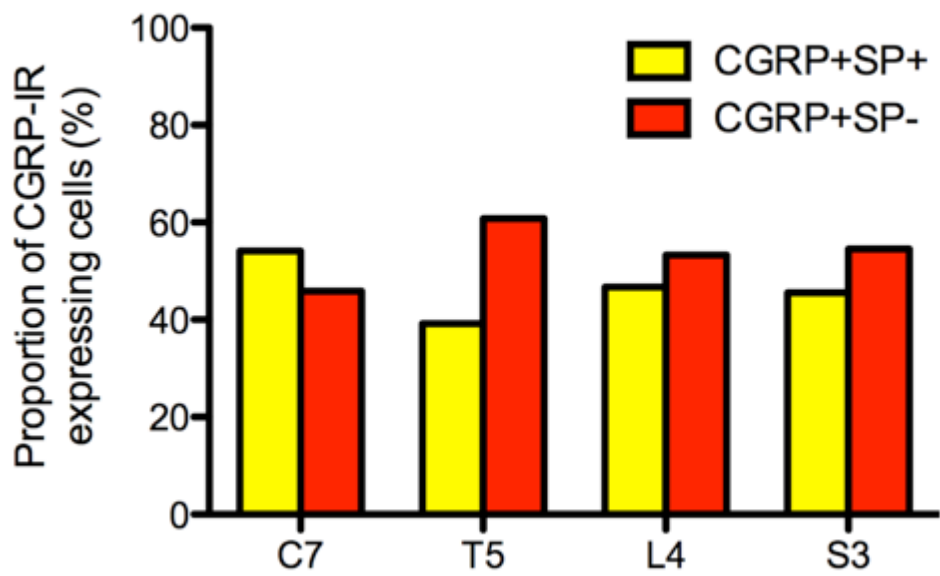
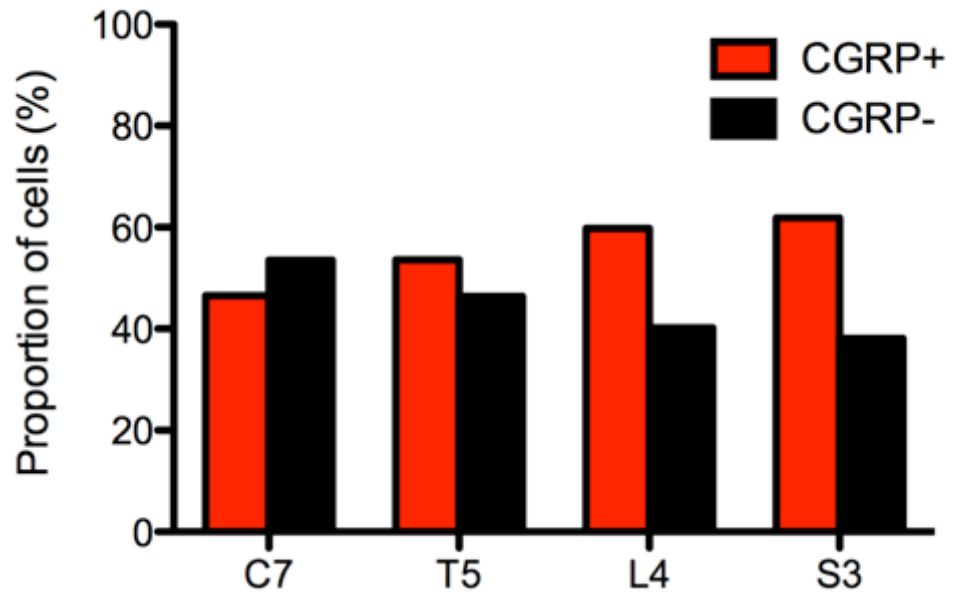


**Figure 3.6: Soma size of neurons in DRG of all spinal levels**

Histogram displayed as depicting the soma size (mean  $\pm$  SEM cross sectional area;  $\mu\text{m}^2$ ) of all neuronal somata in cervical (C7), thoracic (T5), lumbar (L5), and sacral (S3) dorsal root ganglia (DRG). The soma size of neurons were largest in C7 DRG, and L4 DRG neurons were larger than the T5 DRG and S3 DRG neurons (ANOVA:  $F_{(3,3226)} = 38$ ,  $p < 0.001$ ;  $N = 4$  animals;  $n = 3230$  neurons;)

**Figure 3.7: Soma size of neurons expressing CGRP-IR without SP-IR in DRG of all spinal levels**

Histogram (data displayed as mean  $\pm$  SEM) depicting the soma size (cross sectional area;  $\mu\text{m}^2$ ) of neuronal somata that expressed calcitonin gene-related peptide-immunoreactivity (CGRP-IR) with substance P-IR (SP-IR; CGRP<sup>+</sup>SP<sup>+</sup>; yellow bars) or without SP-IR (CGRP<sup>+</sup>SP<sup>-</sup>; red bars) in cervical (C7), thoracic (T5), lumbar (L5), and sacral (S3) dorsal root ganglia (DRG). At all spinal levels CGRP<sup>+</sup>SP<sup>-</sup> neurons were larger than CGRP<sup>+</sup>SP<sup>+</sup> neurons (ANOVA:  $F_{(1,1764)} = 315$ ,  $p < 0.001$ ;  $N = 4$  animals;  $n = 1720$  neurons). CGRP<sup>+</sup>SP<sup>-</sup> neurons were largest at C7, and L4 CGRP<sup>+</sup>SP<sup>-</sup> neurons were larger than S3 CGRP<sup>+</sup>SP<sup>-</sup> neurons (ANOVA:  $F_{(3,1764)} = 33$ ,  $p < 0.001$ ;  $N = 4$  animals;  $n = 1720$  neurons).

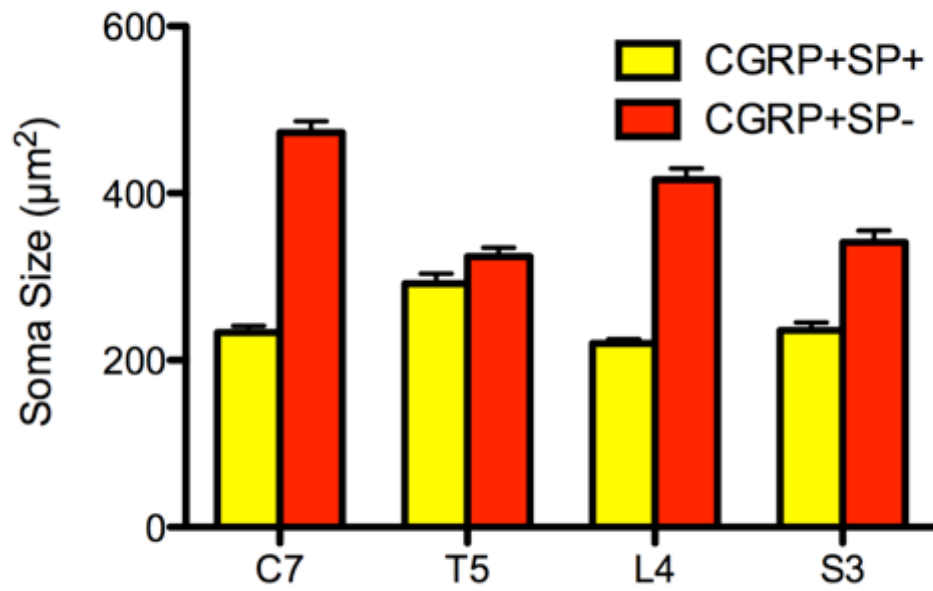
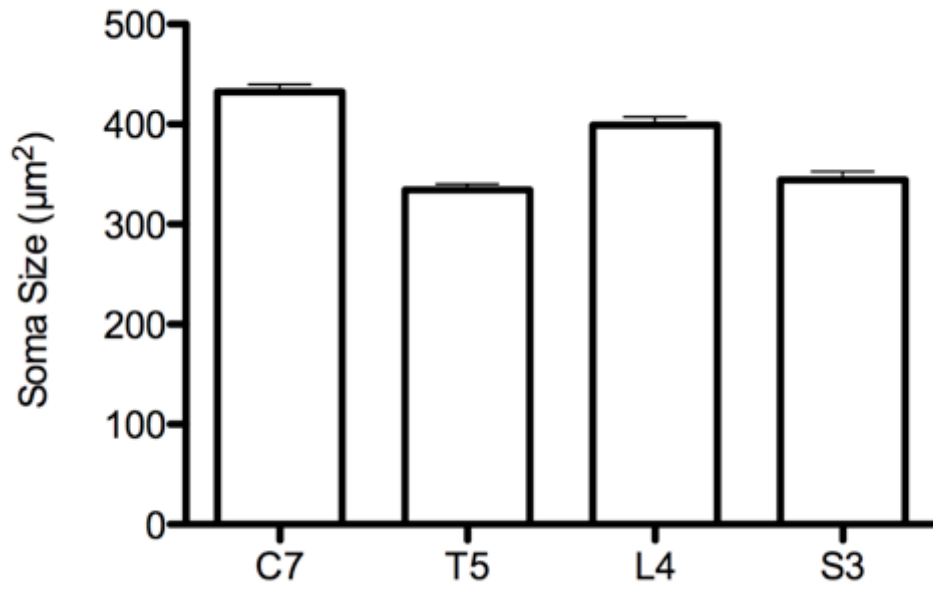


**Figure 3.8: Intensity of CGRP-IR in DRG of all spinal levels**

Histogram (data displayed as mean  $\pm$  SEM) depicting the intensity of calcitonin gene-related peptide-immunoreactivity (CGRP-IR) above the normal background fluorescence of non-immunoreactive neuronal somata in cervical (C7), thoracic (T5), lumbar (L5), and sacral (S3) dorsal root ganglia (DRG). Somata expressing CGRP with substance P (SP; CGRP<sup>+</sup>SP<sup>+</sup>) had higher intensity of CGRP-IR than somata expressing CGRP but not SP (CGRP<sup>+</sup>SP<sup>-</sup>; RM-ANOVA:  $F_{(1,1764)} = 359$ ,  $p < 0.001$ ; N = 4 animals; n = 1720 neurons;)

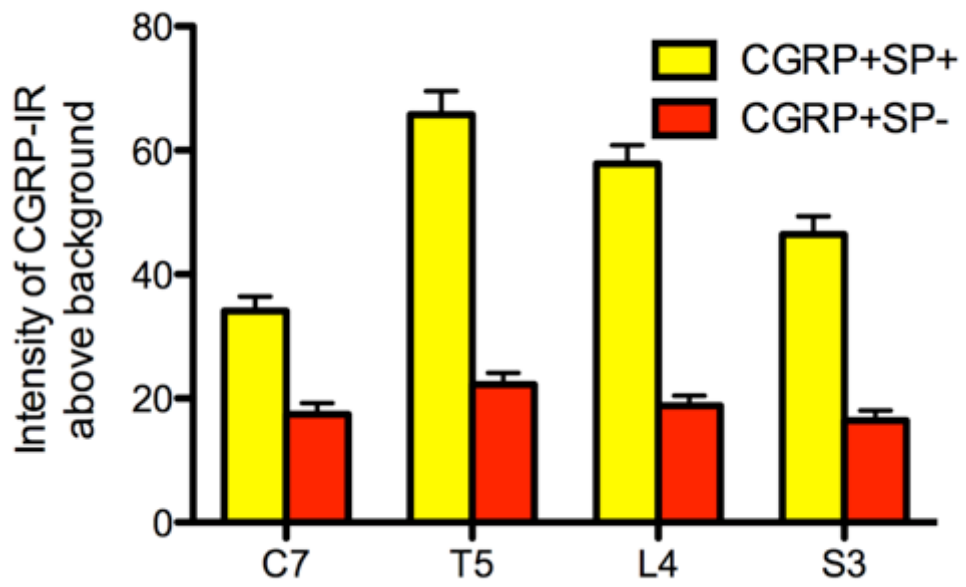


**Figure 3.9: Proportion and size of neuronal somata expressing CGRP-IR in C7 DRG**

**A:** Pie chart depicting the proportion of neuronal somata that expressed calcitonin gene-related peptide-immunoreactivity (CGRP-IR) with substance P-IR (SP-IR; CGRP<sup>+</sup>SP<sup>+</sup>; yellow), expressed CGRP-IR without SP-IR (CGRP<sup>+</sup>SP<sup>-</sup>; red), expressed SP-IR without CGRP-IR (CGRP<sup>-</sup>SP<sup>+</sup>; green) or expressed neither CGRP-IR nor SP-IR (CGRP<sup>-</sup>SP<sup>-</sup>; black) in cervical (C7) dorsal root ganglia (DRG). An equal proportion of CGRP-IR neurons contained (CGRP<sup>+</sup>SP<sup>+</sup>) or lacked (CGRP<sup>+</sup>SP<sup>-</sup>) SP (Chi-Square:  $\chi_1^2 = 3$ ,  $p = 0.1$ ;  $N = 4$  animals,  $n = 418$  neurons).

**B:** Histogram depicting the somata size (mean  $\pm$  SEM of cross sectional area;  $\mu\text{m}^2$ ) of neuronal somata that expressed calcitonin gene-related peptide-immunoreactivity (CGRP-IR) with substance P-IR (SP-IR; CGRP<sup>+</sup>SP<sup>+</sup>; yellow), expressed CGRP-IR without SP-IR (CGRP<sup>+</sup>SP<sup>-</sup>; red) in cervical (C7) dorsal root ganglia (DRG). The soma size of CGRP+SP- neurons were larger than the CGRP+SP+ (ANOVA:  $F_{(1,416)} = 244$ ,  $p < 0.0001$ ;  $N = 4$  animals,  $n = 418$  neurons).

**Figure 3.10: Proportion and size of neuronal somata expressing CGRP-IR in T5 DRG**

**A:** Pie chart depicting the proportion of neuronal somata that expressed calcitonin gene-related peptide-immunoreactivity (CGRP-IR) with substance P-IR (SP-IR; CGRP+SP+; yellow), expressed CGRP-IR without SP-IR (CGRP+SP-; red), expressed SP-IR without CGRP-IR (CGRP-SP+; green) or expressed neither CGRP-IR nor SP-IR (CGRP-SP-; black) in thoracic (T5) dorsal root ganglia (DRG). A higher proportion of CGRP-IR neurons contained (CGRP<sup>+</sup>SP<sup>+</sup>) or lacked (CGRP<sup>+</sup>SP<sup>-</sup>) SP (Chi-Square:  $\chi_1^2 = 22$ ,  $p < 0.001$ ;  $N = 4$  animals,  $n = 464$  neurons).

**B:** Histogram (data displayed as mean  $\pm$  SEM) depicting the somata size (cross sectional area;  $\mu\text{m}^2$ ) of neuronal somata that expressed calcitonin gene-related peptide-immunoreactivity (CGRP-IR) with substance P-IR (SP-IR; CGRP+SP+; yellow bars) or without SP-IR (CGRP+SP-; red bars) in thoracic (T5) dorsal root ganglia (DRG). The soma size of CGRP+SP- neurons were larger than the CGRP+SP+ (ANOVA:  $F_{(1,462)} = 4$ ,  $p < 0.05$ ;  $N = 4$  animals,  $n = 464$  neurons).

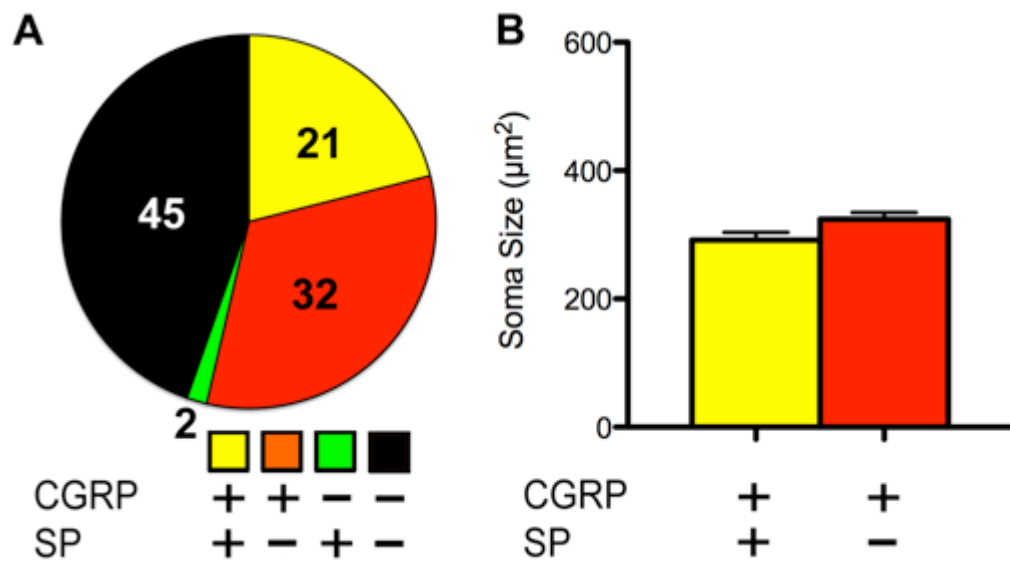
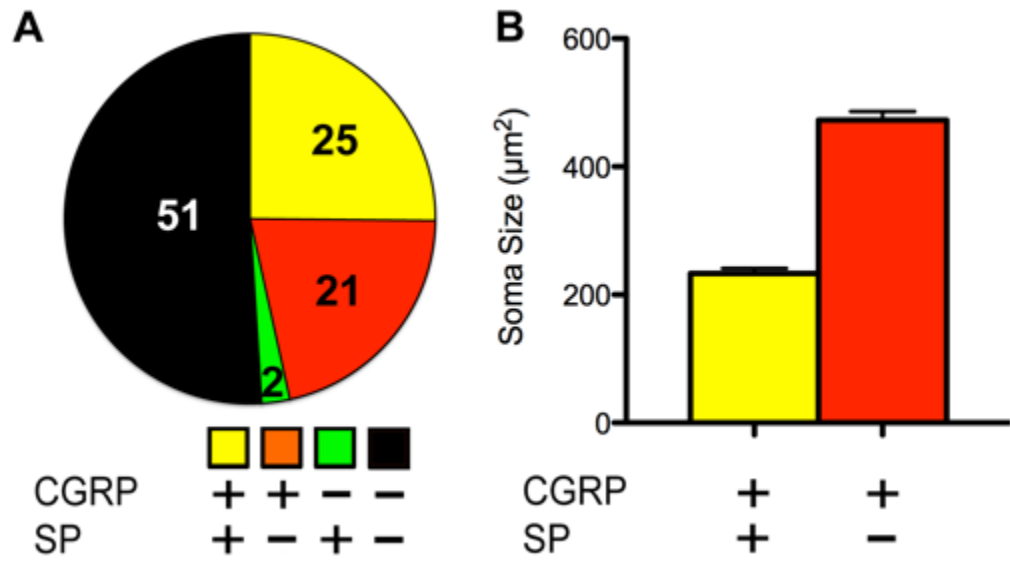


**Figure 3.11: Proportion and size of neuronal somata expressing CGRP-IR in L4 DRG**

**A:** Pie chart depicting the proportion of neuronal somata that expressed calcitonin gene-related peptide-immunoreactivity (CGRP-IR) with substance P-IR (SP-IR; CGRP+SP+; yellow), expressed CGRP-IR without SP-IR (CGRP+SP-; red), expressed SP-IR without CGRP-IR (CGRP-SP+; green) or expressed neither CGRP-IR nor SP-IR (CGRP-SP-; black) in lumbar (L4) dorsal root ganglia (DRG). An equal proportion of CGRP-IR neurons contained (CGRP<sup>+</sup>SP<sup>+</sup>) or lacked (CGRP<sup>+</sup>SP<sup>-</sup>) SP (Chi-Square:  $\chi_1^2 = 2$ ,  $p = 0.1$ ;  $N = 4$  animals,  $n = 508$  neurons).

**B:** Histogram (data displayed as mean  $\pm$  SEM) depicting the somata size (cross sectional area;  $\mu\text{m}^2$ ) of neuronal somata that expressed calcitonin gene-related peptide-immunoreactivity (CGRP-IR) with substance P-IR (SP-IR; CGRP<sup>+</sup>SP<sup>+</sup>; yellow bars) or without SP-IR (CGRP<sup>+</sup>SP<sup>-</sup>; red bars) in lumbar (L4) dorsal root ganglia (DRG). The soma size of CGRP+SP- neurons were larger than the CGRP+SP+ (ANOVA:  $F_{(1,506)} = 166$ ,  $p < 0.0001$ ;  $N = 4$  animals,  $n = 508$  neurons).

**Figure 3.12: Proportion and size of neuronal somata expressing CGRP-IR in S3 DRG**

**A:** Pie chart depicting the proportion of neuronal somata that expressed calcitonin gene-related peptide-immunoreactivity (CGRP-IR) with substance P-IR (SP-IR; CGRP+SP+; yellow), expressed CGRP-IR without SP-IR (CGRP+SP-; red), expressed SP-IR without CGRP-IR (CGRP-SP+; green) or expressed neither CGRP-IR nor SP-IR (CGRP-SP-; black) in sacral (S3) dorsal root ganglia (DRG). An equal proportion of CGRP-IR neurons contained (CGRP<sup>+</sup>SP<sup>+</sup>) or lacked (CGRP<sup>+</sup>SP<sup>-</sup>) SP (Chi-Square:  $\chi_1^2 = 3$ ,  $p = 0.08$ ;  $N = 4$  animals,  $n = 382$  neurons).

**B:** Histogram (data displayed as mean  $\pm$  SEM) depicting the somata size (cross sectional area;  $\mu\text{m}^2$ ) of neuronal somata that expressed calcitonin gene-related peptide-immunoreactivity (CGRP-IR) with substance P-IR (SP-IR; CGRP<sup>+</sup>SP<sup>+</sup>; yellow bars) or without SP-IR (CGRP<sup>+</sup>SP<sup>-</sup>; red bars) in sacral (S3) dorsal root ganglia (DRG). The soma size of CGRP+SP- neurons were larger than the CGRP+SP+ (ANOVA:  $F_{(1,381)} = 36$ ,  $p < 0.0001$ ;  $N = 4$  animals,  $n = 382$  neurons).

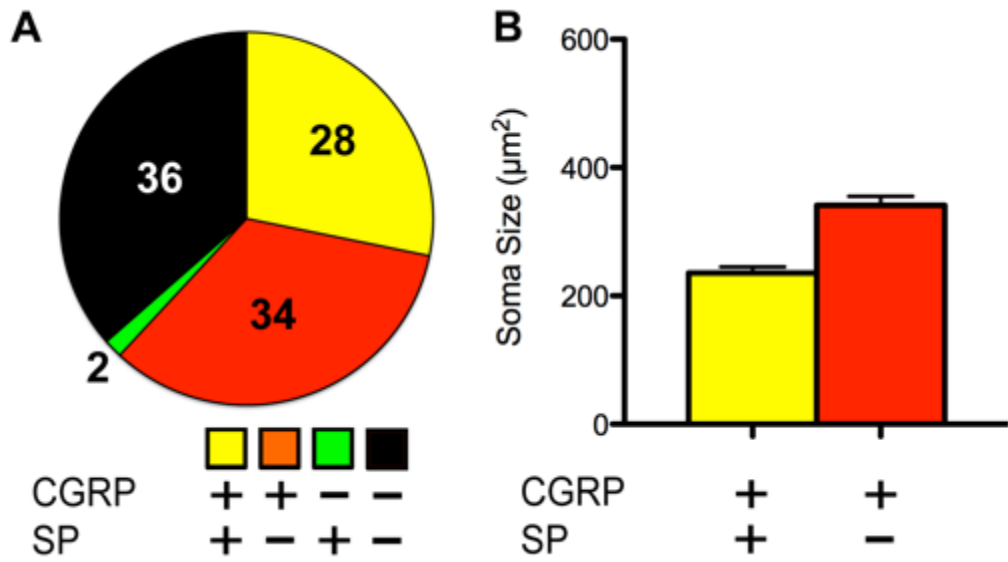
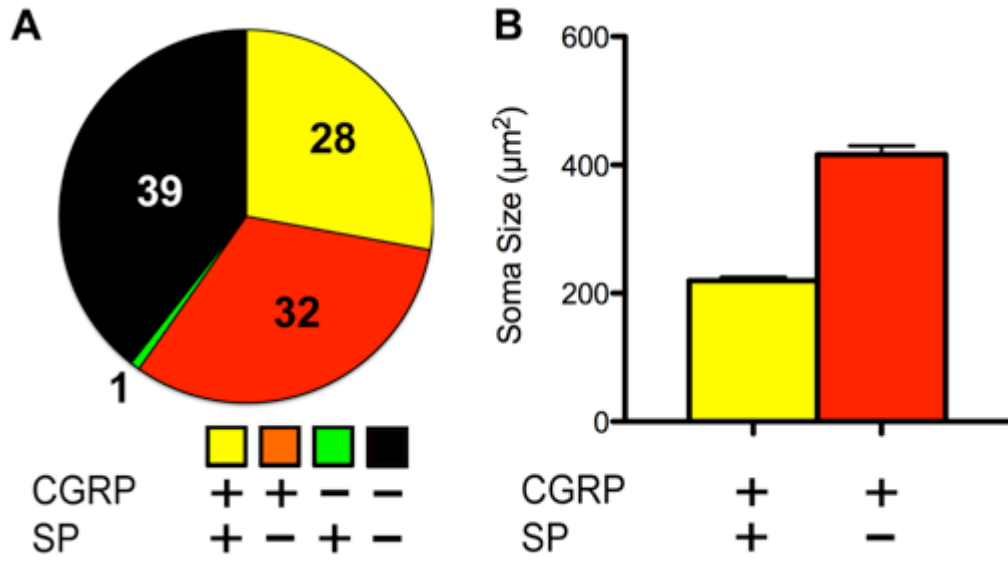


**Figure 3.13: CGRP-IR and SP-IR in the C7, T5, L4 and S3 dorsal horn**

Widefield fluorescence microscopy of mouse cervical (C7; A), thoracic (T5; B), lumbar (L4; C) and sacral (S3; D) dorsal horn double labelled for calcitonin gene-related peptide (CGRP; red) and substance P (SP; green) showing a clear overlap of CGRP-immunoreactivity (IR) and SP-IR (CGRP<sup>+</sup>SP<sup>+</sup>; yellow) in the superficial laminae and some CGRP-IR lacking of SP-IR (CGRP<sup>+</sup>SP<sup>-</sup>; red) in the deeper laminae. Scale bar = 100  $\mu$ m in A (applies to B-D).

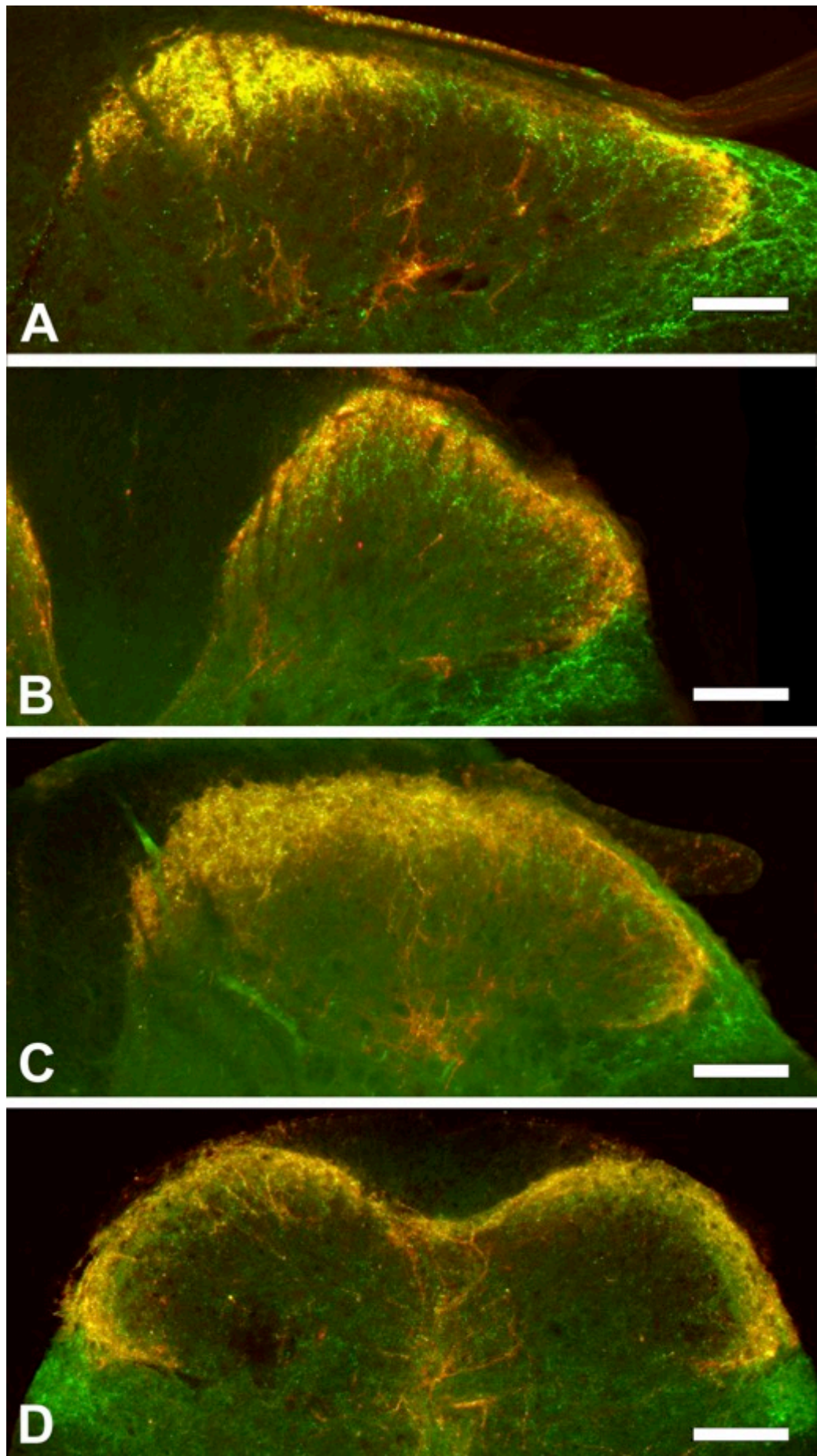


**Figure 3.14: Volume of CGRP-IR boutons in the dorsal horn of all spinal levels**

Histogram (data displayed as mean±SEM) depicting the volume of calcitonin gene-related peptide-immunoreactive (CGRP-IR) voxels in medial and lateral lamina I, and lamina IV/V of cervical (C7; black), thoracic (T5; dark grey), lumbar (L4; light grey) and sacral (S3; white) dorsal horn. There was no difference in the volume of CGRP-IR voxels in medial lamina I, lateral lamina I, or lamina IV/V between the different spinal levels (RM-ANOVA:  $F_{(1,4)} = 0.4$ ,  $p = 0.6$ ;  $n = 5$  animals,  $F_{(1,3)} = 0.02$ ,  $p = 0.9$ ;  $n = 5$  animals and RM-ANOVA:  $F_{(1,4)} = 5$ ,  $p = 0.1$ ;  $n = 5$  animals, respectively). There was no CGRP-IR in lamina IV/V of S3.

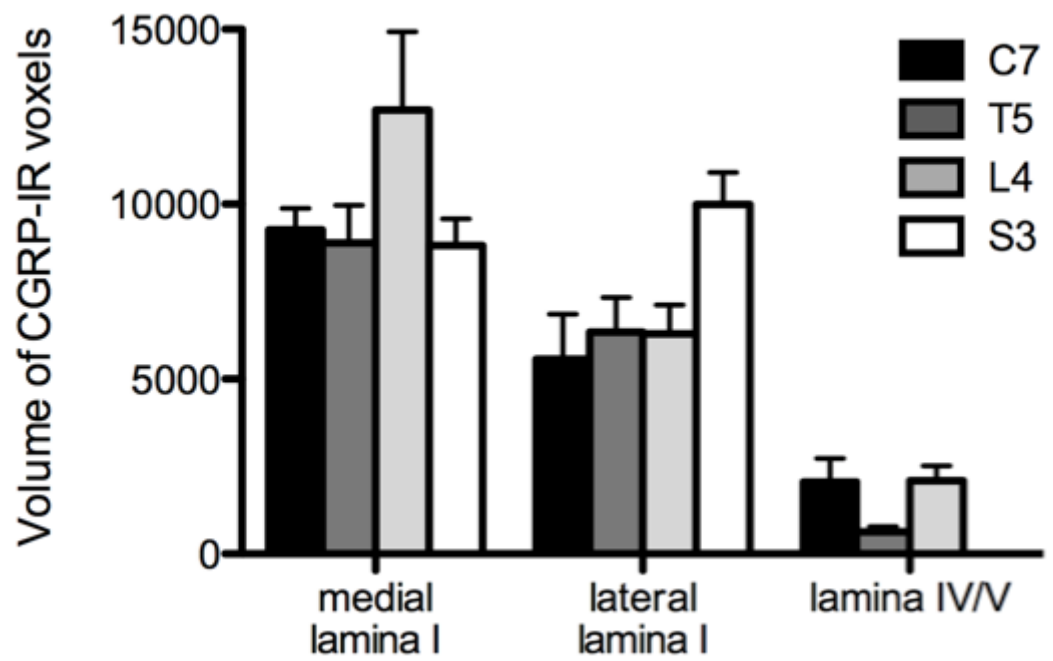


**Figure 3.15: Proportion of CGRP-IR boutons lacking SP-IR in the dorsal horn of all spinal levels**

Histogram (data displayed as mean±SEM) depicting the proportion of calcitonin gene-related peptide-immunoreactive (CGRP-IR) voxels that lacked SP-IR (CGRP<sup>+</sup>SP<sup>-</sup>) in medial and lateral lamina I, and lamina IV/V of cervical (C7; black), thoracic (T5; dark grey), lumbar (L4; light grey) and sacral (S3; white) dorsal horn. There was no difference in the proportion of CGRP-IR voxels that were either CGRP<sup>+</sup>SP<sup>-</sup> terminals in medial lamina I or lamina IV/V (RM-ANOVA:  $F_{(1,4)} = 2$ ,  $p = 0.3$ ;  $n = 5$  animals) between the different levels of the spinal cord. In lateral lamina I there was a higher proportion of CGRP<sup>+</sup>SP<sup>-</sup> terminals in C7 compared to L4 and S3 (RM-ANOVA:  $F_{(1,4)} = 20$ ,  $p = 0.01$ ;  $n = 5$  animals).

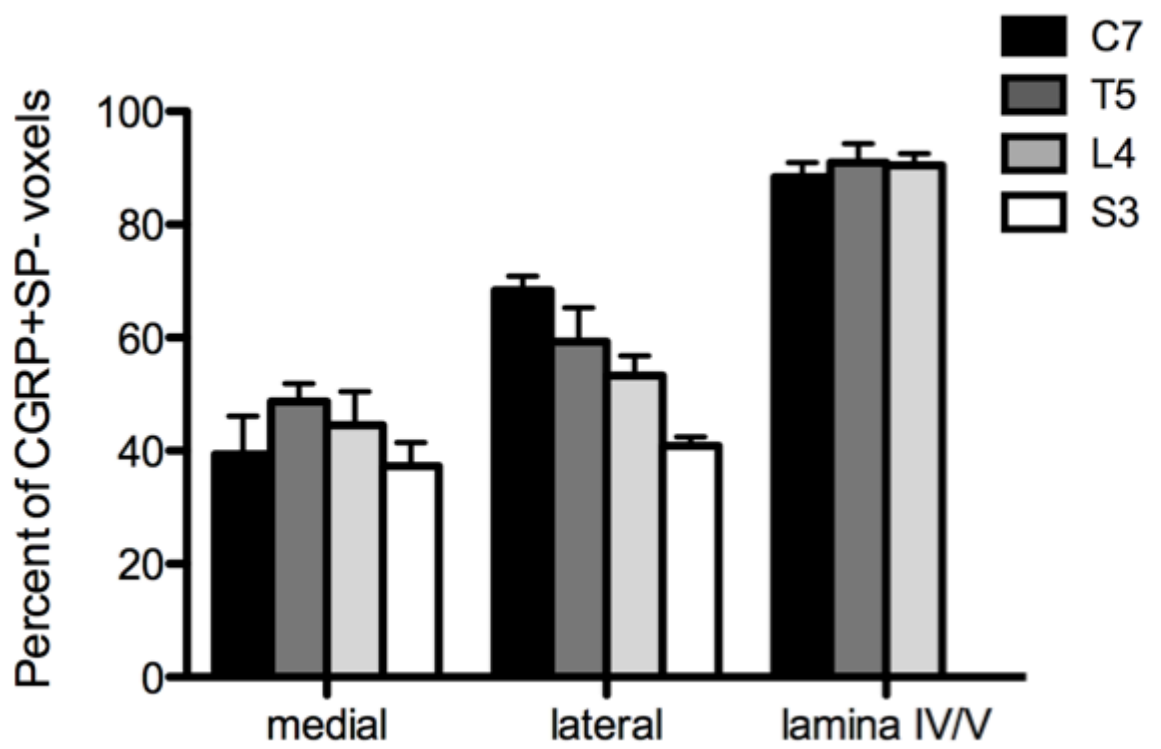
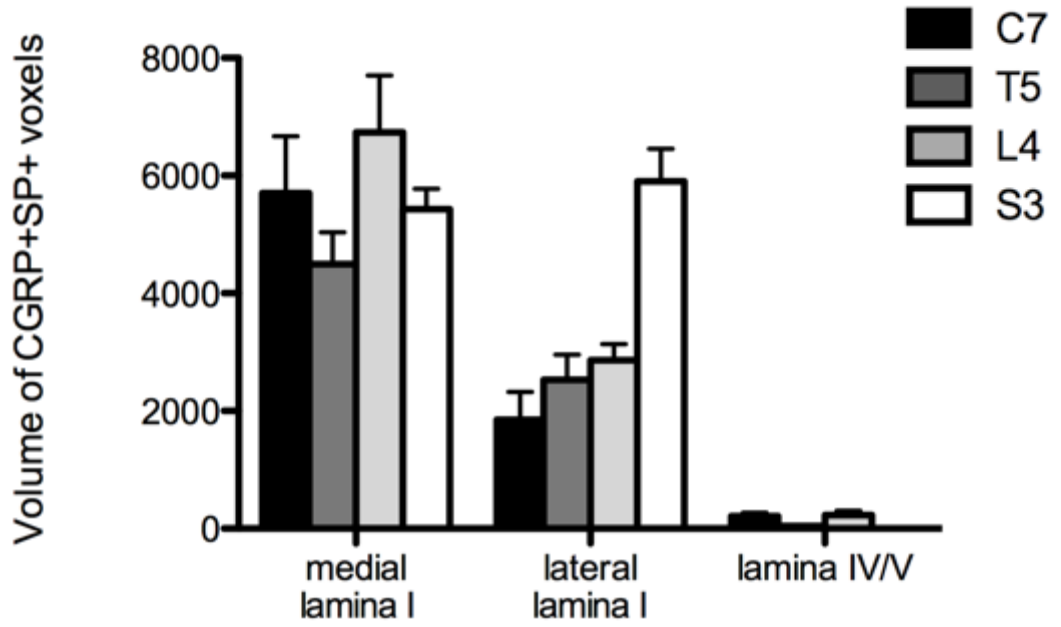
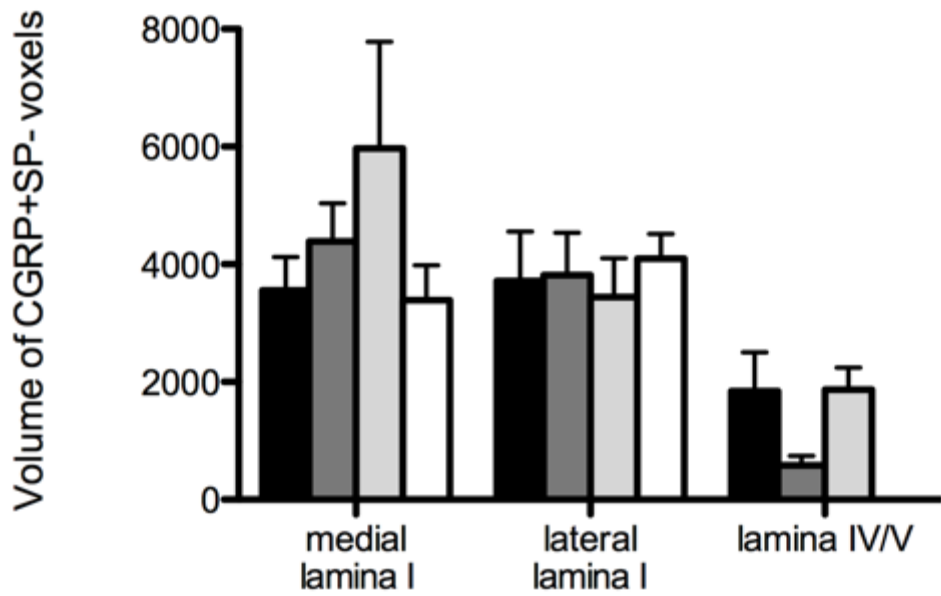


**Figure 3.16: Volume of CGRP-IR boutons containing or lacking SP-IR in the dorsal horn of all spinal levels**

Histogram (data displayed as mean±SEM) depicting the proportion of calcitonin gene-related peptide-immunoreactive (CGRP-IR) voxels that contained substance P-IR (SP-IR; CGRP<sup>+</sup>SP<sup>+</sup>; A) or lacked SP-IR (CGRP<sup>+</sup>SP<sup>-</sup>; B) in medial and lateral lamina I, and lamina IV/V of cervical (C7; black), thoracic (T5; dark grey), lumbar (L4; light grey) and sacral (S3; white) dorsal horn. There was no difference in the volume of CGRP<sup>+</sup>SP<sup>-</sup> voxels or CGRP<sup>+</sup>SP<sup>+</sup> voxels in medial lamina I, lateral lamina I or lamina IV/V (RM-ANOVA:  $F_{(1,4)} = 0$ ,  $p = 1$   $F_{(1,4)} = 0.04$ ,  $p = 0.9$ ;  $n = 5$  animals, and  $F_{(1,4)} = 0.02$ ,  $p = 1$ ;  $n = 5$  animals, respectively) between the different levels of the spinal cord.



**A**



**B**

**Figure 3.17: CGRP-IR and SP-IR in the C7 dorsal horn**

**A:** Widefield fluorescence microscopy of mouse cervical (C7) dorsal horn double labelled for calcitonin gene-related peptide (CGRP; red) and substance P (SP; green) showing a clear overlap of CGRP-immunoreactivity (IR) and SP-IR (CGRP<sup>+</sup>SP<sup>+</sup>; yellow) in the superficial laminae and CGRP-IR lacking of SP-IR (CGRP<sup>+</sup>SP<sup>-</sup>; red) in the deeper laminae. Boxed outlines (1: medial lamina I, 2: lamina IV/V, 3: lateral lamina I) represent dorsal horn regions of high CGRP-IR, further investigated with confocal microscopy. **B-C:** 3D reconstruction of confocal Z-stacks (21 steps of 0.5  $\mu$  m, total depth 10.5  $\mu$  m) of the three regions of the dorsal horn revealing CGRP<sup>+</sup>SP<sup>-</sup> terminals (B<sub>1</sub>- B<sub>3</sub>) and CGRP<sup>+</sup>SP<sup>+</sup> terminals (C<sub>1</sub>- C<sub>3</sub>). Scale bar = 60  $\mu$  m in A and = 20  $\mu$  m in C<sub>3</sub> (applies to B-C).

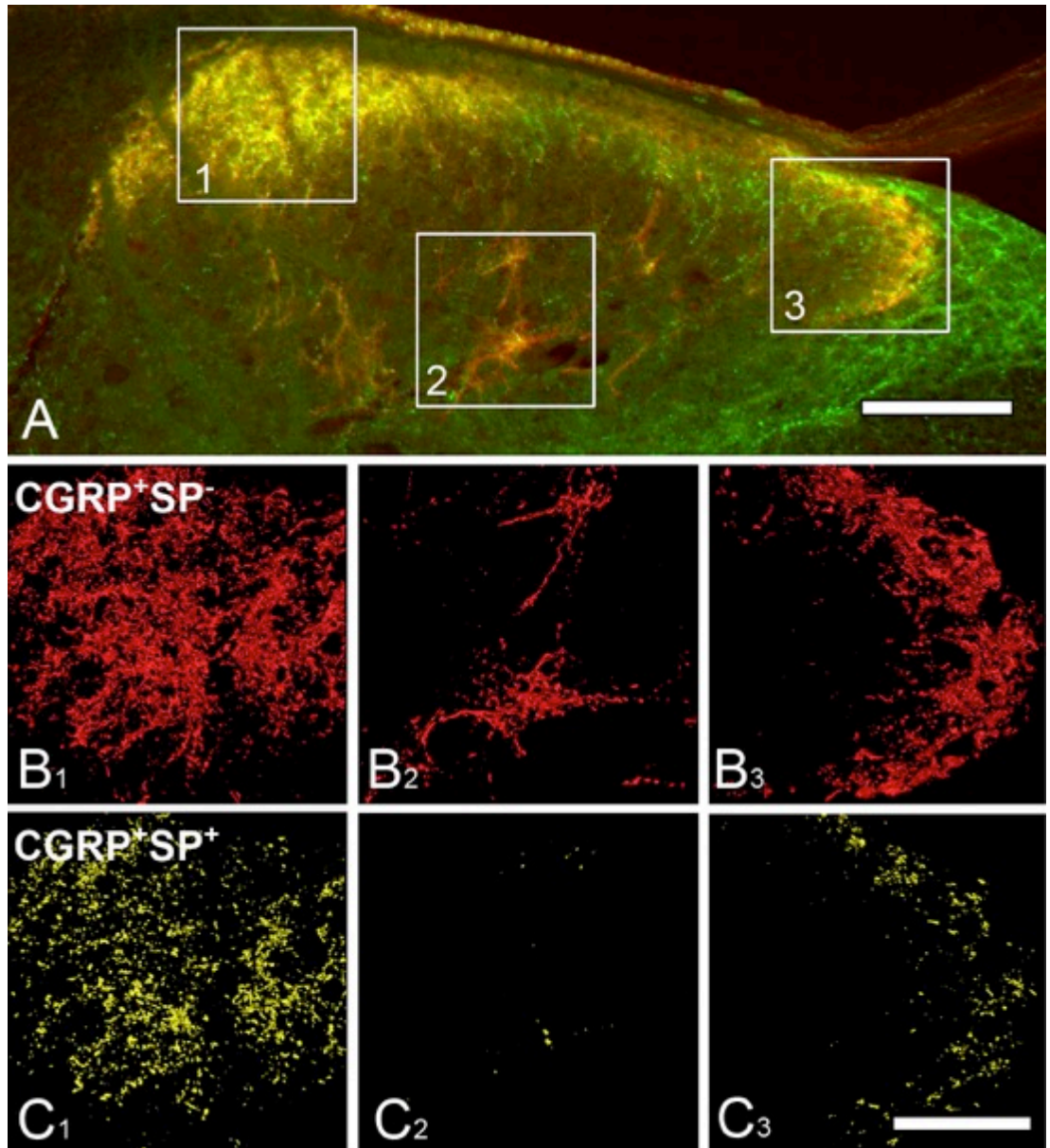


**Figure 3.18: Volume of CGRP-IR terminals in the C7 dorsal horn**

Histogram (data displayed as mean±SEM) depicting the volume of calcitonin gene-related peptide-immunoreactive (CGRP-IR) voxels in laminae I (medial and lateral) and IV/V of the cervical (C7) spinal dorsal horn. Medial lamina I had a higher volume of CGRP-IR voxels compared to lateral lamina I and lamina IV/V, and lateral lamina I had more CGRP-IR voxels than lamina IV/V (RM-ANOVA:  $F_{(1,4)} = 102$ ,  $p = 0.001$ ;  $n = 5$  animals).

**Figure 3.19: Percentage of CGRP-IR terminals that lack SP-IR in the C7 dorsal horn**

Histogram (data displayed as mean±SEM) depicting the proportion of calcitonin gene-related peptide-immunoreactive (CGRP-IR) voxels that either contained SP-IR (CGRP<sup>+</sup>SP<sup>+</sup>; yellow bars) or lacked SP-IR (CGRP<sup>+</sup>SP<sup>-</sup>; red bars) in laminae I (medial and lateral) and IV/V of the cervical (C7) spinal dorsal horn. Lateral lamina I and lamina IV/V had a significantly higher proportion of CGRP<sup>+</sup>SP<sup>-</sup> voxels compared to CGRP<sup>+</sup>SP<sup>+</sup> voxels (RM-ANOVA:  $F_{(1,4)} = 17$ ,  $p = 0.015$ ;  $n = 5$  animals). Lamina IV/V had the highest proportion of CGRP<sup>+</sup>SP<sup>-</sup> voxels compared to medial and lateral lamina I, and lateral lamina I had significantly higher proportion of CGRP<sup>+</sup>SP<sup>-</sup> voxels than medial lamina I (RM-ANOVA:  $F_{(1,4)} = 33$ ,  $p = 0.005$ ;  $n = 5$  animals)

**Figure 3.20: Volume of CGRP-IR terminals lacking SP-IR in the C7 dorsal horn**

Histogram (data displayed as mean±SEM) depicting the volume of calcitonin gene-related peptide-immunoreactive (CGRP-IR) voxels that either contained SP-IR (CGRP<sup>+</sup>SP<sup>+</sup>; yellow bars) or lacked SP-IR (CGRP<sup>+</sup>SP<sup>-</sup>; red bars) in laminae I (medial and lateral) and IV/V of the cervical (C7) spinal dorsal horn. There was a higher volume of CGRP<sup>+</sup>SP<sup>-</sup> voxels compared to CGRP<sup>+</sup>SP<sup>+</sup> voxels in lamina IV/V, but not in lateral or medial lamina I (RM-ANOVA:  $F_{(1,4)} = 320$ ,  $p > 0.001$ ;  $n = 5$  animals). The volume of CGRP<sup>+</sup>SP<sup>-</sup> voxels was highest in medial and lateral lamina I compared to lamina IV/V (RM-ANOVA:  $F_{(1,4)} = 8$ ,  $p = 0.05$ ;  $n = 5$  animals) and the volume of CGRP<sup>+</sup>SP<sup>+</sup> voxels was highest in medial lamina I and lowest in lamina IV/V (RM-ANOVA:  $F_{(1,4)} = 114$ ,  $p < 0.001$ ;  $n = 5$  animals).

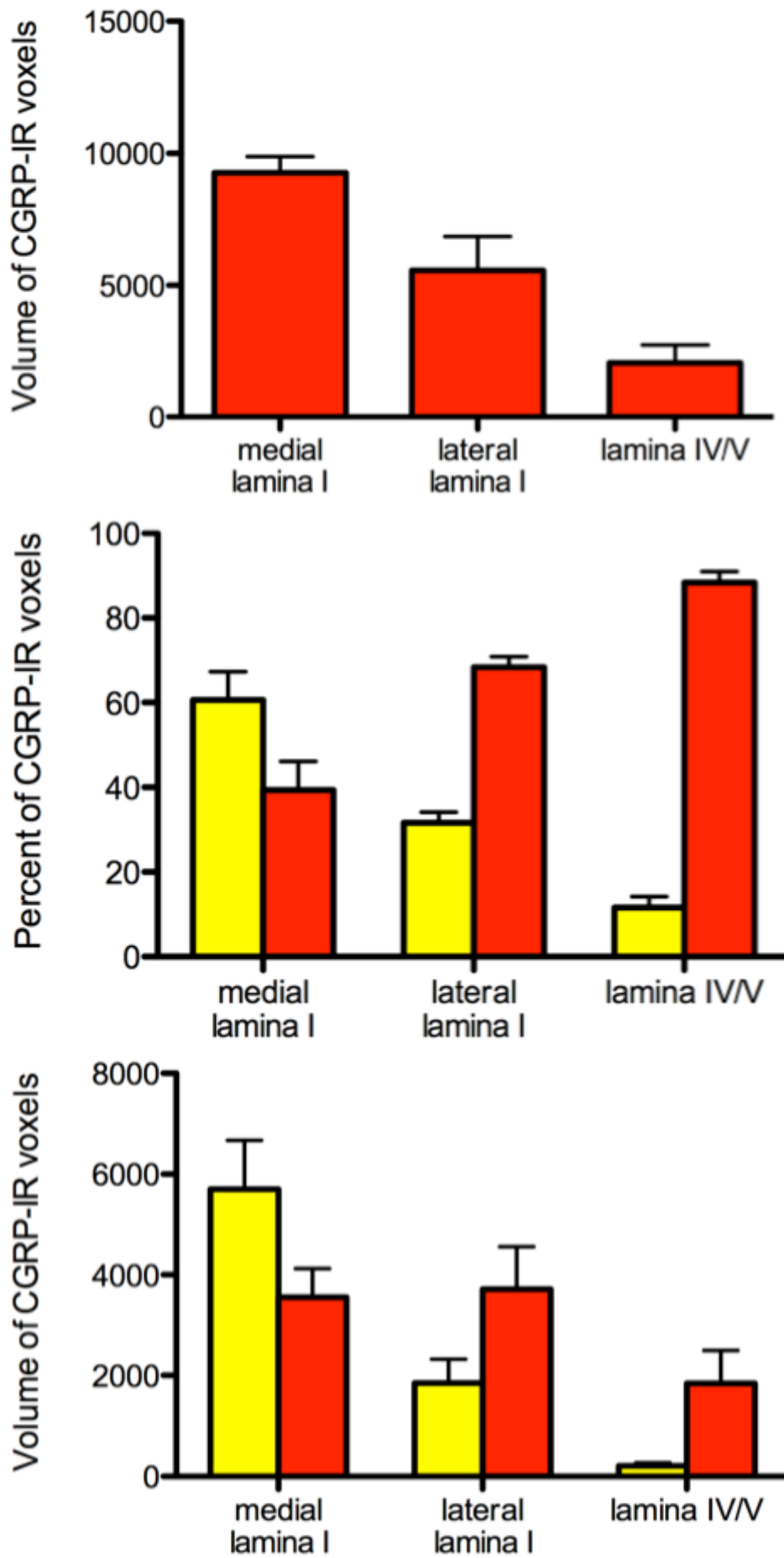


**Figure 3.21: CGRP-IR and SP-IR in the T5 dorsal horn**

**A:** Widefield fluorescence microscopy of mouse thoracic (T5) dorsal horn double labelled for calcitonin gene-related peptide (CGRP; red) and substance P (SP; green) showing a clear overlap of CGRP-immunoreactivity (IR) and SP-IR (CGRP<sup>+</sup>SP<sup>+</sup>; yellow) in the superficial laminae and CGRP-IR lacking of SP-IR (CGRP<sup>+</sup>SP<sup>-</sup>; red) in the deeper laminae. Boxed outlines (1: medial lamina I, 2: lamina IV/V, 3: lateral lamina I) represent dorsal horn regions of high CGRP-IR, further investigated with confocal microscopy. **B-C:** 3D reconstruction of confocal Z-stacks (21 steps of 0.5  $\mu$ m, total depth 10.5  $\mu$ m) of the three regions of the dorsal horn revealing CGRP<sup>+</sup>SP<sup>-</sup> terminals (B<sub>1</sub>- B<sub>3</sub>) and CGRP<sup>+</sup>SP<sup>+</sup> terminals (C<sub>1</sub>- C<sub>3</sub>). Scale bar = 60  $\mu$ m in A and = 20  $\mu$ m in C<sub>3</sub> (applies to B-C).

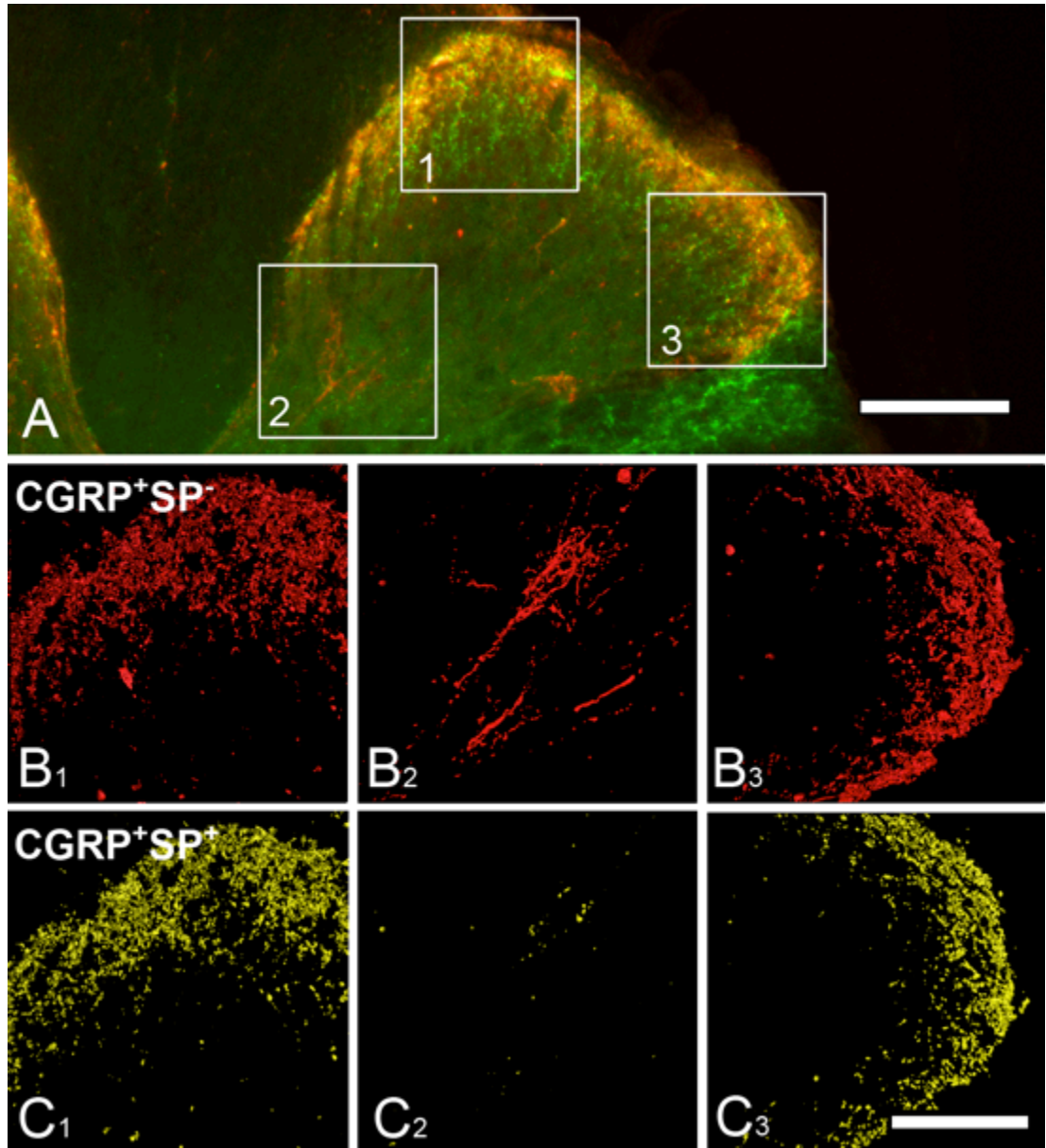


**Figure 3.22: Volume of CGRP-IR terminals in the T5 dorsal horn**

Histogram (data displayed as mean±SEM) depicting the volume of calcitonin gene-related peptide-immunoreactive (CGRP-IR) voxels in laminae I (medial and lateral) and IV/V of the thoracic (T5) spinal dorsal horn. Both medial and lateral lamina I had a significantly higher volume of CGRP-IR voxels compared to lamina IV/V. There was no significant difference between the CGRP-IR voxels in medial and lateral lamina I (RM-ANOVA:  $F_{(1,4)} = 58$ ,  $p = 0.002$ ;  $n = 5$  animals).

**Figure 3.23: Percentage of CGRP-IR terminals that lack SP-IR in the T5 dorsal horn**

Histogram (data displayed as mean±SEM) depicting the proportion of CGRP-IR that either contained SP-IR (CGRP<sup>+</sup>SP<sup>+</sup>; yellow bars) or lacked SP-IR (CGRP<sup>+</sup>SP<sup>-</sup>; red bars) in laminae I (medial and lateral) and IV/V of the thoracic (T5) spinal dorsal horn. Lateral lamina I and lamina IV/V had a higher proportion of CGRP<sup>+</sup>SP<sup>-</sup> voxels compared to CGRP<sup>+</sup>SP<sup>+</sup> voxels (RM-ANOVA:  $F_{(1,4)} = 17$ ,  $p = 0.005$ ;  $n = 5$  animals). Lamina IV/V had the highest proportion of CGRP<sup>+</sup>SP<sup>-</sup> voxels compared to medial and lateral lamina I, and lateral lamina I had significantly higher proportion of CGRP<sup>+</sup>SP<sup>-</sup> voxels than medial lamina I (RM-ANOVA:  $F_{(1,4)} = 33$ ,  $p = 0.005$ ;  $n = 5$  animals).

**Figure 3.24: Volume of CGRP-IR terminals lacking SP-IR in the T5 dorsal horn**

Histogram (data displayed as mean±SEM) depicting the volume of calcitonin gene-related peptide-immunoreactive (CGRP-IR) voxels that either contained SP-IR (CGRP<sup>+</sup>SP<sup>+</sup>; yellow bars) or lacked SP-IR (CGRP<sup>+</sup>SP<sup>-</sup>; red bars) in laminae I (medial and lateral) and IV/V of the thoracic (T5) spinal dorsal horn. There was a higher volume of CGRP<sup>+</sup>SP<sup>-</sup> voxels compared to CGRP<sup>+</sup>SP<sup>+</sup> voxels in lamina IV/V, but not in lateral or medial lamina I (RM-ANOVA:  $F_{(1,4)} = 24$ ,  $p = 0.008$ ;  $n = 5$  animals). The volume of CGRP<sup>+</sup>SP<sup>-</sup> voxels was highest in medial and lateral lamina I compared to lamina IV/V (RM-ANOVA:  $F_{(1,4)} = 30$ ,  $p = 0.005$ ;  $n = 5$  animals) and the volume of CGRP<sup>+</sup>SP<sup>+</sup> voxels was highest in medial lamina I and lowest in lamina IV/V (RM-ANOVA:  $F_{(1,4)} = 371$ ,  $p < 0.001$ ;  $n = 5$  animals).

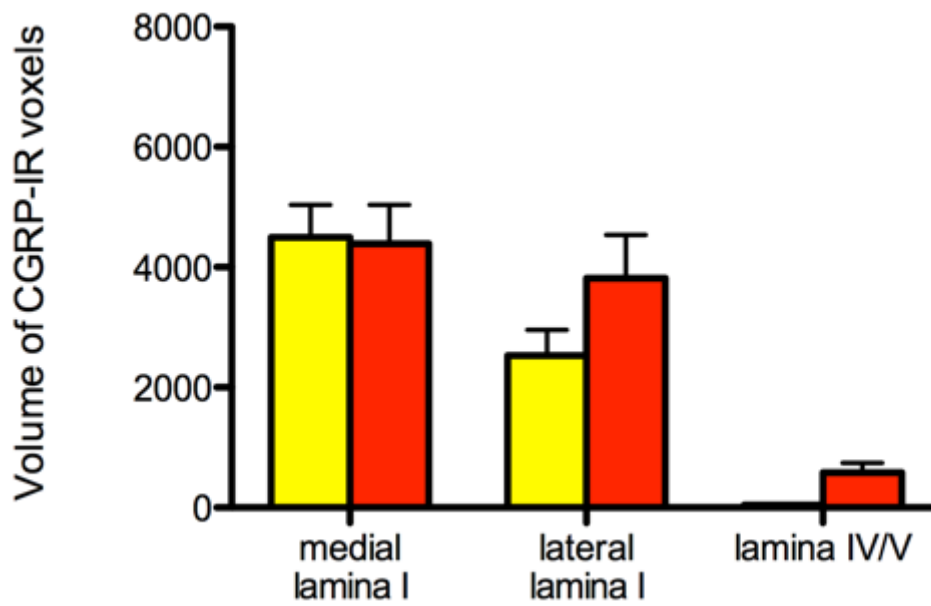
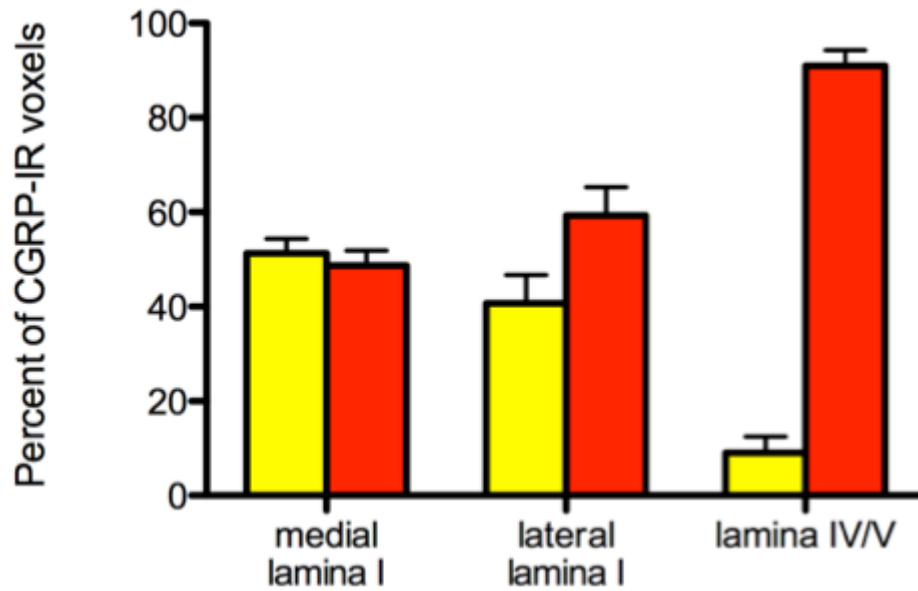
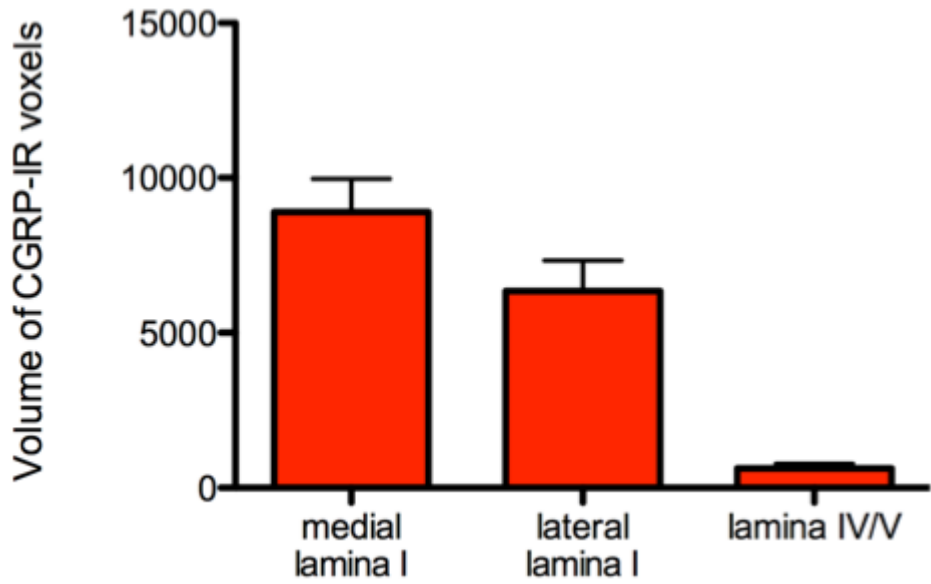


**Figure 3.25: CGRP-IR and SP-IR in the L4 dorsal horn**

**A:** Widefield fluorescence microscopy of mouse lumbar (L4) dorsal horn double labelled for calcitonin gene-related peptide (CGRP; red) and substance P (SP; green) showing a clear overlap of CGRP-immunoreactivity (IR) and SP-IR (CGRP<sup>+</sup>SP<sup>+</sup>; yellow) in the superficial laminae and CGRP-IR lacking of SP-IR (CGRP<sup>+</sup>SP<sup>-</sup>; red) in the deeper laminae. Boxed outlines (1: medial lamina I, 2: lamina IV/V, 3: lateral lamina I) represent dorsal horn regions of high CGRP-IR, further investigated with confocal microscopy. **B-C:** 3D reconstruction of confocal Z-stacks (21 steps of 0.5  $\mu$  m, total depth 10.5  $\mu$  m) of the three regions of the dorsal horn revealing CGRP<sup>+</sup>SP<sup>-</sup> terminals (B<sub>1</sub>- B<sub>3</sub>) and CGRP<sup>+</sup>SP<sup>+</sup> terminals (C<sub>1</sub>- C<sub>3</sub>). Scale bar = 60  $\mu$  m in A and = 20  $\mu$  m in C<sub>3</sub> (applies to B-C).

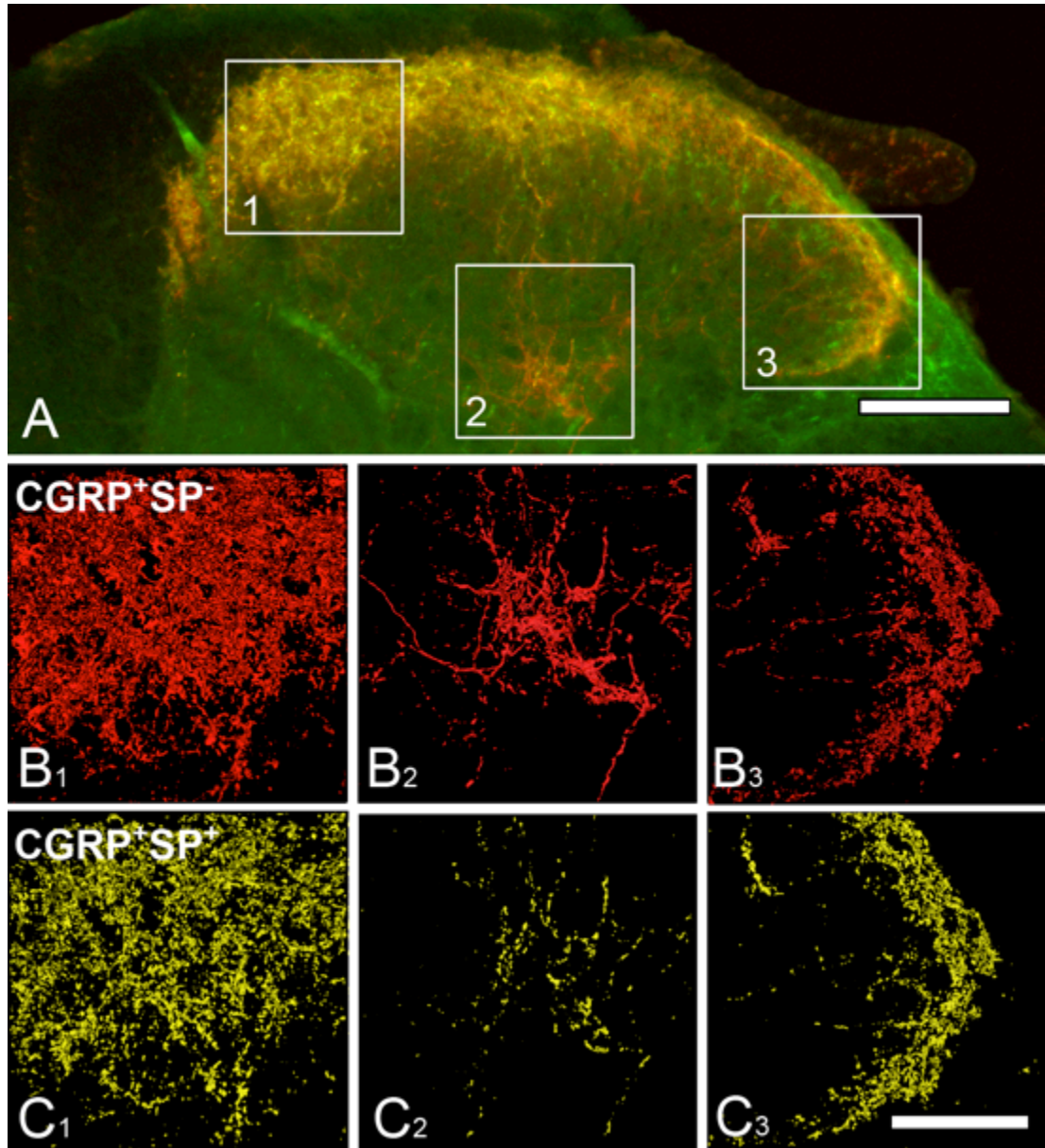


**Figure 3.26: Volume of CGRP-IR terminals in the L4 dorsal horn**

Histogram (data displayed as mean±SEM) depicting the volume of calcitonin gene-related peptide-immunoreactive (CGRP-IR) voxels in laminae I (medial and lateral) and IV/V of the lumbar (L4) spinal dorsal horn. Both medial and lateral lamina I had a significantly higher volume of CGRP-IR voxels compared to lamina IV/V. There was no significant difference between the CGRP-IR voxels in medial and lateral lamina I (RM-ANOVA:  $F_{(1,4)} = 29$ ,  $p = 0.006$ ;  $n = 5$  animals).

**Figure 3.27: Percentage of CGRP-IR terminals that lack SP-IR in the L4 dorsal horn**

The proportion (mean±SEM) of CGRP-IR that either contained SP-IR (CGRP<sup>+</sup>SP<sup>+</sup>; black bars) or lacked SP-IR (CGRP<sup>+</sup>SP<sup>-</sup>; white bars). Lateral lamina I and lamina IV/V had a significantly higher proportion of CGRP<sup>+</sup>SP<sup>-</sup> voxels compared to CGRP<sup>+</sup>SP<sup>+</sup> voxels (RM-ANOVA:  $F_{(1,4)} = 17$ ,  $p = 0.005$ ;  $n = 5$  animals). Lamina IV/V had the highest proportion of CGRP<sup>+</sup>SP<sup>-</sup> voxels compared to medial and lateral lamina I, and lateral lamina I had significantly higher proportion of CGRP<sup>+</sup>SP<sup>-</sup> voxels than medial lamina I (RM-ANOVA:  $F_{(1,4)} = 33$ ,  $p = 0.005$ ;  $n = 5$  animals)

**Figure 3.28: Volume of CGRP-IR terminals lacking SP-IR in the L4 dorsal horn**

Histogram (data displayed as mean±SEM) depicting the volume of calcitonin gene-related peptide-immunoreactive (CGRP-IR) voxels that either contained SP-IR (CGRP<sup>+</sup>SP<sup>+</sup>; yellow bars) or lacked SP-IR (CGRP<sup>+</sup>SP<sup>-</sup>; red bars) in laminae I (medial and lateral) and IV/V of the lumbar (L4) spinal dorsal horn. There was a higher volume of CGRP<sup>+</sup>SP<sup>-</sup> voxels compared to CGRP<sup>+</sup>SP<sup>+</sup> voxels in lamina IV/V, but not in lateral or medial lamina I (RM-ANOVA:  $F_{(1,4)} = 42$ ,  $p = 0.003$ ;  $n = 5$  animals). The volume of CGRP<sup>+</sup>SP<sup>-</sup> voxels was highest in medial and lateral lamina I compared to lamina IV/V (RM-ANOVA:  $F_{(1,4)} = 11$ ,  $p = 0.03$ ;  $n = 5$  animals) and the volume of CGRP<sup>+</sup>SP<sup>+</sup> voxels was highest in medial lamina I and lowest in lamina IV/V (RM-ANOVA:  $F_{(1,4)} = 69$ ,  $p = 0.001$ ;  $n = 5$  animals).

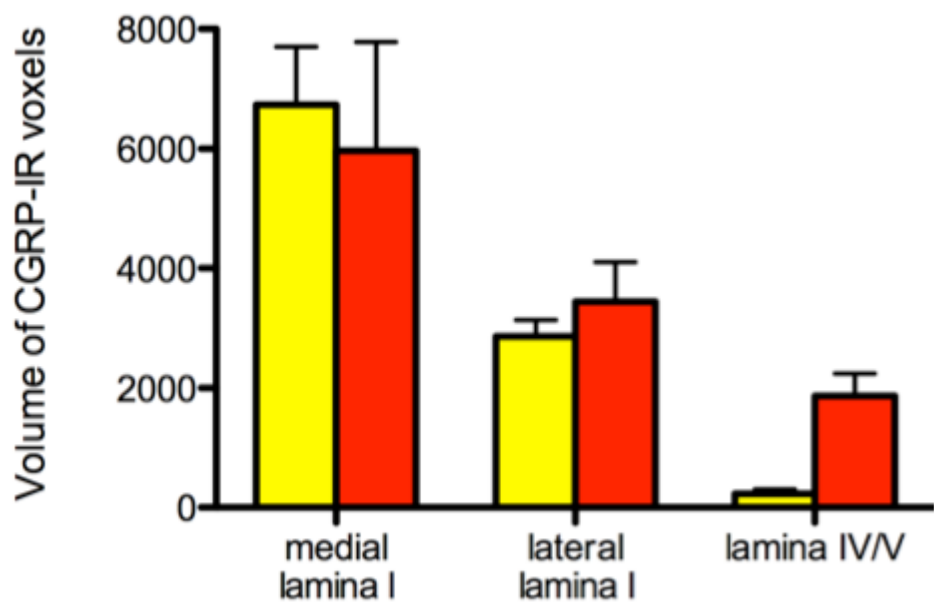
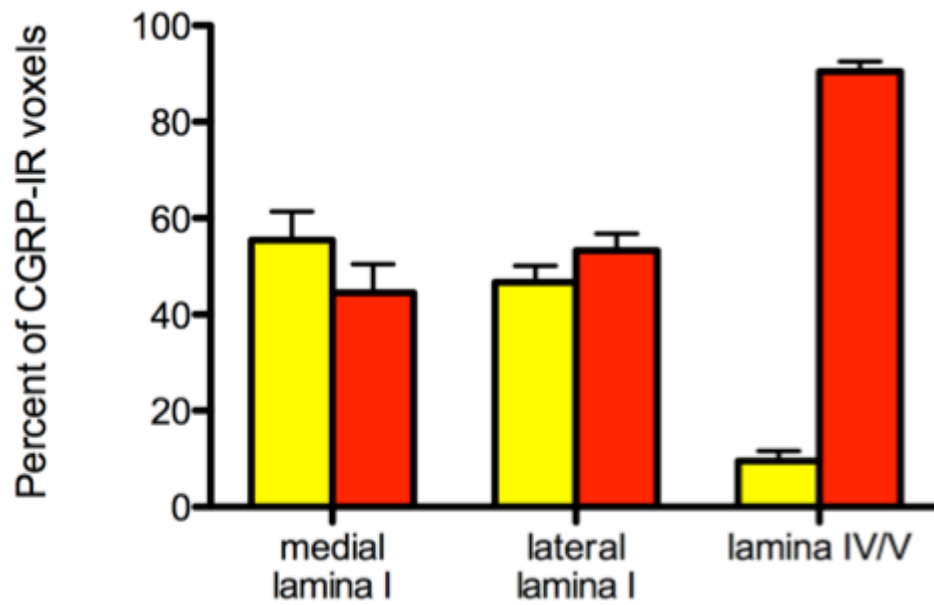
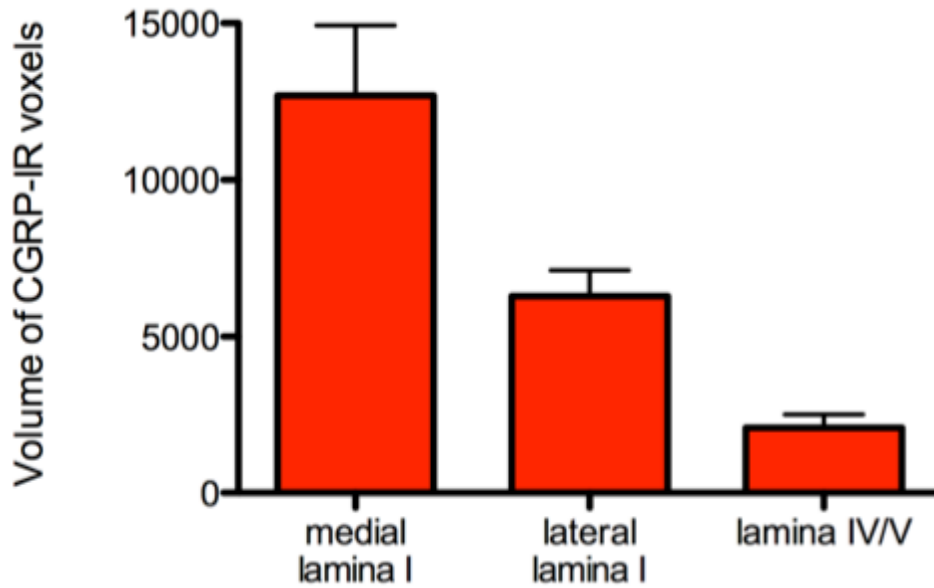


**Figure 3.29: CGRP-IR and SP-IR in the S3 dorsal horn**

**A:** Widefield fluorescence microscopy of mouse sacral (S3) dorsal horns double labelled for calcitonin gene-related peptide (CGRP; red) and substance P (SP; green) showing a clear overlap of CGRP-immunoreactivity (IR) and SP-IR (CGRP<sup>+</sup>SP<sup>+</sup>; yellow) and some CGRP-IR lacking of SP-IR (CGRP<sup>+</sup>SP<sup>-</sup>; red) in the superficial laminae. Boxed outlines (1: medial lamina I and 2: lateral lamina I) represent dorsal horn regions of high CGRP-IR, further investigated with confocal microscopy. **B-C:** 3D reconstruction of confocal Z-stacks (21 steps of 0.5  $\mu$  m, total depth 10.5  $\mu$  m) of the two regions of the dorsal horn revealing CGRP<sup>+</sup>SP<sup>-</sup> terminals (B<sub>1</sub>- B<sub>2</sub>) and CGRP<sup>+</sup>SP<sup>+</sup> terminals (C<sub>1</sub>- C<sub>2</sub>). Scale bar = 100  $\mu$  m in A and = 20  $\mu$  m in C<sub>3</sub> (applies to B-C).

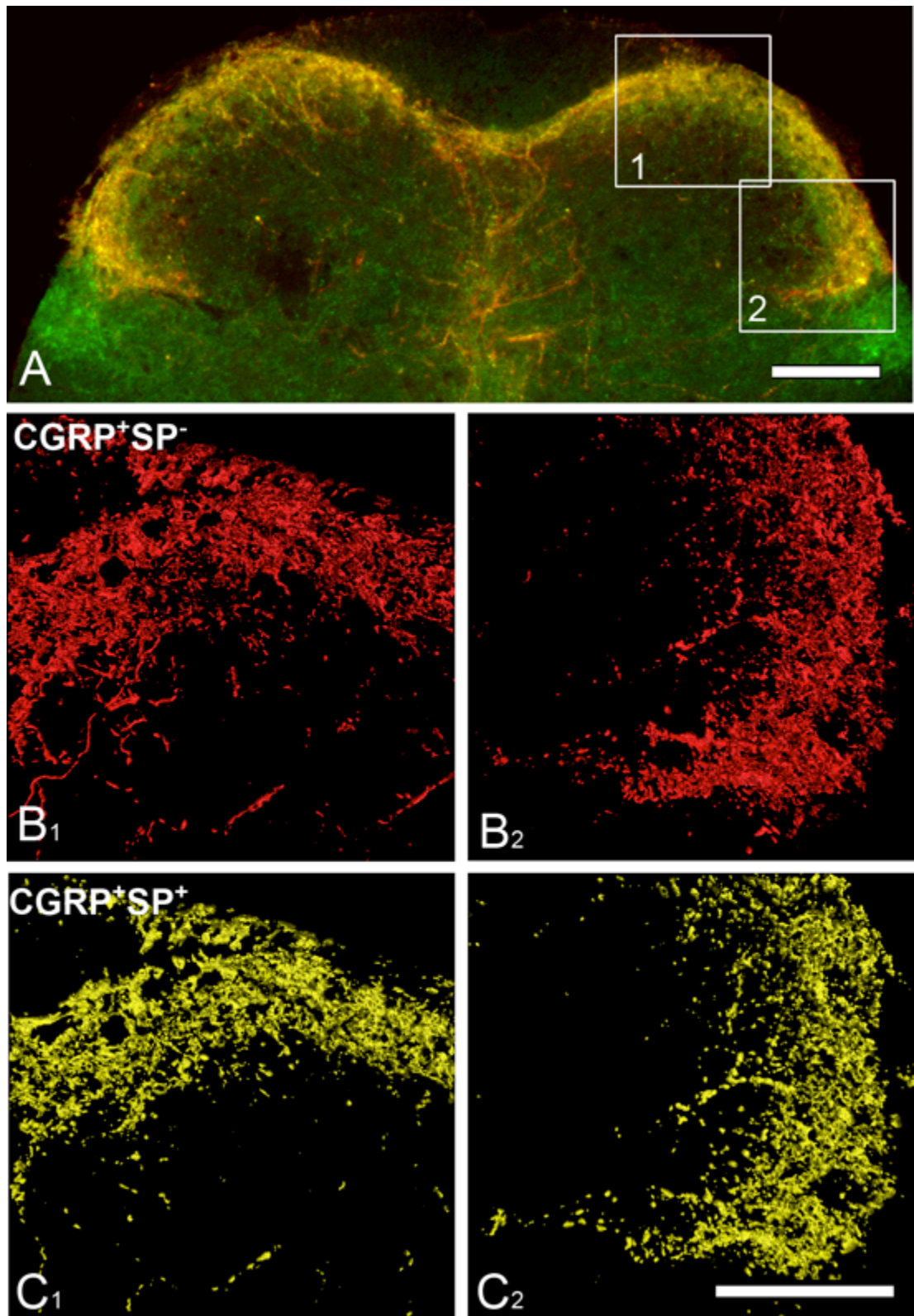


**Figure 3.30: Volume of CGRP-IR terminals in the S3 dorsal horn**

Histogram (data displayed as mean±SEM) depicting the volume of calcitonin gene-related peptide-immunoreactive (CGRP-IR) voxels in medial and lateral lamina I of the sacral (S3) spinal dorsal horn. There was no CGRP-IR detected in lamina IV/V. There was no significant difference between the volume of CGRP-IR voxels in medial or lateral lamina I (Paired t-test:  $t_{(4)} = 1$ ,  $p = 0.4$ ;  $n = 5$  animals).

**Figure 3.31: Percentage of CGRP-IR terminals that lack SP-IR in the S3 dorsal horn**

The proportion (mean±SEM) of CGRP-IR that either contained SP-IR (CGRP<sup>+</sup>SP<sup>+</sup>; yellow bars) or lacked SP-IR (CGRP<sup>+</sup>SP<sup>-</sup>; red bars). Lateral lamina I and lamina IV/V had a significantly higher proportion of CGRP<sup>+</sup>SP<sup>-</sup> voxels compared to CGRP<sup>+</sup>SP<sup>+</sup> voxels (RM-ANOVA:  $F_{(1,4)} = 17$ ,  $p = 0.005$ ;  $n = 5$  animals). Lamina IV/V had the highest proportion of CGRP<sup>+</sup>SP<sup>-</sup> voxels compared to medial and lateral lamina I, and lateral lamina I had significantly higher proportion of CGRP<sup>+</sup>SP<sup>-</sup> voxels than medial lamina I (RM-ANOVA:  $F_{(1,4)} = 33$ ,  $p = 0.005$ ;  $n = 5$  animals)

**Figure 3.32: Volume of CGRP-IR terminals lacking SP-IR in the S3 dorsal horn**

Histogram (data displayed as mean±SEM) depicting the volume of calcitonin gene-related peptide-immunoreactive (CGRP-IR) voxels that either contained SP-IR (CGRP<sup>+</sup>SP<sup>+</sup>; yellow bars) or lacked SP-IR (CGRP<sup>+</sup>SP<sup>-</sup>; red bars) in medial and lateral lamina I of the sacral (S3) spinal dorsal horn. There was a higher volume of CGRP<sup>+</sup>SP<sup>+</sup> voxels compared to CGRP<sup>+</sup>SP<sup>-</sup> voxels (RM-ANOVA:  $F_{(1,4)} = 24$ ,  $p = 0.008$ ;  $n = 5$  animals). There was no difference in the volume of CGRP<sup>+</sup>SP<sup>-</sup> voxels or CGRP<sup>+</sup>SP<sup>+</sup> voxels in medial lamina I or lateral lamina I (RM-ANOVA:  $F_{(1,4)} = 1$ ,  $p = 0.4$ ;  $n = 5$  animals and  $F_{(1,4)} = 1$ ,  $p = 0.5$ ;  $n = 5$  animals, respectively).

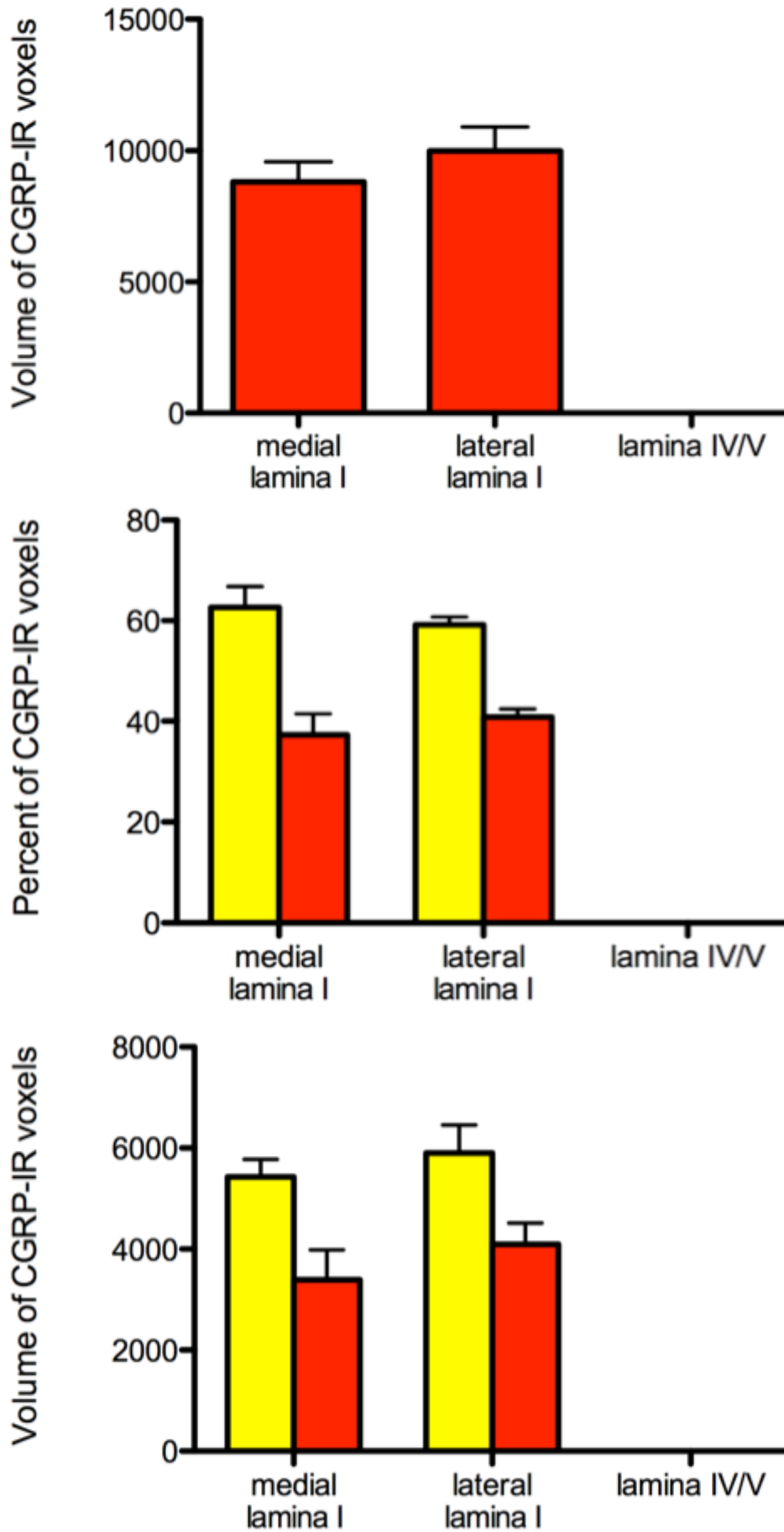


**Figure 3.33: CGRP-IR in dermal papillae of glabrous paw skin**

Wide field microscopy of the innervation of a dermal papillae triple labelled with calcitonin gene-related peptide (CGRP; A), substance P (SP; B) and neuron specific enolase (NSE; C). The overlay (D) shows CGRP-immunoreactive (CGRP-IR) fibres that lacked SP-IR (CGRP<sup>+</sup>SP<sup>-</sup>; red; black arrow) and CGRP-IR fibres that contained SP-IR (CGRP<sup>+</sup>SP<sup>+</sup>; yellow; white arrows). CGRP<sup>+</sup>SP<sup>-</sup> and CGRP<sup>+</sup>SP<sup>+</sup> fibres were detected within the dermis (der) of the dermal papilla and associated with blood vessels (bv). The fibres were also seen penetrating the epidermis (epi) as both free nerve endings and associated with Meissner's corpuscles (mc). Scale bar in D = 60µm (applies to A-D). Abbreviations: epi = epidermis, der = dermis, bv = blood vessel and mc = Meissner's corpuscles

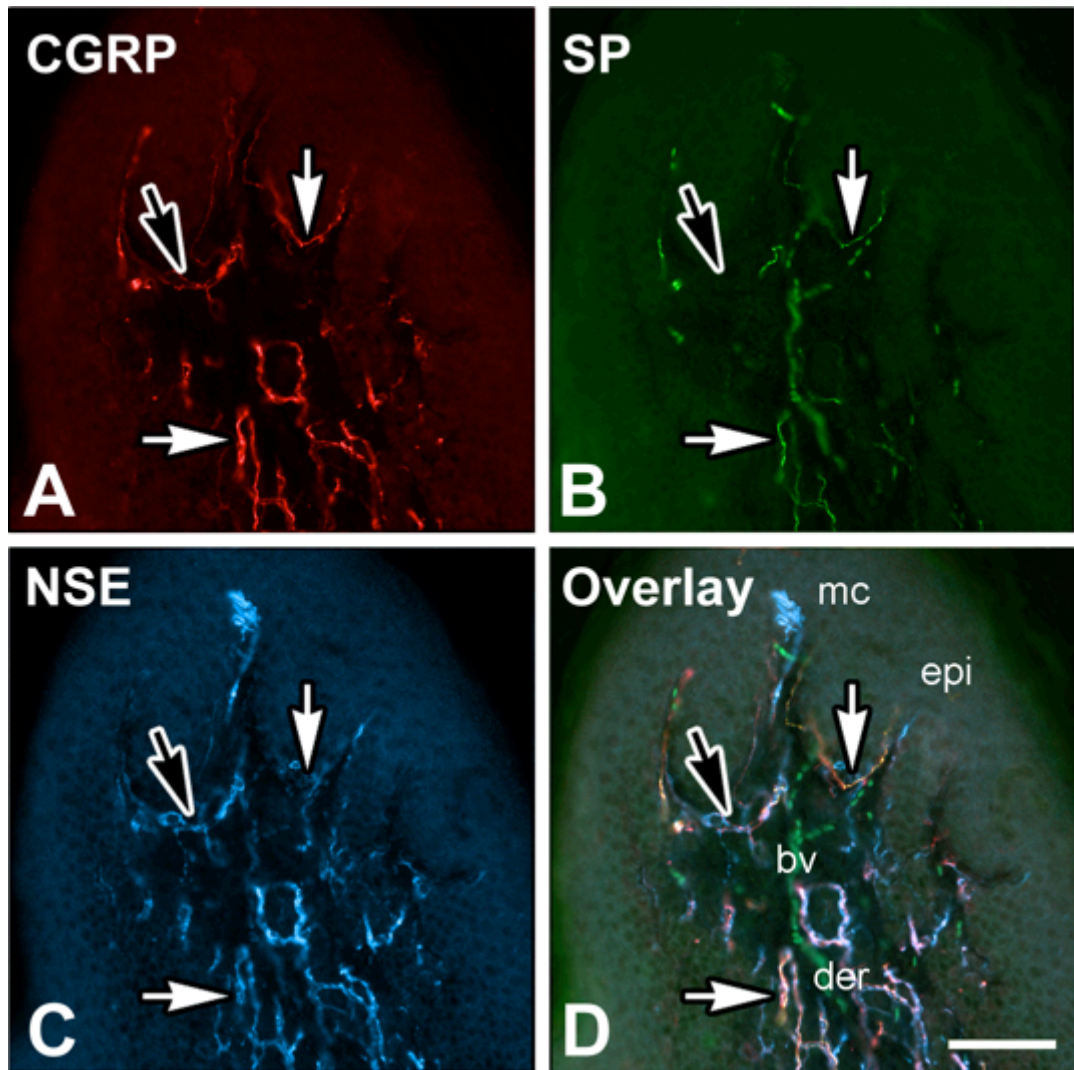


**Figure 3.34: CGRP-IR fibres penetrating the epidermis of glabrous paw skin**

Confocal microscopy of a intraepithelial fibres labelled with calcitonin gene-related peptide (CGRP; A) and substance P (SP; B). The overlay (C) shows CGRP-immunoreactive (CGRP-IR) fibres penetrating the epidermis (epi); one CGRP-IR fibre contained SP-IR (CGRP<sup>+</sup>SP<sup>+</sup>; yellow; white arrows) whilst the other CGRP-IR fibres lacked SP-IR (CGRP<sup>+</sup>SP<sup>-</sup>; red; black arrow). The enlarged inset image (D) displays a closer look at the CGRP+SP<sup>-</sup> intraepithelial fibre. Scale bar in D = 20µm (applies to A-D). Abbreviations: epi = epidermis, and der = dermis

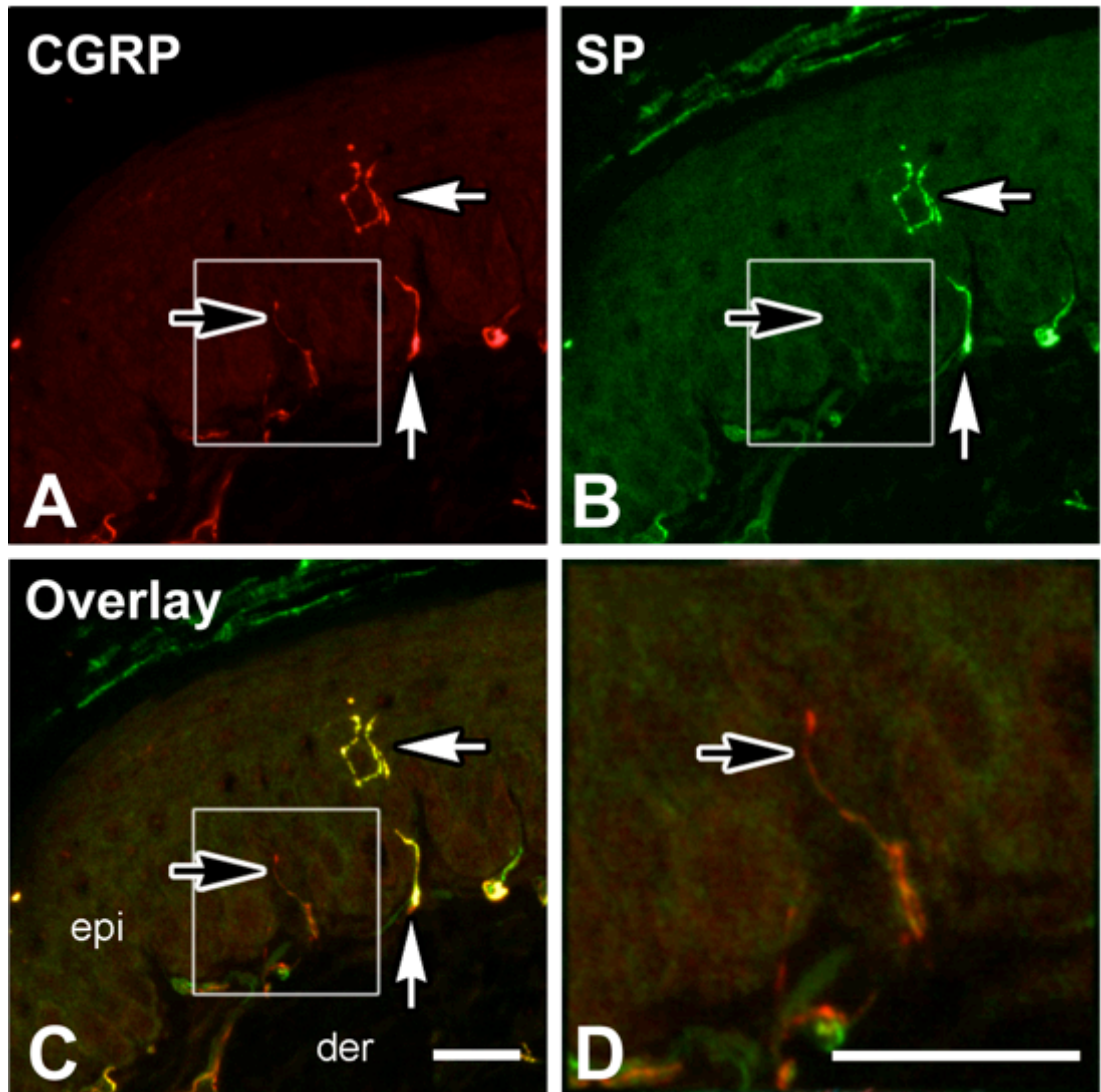


**Figure 3.35: CGRP-IR in Meissner's corpuscles of glabrous paw skin**

Confocal microscopy of a Meissner's corpuscle visualised with neuron specific enolase (NSE; C) and labelled with calcitonin gene-related peptide (CGRP; A) and substance P (SP; B). The overlay (D) shows two CGRP-immunoreactive (CGRP-IR) fibres associated with a Meissner's corpuscle (blue); one CGRP-IR fibre lacked SP-IR (CGRP<sup>+</sup>SP<sup>-</sup>; red; black arrow) whilst the other CGRP-IR fibre contained SP-IR (CGRP<sup>+</sup>SP<sup>+</sup>; yellow; white arrows). Scale bar in D = 20µm (applies to A-D)

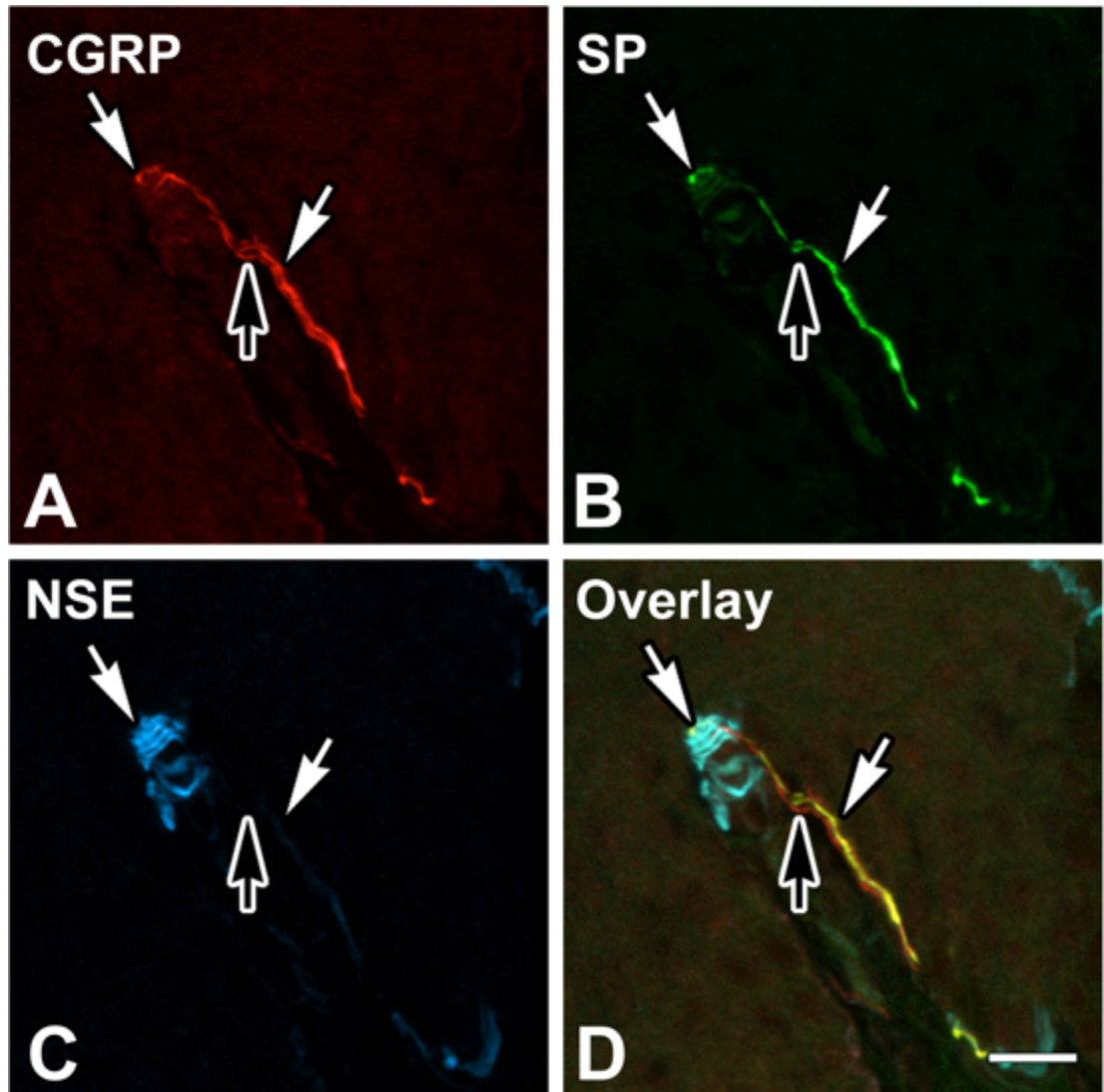


**Figure 3.36: CGRP-IR in hairy paw skin**

Wide field microscopy of the innervation of a hair follicle (hf) triple labelled with calcitonin gene-related peptide (CGRP; A), substance P (SP; B) and neuron specific enolase (NSE; C). The overlay (D) shows circumferential and palisade endings visualised with NSE-immunoreactivity (NSE-IR; blue). Circumferential fibres were seen as fine varicose fibres containing CGRP-IR but not SP-IR (CGRP<sup>+</sup>SP<sup>-</sup>; red; black arrow) superior to a singular circumferential fibre containing CGRP-IR with SP-IR (CGRP<sup>+</sup>SP<sup>+</sup>; white arrow). Scale bar in D = 60 µm (applies to A-D)  
Abbreviations: epi = epidermis, der = dermis, and hf = hair follicle

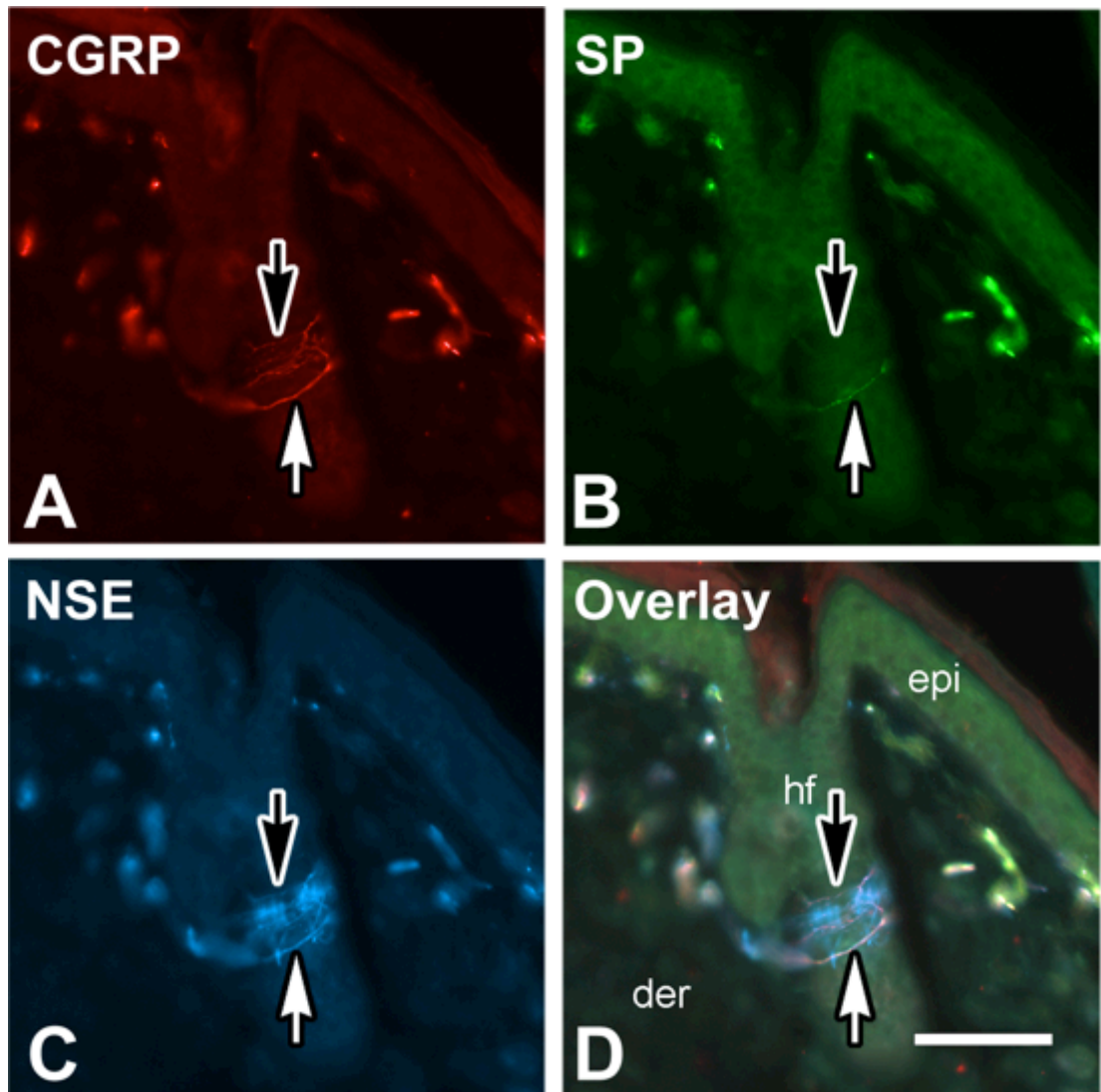
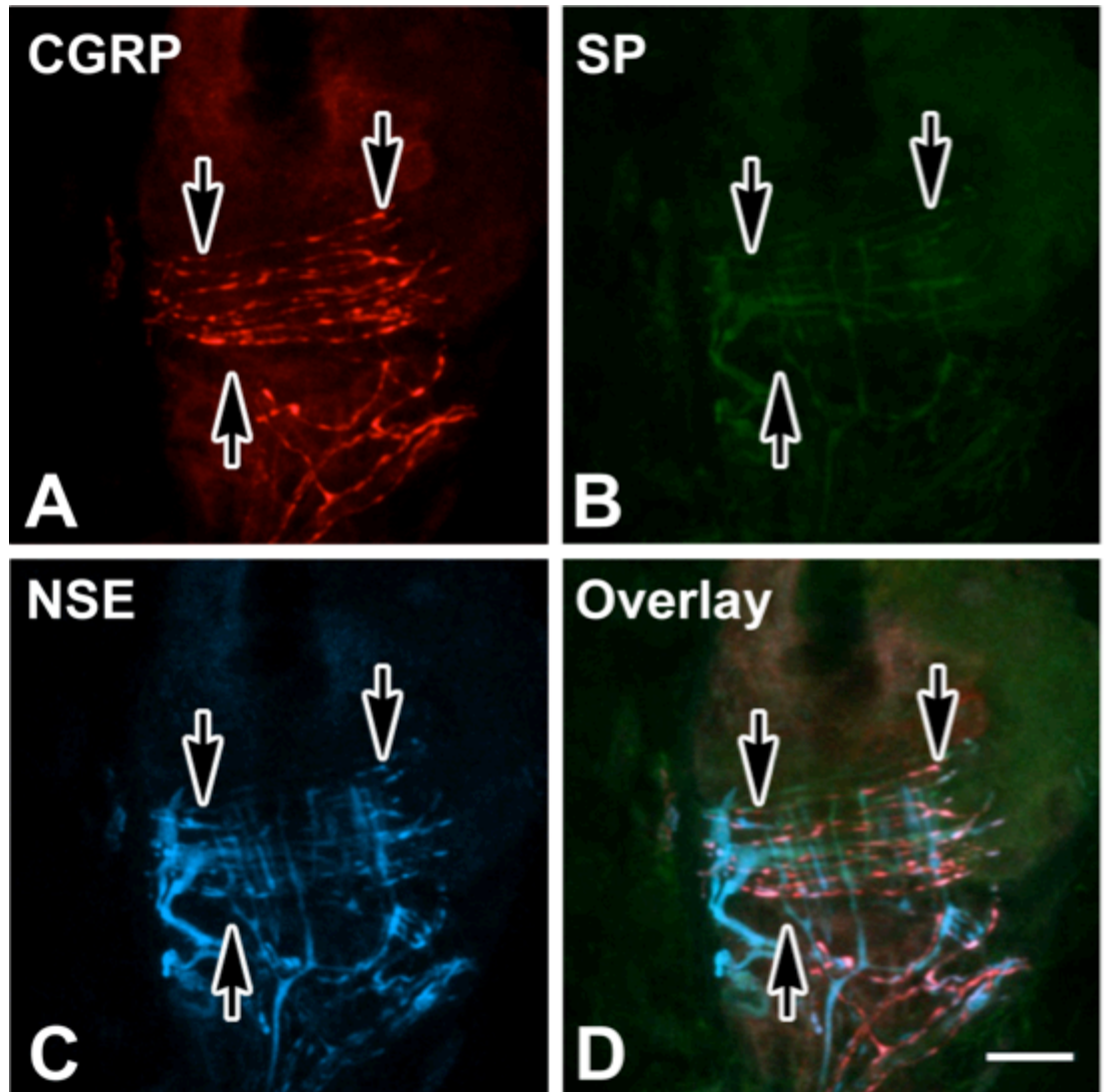


**Figure 3.37: CGRP-IR in hair follicle afferents of hairy paw skin**

Confocal microscopy of a hair follicle afferent visualised with neuron specific enolase (NSE; C) and labelled with calcitonin gene-related peptide (CGRP; A), and substance P (SP; B). The overlay (D) shows circumferential and palisade endings visualised with NSE-immunoreactivity (NSE-IR; blue) with circumferential fibres containing CGRP-IR but not SP-IR (CGRP<sup>+</sup>SP<sup>-</sup>; black arrows). Scale bar in D = 20µm (applies to A-D)





---

**Chapter 4:**  
**Neurochemical profile of**  
**CGRP<sup>+</sup>SP<sup>-</sup> neurons**

---



## 4.1 Background

---

Centrally, CGRP enhances the nociceptive behavioural responses induced by SP by potentiating the release of SP (Oku *et al.*, 1987), inhibiting its degradation (Le Greves *et al.*, 1985) and enhancing the excitability of neurons receiving noxious inputs (Biella *et al.*, 1991; Seybold *et al.*, 2003; Sun *et al.*, 2004; Bird *et al.*, 2006). Without SP, CGRP alone has minimal effects on nociceptive inputs to the spinal cord (Miletic & Tan, 1988). Yet in the previous chapter, we have demonstrated that a significant population of CGRP neurons lack detectable levels of SP. Hence, it is possible that CGRP<sup>+</sup>SP<sup>-</sup> neurons utilise another neurotransmitter, other than SP.

Glutamate is the primary excitatory neurotransmitter in the spinal cord and it is believed that the majority of sensory neurotransmission from primary afferents onto dorsal horn neurons is largely mediated by glutamate (Alvarez *et al.*, 2004). Unfortunately, neurons possess metabolic pools of glutamate that are unrelated to neurotransmission (De Biasi & Rustioni, 1990), which complicates the interpretation of glutamate immunoreactivity. Instead, immunoreactivity to vesicular glutamate transporters (VGluTs) is used. To date there are three VGluTs: VGluT1, VGluT2 and VGluT3 (Bellocchio *et al.*, 1998; Takamori *et al.*, 2000; Bai *et al.*, 2001; Takamori *et al.*, 2001; Herzog *et al.*, 2004). CGRP-IR neurons do not express VGluT1 (Oliveira *et al.*, 2003; Todd *et al.*, 2003; Morris *et al.*, 2005; Brumovsky *et al.*, 2007) or VGluT3 (Morris *et al.*, 2005; Seal *et al.*, 2009; Draxler *et al.*, 2014). There are inconsistent reports of whether CGRP neurons express VGluT2, with some reporting no colocalisation (Morris *et al.*, 2005; Clarke *et al.*, 2011) and others reporting colocalisation (Todd *et al.*, 2003; Brumovsky *et al.*, 2007). Regardless, it has been demonstrated that CGRP expressing neurons lack the protein machinery required for vesicular release of glutamate (Morris *et al.*, 2005). Therefore, it is highly unlikely that CGRP<sup>+</sup>SP<sup>-</sup> neurons utilize glutamate. Others have demonstrated that CGRP neurons also express other peptides: including galanin (GAL) and vasoactive intestinal peptide (VIP; Ju *et al.*, 1987; Hökfelt *et al.*, 1993) (Ju *et al.*, 1987; Hökfelt *et al.*, 1993). Therefore it is possible that CGRP<sup>+</sup>SP<sup>-</sup> neurons utilise another peptide neurotransmitter.

We have also demonstrated that these CGRP<sup>+</sup>SP<sup>-</sup> neurons were distinct from CGRP<sup>+</sup>SP<sup>+</sup> neurons in ways unrelated to SP expression. The soma sizes of

CGRP<sup>+</sup>SP<sup>-</sup> neurons were larger and their central terminations in the dorsal horn were present in deeper lamina than CGRP<sup>+</sup>SP<sup>+</sup> neurons. Hence, it is possible that CGRP<sup>+</sup>SP<sup>-</sup> neurons are distinct from CGRP<sup>+</sup>SP<sup>+</sup> neurons in other ways as well.

CGRP neurons express the capsaicin receptor transient receptor potential vanilloid type 1 (TRPV1; previously VR1: vanilloid receptor). TRPV1 is expressed by small diameter capsaicin sensitive nociceptors (Caterina *et al.*, 1997; Tominaga *et al.*, 1998) and has a clear role in detecting noxious heat (Caterina *et al.*, 1997) and thermal hyperalgesia under inflammation and injury (Caterina *et al.*, 2000; Davis *et al.*, 2000; Levine & Alessandri-Haber, 2007). It is well characterised that CGRP and SP coexist in capsaicin sensitive afferents (Gibbins *et al.*, 1985; Lundberg *et al.*, 1985; Skofitsch & Jacobowitz, 1985; Franco-Cereceda *et al.*, 1987). However, some have noted that not all CGRP neurons are capsaicin sensitive afferents. Guo and colleagues (1999) have demonstrated that not all CGRP neurons contain TRPV1, and Matsuyama and colleagues (1986) demonstrated that the CGRP terminals in lamina IV/V of the spinal dorsal horn are not capsaicin sensitive. Hence, it is not unreasonable to suggest that while CGRP<sup>+</sup>SP<sup>+</sup> neurons most likely express TRPV1, the large diameter CGRP<sup>+</sup>SP<sup>-</sup> neurons may not.

In the previous chapter, we suggested that CGRP<sup>+</sup>SP<sup>-</sup> neurons might be myelinated A-fibre neurons due to their larger size compared to CGRP<sup>+</sup>SP<sup>+</sup> neurons. However, cell size alone is an unreliable indicator as to whether neurons are myelinated or unmyelinated (Hoheisel & Mense, 1987). Neurofilament-200 kDa (NF200, or NF-H; heavy/high neurofilament) is exclusively expressed in neurons with myelinated A-fibre afferents (Lawson & Waddell, 1991), and hence, a more reliable indicator on the myelination of a neuron. CGRP neurons have been demonstrated both express NF200 and possess action potential velocities in the A-fibre range (McCarthy & Lawson, 1990; Ruscheweyh *et al.*, 2007). SP neurons have been shown to lack NF200 and possess action potential velocities in the C-fibre range (McCarthy & Lawson, 1989). Therefore, it is likely that the small diameter CGRP<sup>+</sup>SP<sup>+</sup> neurons will lack NF200 express while the large diameter CGRP<sup>+</sup>SP<sup>-</sup> neurons most likely express NF200.

To further distinguish CGRP<sup>+</sup>SP<sup>-</sup> neurons from CGRP<sup>+</sup>SP<sup>+</sup> neurons, we have used multiple labeling immunohistochemistry to determine the presence of the

Chapter 4: Neurochemical profile of CGRP<sup>+</sup>SP<sup>-</sup> neurons  
neurochemical markers TRPV1 and NF200 in these neurons. TRPV1 was used to distinguish the capsaicin sensitive nociceptors and NF200 was used to distinguish the myelinated neurons. We also used multiple labeling immunohistochemistry to detect the neuropeptides galanin and VIP that have been previously identified in CGRP neurons to determine their presence in CGRP<sup>+</sup>SP<sup>-</sup> neurons.



## 4.2 Materials and Methods

DRG samples were taken from cervical (C7), thoracic (T5), lumbar (L4) and sacral (S3) levels. Samples were fixed, processed through DMSO, embedded in PEG and sectioned using a microtome.

Sections were then triple labelled with anti-CGRP raised in a goat; polyclonal or monoclonal anti-SP raised in rabbit and rat, respectively; and one of either anti-TRPV1 raised in rabbit, and anti-NF200 raised in mouse, anti-GAL raised in rabbit, and anti-VIP raised in rat (see Table 4.1 for more information).

**Table 4.1: Primary and secondary antisera**

Primary antisera			
Antigen	Host	Dilution	Source
CGRP	goat	1:1000	code1780, Arnel, New York, USA
SP	rabbit	1:2000	Incstar (now Immunostar), Wisconsin, USA
SP	rat	1:600	clone NC1/34HL, Sera-Lab, West Sussex, UK
TRPV1	rabbit	1:500	Alomone Labs, Jerusalem, ISR
NF200	mouse	1:2000	Sigma-Aldrich, Missouri, USA
VIP	rabbit	1:1000	Incstar
Galanin	rabbit	1:3000	Peninsula Lab, California, USA
Secondary antisera and streptavidin conjugates			
Cy5 anti sheep IgG	donkey	1:50	Jackson ImmunoResearch, Pennsylvania, USA
FITC anti rabbit IgG	donkey	1:100	Jackson ImmunoResearch
FITC anti rat IgG	donkey	1:50	Jackson ImmunoResearch
Cy3 anti rabbit IgG	donkey	1:100	Jackson ImmunoResearch
Cy3 anti mouse IgG	donkey	1:100	Jackson ImmunoResearch

The specificity of anti-CGRP raised in goat; polyclonal and monoclonal anti-SP raised in rabbit and rat, respectively, have been previously demonstrated in the previous chapter. The specificity of anti-neurofilament 200 (NF200) raised in mice (Tam Tam *et al.*, 2011), anti-GAL raised in rabbit (Morris *et al.*, 1992; Holmgren *et al.*, 1994), and anti-VIP raised in rabbit (Jobling & Gibbins, 1999; Morris *et al.*, 2005) have all been previously demonstrated by our group. The specificity of anti-TRPV1 raised in rabbit was verified with pre-absorption using the corresponding TRPV1 control antigen.

Widefield images of DRG sections were taken with an Olympus BX50 epifluorescence microscope with a 20x objective. Widefield images of DRG were, imported to ImageJ to determine the presence of IR and soma cross-sectional area of sensory neurons. Data were then displayed as mean $\pm$ SEM or total percentages and

the statistical significance was determined using RM-ANOVA with post hoc BMC correction with 95% confidence limits or Chi-Square analysis.

## 4.3 Results

---

### Most CGRP<sup>+</sup>SP<sup>-</sup> neurons lacked TRPV1

TRPV1-IR was detected in neuronal somata and fibres in dorsal root ganglia (DRG) of all spinal levels (C7, T5, L4 and S3). Cytoplasmic TRPV1-IR was uniformly intense in small to medium sized neurons (50-500  $\mu\text{m}^2$ ; Figure 4.1A). There was no correlation between the intensity of TRPV1-IR and the soma size of the neurons (Linear correlation:  $r = 0.03$ ;  $p < 0.0001$ ; Figure 4.2). TRPV1-IR occurred in DRG neurons containing CGRP-IR with SP-IR (CGRP<sup>+</sup>SP<sup>+</sup>TRPV1<sup>+</sup>), CGRP-IR without SP-IR (CGRP<sup>+</sup>SP<sup>-</sup>TRPV1<sup>+</sup>) and neurons lacking CGRP-IR or SP-IR (CGRP<sup>-</sup>SP<sup>-</sup>TRPV1<sup>+</sup>; Figure 4.1).

Overall, TRPV1-IR was detected in neuronal somata in all DRG investigated. TRPV1-IR was present in 46% (1301/2811) of DRG neurons, and there was no difference between the spinal levels (Chi-Square:  $\chi^2_3 = 1$ ,  $p = 0.8$ ;  $N = 5$  animals,  $n = 2811$  neurons; Figure 4.3). TRPV1-IR was expressed in neurons with a mean soma size of  $240 \pm 3 \mu\text{m}^2$  and there was no difference in the soma size of these neurons between the DRG of different levels (ANOVA:  $F_{(2,1297)} = 1$ ,  $p = 0.4$ ,  $N = 5$  animals,  $n = 1301$  neurons; Figure 4.4).

The majority (81%, 1060/1301) of TRPV1-IR neurons contained CGRP-IR. A lower proportion of TRPV1-IR neurons contained CGRP-IR in C7 DRG and higher proportions contained CGRP-IR in L4 and S3 DRG than compared to the other levels (Chi-Square:  $\chi^2_3 = 17$ ,  $p = 0.001$ ;  $N = 5$  animals;  $n = 1301$  neurons). Conversely, the majority (67%; 1060/1574) of CGRP-IR neurons contained TRPV1-IR and this was consistent through the levels (Chi-Square:  $\chi^2_3 = 0.4$ ,  $p = 0.9$ ;  $N = 5$  animals;  $n = 1574$  neurons). Almost all (96%; 706/732) CGRP<sup>+</sup>SP<sup>+</sup> neurons had TRPV1-IR and this was consistent through the levels (Chi-Square:  $\chi^2_3 = 0.1$ ,  $p = 1$ ;  $N = 5$  animals;  $n = 732$  neurons; Figure 4.5). In contrast, only 42% (354/842) of the CGRP<sup>+</sup>SP<sup>-</sup> neurons contained TRPV1-IR. A lower proportion of CGRP<sup>+</sup>SP<sup>-</sup> neurons contained TRPV1-IR in C7 DRG and a higher proportion contained TRPV1-IR in T5 DRG compared to the other levels (Chi-Square:  $\chi^2_3 = 9$ ,  $p = 0.03$ ;  $N = 5$  animals;  $n = 842$  neurons; Figure 4.5). The larger CGRP<sup>+</sup>SP<sup>-</sup> neurons lacked TRPV1. CGRP<sup>+</sup>SP<sup>-</sup>TRPV1<sup>+</sup> neurons were the largest, and CGRP<sup>+</sup>SP<sup>-</sup>TRPV1<sup>+</sup> neurons were larger than

CGRP<sup>+</sup>SP<sup>+</sup>TRPV1<sup>+</sup> neurons (RM-AVONA:  $F_{(3,1536)} = 467$ ,  $p < 0.0001$ ;  $N = 5$  animals,  $n = 1574$  neurons; Figure 4.6)

CGRP<sup>+</sup>SP<sup>-</sup>TRPV1<sup>-</sup> neuronal somata were largest at the C7 and L4 level, and the neurons of T5 were larger than the neurons of S3 (RM-AVONA:  $F_{(6,1536)} = 13$ ,  $p < 0.0001$ ;  $N = 5$  animals,  $n = 1574$  neurons; Figure 4.6). CGRP<sup>+</sup>SP<sup>-</sup>TRPV1<sup>+</sup> were largest at C7, and CGRP<sup>+</sup>SP<sup>+</sup>TRPV1<sup>+</sup> neurons were largest at T5 compared to the other levels (RM-ANOVA:  $F_{(6,1536)} = 13$ ,  $p < 0.0001$ ;  $N = 5$  animals,  $n = 1574$  neurons; Figure 4.6).

### ***TRPV1, CGRP and SP in C7 DRG***

In C7 ( $N = 5$  animals,  $n = 685$  neurons), TRPV1-IR was detected in 43% (297/685 neurons) of DRG neurons. Most (77%; 230/297) of the TRPV1-IR neurons contained CGRP-IR. Conversely, 68% (230/337) of CGRP-IR neurons contained TRPV1-IR. Almost all (95%, 190/201) CGRP<sup>+</sup>SP<sup>+</sup> neurons contained TRPV1-IR, whereas, only 29% (40/139) of CGRP<sup>+</sup>SP<sup>-</sup> neurons contained TRPV1-IR (Figure 4.7).

CGRP<sup>+</sup>SP<sup>-</sup>TRPV1<sup>-</sup> neurons ( $511 \pm 13 \mu\text{m}^2$ ) were the largest of the CGRP-IR neurons, and CGRP<sup>+</sup>SP<sup>-</sup>TRPV1<sup>+</sup> neurons ( $331 \pm 13 \mu\text{m}^2$ ) were larger than CGRP<sup>+</sup>SP<sup>+</sup>TRPV1<sup>+</sup> neurons ( $216 \pm 20 \mu\text{m}^2$ ; ANOVA:  $F_{(2,326)} = 168$ ,  $p < 0.0001$ ,  $N = 5$  animals,  $n = 328$  neurons; Figure 4.8).

### ***TRPV1, CGRP and SP in T5 DRG***

In T5 ( $N = 5$  animals,  $n = 670$  neurons), TRPV1-IR was detected in 52% (349/670) of DRG neurons. Most (75%; 262/349) of the TRPV1-IR neurons contained CGRP-IR. Conversely, most (71%; 262/369) of CGRP-IR neurons contained TRPV1-IR. Almost all (98%, 129/131) CGRP<sup>+</sup>SP<sup>+</sup> neurons contained TRPV1-IR, whereas, 56% (133/238) of CGRP<sup>+</sup>SP<sup>-</sup> neurons contained TRPV1-IR (Figure 4.7).

CGRP<sup>+</sup>SP<sup>-</sup>TRPV1<sup>-</sup> neurons ( $463 \pm 14 \mu\text{m}^2$ ) were the largest of the CGRP-IR neurons, and CGRP<sup>+</sup>SP<sup>-</sup>TRPV1<sup>+</sup> neurons ( $284 \pm 12 \mu\text{m}^2$ ) were larger than CGRP<sup>+</sup>SP<sup>+</sup>TRPV1<sup>+</sup> neurons ( $219 \pm 12 \mu\text{m}^2$ ; ANOVA:  $F_{(2,364)} = 92$ ,  $p < 0.0001$ ,  $N = 5$  animals,  $n = 367$  neurons; Figure 4.8).

***TRPV1, CGRP and SP in L4 DRG***

In L4 (N = 5 animals, n = 845 neurons), TRPV1-IR was detected in 46% (387/845) of DRG neurons. Most (86%; 332/387) of the TRPV1-IR neurons contained CGRP-IR. Conversely, most (67%; 332/495) of CGRP-IR neurons contained TRPV1-IR. Almost all (97%; 230/237) CGRP<sup>+</sup>SP<sup>+</sup> neurons contained TRPV1-IR, whereas, only 40% (102/258) of CGRP<sup>+</sup>SP<sup>-</sup> neurons contained TRPV1-IR (Figure 4.7).

The soma size of CGRP<sup>+</sup>SP<sup>-</sup>TRPV1<sup>-</sup> neurons ( $532 \pm 11 \mu\text{m}^2$ ) were the largest of the CGRP-IR neurons, and CGRP<sup>+</sup>SP<sup>-</sup>TRPV1<sup>+</sup> neurons ( $258 \pm 14 \mu\text{m}^2$ ) were larger than CGRP<sup>+</sup>SP<sup>+</sup>TRPV1<sup>+</sup> neurons ( $214 \pm 9 \mu\text{m}^2$ ; ANOVA:  $F_{(2,485)} = 257$ ,  $p < 0.0001$ , N = 5 animals, n = 488 neurons; Figure 4.8).

***TRPV1, CGRP and SP in S3 DRG***

In S3 (N = 5 animals, n = 611 neurons), TRPV1-IR was detected in 44% (268/611) of DRG neurons. Most (88%; 236/268) of the TRPV1-IR neurons contained CGRP-IR. Conversely, most (64%; 236/371) of CGRP-IR neurons contained TRPV1-IR. Almost all (96%; 157/164) CGRP<sup>+</sup>SP<sup>+</sup> neurons contained TRPV1-IR, whereas, only 39% (79/207) of CGRP<sup>+</sup>SP<sup>-</sup> neurons contained TRPV1-IR (Figure 4.7).

CGRP<sup>+</sup>SP<sup>-</sup>TRPV1<sup>-</sup> neurons ( $412 \pm 13 \mu\text{m}^2$ ) were the largest of the CGRP-IR neurons. There was no difference between the soma size of CGRP<sup>+</sup>SP<sup>-</sup>TRPV1<sup>+</sup> neurons ( $232 \pm 12 \mu\text{m}^2$ ) and CGRP<sup>+</sup>SP<sup>+</sup>TRPV1<sup>+</sup> neurons ( $212 \pm 12 \mu\text{m}^2$ ; RMANOVA:  $F_{(2,361)} = 70$ ,  $p < 0.0001$ , N = 5 animals, n = 364 neurons; Figure 4.8).

**Most CGRP<sup>+</sup>SP<sup>-</sup> neurons expressed NF200**

NF200-IR was detected in neuronal somata and fibres DRG of all spinal levels (C7, T5, L4 and S3). Cytoplasmic NF200-IR was uniformly intense in small to large sized neurons ( $50\text{-}1000 \mu\text{m}^2$ ; Figure 4.9). There was no correlation between the intensity of NF200-IR and the soma size of the neurons (Linear correlation:  $r = 0.06$ ,  $p < 0.0001$ ; N = 5 animals, n = 1562 neurons; Figure 4.10). NF200-IR occurred in DRG neurons containing CGRP-IR with SP-IR (CGRP<sup>+</sup>SP<sup>+</sup>NF200<sup>+</sup>), CGRP-IR without SP-IR (CGRP<sup>+</sup>SP<sup>-</sup>NF200<sup>+</sup>) and neurons lacking CGRP-IR or SP-IR (CGRP<sup>-</sup>SP<sup>-</sup>NF200<sup>+</sup>; Figure 4.9).

Overall, NF200-IR was detected in neuronal somata in all DRG investigated. NF200-IR was present in 71% (1562/2196) of DRG neurons, and there was no difference

between the DRG levels (Chi-Square:  $\chi_3^2 = 1$ ,  $p = 0.8$ ;  $N = 5$  animals;  $n = 2196$ ; Figure 4.11). NF200-IR was expressed in neurons with a mean soma size of  $518 \pm 5 \mu\text{m}^2$ . NF200-IR neurons were largest at L4, and at C7 NF200-IR neurons were larger than T5 and S3 NF200-IR neurons (ANOVA:  $F_{(3,1558)} = 44$ ,  $p < 0.0001$ ,  $N = 5$  animals,  $n = 1562$  neurons; Figure 4.12).

Half (49%; 773/1562) of the NF200-IR neurons contained CGRP-IR and there was no difference in proportions of NF200-IR neurons containing CGRP-IR between levels (Chi-Square:  $\chi_3^2 = 0.2$ ,  $p = 1$ ;  $N = 5$  animals,  $n = 1562$  neurons). Conversely, most (66%; 773/1174) CGRP-IR neurons contained NF200-IR and this was consistent through the levels (Chi-Square:  $\chi_3^2 = 3$ ,  $p = 0.4$ ;  $N = 5$  animals;  $n = 1174$  neurons). Half (50%; 324/654) of the CGRP<sup>+</sup>SP<sup>+</sup> neurons had NF200-IR. A higher proportion of CGRP<sup>+</sup>SP<sup>+</sup> neurons had NF200-IR in T5 DRG and a lower proportion of CGRP<sup>+</sup>SP<sup>+</sup> neurons had NF200-IR in L4 DRG compared to other levels (Chi-Square:  $\chi_3^2 = 9$ ,  $p = 0.04$ ;  $N = 5$  animals,  $n = 654$  neurons; Figure 4.13). In contrast, the majority (86%; 449/520) of CGRP<sup>+</sup>SP<sup>-</sup> neurons contained NF200-IR and there was no difference in proportions of CGRP<sup>+</sup>SP<sup>-</sup> neurons contained NF200-IR between levels (Chi-Square:  $\chi_3^2 = 1$ ,  $p = 0.8$ ;  $N = 5$  animals,  $n = 520$  neurons; Figure 4.13). The CGRP neurons that contained NF200 were larger than those that did not; CGRP<sup>+</sup>SP<sup>-</sup>NF200<sup>+</sup> were larger than CGRP<sup>+</sup>SP<sup>+</sup>NF200<sup>+</sup>, and CGRP<sup>+</sup>SP<sup>-</sup>NF200<sup>-</sup> neurons were larger than CGRP<sup>+</sup>SP<sup>+</sup>NF200<sup>-</sup> neurons (RM-ANOVA:  $F_{(3,1158)} = 173$ ,  $p < 0.0001$ ;  $N = 5$  animals,  $n = 1174$  neurons; Figure 4.14)

The mean soma size of CGRP<sup>+</sup>SP<sup>-</sup>NF200<sup>+</sup> neurons was largest at L4, and mean soma size of CGRP<sup>+</sup>SP<sup>+</sup>NF200<sup>-</sup> and CGRP<sup>+</sup>SP<sup>-</sup>NF200<sup>-</sup> were largest at S3 compared to the other levels (RM-ANOVA:  $F_{(9,1158)} = 8$ ,  $p < 0.0001$ ;  $N = 5$  animals,  $n = 1174$  neurons; Figure 4.14). There was no difference in the size of CGRP<sup>+</sup>SP<sup>+</sup>NF200<sup>+</sup> neurons between the spinal levels.

### ***NF200, CGRP and SP in C7 DRG***

In C7 ( $N = 5$  animals,  $n = 743$  neurons), NF200-IR was detected in 73% (540/743) of DRG neurons. Half (49%; 266/540) of the NF200-IR neurons contained CGRP-IR. Conversely, most (69%; 266/386) CGRP-IR neurons contained NF200-IR. The majority (87%; 144/165) of CGRP<sup>+</sup>SP<sup>-</sup> neurons contained NF200-IR, whereas, 57% (122/221) of CGRP<sup>+</sup>SP<sup>+</sup> neurons contained NF200-IR (Figure 4.15).

As expected, the CGRP<sup>+</sup>SP<sup>+</sup> and CGRP<sup>+</sup>SP<sup>-</sup> neurons that expressed NF200-IR (400±13 μm<sup>2</sup> and 511±12 μm<sup>2</sup>, respectively) were larger than the CGRP<sup>+</sup>SP<sup>+</sup> and CGRP<sup>+</sup>SP<sup>-</sup> neurons that lacked NF200-IR (202±15 μm<sup>2</sup> and 236±32 μm<sup>2</sup>, respectively; ANOVA:  $F_{(3,382)} = 92$ ,  $p < 0.0001$ ;  $N = 5$  animals,  $n = 386$  neurons; Figure 4.16). While CGRP<sup>+</sup>SP<sup>-</sup>NF200<sup>+</sup> neurons were larger than CGRP<sup>+</sup>SP<sup>+</sup>NF200<sup>+</sup> neurons, there was no difference between the sizes of CGRP<sup>+</sup>SP<sup>-</sup>NF200<sup>+</sup> and CGRP<sup>+</sup>SP<sup>-</sup>NF200<sup>-</sup> neurons.

#### ***NF200, CGRP and SP in T5 DRG***

In T5 ( $N = 5$  animals,  $n = 503$  neurons), NF200-IR was detected in 69% (347/503) of DRG neurons. Half (50%; 173/347) of the NF200-IR neurons contained CGRP-IR. Conversely, most (75%; 173/231) CGRP-IR neurons contained NF200-IR. The majority (80%, 116/145) of CGRP<sup>+</sup>SP<sup>-</sup> neurons contained NF200-IR, whereas, 66% (57/86) of CGRP<sup>+</sup>SP<sup>+</sup> neurons contained NF200-IR (Figure 4.15).

CGRP<sup>+</sup>SP<sup>+</sup> and CGRP<sup>+</sup>SP<sup>-</sup> neurons that expressed NF200-IR (433±20 μm<sup>2</sup> and 441±14 μm<sup>2</sup>, respectively) were larger than the CGRP<sup>+</sup>SP<sup>+</sup> and CGRP<sup>+</sup>SP<sup>-</sup> neurons that lacked NF200-IR (231±28 μm<sup>2</sup> and 238±28 μm<sup>2</sup>, respectively; ANOVA:  $F_{(3,227)} = 269$ ,  $p < 0.0001$ ;  $N = 5$  animals,  $n = 231$  neurons; Figure 4.16). There was no difference between the sizes of CGRP<sup>+</sup>SP<sup>-</sup>NF200<sup>+</sup> and CGRP<sup>+</sup>SP<sup>+</sup>NF200<sup>+</sup> neurons, nor was there a difference between the sizes of CGRP<sup>+</sup>SP<sup>-</sup>NF200<sup>+</sup> and CGRP<sup>+</sup>SP<sup>-</sup>NF200<sup>-</sup> neurons.

#### ***NF200, CGRP and SP in L4 DRG***

In L4 ( $N = 5$  animals,  $n = 530$  neurons), NF200-IR was detected in 76% (404/530) of DRG neurons. Half (48%; 194/404) of the NF200-IR neurons contained CGRP-IR. Conversely, most (63%; 194/306) CGRP-IR neurons contained NF200-IR. The majority (94%, 121/129) of CGRP<sup>+</sup>SP<sup>-</sup> neurons contained NF200-IR, whereas, 41% (73/177) of CGRP<sup>+</sup>SP<sup>+</sup> neurons contained NF200-IR (Figure 4.15).

CGRP<sup>+</sup>SP<sup>+</sup> and CGRP<sup>+</sup>SP<sup>-</sup> neurons that expressed NF200-IR (464±18 μm<sup>2</sup> and 595±14 μm<sup>2</sup>, respectively) were larger than the CGRP<sup>+</sup>SP<sup>+</sup> and CGRP<sup>+</sup>SP<sup>-</sup> neurons that lacked NF200-IR (226±15 μm<sup>2</sup> and 240±54 μm<sup>2</sup>, respectively; ANOVA:  $F_{(3,302)} = 116$ ,  $p < 0.0001$ ;  $N = 5$  animals,  $n = 306$  neurons; Figure 4.16). While CGRP<sup>+</sup>SP<sup>-</sup>NF200<sup>+</sup> were larger than CGRP<sup>+</sup>SP<sup>+</sup>NF200<sup>+</sup>, there was no difference between the sizes of CGRP<sup>+</sup>SP<sup>-</sup>NF200<sup>+</sup> and CGRP<sup>+</sup>SP<sup>-</sup>NF200<sup>-</sup> neurons.

### ***NF200, CGRP and SP in S3 DRG***

In S3 (N = 5 animals, n = 420 neurons), NF200-IR was detected in 65% (271/420) of DRG neurons. Half (52%; 140/271) of the NF200-IR neurons contained CGRP-IR. Conversely, more than half (56%; 140/251) of the CGRP-IR neurons contained NF200-IR. The majority (84%, 68/81) of CGRP<sup>+</sup>SP<sup>-</sup> neurons contained NF200-IR, whereas, 42% (72/170) of CGRP<sup>+</sup>SP<sup>+</sup> neurons contained NF200-IR (Figure 4.15).

CGRP<sup>+</sup>SP<sup>+</sup> and CGRP<sup>+</sup>SP<sup>-</sup> neurons that expressed NF200-IR (399±19 μm<sup>2</sup> and 488±19 μm<sup>2</sup>, respectively) were larger than the CGRP<sup>+</sup>SP<sup>+</sup> neurons that lacked NF200-IR (320±16 μm<sup>2</sup>, respectively; ANOVA:  $F_{(3,247)} = 15$ ,  $p < 0.0001$ ; N = 5 animals, n = 251 neurons; Figure 4.16). While CGRP<sup>+</sup>SP<sup>-</sup>NF200<sup>+</sup> neurons were larger than CGRP<sup>+</sup>SP<sup>+</sup>NF200<sup>+</sup>, there was no difference between the sizes of CGRP<sup>+</sup>SP<sup>-</sup>NF200<sup>+</sup> and CGRP<sup>+</sup>SP<sup>-</sup>NF200<sup>-</sup> neurons.

### **Most CGRP<sup>+</sup>SP<sup>-</sup> neurons lacked Galanin**

GAL-IR was detected in neuronal somata and fibres in dorsal root ganglia (DRG) of all spinal levels (C7, T5, L4 and S3; Figure 4.17). Cytoplasmic GAL-IR was uniformly intense in small to medium sized neurons (50-500 μm<sup>2</sup>; Figure 4.17A). There was no correlation between the intensity of GAL-IR and the soma size of the neurons (Linear correlation:  $r = 0.08$ ,  $p < 0.0001$ ; N = 3 animals, n = 342 neurons Figure 4.18). GAL-IR occurred exclusively in DRG neurons containing CGRP-IR with SP-IR (CGRP<sup>+</sup>SP<sup>+</sup>GAL<sup>+</sup>; Figure 4.17).

Overall, GAL-IR was detected in neuronal somata in all DRG investigated. GAL-IR was present in 39% (342/1318) of DRG neurons. A lower proportion of DRG neurons contained GAL-IR in C7 and T5 DRG and a higher proportion contained GAL-IR in S3 DRG compared to other levels (Chi-Square:  $\chi^2_3 = 23$ ,  $p < 0.0001$ ; N = 3 animals, n = 1318 neurons; Figure 4.19). GAL-IR was expressed in neurons with a mean soma size of 283±8 μm<sup>2</sup>. GAL-IR neurons were larger in S3 DRG than compared to GAL-IR neurons in C7 and L4 DRG, and GAL-IR neurons were larger in T5 DRG than C7 DRG ( $F_{(3,338)} = 12$ ,  $p < 0.0001$ ; N = 3 animals, n = 342 neurons; Figure 4.20).

Virtually all (98%, 337/342) GAL-IR neurons contained CGRP-IR and there was no difference between proportions of GAL-IR neurons containing CGRP-IR in the DRG

of different levels (Chi-Square:  $\chi_3^2 = 0.1$ ,  $p = 1$ ,  $N = 3$  animals,  $n = 268$  neurons). Conversely, 40% (337/837) CGRP-IR neurons contained GAL-IR. CGRP-IR neurons containing GAL-IR were more prominent in S3 DRG and less prominent in C7 and T5 DRG than other levels (Chi-Square:  $\chi_3^2 = 18$ ,  $p < 0.0001$ ;  $N = 3$  animals;  $n = 837$  neurons). Most (73%; 325/444) CGRP<sup>+</sup>SP<sup>+</sup> neurons had GAL-IR. A lower proportion of CGRP<sup>+</sup>SP<sup>+</sup> neurons had GAL-IR in C7 and T5 DRG, and a higher proportion of CGRP<sup>+</sup>SP<sup>+</sup> neurons had GAL-IR in S3 DRG (Chi-Square:  $\chi_3^2 = 15$ ,  $p = 0.002$ ,  $N = 3$  animals,  $n = 444$  neurons; Figure 4.21). Almost no (3%; 12/393) CGRP<sup>+</sup>SP<sup>-</sup> neurons contained GAL-IR and there was no difference in this proportion between spinal levels (Chi-Square:  $\chi_3^2 = 1$ ,  $p = 0.9$ ,  $N = 3$  animals,  $n = 444$  neurons; Figure 4.21).

At all spinal levels, CGRP<sup>+</sup>SP<sup>-</sup>GAL<sup>-</sup> neurons were the largest and CGRP<sup>+</sup>SP<sup>+</sup>GAL<sup>-</sup> neurons were larger than CGRP<sup>+</sup>SP<sup>+</sup>GAL<sup>+</sup> neurons (RM-ANOVA:  $F_{(2,810)} = 174$ ,  $p < 0.0001$ ;  $N = 5$  animals,  $n = 821$  neurons; Figure 4.22). S3 DRG lacked CGRP<sup>+</sup>SP<sup>+</sup>GAL<sup>-</sup> neurons, but CGRP<sup>+</sup>SP<sup>-</sup>GAL<sup>-</sup> neurons were still larger than CGRP<sup>+</sup>SP<sup>+</sup>GAL<sup>+</sup> neurons (ANOVA:  $F_{(2,219)} = 92$ ,  $p < 0.0001$ ,  $N = 3$  animals,  $n = 221$  neurons). CGRP<sup>+</sup>SP<sup>-</sup>GAL<sup>-</sup> neurons were larger in L4 DRG than in C7 DRG ( $F_{(3,810)} = 9$ ,  $p < 0.0001$ ;  $N = 5$  animals,  $n = 821$  neurons; Figure 4.22). There was no difference in the size of CGRP<sup>+</sup>SP<sup>-</sup>GAL<sup>-</sup> or CGRP<sup>+</sup>SP<sup>+</sup>GAL<sup>+</sup> neurons between DRG of different levels.

### ***GAL, CGRP and SP in C7 DRG***

In C7 ( $N = 3$  animals,  $n = 336$  neurons), GAL-IR was detected in 17% (56/336) of DRG neurons. All (100%; 56/56) GAL-IR neurons contained CGRP-IR. Conversely, a third (30%; 56/187) of CGRP-IR neurons contained GAL-IR. Most (59%; 53/90) of CGRP<sup>+</sup>SP<sup>+</sup> neurons contained GAL-IR, whereas, very few (3%; 3/97) CGRP<sup>+</sup>SP<sup>-</sup> neurons contained GAL-IR (Figure 4.23).

CGRP<sup>+</sup>SP<sup>-</sup> neurons without GAL-IR ( $457 \pm 23 \mu\text{m}^2$ ) were larger than CGRP<sup>+</sup>SP<sup>+</sup> neurons expressing GAL-IR and CGRP<sup>+</sup>SP<sup>+</sup> neurons lacking GAL-IR ( $235 \pm 28 \mu\text{m}^2$  and  $203 \pm 24 \mu\text{m}^2$ , respectively; ANOVA:  $F_{(2,181)} = 45$ ,  $p < 0.0001$ ,  $N = 3$  animals,  $n = 184$  neurons; Figure 4.24). There was no difference between the mean soma size of CGRP<sup>+</sup>SP<sup>+</sup> neurons express or lacking GAL-IR.

### ***GAL, CGRP and SP in T5 DRG***

In T5 (N = 3 animals, n = 348 neurons), GAL-IR was detected in 15% (54/348) of DRG neurons. Virtually all (98%; 53/54) GAL-IR neurons contained CGRP-IR. Conversely, a third (27%; 53/194) of CGRP-IR neurons contained GAL-IR. Half (55%; 49/88) of CGRP<sup>+</sup>SP<sup>+</sup> neurons contained GAL-IR, whereas, very few (4%; 4/106) CGRP<sup>+</sup>SP<sup>-</sup> neurons contained GAL-IR (Figure 4.23).

CGRP<sup>+</sup>SP<sup>-</sup> neurons without GAL-IR ( $478 \pm 18 \mu\text{m}^2$ ) were larger than CGRP<sup>+</sup>SP<sup>+</sup> neurons expressing GAL-IR and CGRP<sup>+</sup>SP<sup>+</sup> neurons lacking GAL-IR ( $272 \pm 26 \mu\text{m}^2$  and  $313 \pm 29 \mu\text{m}^2$ , respectively; ANOVA:  $F_{(2,187)} = 26$ ,  $p < 0.0001$ , N = 3 animals, n = 190 neurons; Figure 4.24). There was no difference between the mean soma size of CGRP<sup>+</sup>SP<sup>+</sup> neurons expressing or lacking GAL-IR.

### ***GAL, CGRP and SP in L4 DRG***

In L4 (N = 3 animals, n = 334 neurons), GAL-IR was detected in 27% (90/334) of DRG neurons. The majority (98%; 88/90) of GAL-IR neurons contained CGRP-IR. Conversely, 39% (88/228) of CGRP-IR neurons contained GAL-IR. Most (69%; 86/125) CGRP<sup>+</sup>SP<sup>+</sup> neurons contained GAL-IR, whereas, no (1%; 2/103) CGRP<sup>+</sup>SP<sup>-</sup> neurons contained GAL-IR (Figure 4.23).

CGRP<sup>+</sup>SP<sup>-</sup> neurons without GAL-IR ( $562 \pm 19 \mu\text{m}^2$ ) were larger than CGRP<sup>+</sup>SP<sup>+</sup> neurons expressing GAL-IR and CGRP<sup>+</sup>SP<sup>+</sup> neurons lacking GAL-IR ( $231 \pm 21 \mu\text{m}^2$  and  $380 \pm 37 \mu\text{m}^2$ , respectively; ANOVA:  $F_{(2,223)} = 71$ ,  $p < 0.0001$ , N = 3 animals, n = 226 neurons; Figure 4.24). There was no difference between the mean soma size of CGRP<sup>+</sup>SP<sup>+</sup> neurons express or lacking GAL-IR.

### ***GAL, CGRP and SP in S3 DRG***

In S3 (N = 3 animals, n = 300 neurons), GAL-IR was detected in 61% (142/300) of DRG neurons. Almost all (99%; 140/142) GAL-IR neurons contained CGRP-IR. Conversely, most (61%; 140/228) CGRP-IR neurons contained GAL-IR. Virtually all (96%; 137/142) CGRP<sup>+</sup>SP<sup>+</sup> neurons containing GAL-IR, whereas, near zero (3%; 3/87) CGRP<sup>+</sup>SP<sup>-</sup> neurons contained GAL-IR (Figure 4.23).

CGRP<sup>+</sup>SP<sup>-</sup> neurons without GAL-IR ( $522 \pm 16 \mu\text{m}^2$ ) were larger than CGRP<sup>+</sup>SP<sup>+</sup> neurons expressing GAL-IR ( $323 \pm 13 \mu\text{m}^2$ ; ANOVA:  $F_{(2,219)} = 92$ ,  $p < 0.0001$ , N = 3 animals, n = 221 neurons; Figure 4.24).

## Most CGRP+SP- expressed VIP

VIP-IR was detected in neuronal somata and fibres in dorsal root ganglia (DRG) of all spinal levels (C7, T5, L4 and S3), however the VIP-IR appeared more intense in L4 and S3 compared to C7 and T5. VIP-IR was detected in small to large sized neurons (50 to >500  $\mu\text{m}^2$ ; Figure 4.25C). There was no correlation between the intensity of VIP-IR and the soma size of the neurons (linear correlation:  $r = 0.001$ ,  $p = 0.04$ ; Figure 4.26). VIP-IR occurred in DRG neurons containing CGRP-IR with SP-IR (CGRP<sup>+</sup>SP<sup>+</sup>VIP<sup>+</sup>) and CGRP-IR without SP-IR (CGRP<sup>+</sup>SP<sup>-</sup>VIP<sup>+</sup>; Figure 4.25).

Overall, VIP-IR was detected in neuronal somata in all DRG investigated. VIP-IR was present in a third (30%; 319/1064) of DRG neurons. A lower proportion of DRG neurons contained VIP-IR in C7 and T5 DRG and a higher proportion contained VIP-IR in L4 and S3 DRG compared to other levels (Chi-Square:  $\chi_3^2 = 14$ ,  $p = 0.003$ ;  $N = 3$  animals;  $n = 1064$  neurons; Figure 4.27). VIP-IR was expressed in neurons with a mean soma size of  $378 \pm 11 \mu\text{m}^2$ . VIP-IR neurons were largest in T5 DRG, and VIP-IR neurons were larger in L4 DRG than S3 DRG ( $F_{(3,315)} = 13$ ,  $p < 0.0001$ ;  $N = 3$  animals,  $n = 319$  neurons; Figure 4.28). Virtually all (98%; 313/319) VIP-IR neurons contained CGRP-IR in DRG and there was no difference between proportions of VIP-IR neurons containing CGRP-IR in the DRG of different levels (Chi-Square:  $\chi_3^2 = 0.1$ ,  $p = 1$ ;  $N = 3$  animals,  $n = 319$  neurons). Conversely, half (53%; 313/592) of CGRP-IR neurons contained VIP-IR. CGRP-IR neurons containing VIP-IR were more prominent in L4 and S3 DRG and least prominent in C7 and T5 DRG than other levels (Chi-Square:  $\chi_3^2 = 11$ ,  $p = 0.01$ ;  $N = 3$  animals;  $n = 592$  neurons). The majority (81% 214/265) of CGRP<sup>+</sup>SP<sup>+</sup> neurons had VIP-IR and there was no difference between proportions in the DRG of different levels (Chi-Square:  $\chi_3^2 = 4$ ,  $p = 0.2$ ;  $N = 3$  animals;  $n = 265$  neurons; Figure 4.29). Only a third (30%; 99/327) of CGRP<sup>+</sup>SP<sup>-</sup> neurons contained VIP-IR. A lower proportion of CGRP<sup>+</sup>SP<sup>-</sup> neurons contained VIP-IR in C7 and T5 DRG than compared to L4 and S3 DRG (Chi-Square:  $\chi_3^2 = 14$ ,  $p = 0.004$ ;  $N = 3$  animals;  $n = 327$  neurons; Figure 4.29).

At all levels, CGRP<sup>+</sup>SP<sup>-</sup>VIP<sup>+</sup> neurons were the largest, and CGRP<sup>+</sup>SP<sup>-</sup>VIP<sup>-</sup> neurons were larger than CGRP<sup>+</sup>SP<sup>+</sup>VIP<sup>+</sup> and CGRP<sup>+</sup>SP<sup>+</sup>VIP<sup>-</sup> neurons (ANOVA:  $F_{(2,512)} = 31$ ,  $p < 0.0001$ ;  $N = 3$  animals,  $n = 528$  neurons; Figure 4.30). There was no

difference between the size of CGRP<sup>+</sup>SP<sup>+</sup>VIP<sup>+</sup> and CGRP<sup>+</sup>SP<sup>+</sup>VIP<sup>-</sup> neurons. CGRP<sup>+</sup>SP<sup>+</sup>VIP<sup>+</sup> and CGRP<sup>+</sup>SP<sup>+</sup>VIP<sup>-</sup> were larger in T5 DRG than the other levels and CGRP<sup>+</sup>SP<sup>-</sup>VIP<sup>+</sup> neurons were smaller in S3 DRG than the other levels (ANOVA:  $F_{(3,512)} = 12$ ,  $p < 0.0001$ ;  $N = 3$  animals,  $n = 528$  neurons; Figure 4.30). There was no difference between the sizes of CGRP<sup>+</sup>SP<sup>-</sup>VIP<sup>-</sup> neurons between the levels.

#### ***VIP, CGRP and SP in C7 DRG***

In C7 ( $N = 3$  animals,  $n = 241$  neurons), VIP-IR was detected in 24% (59/241) of DRG neurons. Virtually all (97%; 57/59) VIP-IR neurons contained CGRP-IR. Conversely, approximately half (46%; 57/125) of the CGRP-IR neurons contained VIP-IR. The majority (78%; 38/49) of CGRP<sup>+</sup>SP<sup>+</sup> and a quarter (25%; 19/76) of CGRP<sup>+</sup>SP<sup>-</sup> neurons contained VIP-IR (Figure 4.31).

CGRP<sup>+</sup>SP<sup>-</sup> neurons without VIP-IR ( $457 \pm 23 \mu\text{m}^2$ ) and CGRP<sup>+</sup>SP<sup>-</sup> neurons expressing VIP-IR ( $524 \pm 40 \mu\text{m}^2$ ) were larger than CGRP<sup>+</sup>SP<sup>+</sup> neurons expressing VIP-IR ( $235 \pm 28 \mu\text{m}^2$ ) and CGRP<sup>+</sup>SP<sup>+</sup> neurons lacking VIP-IR ( $203 \pm 24 \mu\text{m}^2$ ; ANOVA:  $F_{(3,121)} = 21$ ,  $p < 0.0001$ ,  $N = 3$  animals,  $n = 125$  neurons; Figure 4.32). There was no difference between the mean soma size of CGRP<sup>+</sup>SP<sup>-</sup> neurons expressing or lacking GAL-IR and no difference between CGRP<sup>+</sup>SP<sup>+</sup> neurons expressing or lacking GAL-IR.

#### ***VIP, CGRP and SP in T5 DRG***

In T5 ( $N = 3$  animals,  $n = 292$  neurons), VIP-IR was detected in 17% (49/292) of DRG neurons. All (100%; 49/49) VIP-IR neurons contained CGRP-IR. Conversely, a third (32%; 49/151) of CGRP-IR neurons contained VIP-IR. Most (64%; 30/47) of CGRP<sup>+</sup>SP<sup>+</sup> and 18% (19/104) of CGRP<sup>+</sup>SP<sup>-</sup> neurons contained VIP-IR (Figure 4.31).

There was no difference in the size of CGRP<sup>+</sup>SP<sup>-</sup> neurons lacking VIP-IR ( $464 \pm 22 \mu\text{m}^2$ ), CGRP<sup>+</sup>SP<sup>-</sup> neurons expressing VIP-IR ( $555 \pm 47 \mu\text{m}^2$ ), CGRP<sup>+</sup>SP<sup>+</sup> neurons expressing VIP-IR ( $467 \pm 37 \mu\text{m}^2$ ), or CGRP<sup>+</sup>SP<sup>+</sup> neurons lacking VIP-IR ( $454 \pm 50 \mu\text{m}^2$ ; ANOVA:  $F_{(3,147)} = 1$ ,  $p = 0.3$ ,  $N = 3$  animals,  $n = 151$  neurons; Figure 4.32).

#### ***VIP, CGRP and SP in L4 DRG***

In L4 ( $N = 3$  animals,  $n = 289$  neurons), VIP-IR was detected in 37% (106/289) of DRG neurons. Virtually all (96%; 102/106) VIP-IR neurons contained CGRP-IR. Conversely, most (63%; 102/162) CGRP-IR neurons contained VIP-IR. Most (87%;

62/71) of CGRP<sup>+</sup>SP<sup>+</sup> and 44% (40/91) of CGRP<sup>+</sup>SP<sup>-</sup> neurons contained VIP-IR (Figure 4.31).

CGRP<sup>+</sup>SP<sup>-</sup> neurons expressing VIP-IR ( $564 \pm 29 \mu\text{m}^2$ ) were the largest, and CGRP<sup>+</sup>SP<sup>-</sup> neurons lacking VIP-IR ( $413 \pm 26 \mu\text{m}^2$ ) were larger than CGRP<sup>+</sup>SP<sup>+</sup> neurons expressing VIP-IR ( $282 \pm 23 \mu\text{m}^2$ ) and CGRP<sup>+</sup>SP<sup>+</sup> neurons lacking VIP-IR ( $255 \pm 61 \mu\text{m}^2$ ; ANOVA:  $F_{(3,158)} = 21$ ,  $p < 0.0001$ ,  $N = 3$  animals,  $n = 162$  neurons; Figure 4.32). There was no difference in soma size between CGRP<sup>+</sup>SP<sup>+</sup> neurons expressing or lacking VIP-IR.

### ***VIP, CGRP and SP in S3 DRG***

In S3 ( $N = 3$  animals,  $n = 242$  neurons), VIP-IR was detected in 43% (105/242) of DRG neurons. All (100%; 105/105) VIP-IR neurons contained CGRP-IR. Conversely, half (55%; 84/154) of CGRP-IR neurons contained VIP-IR. The majority (86%; 84/98) of CGRP<sup>+</sup>SP<sup>+</sup> and 38% (21/56) CGRP<sup>+</sup>SP<sup>-</sup> neurons contained VIP-IR (Figure 4.31).

CGRP<sup>+</sup>SP<sup>-</sup> neurons expressing VIP-IR ( $435 \pm 25 \mu\text{m}^2$ ) and CGRP<sup>+</sup>SP<sup>-</sup> neurons lacking VIP-IR ( $386 \pm 20 \mu\text{m}^2$ ) were larger than CGRP<sup>+</sup>SP<sup>+</sup> neurons expressing VIP-IR ( $282 \pm 13 \mu\text{m}^2$ ) and CGRP<sup>+</sup>SP<sup>+</sup> neurons lacking VIP-IR ( $305 \pm 31 \mu\text{m}^2$ ; ANOVA:  $F_{(3,150)} = 13$ ,  $p < 0.0001$ ,  $N = 3$  animals,  $n = 154$  neurons; Figure 4.32). There was no difference between the mean soma size of CGRP<sup>+</sup>SP<sup>-</sup> neurons expressing or lacking GAL-IR and no difference between CGRP<sup>+</sup>SP<sup>+</sup> neurons expressing or lacking GAL-IR.



## 4.4 Discussion

---

The previous chapter, demonstrated distinct immunohistochemical populations of fibres containing significant levels of CGRP-IR without detectable SP-IR in skin, medium size cell bodies in the DRG, and fibres in lateral lamina I and deep lamina IV/V of the dorsal horn. These neurons were present in the dorsal horn and DRG of all spinal levels. This current chapter set out to determine if CGRP-IR neurons lacking detectable SP-IR could be further distinguished from CGRP-IR neurons with SP-IR using a myriad of immunohistochemical markers.

### **Larger CGRP<sup>+</sup>SP<sup>-</sup> neurons are not capsaicin sensitive nociceptors**

TRPV1 (previously VR1: vanilloid receptor) is most notably activated by the vanilloid compound capsaicin (spicy component of chilli peppers), noxious heat ( $\geq 43^{\circ}\text{C}$ ; Caterina *et al.*, 1997) and is also involved in thermal hyperalgesia under inflammation and injury (Caterina *et al.*, 2000; Davis *et al.*, 2000; Levine & Alessandri-Haber, 2007). Thus, TRPV1 expression in sensory neurons is often used as an indicator that the neurons are capsaicin sensitive nociceptors.

It is already well characterised that TRPV1 is expressed in small to medium sized neurons in DRG (Caterina *et al.*, 1997; Tominaga *et al.*, 1998; Guo *et al.*, 1999). While most TRPV1 neurons are peptidergic, expressing the peptides CGRP and SP (Cavanaugh *et al.*, 2011; McCoy *et al.*, 2012), there are also a small proportion of nonpeptidergic TRPV1 neurons that lack these peptides and bind IB4 (Guo *et al.*, 1999; Michael & Priestley, 1999). This current study has further supported these well-documented findings. TRPV1 expression was detected in both small to medium ( $50\text{-}500\ \mu\text{m}^2$ ) neuronal soma sizes and there was a 74% overlap with CGRP-IR. The TRPV1 neurons that lacked CGRP-IR would most likely bind IB4.

It is also well characterised that the reverse is also true: most, but not all, CGRP-IR neurons express TRPV1 (Cavanaugh *et al.*, 2011; McCoy *et al.*, 2012). This current study supports these findings and demonstrated that 67% of CGRP-IR neurons contained TRPV1. The proportion of CGRP-IR neurons that contained or lacked SP has not yet been characterised with regards to TRPV1 expression. In this study we determined that virtually all (96%) the CGRP<sup>+</sup>SP<sup>+</sup> neurons contained TRPV1, yet

less than half (42%) of the CGRP<sup>+</sup>SP<sup>-</sup> neurons expressed TRPV1. The CGRP<sup>+</sup>SP<sup>-</sup>TRPV1<sup>-</sup> neurons were larger than both the CGRP<sup>+</sup>SP<sup>+</sup>TRPV1<sup>+</sup> and CGRP<sup>+</sup>SP<sup>-</sup>TRPV1<sup>+</sup> neurons. Based on their soma sizes, it is probable that CGRP<sup>+</sup>SP<sup>+</sup>TRPV1<sup>+</sup> neurons were unmyelinated C-fibre nociceptors, CGRP<sup>+</sup>SP<sup>-</sup>TRPV1<sup>+</sup> neurons were likely myelinated A $\delta$ -fibre nociceptors and CGRP<sup>+</sup>SP<sup>-</sup>TRPV1<sup>-</sup> neurons were A $\delta$ /A $\beta$  fibre sensory neurons.

In summary, it appears that CGRP-IR expressing neurons can be split up into three subpopulations: the small capsaicin sensitive CGRP neurons that contain SP, the small capsaicin sensitive CGRP neurons that lack SP, and the larger capsaicin insensitive CGRP neurons that lack SP. Both the CGRP<sup>+</sup>SP<sup>+</sup> and CGRP<sup>+</sup>SP<sup>-</sup> neurons that contained TRPV1 are likely to have some role in nociception, in particular the processing of noxious heat and thermal hyperalgesia. In contrast, the larger CGRP<sup>+</sup>SP<sup>-</sup> neurons that lacked TRPV1 expression may not have a role in nociception.

## **CGRP<sup>+</sup>SP<sup>-</sup> neurons are most likely myelinated**

Neurofilament-200kDa (NF200 or NF-H; heavy/high neurofilament) is a component of the cytoskeleton exclusively expressed myelinated neurons (Lawson & Waddell, 1991). In this current study NF200-IR was detected in small, medium and large neurons but predominately detected in the larger neurons. The soma size of neurons is not a reliable determinant of the neurons conduction velocity (Hoheisel & Mense, 1987). A $\delta$ -fibre neurons units had no significant correlation between soma size and conduction velocity, and C fibre units had a negative correlation (Hoheisel & Mense, 1987). Hence, it is likely that while NF200-IR was detected in neurons with small soma sizes, these neurons are still likely to be myelinated.

CGRP neurons have been demonstrated to express both NF200-IR and possess action potential velocities in the A $\alpha$ , A $\beta$ , A $\delta$  and C-fibre range (McCarthy & Lawson, 1990; Ruscheweyh *et al.*, 2007), while SP neurons possess action potential velocities in only the A $\delta$  fibre and C-fibre range and most lack NF200 expression (McCarthy & Lawson, 1989). Consistent with these findings, this current study detected NF200 in most of the CGRP-IR neurons and in half of SP-IR neurons.

The proportion of CGRP-IR neurons that contained or lacked SP has not yet been characterised with regards to NF200 expression. In this study, we determined that almost all the CGRP<sup>+</sup>SP<sup>-</sup> neurons contained NF200, while only half of the CGRP<sup>+</sup>SP<sup>+</sup> neurons contained NF200. As expected, the CGRP neurons that expressed NF200 were larger than CGRP neurons that lacked NF200. The co-expression of NF200 and the size of the CGRP neurons suggest that the CGRP<sup>+</sup>SP<sup>-</sup> neurons were all myelinated A-fibre neurons, whereas half of the CGRP<sup>+</sup>SP<sup>+</sup> neurons were myelinated A $\delta$ -fibre neurons and the other half were unmyelinated C-fibre neurons, which is consistent with previous studies (McCarthy & Lawson, 1989; 1990). The notion that CGRP<sup>+</sup>SP<sup>-</sup> neurons are myelinated is further supported from the findings of the previous chapter that suggested their myelination, namely: their larger soma size, deep lamina IV/V projections and association with typically myelinated peripheral endings in the skin.

Nociceptive neurons are usually thought to be limited to A  $\delta$  and C-fibre classes. Yet, some of the earliest descriptions of nociceptors included A $\alpha$ /  $\beta$  fibre classes which almost certainly originate from large diameter DRG neurons (Burgess & Perl, 1967; Ritter & Mendell, 1992; Djouhri *et al.*, 1998; Djouhri & Lawson, 2001). Here we have demonstrated larger myelinated neurons expressing CGRP, that likely correlate to CGRP expressing A $\alpha$ /  $\beta$  nociceptors characterised Lawson and colleagues (2002).

In summary, it appears that CGRP-IR expressing neurons can be split up into three subpopulations based on their NF200 expression: the small unmyelinated CGRP<sup>+</sup>SP<sup>+</sup> neurons, the medium myelinated CGRP<sup>+</sup>SP<sup>+</sup> neurons, and larger myelinated CGRP<sup>+</sup>SP<sup>-</sup> neurons. The CGRP<sup>+</sup>SP<sup>+</sup>NF200<sup>-</sup>, CGRP<sup>+</sup>SP<sup>+</sup>NF200<sup>+</sup> neurons are likely to be C-fibre and A $\delta$ -fibre neurons, respectively. The larger CGRP<sup>+</sup>SP<sup>-</sup>NF200<sup>+</sup> neurons are most likely A $\beta$ -fibre neurons, neurons that are not commonly associated with nociception.

## **CGRP<sup>+</sup>SP<sup>-</sup> neurons do not co-express GAL under normal conditions**

Galanin (GAL) is an inhibitory neuropeptide present in small to medium sized sensory neurons of the DRG (Ju *et al.*, 1987; Garry *et al.*, 1989; Villar *et al.*, 1991; Ma & Bisby, 1997). GAL has both anti-nociceptive and nociceptive roles, depending on the activation of which specific GAL receptors. Activation of GAL receptor type

1 (GALR1) has an anti-nociceptive effect: causing inhibition of dorsal horn transmission (Yanagisawa *et al.*, 1986), potentiation of the spinal analgesic effect of morphine (Wiesenfeld-Hallin, Xu, Villar, *et al.*, 1990), and an increase in the latency of withdrawal to noxious heat (Cridland & Henry, 1988; Kuraishi *et al.*, 1991). Conversely, activation of GALR2 has a nociceptive effect: causing a reduction in mechanical threshold (Cridland & Henry, 1988; Kuraishi *et al.*, 1991).

In this study, GAL-IR was detected around 39% of DRG neurons and was expressed in predominantly small to medium sized neurons, which was consistent with previous studies in rats (Ju *et al.*, 1987; Garry *et al.*, 1989; Villar *et al.*, 1991; Ma & Bisby, 1997). Under normal conditions GAL expression is low, but is up-regulated after nerve injury (Hökfelt *et al.*, 1987).

GAL-IR has also been detected in CGRP and SP DRG neurons, and GAL-IR terminals have similar distributions to CGRP and SP terminals in the superficial spinal dorsal horn (Ju *et al.*, 1987; Villar *et al.*, 1991). In this current study, GAL-IR was found exclusively in CGRP neurons, but there were a large proportion of CGRP-IR neurons that lacked GAL-IR. All CGRP<sup>+</sup>SP<sup>+</sup> neurons contained GAL-IR whereas all CGRP<sup>+</sup>SP<sup>-</sup> neurons lacked GAL-IR. GAL is antagonistic to CGRP and SP and blocks the excitatory effect CGRP and SP in the dorsal horn (Xu *et al.*, 1990; Hua *et al.*, 2005). However, it appears evident that GAL does not contribute in the same way in CGRP<sup>+</sup>SP<sup>-</sup> neurons. Nevertheless, GAL-IR is up regulated in peptidergic neurons after nerve injury, (Hökfelt *et al.*, 1987) and so GAL may contribute in damaged CGRP<sup>+</sup>SP<sup>-</sup> neurons, although this remains to be characterised.

In summary, all CGRP<sup>+</sup>SP<sup>+</sup> neurons contained GAL-IR and all CGRP<sup>+</sup>SP<sup>-</sup> neurons lacked GAL-IR. Hence, under normal conditions, CGRP<sup>+</sup>SP<sup>-</sup> neurons can be further distinguished from CGRP<sup>+</sup>SP<sup>+</sup> neurons by their absence of GAL-IR.

## **Some CGRP<sup>+</sup>SP<sup>-</sup> neurons co-express VIP**

Vasoactive intestinal peptide (VIP) is as potent vasodilator present in small to medium sized sensory neurons of the DRG (Gibson, Polak, Anand, *et al.*, 1984). VIP has a nociceptive role, and has been shown to decrease the latency of withdrawal to noxious heat (Cridland & Henry, 1988).

In this study, VIP was detected in one third of DRG neurons in small, medium and large neurons, which was consistent with previous studies in rats (McGregor *et al.*, 1984; Shehab & Atkinson, 1986). Like GAL, VIP had higher expression in lumbar and sacral DRG than in cervical and thoracic DRG, which is also consistent with previous findings (Gibson, Polak, Anand, *et al.*, 1984). Also resembling GAL, VIP expression is up regulated after nerve injury (McGregor *et al.*, 1984; Shehab & Atkinson, 1986).

VIP-IR has been demonstrated in both CGRP and SP neurons (Doughty *et al.*, 1991), and has a similar distribution to CGRP and SP terminals in the superficial dorsal horn (Gibson, Polak, Anand, *et al.*, 1984; Liu & Morris, 1999). In this study, VIP was found exclusively in CGRP-IR neurons. Conversely half of the CGRP neurons contained VIP. The majority of CGRP<sup>+</sup>SP<sup>+</sup> neurons contained VIP and a third of CGRP<sup>+</sup>SP<sup>-</sup> neurons contained VIP. The CGRP<sup>+</sup>SP<sup>-</sup>VIP<sup>+</sup> neurons were larger than CGRP<sup>+</sup>SP<sup>-</sup>VIP<sup>-</sup> neurons. VIP may be able to replace the role of CGRP and SP following nerve injury. After peripheral axotomy both CGRP (Noguchi *et al.*, 1990) and SP (Jessell *et al.*, 1979) are down-regulated, conversely, VIP is up-regulated (McGregor *et al.*, 1984; Shehab & Atkinson, 1986). Under normal conditions VIP has been shown to increase the excitability of neurons in nociceptive circuits (Cridland & Henry, 1988), which markedly increased after axotomy (Wiesenfeld-Hallin, Xu, Håkanson, *et al.*, 1990). This increase in the excitatory action of VIP is comparable to the effect that SP has on the nociceptive reflex (Wiesenfeld-Hallin, Xu, Håkanson, *et al.*, 1990). Like GAL, VIP-IR is up regulated in peptidergic neurons after nerve injury (Hökfelt *et al.*, 1987) and so VIP may be expressed in all CGRP-IR neurons, although this remains to be characterised.

In summary, the majority of CGRP<sup>+</sup>SP<sup>+</sup> neurons contained VIP and a third of CGRP<sup>+</sup>SP<sup>-</sup> neurons contained VIP. The expression of VIP in CGRP-IR neurons does not appear to be a reliable neurochemical marker that further distinguishes CGRP<sup>+</sup>SP<sup>-</sup> neurons from CGRP<sup>+</sup>SP<sup>+</sup> neurons. However, VIP expression may divide the CGRP<sup>+</sup>SP<sup>-</sup> neurons into two subpopulations: large CGRP<sup>+</sup>SP<sup>-</sup>VIP<sup>-</sup> neurons and larger CGRP<sup>+</sup>SP<sup>-</sup>VIP<sup>+</sup> neurons.

Overall, it appears that CGRP-IR expressing neurons can be split up into further subpopulations based on their expression of other neurochemical markers besides SP (summarised in Table 4.2): CGRP<sup>+</sup>SP<sup>+</sup> neurons that are small unmyelinated and

medium myelinated capsaicin sensitive neurons that co-expressed GAL-IR and VIP-IR, and CGRP<sup>+</sup>SP<sup>-</sup> neurons that are medium capsaicin-sensitive and large capsaicin insensitive neurons that lack GAL-IR and either expressed or lacked VIP-IR. The capsaicin sensitive CGRP<sup>+</sup>SP<sup>+</sup> and CGRP<sup>+</sup>SP<sup>-</sup> neurons are likely to have some role in nociception, in particular the processing of noxious heat and thermal hyperalgesia. In contrast, it is not yet clear whether the large capsaicin-insensitive CGRP<sup>+</sup>SP<sup>-</sup> neurons have a role in nociception. These large CGRP<sup>+</sup>SP<sup>-</sup> neurons could either suggest that CGRP expression is not limited to nociceptive neurons or nociceptive neurons are not limited to A $\delta$  and C-fibre classes. Based on their expression of NF200, their lack of TRPV1 expression, peripheral endings and their projections to the spinal cord CGRP<sup>+</sup>SP<sup>-</sup> neurons may have a polymodal mechanoreceptor function.

**Table 4.2: Summary of the subpopulations of CGRP expressing neurons**

Soma size	Fibre class	SP	NF200	TRPV1	GAL
Small	C	+	-	+	-
Medium	A $\delta$	+	+	+	+
Medium	A $\delta$	-	+	+	-
Medium	A $\delta$	-	+	-	-
Large	A $\beta$	-	+	-	-

## **4.5 Figures**

---

**Figure 4.1: TRPV1, CGRP and SP-IR in neuronal soma of the C7 DRG**

Widefield fluorescence microscopy of mouse C7 dorsal root ganglia triple labelled for calcitonin gene-related peptide (CGRP; A), substance P (SP; B) and the vanilloid receptor TRPV1 (C). The overlay of A, B and C (D) shows three subpopulations of neurons positive for CGRP-immunoreactivity (IR): neurons containing CGRP-, SP- and TRPV1-IR (CGRP<sup>+</sup>SP<sup>+</sup>TRPV1<sup>+</sup>; white arrows; white in D), neurons containing CGRP- and TRPV1-IR without SP-IR (CGRP<sup>+</sup>SP<sup>-</sup>TRPV1<sup>+</sup>; white arrowheads; magenta in D), and neurons containing CGRP- without TRPV1- and SP-IR (CGRP<sup>+</sup>SP<sup>-</sup>TRPV1<sup>-</sup>; black arrows; red in D). Scale bar = 60 μm in D (applies to A-D).

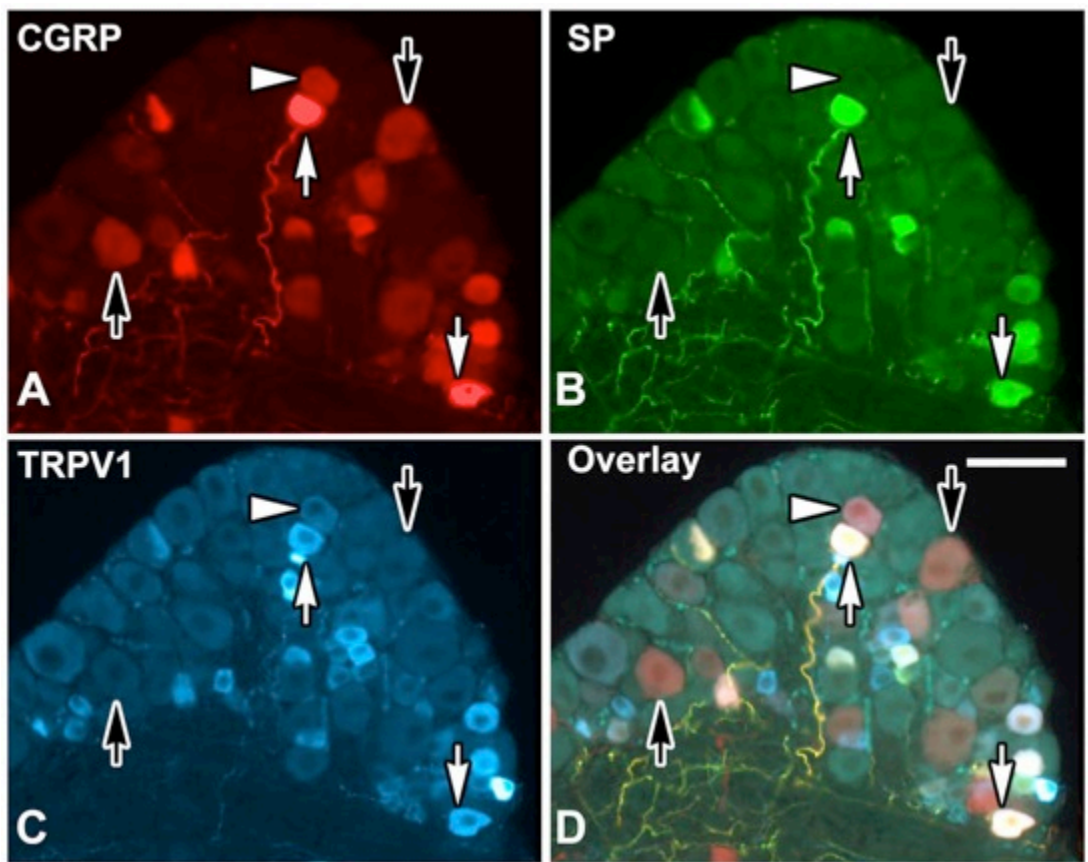


**Figure 4.2: Intensity of TRPV1-IR and soma size in DRG neurons**

Scatter dot plot (dots = cells; line = linear regression with 95% confidence limits) depicting the size of neuronal somata and their intensity of TRPV1-immunoreactivity (TRPV1-IR) more than 2 standard deviations above mean background fluorescence in dorsal root ganglia (DRG) of all spinal levels. There was no correlation between the intensity of TRPV1-IR and the soma size of the neurons (linear correlation:  $r^2 < 0.01$ ,  $p < 0.0001$ ). While the slope of the line is significantly different from zero ( $p < 0.0001$ ), the correlation coefficient ( $r < 0.01$ ) is too small to denote any practical significance.

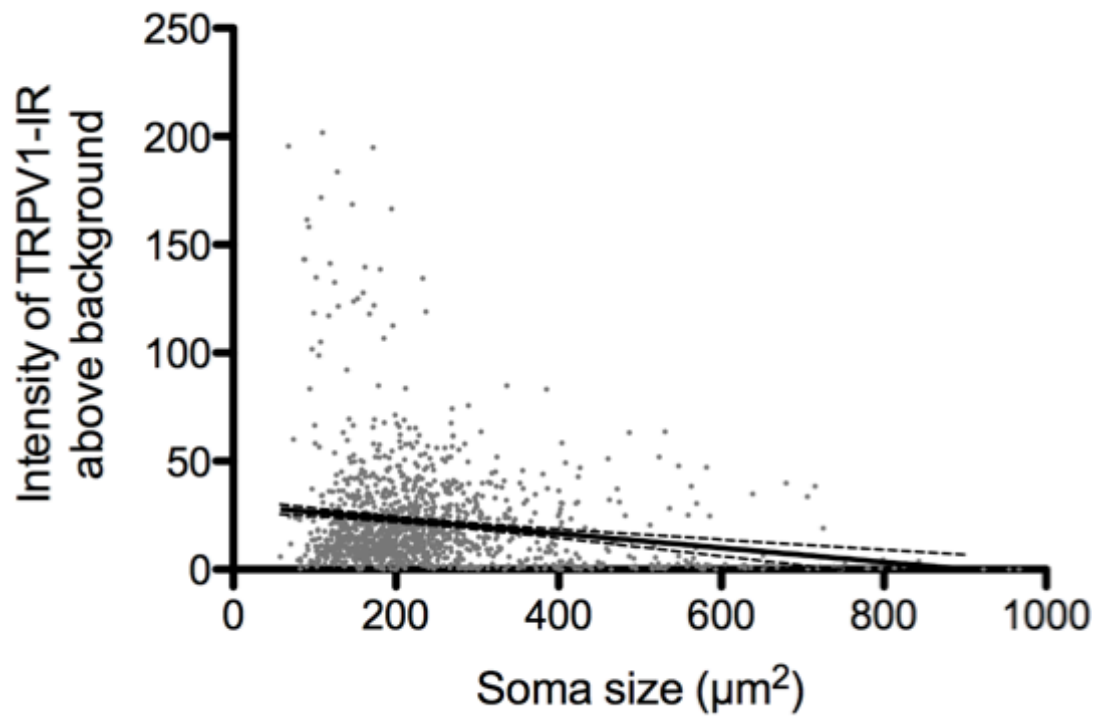


**Figure 4.3: Proportion of neuronal somata expressing TRPV1-IR in DRG of all spinal levels**

Histogram (total percentage) depicting the proportion of neuronal somata that either expressed TRPV1-immunoreactivity (TRPV1-IR; TRPV1+; blue bars) or lacked TRPV1-IR (TRPV1-; black bars) in cervical (C7), thoracic (T5), lumbar (L5), and sacral (S3) dorsal root ganglia (DRG). Overall TRPV1-IR was present in 46% of DRG neurons. There was no difference between the proportions of neuronal somata that expressed TRPV1-IR in the DRG of different levels (Chi-Square:  $\chi^2_3 = 1$ ,  $p = 0.8$ ;  $N = 5$  animals,  $n = 2811$  neurons).

**Figure 4.4: Soma size of neurons expressing TRPV1-IR in DRG of all spinal levels**

Histogram (mean  $\pm$  SEM) depicting the size (cross sectional area;  $\mu\text{m}^2$ ) of neuronal somata that either expressed TRPV1-immunoreactivity (TRPV1-IR; TRPV1+; blue bars) or lacked TRPV1-IR (TRPV1-; black bars) in cervical (C7), thoracic (T5), lumbar (L5), and sacral (S3) dorsal root ganglia (DRG). TRPV1-IR was expressed in neurons with a mean soma size of  $240 \pm 3 \mu\text{m}^2$  and there was no difference in the soma size of neurons that expressed TRPV1-IR between the DRG of different levels (ANOVA:  $F_{(2,1297)} = 1$ ,  $p = 0.4$ ,  $N = 5$  animals,  $n = 1301$  neurons).

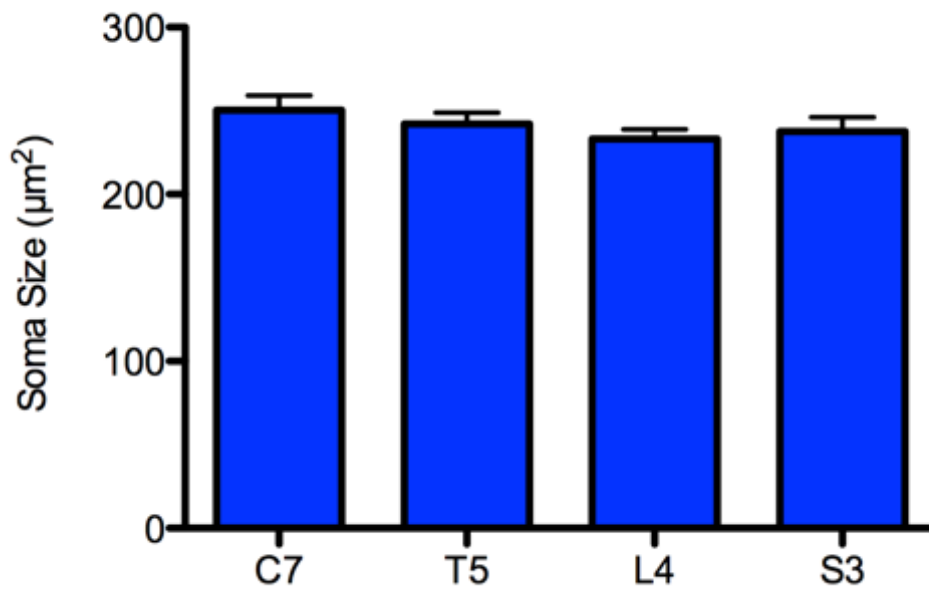
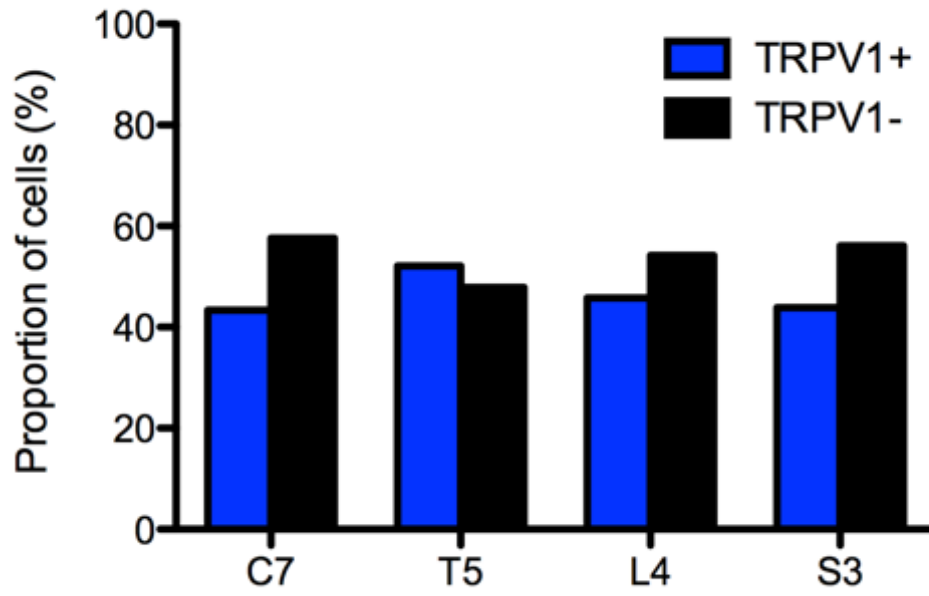


**Figure 4.5: Proportion of CGRP<sup>+</sup>SP<sup>-</sup>TRPV1<sup>-</sup> neurons in DRG of all spinal levels**

Histogram (total percentage) depicting the proportion of neuronal somata that expressed calcitonin gene related peptide-immunoreactivity (CGRP-IR) with substance P-IR (SP-IR) that also expressed TRPV1 (CGRP<sup>+</sup>SP<sup>+</sup>TRPV1<sup>+</sup>; white) or lacked TRPV1-IR (CGRP<sup>+</sup>SP<sup>+</sup>TRPV1<sup>-</sup>; yellow) and the proportion of neuronal somata that expressed CGRP-IR without SP-IR that expressed TRPV1 (CGRP<sup>+</sup>SP<sup>-</sup>TRPV1<sup>+</sup>; magenta), or lacked TRPV1-IR (CGRP<sup>+</sup>SP<sup>-</sup>TRPV1<sup>-</sup>; red) in cervical (C7), thoracic (T5), lumbar (L5), and sacral (S3) dorsal root ganglia (DRG). Virtually all CGRP<sup>+</sup>SP<sup>+</sup> neurons had TRPV1-IR and this was consistent through the levels (Chi-Square:  $\chi^2_3 = 0.1$ ,  $p = 1$ ;  $N = 5$  animals;  $n = 732$  neurons). In contrast, only 42% of the CGRP<sup>+</sup>SP<sup>-</sup> neurons contained TRPV1-IR. A lower proportion of CGRP<sup>+</sup>SP<sup>-</sup> neurons contained TRPV1-IR in C7 DRG and a higher proportion contained TRPV1-IR in T5 DRG than compared to the other levels (Chi-Square:  $\chi^2_3 = 9$ ,  $p = 0.03$ ;  $N = 5$  animals;  $n = 842$  neurons)

**Figure 4.6: Soma size of CGRP<sup>+</sup>SP<sup>-</sup>TRPV1<sup>-</sup> neurons in DRG of all spinal levels**

Histogram (mean  $\pm$  SEM) depicting the size (cross sectional area;  $\mu\text{m}^2$ ) of neuronal somata that expressed calcitonin gene related peptide-immunoreactivity (CGRP-IR) with substance P-IR (SP-IR) and TRPV1-IR (CGRP<sup>+</sup>SP<sup>+</sup>TRPV1<sup>+</sup>; white), CGRP-IR with TRPV1-IR but no SP-IR (CGRP<sup>+</sup>SP<sup>-</sup>TRPV1<sup>+</sup>; magenta), or CGRP-IR without SP-IR and TRPV1-IR (CGRP<sup>+</sup>SP<sup>-</sup>TRPV1<sup>-</sup>; red) in cervical (C7), thoracic (T5), lumbar (L5), and sacral (S3) dorsal root ganglia (DRG). At all levels, CGRP<sup>+</sup>SP<sup>-</sup>TRPV1<sup>-</sup> neurons were the largest, and CGRP<sup>+</sup>SP<sup>-</sup>TRPV1<sup>+</sup> neurons were larger than CGRP<sup>+</sup>SP<sup>+</sup>TRPV1<sup>+</sup> neurons (RM-ANOVA:  $F_{(3,1536)} = 467$ ,  $p < 0.0001$ ;  $N = 5$  animals,  $n = 1574$  neurons). Between the different DRG levels, the soma size of CGRP<sup>+</sup>SP<sup>-</sup>TRPV1<sup>-</sup> neurons were largest at the C7 and L4 level, and the CGRP<sup>+</sup>SP<sup>-</sup>TRPV1<sup>-</sup> neurons of T5 were larger than those of S3 (RM-ANOVA:  $F_{(6,1536)} = 13$ ,  $p < 0.0001$ ). CGRP<sup>+</sup>SP<sup>-</sup>TRPV1<sup>+</sup> neurons were largest at C7, and T5 compared to the other levels (RM-ANOVA:  $F_{(6,1536)} = 13$ ,  $p < 0.0001$ ;  $N = 5$  animals,  $n = 1574$  neurons).

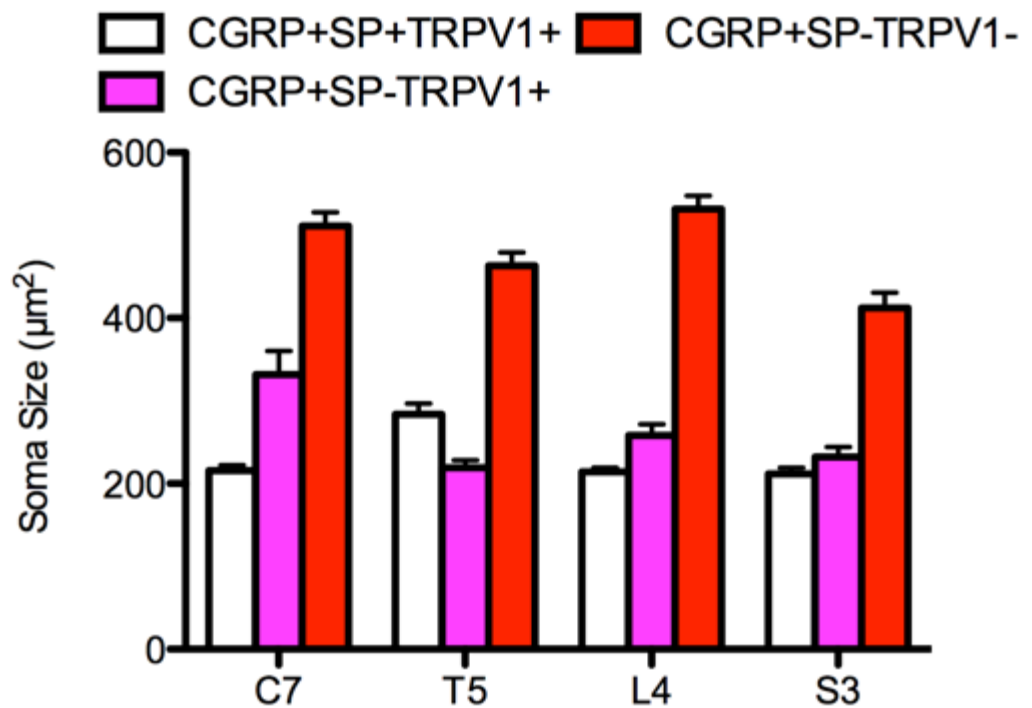
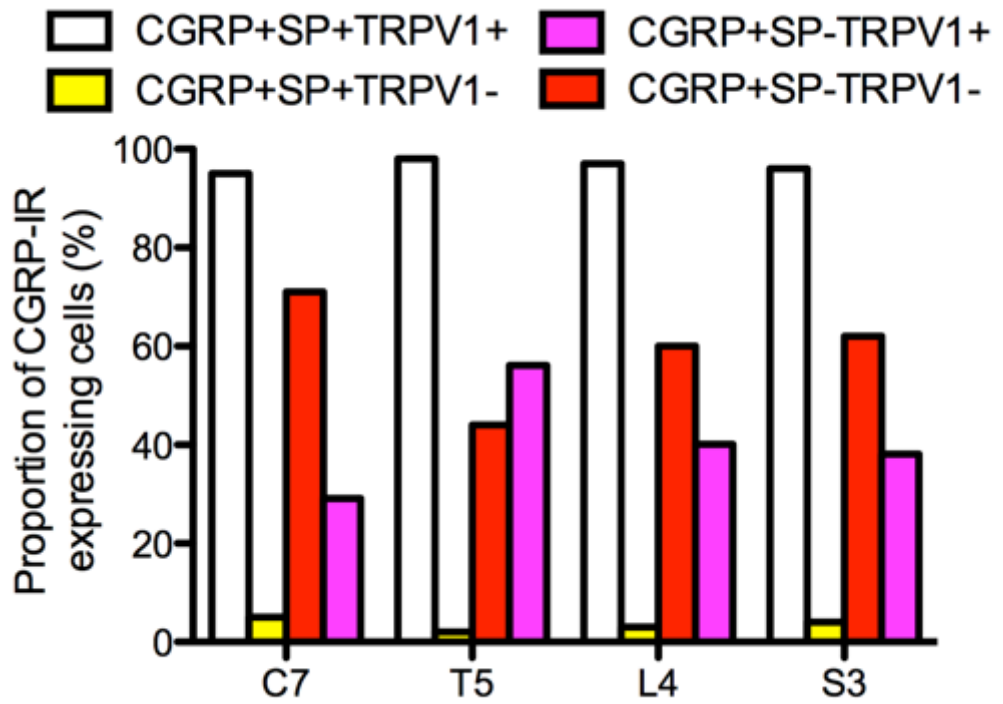


**Figure 4.7: Proportion of CGRP<sup>+</sup>SP<sup>-</sup>TRPV1<sup>-</sup> neurons in individual DRG**

Pie charts (data displayed as percentage) depicting the proportion of neuronal somata that expressed calcitonin gene related peptide-immunoreactivity (CGRP-IR) with substance P-IR (SP-IR) and TRPV1-IR (CGRP<sup>+</sup>SP<sup>+</sup>TRPV1<sup>+</sup>; white), CGRP-IR with TRPV1-IR but no SP-IR (CGRP<sup>+</sup>SP<sup>-</sup>TRPV1<sup>+</sup>; magenta), CGRP-IR without SP-IR and TRPV1-IR (CGRP<sup>+</sup>SP<sup>-</sup>TRPV1<sup>-</sup>; red), TRPV1-IR without CGRP-IR and SP-IR (CGRP<sup>-</sup>SP<sup>-</sup>TRPV1<sup>+</sup>; blue) or expressed neither CGRP-IR, SP-IR nor TRPV1-IR (CGRP<sup>-</sup>SP<sup>-</sup>TRPV1<sup>-</sup>; black) in cervical (C7), thoracic (T5), lumbar (L4) and sacral (S3) dorsal root ganglia (DRG). TRPV1-IR was detected in 43% of C7 DRG neurons (N = 5 animals, n = 685 neurons), 52% of T5 DRG neurons (N = 5 animals, n = 670 neurons), 46% of L4 DRG neurons (N = 5 animals, n = 845 neurons), and 44% of S3 DRG neurons (N = 5 animals, n = 611 neurons). In all DRG, virtually all CGRP<sup>+</sup>SP<sup>+</sup> neurons contained TRPV1-IR, whereas, approximately half of CGRP<sup>+</sup>SP<sup>-</sup> neurons lacked TRPV1-IR.

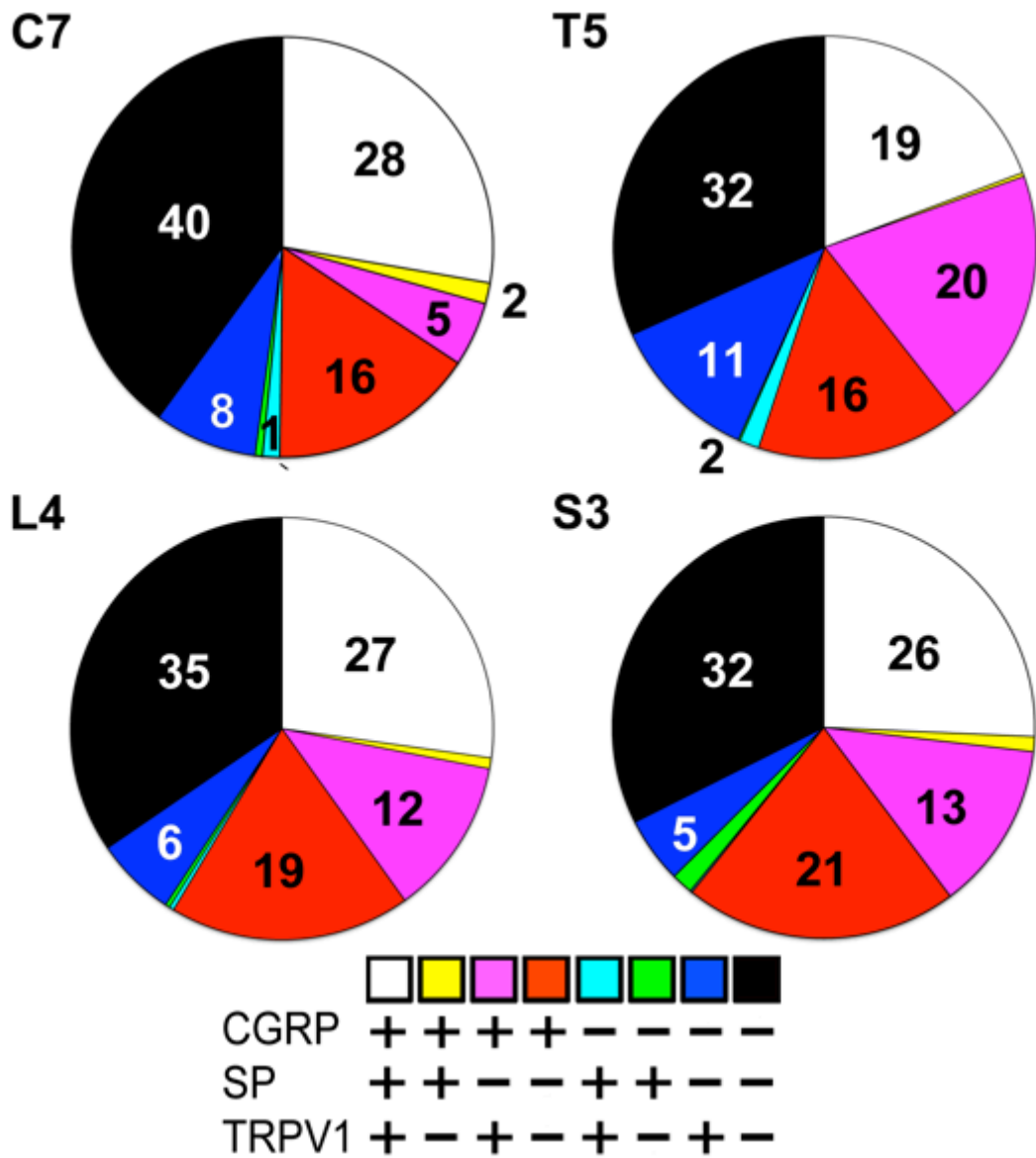


**Figure 4.8: Soma size of CGRP<sup>+</sup>SP<sup>-</sup>TRPV1<sup>-</sup> neurons in individual DRG**

Histograms (mean  $\pm$  SEM) depicting the size (cross sectional area;  $\mu\text{m}^2$ ) of neuronal somata that expressed calcitonin gene related peptide-immunoreactivity (CGRP-IR) with substance P-IR (SP-IR) and TRPV1-IR (CGRP<sup>+</sup>SP<sup>+</sup>TRPV1<sup>+</sup>; white), CGRP-IR with TRPV1-IR but no SP-IR (CGRP<sup>+</sup>SP<sup>-</sup>TRPV1<sup>+</sup>; magenta), CGRP-IR without SP-IR and TRPV1-IR (CGRP<sup>+</sup>SP<sup>-</sup>TRPV1<sup>-</sup>; red) in cervical (C7), thoracic (T5), lumbar (L4) and sacral (S3) dorsal root ganglia (DRG). In C7 and L4 DRG, the CGRP<sup>+</sup>SP<sup>-</sup>TRPV1<sup>-</sup> neurons were largest and the CGRP<sup>+</sup>SP<sup>+</sup>TRPV1<sup>+</sup> neurons were the smallest (ANOVA:  $F_{(2,326)} = 168$ ,  $p < 0.0001$ ;  $N = 5$  animals,  $n = 328$  neurons, and  $F_{(2,485)} = 257$ ,  $p < 0.0001$ ;  $N = 5$  animals,  $n = 488$  neuron, respectively). In T5 DRG, the CGRP<sup>+</sup>SP<sup>-</sup>TRPV1<sup>-</sup> neurons were largest and the CGRP<sup>+</sup>SP<sup>-</sup>TRPV1<sup>+</sup> neurons were the smallest (ANOVA:  $F_{(2,364)} = 92$ ,  $p < 0.0001$ ;  $N = 5$  animals,  $n = 367$  neurons). In S3 DRG, the CGRP<sup>+</sup>SP<sup>-</sup>TRPV1<sup>-</sup> neurons were largest and there was no size difference between CGRP<sup>+</sup>SP<sup>+</sup>TRPV1<sup>+</sup> neurons and CGRP<sup>+</sup>SP<sup>-</sup>TRPV1<sup>+</sup> neurons (ANOVA:  $F_{(2,361)} = 70$ ,  $p < 0.0001$ ;  $N = 5$  animals,  $n = 364$  neurons).

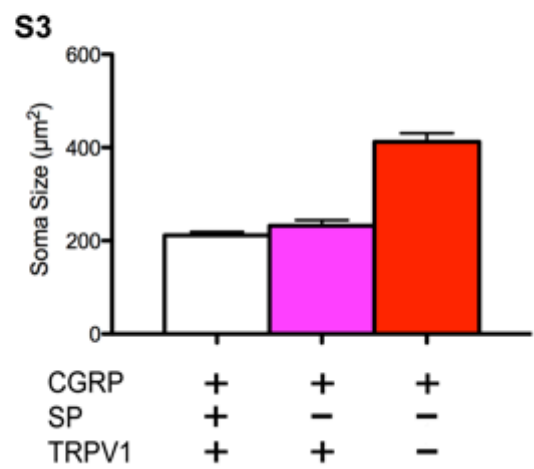
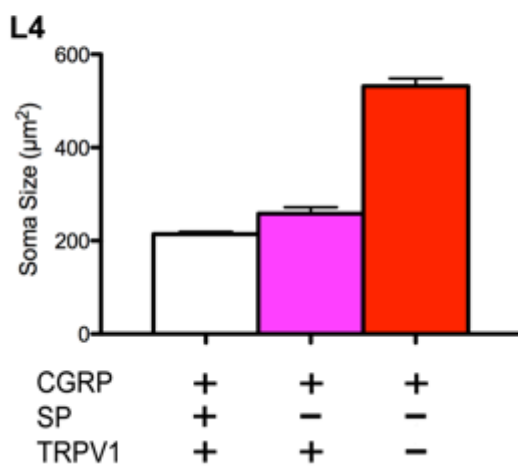
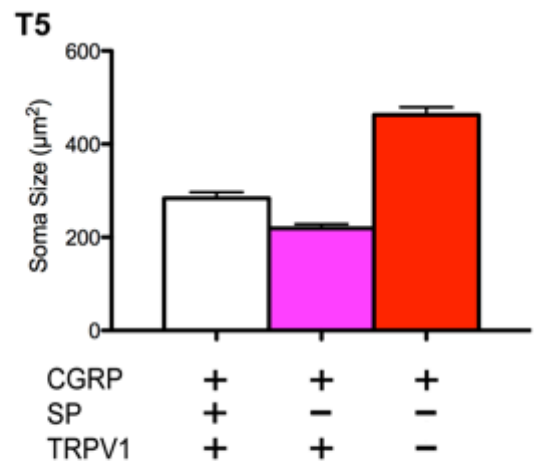
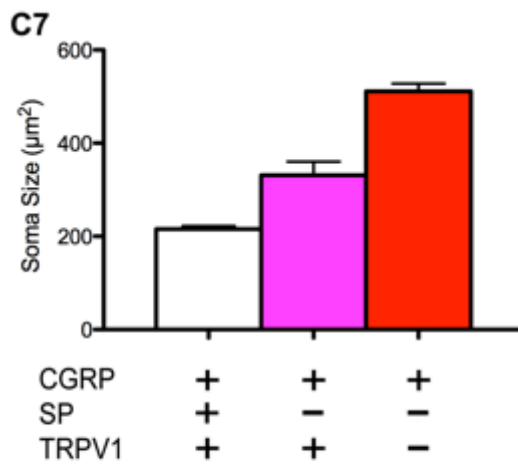


**Figure 4.9: NF200, CGRP and SP-IR in neuronal soma of the C7 DRG**

Widefield fluorescence microscopy of mouse C7 dorsal root ganglia triple labelled for calcitonin gene-related peptide (CGRP; A), substance P (SP; B) and neurofilament-200kDa (NF200; C). The overlay of A, B and C (D) shows three subpopulations of neurons positive for CGRP-immunoreactivity (IR): neurons containing CGRP-, SP- and NF200-IR (CGRP<sup>+</sup>SP<sup>+</sup>NF200<sup>+</sup>; white arrowheads; white in D), neurons containing CGRP- and SP-IR without NF200-IR (CGRP<sup>+</sup>SP<sup>+</sup>NF200<sup>-</sup>; white arrows; yellow in D), and neurons containing CGRP- and NF200 without SP-IR (CGRP<sup>+</sup>SP<sup>-</sup>NF200<sup>-</sup>; black arrows; magenta in D). Scale bar = 60  $\mu$ m in D (applies to A-D).

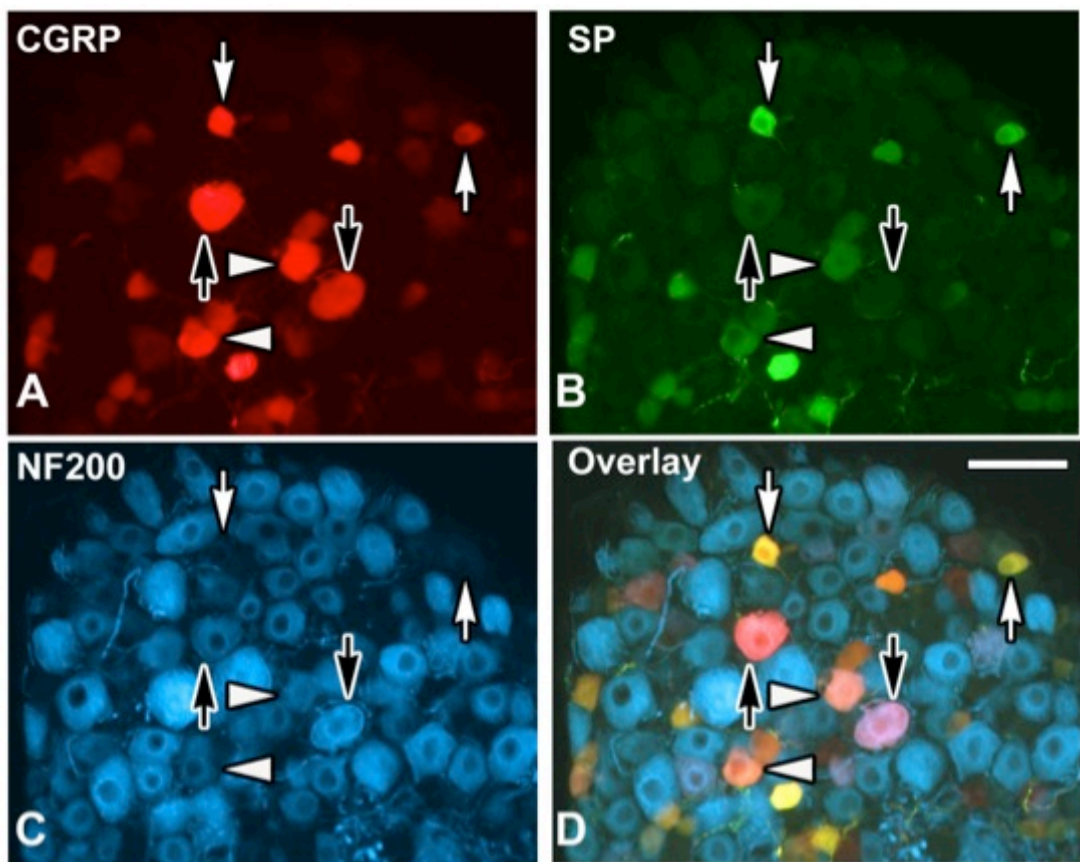


**Figure 4.10: Intensity of NF200-IR and soma size in DRG neurons**

Scatter dot plot (dots = cells; line = linear regression with 95% confidence limits) depicting the size of neuronal somata and their intensity of neurofilament-200kDa-immunoreactivity (NF200-IR) more than 2 standard deviations above background fluorescence in dorsal root ganglia (DRG) of all spinal levels. There was no correlation between the intensity of NF200-IR and the soma size of the neurons (linear correlation:  $r = 0.06$ ,  $p < 0.0001$ ;  $N = 5$  animals,  $n = 1562$  neurons). While the slope of the line is significantly different from zero ( $p < 0.0001$ ), the correlation coefficient ( $r = 0.06$ ) is too small to denote any practical significance.

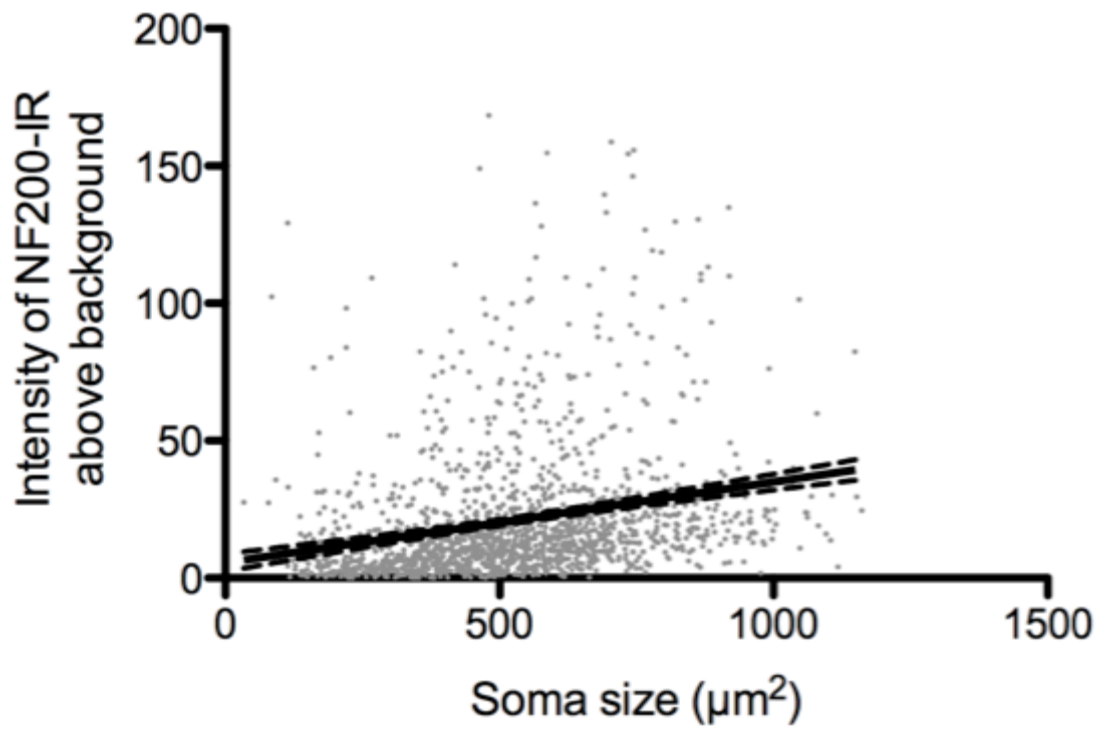


**Figure 4.11: Proportion of neuronal somata expressing NF200-IR in DRG of all spinal levels**

Histogram (total percentage) depicting the proportion of neuronal somata that either expressed neurofilament-200kDa-immunoreactivity (NF200-IR; NF200+; blue bars) or lacked NF200-IR (NF200-; black bars) in cervical (C7), thoracic (T5), lumbar (L4), and sacral (S3) dorsal root ganglia (DRG). Overall NF200-IR was present in 71% of DRG neurons. There was no difference between the proportions of neuronal somata that expressed NF200-IR in the DRG of different levels (Chi-Square:  $\chi^2_3 = 1$ ,  $p = 0.8$ ;  $N = 5$  animals;  $n = 2196$  neurons).

**Figure 4.12: Soma size of neurons expressing NF200-IR in DRG of all spinal levels**

Histogram (data displayed as mean  $\pm$  SEM) depicting the size (cross sectional area;  $\mu\text{m}^2$ ) of neuronal somata that either expressed neurofilament-200kDa-immunoreactivity (NF200-IR; NF200+; blue bars) or lacked NF200-IR (NF200-; black bars) in cervical (C7), thoracic (T5), lumbar (L4), and sacral (S3) dorsal root ganglia (DRG). NF200-IR was expressed in neurons with a mean soma size of  $518 \pm 5 \mu\text{m}^2$ . NF200-IR neurons were largest at L4, and at C7 were larger than NF200-IR neurons of T5 and S3 (ANOVA:  $F_{(3,1558)} = 44$ ,  $p < 0.0001$ ,  $N = 5$  animals,  $n = 1562$  neurons).

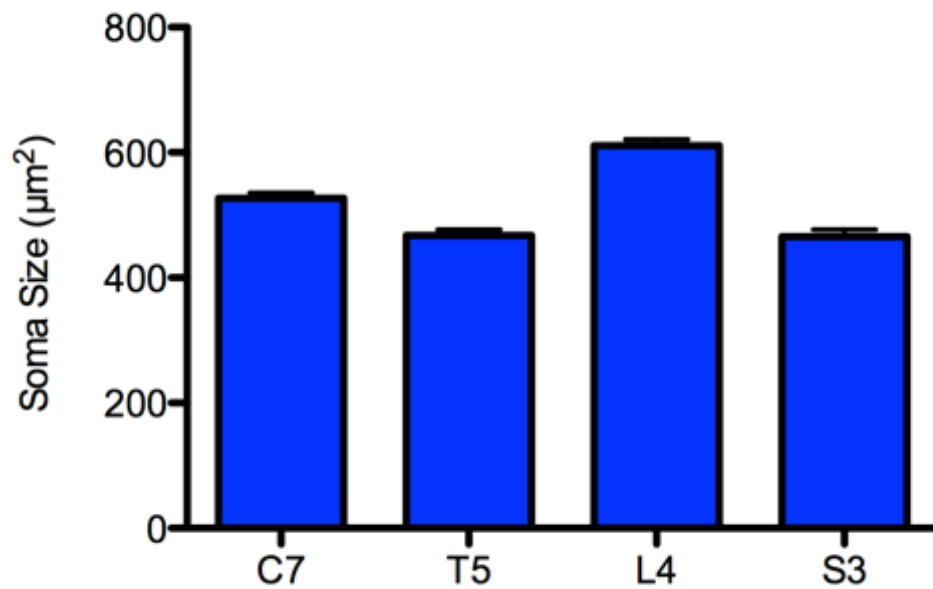
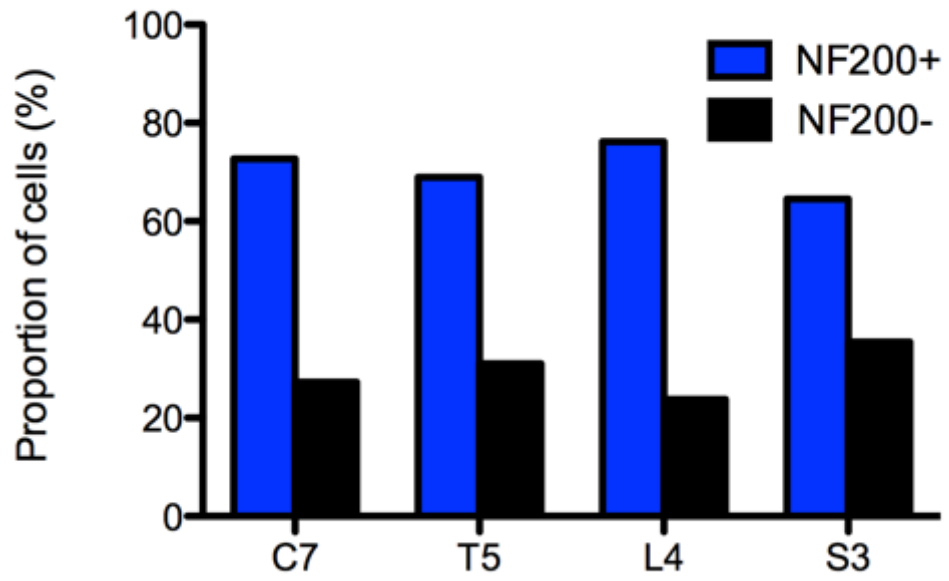


**Figure 4.13: Proportion of CGRP<sup>+</sup>SP<sup>-</sup>NF200<sup>+</sup> neurons in DRG of all spinal levels**

Histogram (total percentage) depicting the proportion of neuronal somata that expressed calcitonin gene related peptide-immunoreactivity (CGRP-IR) and substance P-IR (SP-IR) that also expressed NF200 (CGRP<sup>+</sup>SP<sup>+</sup>NF200<sup>+</sup>; white) or lacked NF200-IR (CGRP<sup>+</sup>SP<sup>+</sup>NF200<sup>-</sup>; yellow) and the proportion of neuronal somata that expressed CGRP-IR without SP-IR that expressed NF200-IR (CGRP<sup>+</sup>SP<sup>-</sup>NF200<sup>+</sup>; magenta), or lacked NF200-IR (CGRP<sup>+</sup>SP<sup>-</sup>NF200<sup>-</sup>; red) in cervical (C7), thoracic (T5), lumbar (L4), and sacral (S3) dorsal root ganglia (DRG). Half of the CGRP<sup>+</sup>SP<sup>+</sup> neurons had NF200-IR. A higher proportion of CGRP<sup>+</sup>SP<sup>+</sup> neurons had NF200-IR in T5 DRG and a lower proportion of CGRP<sup>+</sup>SP<sup>+</sup> neurons had NF200-IR in L4 DRG compared to other levels (Chi-Square:  $\chi^2_3 = 9$ ,  $p = 0.04$ ;  $N = 5$  animals,  $n = 654$  neurons). In contrast, the majority of CGRP<sup>+</sup>SP<sup>-</sup> neurons had NF200-IR and this was consistent between levels (Chi-Square:  $\chi^2_3 = 1$ ,  $p = 0.8$ ;  $N = 5$  animals,  $n = 520$  neurons).

**Figure 4.14: Soma size of CGRP<sup>+</sup>SP<sup>-</sup>NF200<sup>+</sup> neurons in DRG of all spinal levels**

Histogram (data displayed as mean  $\pm$  SEM) depicting the size (cross sectional area;  $\mu\text{m}^2$ ) of neuronal somata that expressed calcitonin gene related peptide-immunoreactivity (CGRP-IR) with substance P-IR (SP-IR) and NF200-IR (CGRP<sup>+</sup>SP<sup>+</sup>NF200<sup>+</sup>; white), with SP-IR but no NF200-IR (CGRP<sup>+</sup>SP<sup>+</sup>NF200<sup>-</sup>; yellow), with NF200-IR but no SP-IR (CGRP<sup>+</sup>SP<sup>-</sup>NF200<sup>+</sup>; magenta), or without SP-IR and NF200-IR (CGRP<sup>+</sup>SP<sup>-</sup>NF200<sup>-</sup>; red) in cervical (C7), thoracic (T5), lumbar (L4), and sacral (S3) dorsal root ganglia (DRG). At all levels, the CGRP neurons that contained NF200 were larger than those that did not, CGRP<sup>+</sup>SP<sup>-</sup>NF200<sup>+</sup> were the largest, and CGRP<sup>+</sup>SP<sup>-</sup>NF200<sup>-</sup> neurons were larger than CGRP<sup>+</sup>SP<sup>+</sup>NF200<sup>-</sup> neurons (RM-ANOVA:  $F_{(3,1158)} = 173$ ,  $p < 0.0001$ ;  $N = 5$  animals,  $n = 1174$  neurons). CGRP<sup>+</sup>SP<sup>-</sup>NF200<sup>+</sup> neurons were largest at L4, and CGRP<sup>+</sup>SP<sup>+</sup>NF200<sup>-</sup> neurons and CGRP<sup>+</sup>SP<sup>-</sup>NF200<sup>-</sup> neurons were largest at S3 compared to the other levels (RM-ANOVA:  $F_{(9,1158)} = 8$ ,  $p < 0.0001$ ;  $N = 5$  animals,  $n = 1174$  neurons). There was no difference in the size of CGRP<sup>+</sup>SP<sup>+</sup>NF200<sup>+</sup> neurons between the spinal levels.

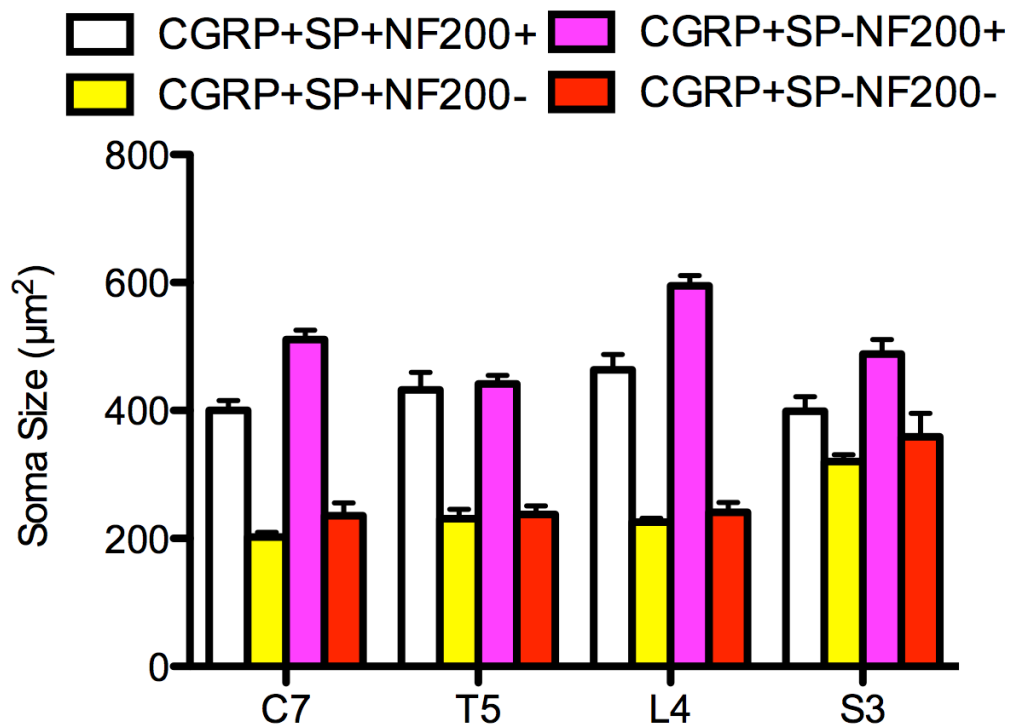
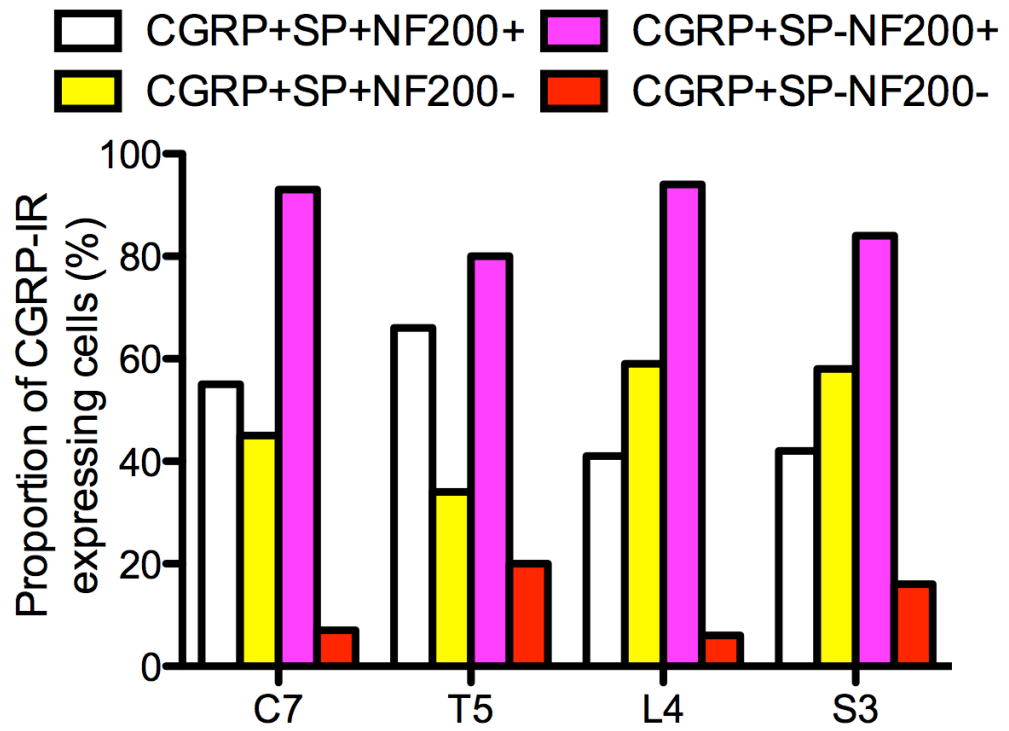


**Figure 4.15: Proportion of CGRP<sup>+</sup>SP<sup>-</sup>NF200<sup>+</sup> neurons in individual DRG**

**A:** Pie chart depicting the proportion of neuronal somata that expressed calcitonin gene related peptide-immunoreactivity (CGRP-IR) with substance P-IR (SP-IR) and neurofilament-200-IR (NF200-IR; CGRP<sup>+</sup>SP<sup>+</sup>NF200<sup>+</sup>; white), CGRP-IR with SP-IR but no NF200-IR (CGRP<sup>+</sup>SP<sup>+</sup>NF200<sup>-</sup>; yellow), CGRP-IR with NF200-IR but no SP-IR (CGRP<sup>+</sup>SP<sup>-</sup>NF200<sup>+</sup>; magenta), CGRP-IR without SP-IR and NF200-IR (CGRP<sup>+</sup>SP<sup>-</sup>NF200<sup>-</sup>; red), NF200-IR without CGRP-IR and SP-IR (CGRP<sup>-</sup>SP<sup>-</sup>NF200<sup>+</sup>; blue), or expressed neither CGRP-IR, SP-IR nor NF200-IR (CGRP<sup>-</sup>SP<sup>-</sup>NF200<sup>-</sup>; black) in cervical (C7), thoracic (T5), lumbar (L4) and sacral (S3) dorsal root ganglia (DRG). NF200-IR was detected in 73% of C7 DRG neurons (N = 5 animals, n = 743 neurons), 69% of T5 DRG neurons (N = 5 animals, n = 503 neurons), 76% of L4 DRG neurons (N = 5 animals, n = 530 neurons), and 65% of S3 DRG neurons (N = 5 animals, n = 420 neurons). In all DRG, the majority of CGRP<sup>+</sup>SP<sup>-</sup> neurons contained NF200-IR, and around half of CGRP<sup>+</sup>SP<sup>+</sup> neurons contained NF200-IR.

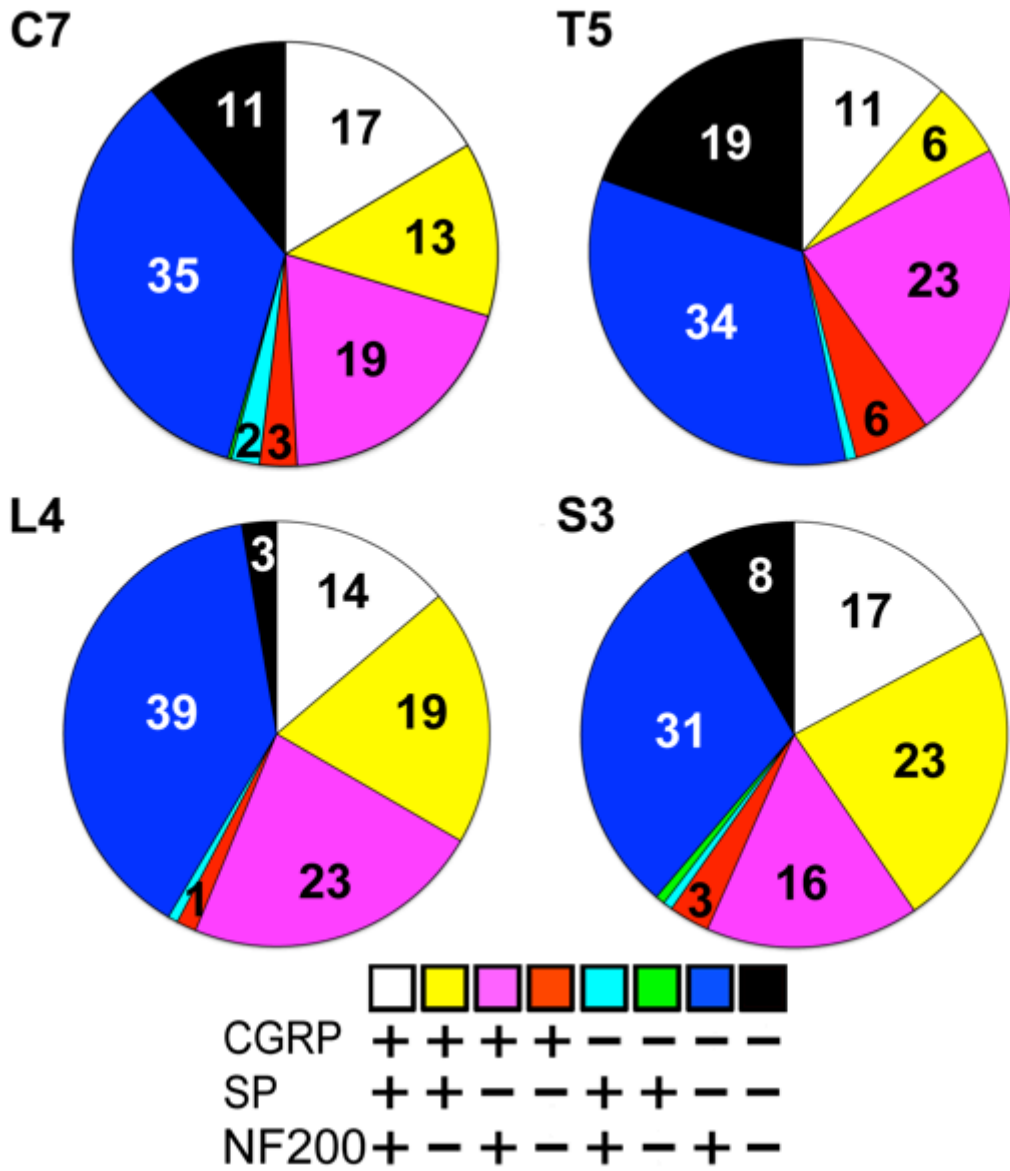


**Figure 4.16: Soma size of CGRP<sup>+</sup>SP<sup>-</sup>NF200<sup>+</sup> neurons in individual DRG**

Histogram (data displayed as mean  $\pm$  SEM) depicting the size (cross sectional area;  $\mu\text{m}^2$ ) of neuronal somata that expressed calcitonin gene related peptide-immunoreactivity (CGRP-IR) with substance P-IR (SP-IR) and neurofilament-200-IR (NF200-IR; CGRP<sup>+</sup>SP<sup>+</sup>NF200<sup>+</sup>; white), CGRP-IR with SP-IR but no NF200-IR (CGRP<sup>+</sup>SP<sup>+</sup>NF200<sup>-</sup>; yellow), CGRP-IR with NF200-IR but no SP-IR (CGRP<sup>+</sup>SP<sup>-</sup>NF200<sup>+</sup>; magenta), CGRP-IR without SP-IR and NF200-IR (CGRP<sup>+</sup>SP<sup>-</sup>NF200<sup>-</sup>; red) in cervical (C7), thoracic (T5), lumbar (L4) and sacral (S3) dorsal root ganglia (DRG). In all DRG, CGRP<sup>+</sup>SP<sup>-</sup>NF200<sup>+</sup> neurons were larger than CGRP<sup>+</sup>SP<sup>+</sup>NF200<sup>+</sup>, CGRP<sup>+</sup>SP<sup>+</sup>NF200<sup>-</sup> and CGRP<sup>+</sup>SP<sup>-</sup>NF200<sup>-</sup> neurons (C7: ANOVA:  $F_{(2,382)} = 92$ ,  $p < 0.0001$ ; N = 5 animals, n = 386 neurons; T5:  $F_{(2,227)} = 269$ ,  $p < 0.0001$ ; N = 5 animals, n = 231 neurons; L4:  $F_{(2,302)} = 116$ ,  $p < 0.0001$ ; N = 5 animals, n = 306 neurons; S3:  $F_{(2,247)} = 15$ ,  $p < 0.0001$ ; N = 5 animals, n = 251 neurons).

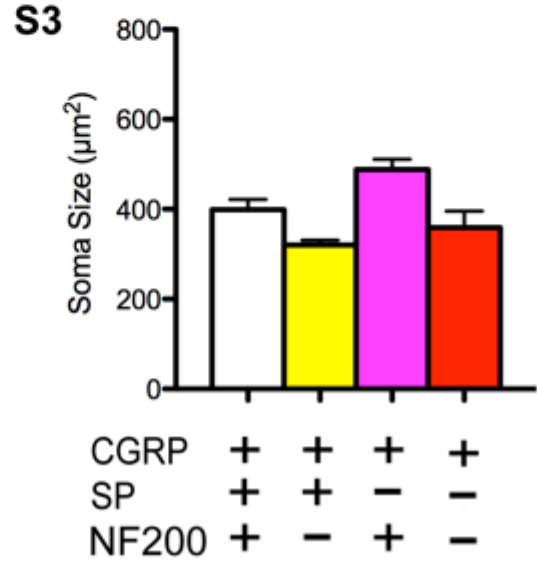
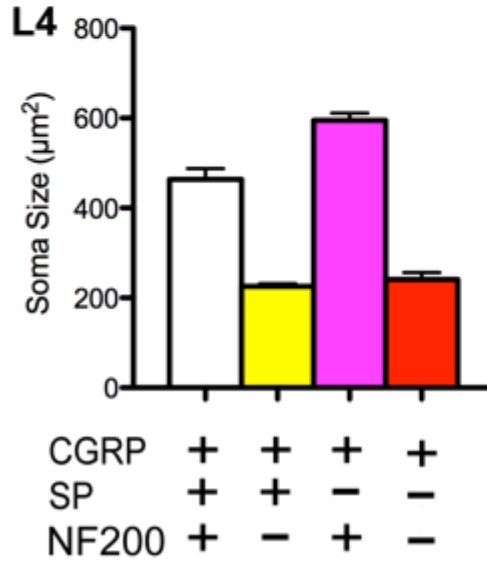
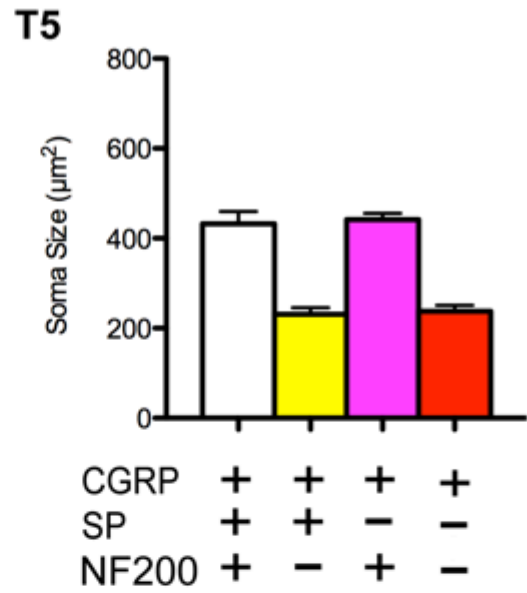
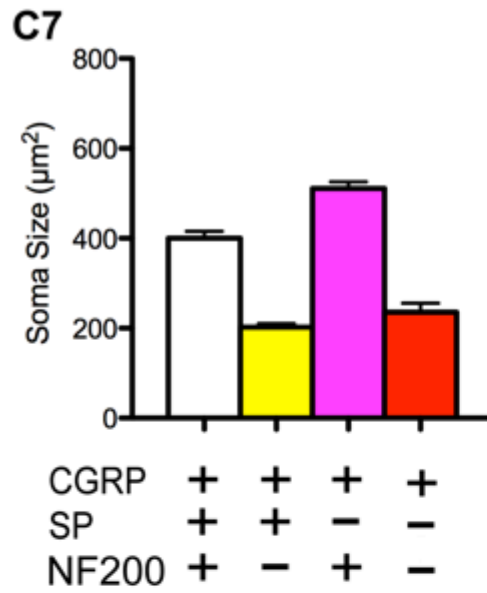


**Figure 4.17: GAL, CGRP and SP-IR in neuronal soma of the L4 DRG**

Widefield fluorescence microscopy of mouse lumbar (L4) dorsal root ganglia (DRG) triple labelled for calcitonin gene-related peptide (CGRP; A), substance P (SP; B) and galanin (GAL; C). The overlay of A, B and C (D) shows three subpopulations of neurons positive for CGRP-immunoreactivity (IR): neurons containing CGRP-, SP- and GAL-IR (CGRP<sup>+</sup>SP<sup>+</sup>GAL<sup>+</sup>; white arrows; white in D), neurons containing CGRP- and SP-IR without GAL-IR (CGRP<sup>+</sup>SP<sup>+</sup>GAL<sup>-</sup>; white arrowheads; yellow in D), and neurons containing CGRP- without SP-IR or GAL-IR (CGRP<sup>+</sup>SP<sup>-</sup>GAL<sup>-</sup>; black arrows; red in D). Scale bar = 60  $\mu$ m in D (applies to A-D).

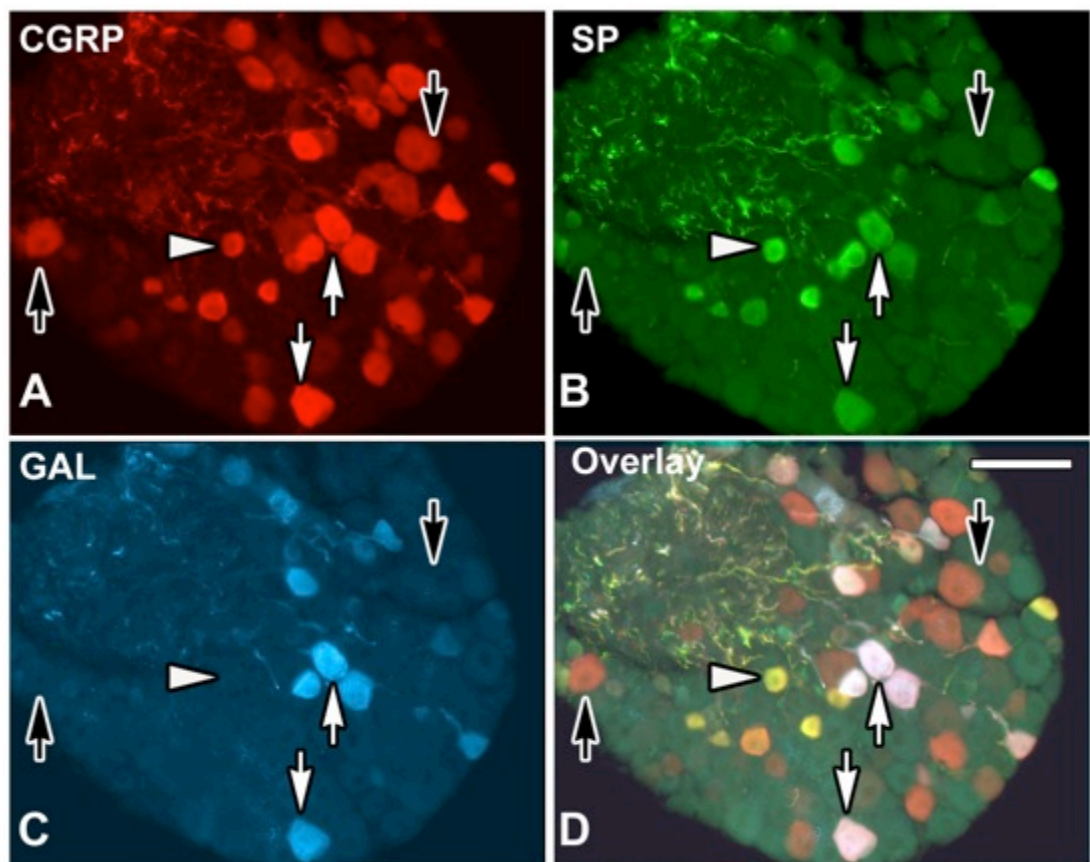


**Figure 4.18: Intensity of GAL-IR and soma size in DRG neurons**

Scatter dot plot (dots = cells; line = linear regression with 95% confidence limits) depicting the size of neuronal somata and their intensity of galanin-immunoreactivity (GAL-IR) more than 2 standard deviations above mean background fluorescence in dorsal root ganglia (DRG) of all spinal levels. There was no correlation between the intensity of GAL-IR and the soma size of the neurons (linear correlation:  $r = 0.08$ ,  $p < 0.0001$ ;  $N = 3$  animals,  $n = 342$  neurons). While the slope of the line is significantly different from zero ( $p < 0.0001$ ), the correlation coefficient ( $r = 0.08$ ) is too small to denote any practical significance.

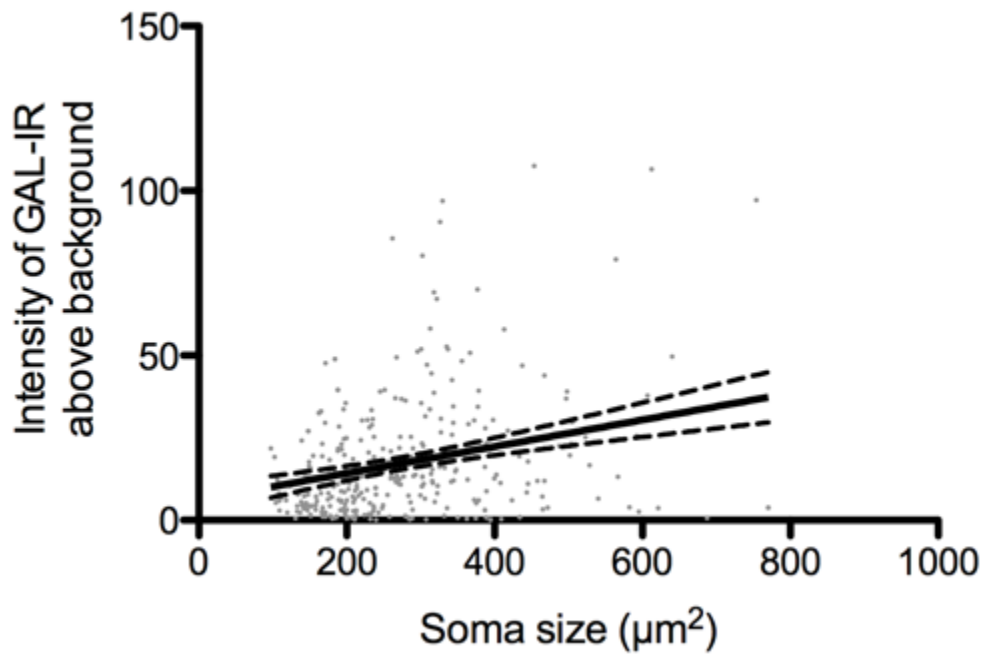


**Figure 4.19: Proportion of neuronal somata expressing GAL-IR in DRG of all spinal levels**

Histogram (total percentage) depicting the proportion of neuronal somata that either expressed galanin-immunoreactivity (GAL-IR; GAL+; blue bars) or lacked GAL-IR (GAL-; black bars) in cervical (C7), thoracic (T5), lumbar (L4), and sacral (S3) dorsal root ganglia (DRG). Overall, GAL-IR was present in 39% of DRG neurons. A lower proportion of DRG neurons contained GAL-IR in C7 and T5 DRG and a higher proportion contained GAL-IR in S3 DRG compared to other levels (Chi-Square:  $\chi^2_3 = 23$ ,  $p < 0.0001$ ; N = 3 animals, n = 1318 neurons).

**Figure 4.20: Size of neuronal somata expressing GAL-IR in DRG of all spinal levels**

Histogram (mean  $\pm$  SEM) depicting the size of neuronal somata that expressed galanin-immunoreactivity (GAL-IR) in cervical (C7), thoracic (T5), lumbar (L4), and sacral (S3) dorsal root ganglia (DRG). GAL-IR was expressed in neurons with a mean soma size of  $283 \pm 8 \mu\text{m}^2$ . GAL-IR neurons were larger in S3 DRG than compared to GAL-IR neurons in C7 and L4 DRG, and GAL-IR neurons were larger in T5 DRG than C7 DRG ( $F_{(3,338)} = 12$ ,  $p < 0.0001$ ; N = 3 animals, n = 342 neurons).

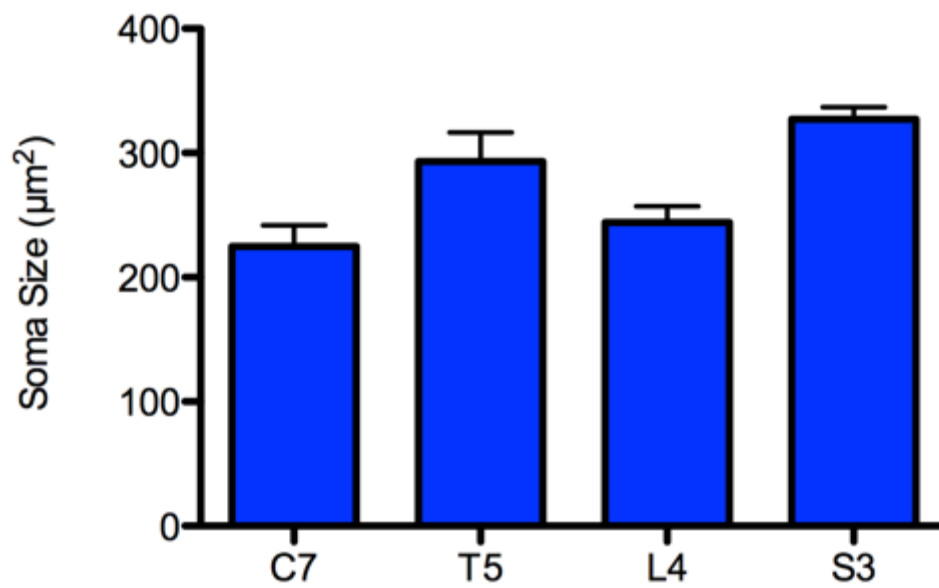
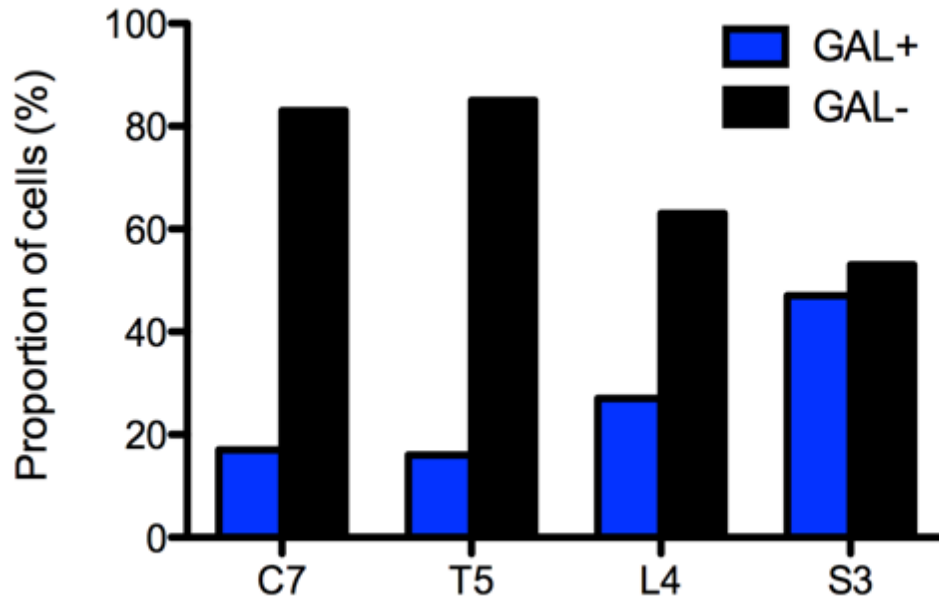


**Figure 4.21: Proportion of CGRP<sup>+</sup>SP<sup>+</sup>GAL<sup>-</sup> neurons in DRG of all spinal levels**

Histogram (data displayed as mean  $\pm$  SEM) depicting the proportion of neuronal somata that expressed calcitonin gene related peptide-immunoreactivity (CGRP-IR) with substance P-IR (SP-IR) that also expressed galanin (GAL; CGRP<sup>+</sup>SP<sup>+</sup>GAL<sup>+</sup>; white) or lacked GAL-IR (CGRP<sup>+</sup>SP<sup>+</sup>GAL<sup>-</sup>; yellow) and the proportion of neuronal somata that expressed CGRP without SP-IR that expressed GAL (CGRP<sup>+</sup>SP<sup>-</sup>GAL<sup>-</sup>; magenta), or lacked GAL-IR (CGRP<sup>+</sup>SP<sup>-</sup>GAL<sup>-</sup>; red) in cervical (C7), thoracic (T5), lumbar (L4), and sacral (S3) dorsal root ganglia (DRG). Most CGRP<sup>+</sup>SP<sup>+</sup> neurons had GAL-IR. A lower proportion of CGRP<sup>+</sup>SP<sup>+</sup> neurons had GAL-IR in C7 and T5 DRG, and a higher proportion of CGRP<sup>+</sup>SP<sup>+</sup> neurons had GAL-IR in S3 DRG (Chi-Square:  $\chi^2_3 = 15$ ,  $p = 0.002$ ,  $N = 3$  animals,  $n = 444$  neurons). Almost no CGRP<sup>+</sup>SP<sup>-</sup> neurons contained GAL-IR and there was no difference in DRG of all spinal levels (Chi-Square:  $\chi^2_3 = 1$ ,  $p = 0.9$ ,  $N = 3$  animals,  $n = 444$  neurons)

**Figure 4.22: Soma size of CGRP<sup>+</sup>SP<sup>-</sup>GAL<sup>-</sup> neurons in DRG of all spinal levels**

Histogram (data displayed as mean  $\pm$  SEM) depicting the size (cross sectional area;  $\mu\text{m}^2$ ) of neuronal somata that expressed calcitonin gene related peptide-immunoreactivity (CGRP-IR) with substance P-IR (SP-IR) and galanin-IR (GAL-IR; CGRP<sup>+</sup>SP<sup>+</sup>GAL<sup>+</sup>; white), with SP-IR but no GAL-IR (CGRP<sup>+</sup>SP<sup>+</sup>GAL<sup>-</sup>; magenta), or without SP-IR and GAL-IR (CGRP<sup>+</sup>SP<sup>-</sup>GAL<sup>-</sup>; red, or without SP-IR and GAL-IR (CGRP<sup>+</sup>SP<sup>-</sup>GAL<sup>-</sup>; red) in cervical (C7), thoracic (T5), lumbar (L5), and sacral (S3) dorsal root ganglia (DRG). At all spinal levels, CGRP<sup>+</sup>SP<sup>-</sup>GAL<sup>-</sup> neurons were the largest and CGRP<sup>+</sup>SP<sup>+</sup>GAL<sup>-</sup> neurons were larger than CGRP<sup>+</sup>SP<sup>+</sup>GAL<sup>+</sup> neurons (RM-ANOVA:  $F_{(2,810)} = 174$ ,  $p < 0.0001$ ;  $N = 5$  animals,  $n = 821$  neurons). S3 DRG lacked CGRP<sup>+</sup>SP<sup>+</sup>GAL<sup>-</sup> neurons. CGRP<sup>+</sup>SP<sup>-</sup>GAL<sup>-</sup> neurons were larger in L4 DRG than in C7 DRG ( $F_{(3,810)} = 9$ ,  $p < 0.0001$ ;  $N = 5$  animals,  $n = 821$  neurons). There was no difference in the size of CGRP<sup>+</sup>SP<sup>-</sup>GAL<sup>-</sup> or CGRP<sup>+</sup>SP<sup>+</sup>GAL<sup>+</sup> neurons between DRG of different levels.

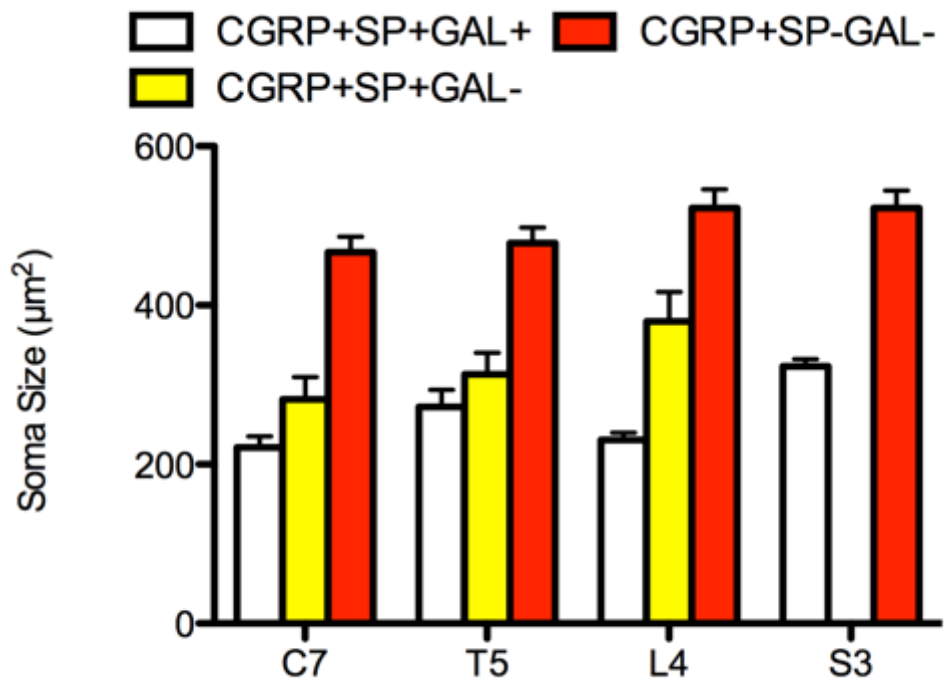
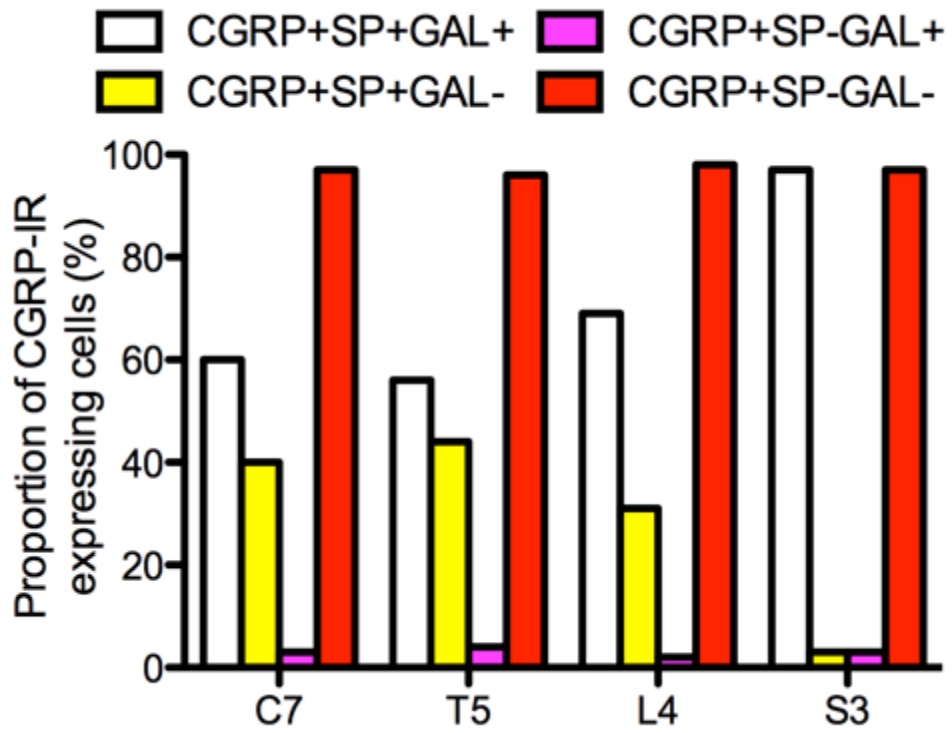


**Figure 4.23: Proportion of CGRP<sup>+</sup>SP<sup>-</sup>GAL<sup>-</sup> neurons in individual DRG**

**A:** Pie chart depicting the proportion of neuronal somata that expressed calcitonin gene related peptide-immunoreactivity (CGRP-IR) with substance P-IR (SP-IR) and galanin-IR (GAL-IR; CGRP<sup>+</sup>SP<sup>+</sup>GAL<sup>+</sup>; white), CGRP-IR with SP-IR but no GAL-IR (CGRP<sup>+</sup>SP<sup>+</sup>GAL<sup>-</sup>; yellow), CGRP-IR without SP-IR and GAL-IR (CGRP<sup>+</sup>SP<sup>-</sup>GAL<sup>-</sup>; red), GAL-IR without CGRP-IR and SP-IR (CGRP<sup>-</sup>SP<sup>-</sup>GAL<sup>+</sup>; blue), or expressed neither CGRP-IR, SP-IR nor NF200-IR (CGRP<sup>-</sup>SP<sup>-</sup>GAL<sup>-</sup>; black) in cervical (C7), thoracic (T5), lumbar (L5), and sacral (S3) dorsal root ganglia (DRG). GAL-IR was detected in 17% of C7 DRG neurons (N = 3 animals, n = 348 neurons), 15% of T5 DRG neurons (N = 3 animals, n = 348 neurons), 27% of L4 DRG neurons (N = 3 animals, n = 334 neurons) and 61% of S3 DRG neurons (N = 3 animals, n = 300 neurons) In C7, T5 and L4 DRG most CGRP<sup>+</sup>SP<sup>+</sup> neurons contained GAL-IR, and in S4 DRG virtually all CGRP<sup>+</sup>SP<sup>+</sup> neurons contained GAL-IR. In all DRG near zero CGRP<sup>+</sup>SP<sup>-</sup> neurons contained GAL-IR.

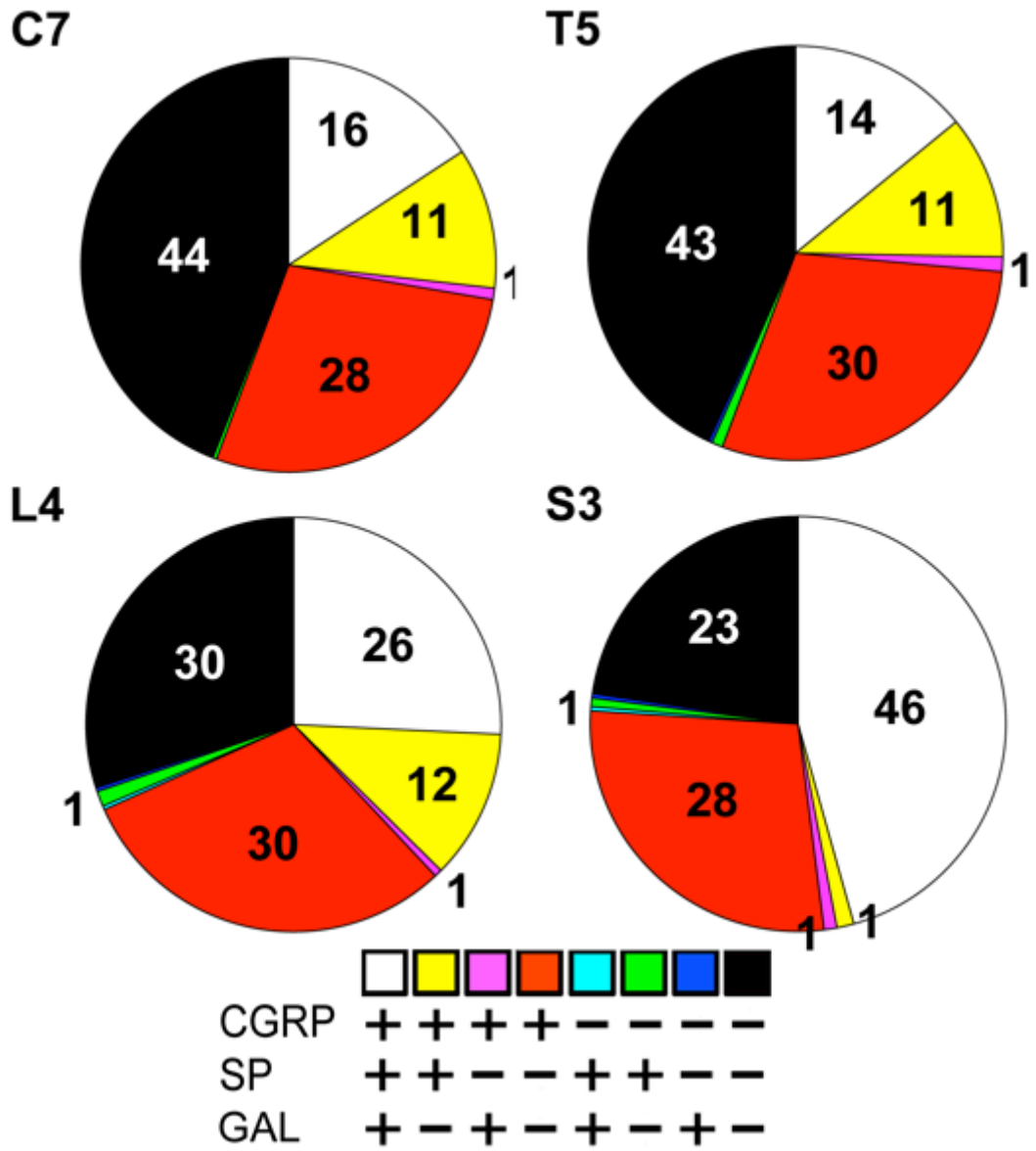


**Figure 4.24: Proportion and soma size of CGRP<sup>+</sup>SP<sup>-</sup>GAL<sup>-</sup> neurons in DRG of all spinal levels**

Histogram (data displayed as mean  $\pm$  SEM) depicting the size (cross sectional area;  $\mu\text{m}^2$ ) of neuronal somata that expressed calcitonin gene related peptide-immunoreactivity (CGRP-IR) with substance P-IR (SP-IR) and galanin-IR (GAL-IR; CGRP<sup>+</sup>SP<sup>+</sup>GAL<sup>+</sup>; white), CGRP-IR with SP-IR but no GAL-IR (CGRP<sup>+</sup>SP<sup>+</sup>GAL<sup>-</sup>; yellow), CGRP-IR without SP-IR and GAL-IR (CGRP<sup>+</sup>SP<sup>-</sup>GAL<sup>-</sup>; red) in cervical (C7), thoracic (T5), lumbar (L4) and sacral (S3) dorsal root ganglia (DRG).. In all DRG, CGRP<sup>+</sup>SP<sup>-</sup>GAL<sup>-</sup> neurons were the largest and there was no difference between the mean soma size of CGRP<sup>+</sup>SP<sup>+</sup>GAL<sup>+</sup> and CGRP<sup>+</sup>SP<sup>+</sup>GAL<sup>-</sup> neurons (C7: ANOVA:  $F_{(2,187)} = 26$ ,  $p < 0.0001$ ,  $N = 3$  animals,  $n = 190$  neurons; T5:  $F_{(2,181)} = 45$ ,  $p < 0.0001$ ,  $N = 3$  animals,  $n = 184$  neurons; L4:  $F_{(2,223)} = 71$ ,  $p < 0.0001$ ,  $N = 3$  animals,  $n = 226$  neurons; S3:  $F_{(2,219)} = 92$ ,  $p < 0.0001$ ,  $N = 3$  animals,  $n = 221$  neurons). There were no CGRP<sup>+</sup>SP<sup>+</sup>GAL<sup>-</sup> neurons in S3 DRG.

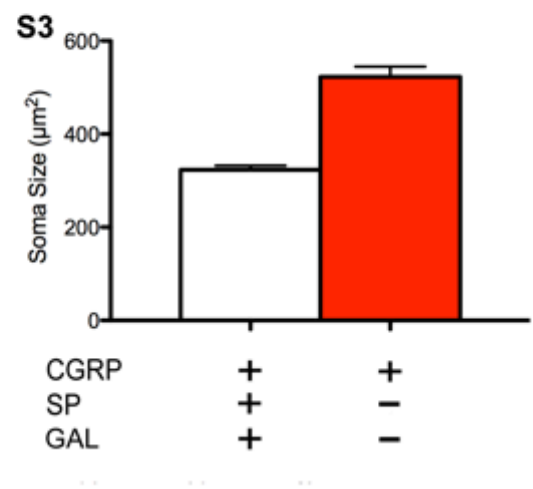
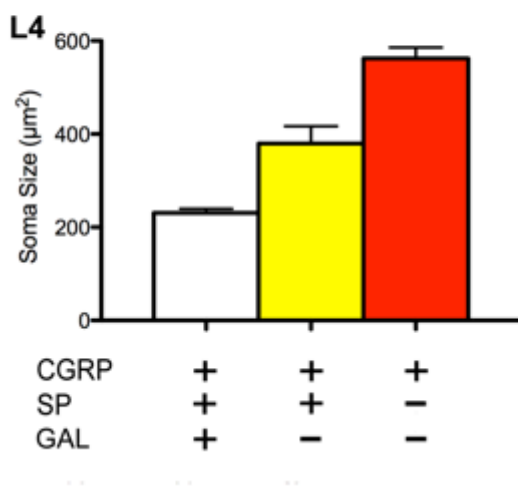
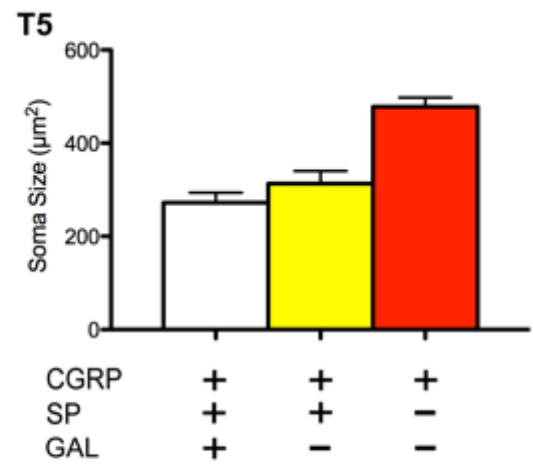
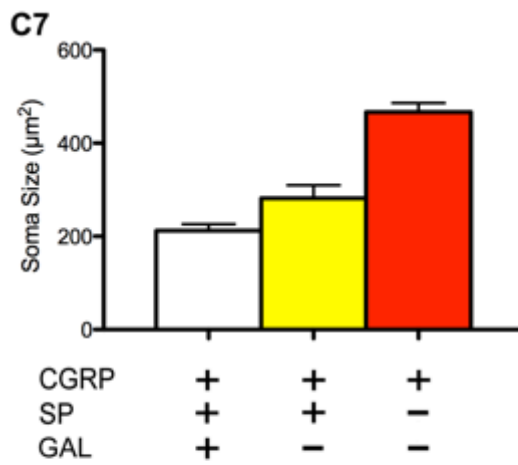


**Figure 4.25: VIP, CGRP and SP-IR in neuronal soma of the S3 DRG**

Widefield fluorescence microscopy of mouse sacral (S3) dorsal root ganglia (DRG) triple labelled for calcitonin gene-related peptide (CGRP; A), substance P (SP; B) and the vasoactive intestinal peptide (VIP; C). The overlay of A, B and C (D) shows four subpopulations of neurons positive for CGRP-immunoreactivity (IR): neurons containing CGRP-, SP- and VIP-IR (CGRP<sup>+</sup>SP<sup>+</sup>VIP<sup>+</sup>; white arrows; white in D) and neurons containing CGRP- and VIP-IR without SP-IR (CGRP<sup>+</sup>SP<sup>-</sup>VIP<sup>+</sup>; black arrows; magenta in D). Scale bar = 60  $\mu$ m in D (applies to A-D).

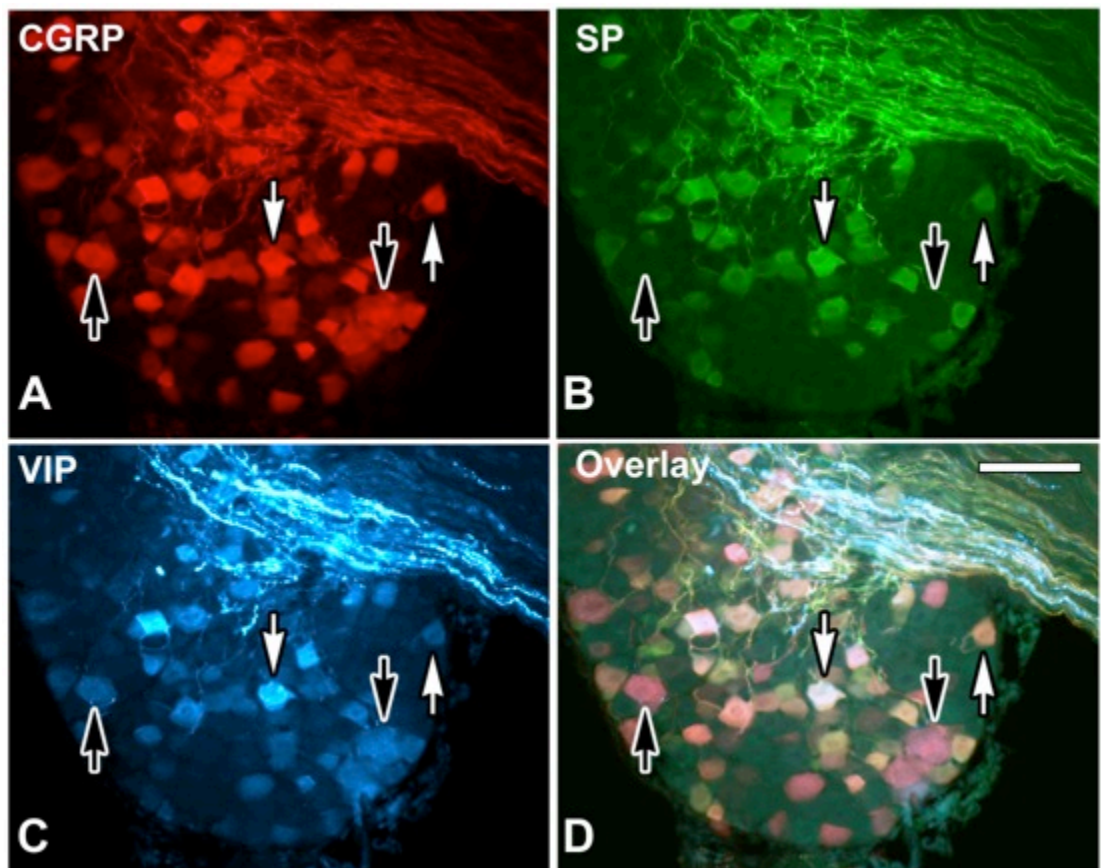


**Figure 4.26: Intensity of VIP-IR and soma size in DRG neurons**

Scatter dot plot (dots = cells; line = linear regression with 95% confidence limits) depicting the size of neuronal somata and their intensity of vasoactive intestinal peptide-immunoreactivity (VIP-IR) more than 2 standard deviations above mean background fluorescence in dorsal root ganglia (DRG) of all spinal levels. There was no correlation between the intensity of VIP-IR and the soma size of the neurons (linear correlation:  $r = 0.01$ ,  $p = 0.04$ ;  $N = 3$  animals,  $n = 313$  neurons). While the slope of the line is significantly different from zero ( $p = 0.04$ ), the correlation coefficient ( $r = 0.01$ ) is too small to denote any practical significance.

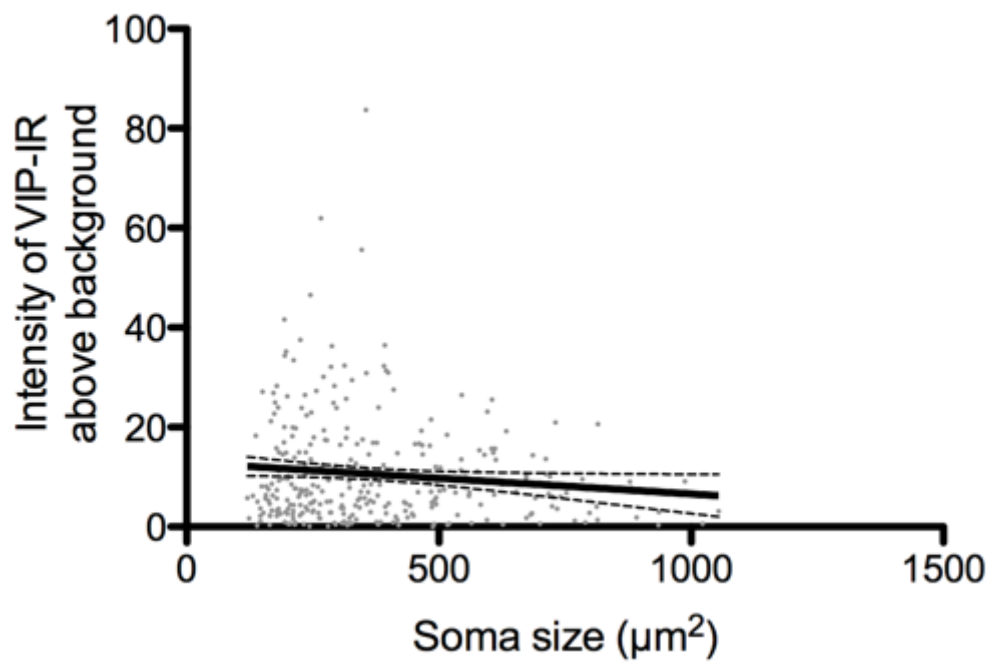


**Figure 4.27: Proportion of neuronal somata expressing VIP-IR in DRG of all spinal levels**

Histogram (data displayed as mean  $\pm$  SEM) depicting the proportion of neuronal somata that either expressed vasoactive intestinal peptide-immunoreactivity (VIP-IR; VIP+; blue bars) or lacked VIP-IR (VIP-; black bars) in cervical (C7), thoracic (T5), lumbar (L4), and sacral (S3) dorsal root ganglia (DRG). Overall, VIP-IR was present in a third of DRG neurons. A lower proportion of DRG neurons contained VIP-IR in C7 and T5 DRG and a higher proportion contained VIP-IR in L4 and S3 DRG compared to other levels (Chi-Square:  $\chi^2_3 = 14$ ,  $p = 0.003$ ;  $N = 3$  animals;  $n = 1064$  neurons).

**Figure 4.28: Soma size of neurons expressing VIP-IR in DRG of all spinal levels**

Histogram (mean  $\pm$  SEM) depicting the size (cross sectional area;  $\mu\text{m}^2$ ) of neuronal somata that either expressed vasoactive intestinal peptide-immunoreactivity (VIP-IR; VIP+; blue bars) or lacked VIP-IR (VIP-; black bars) in cervical (C7), thoracic (T5), lumbar (L4), and sacral (S3) dorsal root ganglia (DRG). VIP-IR was expressed in neurons with a mean soma size of  $378 \pm 11 \mu\text{m}^2$ . VIP-IR neurons were largest in T5 DRG, and GAL-IR neurons were larger in L4 DRG than S3 DRG ( $F_{(3,315)} = 13$ ,  $p < 0.0001$ ;  $N = 3$  animals,  $n = 319$  neurons).

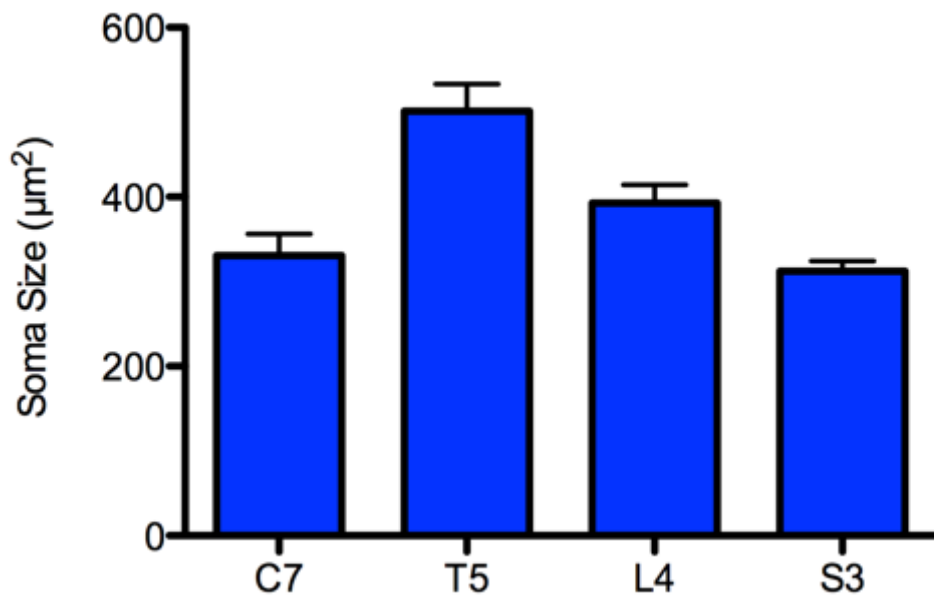
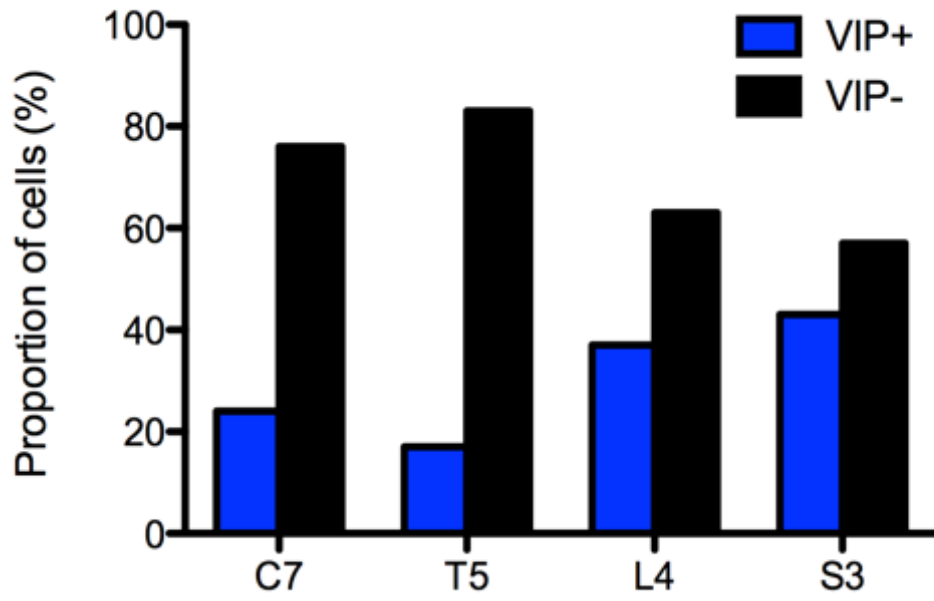


**Figure 4.29: Proportion of CGRP<sup>+</sup>SP<sup>-</sup>VIP<sup>-</sup> neurons in DRG of all spinal levels**

Histogram (total percentage) depicting the proportion of neuronal somata that expressed calcitonin gene related peptide-immunoreactivity (CGRP-IR) with substance P-IR (SP-IR) that also vasoactive intestinal peptide (VIP; CGRP<sup>+</sup>SP<sup>+</sup>VIP<sup>+</sup>; white) or lacked VIP (CGRP<sup>+</sup>SP<sup>+</sup>VIP<sup>-</sup>; yellow) and the proportion of neuronal somata that expressed CGRP without SP-IR that expressed VIP-IR (CGRP<sup>+</sup>SP<sup>-</sup>VIP<sup>+</sup>; magenta) or lacked VIP-IR (CGRP<sup>+</sup>SP<sup>-</sup>VIP<sup>-</sup>; red) in cervical (C7), thoracic (T5), lumbar (L4), and sacral (S3) dorsal root ganglia (DRG). The majority CGRP<sup>+</sup>SP<sup>-</sup> neurons had VIP-IR and this was consistent between the DRG of different levels (Chi-Square:  $\chi^2_3 = 4$ ,  $p = 0.2$ ;  $N = 3$  animals;  $n = 265$  neurons). Only a third of CGRP<sup>+</sup>SP<sup>-</sup> neurons contained GAL-IR. A lower proportion of CGRP<sup>+</sup>SP<sup>-</sup> neurons contained VIP-IR in C7 and T5 DRG than compared to L4 and S3 DRG (Chi-Square:  $\chi^2_3 = 14$ ,  $p = 0.004$ ;  $N = 3$  animals;  $n = 327$  neurons).

**Figure 4.30: Soma size of CGRP<sup>+</sup>SP<sup>-</sup>TRPV1<sup>-</sup> neurons in DRG of all spinal levels**

Histogram (mean  $\pm$  SEM) depicting the size (cross sectional area;  $\mu\text{m}^2$ ) of neuronal somata that expressed calcitonin gene related peptide-immunoreactivity (CGRP-IR) with substance P-IR (SP-IR) and vasoactive intestinal peptide-IR (VIP-IR; CGRP<sup>+</sup>SP<sup>+</sup>VIP<sup>+</sup>; white), with SP-IR but no VIP-IR (CGRP<sup>+</sup>SP<sup>+</sup>VIP<sup>-</sup>; yellow), with VIP-IR but no SP-IR (CGRP<sup>+</sup>SP<sup>-</sup>VIP<sup>+</sup>; magenta), without SP-IR and VIP-IR (CGRP<sup>+</sup>SP<sup>-</sup>VIP<sup>-</sup>; red) in cervical (C7), thoracic (T5), lumbar (L4), and sacral (S3) dorsal root ganglia (DRG). At all levels, CGRP<sup>+</sup>SP<sup>-</sup>VIP<sup>+</sup> neurons were the largest, and CGRP<sup>+</sup>SP<sup>-</sup>VIP<sup>-</sup> neurons were larger than CGRP<sup>+</sup>SP<sup>+</sup>VIP<sup>+</sup> and CGRP<sup>+</sup>SP<sup>+</sup>VIP<sup>-</sup> neurons (ANOVA:  $F_{(2,512)} = 31$ ,  $p < 0.0001$ ;  $N = 3$  animals,  $n = 528$  neurons). There was no difference between the size of CGRP<sup>+</sup>SP<sup>+</sup>VIP<sup>+</sup> and CGRP<sup>+</sup>SP<sup>+</sup>VIP<sup>-</sup> neurons. CGRP<sup>+</sup>SP<sup>+</sup>VIP<sup>+</sup> and CGRP<sup>+</sup>SP<sup>+</sup>VIP<sup>-</sup> neurons were larger in T5 DRG than the other levels and CGRP<sup>+</sup>SP<sup>-</sup>VIP<sup>+</sup> neurons were smaller in S3 DRG than the other levels (ANOVA:  $F_{(3,512)} = 12$ ,  $p < 0.0001$ ;  $N = 3$  animals,  $n = 528$  neurons). There was no difference between the sizes of CGRP<sup>+</sup>SP<sup>-</sup>VIP<sup>-</sup> neurons between the levels.

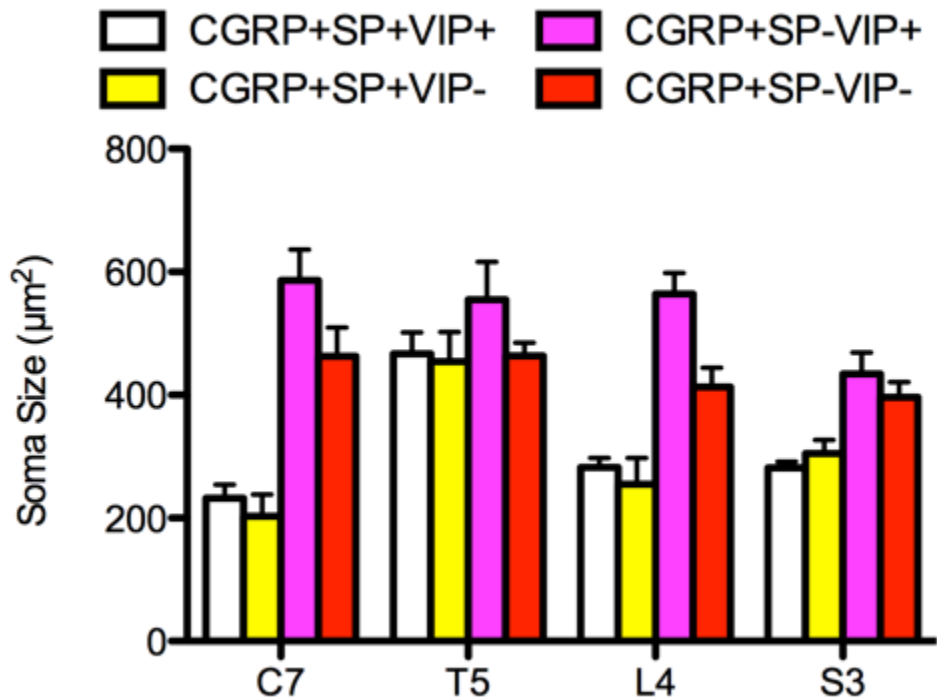
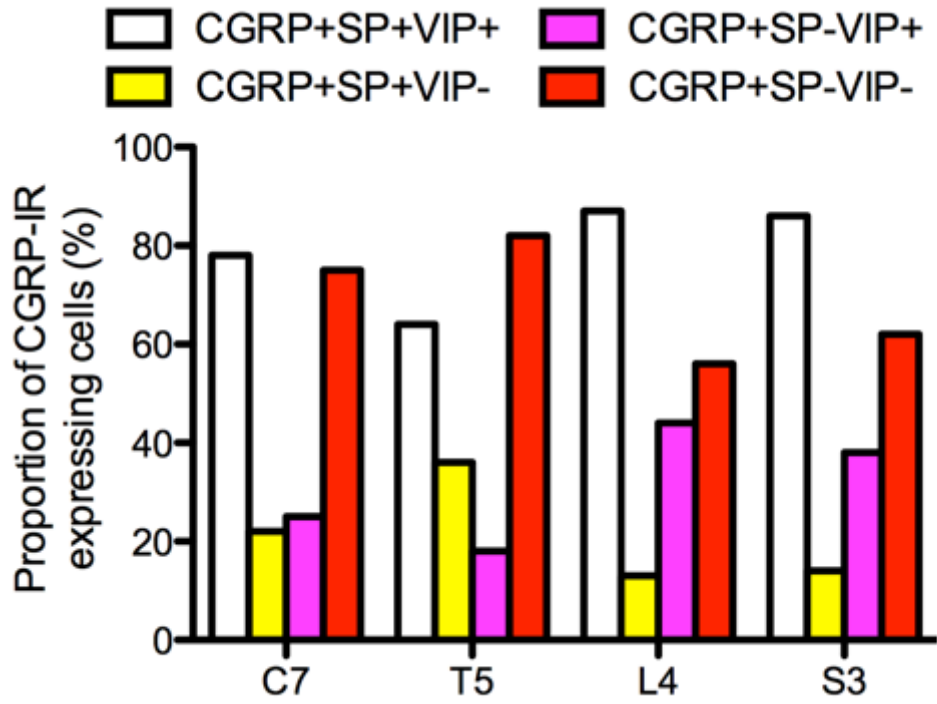


**Figure 4.31: Proportion of CGRP<sup>+</sup>SP<sup>-</sup>VIP<sup>-</sup> neurons in individual DRG**

Pie chart depicting the proportion of neuronal somata that expressed calcitonin gene related peptide-immunoreactivity (CGRP-IR) with substance P-IR (SP-IR) and vasoactive intestinal peptide-IR (VIP-IR; CGRP<sup>+</sup>SP<sup>+</sup>VIP<sup>+</sup>; white), CGRP-IR with SP-IR but no VIP-IR (CGRP<sup>+</sup>SP<sup>+</sup>VIP<sup>-</sup>; yellow), CGRP-IR with VIP-IR but no SP-IR (CGRP<sup>+</sup>SP<sup>-</sup>VIP<sup>+</sup>; magenta), CGRP-IR without SP-IR and VIP-IR (CGRP<sup>+</sup>SP<sup>-</sup>VIP<sup>-</sup>; red), or expressed neither CGRP-IR, SP-IR nor VIP-IR (CGRP<sup>-</sup>SP<sup>-</sup>VIP<sup>-</sup>; black) in cervical (C7), thoracic (T5), lumbar (L4), and sacral (S3) dorsal root ganglia (DRG)

VIP-IR was detected in 24% (59/241) of C7 DRG neurons (N = 3 animals, n = 241 neurons), 17% of T5 DRG neurons (N = 3 animals, n = 292 neurons), 37% of L4 DRG neurons (N = 3 animals, n = 289 neurons), and 43% of S3 DRG neurons (N = 3 animals, n = 242 neurons). In all levels, at least half the CGRP<sup>+</sup>SP<sup>+</sup> neurons had VIP-IR and most of the CGRP<sup>+</sup>SP<sup>-</sup> neurons lacked VIP-IR.

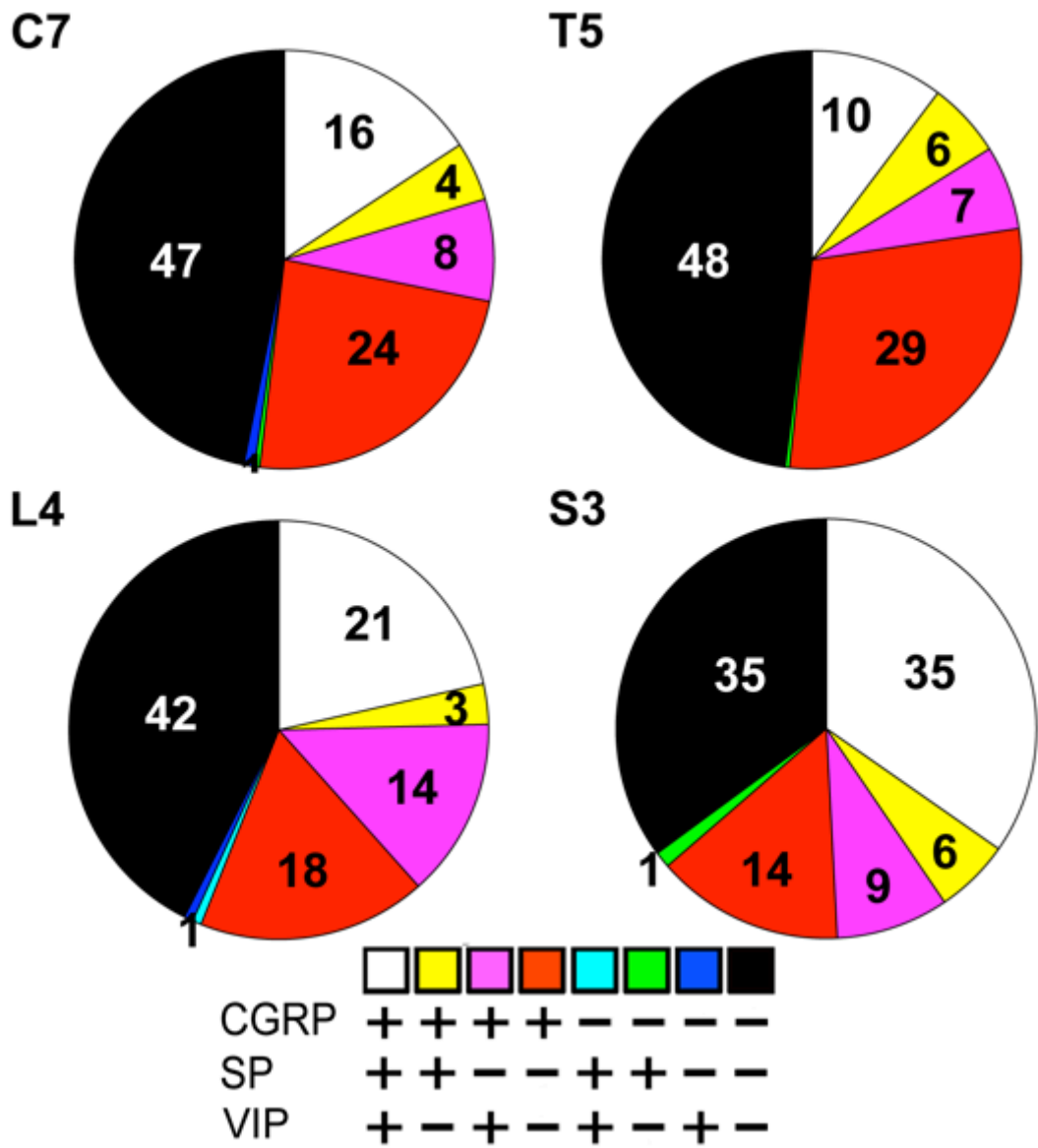
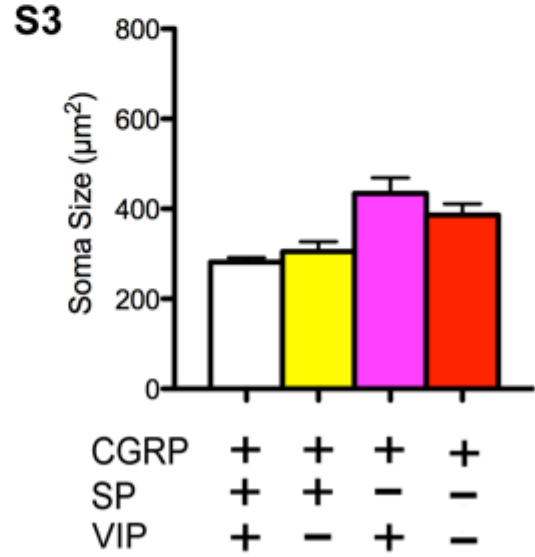
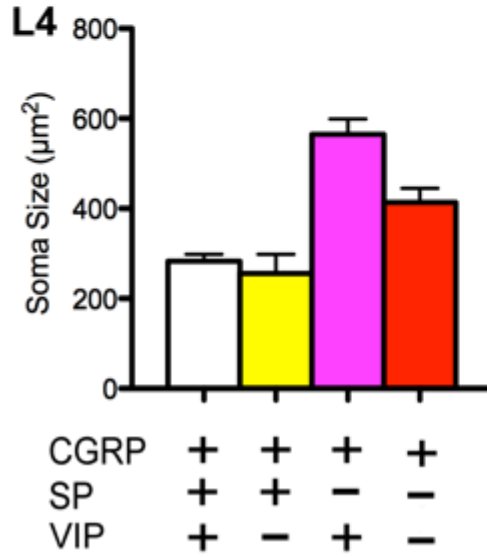
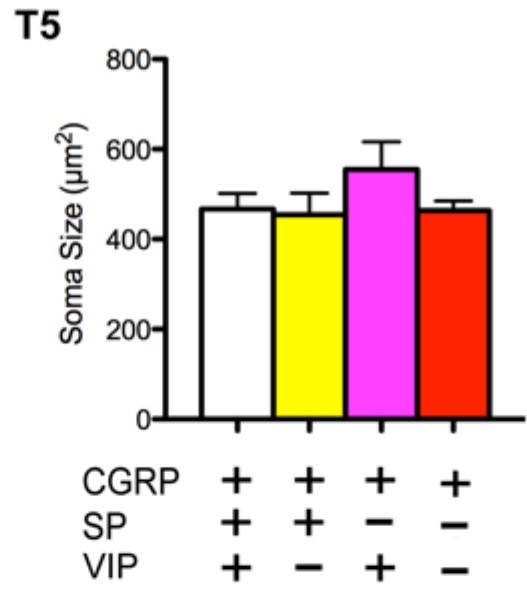
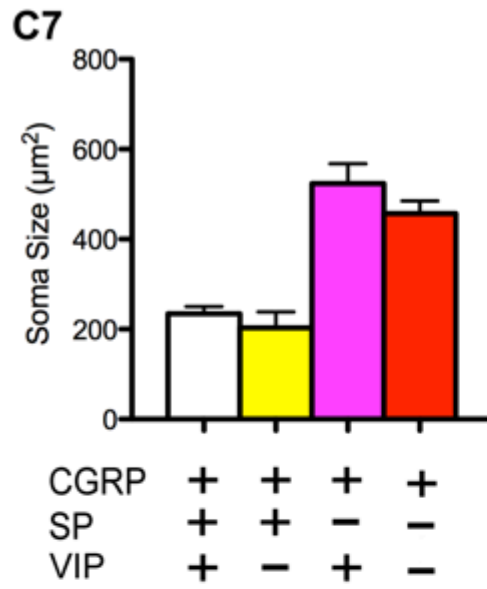


**Figure 4.32: Soma size of CGRP<sup>+</sup>SP<sup>-</sup>VIP<sup>-</sup> neurons in individual DRG**

Histogram (mean  $\pm$  SEM) depicting the size (cross sectional area;  $\mu\text{m}^2$ ) of neuronal somata that expressed calcitonin gene related peptide-immunoreactivity (CGRP-IR) with substance P-IR (SP-IR) and vasoactive intestinal peptide-IR (VIP-IR; CGRP<sup>+</sup>SP<sup>+</sup>VIP<sup>+</sup>; white), CGRP-IR with SP-IR but no VIP-IR (CGRP<sup>+</sup>SP<sup>+</sup>VIP<sup>-</sup>; yellow), CGRP-IR with VIP-IR but no SP-IR (CGRP<sup>+</sup>SP<sup>-</sup>VIP<sup>+</sup>; magenta), CGRP-IR without SP-IR and VIP-IR (CGRP<sup>+</sup>SP<sup>-</sup>VIP<sup>-</sup>; red) in cervical (C4), thoracic (T5), lumbar (L4) or sacral (S3) dorsal root ganglia (DRG). In both C7 and S3 DRG CGRP<sup>+</sup>SP<sup>-</sup>VIP<sup>+</sup> and CGRP<sup>+</sup>SP<sup>-</sup>VIP<sup>-</sup> neurons were larger than CGRP<sup>+</sup>SP<sup>+</sup>VIP<sup>+</sup> and CGRP<sup>+</sup>SP<sup>+</sup>VIP<sup>-</sup> neurons (C7: ANOVA:  $F_{(3,121)} = 21$ ,  $p < 0.0001$ ,  $N = 3$  animals,  $n = 125$  neurons; S3:  $F_{(3,150)} = 13$ ,  $p < 0.0001$ ,  $N = 3$  animals,  $n = 154$  neurons). In L4 DRG, CGRP<sup>+</sup>SP<sup>-</sup>VIP<sup>+</sup> neurons were the largest, and CGRP<sup>+</sup>SP<sup>-</sup>VIP<sup>-</sup> neurons were larger than CGRP<sup>+</sup>SP<sup>+</sup>VIP<sup>+</sup> and CGRP<sup>+</sup>SP<sup>+</sup>VIP<sup>-</sup> neurons (ANOVA:  $F_{(3,158)} = 21$ ,  $p < 0.0001$ ,  $N = 3$  animals,  $n = 162$  neurons). In T5 DRG, there was no difference in the size of any of the neurons (ANOVA:  $F_{(3,147)} = 1$ ,  $p = 0.3$ ,  $N = 3$  animals,  $n = 151$  neurons).





---

**Chapter 5:  
Retrograde tracing of  
CGRP<sup>+</sup>SP<sup>-</sup> muscle  
afferents**

---



## 5.1 Background

---

In previous chapters, we have demonstrated CGRP without SP (CGRP<sup>+</sup>SP<sup>-</sup>) neurons in the DRG with large soma sizes and CGRP<sup>+</sup>SP<sup>-</sup> peripheral fibres penetrating the epithelium and encircling hair follicles in paw skin. McCarthy and Lawson (1990) have also demonstrated CGRP-IR present in both small and large somata of the DRG and ascertained that the smaller somata had C-fibre conduction velocities whereas, the larger somata had A-fibre conduction velocities. McCarthy and Lawson (1989) demonstrated that SP-IR was only present in small somata of the DRG with C-fibre conduction velocities, hence it is most likely that the large CGRP<sup>+</sup>SP<sup>-</sup> neurons of our study were A-fibre neurons. While it is mostly nociceptive C-fibre units that contain CGRP-IR, nociceptive A $\delta$  fibres, and A $\alpha$ /A $\beta$  fibres also contain CGRP-IR (Lawson *et al.*, 2002). Based on these findings it is most likely that CGRP<sup>+</sup>SP<sup>-</sup> fibres penetrating the epidermis were A $\delta$  fibres (possibly nociceptive) and that the CGRP<sup>+</sup>SP<sup>-</sup> fibres encircling the hair follicle were A $\alpha$ /A $\beta$  G-hair units. While the cutaneous afferents have been extensively investigated, muscle afferents potentially responsible for nociception are poorly neurochemically characterised.

In the muscle, nociceptors are classified differently from nociceptors of the skin and viscera. C-fibre afferents and A $\delta$ -fibre afferents correlate with group IV and III muscle afferents, respectively, however differences between muscle and cutaneous pain suggest the underlying mechanisms may not be identical (Mense, 2008). While cutaneous nociception is characterised by a distinct first and second pain, muscular nociception has only a single pain (Mense, 2008). Pain quality is also different, cutaneous pain is well localized and described as stabbing, burning or cutting, while muscle pain tends to be referred and described as tearing, cramping or pressing (Mense, 2008). Muscle nociceptors are specialized to respond to stimuli associated with actual or potential damage to muscle, including trauma, high mechanical load and chemical agents such as pro-inflammatory cytokines or high levels of metabolites (Mense, 2009; Jankowski *et al.*, 2013).

Muscle tissue is innervated by a number of different fibre classes. Group I (corresponding to cutaneous A $\alpha$ -fibres) and II (corresponding to cutaneous A $\beta$ -fibres) fibres are mainly proprioceptive. Proprioceptors include the muscle spindles (or stretch receptors) that are innervated by both group Ia and II fibres, and Golgi tendon organs that are innervated by group Ib fibres. Muscle tissue is also richly

innervated by free nerve endings. However, free nerve endings are not as well characterised as those innervating the skin, and there is no definitive correlation between the morphology and function of free nerve endings in muscle tissue (Jankowski *et al.*, 2013). Nociceptors are restricted to the slowly conducting group III and group IV in muscle. Group III nociceptors are mainly mechanically sensitive and group IV are chemically sensitive (Kaufman & Rybicki, 1987; Jankowski *et al.*, 2013). Not all group III fibres are nociceptors, but the majority of group IV fibres are nociceptors (Jankowski *et al.*, 2013).

Recently, we have demonstrated that CGRP<sup>+</sup>SP<sup>-</sup> fibres were present in the gastrocnemius muscle of mice (Gillan, 2012). These fibres were seen within the connective tissue, associated with blood vessels, or freely distributed in the muscle tissue with no obvious associations with other structures (Gillan, 2012). The origins of these primary afferents have not been investigated. In order to determine the origin of the muscular afferents in the gastrocnemius muscle, we used a retrograde tracing technique to visualize the somata of these afferents in dorsal root ganglia (DRG). The size and neurochemical profile of retrogradely labelled somata was determined with multiple-labelling immunohistochemistry to give an indication of their possible function.

## 5.2 Materials and Methods

---

Mice were anaesthetized with a constant flow of isoflurane (Veterinary Companies Australia NSW, Australia) and medical oxygen through an attached nose cone. The right hind leg of the animal was shaved and wiped with ethanol. A 25G needle was used to first break the skin, in distal end of the calf, and then a Hamilton syringe was used to inject either cholera toxin subunit B (CTXb) conjugated to biotin (CTXb-biotin; 1 mg/mL; Molecular Probes, VIC, Australia) or CTXb-Alexa Fluor-555 (1 mg/mL; Molecular Probes). Four injections of 5  $\mu$ L (for a total volume of 20  $\mu$ L) of CTXb were injected into multiple sites of the gastrocnemius muscle. The injection site was then cleaned with ethanol and sealed with a droplet of liquid Opsite (Smith and Nephew, Hull, England). Mice were allowed to recover and their health was monitored for 7 days.

After 7 days, mice were euthanized and their right gastrocnemius muscle, lumbar spinal cord, and both ipsilateral and contralateral L3-L5 DRGs were removed. Spinal cord and DRG samples were fixed, processed through DMSO, embedded in PEG and sectioned using a microtome. Muscle samples were fixed, processed through xylene and sectioned using a cryostat. Sections were double labelled with anti-CGRP raised in a goat (1:1000; code 1780, Arnel, New York, USA) and anti-SP raised in a rabbit (1:2000; Incstar [now Immunostar], Wisconsin, USA).

Muscle, spinal cord and DRG sections were assessed for CTXb labelling. Widefield images of DRG sections were taken with a 20x objective and imported to ImageJ to determine the presence or absence of IR and their soma cross-sectional area. Data was then displayed as mean $\pm$ SEM and RMANOVA with post hoc BMC correction with 95% confidence limits was used to determine the statistical significance.



## 5.3 Results

---

After injection of CTXb into the left gastrocnemius, CTXb labelled nerve fibres of the injected gastrocnemius, and neuronal somata of the ipsilateral L3, L4 and L5 DRG. CTXb did not label nerve fibres in the contralateral gastrocnemius, or neuronal somata of contralateral L3-L5 DRG, or fibres in the dorsal horn of the spinal cord.

CTXb labelled neuronal somata most frequently in the L4 DRG. In the L4 DRG (N = 4 animals, n = 597 neurons; Figure 5.1), CTXb labelled neuronal somata but not fibres. CTXb labelling was uniformly intense in the cytoplasm of small (50-250  $\mu\text{m}^2$ ) to medium sized neurons (250-500  $\mu\text{m}^2$ ), but less intense and more granular in larger neurons (> 500  $\mu\text{m}^2$ ; Figure 5.1A). CTXb labelled 10% of the neurons in the L4 DRG (62/597 neurons, Fig. 1). CTXb-labelled neurons were more prominent in small sized neurons (34/62) compared to medium (11/62) and large neurons (16/62; Chi-Square:  $\chi^2_3 = 1$ , p = 0.0004; N = 4 animals; n = 62 neurons; Figure 5.2)

Some of these CTXb-labelled neurons contained CGRP-IR (Figure 5.3). Most (53%; 33/62) CTXb-labelled neurons were CGRP<sup>+</sup>SP<sup>-</sup> neurons (Chi-Square:  $\chi^2_3 = 30$ , p < 0.0001; N = 4 animals; n = 62; Figure 5.4). 24% (15/62 neurons) of CTXb labelled neurons were CGRP<sup>+</sup>SP<sup>+</sup> neurons, and 21% (13/62 neurons) lacked both peptides (CGRP<sup>-</sup>SP<sup>-</sup>; Figure 5.4). The CTXb labelled neurons that were CGRP<sup>+</sup>SP<sup>-</sup> were significantly larger (455±49  $\mu\text{m}^2$ ) than the CTXb labelled neurons that were CGRP<sup>+</sup>SP<sup>+</sup> (184±21  $\mu\text{m}^2$ ), or CGRP<sup>-</sup>SP<sup>-</sup> (249±76  $\mu\text{m}^2$ ; ANOVA:  $F_{(2,62)} = 7$ , p < 0.01; N = 4 animals, n = 62 neurons; Figure 5.5).

Of the CGRP-IR containing neurons 12% (48/390 neurons) were labelled with CTXb (Figure 5.6A). 13% (33/262 neurons) of CGRP<sup>+</sup>SP<sup>-</sup> neurons (Figure 5.6D), and 12% (15/128) of CGRP<sup>+</sup>SP<sup>+</sup> (Figure 5.6C) neurons were labelled with CTXb. Only 6% (13/205 neurons) of CGRP<sup>-</sup>SP<sup>-</sup> neurons were labelled with CTXb (Figure 5.6B).



## 5.4 Discussion

---

Previous chapters have demonstrated distinct immunohistochemical populations of cutaneous CGRP<sup>+</sup>SP<sup>-</sup> fibres with medium-large cell bodies in the DRG, and central terminals in lateral lamina I and deep lamina IV/V of the dorsal horn. These neurons were further distinguished from CGRP<sup>+</sup>SP<sup>+</sup> neurons by lacking detectable levels of TRPV1 and expressing NF200. We have also previously shown the presence of these CGRP<sup>+</sup>SP<sup>-</sup> fibres in muscle tissue (Gillan, 2012) and this current chapter has set out to characterise the origin of these fibres in the DRG using a retrograde tracer.

CTXb injections were very localised in the gastrocnemius tissue and consequently only a small number of DRG neurons were labelled with CTXb. The majority of CTXb labelled neurons had small somata (50-250  $\mu\text{m}^2$ ) with some medium (250-500  $\mu\text{m}^2$ ) and large (> 500  $\mu\text{m}^2$ ) neurons labelled with CTXb. While very few studies have retrogradely labelled sensory afferents from skeletal muscle, those that had, obtained similar number and size profiles to this present study, with a larger proportion of smaller neurons (Chyczewski *et al.*, 2006; Pierce *et al.*, 2006). Chyczewski and colleagues (2006) injected Fast Blue into the porcine longissimus dorsi muscle, and Pierce and colleagues (2006) injected CTXb into the levator ani muscle of monkeys.

There were three subpopulations of DRG neurons innervating the gastrocnemius: CGRP<sup>+</sup>SP<sup>+</sup> neurons, CGRP<sup>+</sup>SP<sup>-</sup> neurons, and CGRP<sup>-</sup>SP<sup>-</sup>. The peripheral fibres of these subpopulations were evident in the gastrocnemius muscle as free nerve fibres (Gillan, 2012). Unlike cutaneous afferents, there is no definitive correlation between the morphology and function of free nerve endings of muscular afferents (Jankowski *et al.*, 2013). Nociceptors are restricted to the slowly conducting group III (corresponding to cutaneous A $\delta$ -fibres) and group IV (corresponding to cutaneous C-fibres) in muscle. In DRG, the CTXb-labelled CGRP<sup>+</sup>SP<sup>-</sup> neurons were larger than the CTXb-labelled CGRP<sup>+</sup>SP<sup>+</sup> neurons, and were probably A $\beta$ /A $\delta$ -fibre (group II/III) neurons (McCarthy & Lawson, 1990).

Group II afferents innervate muscle spindles and are not often associated with nociception. Although not analysed, CGRP<sup>+</sup>SP<sup>-</sup> fibres were seen once in association with muscle spindles (Gillan, 2012), however CGRP is very rarely seen associated with muscle spindles (Hoheisel *et al.*, 1994). Hence it is unlikely that the CTXb-

labelled CGRP<sup>+</sup>SP<sup>-</sup> neurons were group II afferents and more likely that these neurons were group III afferents. Most group III afferents are mechanically sensitive (Kaufman & Rybicki, 1987; Jankowski *et al.*, 2013). Not all group III afferents are nociceptive and many respond to non-noxious tendon stretch and probing of their receptive fields (Kaufman *et al.*, 1983; Mense & Meyer, 1985). Nociceptive group III afferents have an increasing response to tetanic contractions (maximum contraction possible) that decreases as the contraction is released (Kaufman *et al.*, 1983; Mense & Meyer, 1985). The nociceptive group III afferents appear to protect the muscle from damage from prolonged contraction. From our results it cannot be concluded whether the CTXb-labelled CGRP<sup>+</sup>SP<sup>-</sup> neurons were nociceptive or non-nociceptive group III afferents.

The CTXb-labelled CGRP<sup>+</sup>SP<sup>+</sup> and CGRP<sup>-</sup>SP<sup>-</sup> neurons were smaller than the CTXb-labelled CGRP<sup>+</sup>SP<sup>-</sup> neurons. The CTXb-labelled CGRP<sup>+</sup>SP<sup>+</sup> neurons were most likely C-fibre (group IV) neurons (McCarthy & Lawson, 1989) and, as these neurons were the same size as the CTXb-labelled CGRP<sup>-</sup>SP<sup>-</sup> neurons, it is likely that these CGRP<sup>-</sup>SP<sup>-</sup> neurons were also group IV neurons. Group IV neurons in muscle can be categorised as either metaboreceptors or metabo-nociceptors (Light *et al.*, 2008; Jankowski *et al.*, 2013). Metaboreceptors contribute to the sensation of fatigue (Light *et al.*, 2008; Jankowski *et al.*, 2013), whereas metabo-nociceptors serve a nociceptive function (Light *et al.*, 2008; Jankowski *et al.*, 2013). It is probable that the CTXb-labelled CGRP<sup>+</sup>SP<sup>+</sup> neurons were metabo-nociceptors as all SP containing primary afferent fibres are presumed nociceptive (Lawson *et al.*, 1997). Metabo-nociceptors were also demonstrated to express TRPV1 (Light *et al.*, 2008; Jankowski *et al.*, 2013) and we have previously demonstrated all CGRP<sup>+</sup>SP<sup>+</sup> neurons expressed TRPV1. The metaboreceptors expressed the purinergic P2X3 receptor (Jankowski *et al.*, 2013), which is not expressed by peptidergic neurons. Hence, the nonpeptidergic CTXb-labelled CGRP<sup>-</sup>SP<sup>-</sup> neurons may have been metaboreceptors.

Cutaneous CGRP<sup>+</sup>SP<sup>-</sup> fibres were most likely A $\alpha$ /A $\beta$  fibre G-hair units and A $\delta$  fibre mechanoreceptors (possibly nociceptive). This current study has demonstrated that CGRP<sup>+</sup>SP<sup>-</sup> fibres also innervate muscle tissue and these fibres were most likely group III mechanoreceptors (possibly nociceptive). Both cutaneous and muscular CGRP<sup>+</sup>SP<sup>-</sup> afferents appear to be mechanoreceptors and it is not yet clear whether they have a role in nociception.

## **5.5 Figures**

---

**Figure 5.1: CTXb labelled neuronal somata in L4 DRG**

Widefield fluorescence microscopy of cholera toxin subunit B (CTXb) labelling in neuronal somata of the L4 dorsal root ganglia (DRG) ipsilateral (ipsi; A) and contralateral (contra; B) to the injection of CTXb. CTXb labelled neurons of the ipsilateral DRG in both small (white arrows) and large (black arrows) diameter neuronal somata. In large soma the CTXb labelling was more granular. No CTXb labelling was detected in the contralateral DRG. Scale bar = 60  $\mu\text{m}$  in both A and B

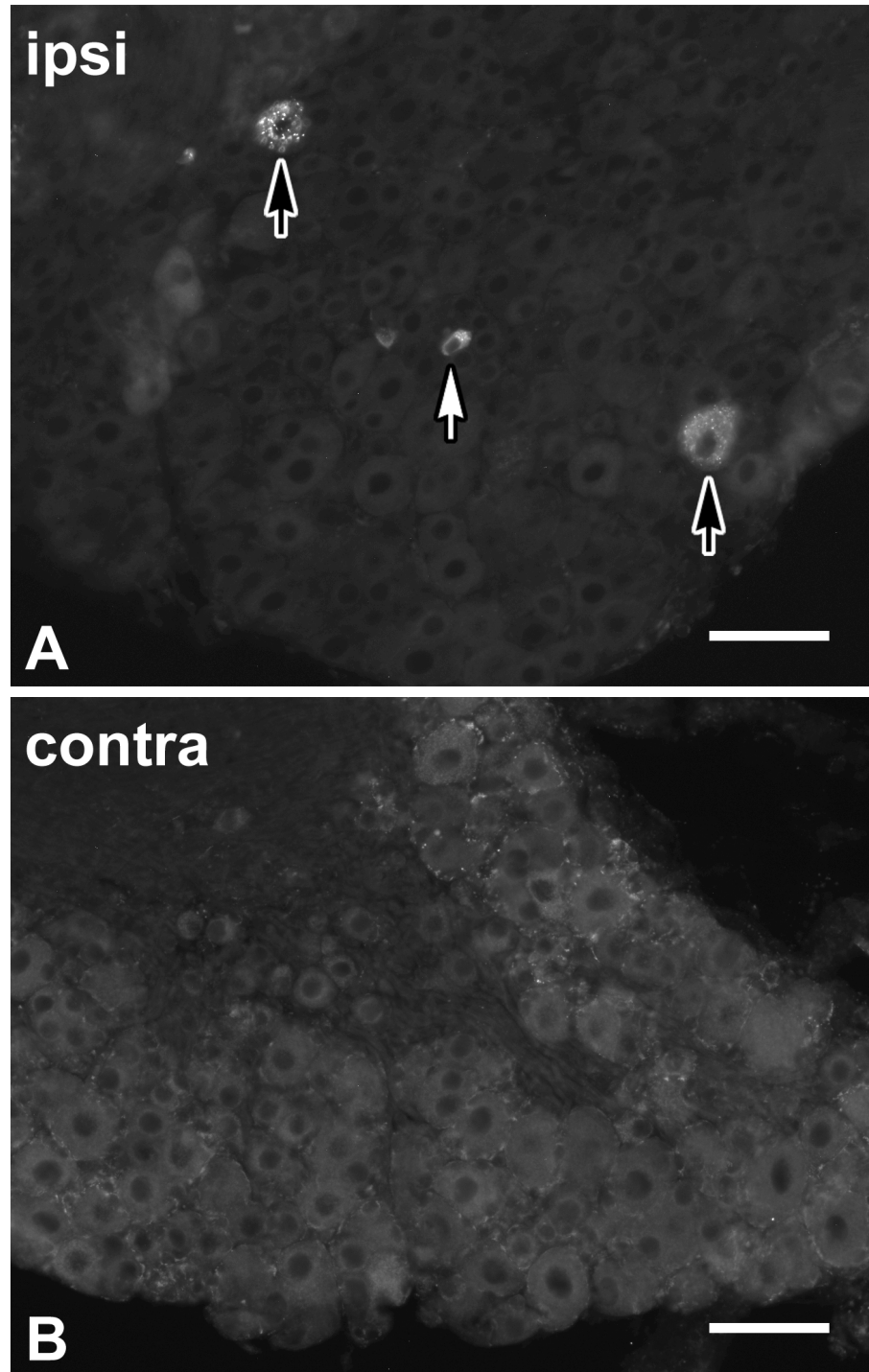


**Figure 5.2: CTXb labelled neuronal somata of various sizes in L4 DRG**

Frequency histogram depicting the size profile of cholera toxin subunit B (CTXb) labelled somata in the L4 dorsal root ganglia (DRG). CTXb-labelled neurons were more prominent in small sized neurons (50-250  $\mu\text{m}^2$ ; dark grey shaded area) compared to medium (250-500  $\mu\text{m}^2$ ; light grey shaded area) and large neurons (> 500  $\mu\text{m}^2$ ; white area; Chi-Square:  $\chi^2_2 = 13.8$ ,  $p = 0.001$ ;  $N = 4$  animals;  $n = 62$  neurons)

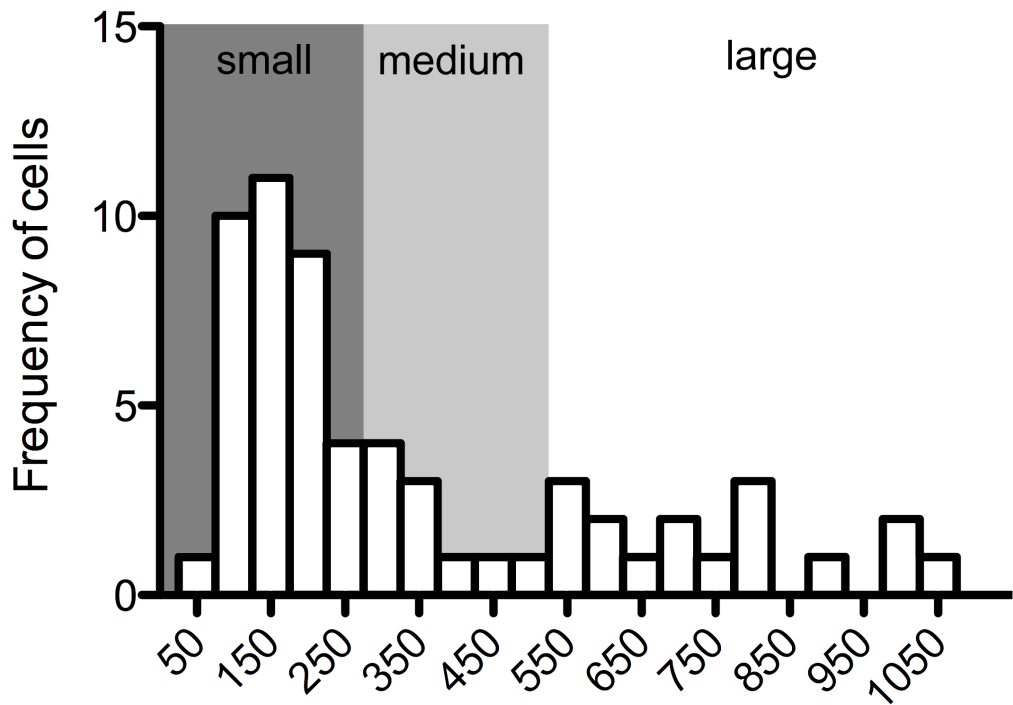


**Figure 5.3: CTXb labelled neurons expressing CGRP-IR in L4 DRG**

Widefield fluorescence microscopy of mouse L4 dorsal root ganglia (DRG) ipsilateral to the injection of cholera toxin subunit B (CTXb) and triple labelled for calcitonin gene-related peptide (CGRP; A; red), substance P (SP; B; green) and CTXb (C; blue). The overlay (D) shows a CTXb labelled neuron containing CGRP-immunoreactivity (IR) without SP-IR (CGRP<sup>+</sup>SP<sup>-</sup>; black arrow), containing CGRP-IR with SP-IR (CGRP<sup>+</sup>SP<sup>+</sup>; white arrow), and containing neither CGRP-IR or SP-IR (CGRP<sup>+</sup>SP<sup>-</sup>; white arrowhead). Scale bar = 60  $\mu$ m in D (applies to A-D)

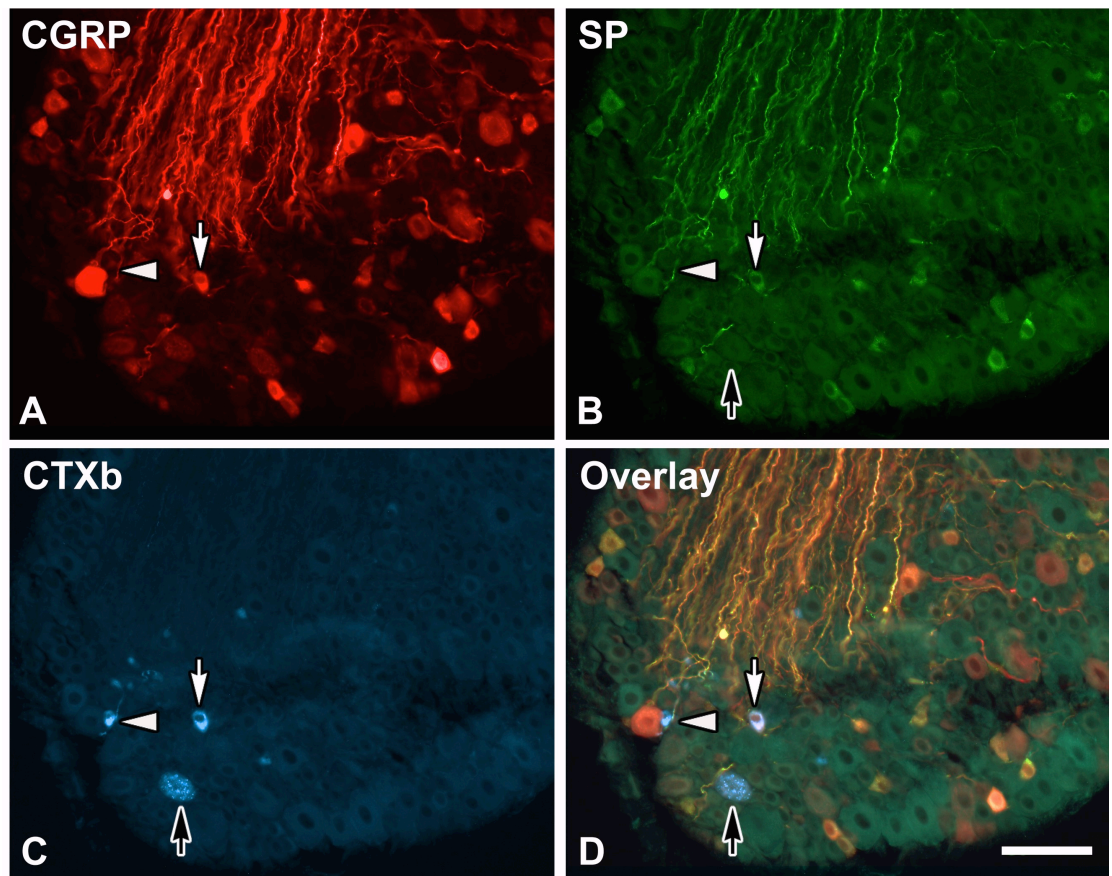


**Figure 5.4: Proportion of CTXb labelled neurons expressing CGRP-IR -IR in L4 DRG**

A pie chart depicting the proportion of neuronal somata labelled with cholera toxin subunit B (CTXb) that also contained calcitonin gene related peptide-immunoreactivity (CGRP-IR) but not substance P-IR (SP; CGRP<sup>+</sup>SP<sup>-</sup>; red area), CGRP-IR with SP-IR (CGRP<sup>+</sup>SP<sup>+</sup>; yellow area), SP-IR without CGRP-IR (CGRP<sup>-</sup>SP<sup>+</sup>; green area), or neither peptide (CGRP<sup>-</sup>SP<sup>-</sup>; black area) in L4 dorsal root ganglia (DRG). Most of the neuronal somata labelled with CTXb were CGRP<sup>+</sup>SP<sup>-</sup> (Chi-Square:  $\chi^2_3 = 30$ ,  $p < 0.0001$ ;  $N = 4$  animals;  $n = 62$ )

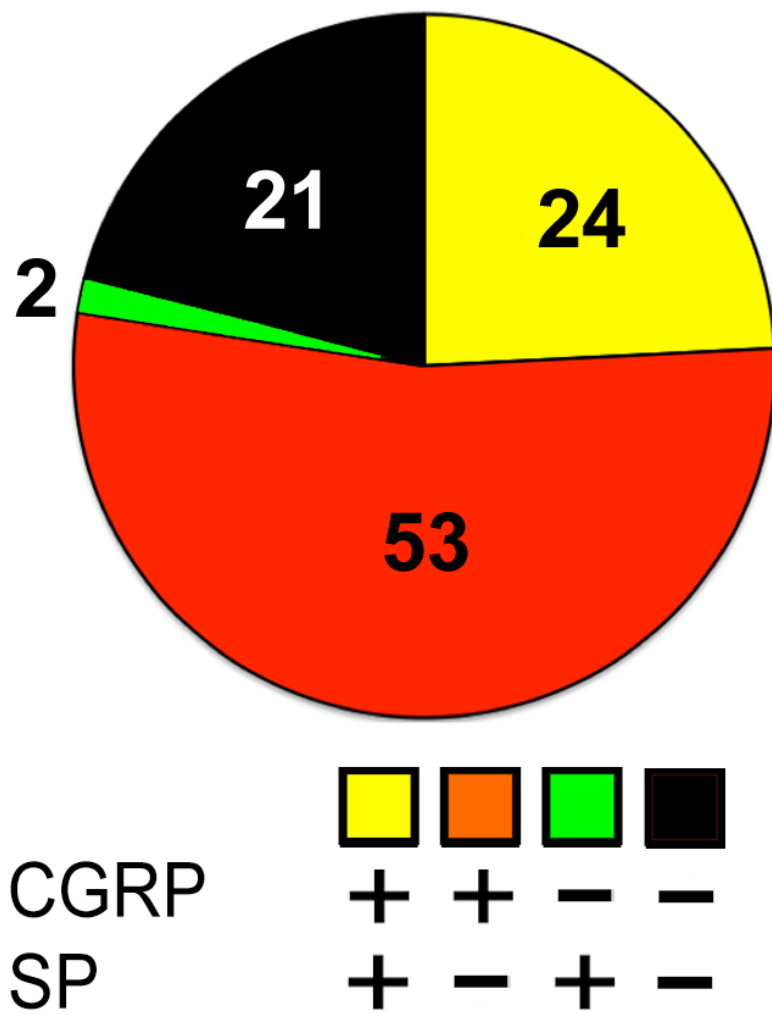
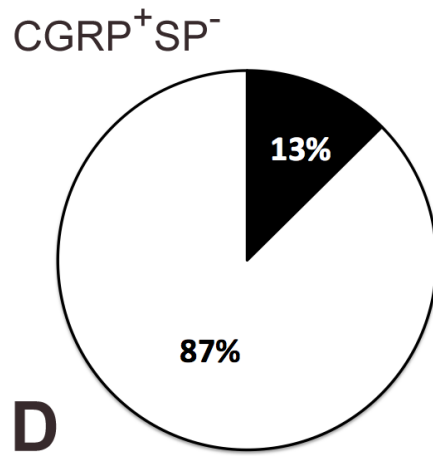
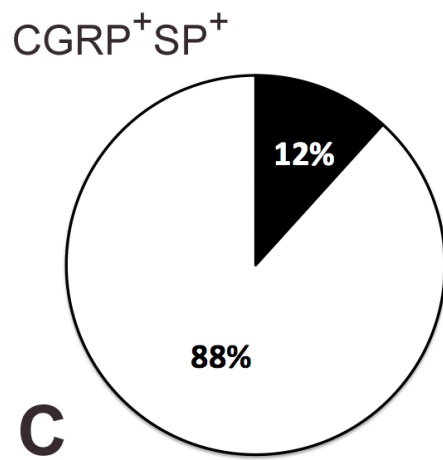
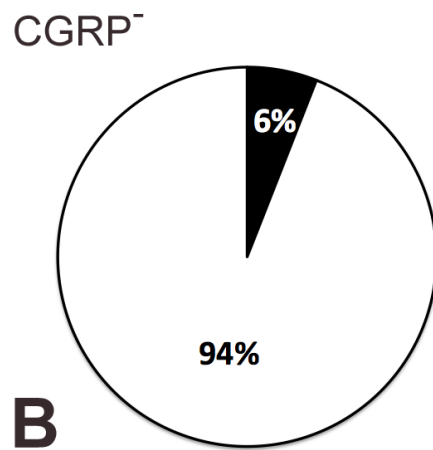
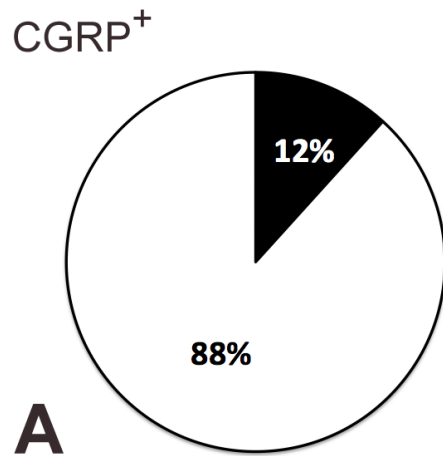
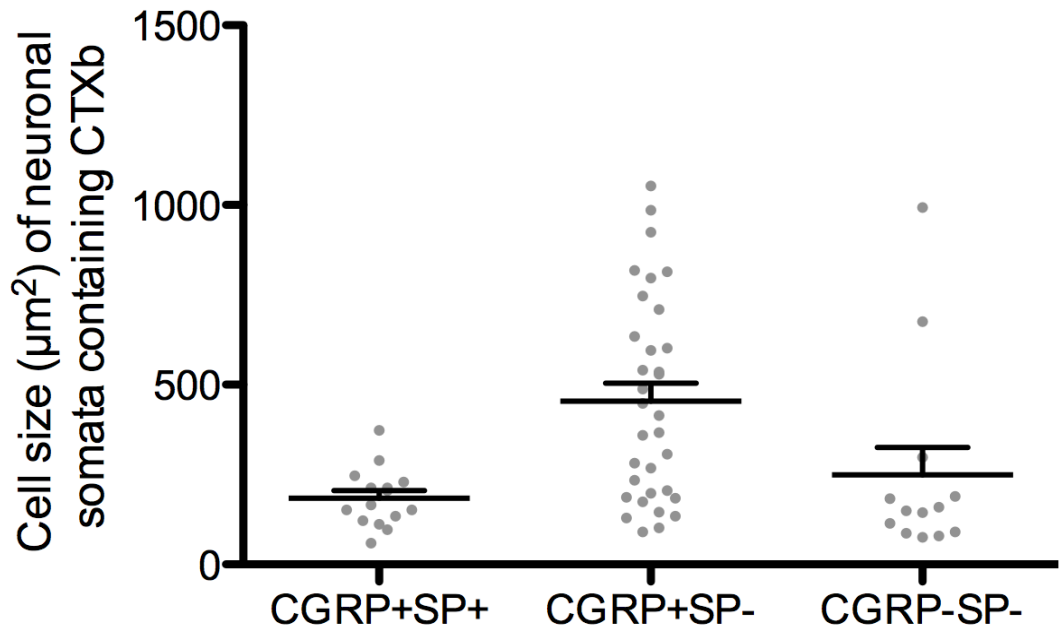


**Figure 5.5: The somata size of CTXb labelled neurons in L4 DRG**

Scatter dot plot depicting the cross sectional area ( $\mu\text{m}^2$ ; lines = mean $\pm$ SEM; dots = single cell sizes) of cholera toxin subunit B (CTXb) labelled neurons that contained calcitonin gene related peptide-IR (CGRP) with substance P-IR (SP; CGRP<sup>+</sup>SP<sup>+</sup>), CGRP-IR without SP-IR (CGRP<sup>+</sup>SP<sup>-</sup>), or lacked peptide expression (CGRP<sup>-</sup>SP<sup>-</sup>) in L4 dorsal root ganglia (DRG). CTXb labelled CGRP<sup>+</sup>SP<sup>-</sup> neurons were significantly larger than the CTXb labelled CGRP<sup>+</sup>SP<sup>+</sup> or CGRP<sup>-</sup>SP<sup>-</sup> neurons. RMANOVA:  $F_{(2,62)} = 7$ ,  $p < 0.01$ ; N = 4 animals, n = 62 neurons

**Figure 5.6: Proportion CGRP-IR labelled with CTXb in L4 DRG**

Pie charts depicting the proportion of neuronal somata containing calcitonin gene related peptide-immunoreactivity (CGRP-IR; CGRP<sup>+</sup>; A); lacking CGRP-IR (CGRP<sup>-</sup>; B); containing CGRP-IR with substance P-IR (SP; CGRP<sup>+</sup>SP<sup>+</sup>; C); or containing CGRP-IR without SP-IR (CGRP<sup>+</sup>SP<sup>-</sup>; D) that were labelled with cholera toxin subunit B (CTXb; black area) in L4 dorsal root ganglia (DRG). Only a small portion of the IR neuronal somata were labelled with CTXb. N= 4 animals, n = 390 neurons in A; N= 4 animals, n = 205 neurons in B; N= 4 animals, n = 128 neurons in C; N= 4 animals, n = 262 neurons in D





---

**Chapter 6:  
Anterograde tracing of  
CGRP<sup>+</sup>SP<sup>-</sup> spinal  
afferents**

---



## 6.1 Background

---

The general assumption that CGRP-IR fibres in the dorsal horn are entirely primary afferent in origin came from lesion studies in the rat (Gibson, Polak, Bloom, *et al.*, 1984; Chung *et al.*, 1988), cat (Gibson, Polak, Bloom, *et al.*, 1984; Traub *et al.*, 1989) and mouse (Tie-Jun *et al.*, 2001). In these studies the dorsal roots were transected and CGRP-IR fibres that remained in the dorsal horn were analysed either qualitatively (Chung *et al.*, 1988; Traub *et al.*, 1989; Tie-Jun *et al.*, 2001) or quantitatively (Gibson, Polak, Bloom, *et al.*, 1984). In both instances there was a dramatic but incomplete loss of CGRP-IR fibres in the dorsal horn. The remaining CGRP-IR fibres were found in both the superficial and deeper laminae of the spinal cord (Traub *et al.*, 1989) and concluded to possibly originate from dorsal roots several segments rostral or caudal from the investigated spinal segment (Traub *et al.*, 1989; McNeill *et al.*, 1991). However, others have concluded that some of the remaining CGRP-IR fibres may be from intrinsic interneurons of the dorsal horn (Conrath *et al.*, 1989). While it is evident that a large proportion of the CGRP-IR fibres in the spinal cord is primary afferent in origin, it is also clear that some CGRP-IR fibres may not be.

CGRP-IR fibres in the dorsal horn are primarily studied in lamina I, as lamina I is predominately associated with nociception. However, CGRP-IR fibres are also present in lamina IV/V, but have been seldom investigated (Matsuyama *et al.*, 1986). Neurons of lamina IV/V receive mostly non-nociceptive input and respond to light mechanical touch (Cervero *et al.*, 1988), though there are also wide dynamic range neurons that can respond to noxious stimuli (Mendell & Wall, 1965; Hillman & Wall, 1969; Light & Durkovic, 1984). The CGRP-IR fibres of lamina IV/V are insensitive to capsaicin, in contrast to the fibres of lamina I that are capsaicin sensitive (Matsuyama *et al.*, 1986). This suggests that the CGRP-IR fibres of lamina IV/V may be functionally different from the CGRP-IR fibres of the superficial lamina. The previous experimental chapters have demonstrated that CGRP-IR neurons lacking SP-IR (CGRP<sup>+</sup>SP<sup>-</sup>) also lacked the capsaicin receptor TRPV1 and that lamina IV/V had the highest proportion of CGRP<sup>+</sup>SP<sup>-</sup> fibres. Therefore it is not unreasonable to predict that these CGRP<sup>+</sup>SP<sup>-</sup> neurons project to lamina IV/V.

## Chapter 6: Anterograde tracing of CGRP<sup>+</sup>SP<sup>-</sup> spinal afferents

In order to better characterise the lamina IV/V projections of CGRP<sup>+</sup>SP<sup>-</sup> neurons, we used an anterograde tracing technique to visualize their afferent terminals and determine their association with other afferent terminals. This technique was originally developed by Tassicker and colleagues (1999) and utilized the small polar molecule biotinamide (Neurobiotin) for the rapid labelling of severed axons *in vitro* into the guinea pig small intestine. We adapted this to map central projections of afferent fibres in the lumbar spinal cord of mice (Clarke *et al.*, 2011) and had made previous attempts with limited success in the cervical spinal cord of mice (Kestell, 2009). Subsequently, the concentration of 1% NB was increased to 5% and compared to L4.

In the previous chapters, we have demonstrated the existence of CGRP<sup>+</sup>SP<sup>-</sup> fibres in the forepaw and hindpaw skin of mice. The forepaw and hindpaw skin are innervated by afferents of cervical and lumbar spinal segments. Hence, in the current chapter we have mapped the central projections of cervical and lumbar primary afferents into their respective dorsal horns.

## 6.2 Materials and Methods

---

Both the 7<sup>th</sup> cervical (C7) and 4<sup>th</sup> lumbar (L4) spinal nerves were prepared for anterograde tracing. The L4 spinal nerve was relatively simple to prepare in comparison to the C7 nerve. In preparations focusing on the L4 nerve the lumbar vertebral column was removed and transferred to a Petri dish containing HEPES buffered balanced salt solution (HBBS solution; 146 mM sodium chloride; 4.7 mM potassium chloride; 0.6 mM magnesium sulphate; 0.13 mM sodium phosphate; 1.6 mM sodium bicarbonate; 7.8 mM D-glucose; 20 mM HEPES; 0.1 mM ascorbic acid; 2.5 mM calcium chloride) constantly bubbled with oxygen. The ventral surface of the vertebral column was exposed and the spinal cord with attached lumbosacral plexus was isolated and severed from the DRG. The lumbosacral plexus was pinned out and the L4 spinal nerve was identified and other nerves of the plexus were removed.

In preparations focusing on the C7 nerve the entire upper half of the animal was separated and transferred to a Petri dish containing HBBS solution constantly bubbled with oxygen. The ventral surface of the spinal cord was exposed before dissecting the brachial plexus to ensure the spinal cord had immediate access to the oxygenated HBBS solution. The head was removed and the terminal branches of the brachial plexus were severed at the elbow and dissected back to the spinal cord. The vertebral column, dura mater, the pedicles and vertebral arch were removed. The isolated spinal cord and brachial plexus were pinned out and the C7 spinal nerve was identified and other nerves of the plexus were removed.

Spinal cord and attached nerves of interest were transferred to a Petri dish modified with a small inner chamber embedded in the Sylgard flooring. Due to the differences between the length of the C7 and L4 dorsal roots, there were slight variations to the procedure. In L4 nerve preparations, the ventral root was removed and the dorsal root was extended inside the small inner chamber. However, in C7 nerve preparations the dorsal root was too short and so the ventral root was cut and the remaining C7 nerve was extended in the small inner chamber (Figure 6.1). In L4 nerve preparations, only the L4 dorsal root and spinal cord were part of the tracing set up, whereas in C7 nerve preparations the C7 spinal nerve, DRG, dorsal root and spinal cord were part of the tracing set up.

The inner chamber was then sealed with a small cover slip and silicon grease (Stennick Scientific, SA, Australia) to prevent the exchange of solutions between the inner and outer chambers. The nerve/dorsal root ending was washed three times with Artificial Intracellular Solution (AIS: 136.7 mM L-glutamate; 7 mM magnesium chloride; 5 mM D-glucose; 1 mM EGTA; 20 mM HEPES; 5 mM ATP; 0.02% Saponin; 1% DMSO; 1% penicillin; 1% streptomycin; 1% gentamicin) and later replaced with a droplet of 5% NB (*N*-[2-aminoethyl] biotinamide hydrochloride; Vector Laboratories, California, USA) diluted in AIS. We (Clarke et al 2011; Kestell 2009) had previously used a droplet of 1% with limited success and so this five-fold increase concentration was anticipated to improve labelling. A fresh transection was then made to the nerve ending/dorsal root within the NB droplet. The inner chamber was subsequently filled with paraffin oil (Faulding Pharmaceuticals, SA, Australia) to maintain the position of the NB droplet and its contact with the nerve/dorsal root ending.

The outer chamber was filled with Dulbecco's Modified Eagle Medium F12 (DMEM/F12) basal media (Sigma-Aldrich, Missouri, USA) containing 10% fetal calf serum (Gibco, VIC, Australia); 2.8mM filtered calcium chloride; 1% Penicillin (Invitrogen, VIC, Australia); 1% Streptomycin (Gibco). The dish was finally placed on a slow speed shaker in a humidified carbon dioxide incubator at 37°C for 4 hours.

Spinal cord was fixed, processed through DMSO, embedded in PEG and sectioned using a microtome. Every 5th section of spinal cord was first tested for the extent of NB labelling with streptavidin conjugated to Cy3 (SA-Cy3; Jackson ImmunoResearch, Missouri, USA). Sections were further analysed based on the extent of NB labelling. Adjacent sections of the chosen sections were then triple labelled with anti-CGRP raised in a goat (1:1000; code 1780, Arnel, New York, USA) and anti-SP raised in a rabbit (1:2000; Incstar [now Immunostar], Wisconsin, USA) and NB was visualised with SA-DTAF (Jackson ImmunoResearch).

Widefield images of spinal cord sections were taken with an Olympus BX50 epifluorescence microscope with a 20x objective. Confocal Z-stacks of spinal cord sections, consisting of 21 optical sections 0.5 µm apart (total depth 10.5 µm), were taken with the Leica SP5 confocal microscope with a 63x N.A. 1.4 oil immersion objective with 2x digital zoom.

Confocal Z-stacks of spinal cord were imported to Avizo for 3D reconstruction and analysis. The volume of CGRP-IR boutons that either contained or lacked SP-IR was first calculated using the AND (A&B) operator and the NOT (A-B) operator between the CGRP and SP data sets. For illustration purposes, NB-labelled primary afferents are shown as volume rendered data sets, while subsets of CGRP-IR and SP-IR fibres (total immunoreactivity and those anterogradely labelled with NB) were displayed with isosurface rendering. The volume of each 3D data set (total anterogradely labelled fibres; total and anterogradely labelled subsets of CGRP-IR fibres with and without SP-IR fibres) was calculated. Data were then displayed as mean±SEM and RM-ANOVA with post hoc BMC correction with 95% confidence limits was used to determine the statistical significance.



## 6.3 Results

---

### **NB labelled fibres in C7 dorsal horn**

After application to the distal cut end of the C7 ventral ramus, NB could be detected in the majority of cells of the C7 DRG (Figure 6.2). In the dorsal horn, NB preferentially labelled large diameter, presumably myelinated fibres (Figure 6.3). NB-labelled fibres entered the dorsal horn via large tracts in the medial superficial dorsal horn and could be detected in Lissauer's tract and the dorsal funiculus of the spinal cord (Figure 6.3). Individual NB-labelled fibres penetrated as far as the ventral horn, whilst other NB-labelled fibres ramified at the level of lamina IV/V and projected towards the nucleus proprius (Figure 6.3). Very few NB-labelled fibres were observed in lamina I (Figure 6.3). No CGRP somata were observed in the dorsal horn.

Quantitatively, lateral lamina I had fewer NB-labelled voxels compared to medial lamina I and lamina IV/V (RM-ANOVA:  $F_{(1,4)} = 17$ ,  $p < 0.01$ ;  $n = 5$  animals; Figure 6.4). However, in medial lamina I, most of the NB-labelled fibres were large diameter axons in penetrating fibre tracts (Figure 6.3). Hence lamina IV/V had the highest density of varicose NB-labelled fibres.

#### ***NB labelled CGRP-IR neuronal somata in C7 DRG and CGRP-IR fibres in C7 dorsal horn***

In the C7 DRG NB-labelled neuronal somata and fibres that also contained CGRP-IR. While some NB-labelled somata were CGRP<sup>+</sup>SP<sup>-</sup> very few NB-labelled somata were CGRP<sup>+</sup>SP<sup>+</sup> (Figure 6.5).

In the C7 dorsal horn, very few NB-labelled voxels contained CGRP-IR (Figure 6.6). Lateral lamina I (Figure 6.6B<sub>3</sub>) had the least amount of NB-labelled voxels that contained CGRP-IR compared to medial lamina I (Figure 6.6B<sub>1</sub>) and lamina IV/V (RM-ANOVA:  $F_{(1,4)} = 15$ ,  $p = 0.02$ ;  $n = 5$  animals; Figure 6.6B<sub>2</sub> and Figure 6.7). In these laminae there was no difference between the volume of NB-labelled voxels that contained either CGRP<sup>+</sup>SP<sup>+</sup> or CGRP<sup>+</sup>SP<sup>-</sup> (RM-ANOVA:  $F_{(1,4)} = 4$ ,  $p = 0.13$ ;  $n = 5$  animals; Figure 6.7).

#### ***NB labelled a small proportion of CGRP-IR fibres in C7 dorsal horn***

As the volume of NB was significantly different in the different dorsal horn regions, it was more accurate to analyse the volume of NB-labelled fibres that contained CGRP-IR as a proportion of the total NB-labelled fibres. Only a low proportion of NB-labelled voxels contained CGRP-IR in the C7 dorsal horn. In medial lamina I, only 4±2% of NB-labelled voxels contained CGRP-IR. Although lateral lamina I had the largest volume of NB-labelled voxels compared with the other dorsal horn regions, lateral lamina I had the highest proportion of NB-labelled voxels containing CGRP-IR (30±5%) compared to the other dorsal horn regions (RM-ANOVA:  $F_{(2,8)} = 13$ ,  $p = 0.03$ ;  $n = 5$  animals; Figure 6.8). Lamina IV/V had the highest density of NB-labelled fibres, yet only 6±3% of NB voxels here contained CGRP-IR. Overall there was no difference between the proportion of NB-labelled voxels that were either CGRP<sup>+</sup>SP<sup>+</sup> or CGRP<sup>+</sup>SP<sup>-</sup> (RM-ANOVA:  $F_{(1,4)} = 1.6$   $p = 0.28$ ;  $n = 5$  animals; Figure 6.8).

***A small proportion of CGRP-IR fibres were labelled with NB in C7 dorsal horn***

In the C7 dorsal horn only 2±0% of the CGRP-IR in medial lamina I and 1±0% of the CGRP-IR in lateral lamina I were within NB-labelled voxels. Lamina IV/V had the highest proportion of CGRP-IR within NB-labelled voxels (7±3%) of the three dorsal horn regions (RM-ANOVA:  $F_{(1,4)} = 9$   $p = 0.04$ ;  $n = 5$  animals; Figure 6.9).

**NB labelled more fibres in L4 dorsal horn compared to C7 dorsal horn**

After application to the L4 dorsal root NB could be detected in the dorsal horn. NB labelled both small and large diameter fibres. NB-labelled fibres entered the dorsal horn via large tracts in the medial superficial dorsal horn and could be detected in Lissauer's tract, the dorsal funiculus, lamina IV/V and as far as the ventral horn (Figure 6.10).

Quantitatively, lateral lamina I had fewer NB-labelled fibres compared to the other dorsal horn regions (RM-ANOVA:  $F_{(1,4)} = 25$ ,  $p < 0.01$ ;  $n = 5$  animals; Figure 6.11). The L4 dorsal horn had more NB-labelled fibres compared to the C7 dorsal horn, particularly in lamina I (RM-ANOVA:  $F_{(1,4)} = 10$ ,  $p = 0.03$ ;  $n = 10$  animals; Figure 6.12).

***NB labelled more CGRP-IR fibres in L4 dorsal horn compared to C7 dorsal horn***

In the L4 dorsal horn, a higher volume of NB-filled voxels contained CGRP-IR in medial lamina I (Figure 6.13B<sub>1</sub>) compared to lateral lamina I (Figure 6.13B<sub>3</sub>) and lamina IV (Figure 6.13B<sub>2</sub>; RM-ANOVA:  $F_{(1,4)} = 14$ ,  $p = 0.02$ ;  $n = 5$  animals; Figure 6.14). While the volume of NB-labelled voxels that were CGRP<sup>+</sup>SP<sup>+</sup> showed a similar distribution (RM-ANOVA:  $F_{(1,4)} = 13$ ,  $p = 0.02$ ;  $n = 5$  animals; Figure 6.14), there was no difference in the volume of NB-labelled voxels that were CGRP<sup>+</sup>SP<sup>-</sup> in the dorsal horn regions (RM-ANOVA:  $F_{(1,4)} = 1$ ,  $p = 0.39$ ;  $n = 5$  animals; Figure 6.14). Overall, a higher volume of NB-labelled voxels were CGRP<sup>+</sup>SP<sup>+</sup> than CGRP<sup>+</sup>SP<sup>-</sup> in the L4 dorsal horn (RM-ANOVA:  $F_{(1,4)} = 12$ ,  $p = 0.03$ ;  $n = 5$  animals; Figure 6.14).

A higher total volume of NB-labelled voxels contained CGRP-IR in medial and lateral lamina I of the L4 dorsal horn compared to the C7 dorsal horn (RM-ANOVA:  $F_{(1,8)} = 12$ ,  $p < 0.01$ ;  $n = 10$  animals; Figure 6.15). This was true for both CGRP<sup>+</sup>SP<sup>+</sup> fibres (RM-ANOVA:  $F_{(1,8)} = 11$ ,  $p = 0.01$ ;  $n = 10$  animals; Figure 6.15A) and CGRP<sup>+</sup>SP<sup>-</sup> fibres (RM-ANOVA:  $F_{(1,8)} = 6$ ,  $p = 0.04$ ;  $n = 10$  animals; Figure 6.15B). There was no difference in the volume of NB-labelled voxels containing CGRP-IR in lamina IV/V of the L4 dorsal horn compared to the C7 dorsal horn.

***NB labelled a higher proportion of CGRP-IR fibres in L4 dorsal horn compared to C7 dorsal horn***

Medial and lateral lamina I had a higher proportion of NB-labelled voxels that contained CGRP-IR ( $59 \pm 7\%$  and  $62 \pm 7\%$ , respectively) compared to lamina IV/V ( $4 \pm 1\%$ ; RM-ANOVA:  $F_{(1,4)} = 53$ ,  $p < 0.01$ ;  $n = 5$  animals; Figure 6.16). Overall there was a higher proportion of NB-labelled fibres that contained CGRP<sup>+</sup>SP<sup>+</sup> than CGRP<sup>+</sup>SP<sup>-</sup>, particularly in medial lamina I (RM-ANOVA:  $F_{(1,4)} = 35$ ,  $p < 0.01$ ;  $n = 5$  animals; Figure 6.16).

A higher proportion of NB-labelled voxels contained CGRP-IR in the L4 dorsal horn compared to the C7 dorsal horn, particularly in medial and lateral lamina I (RM-ANOVA:  $F_{(1,8)} = 17$ ,  $p < 0.01$ ;  $n = 10$  animals; Figure 6.17). While the proportion of NB-labelled voxels that were CGRP<sup>+</sup>SP<sup>+</sup> showed a similar pattern (RM-ANOVA:  $F_{(1,8)} = 48$ ,  $p < 0.01$ ;  $n = 10$  animals; Figure 6.17), there was no difference in the volume of NB-labelled voxels that were CGRP<sup>+</sup>SP<sup>-</sup> in the two dorsal horns (RM-ANOVA:  $F_{(1,8)} = 3$ ,  $p = 0.15$ ;  $n = 10$  animals; Figure 6.17).

***A higher proportion of CGRP-IR fibres was labelled with NB in L4 dorsal horn compared to C7 dorsal horn***

In the L4 dorsal horn, almost equal proportions of the CGRP-IR in lateral lamina I and lamina IV/V were contained within NB-labelled voxels (13±3% and 13±5%, respectively). Medial lamina I had the highest proportion of CGRP-IR contained within NB-labelled voxels (26±5%) compared to the other dorsal horn regions (RM-ANOVA:  $F_{(1,4)} = 12$   $p = 0.03$ ;  $n = 5$  animals; Figure 6.18).

A higher proportion of CGRP-IR was contained within NB-labelled voxels in lamina IV/V of the L4 dorsal horn compared to the C7 dorsal horn (RM-ANOVA:  $F_{(1,8)} = 13$   $p < 0.01$ ;  $n = 10$  animals; Figure 6.19). Both the proportion of CGRP<sup>+</sup>SP<sup>+</sup> and CGRP<sup>+</sup>SP<sup>-</sup> labelled with NB showed a similar pattern (RM-ANOVA:  $F_{(1,8)} = 12$ ,  $p = 0.009$ ;  $n = 10$  animals; Figure 6.19A, and RM-ANOVA:  $F_{(1,8)} = 12$ ,  $p = 0.008$ ;  $n = 10$  animals; Figure 6.19B, respectively).

**NB labelled more VGluT1-IR fibres than CGRP-IR fibres in lamina IV/V**

In both C7 and L4 dorsal horns, lamina IV/V contained a high density of VGluT1-IR fibres (Figure 6.20). None of this VGluT1-IR colocalised with CGRP-IR, but did colocalise with NB-labelled voxels (Figure 6.21 and Figure 6.22). While not in the same voxels, the CGRP-IR positive NB-labelled voxels were situated in very close proximity to the VGluT1-IR positive NB-labelled voxels (Figure 6.20). At both spinal levels, a higher proportion of NB-labelled voxels were positive for VGluT1-IR compared to CGRP-IR (C7: 21±2% and 6±3%, respectively; Paired t-test:  $t_{(3)} = 4$ ,  $p = 0.04$ ;  $n = 3$  animals; Figure 6.21; L4: 24±5% and 6±1%, respectively; Paired t-test:  $t_{(3)} = 4$ ,  $p = 0.04$ ;  $n = 4$  animals; Figure 6.22). There was no difference between the proportion of NB-labelled voxels containing VGluT1-IR between C7 and L4 dorsal horns (RM-ANOVA:  $F_{(1,4)} = 2$ ,  $p = 0.2$ ;  $n = 6$  animals; Figure 6.23).

## 6.4 Discussion

---

Previous chapters have demonstrated distinct immunohistochemical populations of CGRP<sup>+</sup>SP<sup>-</sup> fibres in both skin and muscle tissue, medium size cell bodies in the DRG, and fibres in lateral lamina I and deep lamina IV/V of the dorsal horn. These neurons were present in the dorsal horn and DRG of all spinal levels, and were further distinguished from CGRP<sup>+</sup>SP<sup>+</sup> neurons by lacking detectable levels of TRPV1-IR and expressing NF200-IR. The previous chapter demonstrated that a small proportion of the CGRP<sup>+</sup>SP<sup>-</sup> neurons had peripheral projections to muscle tissue. This chapter set out to characterise the central terminations of these neurons in the dorsal horn of the spinal cord using an anterograde tracer.

### **NB labelled more afferents in L4 dorsal horn compared to C7 dorsal horn**

In C7 tracing preparations, there was a marked increase in NB labelling of the dorsal horn when using 5% compared to the 1% that was previously used (Clarke et al 2011; Kestell 2009). NB labelled both cell bodies in the DRG and fibres in the dorsal horn of the spinal cord. NB labelled fibres within Lissauer's tract and the dorsal horn in a distribution that has been previously described for many larger neurons (Nyberg & Blomqvist, 1985; Arvidsson & Pfaller, 1990). Although there was some smaller fibre labelling of lamina IV/V, this was a vast underrepresentation of the smaller fibres as a whole. NB appeared to label only larger neurons in both the C7 DRG and the C7 dorsal horn.

In L4 tracing preparations, NB labelled both large and smaller fibres in a distribution consistent with our previous studies (Clarke *et al.*, 2011). NB labelled a substantially higher number of fibres in L4 dorsal horn compared to the C7 dorsal horn. This difference was most noticeable in lamina I and appeared to be due to labelling finer fibres in the L4 dorsal horn but not in the C7 dorsal horn.

The preferential labelling of larger myelinated fibres in C7 compared to L4 dorsal horns may be due to the different lengths of their dorsal roots. Lumbar segments of spinal cord had long dorsal roots and allowed the NB droplet to be placed proximal to the DRG. However, cervical segments had very short dorsal roots and limited the placement of the NB droplet distal to the DRG. Therefore, NB had to first fill fibres

of the spinal nerve, cell bodies of the DRG, and fibres of the dorsal and ventral roots, before filling fibres of the C7 dorsal horn. In comparison NB only had to fill fibres of the dorsal root before filling fibres of L4 dorsal horn. Therefore more NB ended up in the dorsal horn of the L4 dorsal horn than compared to the C7 dorsal horn and could account for the differences seen here.

NB was not an effective anterograde tracer in C7 tracing preparations. Conversely, NB was an effective anterograde tracer in L4 tracing preparations, and advantageous over the traditional HRP-based axonal tracing for a number of reasons. Firstly, the current results and previous results from our laboratory (Clarke *et al* 2011) have demonstrated that NB labels most if not all the spinal projections from the application site including unmyelinated fibres projecting to the dorsal horn of lumbar spinal cord that are not labelled with HRP-based tracers. This was not evident C7 tracing preparations. Secondly, it is possible to combine this marker with up to four other fluorescent labels to neurochemically profile the labelled fibres, such as done in this study.

## **CGRP<sup>+</sup>SP<sup>-</sup> fibres of lamina IV/V are primary afferent and most likely larger myelinated afferents**

While few in number, NB labelled CGRP-IR fibres in the C7 dorsal horn. Few NB labelled CGRP-IR fibres were detected in medial and lateral lamina I, and most abundant in the lamina IV/V. While many of the CGRP-IR fibres were labelled with NB in lamina IV/V, there were many fibres labelled with NB that were unlabelled by CGRP-IR. CGRP<sup>+</sup>SP<sup>+</sup> fibres and CGRP<sup>+</sup>SP<sup>-</sup> fibres were labelled with NB equally throughout the C7 dorsal horn. Assuming that CGRP-IR is of primary afferent origin, the proportion of CGRP-IR fibres labelled with NB fibres could be used as a guide to determine how effective NB was at tracing the peptidergic afferents. The proportion of CGRP-IR fibres labelled with NB in the C7 dorsal horn suggests that a vast underrepresentation of the fibres had been labelled. The lack of fine CGRP-IR fibres labelled in lamina I of the C7 dorsal horn further supports the notion that NB was not able to label fine fibres in the C7 dorsal horn and instead preferentially labelled larger fibres.

There was a considerably higher number and proportion of CGRP-IR fibres labelled with NB in L4 dorsal horn than the C7 dorsal horn. NB-labelled CGRP-IR fibres

mostly in lamina I and the majority of these were CGRP<sup>+</sup>SP<sup>+</sup> fibres. This data suggests that NB labelling in the L4 dorsal horn was effective at labelling the fine CGRP-IR fibres that had not been labelled with NB in the C7 dorsal horn. In contrast, there was no difference in the proportion of NB-labelled CGRP<sup>+</sup>SP<sup>-</sup> fibres between the two levels in both lamina I and IV/V. This lack of difference suggests that CGRP<sup>+</sup>SP<sup>-</sup> fibres were larger fibres than CGRP<sup>+</sup>SP<sup>+</sup> fibres. The larger fibre size of CGRP<sup>+</sup>SP<sup>-</sup> fibres suggests they are myelinated afferents. This matches our previous conclusions based on the soma size of CGRP<sup>+</sup>SP<sup>-</sup> neurons, their NF200 expression and work by McCarthy and Lawson (1990).

While it is true that we did not see a complete overlap of NB labelled fibres containing CGRP-IR or CGRP-IR fibres labelled with NB, it was not expected for a number of reasons. Firstly, CGRP-IR afferents only represent a small population of primary afferent fibres. Secondly, NB labelled the entire primary afferent fibre, whereas CGRP is mainly present in the varicosities of the fibres. Lastly, it has been demonstrated that CGRP-IR fibres originate from dorsal roots several segments rostral or caudal from the investigated spinal segment (Traub *et al.*, 1989; McNeill *et al.*, 1991) and we only traced one root.

While it is evident in the literature that a large proportion of the CGRP-IR fibres in the spinal cord are primary afferent in origin, there are a small population that is not (Traub *et al.*, 1989). It has been suggested that the remaining CGRP-IR originates from dorsal roots several segments rostral or caudal from the investigated spinal segment (Traub *et al.*, 1989; McNeill *et al.*, 1991) or from intrinsic interneurons of the dorsal horn (Conrath *et al.*, 1989). However, no CGRP was observed in any somata of the dorsal horn in this study and hence unlikely to be of interneuron origin. Most of these studies also focus on the superficial lamina. In this current study we have demonstrated that CGRP-IR terminals in lamina IV/V are labelled with NB, and are hence of primary afferent origin.

### **CGRP<sup>+</sup>SP<sup>-</sup> fibres of lamina IV/V are most likely lightly myelinated mechanoreceptors projecting to wide-dynamic range neurons**

Most large diameter mechanoreceptors express the vesicular glutamate transporter, VGluT1. However CGRP-IR neurons, including CGRP<sup>+</sup>SP<sup>-</sup> neurons, do not

(Oliveira *et al.*, 2003; Morris *et al.*, 2005; Brumovsky *et al.*, 2011), an observation confirmed with the current results. This suggests that most CGRP<sup>+</sup>SP<sup>-</sup> neurons are not a subset of conventional glutamatergic low-threshold, myelinated mechanoreceptors, such as those innervating the skin or muscle spindles. On the other hand, most large myelinated mechanoreceptors express high level of the cytoskeletal protein; NF200 (Lawson & Waddell, 1991) and we have confirmed in previous chapters that CGRP<sup>+</sup>SP<sup>-</sup> neurons also are NF200-positive. Hence it is likely that CGRP<sup>+</sup>SP<sup>-</sup> neurons are neurochemically unique population of mechanoreceptors that most likely corresponding to A $\beta$  or A $\delta$  neurons (McCarthy & Lawson, 1990; Ruscheweyh *et al.*, 2007).

Unlike CGRP-IR, VGluT1-IR in the spinal cord is not entirely of primary afferent origin (Persson *et al.*, 2006). Hence NB was required to label the primary afferent terminals of VGluT1. In lamina IV/V, CGRP<sup>+</sup>SP<sup>-</sup> fibres were in close proximity to VGluT1-IR fibres that were well labelled with NB. Lamina IV/V contains both low threshold and wide dynamic range mechanoreceptive neurons and receive mostly non-nociceptive input, and respond to light mechanical touch (Cervero *et al.*, 1988). Nevertheless, wide dynamic range neurons responding to noxious stimuli are also present in lamina IV (Mendell & Wall, 1965; Hillman & Wall, 1969; Light & Durkovic, 1984). Lamina V neurons receive inputs from A $\beta$ - and A $\delta$ -fibres and polysynaptic inputs from C-fibres terminating in the superficial dorsal horn (Willis & Coggeshall, 1991). This pattern of termination of the CGRP<sup>+</sup>SP<sup>-</sup> fibres is consistent with their postulated function as lightly myelinated mechanoreceptors. As CGRP<sup>+</sup>SP<sup>-</sup> fibres were neurochemically distinct from classical low-threshold glutamatergic mechanoreceptors it is likely that these fibres project to the wide dynamic range neurons of lamina IV/V.

## **6.5 Figures**

---

**Figure 6.1: C7 anterograde tracing set up**

The brachial plexus was transected at the C5-6 and C8-T1 roots (A; dotted lines). The brachial plexus with attached spinal cord was transferred to a smaller dish containing HEPES buffered balanced salt solution and an embedded internal chamber (B). The remaining plexus was pulled into the inner chamber (i), the chamber was then sealed and the HEPES buffered balanced salt solution was removed from within the chamber (ii). In artificial intracellular solution (AIS) the brachial plexus was dissected back to the shortest possible branch of C7 and washed in AIS (iii). The AIS droplet was then replaced with a droplet of Neurobiotin held in place with paraffin oil. The external HEPES buffered balanced salt solution replaced with Dulbecco's Modified Eagle Medium F12 (DMEM/F12) basal media (iv).

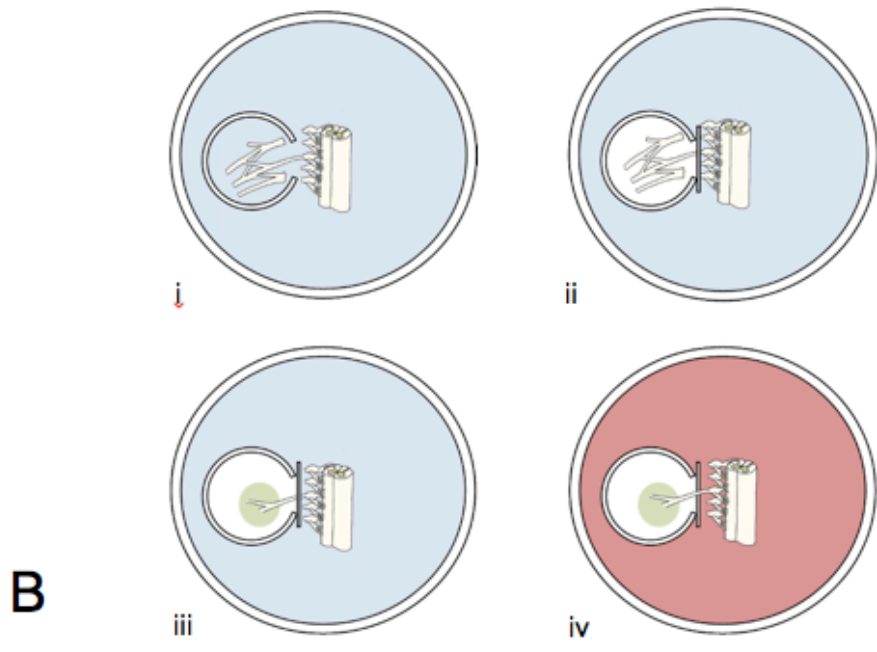
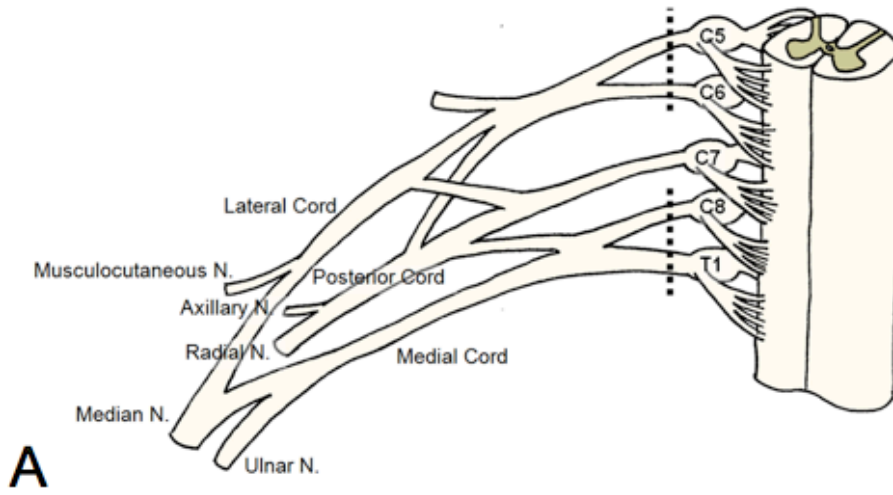


**Figure 6.2: NB labelled neuronal somata in the C7 DRG**

Widefield fluorescence microscopy of the mouse C7 dorsal root ganglia (DRG) showing Neurobiotin (NB) labelled fibres and somata. NB-immunoreactivity could be detected in the majority of the somata. Scale bar = 100  $\mu$ m

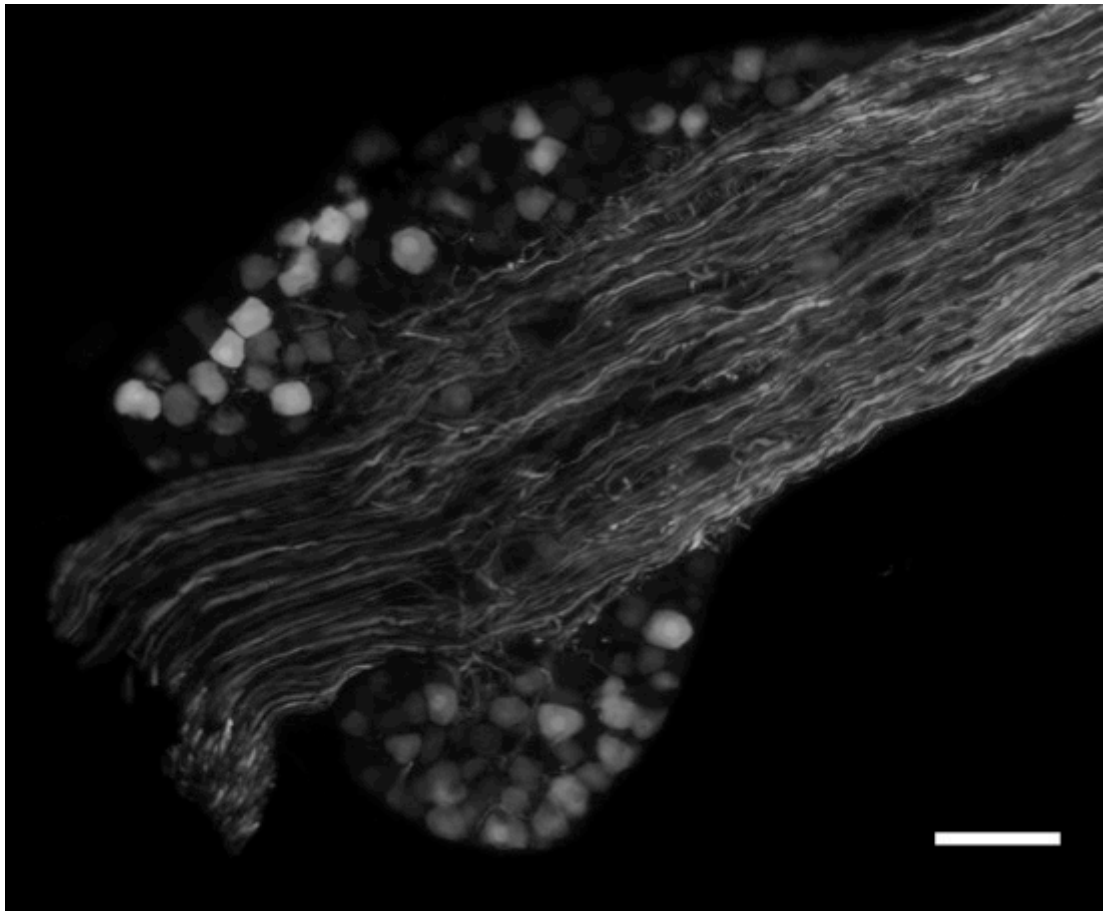


**Figure 6.3: NB labelled fibres in the C7 dorsal horn**

Montage of wide-field fluorescence micrographs of the mouse C7 spinal cord showing Neurobiotin (NB) labelled fibres. NB-labelled fibres can be seen in the dorsal root (DR) and heading toward the dorsal funiculus (DF). Around the DF NB-labelled fibres can be seen penetrating the dorsal horn (DH), with some penetrating as far as the ventral horn (VH). Very few fibres were seen terminating in the superficial lamina. In this particular preparation the ventral roots (VR) were not cut and NB-labelled fibres can be seen entering the VH but not filling any neuronal cell bodies. Scale bar = 100  $\mu$ m

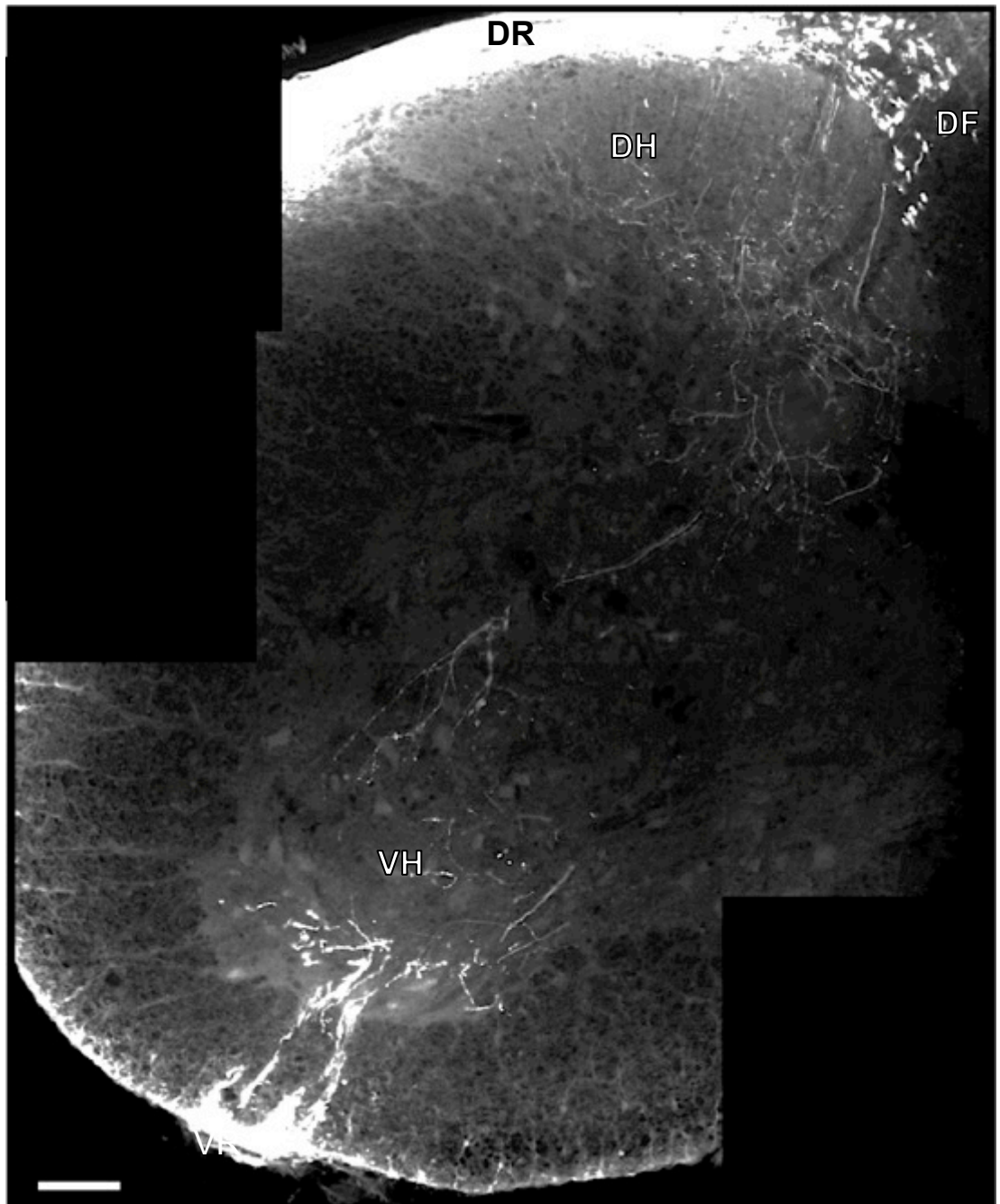


**Figure 6.4: Volume of NB labelled fibres in the C7 dorsal horn**

Histogram (data displayed as mean  $\pm$  SEM) depicting the volume (voxels) of Neurobiotin (NB) labelled fibres in medial and lateral lamina I, and lamina IV/V of the mouse C7 dorsal horn. Lateral lamina I had fewer NB-labelled fibres compared to medial lamina I and lamina IV/V (RM-ANOVA:  $F_{(1,4)} = 17$ ,  $p < 0.01$ ;  $n = 5$  animals).

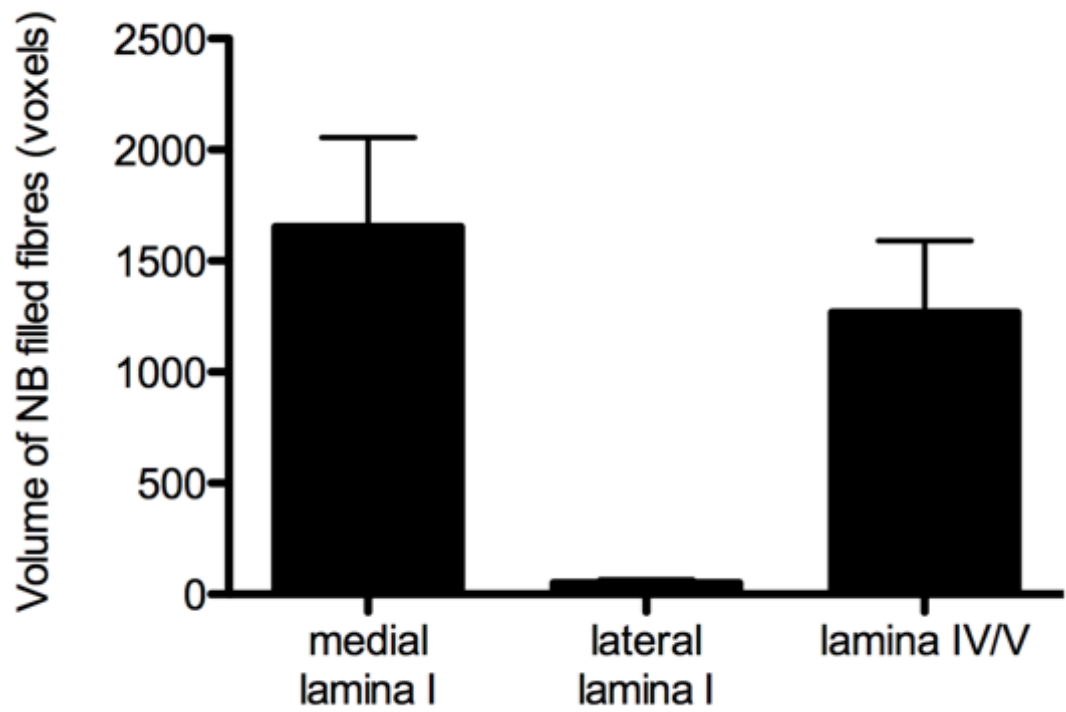


**Figure 6.5: NB labelled neuronal somata in C7 DRG**

Widefield fluorescence microscopy of mouse C7 dorsal root ganglia (DRG) triple labelled for calcitonin gene-related peptide (CGRP; A), substance P (SP; B) and Neurobiotin (NB; C). The overlay (D) shows NB mainly labelled larger DRG neurons with some filled neurons containing CGRP-immunoreactivity (IR) without SP-IR (CGRP<sup>+</sup>SP<sup>-</sup>; black arrowhead). However, not all CGRP<sup>+</sup>SP<sup>-</sup> neurons were labelled (black arrows) and very few CGRP-IR neurons containing SP-IR were labelled with NB (white arrows). Scale bar = 60  $\mu$ m in D (applies to A-D)

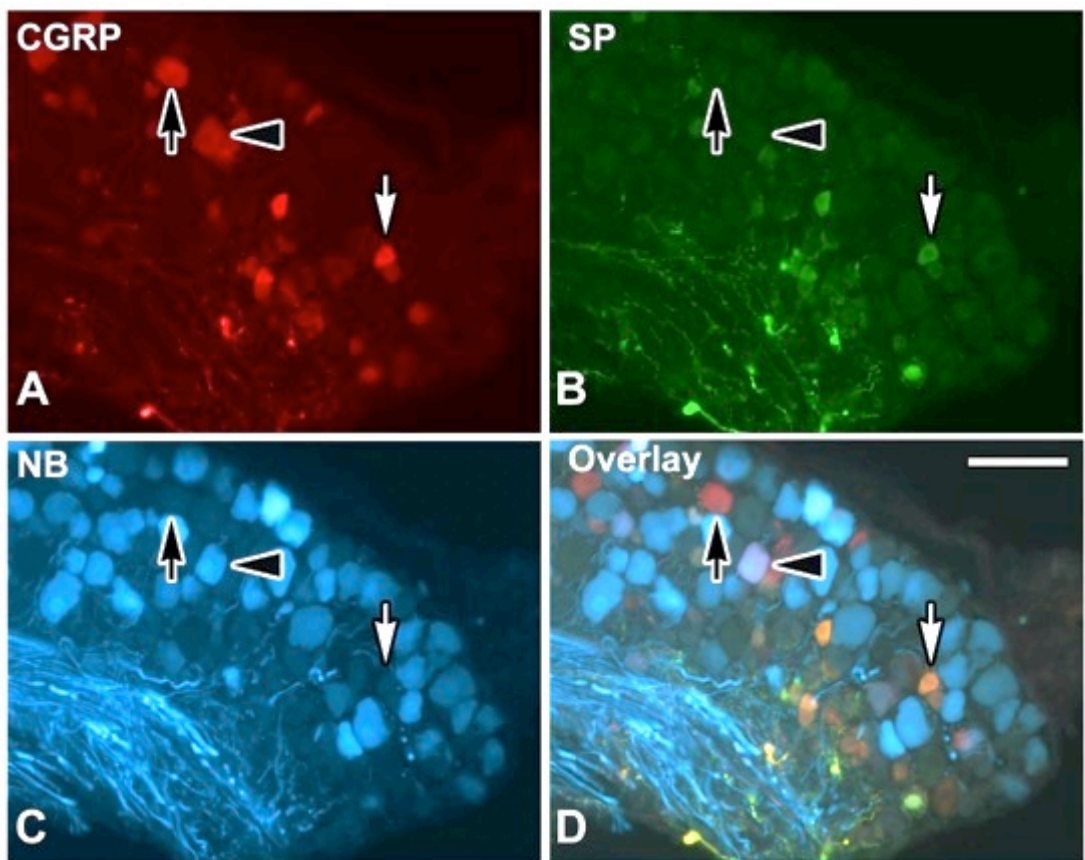


**Figure 6.6: NB labelled fibres in the C7 dorsal horn in association with CGRP-IR terminals**

**A:** Wide field fluorescence microscopy of mouse C7 dorsal horn triple labelled for Neurobiotin (NB; blue), calcitonin gene-related peptide (CGRP; red) and substance P (SP) showing fibres labelled with NB throughout the dorsal horn. Boxed outlines (1-3) represent the dorsal horn regions (1: medial lamina I; 2: lamina IV/V; 3: lateral lamina I) of high CGRP-immunoreactivity (IR) further investigated with confocal microscopy. **B<sub>1</sub>- C<sub>3</sub>:** 3D reconstruction of confocal Z-stacks (21 steps of 0.5  $\mu\text{m}$ ; total volume 10.5  $\mu\text{m}$ ) of the three dorsal horn regions using Avizo. **B<sub>1</sub>- B<sub>3</sub>:** 3D reconstruction of NB labelled fibres (blue) in association with CGRP-IR terminals with SP-IR (CGRP<sup>+</sup>SP<sup>+</sup>, yellow) and without SP-IR (CGRP<sup>+</sup>SP<sup>-</sup>, red). **C<sub>1</sub>- C<sub>3</sub>:** 3D reconstruction of NB labelled fibres showing only the CGRP<sup>+</sup>SP<sup>+</sup> (white, black arrows) and CGRP<sup>+</sup>SP<sup>-</sup> (magenta, white arrows) terminals that were within the NB labelled fibres. Lamina IV/V (2) had a substantially greater number of fibres labelled with NB containing CGRP-IR than medial (1) and lateral (3) lamina I. Scale bar = 60  $\mu\text{m}$  in A; 20  $\mu\text{m}$  in C<sub>3</sub> (applies to B-C)

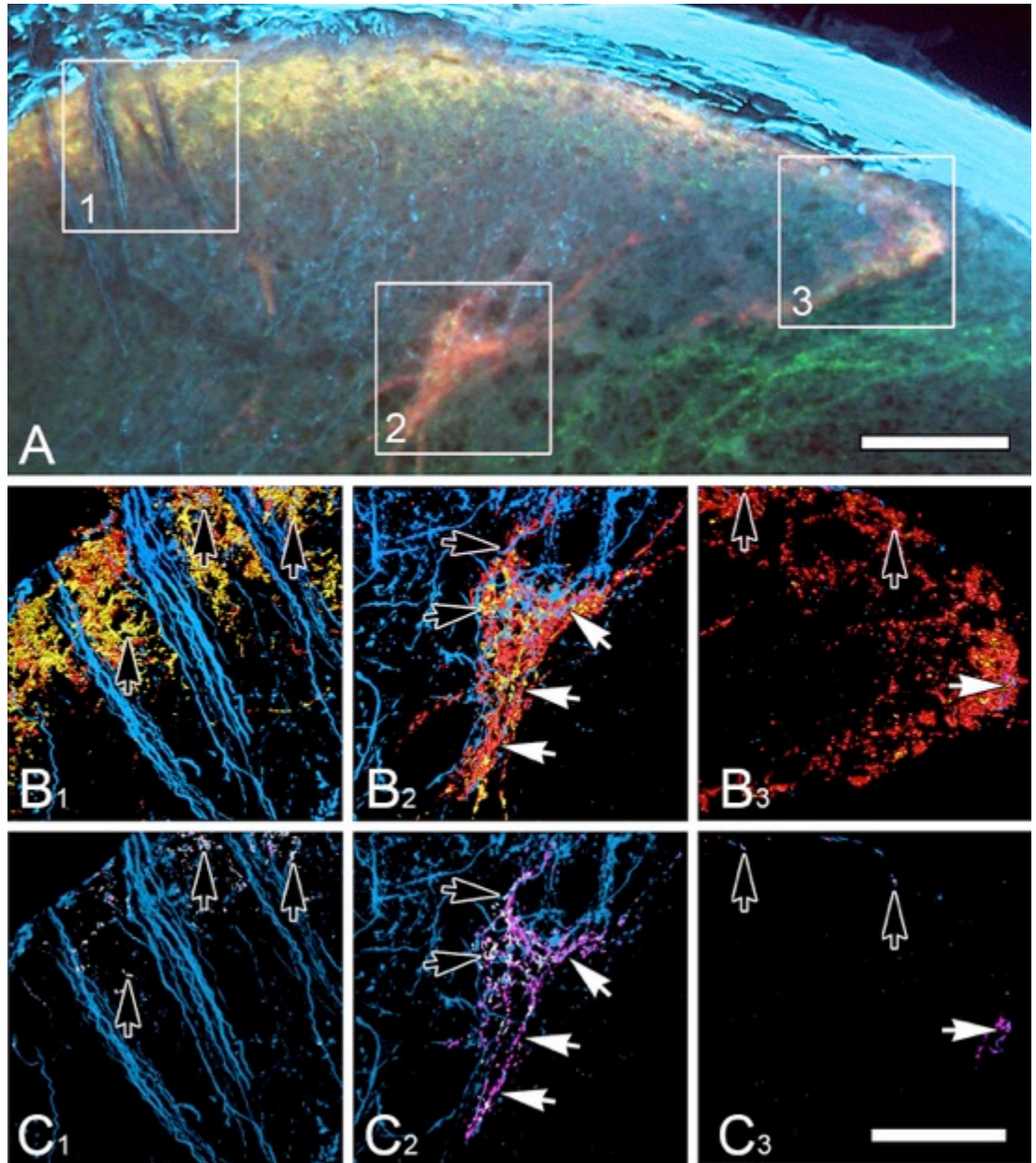


**Figure 6.7: Volume of NB labelled fibres that contained CGRP-IR in the C7 dorsal horn**

Histogram (data displayed as mean  $\pm$  SEM) depicting the volume (voxels) of Neurobiotin (NB) labelled fibres that contained calcitonin gene related peptide (CGRP) with substance P (SP; CGRP<sup>+</sup>SP<sup>+</sup>; yellow) and fibres that contained CGRP without SP (CGRP<sup>+</sup>SP<sup>-</sup>; red) in medial and lateral lamina I, and lamina IV/V of the mouse C7 dorsal horn. Lateral lamina I had the least amount of NB-labelled voxels that contained CGRP-IR compared to medial lamina I and lamina IV/V (RM-ANOVA:  $F_{(1,4)} = 15$ ,  $p = 0.02$ ;  $n = 5$  animals). There was no significant difference between the volume of NB-labelled fibres that contained either CGRP<sup>+</sup>SP<sup>+</sup> or CGRP<sup>+</sup>SP<sup>-</sup> (RM-ANOVA:  $F_{(1,4)} = 4$ ,  $p = 0.1$ ;  $n = 5$  animals).

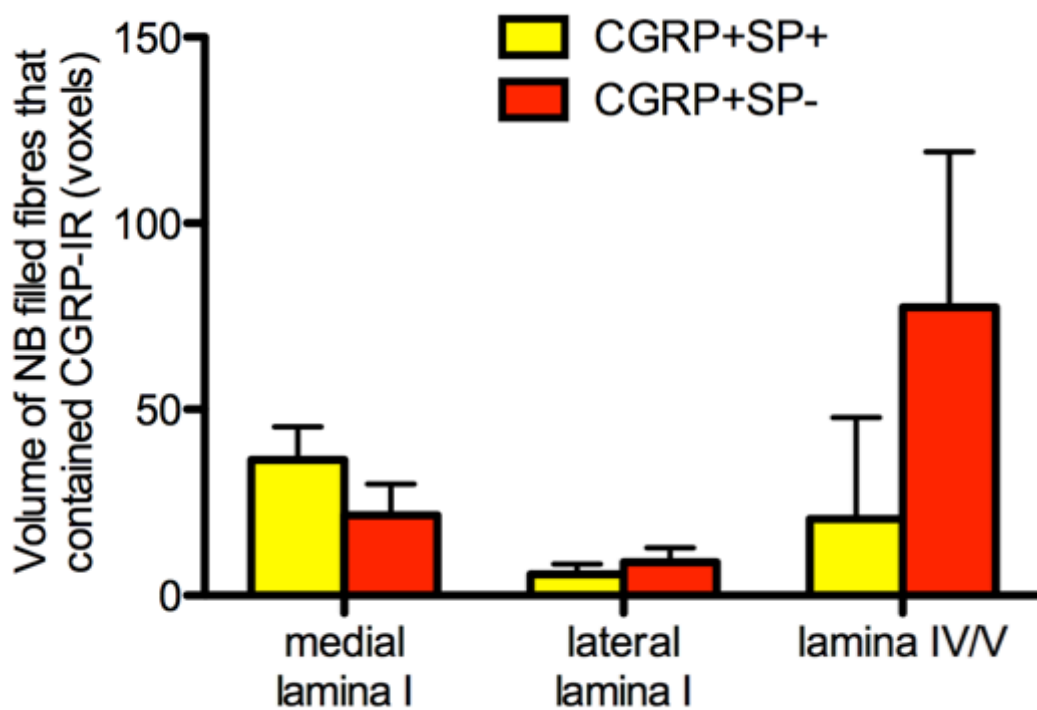


**Figure 6.8: Proportion of NB labelled fibres that contained CGRP-IR in the C7 dorsal horn**

Histogram (data displayed as mean  $\pm$  SEM) depicting the proportion (%) of Neurobiotin (NB) labelled fibres that contained calcitonin gene related peptide (CGRP) with substance P (SP; CGRP<sup>+</sup>SP<sup>+</sup>; yellow) and fibres that contained CGRP without SP (CGRP<sup>+</sup>SP<sup>-</sup>; red) in medial and lateral lamina I, and lamina IV/V of the mouse C7 dorsal horn. Lateral lamina I had the highest level of NB-labelled fibres containing CGRP-IR than the other lamina areas (RM-ANOVA:  $F_{(2,8)} = 13$ ,  $p = 0.03$ ;  $n = 5$  animals). Overall there was no significant difference between the proportion of NB-labelled fibres that contained either CGRP<sup>+</sup>SP<sup>+</sup> or CGRP<sup>+</sup>SP<sup>-</sup> (RM-ANOVA:  $F_{(1,4)} 1.6$   $p = 0.3$ ;  $n = 5$  animals).

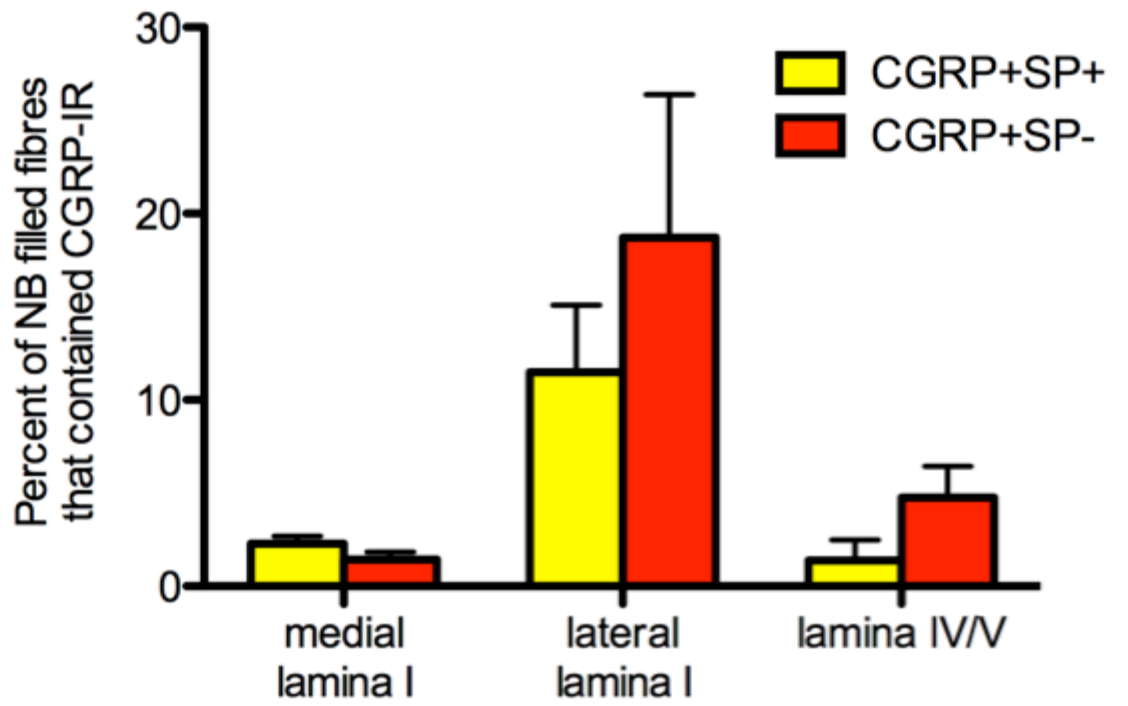


**Figure 6.9: Proportion of CGRP-IR within NB labelled fibres in the C7 dorsal horn**

Histogram (data displayed as mean  $\pm$  SEM) depicting the proportion (%) of fibres that contained calcitonin gene related peptide (CGRP) with substance P (SP; CGRP<sup>+</sup>SP<sup>+</sup>; yellow) and fibres that contained CGRP without SP (CGRP<sup>+</sup>SP<sup>-</sup>; red) that were labelled with Neurobiotin (NB) in medial and lateral lamina I, and lamina IV/V of the mouse C7 dorsal horn. Lamina IV/V had the highest proportion of CGRP-IR that was within NB-labelled fibres compared to medial and lateral lamina I (RM-ANOVA:  $F_{(1,4)} = 9$   $p = 0.04$ ;  $n = 5$  animals).

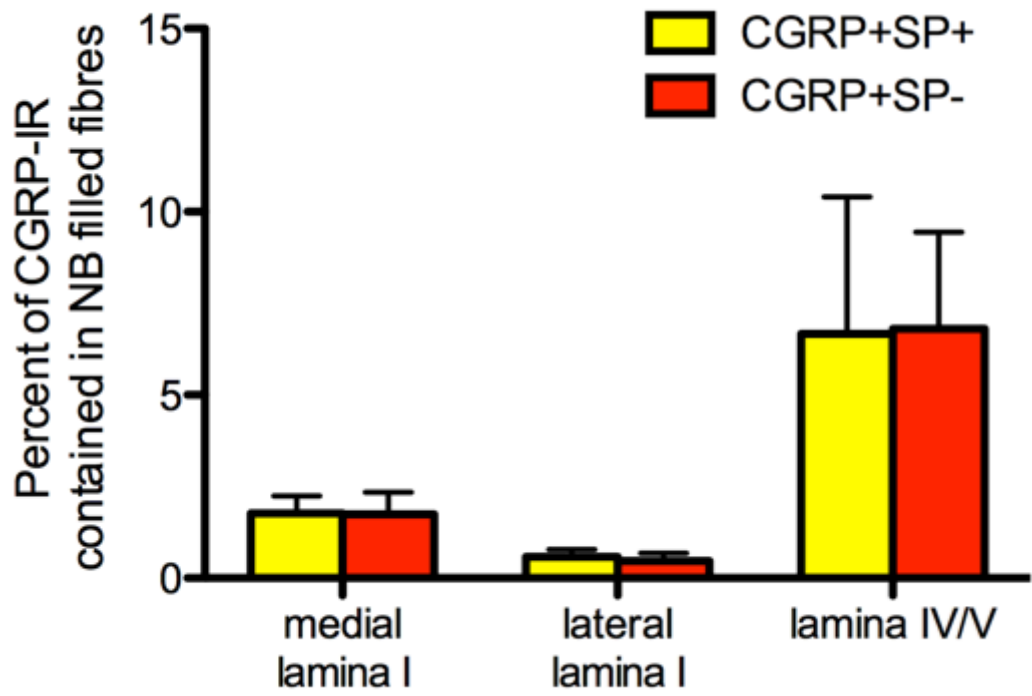


**Figure 6.10: NB labelled fibres in the L4 dorsal horn**

Montage of wide-field fluorescence micrographs of the mouse L4 spinal cord showing Neurobiotin (NB) labelled fibres. NB-labelled fibres can be seen in the dorsal root (DR) and heading toward the dorsal funiculus (DF). Around the DF NB-labelled fibres can be seen penetrating the dorsal horn (DH), with some penetrating as far as the ventral horn (VH). Fibres were seen terminating in the superficial lamina in the medial, mid and lateral parts of the superficial lamina. Scale bar = 60  $\mu$ m

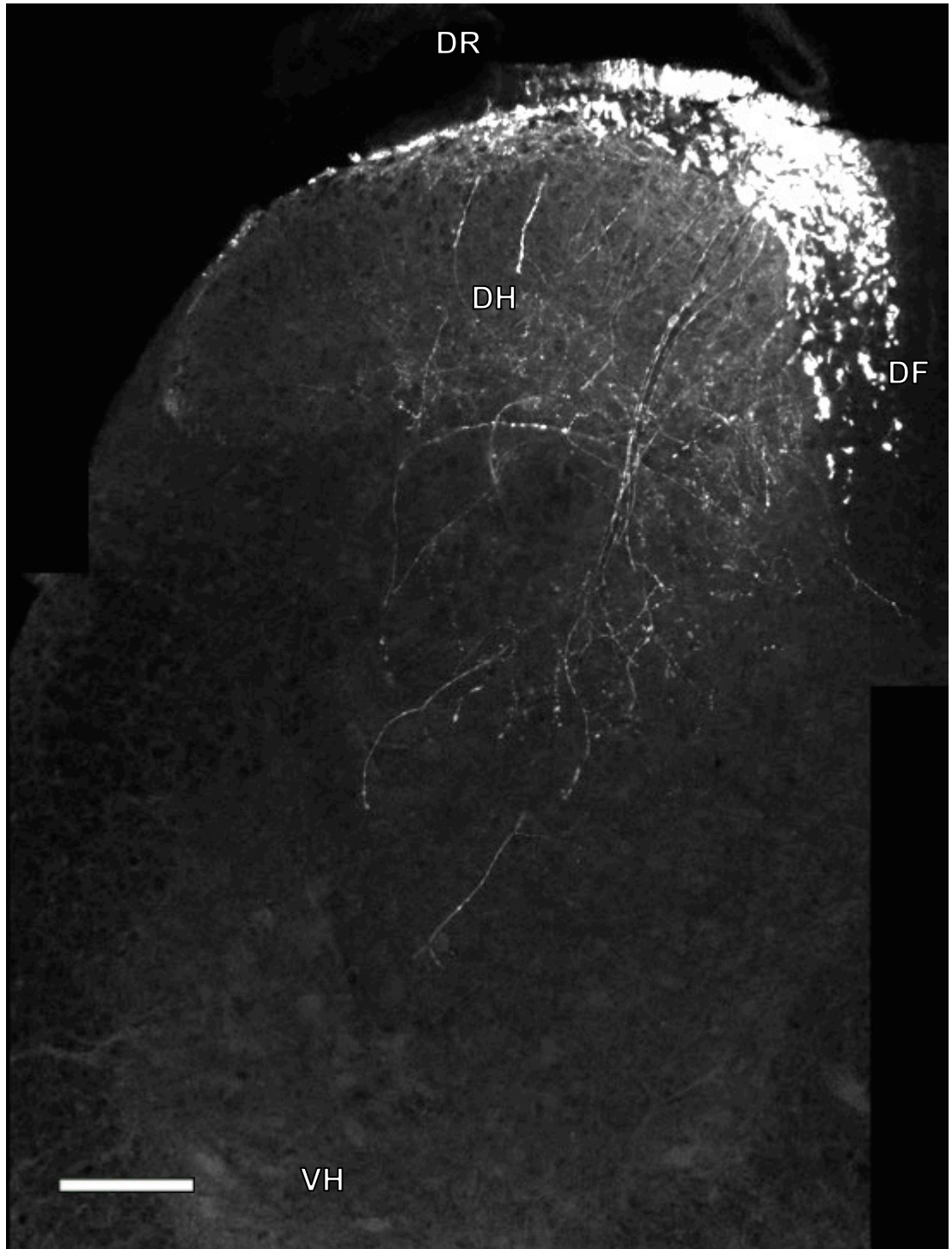


**Figure 6.11: Volume of NB labelled fibres in the L4 dorsal horn**

Histogram (data displayed as mean  $\pm$  SEM) depicting the volume (voxels) of Neurobiotin (NB) labelled fibres in medial and lateral lamina I, and lamina IV/V of the mouse L4 dorsal horn. Lateral lamina I had significantly fewer NB-labelled fibres compared to medial lamina I and lamina IV/V (RM-ANOVA:  $F_{(1,4)} = 25$ ,  $p < 0.01$ ;  $n = 5$  animals).

**Figure 6.12: Volume of NB labelled fibres in the C7 dorsal horn compared to the L4 dorsal horn**

Histogram (data displayed as mean  $\pm$  SEM) depicting the volume (voxels) of Neurobiotin (NB) labelled fibres in medial and lateral lamina I, and lamina IV/V of the mouse C7 dorsal horn (black) compared to the L4 dorsal horn (white). The L4 dorsal horn had significantly more NB-labelled fibres compared to the C7 dorsal horn (RM-ANOVA:  $F_{(1,4)} = 10$ ,  $p = 0.03$ ;  $n = 10$  animals).

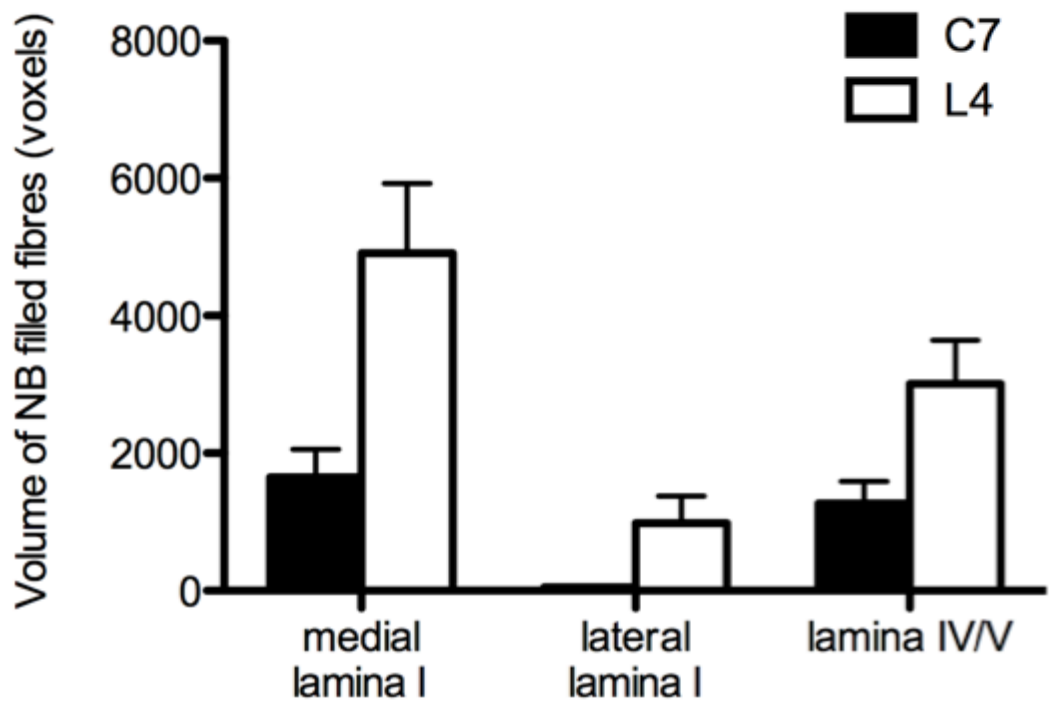
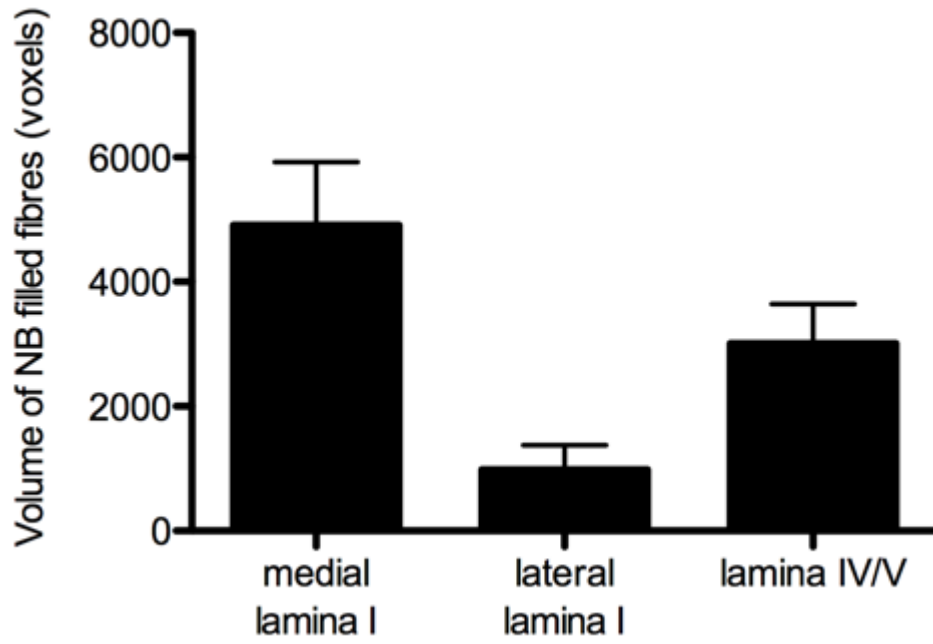


**Figure 6.13: NB labelled fibres in the L4 dorsal horn in association with CGRP-IR terminals**

**A:** Wide field fluorescence microscopy of mouse L4 dorsal horn triple labelled for Neurobiotin (NB; blue), calcitonin gene-related peptide (CGRP; red) and substance P (SP; green) showing fibres labelled with NB throughout the dorsal horn. Boxed outlines (1-3) represent the dorsal horn regions (medial and lateral lamina I, and lamina IV/V) of high CGRP-immunoreactivity (IR) further investigated with confocal microscopy. **B<sub>1</sub>- C<sub>3</sub>:** 3D reconstruction of confocal Z-stacks (21 steps of 0.5µm) of the three dorsal horn regions using Avizo. **B<sub>1</sub>- B<sub>3</sub>:** The 3D reconstruction of fibres labelled with NB (blue) in association with CGRP-IR terminals with (CGRP<sup>+</sup>SP<sup>+</sup>, yellow) and without SP-IR (CGRP<sup>+</sup>SP<sup>-</sup>, red). **C<sub>1</sub>- C<sub>3</sub>:** The 3D reconstructions of fibres labelled with NB showing only the CGRP<sup>+</sup>SP<sup>+</sup> (white, black arrows) and CGRP<sup>+</sup>SP<sup>-</sup> (magenta, white arrows) terminals that also contained NB labelling. Scale bar = 60 µm in A; 20 µm in C<sub>3</sub> (applies to B-C)

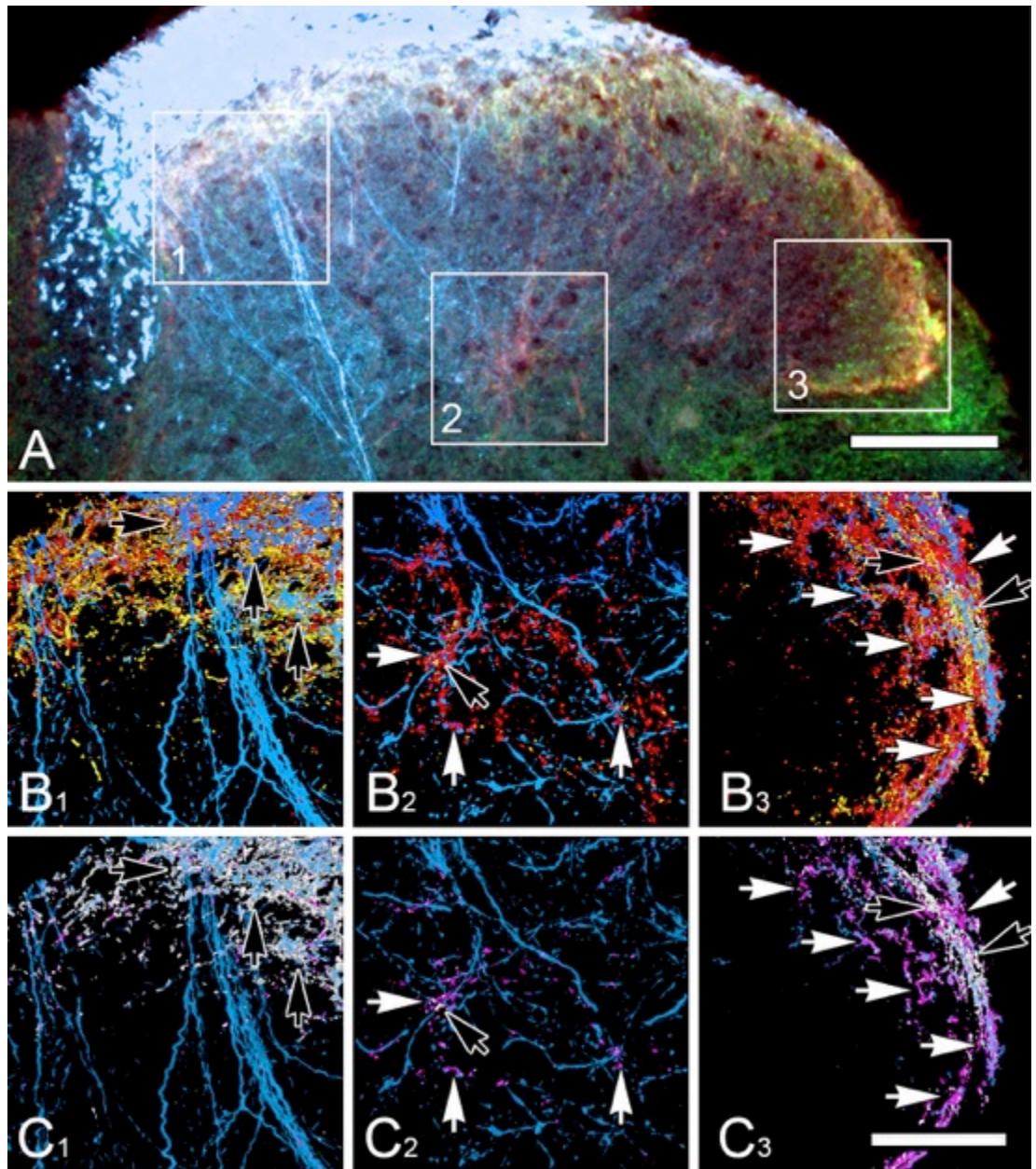


**Figure 6.14: Volume of NB labelled fibres that contained CGRP-IR in the L4 dorsal horn**

Histogram (data displayed as mean  $\pm$  SEM) depicting the volume (in pixels<sup>3</sup> or voxels) of Neurobiotin (NB) labelled fibres that contained calcitonin gene related peptide (CGRP) with substance P (SP; CGRP<sup>+</sup>SP<sup>+</sup>; yellow) and fibres that contained CGRP without SP (CGRP<sup>+</sup>SP<sup>-</sup>; red) in medial and lateral lamina I, and lamina IV/V of the mouse L4 dorsal horn. There was a higher volume of NB-labelled fibres that contained CGRP<sup>+</sup>SP<sup>+</sup> in medial lamina I compared to lateral lamina I and lamina IV (RM-ANOVA:  $F_{(1,4)} = 13$ ,  $p = 0.02$ ;  $n = 5$  animals). There was no significant difference in the volume of NB-labelled fibres containing CGRP<sup>+</sup>SP<sup>-</sup> in any of the lamina (RM-ANOVA:  $F_{(1,4)} = 1$ ,  $p = 0.4$ ;  $n = 5$  animals). Overall, there was a higher volume of NB-labelled fibres containing CGRP<sup>+</sup>SP<sup>+</sup> than CGRP<sup>+</sup>SP<sup>-</sup> voxels in the L4 dorsal horn (RM-ANOVA:  $F_{(1,4)} = 12$ ,  $p = 0.03$ ;  $n = 5$  animals).

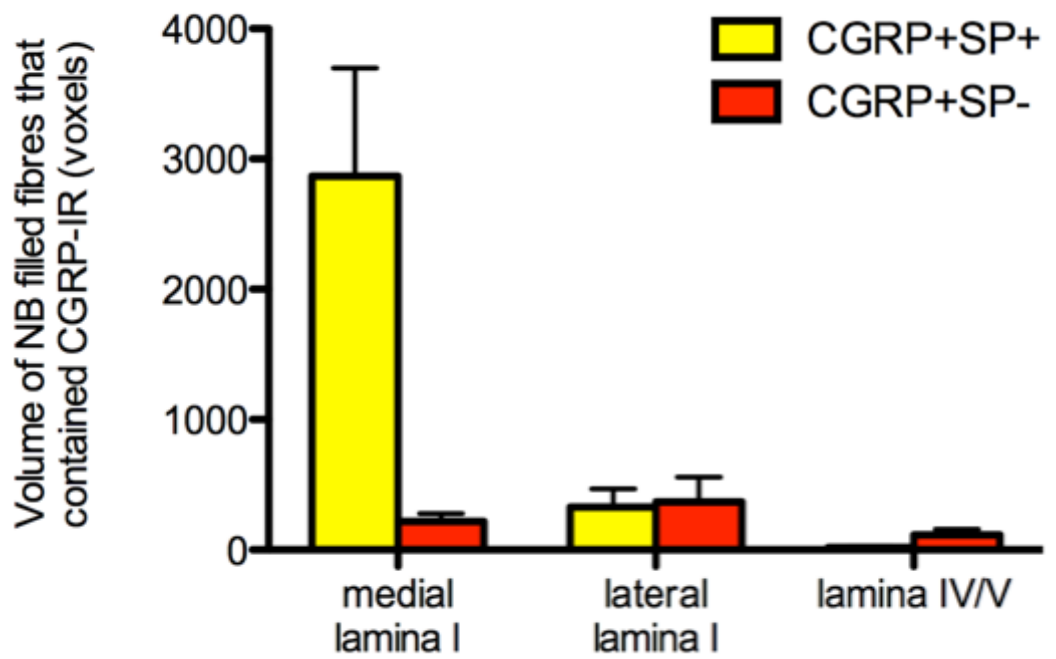


**Figure 6.15: Volume of NB labelled fibres that contained CGRP-IR in the C7 dorsal horn compared to the L4 dorsal horn**

Histogram (data displayed as mean  $\pm$  SEM) depicting the volume (in pixels<sup>3</sup> or voxels) of Neurobiotin (NB) labelled fibres that contained calcitonin gene related peptide (CGRP) with substance P (SP; CGRP<sup>+</sup>SP<sup>+</sup>; A) and fibres that contained CGRP without SP (CGRP<sup>+</sup>SP<sup>-</sup>; B) in medial and lateral lamina I, and lamina IV/V of the mouse C7 dorsal horn (black) compared to the L4 dorsal horn (white). Overall, there were more NB-labelled fibres that contained CGRP-IR in medial and lateral lamina I of the L4 dorsal horn compared to the C7 dorsal horn (RM-ANOVA:  $F_{(1,8)} = 12$ ,  $p < 0.01$ ;  $n = 10$  animals). This was true for both CGRP<sup>+</sup>SP<sup>+</sup> fibres (A: RM-ANOVA:  $F_{(1,8)} = 11$ ,  $p = 0.01$ ;  $n = 10$  animals) and CGRP<sup>+</sup>SP<sup>-</sup> fibres (B: RM-ANOVA:  $F_{(1,8)} = 6$ ,  $p = 0.04$ ;  $n = 10$  animals).

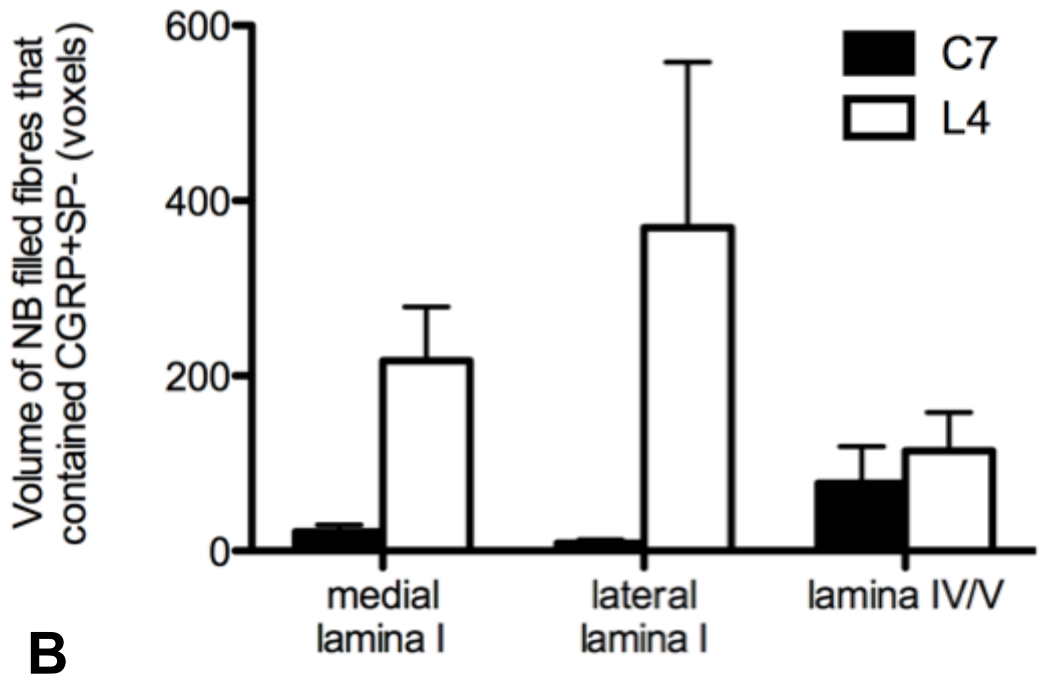
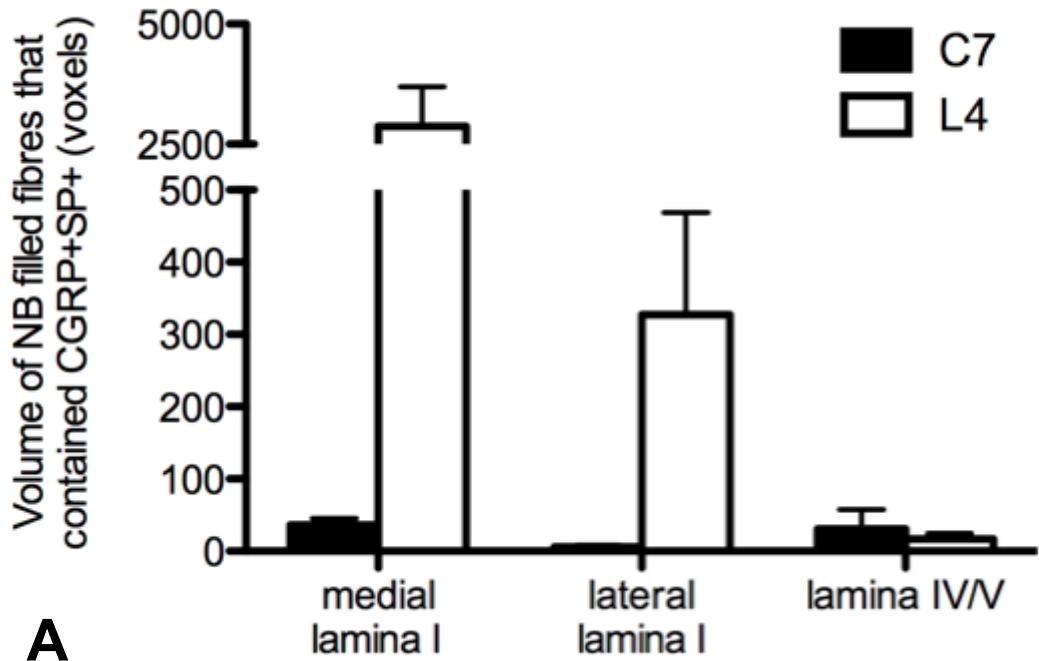


**Figure 6.16: Proportion of NB labelled fibres that contained CGRP-IR in the L4 dorsal horn**

Histogram (data displayed as mean  $\pm$  SEM) depicting the proportion (%) of Neurobiotin (NB) labelled fibres that contained calcitonin gene related peptide (CGRP) with substance P (SP; CGRP<sup>+</sup>SP<sup>+</sup>; yellow) and fibres that contained CGRP without SP (CGRP<sup>+</sup>SP<sup>-</sup>; red) in medial and lateral lamina I, and lamina IV/V of the mouse L4 dorsal horn. There was a significantly higher proportion of NB-labelled fibres that contained CGRP<sup>+</sup>SP<sup>+</sup> than CGRP<sup>+</sup>SP<sup>-</sup> (RM-ANOVA:  $F_{(1,4)} = 35$   $p < 0.01$ ;  $n = 5$  animals).

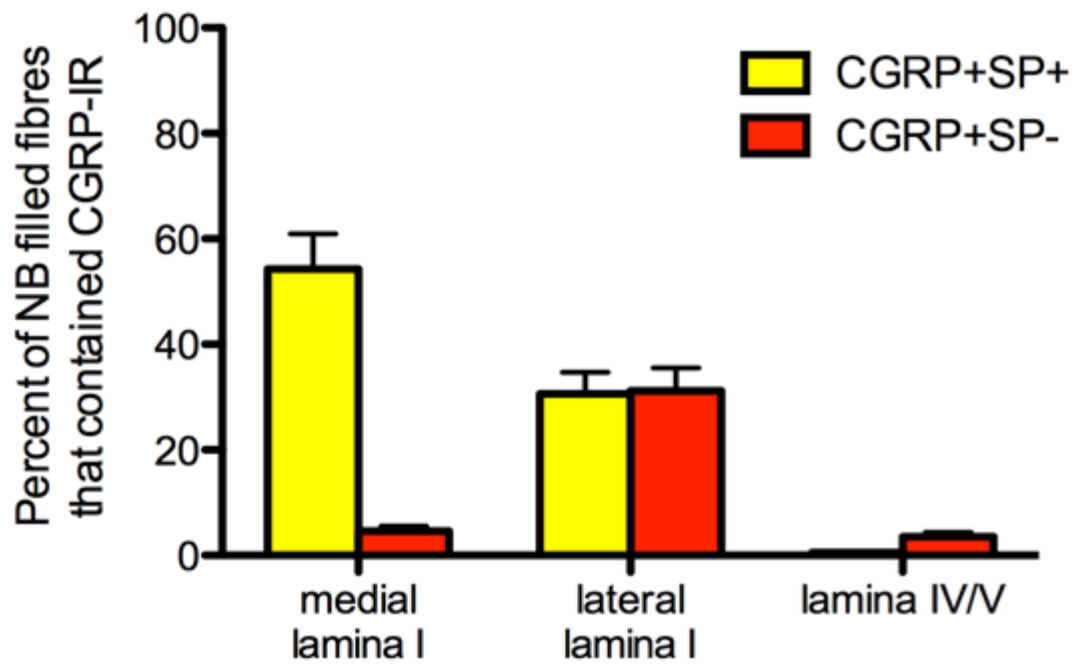


**Figure 6.17: Proportion of NB labelled fibres that contained CGRP-IR in the C7 dorsal horn compared to the L4 dorsal horn**

Histogram (data displayed as mean  $\pm$  SEM) depicting the proportion (%) of Neurobiotin (NB) labelled fibres that contained calcitonin gene related peptide (CGRP) with substance P (SP; CGRP<sup>+</sup>SP<sup>+</sup>; A) and fibres that contained CGRP without SP (CGRP<sup>+</sup>SP<sup>-</sup>; B) in medial and lateral lamina I, and lamina IV/V of the mouse C7 dorsal horn (black) compared to the L4 dorsal horn (white). There was a higher proportion of NB-labelled voxels that contained CGRP-IR in the L4 dorsal horn compared to the C7 dorsal horn, particularly in medial and lateral lamina I (RM-ANOVA:  $F_{(1,8)} = 17$ ,  $p < 0.01$ ;  $n = 10$  animals) While the proportion of NB-labelled voxels that were CGRP<sup>+</sup>SP<sup>+</sup> showed a similar pattern (A: RM-ANOVA:  $F_{(1,8)} = 48$ ,  $p < 0.0001$ ;  $n = 10$  animals), there was no difference in the volume of NB-labelled voxels that were CGRP<sup>+</sup>SP<sup>-</sup> in the two dorsal horns (B: RM-ANOVA:  $F_{(1,8)} = 3$ ,  $p = 0.15$ ;  $n = 10$  animals).

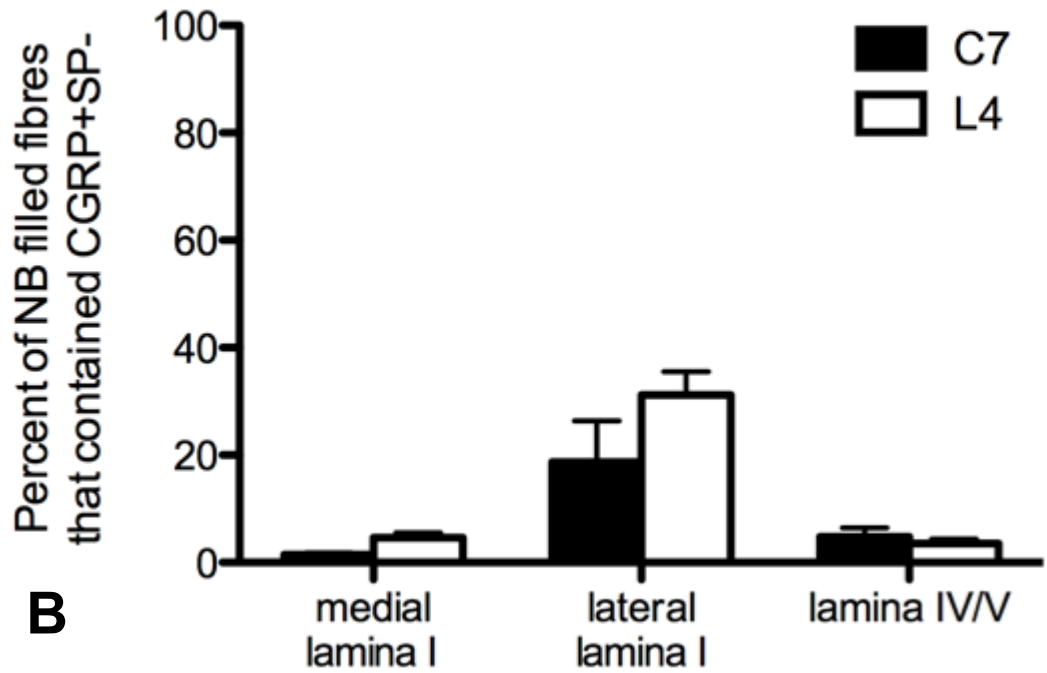
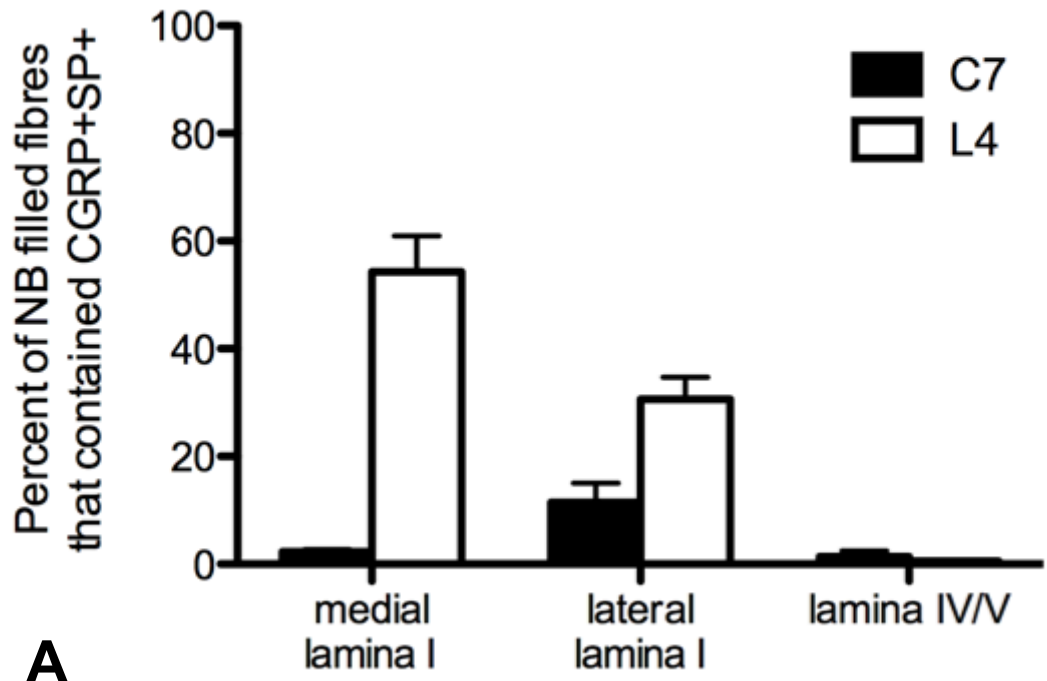


**Figure 6.18: Proportion of CGRP-IR within NB labelled fibres in the L4 dorsal horn**

Histogram (data displayed as mean  $\pm$  SEM) depicting the proportion (%) of fibres that contained calcitonin gene related peptide (CGRP) with substance P (SP; CGRP<sup>+</sup>SP<sup>+</sup>; yellow) and fibres that contained CGRP without SP (CGRP<sup>+</sup>SP<sup>-</sup>; red) that were labelled with Neurobiotin (NB) in medial and lateral lamina I, and lamina IV/V of the mouse L4 dorsal horn. Medial lamina I had the highest proportion of CGRP-IR contained within NB-labelled fibres compared to lateral lamina I and lamina IV/V (RM-ANOVA:  $F_{(1,4)} = 12$   $p = 0.03$ ;  $n = 5$  animals).

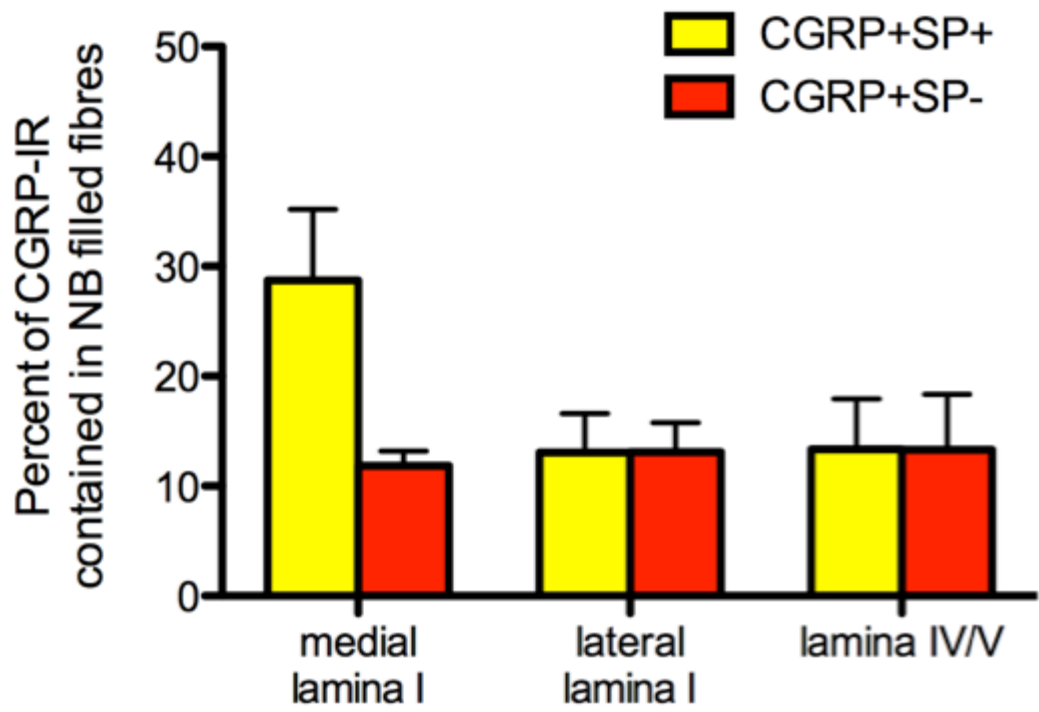


**Figure 6.19: Proportion of CGRP-IR within NB labelled fibres in the C7 dorsal horn compared to the L4 dorsal horn**

Histogram (data displayed as mean  $\pm$  SEM) depicting the proportion (%) of fibres that contained calcitonin gene related peptide (CGRP) with substance P (SP; CGRP<sup>+</sup>SP<sup>+</sup>; A) and fibres that contained CGRP without SP (CGRP<sup>+</sup>SP<sup>-</sup>; B) that were labelled with Neurobiotin (NB) in medial and lateral lamina I, and lamina IV/V of the mouse C7 dorsal horn (black) compared L4 dorsal horn (white). A significantly higher proportion of CGRP-IR (both CGRP<sup>+</sup>SP<sup>+</sup> and CGRP<sup>+</sup>SP<sup>-</sup>) in the L4 dorsal horn was contained within NB-labelled fibres compared to the proportion of CGRP-IR within NB-labelled fibres in the C7 dorsal horn (RM-ANOVA:  $F_{(1,8)} = 13$   $p < 0.01$ ;  $n = 10$  animals)

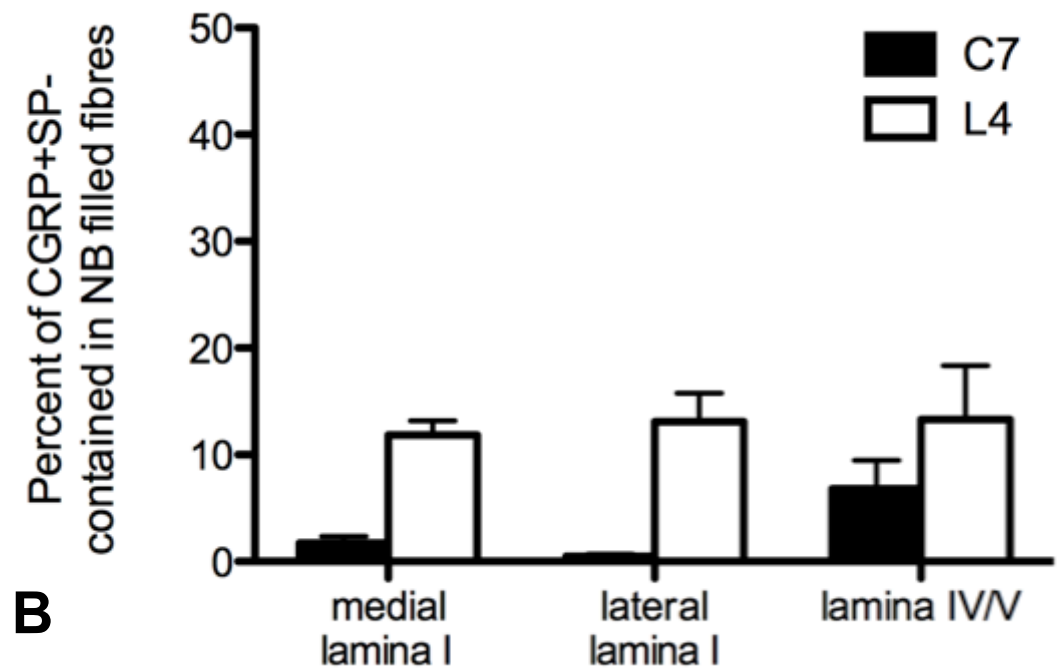
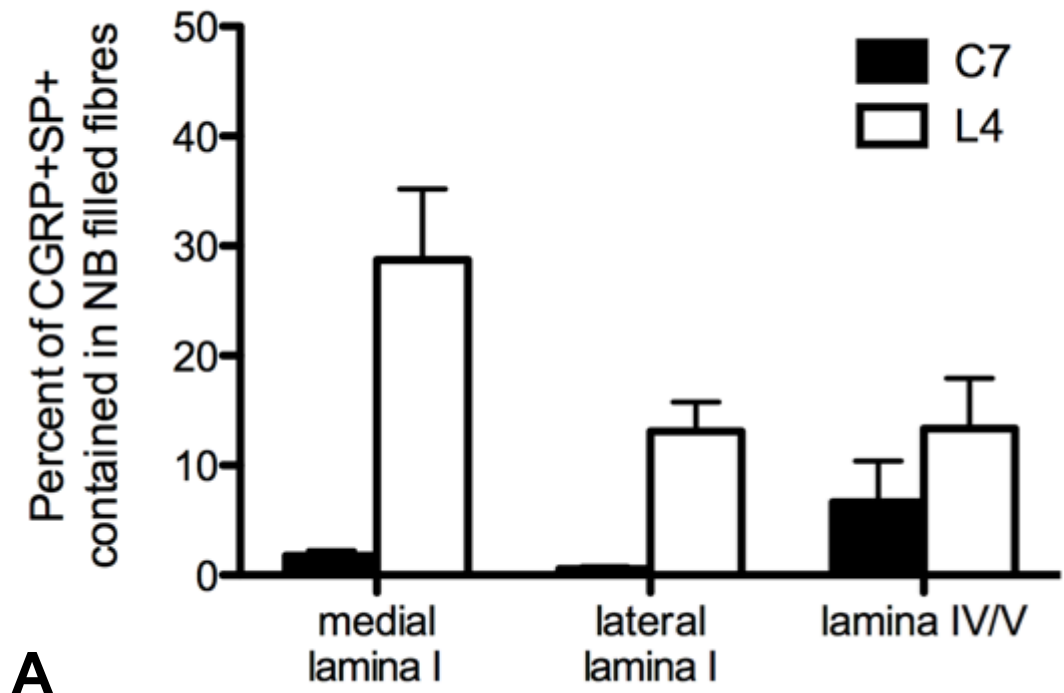


**Figure 6.20: NB labelled fibres in the L4 dorsal horn in association with CGRP-IR and VGluT1-IR terminals**

**A:** Wide field fluorescence microscopy of mouse L4 dorsal horn triple labelled for Neurobiotin (NB; blue), calcitonin gene-related peptide (CGRP; red) and vesicular glutamate transporter 1 (VGluT1; green) showing fibres labelled with NB throughout the dorsal horn. The boxed outline represents lamina IV/V that was further investigated with confocal microscopy. **B- C:** 3D reconstruction of confocal Z-stacks (21 steps of 0.5µm) of lamina IV/V using Avizo. **B:** The 3D reconstruction of fibres labelled with NB (blue) in association with CGRP-IR terminals and without VGluT1-IR terminals. **C:** The 3D reconstructions of fibres labelled with NB showing only the CGRP-IR (magenta) and VGluT1-IR (cyan) terminals that also contained NB labelling. The C7 dorsal horn was not visibly different from the L4 dorsal horn.

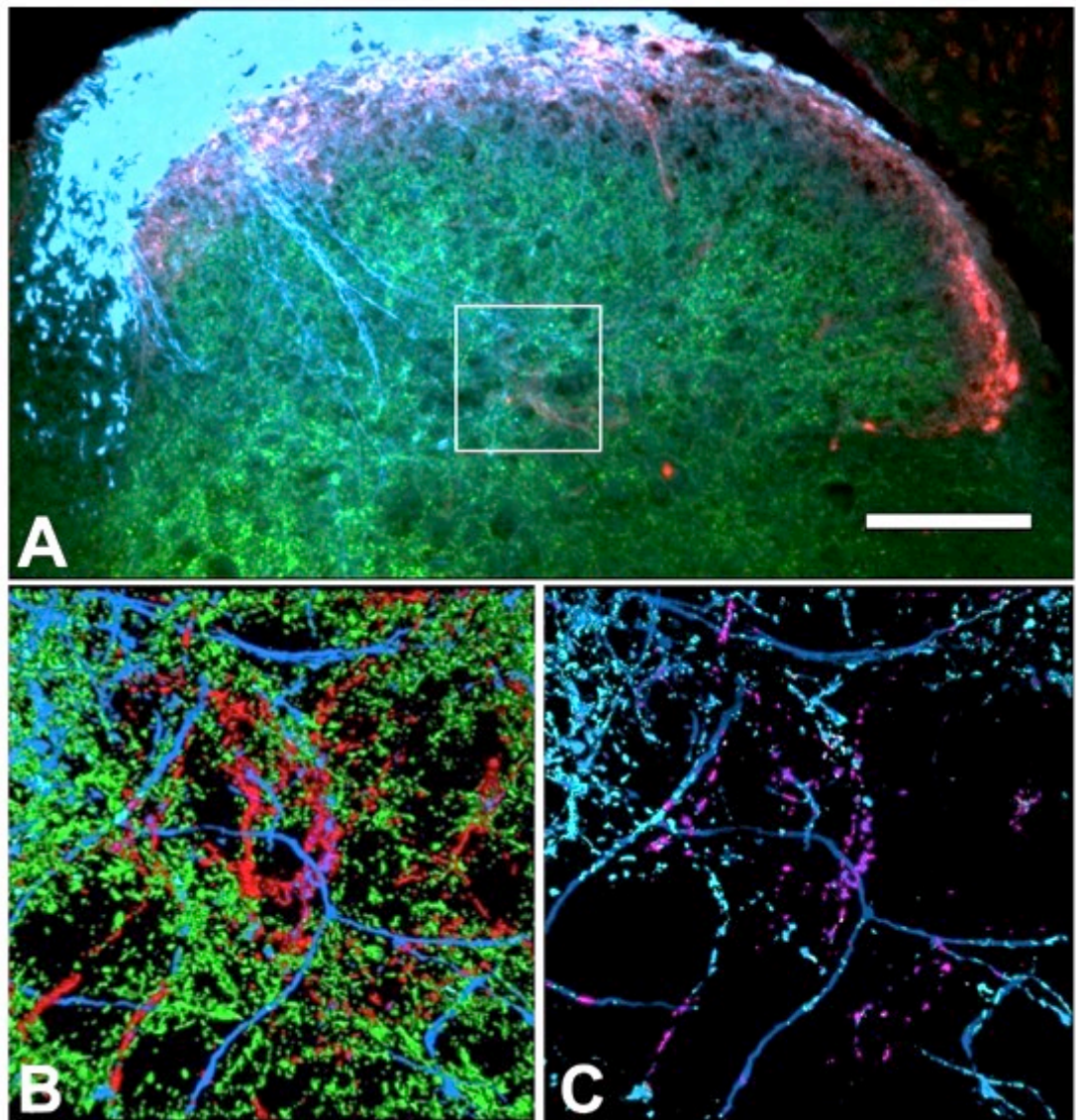


**Figure 6.21: Proportion of NB-labelled fibres containing VGluT-IR compared to CGRP-IR in C7 dorsal horn**

Histogram (data displayed as mean  $\pm$  SEM) depicting the proportion (%) of Neurobiotin (NB) labelled fibres that contained calcitonin gene related peptide-immunoreactivity (CGRP-IR; red) or lacked vesicular glutamate transporter 1-IR (VGluT1-IR; green) in lamina IV/V of the C7 dorsal horn. Significantly more NB-labelled fibres contained VGluT1-IR than CGRP-IR (Paired t-test:  $t_{(3)}=4$ ,  $p = 0.04$ ;  $n = 3$  animals).

**Figure 6.22: Proportion of NB-labelled fibres containing VGluT-IR compared to CGRP-IR in L4 dorsal horn**

Histogram (data displayed as mean  $\pm$  SEM) depicting the proportion (%) of Neurobiotin (NB) labelled fibres that contained calcitonin gene related peptide-immunoreactivity (CGRP-IR; red) or lacked vesicular glutamate transporter 1-IR (VGluT1-IR; green) in lamina IV/V of the C7 dorsal horn. Significantly more NB-labelled fibres contained VGluT1-IR than CGRP-IR (Paired t-test:  $t_{(3)}=4$ ,  $p=0.04$ ;  $n = 4$  animals).

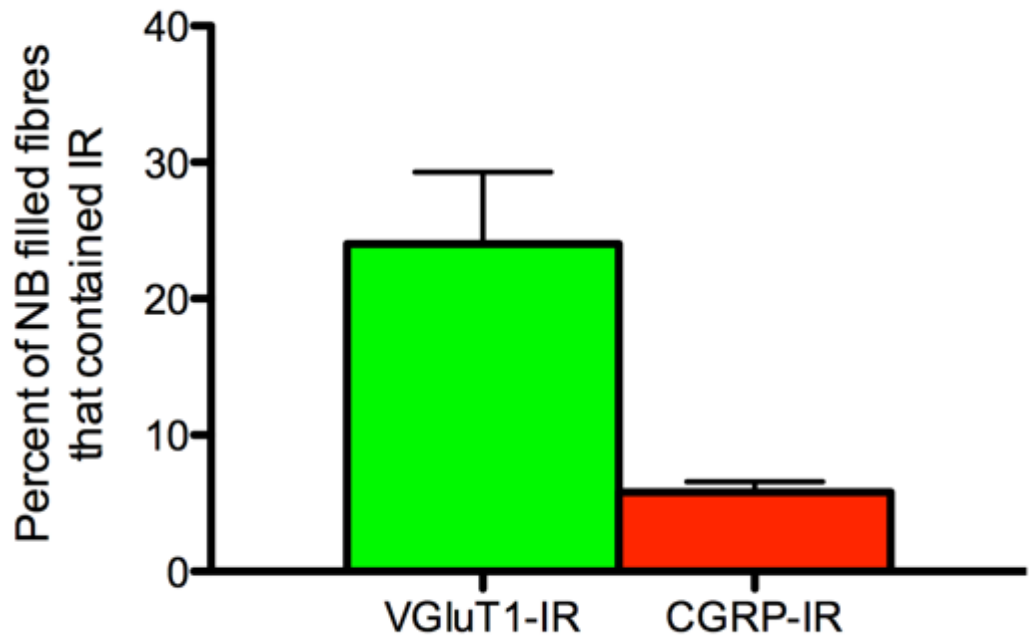
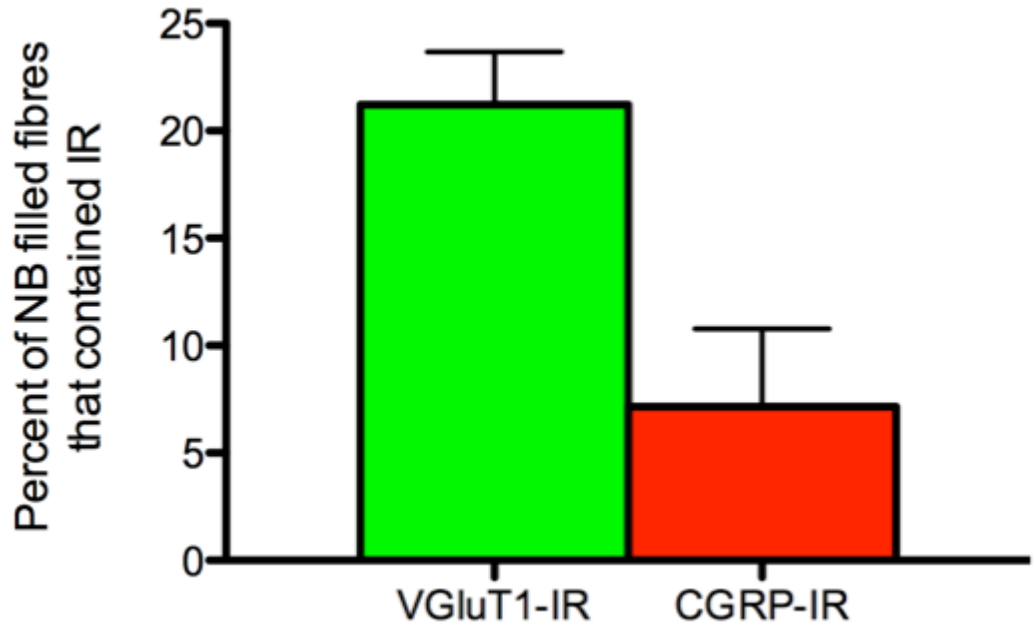
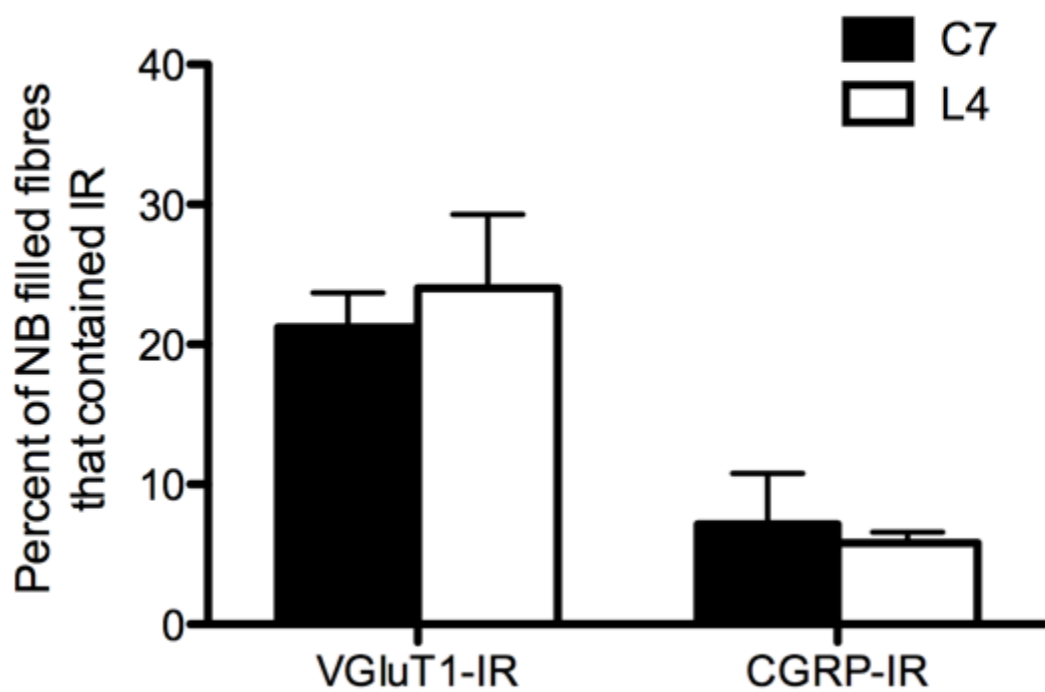


**Figure 6.23: Proportion of NB-labelled fibres containing VGluT-IR or CGRP-IR in C7 dorsal horn compared to L4 dorsal horn**

Histogram (data displayed as mean  $\pm$  SEM) depicting the proportion (%) of Neurobiotin (NB) labelled fibres that contained calcitonin gene related peptide-immunoreactivity (CGRP-IR) or vesicular glutamate transporter 1-IR (VGluT1-IR) in lamina IV/V of the C7 dorsal horn (black) compared to the L4 dorsal horn (white). There was no significant difference between the amount of NB-labelled fibres containing VGluT1-IR in C7 or L4 dorsal horns (RM-ANOVA:  $F_{(1,4)} = 2$ ,  $p = 0.2$ ;  $n = 6$  animals).





---

**Chapter 7:  
Relationship of CGRP<sup>+</sup>SP<sup>-</sup>  
terminals with nociceptive  
dorsal horn neurons**

---



## 7.1 Background

---

Within the spinal cord, CGRP enhances the nociceptive behavioural responses induced by SP, by potentiating the release of SP (Oku *et al.*, 1987), inhibiting its degradation (Le Greves *et al.*, 1985) and enhancing the excitability of neurons receiving noxious inputs (Biella *et al.*, 1991; Seybold *et al.*, 2003; Sun *et al.*, 2004; Bird *et al.*, 2006). CGRP alone has minimal effects on nociceptive inputs to the spinal cord (Miletic & Tan, 1988). Yet, in previous chapters, we have demonstrated that CGRP neurons exist that lack any detectable SP (CGRP<sup>+</sup>SP<sup>-</sup> neurons) in DRG, the spinal dorsal horn, and skin and muscle. These neurons were neurochemically distinct from CGRP<sup>+</sup>SP<sup>+</sup> neurons. With large cell bodies, NF200 expression and central terminals in lamina IV/V we have suggested that CGRP<sup>+</sup>SP<sup>-</sup> neurons were myelinated A $\beta$ -fibres, but were not classical VGluT1 expressing mechanoreceptors. Their lack of TRPV1 expression also suggests they are not capsaicin sensitive. Hence, it is likely that the function of CGRP<sup>+</sup>SP<sup>-</sup> neurons is distinct from CGRP<sup>+</sup>SP<sup>+</sup> neurons. However, this function is unknown.

One method to determine neuronal function is to use markers for neuronal activation, which can then be detected immunohistochemically in the spinal cord. The most common markers for neuronal activation are components of the mitogen activated kinase (MAPK) pathway (Figure 7.1). These include phosphorylation of the extracellular signal-regulated kinases 1/2 (ERK1/2, also known as MAPK1/2), the phosphorylation of cAMP-response element binding protein (CREB), and the production of the c-Fos protein. Briefly, the MAPK pathway begins with an extracellular ligand binding to a receptor that activates Ras and causes a kinase cascade. Ras activates RAF kinase (or MAP3K: MAPK kinase kinase). RAF kinase then phosphorylates MEK (or MAP2K: MAPK kinase) which in turn phosphorylates the last of the kinases: ERK (or MAPK). Upon activation, phosphorylated ERK (pERK) activates several transcriptional factors including CREB (Ji & Rupp, 1997). CREB is phosphorylated and translocated into the nucleus where it regulates the transcription of several genes including *c-fos* (Sheng & Greenberg, 1990). The transcription of the *c-fos* gene produces the c-Fos protein. pERK, phosphorylated CREB (pCREB) and the protein c-Fos can all be detected immunohistochemically to detect activated neurons.

c-Fos is the most widely used neuronal activation marker in the study of the neurons involved in nociception (Bullit *et al* 1992; Coggeshall 2005; Harris 1998). c-Fos is the protein product of the proto-oncogene *c-fos*, and forms a complex with Jun to induce gene transcription (Gao & Ji, 2009). Hunt and colleagues (1987) were first to report a marked induction of c-Fos in the superficial dorsal horn after peripheral noxious stimulation of rat hindpaw. c-Fos expression is specific, robust and its detection with immunohistochemistry is relatively simple (Gao & Ji, 2009). However, as the protein c-Fos is a product of gene expression, peak induction time (1-2 hours) and the return to baseline (8-24 hours) is slow. Consequently using c-Fos as a marker for neuronal activation is restricted to *in vivo* use (Hunt *et al.*, 1987; Presley *et al.*, 1990; Williams *et al.*, 1990).

Ji and colleagues (1999) first detected an increase in pERK expression in the superficial laminae of the spinal cord after noxious stimulation of the hindpaw. Like c-Fos expression, pERK expression is also very robust and requires high-threshold noxious stimuli (Gao & Ji, 2009). pERK expression is suppressed by analgesic compounds (Karim *et al.*, 2001; Kawasaki *et al.*, 2006), demonstrating that, like c-Fos, pERK can also be used as a marker for the activation of dorsal horn neurons following nociceptive activity. Unlike c-Fos, pERK is an early stage intracellular messenger, and hence the peak induction time (2-10 minutes) and return to base levels (1-2 hours) is much more rapid (Ji *et al.*, 1999). Consequently, pERK can be used as a marker for neuronal activation *ex vivo/in vitro* in spinal cord slices (Kawasaki *et al.*, 2004). Importantly, the role of pERK in pain regulation has been demonstrated in central sensitisation (Ji *et al.*, 1999; Karim *et al.*, 2001).

pCREB expression is tightly linked to pERK expression, and hence using pCREB as a marker for neuronal activation shares many of the advantages of using pERK. Like pERK, Ji and Rupp (1997) first detected an increase in pCREB expression in the dorsal horn of the spinal cord after noxious stimulation of the hindpaw. The peak induction time (2-10 minutes) and return to baseline (1-2 hours) of pCREB expression was the same time frame as pERK expression (Ji & Rupp, 1997; Kawasaki *et al.*, 2004; Song *et al.*, 2005). Consequently, pCREB can also be used as a marker for neuronal activation *ex vivo/in vitro* in spinal cord slices (Kawasaki *et al.*, 2004). However, pERK is not necessary for pCREB induction, and other protein

kinases play a role in CREB phosphorylation (Lonze & Ginty, 2002). Therefore, while pERK may be nociceptive-specific, pCREB is not.

pERK and pCREB have clear advantages over c-Fos as markers for neuronal activation. Namely, their timescale of induction onset and return to base make them both suitable for *ex vivo/in vitro* work. pERK is nociceptive-specific and hence will label only the activated nociceptive dorsal horn neurons after stimulation, whereas pCREB is not and should hence label more activated dorsal horn neurons. Using these two markers we should be able to detect activated dorsal horn neurons *in vitro* and determine the relationship of the central terminals of CGRP<sup>+</sup>SP<sup>-</sup> neurons to noxiously activated dorsal horn neurons and hence their possible involvement in nociception.

To investigate the relationship of CGRP<sup>+</sup>SP<sup>-</sup> neurons to noxiously activated dorsal horn neurons we adapted techniques from Kawasaki and colleagues (2004) and coupled them with multiple labeling immunohistochemistry and high-resolution confocal microscopy. We used two different stimulation parameters. Stimulation with capsaicin to activate dorsal horn neurons receiving input from classical peptidergic nociceptors expressing TRPV1 receptors, and electrical stimulation to activate dorsal horn neurons receiving input from any primary afferent from the stimulated dorsal root. We then used multiple labeling immunohistochemistry and high-resolution confocal microscopy to determine whether CGRP<sup>+</sup>IR terminals were close enough to be in potential contact with the activated pERK/pCREB dorsal horn neurons.



## 7.2 Materials and Methods

---

Lumbar spinal cord samples were isolated in low calcium high magnesium HEPES buffered balanced salt solution (LCHM-HBBS solution; 146 mM sodium chloride; 4.7 mM potassium chloride; 10 mM magnesium sulphate; 0.13 mM sodium phosphate; 1.6 mM sodium bicarbonate; 7.8 mM D-glucose; 20 mM HEPES; 0.1 mM ascorbic acid; 0.5 mM calcium chloride) on ice. The spinal cord was cut into smaller transverse segments (around 2-3 cm long) and placed onto a small polystyrene block saturated with LCHM-HBBS solution. The spinal nerves were arranged perpendicular to the spinal cord and the excess LCHM-HBBS solution was removed. The polystyrene block was then fixed with cyanoacrylate glue to a metal chuck with cork backing. To hold the position of the spinal cord, the caudal surface of the spinal cord was also fixed to the chuck. The spinal cord was then sliced at 500  $\mu\text{m}$  on a vibrating microtome at 4°C.

Slices were then placed into HEPES buffered balanced salt solution (HBBS solution; 146 mM sodium chloride; 4.7 mM potassium chloride; 0.6 mM magnesium sulphate; 0.13 mM sodium phosphate; 1.6 mM sodium bicarbonate; 7.8 mM D-glucose; 20 mM HEPES; 0.1 mM ascorbic acid; 2.5 mM calcium chloride) and incubated for 3 hours at 37°C to allow for the dephosphorylation of any ERK/CREB phosphorylated as a result of neuronal activation during spinal cord dissection and slice preparation (Kawasaki *et al.*, 2004). Slices that contained an intact dorsal root were used for electrical stimulation and those that did not were used for pharmacological stimulation.

***Capsaicin stimulation:*** Stock solutions of  $10^{-2}$  M capsaicin were created by dissolving 30 mg of capsaicin powder in a 10 mL of 10% Tween80 / 90% ethanol solution. Stock solutions were diluted in HBBS solution to the working concentration of  $10^{-6}$  M capsaicin. To ensure Tween80 and ethanol had no effect on the activity of the dorsal horn neurons two controls were used. The vehicle control used the stock solution of 10% Tween80 and ethanol mixture (without any capsaicin) diluted in HBBS solution, and the saline control contained only HBBS solution.

Slices lacking dorsal roots were transferred into three 2 mL vials containing HBBS solution for 3 hours at 37°C. After 3 hours, the HBBS solution of each vial was

replaced with one of either the 10<sup>-6</sup> M capsaicin solution, the vehicle control or saline control solutions. Slices were left in these solutions for 10 minutes at 37°C. Slices were then fixed, processed through DMSO, PEG embedded and sectioned on a microtome.

**Electrical Stimulation:** Slices with roots were transferred into a Petri dish with a constant flow of oxygenated HBBS solution at 37°C. Dorsal roots of slices were pulled into a suction electrode that was connected to Grass S44 stimulator (Grass Medical Instruments, Quincy, MA, USA) controlled by a Master-8 programmable pulse generator (AMPI, Jerusalem, Israel).

After 3 hours, the seal of the suction electrode on the dorsal root was checked before stimulation. The seal was deemed acceptable if the dorsal root was still within the suction electrode prior to stimulation. The stimulation parameters were adapted from Kawasaki et al (2004): attached dorsal roots were stimulated with three trains of 50 pulses (each pulse was 90 V for 0.5 ms) at 50Hz for one second with 10-second inter-train interval. After 2 minutes, slices were then fixed, processed through DMSO, PEG embedded and sectioned on a microtome. While the method used was similar to the work of Kawasaki et al (2004), which measured the current drawn (1000 µA), our validations simply involved increasing the potential difference (V) of the suction electrode until activation occurred at 90 V. These preliminary experiments were merely intended to demonstrate that electrical stimulation was a viable means of stimulating both A-fibre and C-fibre afferents.

For counts of activated dorsal horn cells, sections were then double labelled with DAPI (1:1000; Cell Signalling, Massachusetts, USA) to visualise all dorsal horn cells and one of either anti-pERK1/2 raised in rabbit (1:500; Cell Signalling, Massachusetts, USA) or anti-pCREB raised in rabbit (1:500; Cell Signalling) to visualise the activated subset of neurons. Manual cell counts were performed on widefield images of spinal cord sections that were taken with an Olympus BX50 epifluorescence microscope with a 20x objective. Counts were displayed as either a total number of pERK/pCREB positive neurons, or as proportion of all dorsal horn neurons that were pERK/pCREB positive.

To determine the association of CGRP<sup>+</sup>SP<sup>-</sup> terminals with the pERK/pCREB positive cells, adjacent sections were triple labelled with anti-CGRP raised in a goat (1:1000;

code 1780, Arnel, New York, USA), anti-SP raised in a rat (1:600; clone NC1/34HL, Sera-Lab, West Sussex, UK) and one of either rabbit anti-pERK1/2 or rabbit anti-pCREB. Confocal Z-stacks of spinal cord sections, consisting of 21 optical sections 0.5  $\mu\text{m}$  apart (total depth 10.5  $\mu\text{m}$ ), were taken with a Leica confocal microscope with a 63x N.A. 1.4 oil immersion objective with 3x digital zoom. Confocal Z-stacks of spinal cord were imported to Avizo for 3D reconstruction and analysis. Each detection channel was first 3D-median filtered (kernel size 3) to reduce single pixel noise and 3D thresholds were optimised to select specific labelling of axonal boutons above background labelling and intervaricose axons. Identical thresholds were used for each of the analysed regions within a spinal cord section and the respective thresholds for each channel were set to be consistent between sections and between experiments. The volume of CGRP-IR boutons that either contained or lacked SP-IR was first calculated using the AND (A&B) operator and the NOT (A-B) operator between the CGRP and SP data sets. The CGRP and SP contacts onto pERK/pCREB cells were defined as CGRP/SP data sets that were colocalised with the pERK/pCREB cells using the A&B operator. For illustration purposes, pERK/pCREB positive cells were shown as volume rendered data sets, while subsets of CGRP-IR and SP-IR boutons (total immunoreactivity and those contacting pERK/pCREB positive cells) were displayed with isosurface rendering. For quantification purposes only CGRP/SP data sets that were colocalised with pERK/pCREB positive cells were displayed and the pERK/pCREB cells were manually scored for the presence of CGRP<sup>+</sup>SP<sup>+</sup>, CGRP<sup>+</sup>SP<sup>-</sup> and CGRP<sup>-</sup>SP<sup>+</sup> contacts.

Data were then displayed as mean $\pm$ SEM and RM-ANOVA and M-ANOVA with post hoc BMC correction with 95% confidence limits were used to determine the statistical significance.



## 7.3 Results

---

### **pERK and pCREB levels were increased after stimulation of afferents with capsaicin**

Very few cells expressed pERK-IR in the dorsal horn of the spinal cord in vehicle and saline controls (Figure 7.2B and C). In dorsal horns stimulated with capsaicin, pERK-IR cells were observed in the superficial lamina (lamina I/II; Figure 7.2A).

The number of dorsal horn cells expressing pERK-IR after capsaicin stimulation were higher than vehicle and saline controls (ANOVA:  $F_{(2,4)} = 68$ ,  $p < 0.0001$ ,  $n = 6$  animals, Figure 7.3). After capsaicin stimulation  $40 \pm 4$  cells per dorsal horn expressed pERK-IR compared to  $3 \pm 1$  cells and  $1 \pm 1$  cell per dorsal horn in vehicle and saline controls, respectively. To determine the proportion of dorsal horn cells expressing pERK-IR, dorsal horn cells were visualised using DAPI staining. The proportion of dorsal horn cells expressing pERK-IR after capsaicin stimulation were higher than vehicle and saline controls (ANOVA:  $F_{(2,4)} = 73$ ,  $p < 0.0001$ ,  $n = 5$  animals, Figure 7.4). After capsaicin stimulation 6% (239/3997) of dorsal horn cells expressed pERK-IR compared to 0% in both the vehicle and saline controls (20/3815 and 10/3756, respectively).

Similarly to pERK-IR, very few dorsal horn cells were observed expressing pCREB-IR in the dorsal horn of the spinal cord in vehicle and saline controls (Figure 7.5B and C). In dorsal horns stimulated with capsaicin, pCREB-IR cells were observed in the superficial lamina (lamina I/II; Figure 7.5A).

Both the total number and the proportion of dorsal horn cells (visualised by DAPI) expressing pCREB-IR after capsaicin stimulation were higher than vehicle and saline controls (ANOVA:  $F_{(2,4)} = 57$ ,  $p < 0.0001$ ,  $n = 5$  animals, Figure 7.6 and  $F_{(2,4)} = 67$ ,  $p < 0.0001$ ,  $n = 5$  animals, Figure 7.7, respectively). After capsaicin stimulation  $130 \pm 15$  cells per dorsal horn (20% of dorsal horn cells; 651/3321) expressed pCREB-IR compared to  $3 \pm 1$  cells (0%; 17/3327) and  $1 \pm 1$  cell per dorsal horn (0%; 8/3452) in vehicle and saline controls, respectively.

Compared to pERK-IR, there were 2-3 times higher number and proportion of pCREB-IR expressing cells after capsaicin stimulation of afferents (RM-ANOVA:

$F_{(1,9)} = 29$ ,  $p = 0.0007$ ,  $n = 5$  animals, Figure 7.8 and  $F_{(1,9)} = 32$ ,  $p = 0.0005$ ,  $n = 5$  animals, Figure 7.9, respectively).

## **Capsaicin stimulated afferents activated dorsal horn neurons that received contacts from CGRP<sup>+</sup>SP<sup>-</sup> afferents**

From previous chapters we know that CGRP-IR terminals are found in lamina I/II and lamina IV/V. After chemical stimulation with capsaicin, both pERK-IR and pCREB-IR cells were restricted to lamina I/II of the dorsal horn (Figure 7.10A). In these laminae the pERK-IR and pCREB cells were in close proximity to the CGRP-IR terminals. There were no pERK-IR or pCREB-IR cells in lamina IV/V, and hence the CGRP-IR terminals of lamina IV/V were not in close association with any pERK-IR or pCREB-IR cells. Using our multiple labelling immunohistochemistry and high-resolution confocal microscopy we were able to visualize individual pERK expressing cells and examine their close association or contacts (which we defined earlier as CGRP/SP data sets that were colocalised with the pERK/pCREB cells at this resolution) with primary afferent terminals containing CGRP-IR.

Confocal analysis (Figure 7.10B) and 3D reconstructions (Figure 7.10C) revealed that pERK-IR cells of lamina I did make contacts with CGRP-IR and SP-IR terminals. pERK-IR cells received contacts from CGRP-IR terminals that also contained SP-IR, CGRP-IR terminals that lacked SP-IR, and SP-IR terminals that lacked CGRP-IR. A higher proportion of cells had CGRP<sup>+</sup>SP<sup>-</sup> (90%; 140/156) and CGRP<sup>-</sup>SP<sup>+</sup> (82%; 128/156) contacts compared to CGRP<sup>+</sup>SP<sup>+</sup> (54%, 84/156) contacts and a higher proportion of cells had CGRP<sup>+</sup>SP<sup>+</sup> contacts than cells that had no contacts (3%; 5/156; ANOVA  $F_{(3,11)} = 54$ ,  $p < 0.0001$ ,  $n = 3$  animals; Figure 7.11).

Many of these cells received contacts from multiple terminals. 47% (73/156) of pERK-IR cells in lamina I had contacts from all three classes of peptidergic terminals (CGRP<sup>+</sup>SP<sup>-</sup>, CGRP<sup>+</sup>SP<sup>+</sup> and CGRP<sup>-</sup>SP<sup>+</sup>); and 28% (44/156) had contacts from CGRP<sup>+</sup>SP<sup>-</sup> and CGRP<sup>-</sup>SP<sup>+</sup> terminals. No other combination differed significantly from zero (ANOVA:  $F_{(7,23)} = 16$   $p < 0.0001$ ,  $n = 3$  animals Figure 7.12).

## **pERK and pCREB levels increased after electrical stimulation of afferents**

Very few dorsal horn cells were observed expressing pERK-IR in the dorsal horn of the spinal cord in saline controls (Figure 7.13). After electrical stimulation of the attached dorsal root, pERK-IR cells were observed in the superficial lamina (lamina I/II). There was also an increase in pERK-IR that was not restricted to dorsal horn cells, and did not colocalise with DAPI staining. This extra-somatic pERK-IR was confined to lamina I/II of the dorsal horn and could possibly be labelling terminals of the dorsal horn (Figure 7.13). Unfortunately, this extra-somatic pERK-IR was too intense and widespread and so pERK-IR cells were not easily identified. Consequently, it was not possible to quantify the number of pERK-IR neurons.

Similarly to pERK-IR, very few dorsal horn cells were observed expressing pCREB-IR in the dorsal horn of the spinal cord in saline controls (Figure 7.14). After electrical stimulation of the attached dorsal root, pCREB-IR cells were observed in the lamina I-III. Unlike pERK-IR, there was no extra-somatic pCREB-IR detected.

Both the number and the proportion of dorsal horn cells (visualised by DAPI) expressing pCREB-IR after the electrical stimulation of afferents was higher than saline controls (paired *t*-test:  $t_{(4)} = 12$ ,  $p = 0.0003$ ,  $n = 3$  animals, Figure 7.15 and  $t_{(4)} = 12$ ,  $p = 0.0002$ ,  $n = 3$  animals, Figure 7.16, respectively). After electrical stimulation of afferents,  $184 \pm 19$  cells per dorsal horn (28% of dorsal horn cells; 920/3318) expressed pCREB-IR compared to  $10 \pm 3$  cells per dorsal horn (1%; 48/3285) in saline controls.

Compared to capsaicin stimulation, there were a higher number and proportion of pCREB-IR expressing cells after electrical stimulation of afferents (RM-ANOVA  $F_{(3,19)} = 63$ ,  $p < 0.0001$ ,  $n = 3$  animals, Figure 7.17 and  $F_{(3,19)} = 65$ ,  $p < 0.0001$ ,  $n = 3$  animals, Figure 7.18, respectively).

## **Electrical stimulated afferents activated cells that received contacts from CGRP<sup>+</sup>SP<sup>-</sup> afferents**

After electrical stimulation of the attached dorsal root, pCREB-IR cells were restricted to lamina I-III of the dorsal horn (Figure 7.10A). In lamina I pCREB cells

were in close proximity to the CGRP-IR terminals. There were no pCREB-IR cells in lamina IV/V, and hence the CGRP-IR terminals of lamina IV/V were not in close association with any pCREB-IR cells.

Confocal analysis (Figure 7.10B) and 3D reconstructions (Figure 7.10C) revealed that pCREB-IR cells of lamina I did make contacts with CGRP-IR and SP-IR terminals. pCREB-IR cells received contacts from CGRP<sup>+</sup>SP<sup>+</sup> terminals, CGRP<sup>+</sup>SP<sup>-</sup> terminals and CGRP<sup>-</sup>SP<sup>+</sup> terminals. 76% (237/313) of cells had contacts from CGRP<sup>+</sup>SP<sup>-</sup> terminals, 58% (183/313) from CGRP<sup>+</sup>SP<sup>+</sup> terminals, 52% (164/313) from CGRP<sup>-</sup>SP<sup>+</sup> terminals, and 17% made no contacts. A higher proportion of cells had CGRP<sup>+</sup>SP<sup>-</sup> contacts than cells that had no such contacts (ANOVA  $F_{(3,11)} = 8$ ,  $p = 0.01$ ,  $n = 3$  animals, Figure 7.20)

Many of these cells received contacts from multiple classes of terminals. 32% (101/321 cells) of pCREB-IR cells in lamina I had contacts from all three classes of peptidergic terminals (CGRP<sup>+</sup>SP<sup>-</sup>, CGRP<sup>+</sup>SP<sup>+</sup> and CGRP<sup>-</sup>SP<sup>+</sup>); 24% (75/313) had contacts from CGRP<sup>+</sup>SP<sup>-</sup> and CGRP<sup>+</sup>SP<sup>+</sup> terminals; 15% (47/313) from CGRP<sup>+</sup>SP<sup>-</sup> and CGRP<sup>-</sup>SP<sup>+</sup> terminals; and 19% (59/313) had no contacts from any sources. No other combination differed significantly from zero (ANOVA:  $F_{(3,23)} = 5$   $p = 0.006$ ,  $n = 3$  animals, Figure 7.21)

There was a lower proportion of cells with CGRP<sup>-</sup>SP<sup>+</sup> contacts and a higher proportion of cells with no contacts after electrical stimulation compared to after capsaicin stimulation (ANOVA  $F_{(3,23)} = 39$ ,  $p < 0.0001$ ,  $n = 6$  animals). There was no difference in the proportion of cells that received contacts from CGRP<sup>+</sup>SP<sup>-</sup> or CGRP<sup>+</sup>SP<sup>+</sup> terminals between capsaicin or electrical stimulation.

## 7.4 Discussion

---

In previous chapters we have demonstrated a prominent population of CGRP<sup>+</sup>SP<sup>-</sup> neurons in DRG, with central terminals in the dorsal horn, and peripheral fibres in skin and muscle tissue. In DRG, CGRP<sup>+</sup>SP<sup>-</sup> neurons were distinct from CGRP<sup>+</sup>SP<sup>+</sup> neurons based on their larger cell bodies, positive NF200-IR and lack of TRPV1 expression. CGRP<sup>+</sup>SP<sup>-</sup> neurons were also differentiated from CGRP<sup>+</sup>SP<sup>+</sup> neurons by deep lamina IV/V projections in the dorsal horn that were close to projections of classical mechanoreceptors. All of these data has so far suggested that CGRP<sup>+</sup>SP<sup>-</sup> neurons might be a subset of myelinated A $\beta$ -fibre neurons. In this current chapter we hoped to determine their function through investigation of the relationship of the central terminals of CGRP<sup>+</sup>SP<sup>-</sup> neurons with nociceptive dorsal horn neurons.

### **Capsaicin stimulation induced pERK and pCREB expression in dorsal horn neurons**

We can be certain that pERK/pCREB is directly induced in postsynaptic neurons by neurotransmitters released from primary afferents in response to capsaicin for two reasons. Firstly, the TRPV1 receptor is not expressed by intrinsic dorsal horn neurons and is restricted to the primary afferent terminals of the dorsal horn (Szallasi *et al.*, 1995; Caterina *et al.*, 1997; Tominaga *et al.*, 1998). Consequently, capsaicin is not able to directly activate the dorsal horn neurons and induce pERK/pCREB. Secondly, pERK/pCREB is not induced by polysynaptic activation after capsaicin application (Kawasaki *et al.*, 2004). Hence, the pERK-IR in the spinal cord is induced by monosynaptic input from capsaicin sensitive primary afferent fibres.

Bath application of capsaicin onto the spinal cord slices *in vitro* increased the expression of pERK and pCREB in neurons of lamina I/II in spinal dorsal horn, consistent with previous pERK studies of intraplantar capsaicin injection *in vivo* (Ji *et al.*, 1999; Kawasaki *et al.*, 2004) and bath application *in vitro* (Kawasaki *et al.*, 2004), and pCREB studies with intraplantar capsaicin injection *in vivo* (Wu *et al.*, 2002) and bath application *in vitro* (Kawasaki *et al.*, 2004). Capsaicin stimulation induced a higher number of neurons expressing pCREB than pERK. pCREB expression can induced by protein kinases other than pERK (Lonze & Ginty, 2002). While pERK neurons are nociceptive specific (Gao & Ji, 2009) the higher number of

pCREB expressing dorsal horn neurons suggest that pERK-IR does not represent the entire population nociceptive dorsal horn neurons activated by capsaicin sensitive afferents.

## **Electrical stimulation of dorsal roots induced pERK and pCREB expression in dorsal horn neurons**

The electrical stimulation parameters used in this study were adapted from similar studies by Kawasaki and colleagues (2004). Kawasaki and colleagues (2004) stimulated attached dorsal roots with three trains of 50 pulses (each pulse was 90 V for 0.5 ms) at 50Hz for one second with 10-second inter-train interval. This stimulation intensity also activated A $\beta$  and A $\delta$  fibers. However pERK is not activated by A $\beta$ -fiber stimulation and only very slightly by A $\delta$ -fiber stimulation (Ji *et al.*, 1999).

Consistent with Kawasaki and colleagues (2004) electrical stimulation of the attached dorsal root increased the expression of pERK in lamina I/II and pCREB in neurons of lamina I-III of the spinal dorsal horn. Electrical stimulation induced a higher expression of pCREB than pERK. CREB is not just restricted to neurons expressing ERK (Lonze & Ginty, 2002). As the stimulation intensity used also activated A $\beta$  and A $\delta$  fibers (Kawasaki *et al.*, 2004) the higher expression of pCREB may have been induced in dorsal horn neurons receiving input from A $\beta$  and/or A $\delta$  fibers.

Together, the results of capsaicin and electrical stimulation of afferents suggest that, in agreement with previous studies (Ji *et al.*, 1999; Kawasaki *et al.*, 2004), pERK is a suitable neuronal activation marker for of a subset of nociceptive dorsal horn neurons, whereas pCREB appears to be a neuronal activation marker a more widespread neuronal population that includes the subset of nociceptive neurons that express pERK.

## **pERK expressing dorsal horn cells activated by capsaicin sensitive nociceptors received convergent contacts from CGRP<sup>+</sup>SP<sup>-</sup> afferents in lamina I**

Consistent with previous studies (Ji *et al.*, 1999; Kawasaki *et al.*, 2004) neurons expressing pERK were mainly present in lamina I/II of the dorsal horn after capsaicin stimulation. As we have previously demonstrated, lamina I/II also contains primary afferent CGRP<sup>+</sup>SP<sup>-</sup> terminals. Together with our multiple labelling immunohistochemistry and high-resolution confocal microscopy we were able to visualize individual pERK expressing cells and examine their close associations or contacts with primary afferent CGRP<sup>+</sup>SP<sup>-</sup> terminals.

In this study we have defined the term contacts as CGRP- and SP-IR that colocalised with the pERK/pCREB cells within the limits of our high-resolution confocal microscope. As confocal stacks were taken at a resolution of 8.234 pixels/ $\mu\text{m}$ , our definition of contacts was pixels that were within 0.25  $\mu\text{m}$  of one another. However, to determine physical contacts or functioning synapses we would have to use electron microscopy as the size of closed synapses are a distance of 20-50 nm between the pre- and post-synaptic neuron (Zoli *et al.*, 1999). Our group has previously compared IR contacts identified with confocal microscopy and determined, using electron microscopy, that the majority of IR contacts were synapses (Murphy *et al.*, 1998; Gibbins *et al.*, 2003). Hence, our definition of contact is able to determine a direct synapse between an IR terminal and an activated pERK/pCREB cell.

In this study the capsaicin-induced pERK expressing cells of lamina I received contacts from multiple classes of terminals, either: pERK expressing cells that received contacts from CGRP<sup>+</sup>SP<sup>+</sup>, CGRP<sup>+</sup>SP<sup>-</sup> and CGRP<sup>-</sup>SP<sup>+</sup> terminals, and pERK expressing cells that received contacts from CGRP<sup>+</sup>SP<sup>-</sup> and CGRP<sup>-</sup>SP<sup>+</sup> terminals. As we have discussed in previous chapters, CGRP in the dorsal horn is entirely of primary afferent origin and hence both the CGRP<sup>+</sup>SP<sup>+</sup> and CGRP<sup>+</sup>SP<sup>-</sup> terminals are terminals of primary afferent neurons. However, as we have demonstrated in previous chapters CGRP<sup>-</sup>SP<sup>+</sup> terminals are terminals of intrinsic dorsal horn neurons.

CGRP<sup>+</sup>SP<sup>+</sup> afferent terminals most likely induced pERK expression in the cells that received input from CGRP<sup>+</sup>SP<sup>+</sup>, CGRP<sup>+</sup>SP<sup>-</sup> and CGRP<sup>-</sup>SP<sup>+</sup> terminals in lamina I. As

we have previously demonstrated, the CGRP<sup>+</sup>SP<sup>+</sup> neurons contained the capsaicin sensitive receptor TRPV1 and had central terminations in lamina I. This suggests that the capsaicin sensitive CGRP<sup>+</sup>SP<sup>+</sup> afferents were stimulated by the application of capsaicin, releasing CGRP and SP, which activated the postsynaptic dorsal horn neurons in contact with the CGRP<sup>+</sup>SP<sup>+</sup> terminals and induced pERK expression. SP activates the dorsal horn neurons (Salter & Henry, 1991) and CGRP potentiates the effects of SP (Seybold, 2009).

CGRP<sup>-</sup>SP<sup>+</sup> fibres were most likely from descending supraspinal pathways. SP is also found in intrinsic spinal neurons, including supraspinal structures involved in descending pain control (Beitz, 1982; Skirboll *et al.*, 1983). Many PAG neurons possess neurokinin 1 (NK1) receptors, the primary binding site for substance P (Commons & Valentino, 2002). Both pro- and anti-nociceptive properties have been attributed to the NK1 receptor (Holden *et al.*, 2002; Suzuki *et al.*, 2002). Therefore these descending CGRP<sup>-</sup>SP<sup>+</sup> fibres most likely facilitated or inhibited dorsal horn neurons that were activated by the primary afferent CGRP<sup>+</sup>SP<sup>+</sup> or CGRP<sup>+</sup>SP<sup>-</sup> neurons.

CGRP<sup>+</sup>SP<sup>-</sup> afferent terminals most likely induced pERK expression in the cells that received input from CGRP<sup>+</sup>SP<sup>-</sup> and CGRP<sup>-</sup>SP<sup>+</sup> terminals in lamina I. As we have already discussed, the CGRP<sup>-</sup>SP<sup>+</sup> terminals are not of primary afferent origin. Consequently, these terminals would lack the TRPV1 receptor and not be activated by capsaicin (Szallasi *et al.*, 1995; Caterina *et al.*, 1997; Tominaga *et al.*, 1998). We have previously demonstrated that some CGRP<sup>+</sup>SP<sup>-</sup> neurons contained the TRPV1 receptor. This suggests that CGRP<sup>+</sup>SP<sup>-</sup>TRPV1<sup>+</sup> afferents were stimulated by the application of capsaicin and induced pERK expression in the postsynaptic dorsal horn neurons in contact with CGRP<sup>+</sup>SP<sup>+</sup> terminals. However, CGRP alone has minimal effects on the excitability of neurons in the dorsal horn (Miletic & Tan, 1988) and instead, functions to enhance SP-mediated transmission (Seybold, 2009). Hence it is unlikely that CGRP alone was capable of inducing pERK expression in the postsynaptic dorsal horn neurons.

CGRP<sup>+</sup>SP<sup>-</sup> afferent terminals may have induced pERK expression in dorsal horn neurons through the use of another neurotransmitter, which activated the postsynaptic dorsal horn neurons. However, we have already shown that CGRP<sup>+</sup>SP<sup>-</sup>

neurons lack the vesicular glutamate transporters (VGluT1 and VGluT2) and lack the protein machinery to utilize glutamate (Morris *et al.*, 2005). In previous chapters we demonstrated that CGRP<sup>+</sup>SP<sup>-</sup> neurons did express VIP. VIP shares similar features to CGRP and is considered a neuromodulator. Under normal conditions VIP increases the excitability of neurons in nociceptive circuits (Cridland & Henry, 1988). This excitatory action of VIP is markedly increased in injury models to a level comparable to the effect that SP has on nociceptive neurons (Wiesenfeld-Hallin, Xu, Håkanson, *et al.*, 1990). Hence VIP may be able to replace the role of CGRP and SP following nerve injury.

CGRP<sup>+</sup>SP<sup>-</sup> afferent terminals may have had a modulatory role in the capsaicin-induced expression of pERK in the dorsal horn neurons. We have demonstrated that almost all pERK expressing neurons had contacts from multiple classes of IR terminals, and that most of these included CGRP<sup>+</sup>SP<sup>-</sup> terminals. We already know that CGRP enhances the excitability of neurons receiving nociceptive inputs (Biella *et al.*, 1991; Seybold *et al.*, 2003; Sun *et al.*, 2004; Bird *et al.*, 2006). So rather than CGRP enhancing the effects of a neurotransmitter from within the same afferent terminal, CGRP may have been released and enhanced the excitability of the pERK expressing dorsal horn neuron. Another convergent afferent terminal on the single postsynaptic dorsal horn neuron may have activated this neurons and induced pERK expression.

### **pCREB expressing dorsal horn cells activated by electrically stimulated afferents nociceptors received contacts from CGRP<sup>+</sup>SP<sup>-</sup> afferents in lamina I**

Electrical stimulation of the attached dorsal root induced pERK expression in neurons of lamina I. Unfortunately, there was also an increase in extra-somatic pERK-IR that was too intense and widespread and so pERK-IR cells were not easily identified. Hence, their relationship to CGRP<sup>+</sup>SP<sup>-</sup> terminals could not be investigated. Fortunately, there was no extra-somatic pCREB after electrical stimulation of the attached dorsal root, and so we were able to identify individual pCREB expressing neurons.

Consistent with previous studies (Ji *et al.*, 1999; Kawasaki *et al.*, 2004) neurons expressing pCREB were mainly present in lamina I-III of the dorsal horn after

electrical stimulation of the attached dorsal root. Much like pERK neurons after capsaicin stimulation, the pCREB neurons were in close proximity with the primary afferent CGRP<sup>+</sup>SP<sup>-</sup> terminals of lamina I. We were able to visualize individual pCREB expressing cells and examine their contacts with these primary afferent CGRP<sup>+</sup>SP<sup>-</sup> terminals using our multiple labelling immunohistochemistry and high-resolution confocal microscopy.

In lamina I, the electrically induced pCREB expressing neurons shared many similarities with capsaicin-induced pERK expressing neurons. Most pCREB expressing neurons had contacts from multiple classes of terminals, either: pCREB expressing cells that received contacts from CGRP<sup>+</sup>SP<sup>+</sup>, CGRP<sup>+</sup>SP<sup>-</sup> and CGRP<sup>-</sup>SP<sup>+</sup> terminals; CGRP<sup>+</sup>SP<sup>+</sup> and CGRP<sup>+</sup>SP<sup>-</sup> terminals; CGRP<sup>+</sup>SP<sup>-</sup> and CGRP<sup>-</sup>SP<sup>+</sup> terminals; or received no contact from any of the classes of terminals.

It is likely that most of the electrically induced pCREB neurons of lamina I that received contacts from CGRP<sup>+</sup>SP<sup>+</sup> terminals were the same neurons capsaicin induced pERK that received contacts from CGRP<sup>+</sup>SP<sup>+</sup> terminals. As we have previously mentioned, all CGRP<sup>+</sup>SP<sup>+</sup> neurons contained TRPV1 and studies have shown that many CREB expressing neurons also express ERK (Ji *et al.*, 1999; Kawasaki *et al.*, 2004). Conversely, CREB is not just restricted to neurons expressing ERK (Lonze & Ginty, 2002) and so electrical stimulation induced pCREB expression in neurons in lamina I that had no contacts from CGRP or SP terminals.

## **CGRP<sup>+</sup>SP<sup>-</sup> afferents in lamina IV/V must have a different function to lamina I**

Our previous chapters have demonstrated that CGRP<sup>+</sup>SP<sup>-</sup> neurons are a distinct subpopulation of CGRP neurons that are separate from CGRP<sup>+</sup>SP<sup>+</sup> neurons. While all CGRP<sup>+</sup>SP<sup>+</sup> neurons contained the capsaicin receptor TRPV1, only small CGRP<sup>+</sup>SP<sup>-</sup> neurons contained TRPV1. Not only did these large CGRP<sup>+</sup>SP<sup>-</sup> neurons lack TRPV1, they also expressed the marker for large myelinated neurons: NF200. We have also demonstrated that CGRP<sup>+</sup>SP<sup>-</sup> neurons had dual central terminations in lamina I and in close association with classical mechanoreceptors of lamina IV/V. These observations suggest that CGRP<sup>+</sup>SP<sup>-</sup> neurons may be able to be further

subdivided into capsaicin sensitive nociceptors with central terminals in lamina I, and capsaicin insensitive mechanoreceptors with central terminals in lamina IV/V.

These current results demonstrate that the CGRP<sup>+</sup>SP<sup>-</sup> afferents of lamina I were functionally different from the CGRP<sup>+</sup>SP<sup>-</sup> afferents of lamina IV/V. In lamina I, both capsaicin stimulation and electrical stimulation induced pERK/pCREB expression in dorsal horn neurons that received contacts from CGRP<sup>+</sup>SP<sup>-</sup> afferent terminals. However, both capsaicin stimulation and electrical stimulation failed to induce pERK/pCREB expression in dorsal horn neurons of lamina IV/V. Dorsal horn neurons of lamina IV/V do express ERK/CREB (Kawasaki *et al.*, 2004; Song *et al.*, 2005) and hence pERK/pCREB should be induced in these neurons given the correct stimulus. This suggests that the CGRP<sup>+</sup>SP<sup>-</sup> afferents of lamina IV/V were not activated by capsaicin stimulation or electrical stimulation and are hence functionally different from CGRP<sup>+</sup>SP<sup>-</sup> afferents of lamina I.

Lamina IV/V contains both low threshold and wide dynamic range mechanoreceptive neurons and receive mostly non-nociceptive input, and respond to light mechanical touch (Cervero *et al.*, 1988). Nevertheless, wide dynamic range neurons responding to noxious stimuli are also present in lamina IV (Mendell & Wall, 1965; Hillman & Wall, 1969; Light & Durkovic, 1984). CGRP increases the excitability of wide dynamic range neurons in the deep dorsal horn and probably contributes to mechanical hyperalgesia (Yu *et al.*, 2002; Sun *et al.*, 2004).

In summary, some smaller CGRP<sup>+</sup>SP<sup>-</sup> neurons contain TRPV1 and have terminals in lamina I that appear to have a modulatory role in nociceptive circuits. Larger CGRP<sup>+</sup>SP<sup>-</sup> neurons lack TRPV1 and have terminals in lamina IV/V that appear to have a different function to the CGRP<sup>+</sup>SP<sup>-</sup> terminals of lamina I. While this function was not determined it is likely that it is involved in mechanical hyperalgesia. Once again, these observations are consistent with the prediction that larger some CGRP<sup>+</sup>SP<sup>-</sup> neurons are high-threshold mechanoreceptors with a predominant (although not exclusive) projection to wide dynamic range neurons in the deep dorsal horn.



## **7.5 Figures**

---

**Figure 7.1: MAPK/ERK signal transduction pathways**

The MAPK pathway begins with an extracellular ligand binding to a receptor that activates Ras and causes a kinase cascade. Ras activates RAF kinase (or MAP3K: MAPK kinase kinase). RAF kinase then phosphorylates MEK (or MAP2K: MAPK kinase) which in-turn phosphorylates the last of the kinases: ERK (or MAPK). Upon activation, phosphorylated ERK (pERK) activates several transcriptional factors including CREB (Ji & Rupp, 1997). CREB is phosphorylated and translocated into the nucleus where it regulates the transcription of several genes including *c-fos* (Sheng & Greenberg, 1990). The transcription of the *c-fos* gene produces the c-Fos protein, which itself is a transcription factor that further regulates gene transcription. Figure taken from Ji and Woolf (2001). In this project the phosphorylation of ERK and CREB are used as markers of neuronal activation (highlighted by a red circle).

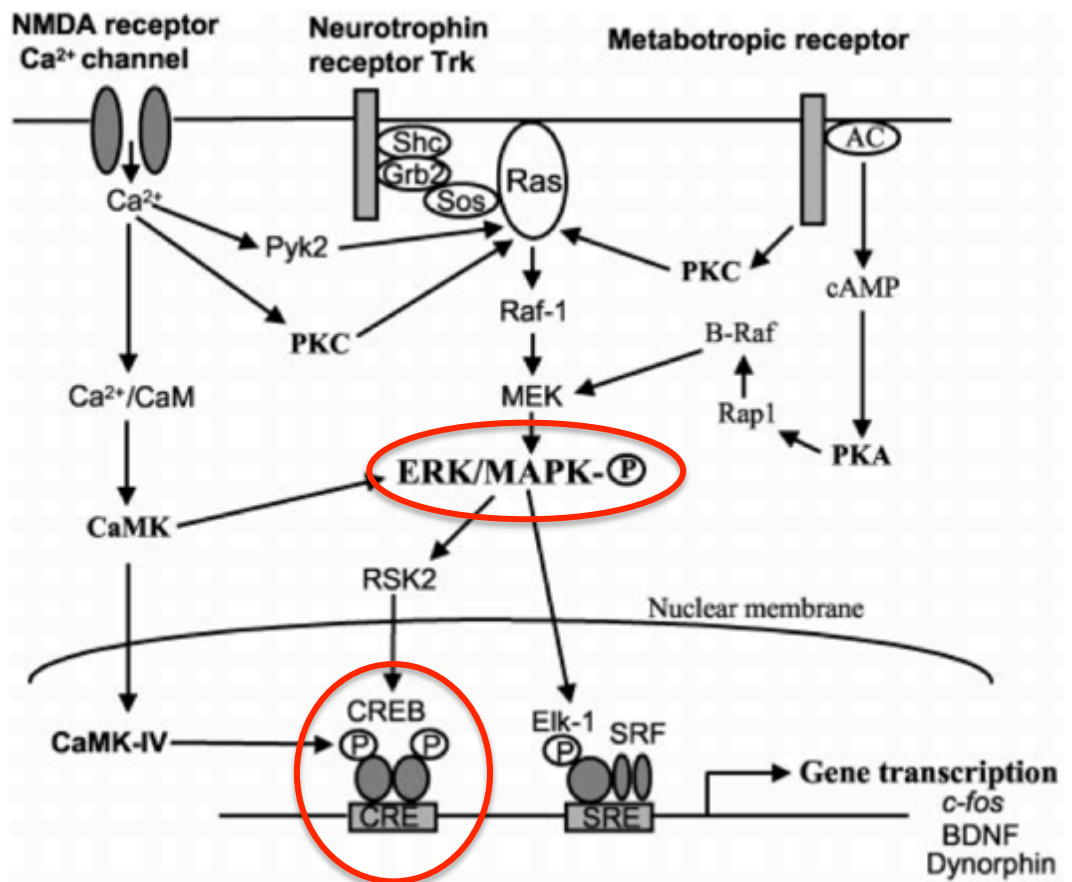


**Figure 7.2: pERK levels in lumbar dorsal horn after stimulation with capsaicin**

Widefield fluorescence microscopy of mouse lumbar dorsal horn labelled for phosphorylated extracellular-signal-regulated kinase (pERK) showing pERK-immunoreactivity (pERK-IR) in dorsal horn cells after stimulation with  $10^{-6}$  M of capsaicin (A), or no stimulation in vehicle (B) and saline controls (C). After capsaicin stimulation (A), pERK-IR cells were observed in the superficial lamina (lamina I/II). Very few dorsal horn cells were observed with pERK-IR in the dorsal horn of vehicle (B) and saline controls (C). Scale bar = 60  $\mu$ m in C (applies to A-C)

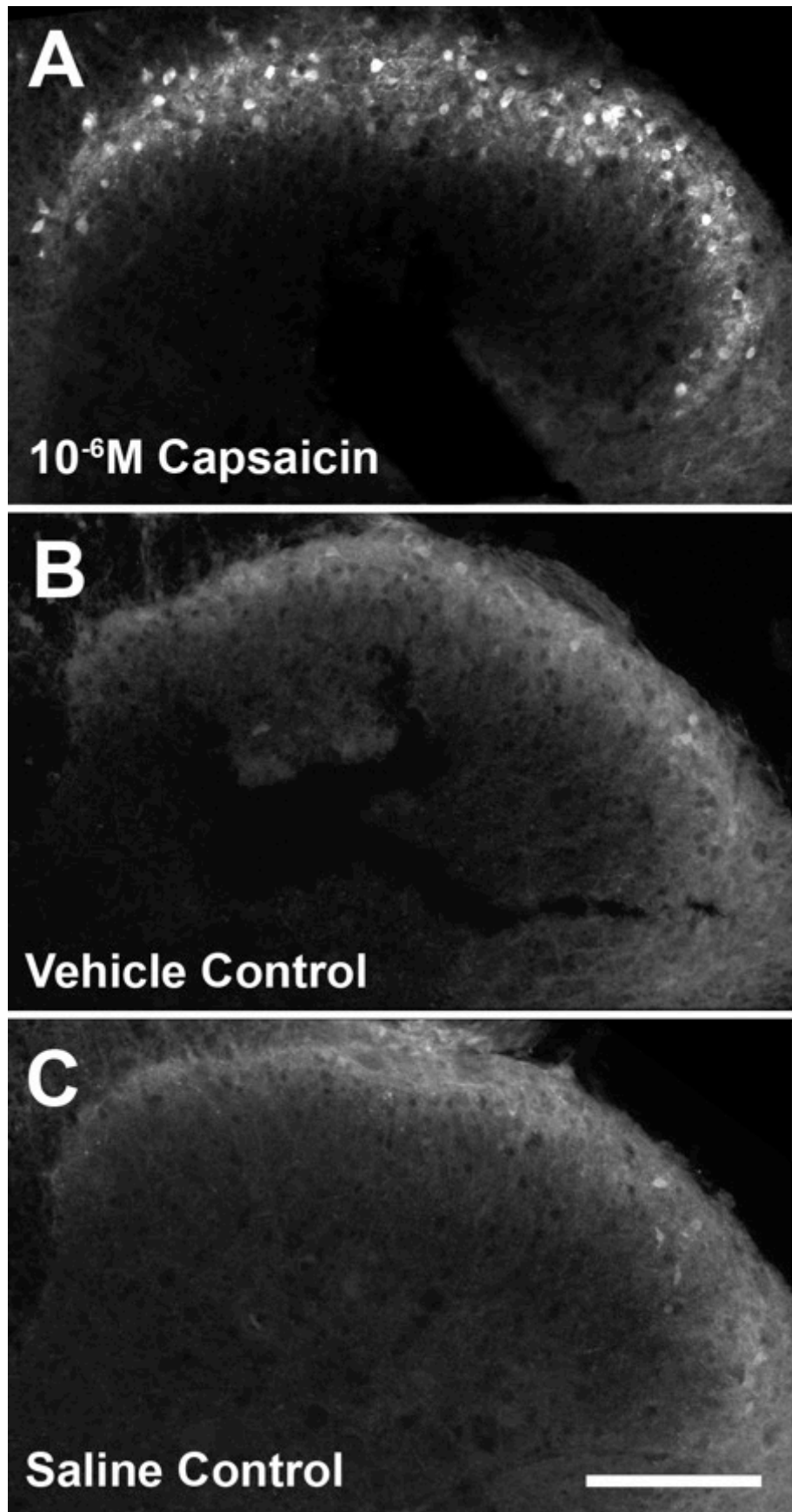


**Figure 7.3: Number of pERK-IR cells in the dorsal horn after stimulation with capsaicin**

Histogram (data displayed as mean±SEM) depicting the number of cells showing phosphorylated extracellular-signal-regulated kinase-immunoreactivity (pERK-IR) in dorsal horn cells after stimulation with 10<sup>-6</sup> M of capsaicin, or no stimulation in vehicle and saline controls. The number of dorsal horn cells expressing pERK-IR after capsaicin stimulation was higher than vehicle and saline controls (ANOVA:  $F_{(2,4)} = 68$ ,  $p < 0.0001$ ,  $n = 6$  animals).

**Figure 7.4: Proportion of pERK-IR cells in the dorsal horn after stimulation with capsaicin**

Histogram (data displayed as mean±SEM) depicting the proportion of dorsal horn cells (visualised with DAPI staining) showing phosphorylated extracellular-signal-regulated kinase-immunoreactivity (pERK-IR) in dorsal horn cells after stimulation with 10<sup>-6</sup> M of capsaicin or no stimulation in vehicle and saline controls. The proportion of dorsal horn cells expressing pERK-IR after capsaicin stimulation was higher than vehicle and saline controls (ANOVA:  $F_{(2,4)} = 73$ ,  $p < 0.0001$ ,  $n = 5$  animals).

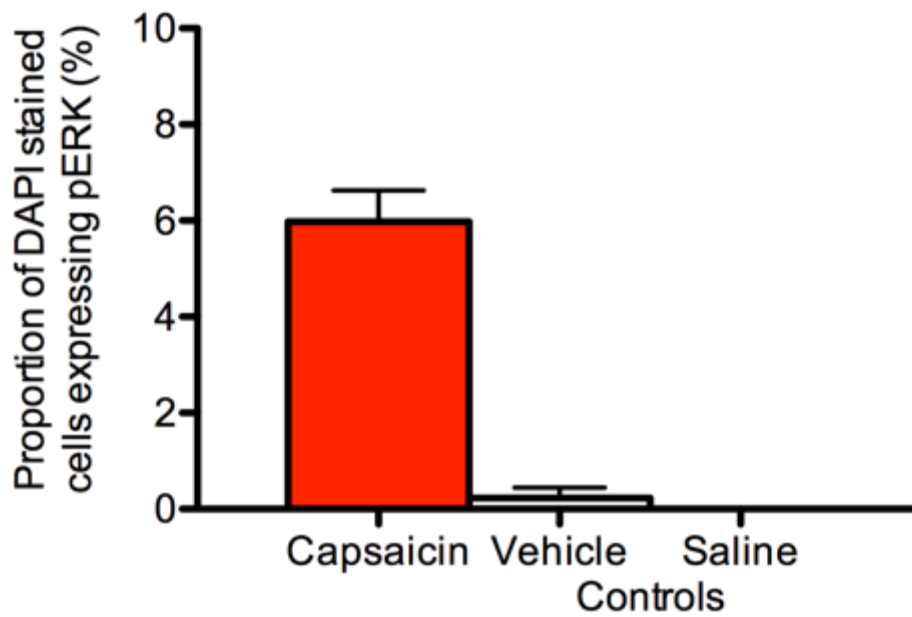
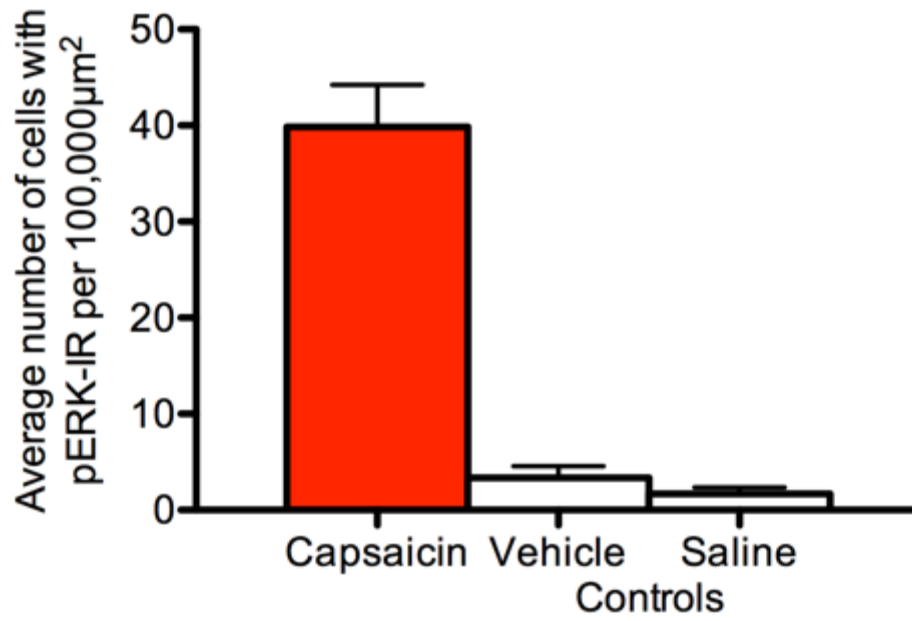


**Figure 7.5: pCREB-IR levels in lumbar dorsal horn after stimulation with capsaicin**

Widefield fluorescence microscopy of mouse lumbar dorsal horn labelled for phosphorylated cAMP response element-binding protein (pCREB) showing pCREB-immunoreactivity (pCREB-IR) in dorsal horn cells after stimulation with  $10^{-6}$  M capsaicin (A), or no stimulation in vehicle (B) and saline controls (C). After capsaicin stimulation (A), pCREB-IR cells were observed in the superficial lamina (lamina I/II). Very few dorsal horn cells were observed with pCREB-IR in the dorsal horn of vehicle (B) and saline controls (C). Scale bar = 60  $\mu$ m in C (applies to A-C)

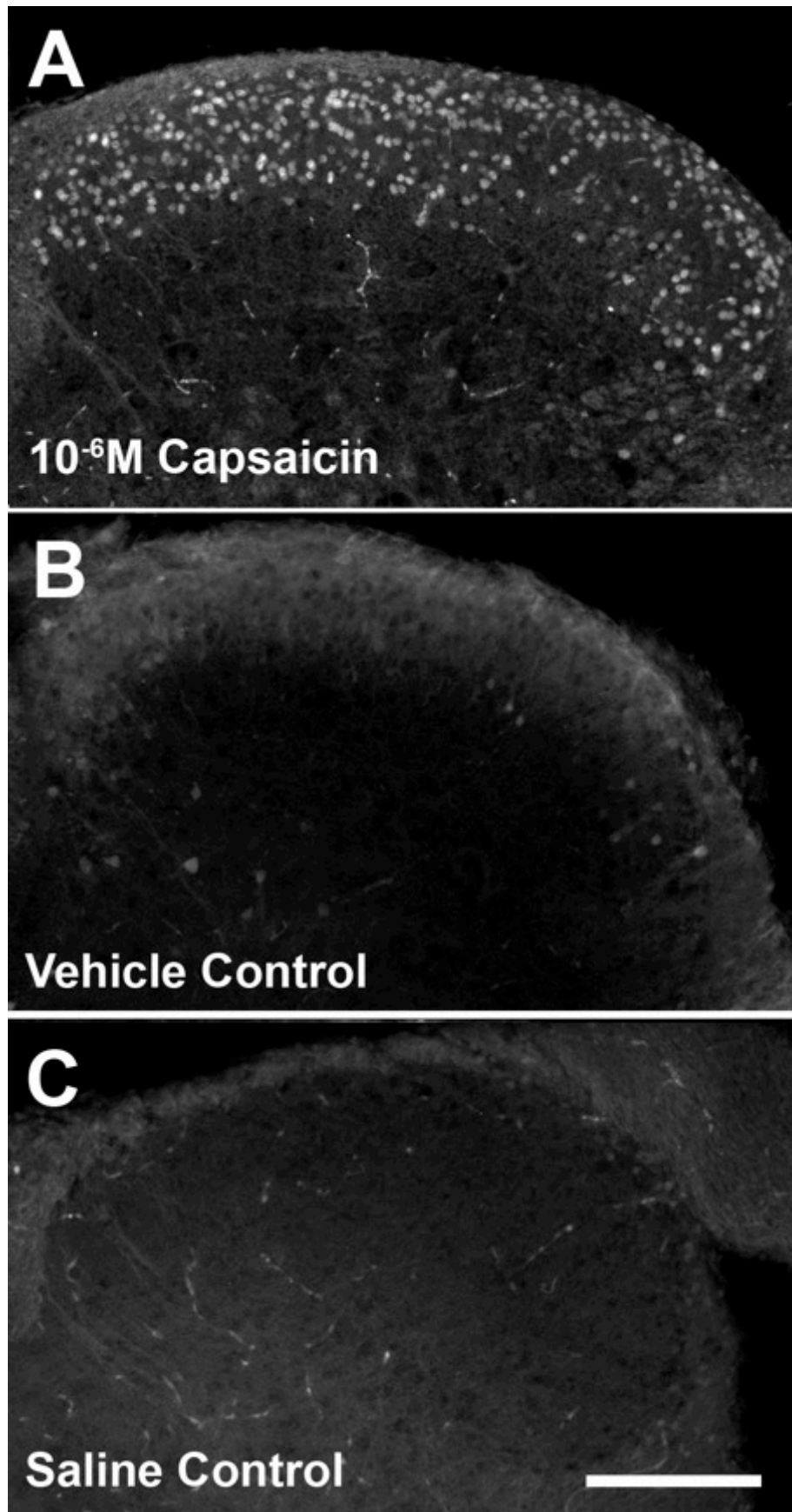


**Figure 7.6: Number of pCREB-IR cells in the dorsal horn after stimulation with capsaicin**

Histogram (data displayed as mean±SEM) depicting the number of cells showing phosphorylated cAMP response element-binding protein-immunoreactivity (pCREB-IR) in dorsal horn cells after stimulation with 10<sup>-6</sup> M of capsaicin, or no stimulation in vehicle and saline controls. The number of dorsal horn cells expressing pCREB-IR after capsaicin stimulation was higher than vehicle and saline controls (ANOVA:  $F_{(2,4)} = 57$ ,  $p < 0.0001$ ,  $n = 5$  animals).

**Figure 7.7: Proportion of pCREB-IR cells in the dorsal horn after stimulation with capsaicin**

Histogram (data displayed as mean±SEM) depicting the proportion of dorsal horn cells (visualised with DAPI staining) showing phosphorylated cAMP response element-binding protein -immunoreactivity (pCREB-IR) in dorsal horn cells after stimulation with 10<sup>-6</sup> M of capsaicin, or no stimulation in vehicle and saline controls. The proportion of dorsal horn cells expressing pCREB-IR after capsaicin stimulation was higher than vehicle and saline controls (RM-ANOVA:  $F_{(2,4)} = 67$ ,  $p < 0.0001$ ,  $n = 5$  animals).

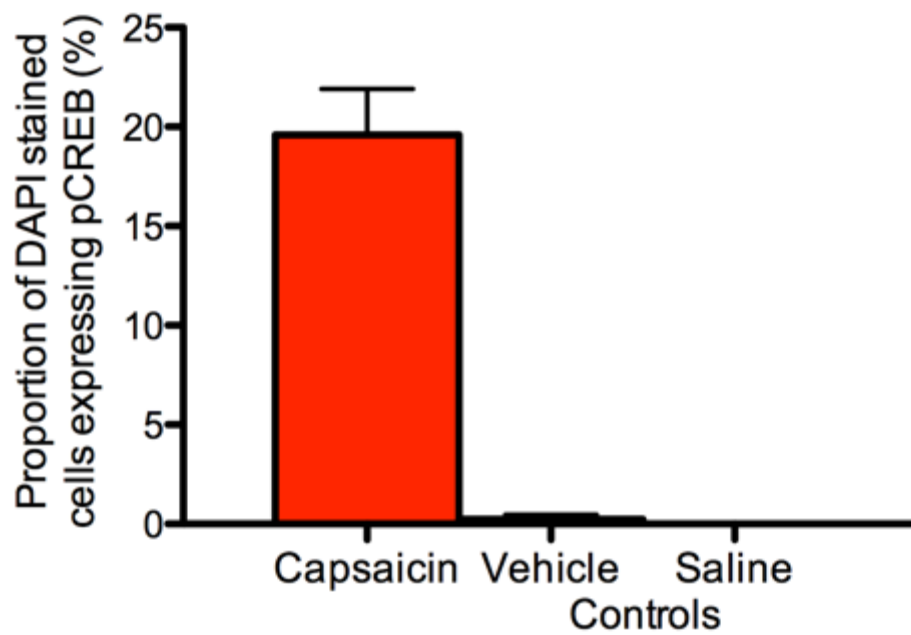
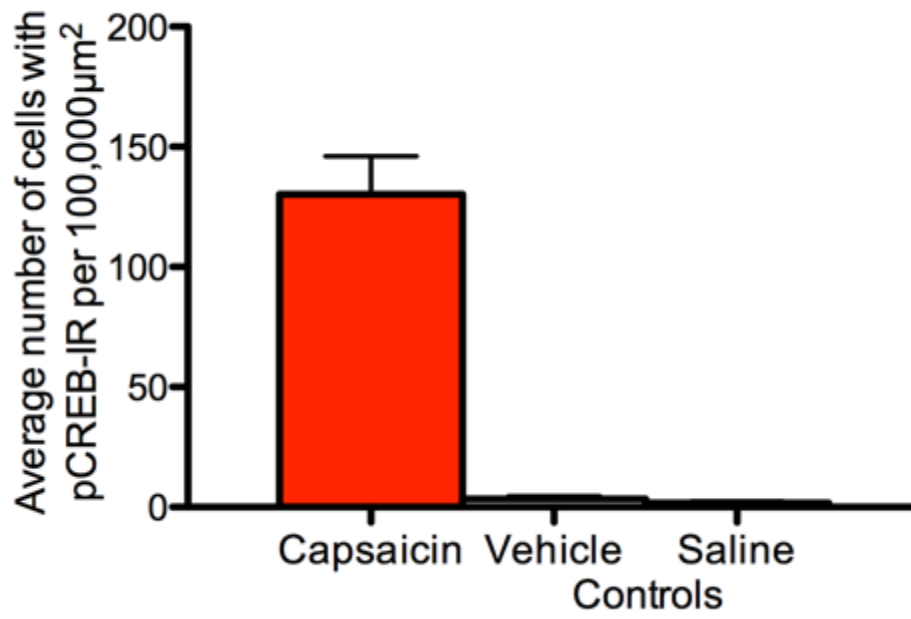


**Figure 7.8: Number of pERK-IR cells compared to the number of pCREB-IR cells in the dorsal horn after stimulation with capsaicin**

Histogram (data displayed as mean±SEM) depicting the number of cells showing phosphorylated extracellular-signal-regulated kinase-immunoreactivity (pERK-IR) compared to the number of cells showing phosphorylated cAMP response element-binding protein-IR (pCREB-IR) in dorsal horn cells after stimulation with 10<sup>-6</sup> M of capsaicin, or no stimulation in vehicle and saline controls. The number of dorsal horn cells expressing pCREB-IR was higher than the number of cells expressing pERK-IR after capsaicin stimulation (RM-ANOVA:  $F_{(1,9)} = 29$ ,  $p = 0.0007$ ,  $n = 5$  animals). There was no difference in the number of pERK-IR cells compared to the number pCREB-IR cells in the vehicle and saline controls.

**Figure 7.9: Proportion of pERK-IR cells compared to the proportion of pCREB-IR cells in the dorsal horn after stimulation with capsaicin**

Histogram (data displayed as mean±SEM) depicting the proportion of dorsal horn cells (visualised with DAPI staining) phosphorylated extracellular-signal-regulated kinase-immunoreactivity (pERK-IR) compared to the proportion of dorsal horn cells showing phosphorylated cAMP response element-binding protein-IR (pCREB-IR) in dorsal horn cells after stimulation with 10<sup>-6</sup> M of capsaicin, or no stimulation in vehicle and saline controls. The proportion of dorsal horn cells expressing pCREB-IR after capsaicin stimulation was higher than vehicle and saline controls (RM-ANOVA:  $F_{(1,9)} = 32$ ,  $p = 0.0005$ ,  $n = 5$  animals). There was no difference in the proportion of pERK-IR cells compared to the proportion of pCREB-IR cells in the vehicle and saline controls.

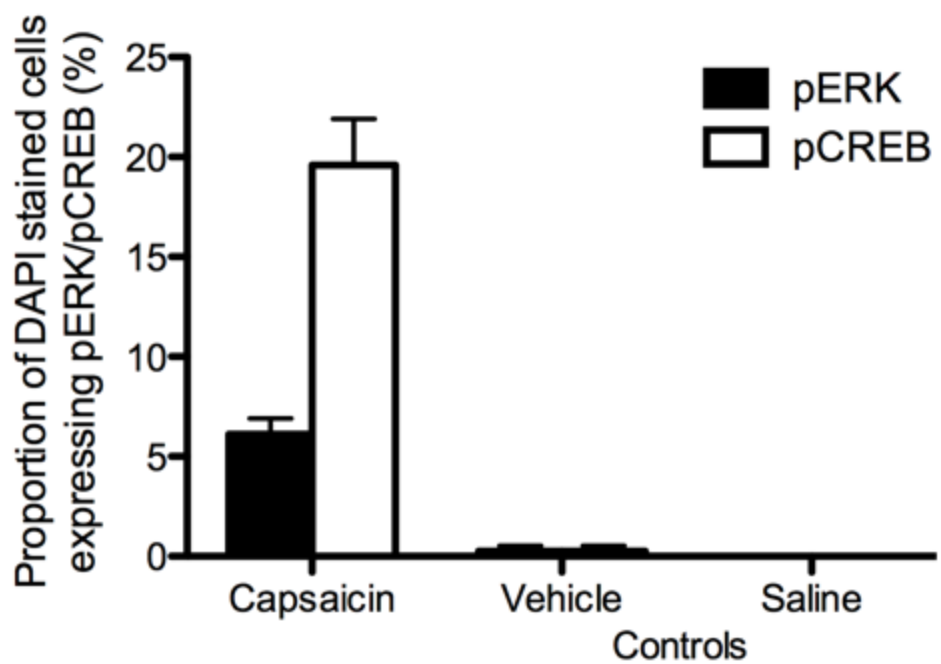
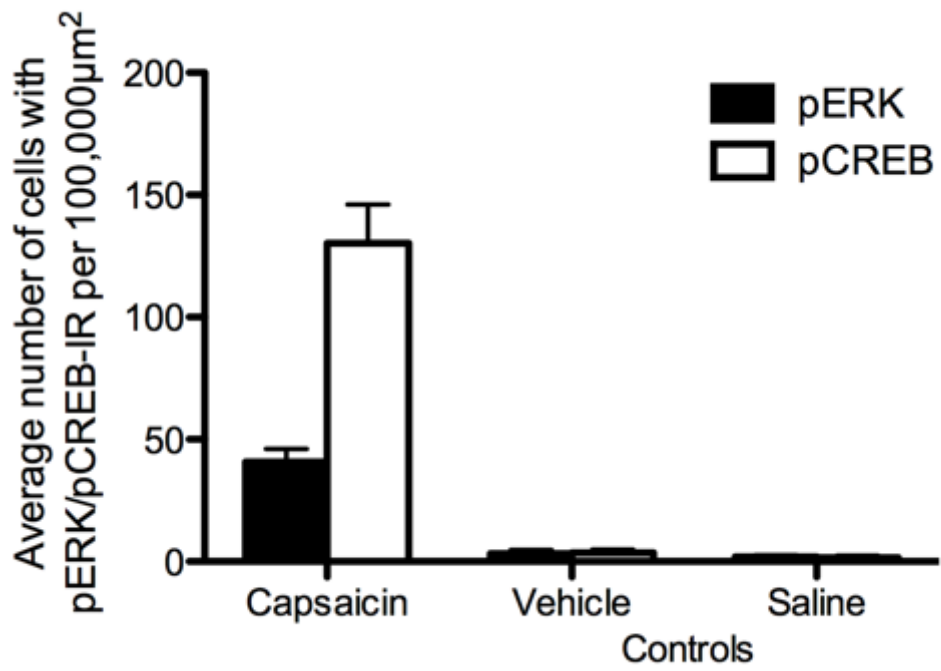


**Figure 7.10: CGRP<sup>-</sup>IR terminals and pERK-IR cells in lumbar dorsal horn stimulated with capsaicin**

**A:** Widefield fluorescence microscopy of mouse lumbar dorsal horn after stimulation with  $10^{-6}$  M of capsaicin, triple labelled for phosphorylated extracellular-signal-regulated kinase (pERK; white), calcitonin gene-related peptide (CGRP; red) and substance P (SP; green) showing overlap of CGRP-IR terminals and pERK-IR cells in lamina I. **B:** Confocal Z-stacks (21 steps of  $0.5 \mu\text{m}$ , total depth  $10.5 \mu\text{m}$ ) showing a pERK-IR cell (white) surrounded by CGRP terminals that contained SP (CGRP<sup>+</sup>SP<sup>+</sup>; yellow), CGRP terminals that lacked SP (CGRP<sup>+</sup>SP<sup>-</sup>; red) and SP terminals that lacked SP (CGRP<sup>-</sup>SP<sup>+</sup>; green) in lateral lamina I. **C:** 3D reconstruction of the confocal Z-stack showing pERK-IR cells (white) and only the CGRP-IR and SP-IR terminals in contact with pERK-IR cells. It shows that this particular pERK-IR cell had CGRP<sup>+</sup>SP<sup>+</sup> (yellow), CGRP<sup>+</sup>SP<sup>-</sup> (red) and CGRP<sup>-</sup>SP<sup>+</sup> (green) terminal contacts. Scale bar =  $60 \mu\text{m}$  in A and =  $20 \mu\text{m}$  in B (applies to B-C).

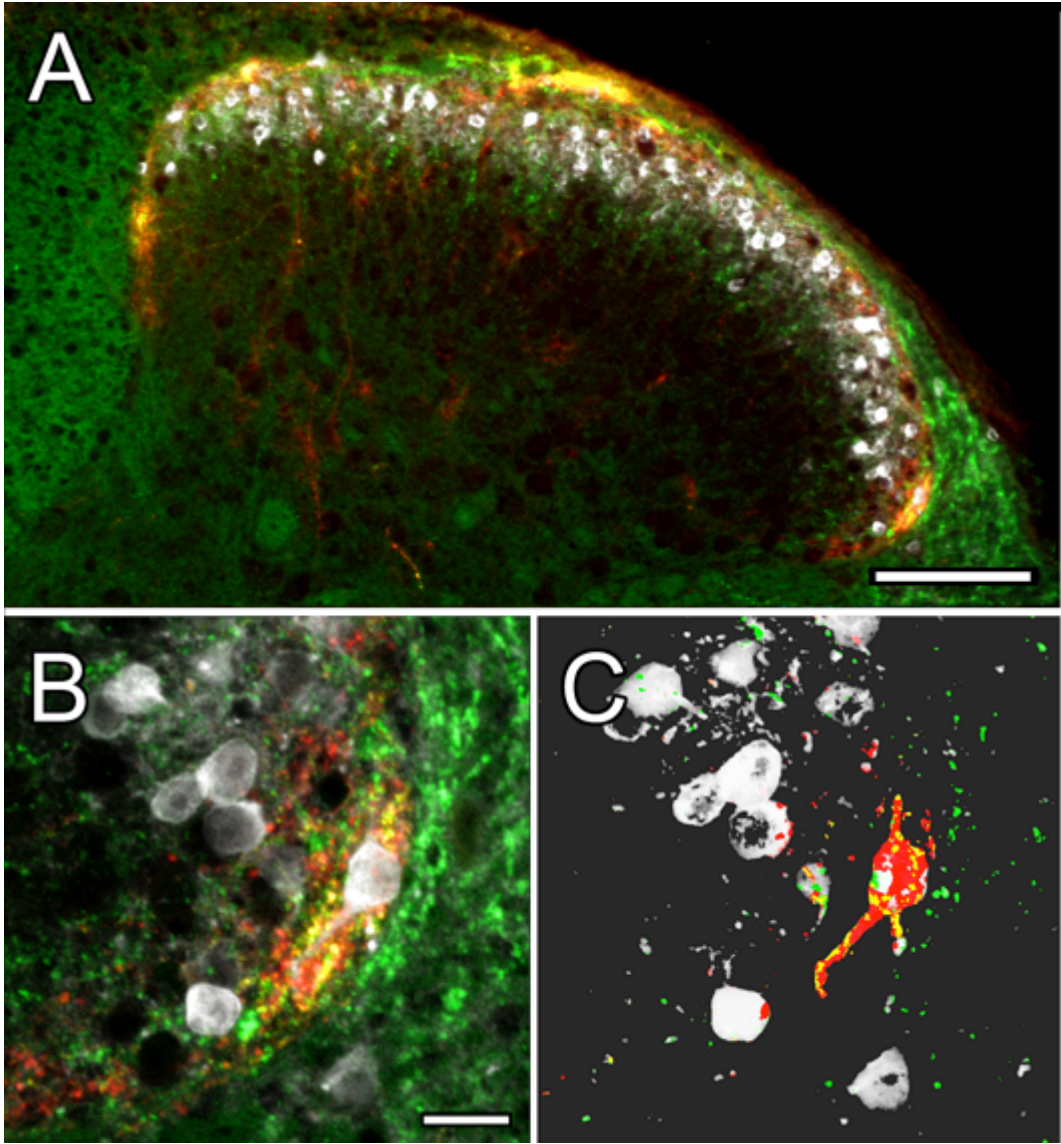


**Figure 7.11: Peptidergic contacts onto pERK-IR cells in lumbar dorsal horn after stimulation with capsaicin**

Histogram (data displayed as mean±SEM) depicting the proportion of cells expressing phosphorylated extracellular-signal-regulated kinase (pERK) that received contacts from calcitonin gene-related peptide-immunoreactive (CGRP) terminals that lacked substance P (SP; CGRP<sup>+</sup>SP<sup>-</sup>; red), CGRP terminals that contained SP (CGRP<sup>+</sup>SP<sup>+</sup>; yellow), SP terminals that lacked CGRP (CGRP<sup>-</sup>SP<sup>+</sup>) or no contacts after capsaicin stimulation. While most cells received peptidergic contacts, a higher proportion of pERK-IR cells had CGRP<sup>+</sup>SP<sup>-</sup> and CGRP<sup>-</sup>SP<sup>+</sup> contacts than CGRP<sup>+</sup>SP<sup>+</sup> contacts and a higher proportion of cells had CGRP<sup>+</sup>SP<sup>+</sup> contacts than cells that had no contacts (RM-ANOVA  $F_{(3,11)} = 54$ ,  $p < 0.0001$ ,  $n = 3$  animals).

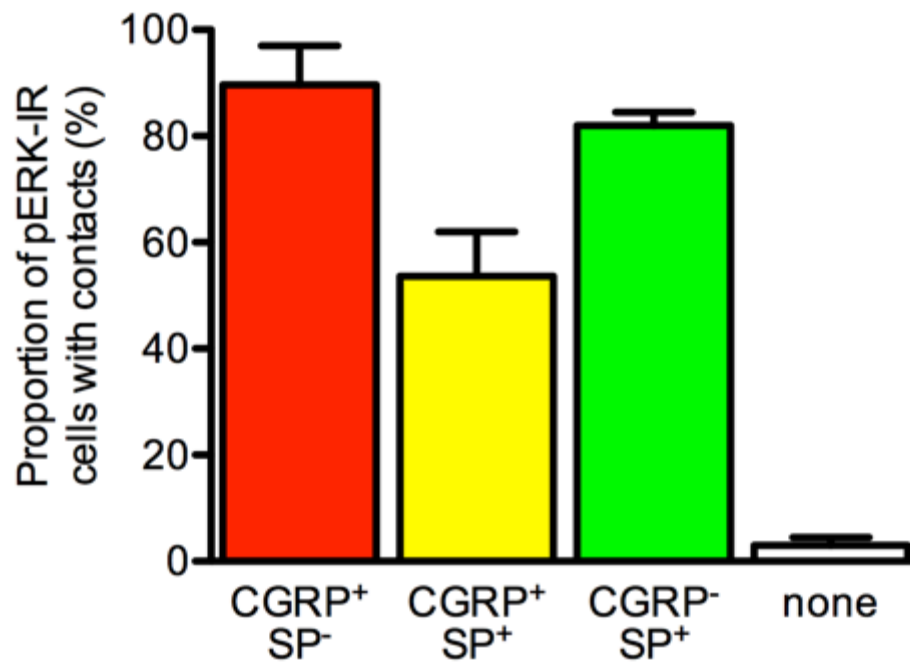


**Figure 7.12: Multiple peptidergic contacts onto pERK-IR cells in lumbar dorsal horn after stimulation with capsaicin**

Histogram (data displayed as mean±SEM) depicting the proportion of cells expressing phosphorylated extracellular-signal-regulated kinase (pERK) that received multiple contacts from calcitonin gene-related peptide-immunoreactive (CGRP) terminals that lacked substance P (SP; CGRP<sup>+</sup>SP<sup>-</sup>; red), CGRP terminals that contained SP (CGRP<sup>+</sup>SP<sup>+</sup>; yellow), SP terminals that lacked CGRP (CGRP<sup>-</sup>SP<sup>+</sup>) or no contacts (white) after capsaicin stimulation. 47% of pERK-IR cells in lamina I had contacts from all three classes of peptidergic terminals (CGRP<sup>+</sup>SP<sup>-</sup>, CGRP<sup>+</sup>SP<sup>+</sup> and CGRP<sup>-</sup>SP<sup>+</sup>); and 28% had contacts from CGRP<sup>+</sup>SP<sup>-</sup> and CGRP<sup>-</sup>SP<sup>+</sup> terminals. No other combination differed significantly from zero (RM-ANOVA  $F_{(7,23)} = 16$   $p < 0.0001$ ,  $n = 3$  animals)

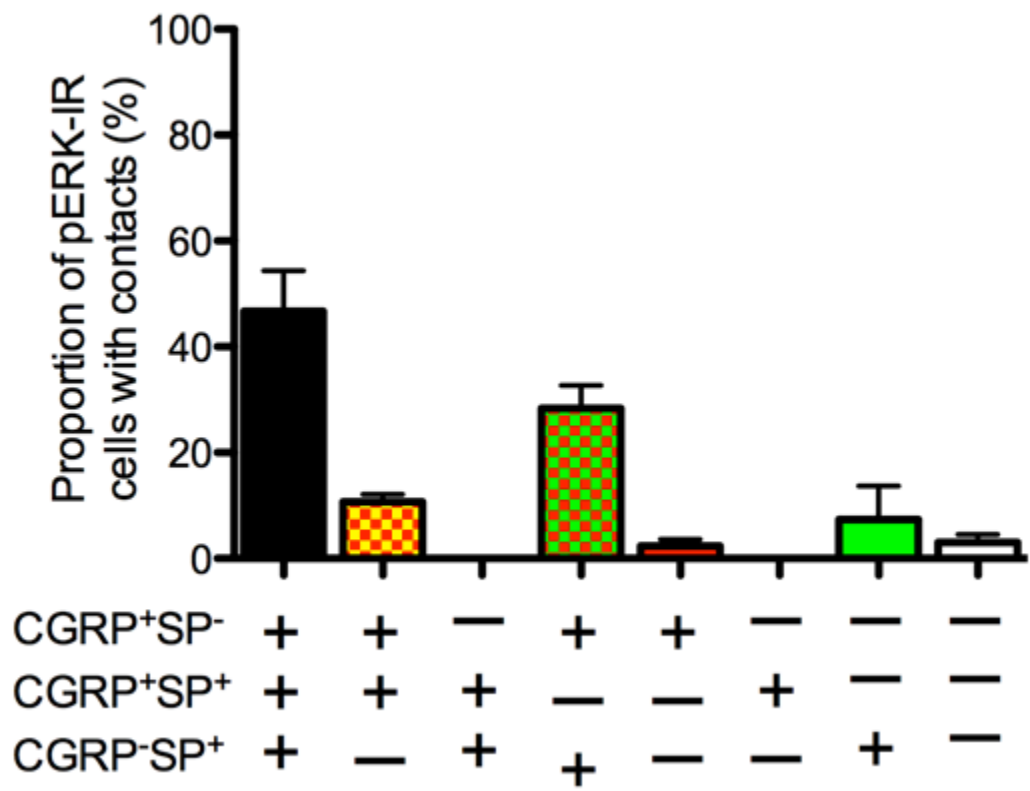


**Figure 7.13: pERK levels in lumbar dorsal horn after electrical stimulation of afferent fibres**

Widefield fluorescence microscopy of mouse lumbar dorsal horn labelled for phosphorylated extracellular-signal-regulated kinase (pERK) showing pERK-immunoreactivity (pERK-IR) in dorsal horn cells after electrical stimulation of the attached dorsal root (three trains of fifty 90V pulses at 50 Hz with 10 sec interval; A), or after no stimulation (control; B). Very few dorsal horn cells were observed with pERK-IR in the dorsal horn of control (B). After electrical stimulation of afferent fibres (A), pERK-IR cells were observed in the lamina I-III, however individual cells were not easily distinguished. Scale bar = 60  $\mu$ m in C (applies to A-C)

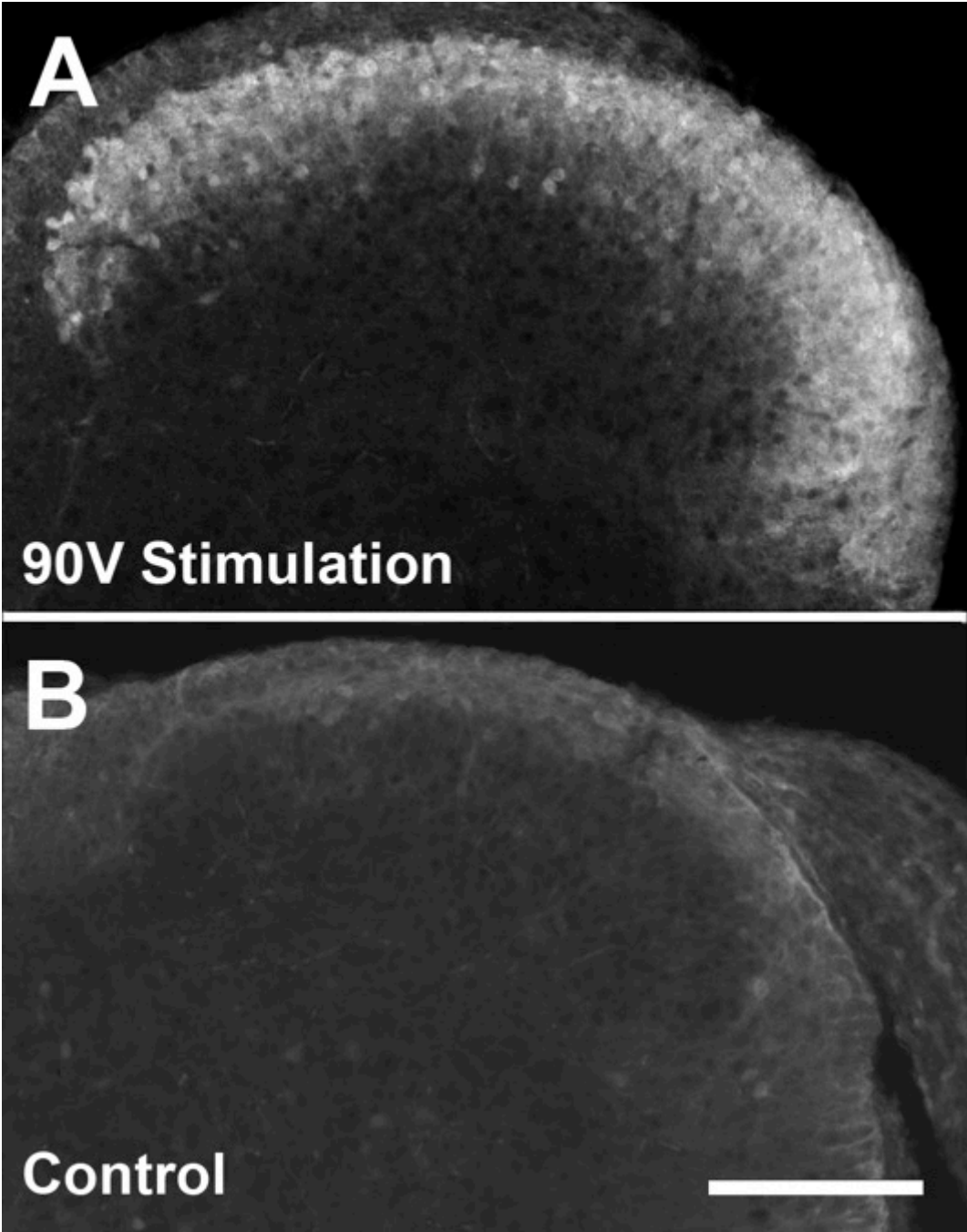


**Figure 7.14: pCREB levels in lumbar dorsal horn after electrical stimulation of afferent fibres**

Widefield fluorescence microscopy of mouse lumbar dorsal horn labelled for phosphorylated cAMP response element-binding protein (pCREB) showing pCREB-immunoreactivity (pCREB-IR) in dorsal horn cells after Electrical stimulation (three trains of fifty 90V pulses at 50 Hz with 10 sec interval) of the attached dorsal root at (A), or after no stimulation (control; B). Very few dorsal horn cells were observed with pCREB-IR in the dorsal horn of control (B). After electrical stimulation of afferent fibres (A), pCREB-IR cells were observed in the lamina I-III. Scale bar = 60  $\mu$ m in B (applies to A-B)

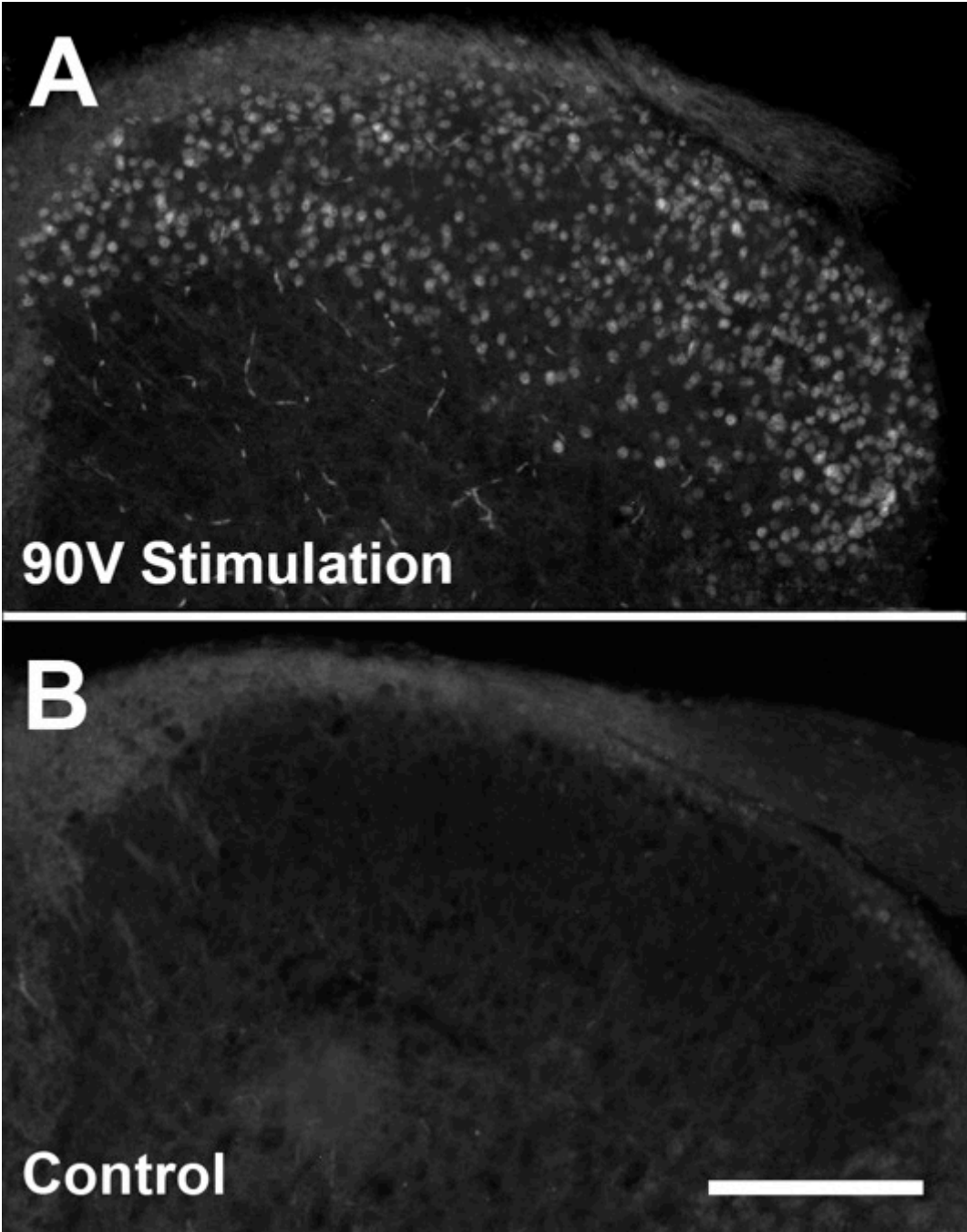


**Figure 7.15: Number of pCREB-IR cells in the dorsal horn after electrical stimulation of afferent fibres**

Histogram (data displayed as mean±SEM) depicting the number of cells showing phosphorylated cAMP response element-binding protein-immunoreactivity (pCREB-IR) in dorsal horn cells after electrical stimulation (three trains of fifty 90V pulses at 50 Hz with 10 sec interval) of the attached dorsal root or no stimulation (control). The number of dorsal horn cells expressing pCREB-IR after electrical stimulation of afferent fibres was higher than control (paired *t*-test:  $t_{(4)} = 11$ ,  $p = 0.0003$ ,  $n = 5$  animals).

**Figure 7.16: Proportion of pCREB-IR cells in the dorsal horn after electrical stimulation of afferent fibres**

Histogram (data displayed as mean±SEM) depicting the proportion of dorsal horn cells (visualised with DAPI staining) showing phosphorylated cAMP response element-binding protein-immunoreactivity (pCREB-IR) in dorsal horn after electrical stimulation (three trains of fifty 90V pulses at 50 Hz with 10 sec interval) of the attached dorsal root or no stimulation (control). The proportion of dorsal horn cells expressing pCREB-IR after electrical stimulation of afferent fibres was higher than controls (paired *t*-test:  $t_{(4)} = 12$ ,  $p = 0.0002$ ,  $n = 5$  animals).

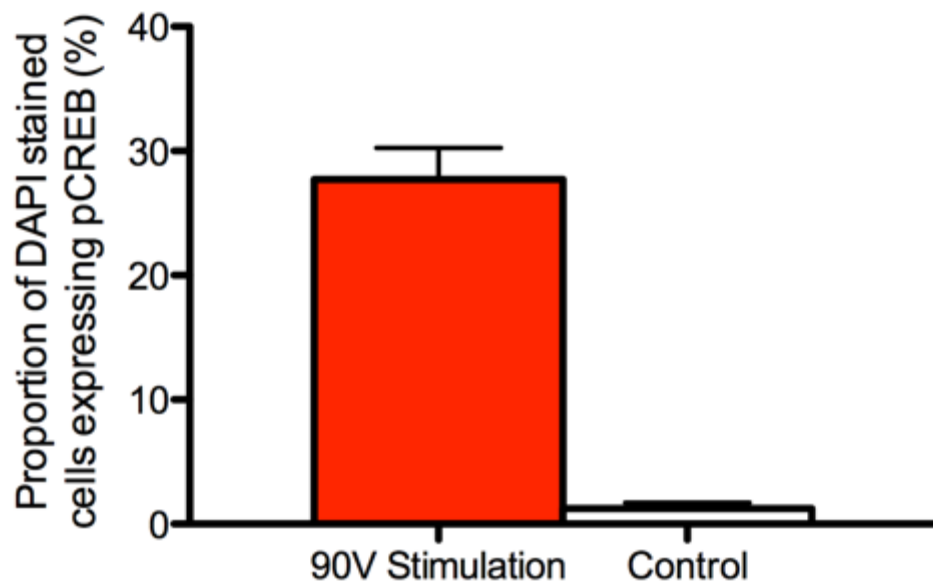
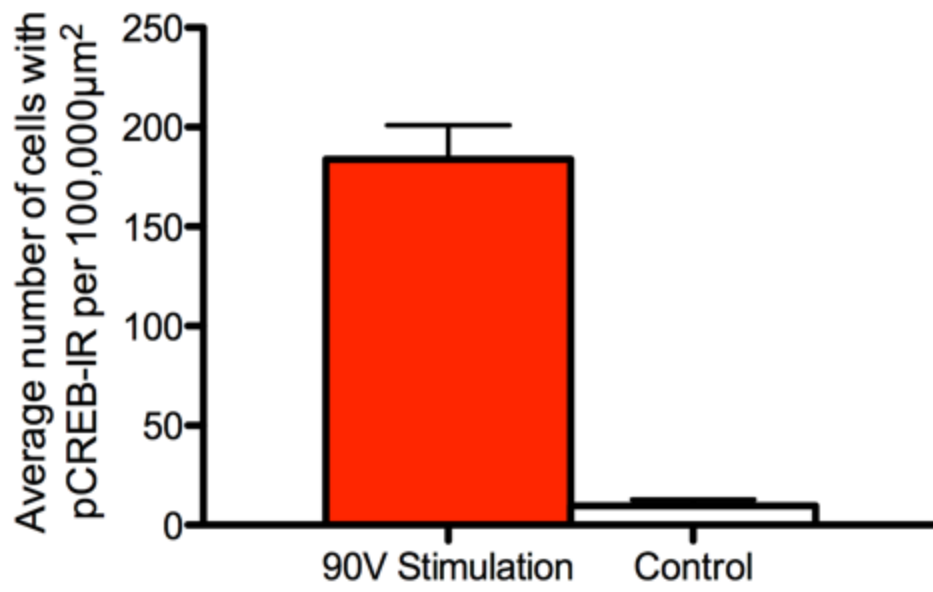


**Figure 7.17: Number of pCREB-IR cells in the dorsal horn after electrical stimulation of afferent fibres compared to the number of pCREB-IR cells after capsaicin stimulation**

Histogram (data displayed as mean±SEM) depicting the number of cells showing phosphorylated cAMP response element-binding protein-immunoreactivity (pCREB-IR) in dorsal horn cells after electrical stimulation (three trains of fifty 90V pulses at 50 Hz with 10 sec interval) of the attached dorsal root compared to stimulation with 10<sup>-6</sup> M capsaicin. Both electrical stimulation of afferent fibres and stimulation with capsaicin increased the number of dorsal horn cells expressing pCREB-IR to levels higher than controls. Electrical stimulation of afferent fibres increased the number of dorsal horn cells expressing pCREB-IR higher than stimulation with capsaicin (RM-ANOVA:  $F_{(3,19)} = 63$   $p < 0.0001$ ,  $n = 10$  animals).

**Figure 7.18: Proportion of pCREB-IR cells in the dorsal horn after electrical stimulation of afferent fibres compared to the number of pCREB-IR cells after capsaicin stimulation**

Histogram (data displayed as mean±SEM) depicting the proportion of dorsal horn cells (visualised with DAPI staining) showing phosphorylated cAMP response element-binding protein -immunoreactivity (pCREB-IR) in dorsal horn after electrical stimulation (three trains of fifty 90V pulses at 50 Hz with 10 sec interval) of the attached dorsal root compared to stimulation with 10<sup>-6</sup> M capsaicin. Both electrical stimulation of afferent fibres and stimulation with capsaicin increased the proportion of dorsal horn cells expressing pCREB-IR to levels higher than controls. Electrical stimulation of afferent fibres increased the proportion of dorsal horn cells expressing pCREB-IR higher than stimulation with capsaicin (RM-ANOVA  $F_{(3,19)} = 65$   $p < 0.0001$ ,  $n = 10$  animals)

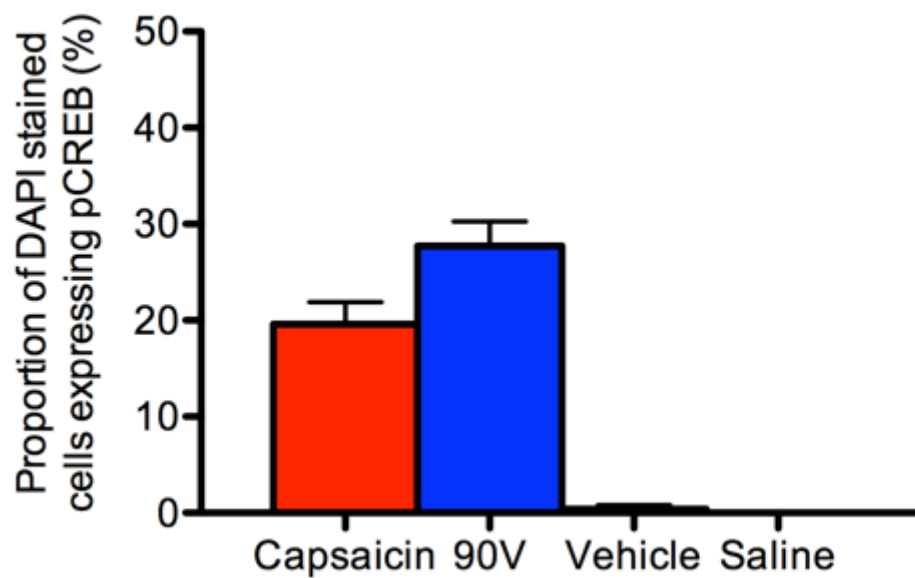
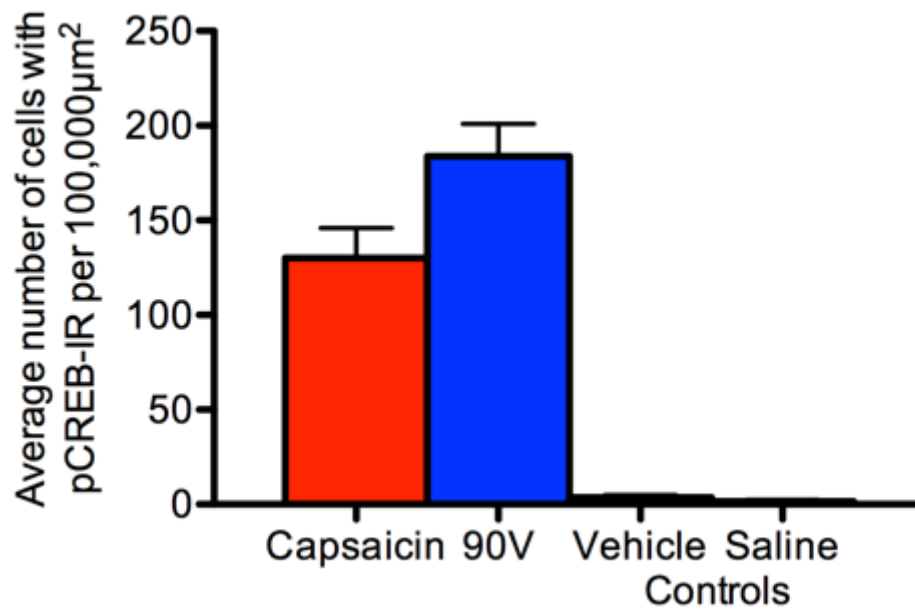


**Figure 7.19: CGRP<sup>-</sup>IR terminals and pCREB<sup>-</sup>IR cells in lumbar dorsal horn electrical stimulation of afferent fibres**

**A:** Widefield fluorescence microscopy of mouse lumbar dorsal horn, after electrical stimulation (three trains of fifty 90V pulses at 50 Hz with 10 sec interval) of the attached dorsal root, triple labelled for phosphorylated cAMP response element-binding protein-immunoreactivity (pCREB; white), calcitonin gene-related peptide (CGRP; red) and substance P (SP; green) showing overlap of CGRP-IR terminals and pCREB-IR cells in lamina I. **B:** Confocal Z-stacks (21 steps of 0.5  $\mu$  m, total depth 10.57  $\mu$  m) pCREB-IR cell surrounded by CGRP terminals that contained SP (CGRP<sup>+</sup>SP<sup>+</sup>; yellow), CGRP terminals that lacked SP (CGRP<sup>+</sup>SP<sup>-</sup>; red) and SP terminals that lacked SP (CGRP<sup>-</sup>SP<sup>+</sup>; green) in lateral lamina I of the dorsal horn. **C:** 3D reconstruction of the confocal Z-stack showing pCREB-IR cells (white) and only the CGRP-IR and SP-IR terminals in contact with pCREB-IR cells demonstrating cells with CGRP<sup>+</sup>SP<sup>+</sup> (yellow), CGRP<sup>+</sup>SP<sup>-</sup> (red) and CGRP<sup>-</sup>SP<sup>+</sup> (green) contacts. Scale bar = 60  $\mu$  m in A and = 10  $\mu$  m in B (applies to B-C).

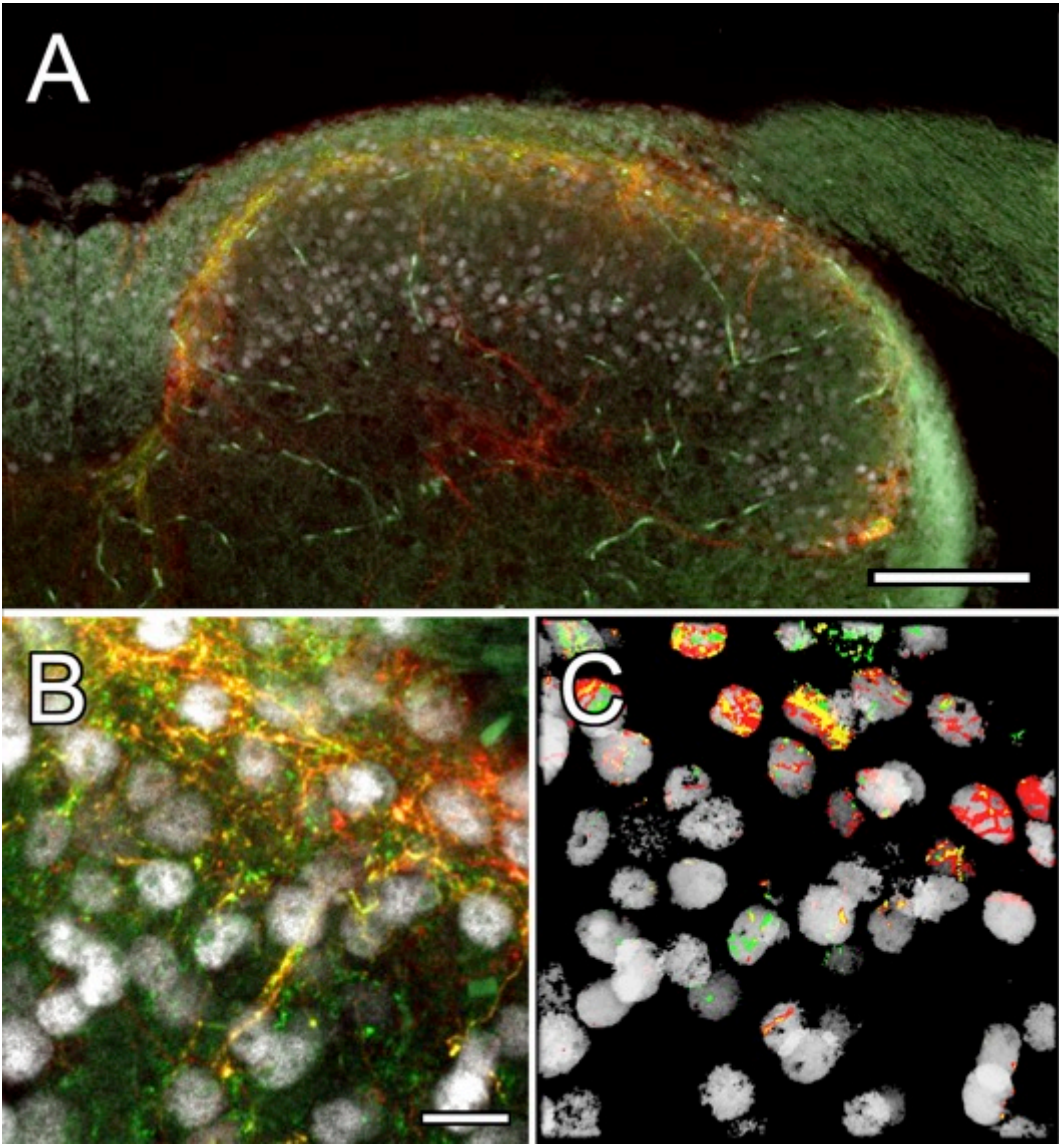


**Figure 7.20: Peptidergic contacts onto pCREB<sup>+</sup>IR cells in the dorsal horn after electrical stimulation of afferent fibres**

Histogram (data displayed as mean±SEM) depicting the proportion of cells expressing phosphorylated cAMP response element-binding protein (pCREB) induced by electrical stimulation (three trains of fifty 90V pulses at 50 Hz with 10 sec interval) of the attached dorsal root that received contacts from calcitonin gene-related peptide-immunoreactive (CGRP) terminals that lacked substance P (SP; CGRP<sup>+</sup>SP<sup>-</sup>; red), CGRP terminals that contained SP (CGRP<sup>+</sup>SP<sup>+</sup>; yellow), SP terminals that lacked CGRP (CGRP<sup>-</sup>SP<sup>+</sup>; green) or no contacts. Not all cells received peptidergic contacts, but a higher proportion of cells had CGRP<sup>+</sup>SP<sup>-</sup> contacts than cells that had no contacts (RM-ANOVA  $F_{(3,11)} = 8$ ,  $p = 0.01$ ,  $n = 3$  animals).

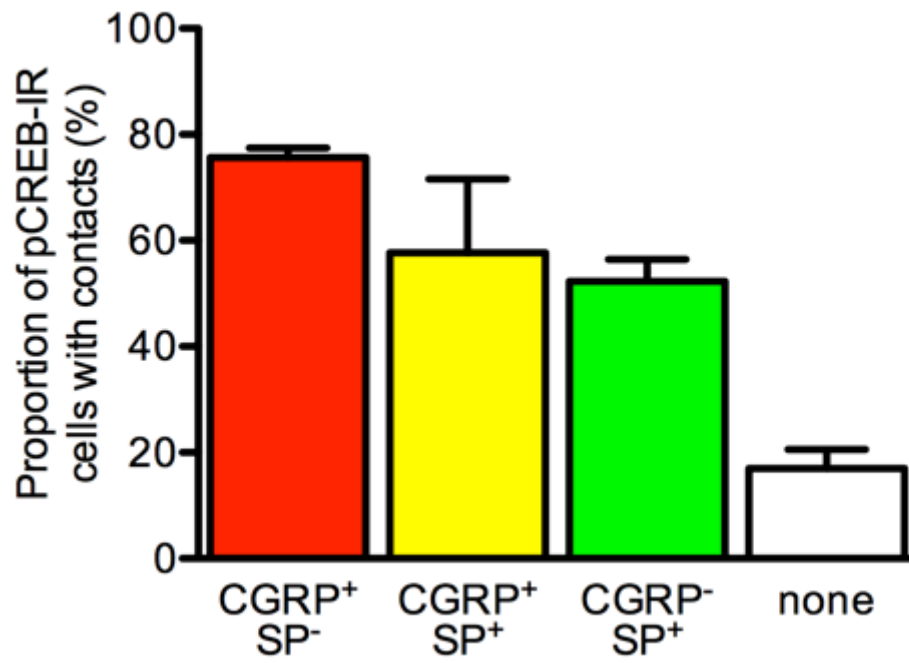
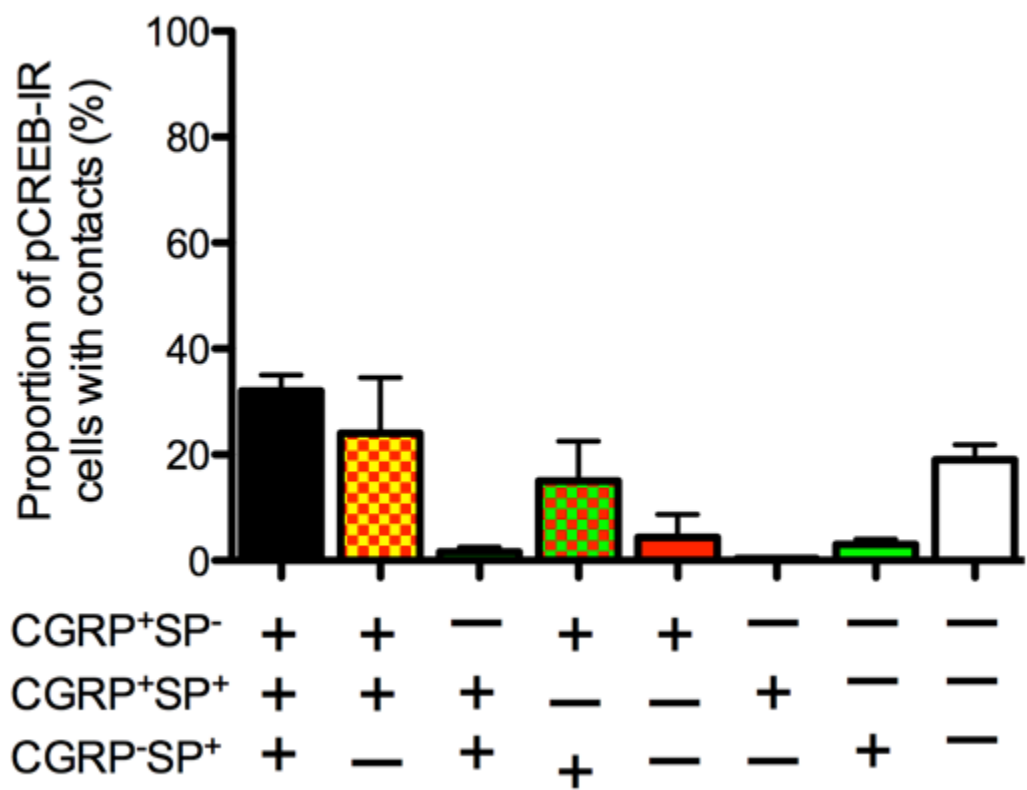


**Figure 7.21: Multiple peptidergic contacts onto electrically induced pCREB-IR neurons in the dorsal horn**

Histogram (data displayed as mean±SEM) depicting the proportion of cells expressing phosphorylated cAMP response element-binding protein (pCREB) induced by electrical stimulation (three trains of fifty 90V pulses at 50 Hz with 10 sec interval) of the attached dorsal root that received multiple contacts from calcitonin gene-related peptide-immunoreactive (CGRP) terminals that lacked substance P (SP; CGRP<sup>+</sup>SP<sup>-</sup>; red), CGRP terminals that contained SP (CGRP<sup>+</sup>SP<sup>+</sup>; yellow), SP terminals that lacked CGRP (CGRP<sup>-</sup>SP<sup>+</sup>) or no contacts. 32% of pCREB-IR cells in lamina I had contacts from all three classes of peptidergic terminals (CGRP<sup>+</sup>SP<sup>-</sup>, CGRP<sup>+</sup>SP<sup>+</sup> and CGRP<sup>-</sup>SP<sup>+</sup>); 24% had contacts from CGRP<sup>+</sup>SP<sup>-</sup> and CGRP<sup>+</sup>SP<sup>+</sup> terminals; 15% from CGRP<sup>+</sup>SP<sup>-</sup> and CGRP<sup>-</sup>SP<sup>+</sup> terminals; and 19% had no contacts from any sources. No other combination was significantly different from zero (RM-ANOVA  $F_{(3,23)} = 5$   $p = 0.006$  ,  $n = 3$  animals)





---

# **Chapter 8: Discussion and Conclusions**

---



Normal reactions to painful stimuli are clearly protective sensations required for our survival and wellbeing. Chronic pain, however, becomes maladaptive, serves no protective role and instead severely limits everyday life and general well being. Unfortunately, chronic pain is not entirely understood. While there is a basic level of understanding of the neural processing behind pain, the properties of nociceptors, and their projections into the spinal cord remain incompletely characterised, both with regard to their normal functions and to their contributions to chronic pain.

One of the largest problems limiting our current understanding of nociception is the widespread use of oversimplified classification schemes that include the assumption that nociceptors are restricted to either small diameter lightly myelinated A $\delta$ -fibre or unmyelinated C-fibre afferent neurons. However, it has been shown that larger myelinated A $\alpha$ / $\beta$ -fibre afferent neurons can also be nociceptive (Djouhri & Lawson, 2004). Some (Julius & Basbaum, 2001; Basbaum *et al.*, 2009) also claim that the C-fibre nociceptors are either peptidergic or nonpeptidergic. Yet some peptides are expressed by A $\alpha$ -, A $\beta$ -, A $\delta$ - and C-fibre neurons (McCarthy & Lawson, 1990) and there is an overlap of marker expression between peptidergic and nonpeptidergic neurons (Ringkamp & Meyer, 2007; Priestley, 2009). Furthermore, several nociceptor subpopulations do not express neuropeptides or bind IB4, which is the standard marker for nonpeptidergic neurons. Examples include presumptive nociceptors that: express high levels of vesicular glutamate transporter 2 (VGluT2; Morris *et al.*, 2005; Clarke *et al.*, 2011); express TRPM8 (TRPM8; Peier, Reeve, *et al.*, 2002; Dhaka *et al.*, 2008); a population that express the capsaicin receptor, TRPV1 (Bráz & Basbaum, 2010); and small groups that express Mas-related G-protein coupled receptor member D (Mrgprd) and TRPA1 (Cavanaugh *et al.*, 2009).

One of the standard markers for peptidergic neurons is CGRP, which is often expressed in DRG neurons that also express SP (Gibson, Polak, Bloom, *et al.*, 1984; Wiesenfeld-Hallin *et al.*, 1984). Functionally, CGRP enhances the nociceptive behavioural responses induced by SP (Wiesenfeld-Hallin *et al.*, 1984) by potentiating the release of SP (Oku *et al.*, 1987), inhibiting its degradation (Le Greves *et al.*, 1985) and enhancing the excitability of neurons receiving noxious inputs (Biella *et al.*, 1991; Seybold *et al.*, 2003; Sun *et al.*, 2004; Bird *et al.*, 2006). CGRP is often used as the marker for these peptidergic nociceptors as, unlike SP, CGRP terminals

in the dorsal horn appear to be primarily of primary afferent origin (Gibson, Polak, Bloom, *et al.*, 1984; Franco-Cereceda *et al.*, 1987; Chung *et al.*, 1988; Hammond & Ruda, 1989; Traub *et al.*, 1989; Tie-Jun *et al.*, 2001). However, CGRP expression is not restricted to this class of peptidergic nociceptor.

Even though research suggest that both CGRP and SP are required for nociception, there are also long-standing reports of sensory neurons that contain CGRP without SP causing some confusion (Gibbins, Wattchow, *et al.*, 1987; Tamatani *et al.*, 1989; McCarthy & Lawson, 1990; Morris *et al.*, 2005; Kestell, 2009). Furthermore, while often overlooked, CGRP is expressed in DRG neurons of all soma sizes, including A $\alpha$ - and A $\beta$ - fibre neurons (McCarthy & Lawson, 1990). Therefore the role of CGRP without SP is unclear. Without SP, CGRP alone has been shown to have minimal effects on nociceptive inputs to the spinal cord (Miletic & Tan, 1988) and so the function of this population of overlooked peptidergic neurons is unknown, with no attempts (to date) to characterise them. Despite this confusing aspect, CGRP is still routinely used as a marker for peptidergic nociceptors because CGRP<sup>+</sup>SP<sup>+</sup> neurons are nociceptive (Lawson *et al.*, 1997). However the function of the CGRP<sup>+</sup>SP<sup>-</sup> neurons is unknown and so the categorical value of CGRP as a marker must be questioned. The aim of the research is therefore to establish whether CGRP is a completely reliable marker for peptidergic nociceptors, and whether it could lead to an over-representation of the peptidergic nociceptor population. However, the significance of these research questions depends upon just how prominent the CGRP<sup>+</sup>SP<sup>-</sup> neurons are. The research reported upon in this thesis therefore aimed to determine:

- If CGRP<sup>+</sup>SP<sup>-</sup> neurons are a prominent population of neurons;
- If CGRP<sup>+</sup>SP<sup>-</sup> neurons are most likely myelinated;
- If larger CGRP<sup>+</sup>SP<sup>-</sup> neurons are not capsaicin sensitive nociceptors;
- If larger CGRP<sup>+</sup>SP<sup>-</sup> neurons are not classical mechanoreceptors;
- How CGRP<sup>+</sup>SP<sup>-</sup> neurons function without SP?
- What is the possible role of CGRP<sup>+</sup>SP<sup>-</sup> neurons?

## **CGRP<sup>+</sup>SP<sup>-</sup> neurons are a prominent population of neurons**

Results from the research undertaken as part of this study revealed that in cervical, thoracic, lumbar and sacral DRG, CGRP-IR was detected in a large number of neuronal somata, which was consistent with previous reports (Gibson, Polak, Bloom, *et al.*, 1984; Wiesenfeld-Hallin *et al.*, 1984; McCarthy & Lawson, 1990; Morris *et al.*, 2005). These CGRP expressing somata could be subdivided based on their expression of SP. In all DRG investigated CGRP<sup>+</sup>SP<sup>-</sup> neurons were detected just as frequently as CGRP<sup>+</sup>SP<sup>+</sup> neurons, and in T5 DRG CGRP<sup>+</sup>SP<sup>-</sup> neurons were more numerous than CGRP<sup>+</sup>SP<sup>+</sup> neurons. In these DRG the cross sectional area of CGRP<sup>+</sup>SP<sup>-</sup> neuronal somata were more than twice the cross sectional area of CGRP<sup>+</sup>SP<sup>+</sup> neuronal soma in the DRG.

Results of this work also revealed that in the cervical, thoracic, lumbar and sacral dorsal horn, CGRP-IR terminals were detected in lamina I/II and lamina IV/V, which is also consistent with previous research (Gibson, Polak, Bloom, *et al.*, 1984; Wiesenfeld-Hallin *et al.*, 1984; Carlton *et al.*, 1988; Merighi *et al.*, 1988; Fried *et al.*, 1989). The CGRP-IR expressing terminals were subdivided based on their SP expression and so to quantify the amount of CGRP<sup>+</sup>SP<sup>-</sup> this research used confocal microscopy and focused on the medial and lateral region of lamina I/II and in lamina IV/V. It was found that there were equal proportions of CGRP<sup>+</sup>SP<sup>-</sup> and CGRP<sup>+</sup>SP<sup>+</sup> terminals in medial lamina I. However, there was an observable higher proportion of CGRP<sup>+</sup>SP<sup>-</sup> terminals than CGRP<sup>+</sup>SP<sup>+</sup> terminals in lateral lamina I; and lamina IV/V contained only CGRP<sup>+</sup>SP<sup>-</sup> terminals. Overall, there were higher proportions of CGRP<sup>+</sup>SP<sup>-</sup> terminals than CGRP<sup>+</sup>SP<sup>+</sup> terminals in the dorsal horn of the spinal cord.

In the forepaw and hindpaw skin, CGRP-IR fibres were observed penetrating the epidermis, encircling hair follicles, and associated with blood vessels and Meissner's corpuscles. All of these results are consistent with previous research (Gibbins *et al.*, 1985; Ishida-Yamamoto *et al.*, 1988; Kruger *et al.*, 1989). Once again, the CGRP expressing nerve fibres were subdivided based on their expression of SP. Results revealed that CGRP<sup>+</sup>SP<sup>-</sup> neurons were evident, penetrating the epidermis, associated with blood vessels and Meissner's corpuscles, just as frequently as CGRP<sup>+</sup>SP<sup>+</sup> neurons. CGRP<sup>+</sup>SP<sup>-</sup> fibres we also observed encircled around hair follicles.

CGRP neurons from L4 DRG were observed innervating gastrocnemius muscle. This is consistent with previous findings of CGRP fibres in gastrocnemius muscle (Reinert *et al.*, 1998; Hoheisel *et al.*, 2005; Gillan, 2012). Again, CGRP neurons were subdivided based on their expression of SP. Results revealed that CGRP<sup>+</sup>SP<sup>-</sup> neurons innervating the gastrocnemius muscle outnumbered CGRP<sup>+</sup>SP<sup>+</sup> neurons. This finding matched similar observations of the nerve fibres in the gastrocnemius muscle (Gillan, 2012).

Therefore, while this work has not discovered the existence of CGRP<sup>+</sup>SP<sup>-</sup> neurons (Gibbins, Wattchow, *et al.*, 1987; Tamatani *et al.*, 1989; McCarthy & Lawson, 1990; Morris *et al.*, 2005), it has demonstrated that CGRP<sup>+</sup>SP<sup>-</sup> neurons are a very prominent population of neurons with the following salient observations.

- CGRP<sup>+</sup>SP<sup>-</sup> neurons outnumbered CGRP<sup>+</sup>SP<sup>+</sup> neurons;
- In DRG, CGRP<sup>+</sup>SP<sup>-</sup> neurons had larger soma sizes than CGRP<sup>+</sup>SP<sup>+</sup> neurons;
- In DRG, more CGRP<sup>+</sup>SP<sup>-</sup> neurons innervated gastrocnemius muscle than CGRP<sup>+</sup>SP<sup>+</sup> neurons
- In the skin, CGRP<sup>+</sup>SP<sup>-</sup> fibres had a similar, but not identical, distribution to CGRP<sup>+</sup>SP<sup>+</sup> fibres;
- In the dorsal horn, CGRP<sup>+</sup>SP<sup>-</sup> terminals were detected in both lamina I/II and lamina IV/V;
- In lamina I, CGRP<sup>+</sup>SP<sup>-</sup> terminals had a similar distribution to CGRP<sup>+</sup>SP<sup>+</sup> terminals, however CGRP<sup>+</sup>SP<sup>-</sup> terminals outnumbered CGRP<sup>+</sup>SP<sup>+</sup> terminals in lateral lamina I.
- In lamina IV/V there were only CGRP<sup>+</sup>SP<sup>-</sup> terminals.

Consequently, CGRP is expressed by two prominent populations of sensory neurons: CGRP<sup>+</sup>SP<sup>+</sup> neurons that are the peptidergic nociceptors; and CGRP<sup>+</sup>SP<sup>-</sup> neurons. Hence, it has been demonstrated that CGRP is not a reliable marker for peptidergic nociceptors as it does lead to an over-representation of this population.

## **CGRP<sup>+</sup>SP<sup>-</sup> neurons are most likely myelinated**

Results of this study demonstrated that the soma size of CGRP<sup>+</sup>SP<sup>-</sup> neurons was more than twice the soma size of CGRP<sup>+</sup>SP<sup>+</sup> neurons in DRG. Therefore it is possible that CGRP<sup>+</sup>SP<sup>-</sup> neurons are myelinated A-fibre neurons. However, cell size

alone is an unreliable indicator of the myelination of a neuron (Hoheisel & Mense, 1987). Soma size is related by not only by the diameter of the neuronal axon but also by the overall length and degree of branching of the axon (Sugimoto *et al.*, 1988; Hildebrand *et al.*, 1995; Paik *et al.*, 2010). NF200 is typically used as a marker for myelination as it is believed to be exclusively expressed in neurons with myelinated A-fibre afferents (Lawson & Waddell, 1991). The proportion of CGRP<sup>+</sup>SP<sup>-</sup> neurons that expressed NF200 has not yet been characterised.

Some CGRP expressing neurons contain NF200 (McCarthy & Lawson, 1990; Ruscheweyh *et al.*, 2007; McCoy *et al.*, 2012). The research undertaken here demonstrated that the majority of CGRP<sup>+</sup>SP<sup>-</sup> neurons contained NF200, while only half of the CGRP<sup>+</sup>SP<sup>+</sup> neurons contained NF200. As expected, the CGRP neurons that expressed NF200 were larger than CGRP neurons that lacked NF200. This suggests that the majority of CGRP<sup>+</sup>SP<sup>-</sup> neurons were myelinated and half of CGRP<sup>+</sup>SP<sup>+</sup> neurons were unmyelinated. The CGRP<sup>+</sup>SP<sup>-</sup> neurons from L6 DRG innervating the gastrocnemius were also comparable in size to the CGRP<sup>+</sup>SP<sup>-</sup> neurons that contained NF200 and were therefore likely myelinated.

Unfortunately, NF200 may not be a reliable marker for myelinated neurons. Through this work and the work of others (Lawson *et al.*, 1984; Price, 1985; Goldstein *et al.*, 1991; Perry & Lawson, 1993), it was observed that NF200 was also expressed in many neurons with small soma sizes. While small somata are assumed to have unmyelinated fibres, others have been previously demonstrated that some neurons with small somata have A $\alpha$ /A $\beta$  conduction velocities (Hoheisel *et al.*, 1994; Lawson *et al.*, 1996). So the smaller neurons labelled by NF200 may well be myelinated. However, some unmyelinated fibres (Bae *et al.*, 2014) and some neurons with C-fibre conduction velocities have also been demonstrated to express NF200 (Ruscheweyh *et al.*, 2007). Thus, it appears that NF200 is not a reliable marker for myelinated neurons and that a more reliable method of determining the myelination of a neuron would be to establish the conduction velocity for that neuron. Fortunately, this has already been done before by McCarthy and Lawson (1990) who demonstrated CGRP-IR in both small and large somata of the DRG, and established that the smaller somata had C-fibre conduction velocities and lacked NF200 whereas, the larger somata had A-fibre conduction velocities and expressed NF200. McCarthy and Lawson (1989) also demonstrated that SP-IR was only present in small somata

of the DRG. Most SP expressing somata lacked NF200 and had C-fibre conduction velocities, whilst others contained NF200 and had A $\delta$ -fibre conduction velocities (McCarthy & Lawson, 1989). This would suggest that the majority of CGRP<sup>+</sup>SP<sup>-</sup> neurons were myelinated and that some CGRP<sup>+</sup>SP<sup>+</sup> neurons were myelinated, which matches the NF200 data from this research. Therefore, given the conduction velocities determined by McCarthy and Lawson (1989; 1990) it is likely that the majority of CGRP<sup>+</sup>SP<sup>-</sup> neurons were myelinated.

The notion that CGRP<sup>+</sup>SP<sup>-</sup> neurons are myelinated is further supported by their central terminations. In this study it was demonstrated that CGRP<sup>+</sup>SP<sup>-</sup> terminals were prominent in lamina I and lamina IV/V of the spinal dorsal horn. Lamina I neurons receive inputs from A $\delta$ - and C-fibres whereas lamina IV/V neurons receive inputs from A $\beta$ - and A $\delta$ - and C-fibres (Willis & Coggeshall, 1991). In this current research, Neurobiotin (NB) was used to label these CGRP<sup>+</sup>SP<sup>-</sup> terminals in both C7 and L4 dorsal horn. In the L4 dorsal horn NB labelled both fine and larger diameter fibres in lamina I and lamina IV/V. However, in the C7 dorsal horn NB appeared to preferentially label larger fibres, filling mainly fibres in lamina IV/V. Most of the finer fibres filled in lamina I of the L4 dorsal horn were CGRP<sup>+</sup>SP<sup>+</sup> fibres. There was no difference in the amount of NB-labelled CGRP<sup>+</sup>SP<sup>-</sup> fibres in both laminae I and IV/V between the C7 or L4 dorsal horns. This lack of difference suggested that CGRP<sup>+</sup>SP<sup>-</sup> fibres were larger fibres than CGRP<sup>+</sup>SP<sup>+</sup> fibres of lamina I, as NB did not label finer fibres in C7. The larger fibre size of CGRP<sup>+</sup>SP<sup>-</sup> fibres suggests that they are myelinated afferents.

In summary, CGRP-IR expressing neurons can be split up into three subpopulations based on their NF200 expression: CGRP<sup>+</sup>SP<sup>+</sup>NF200<sup>-</sup> neurons, CGRP<sup>+</sup>SP<sup>+</sup>NF200<sup>+</sup> neurons and CGRP<sup>+</sup>SP<sup>-</sup>NF200<sup>+</sup> neurons. The CGRP<sup>+</sup>SP<sup>+</sup>NF200<sup>-</sup> neurons are likely small unmyelinated C-fibre neurons; CGRP<sup>+</sup>SP<sup>+</sup>NF200<sup>+</sup> neurons are likely medium myelinated A $\delta$ -fibre neurons, and the CGRP<sup>+</sup>SP<sup>-</sup>NF200<sup>+</sup> neurons are likely larger myelinated A $\delta$ /A $\beta$ -fibre neurons. The existence of large CGRP<sup>+</sup>SP<sup>-</sup> neurons could be interpreted in two ways: either CGRP expression is not limited to nociceptive neurons; or nociceptive neurons are not limited to A  $\delta$  and C-fibre classes. Although often overlooked, some of the earliest descriptions of nociceptors included A $\alpha$ /  $\beta$  fibre classes which almost certainly originate from large diameter DRG neurons (Burgess & Perl, 1967; Ritter & Mendell, 1992; Djouhri *et al.*, 1998; Djouhri &

Lawson, 2001). Indeed, a more recent study has shown that some DRG neurons with myelinated fibres in the  $A\alpha/\beta$  range both contain CGRP and possess nociceptive properties (Lawson *et al.*, 2002).

### **Larger CGRP<sup>+</sup>SP<sup>-</sup> neurons are not capsaicin sensitive nociceptors**

In this study it was determined that CGRP<sup>+</sup>SP<sup>-</sup> neurons express NF200, which is usually expressed by large myelinated mechanoreceptors (Lawson & Waddell, 1991). Hence, CGRP<sup>+</sup>SP<sup>-</sup> neurons may not be peptidergic nociceptors. Peptidergic nociceptors are often capsaicin sensitive. Capsaicin activates the vanilloid receptor TRPV1 ( $\geq 43^\circ\text{C}$ ; Caterina *et al.*, 1997). Thus, TRPV1 expression in sensory neurons is often used as an indicator that the neurons are capsaicin sensitive nociceptors. TRPV1 is expressed in small to medium sized neurons in DRG (Caterina *et al.*, 1997; Tominaga *et al.*, 1998; Guo *et al.*, 1999). Most TRPV1 neurons are peptidergic and express CGRP and SP (Cavanaugh *et al.*, 2011; McCoy *et al.*, 2012). The reverse is also true: most, but not all, CGRP-IR neurons express TRPV1 (Cavanaugh *et al.*, 2011; McCoy *et al.*, 2012). The proportion of CGRP<sup>+</sup>SP<sup>-</sup> neurons that express TRPV1 has not yet been characterised.

Results determined that virtually all CGRP<sup>+</sup>SP<sup>+</sup> neurons contained TRPV1. In contrast, less than half of the CGRP<sup>+</sup>SP<sup>-</sup> neurons expressed TRPV1. The CGRP<sup>+</sup>SP<sup>-</sup>TRPV1<sup>-</sup> neurons were larger than both the CGRP<sup>+</sup>SP<sup>+</sup>TRPV1<sup>+</sup> and CGRP<sup>+</sup>SP<sup>-</sup>TRPV1<sup>+</sup> neurons. Based on their soma sizes and work by McCarthy and Lawson (McCarthy & Lawson, 1989; 1990), it is probable that CGRP<sup>+</sup>SP<sup>+</sup>TRPV1<sup>+</sup> neurons were unmyelinated C-fibre nociceptors, CGRP<sup>+</sup>SP<sup>-</sup>TRPV1<sup>+</sup> neurons were likely myelinated A $\delta$ -fibre nociceptors and CGRP<sup>+</sup>SP<sup>-</sup>TRPV1<sup>-</sup> neurons were A $\delta$ /A $\beta$  fibre sensory neurons.

In summary, CGRP expressing neurons can be split up into three subpopulations: small CGRP<sup>+</sup>SP<sup>+</sup>TRPV1<sup>+</sup> neurons; small CGRP<sup>+</sup>SP<sup>-</sup>TRPV1<sup>+</sup> neurons; and larger CGRP<sup>+</sup>SP<sup>-</sup>TRPV1<sup>-</sup> neurons. CGRP<sup>+</sup>SP<sup>+</sup>TRPV1<sup>+</sup> and CGRP<sup>+</sup>SP<sup>-</sup>TRPV1<sup>+</sup> neurons have central projections in lamina I and are most likely nociceptive. However, the larger CGRP<sup>+</sup>SP<sup>-</sup>TRPV1<sup>-</sup> neurons have central projections in lamina IV/V and may not have a role in nociception.

## **Larger CGRP<sup>+</sup>SP<sup>-</sup> neurons are not classical mechanoreceptors**

This study has determined that there are two subpopulations of CGRP<sup>+</sup>SP<sup>-</sup> neurons: small CGRP<sup>+</sup>SP<sup>-</sup> neurons that express TRPV1 and larger CGRP<sup>+</sup>SP<sup>-</sup> neurons that lack TRPV1. The lack of TRPV1 expression in the larger CGRP<sup>+</sup>SP<sup>-</sup> neurons suggests that these neurons are not peptidergic nociceptors. CGRP<sup>+</sup>SP<sup>-</sup> fibres were associated with sensory endings that are typically associated with mechanoreceptors and express NF200, which is usually expressed by large myelinated mechanoreceptors (Lawson & Waddell, 1991). This gives rise to the question as to whether these larger CGRP<sup>+</sup>SP<sup>-</sup> neurons that lack TRPV1 expression mechanoreceptors?

CGRP<sup>+</sup>SP<sup>-</sup> fibres were closely associated with hair follicle afferents. Hair follicle afferents form a piloneural complex: a combination of sensory endings that form an ensemble around hair follicles at the mid-level of the hair shaft. The piloneural complex consists of a palisade of blade-like lanceolate endings, and circumferentially oriented endings (Rice & Albrecht, 2007). While it has been previously documented that both CGRP and SP fibres encircle hair follicles (Kruger *et al.*, 1989; Fundin *et al.*, 1997; Rice *et al.*, 1997), results here have demonstrated that CGRP<sup>+</sup>SP<sup>-</sup> fibres encircled hair follicles at the level of the palisade nerve endings. While they did not explicitly characterise their endings, Lawson and colleagues (2002) have also demonstrated CGRP<sup>+</sup>SP<sup>-</sup> fibres associated with hair follicles and determined that these fibres were non-nociceptive moderately rapidly adapting mechanoreceptors that responded to hair movement. Unlike, Lawson and colleagues (2002), it was also demonstrated here that often a single CGRP<sup>+</sup>SP<sup>+</sup> fibre encircled the hair follicle inferior to the circumferential CGRP<sup>+</sup>SP<sup>-</sup> fibres. As all SP containing primary afferent fibres are presumed nociceptive (Lawson *et al.*, 1997), it is likely that the single CGRP<sup>+</sup>SP<sup>+</sup> fibre is associated with noxious distortion of the hair follicle.

CGRP<sup>+</sup>SP<sup>-</sup> fibres were also closely associated with Meissner's corpuscles. Meissner's corpuscles contain a coiled arrangement of endings from at least three types of separate fibres: A $\alpha$ / $\beta$  fibres and peptidergic and non-peptidergic C-fibres (Paré *et al.*, 2001). CGRP and SP are associated with some Meissner's corpuscles (Ishida-Yamamoto *et al.*, 1988; Kruger *et al.*, 1989; Paré *et al.*, 2001), however it was shown here that both CGRP<sup>+</sup>SP<sup>+</sup> and CGRP<sup>+</sup>SP<sup>-</sup> fibres are associated with the

Meissner's corpuscles. The A $\alpha$ / $\beta$  fibres of the Meissner's corpuscle described by Paré and colleagues (2001) expressed CGRP and NF200, and are hence likely the CGRP<sup>+</sup>SP<sup>-</sup> fibres that have demonstrated in this current study. These A $\alpha$ / $\beta$  fibres are believed to be the low-threshold mechanoreceptive endings of the Meissner's corpuscle. These A $\alpha$ / $\beta$  fibres are closely intertwined with endings from peptidergic C-fibres (Paré *et al.*, 2001). These peptidergic fibres lacked NF200 and expressed both CGRP and SP (Paré *et al.*, 2001), and are hence likely the CGRP<sup>+</sup>SP<sup>+</sup> fibres that have demonstrated in this current study. Again, as all SP containing primary afferent fibres are presumed nociceptive (Lawson *et al.*, 1997), it is likely that the CGRP<sup>+</sup>SP<sup>+</sup> fibres are nociceptive. While Meissner's corpuscles are activated by innocuous light touch, it is now believed that they can also be nociceptive (Paré *et al.*, 2001).

This study has demonstrated that CGRP<sup>+</sup>SP<sup>-</sup> neurons have dual central projections to the superficial and deep laminae of the dorsal horn of the spinal cord. While the superficial dorsal horn (laminae I/II) is most commonly associated with nociception, the deeper laminae (laminae IV/V) are commonly associated with low threshold mechanoreceptors. Lamina IV/V neurons receive mostly non-nociceptive input (Cervero *et al.*, 1988) and contains both low threshold mechanoreceptive and wide dynamic range neurons (Mendell & Wall, 1965; Hillman & Wall, 1969; Light & Durkovic, 1984). Low threshold mechanoreceptors express vesicular glutamate transporter 1 (VGLUT1; Alvarez *et al.*, 2004) and so in this study the primary afferent terminals of VGluT1-IR mechanoreceptors were compared with the CGRP<sup>+</sup>SP<sup>-</sup> terminals of lamina IV/V. Results determined that while CGRP<sup>+</sup>SP<sup>-</sup> fibres were in close proximity to primary afferent terminals of VGluT1-IR there was no colocalisation between CGRP and VGluT1-IR. This is consistent with others who have demonstrated that CGRP-IR neurons lack VGluT1-IR (Oliveira *et al.*, 2003; Todd *et al.*, 2003; Morris *et al.*, 2005; Brumovsky *et al.*, 2007). Hence CGRP<sup>+</sup>SP<sup>-</sup> fibres of lamina IV/V are not classical VGluT1 mechanoreceptors, and maybe be an unidentified class of mechanoreceptor. As lamina IV/V also contain wide dynamic range neurons that respond to noxious and innocuous stimuli (Mendell & Wall, 1965; Hillman & Wall, 1969; Light & Durkovic, 1984), therefore CGRP<sup>+</sup>SP<sup>-</sup> fibres of lamina IV/V may still have a role in nociception.

In summary, the larger CGRP<sup>+</sup>SP<sup>-</sup> neurons that lack TRPV1 are most likely not peptidergic nociceptors. Their expression of NF200, association with hair follicle

afferents and Meissner's corpuscles, and deep dorsal horn projections suggest these neurons may be low threshold mechanoreceptors. However, low threshold mechanoreceptors usually contain VGlut1 (Alvarez *et al.*, 2004) and CGRP-IR neurons, including CGRP<sup>+</sup>SP<sup>-</sup> neurons, do not (Oliveira *et al.*, 2003; Todd *et al.*, 2003; Morris *et al.*, 2005; Brumovsky *et al.*, 2007). This suggests that these larger CGRP<sup>+</sup>SP<sup>-</sup> neurons are not a subset of classical VGlut1-IR low-threshold, myelinated mechanoreceptors. Hence it is likely that these larger CGRP<sup>+</sup>SP<sup>-</sup> neurons are a neurochemically unique population of mechanoreceptors that most likely corresponding to A $\beta$  or A $\delta$  neurons (McCarthy & Lawson, 1990; Ruscheweyh *et al.*, 2007).

## **How do CGRP<sup>+</sup>SP<sup>-</sup> neurons function without SP?**

This study has demonstrated that CGRP<sup>+</sup>SP<sup>-</sup> neurons are a very prominent population of neurons and can be subdivided into two subpopulations based on their expression of TRPV1. However, without SP, CGRP has minimal effects on nociceptive inputs to the spinal cord (Miletic & Tan, 1988). To investigate how capsaicin sensitive CGRP<sup>+</sup>SP<sup>-</sup> neurons might function pERK/pCREB was used as a marker of neuronal activation and viable dorsal horn slices were stimulated with capsaicin and electrical stimulation of the attached dorsal root. TRPV1 expression is restricted to the primary afferent terminals of the dorsal horn (Szallasi *et al.*, 1995; Caterina *et al.*, 1997; Tominaga *et al.*, 1998) and pERK/pCREB is not induced by polysynaptic activation after capsaicin application (Kawasaki *et al.*, 2004). Therefore, any pERK/pCREB induced in the spinal cord is induced by monosynaptic input from capsaicin sensitive primary afferent fibres.

Consistent with previous studies (Ji *et al.*, 1999; Kawasaki *et al.*, 2004) results here demonstrated that capsaicin stimulation induced pERK/pCREB expression in dorsal horn neurons of lamina I/II in the dorsal horn. Capsaicin stimulation failed to induce pERK/pCREB expression in dorsal horn neurons of lamina IV/V. Dorsal horn neurons of lamina IV/V do express ERK/CREB (Kawasaki *et al.*, 2004; Song *et al.*, 2005) and hence pERK/pCREB should be induced in these neurons given the correct stimulus. Consistent with Kawasaki and colleagues (2004) electrical stimulation of the attached dorsal root induced pERK expression in neurons of lamina I/II and pCREB expression in neurons of lamina I-III of the spinal dorsal horn. Surprisingly,

there was no pERK/pCREB expression in dorsal horn neurons of lamina IV/V. This suggests that the CGRP<sup>+</sup>SP<sup>-</sup> neurons of laminae IV/V were functionally different from the CGRP<sup>+</sup>SP<sup>-</sup> neurons of laminae I/II.

The capsaicin-induced pERK expression in dorsal horn neurons of lamina I received contacts from multiple classes of primary afferent terminals. Some received input from CGRP<sup>+</sup>SP<sup>+</sup> and CGRP<sup>+</sup>SP<sup>-</sup> terminals and others from just CGRP<sup>+</sup>SP<sup>-</sup> terminals. The electrically induced pCREB expressing neurons shared many similarities with capsaicin-induced pERK expressing neurons. As many CREB expressing neurons also express ERK (Ji *et al.*, 1999; Kawasaki *et al.*, 2004) it is likely that most of the electrically induced pCREB neurons of lamina I were the same neurons as the capsaicin induced pERK neurons of lamina I.

pERK/pCREB expressing dorsal horn neurons that received contacts from CGRP<sup>+</sup>SP<sup>+</sup> terminals were most likely activated by SP. CGRP<sup>+</sup>SP<sup>+</sup> neurons express TRPV1 and hence were able to be stimulated by capsaicin (Szallasi *et al.*, 1995; Caterina *et al.*, 1997; Tominaga *et al.*, 1998). Both capsaicin and electrical stimulation causes the release of CGRP and SP in the dorsal horn (Franco-Cereceda *et al.*, 1987; Morton & Hutchison, 1989). SP activates the dorsal horn neurons receiving CGRP<sup>+</sup>SP<sup>+</sup> contacts (Salter & Henry, 1991) and CGRP potentiates the effects of SP (Seybold, 2009). This neuronal activation then induces pERK/pCREB expression in the postsynaptic dorsal horn neuron.

Many CGRP<sup>+</sup>SP<sup>-</sup> neurons also expressed TRPV1 and have terminals in lamina I. Consequently, both capsaicin and electrical stimulation of these neurons would cause the release of CGRP in the dorsal horn (Franco-Cereceda *et al.*, 1987; Morton & Hutchison, 1989). Yet, CGRP alone has minimal effects on the excitability of dorsal horn neurons (Miletic & Tan, 1988; Biella *et al.*, 1991). So it is unlikely that CGRP alone was able to directly activate and induce pERK/pCREB expression in the postsynaptic dorsal horn neurons. The CGRP<sup>+</sup>SP<sup>-</sup> afferent terminals may have induced pERK/pCREB expression in dorsal horn neurons through the use of another neurotransmitter, which activated the postsynaptic dorsal horn neurons.

CGRP has been shown to enhance the release of other excitatory neurotransmitters such as glutamate (Kangrga & Randic, 1990). Glutamate is the primary excitatory neurotransmitter in the spinal cord and it is believed that the majority of sensory

neurotransmission from primary afferents onto dorsal horn neurons is largely mediated by glutamate (Alvarez *et al.*, 2004). Unfortunately, neurons possess metabolic pools of glutamate that are unrelated to neurotransmission (De Biasi & Rustioni, 1990), which complicates the interpretation of glutamate immunoreactivity. Instead, immunoreactivity to vesicular glutamate transporters (VGluTs) is used. To date there are three VGluTs: VGluT1, VGluT2 and VGluT3 (Bellocchio *et al.*, 1998; Takamori *et al.*, 2000; Bai *et al.*, 2001; Takamori *et al.*, 2001; Herzog *et al.*, 2004). VGluT1 and VGluT2 are expressed by separate populations of primary afferents (Alvarez *et al.*, 2004). VGluT1 is expressed by cutaneous and muscle mechanoreceptors and VGluT2 by small fibre nociceptors. (Alvarez *et al.*, 2004). VGluT3 is expressed by small C-fibre mechanoreceptors (Seal *et al.*, 2009). CGRP-IR neurons do not express VGluT1 (Oliveira *et al.*, 2003; Todd *et al.*, 2003; Morris *et al.*, 2005; Brumovsky *et al.*, 2007) or VGluT3 (Morris *et al.*, 2005; Seal *et al.*, 2009; Draxler *et al.*, 2014). There are inconsistent reports of whether CGRP neurons express VGluT2, with some reporting no colocalisation (Morris *et al.*, 2005; Clarke *et al.*, 2011) and others reporting colocalisation (Todd *et al.*, 2003; Brumovsky *et al.*, 2007). Regardless, it has been demonstrated that CGRP expressing neurons lack the protein machinery required for vesicular release of glutamate (Morris *et al.*, 2005). Therefore, it is highly unlikely that CGRP<sup>+</sup>SP<sup>-</sup> neurons utilize glutamate.

Others have suggested that CGRP<sup>+</sup>SP<sup>-</sup> neurons express other peptides, such as galanin or VIP (Ju *et al.*, 1987; Hökfelt *et al.*, 1993). In this study it has been demonstrated that only CGRP<sup>+</sup>SP<sup>+</sup> neurons expressed galanin, but some CGRP<sup>+</sup>SP<sup>-</sup> neurons did express VIP. VIP shares similar features to CGRP and is considered a neuromodulator. Under normal conditions VIP increases the excitability of neurons in nociceptive circuits (Cridland & Henry, 1988). This excitatory action of VIP is markedly increased in injury models (Wiesenfeld-Hallin, Xu, Håkanson, *et al.*, 1990) to a level comparable to the effect that SP has on nociceptive neurons (Wiesenfeld-Hallin, Xu, Håkanson, *et al.*, 1990). Hence, VIP may be able to replace the role of SP following nerve injury. However, not all CGRP<sup>+</sup>SP<sup>-</sup> neurons express VIP.

Another possibility is that CGRP<sup>+</sup>SP<sup>-</sup> neurons enhance the excitability of dorsal horn neurons and the dorsal horn neurons are activated via convergent axons of other primary afferents. In this study it was demonstrated that almost all pERK/pCREB-expressing neurons had contacts from multiple classes of IR terminals, and that most

of these included CGRP<sup>+</sup>SP<sup>-</sup> terminals. It is already known that CGRP enhances the excitability of neurons receiving nociceptive inputs (Biella *et al.*, 1991; Seybold *et al.*, 2003; Sun *et al.*, 2004; Bird *et al.*, 2006). So rather than CGRP enhancing the effects of a neurotransmitter from within the same afferent terminal, CGRP may have been released and enhanced the excitability of the pERK/pCREB expressing dorsal horn neuron and enhanced the effects of a neurotransmitter from another convergent afferent terminal.

In summary, the central projections of CGRP<sup>+</sup>SP<sup>-</sup> afferents in laminae I/II are functionally different from the CGRP<sup>+</sup>SP<sup>-</sup> afferents of laminae V/IV. The CGRP<sup>+</sup>SP<sup>-</sup> afferents in laminae I/II made contacts with dorsal horn neurons expressing capsaicin-induced pERK/pCREB. Therefore it is likely that the CGRP<sup>+</sup>SP<sup>-</sup> afferents in laminae I/II were the central projections of the capsaicin sensitive CGRP<sup>+</sup>SP<sup>-</sup> neurons. It is likely that these CGRP<sup>+</sup>SP<sup>-</sup> afferents of laminae I/II had a modulatory role in the in the capsaicin-induced pERK/pCREB expression in dorsal horn neurons. Capsaicin failed to induced pERK/pCREB expression in the dorsal horn neurons of lamina IV/V. Therefore it is likely that the CGRP<sup>+</sup>SP<sup>-</sup> afferents in lamina IV/V are the central projections of the capsaicin insensitive CGRP<sup>+</sup>SP<sup>-</sup> neurons.

Furthermore, without SP, CGRP is only able to enhance to nociceptive input to dorsal horn neurons (Biella *et al.*, 1991; Seybold *et al.*, 2003; Sun *et al.*, 2004; Bird *et al.*, 2006). CGRP<sup>+</sup>SP<sup>-</sup> neurons do not appear utilise glutamate or galanin as a neurotransmitter that is capable of activating dorsal horn neurons. CGRP<sup>+</sup>SP<sup>-</sup> neurons can utilise VIP that may be able to replace SP in certain conditions, however not all CGRP<sup>+</sup>SP<sup>-</sup> neurons express VIP. Hence, CGRP<sup>+</sup>SP<sup>-</sup> neurons may just simply enhance the excitability of dorsal horn neurons that are activated by convergent input.

## **What is the possible role of CGRP<sup>+</sup>SP<sup>-</sup> neurons?**

### ***Capsaicin sensitive CGRP<sup>+</sup>SP<sup>-</sup> neurons likely have a role in central sensitisation and hyperalgesia***

In this study it has been demonstrated that there are medium myelinated A $\delta$ -fibre CGRP<sup>+</sup>SP<sup>-</sup> neurons that expressed TRPV1 and had central projections to laminae I/II of the dorsal horn. This study has demonstrated that these neurons made convergent contacts onto nociceptive dorsal horn neurons in laminar I/II, however, without SP it

is unlikely that CGRP was able to directly activate these neurons. Hence, it is doubtful that these CGRP<sup>+</sup>SP<sup>-</sup> neurons are involved in acute nociception. However, their modulatory effects in lamina I may contribute to the central sensitisation resulting in hyperalgesia.

In this work pERK/pCREB markers were used for neuronal activation, however pERK/pCREB is also believed to play a role in central sensitisation (Ji & Woolf, 2001). Results demonstrated that the majority of the pERK/pCREB expressing neuronal cell bodies received convergent input from CGRP<sup>+</sup>SP<sup>-</sup> terminals. It is known that CGRP enhances the excitability of neurons receiving nociceptive inputs (Biella *et al.*, 1991; Seybold *et al.*, 2003; Sun *et al.*, 2004; Bird *et al.*, 2006) but suggested that CGRP alone was not enough to generate an action potential in the postsynaptic dorsal horn neuron as CGRP has minimal effects on nociceptive inputs to the spinal cord (Miletic & Tan, 1988). However, activation of the CGRP receptor has been demonstrated to activate cAMP and initiate the MAPK/ERK pathway (Parameswaran *et al.*, 2000; Seybold *et al.*, 2003). This would lead to changes in gene transcription and changes in the excitability of the dorsal horn neuron. For example the pERK has been demonstrated to contribute to the increased expression of spinal NK1 receptors during peripheral inflammation (Ji, Befort, *et al.*, 2002), which would result in central sensitisation. ERK has also been demonstrated to play a role in increased levels of spinal dynorphin (Ji, Befort, *et al.*, 2002), which has been demonstrated to further sensitise dorsal horn neurons and is possibly involved in neuropathic pain states (Ossipov & Porreca, 2007). The CGRP antagonist CGRP8-37 significantly attenuates heat hyperalgesia (Yu, Hansson, & Lundberg, 1996) and even abolishes heat hyperalgesia (Bennett *et al.*, 2000) in nerve injury models.

***Larger capsaicin insensitive CGRP<sup>+</sup>SP<sup>-</sup> neurons might have a role in mechanical allodynia***

In this study it has been demonstrated that there are myelinated A $\beta$ -fibre CGRP<sup>+</sup>SP<sup>-</sup> neurons that lack TRPV1 and have central terminations in lamina IV/V. Results determined that these neurons were not activated by capsaicin in lamina IV/V, and were hence functionally different from the capsaicin-sensitive A  $\delta$  -fibre CGRP<sup>+</sup>SP<sup>-</sup> neurons of laminae I/II. The role of the larger myelinated A $\delta$ /A $\beta$ -fibre CGRP<sup>+</sup>SP<sup>-</sup> neurons was not determined in this study. While this role is most likely innocuous in

nature, there is evidence to suggest that these neurons could contribute to mechanical allodynia.

Mechanical allodynia is “*pain due to a mechanical stimulus that does not normally provoke pain*” (Merskey & Bogduk, 1994) and is believed to be mediated largely by A $\beta$ -fibre neurons. These larger CGRP<sup>+</sup>SP<sup>-</sup> neurons are most likely A $\beta$ -fibre neurons, due to both their soma size and expression of NF200, and their association with hair follicles and Meissner’s corpuscles. Based on data from McCarthy and Lawson (1990) the large NF200 expressing CGRP<sup>+</sup>SP<sup>-</sup> neurons are A $\alpha$ / $\beta$ -fibres. Based on data from Lawson and colleagues (2002) CGRP<sup>+</sup>SP<sup>-</sup> fibres associated with hair follicles were A $\beta$ -fibres. Finally, based on data from Paré and colleagues (2001) the CGRP<sup>+</sup>SP<sup>-</sup> fibres associated with Meissner’s corpuscles were A $\alpha$ / $\beta$ -fibres. While under normal conditions, these CGRP<sup>+</sup>SP<sup>-</sup> fibres are non-nociceptive, inflammation or neurological damage could potentially result in mechanical hyperalgesia and allodynia. CGRP has been demonstrated to be involved in the sensitisation of mechanical nociceptive dorsal horn neurons (Sun *et al.*, 2004) and in the generation and maintenance of tactile allodynia (Sun *et al.*, 2003). The CGRP antagonist CGRP8-37 delays the onset of mechanical allodynia (Lee & Kim, 2007), reduces the severity (Yu, Hansson, & Lundberg, 1996) and can even reverse mechanical allodynia (Jang, 2004).

The myelinated A $\beta$ -fibre CGRP<sup>+</sup>SP<sup>-</sup> neurons that lacked TRPV1 had central terminations in lamina IV/V. Lamina IV/V contains both low threshold mechanoreceptive and wide dynamic range neurons (Cervero *et al.*, 1988). Wide dynamic range neurons respond to both innocuous and noxious stimuli (Mendell & Wall, 1965; Hillman & Wall, 1969; Light & Durkovic, 1984). CGRP can increase the excitability of wide dynamic range neurons in the deep dorsal horn and probably contributes to mechanical hyperalgesia (Yu *et al.*, 2002; Sun *et al.*, 2004). CGRP is also down-regulated in injured DRG neurons but up-regulated in adjacent spared neurons projecting to lamina III-V of dorsal horn (Ma & Bisby, 1998; Miki *et al.*, 1998; Ma *et al.*, 1999), suggesting a role in mediating the tactile allodynia caused by nerve injury (Sun *et al.*, 2001; Ossipov *et al.*, 2002).

In summary, it is unlikely that CGRP<sup>+</sup>SP<sup>-</sup> neurons are involved in acute nociception. The medium myelinated A $\delta$ -fibre CGRP<sup>+</sup>SP<sup>-</sup>TRPV1<sup>+</sup> neurons with central

projections to laminae I/II of the dorsal horn most likely had modulatory effects in lamina I that may contribute to the central sensitisation resulting in hyperalgesia. The larger myelinated A $\alpha$ / $\beta$ -fibre CGRP<sup>+</sup>SP<sup>-</sup>TRPV1<sup>-</sup> neurons with central projections to laminae IV/V of the dorsal horn were most likely non-nociceptive mechanoreceptors but may synapse on wide dynamic range neurons and could contribute to mechanical allodynia.

## Future directions

It is extremely challenging to distinguish the release of CGRP from the CGRP<sup>+</sup>SP<sup>-</sup> or CGRP<sup>+</sup>SP<sup>+</sup> afferents due to their similar distributions in lamina I/II. Although CGRP causes no acute behavioural effect when injected by itself (Wiesenfeld-Hallin *et al.*, 1984; Gamse & Saria, 1986), intrathecal administration of CGRP causes hyperalgesia to mechanical stimuli (Oku *et al.*, 1987), and intrathecal injection of CGRP antiserum decreases thermal and mechanical hyperalgesia during peripheral inflammation (Kawamura *et al.*, 1989; Kuraishi *et al.*, 1991). In the spinal cord, noxious thermal, mechanical, or electrical stimulation evoke the release of CGRP within the superficial dorsal horn (Morton & Hutchison, 1989; 1990). However, these effects could be mediated in part by CGRP receptors on terminals of primary afferent neurons that facilitate the release of SP (Oku *et al.*, 1987; Ryu *et al.*, 1988). In future, the use of pERK/pCREB as marker for neuronal activation in viable spinal cord slices could be coupled with different receptor antagonists to investigate what neurotransmitters were involved in the activation of pERK/pCREB cells. For example NK1 receptor antagonists could determine if this involvement was dependent on CGRP potentiating the effects of other transmitters or whether CGRP was capable of this alone. Further neurochemical characterisation of CGRP<sup>+</sup>SP<sup>-</sup> neurons could also determine any other potential neurotransmitters and peptides that could be utilized by these neurons.

## Summary

Therefore, while this research did not discover the existence of CGRP<sup>+</sup>SP<sup>-</sup> neurons (Gibbins, Wattchow, *et al.*, 1987; Tamatani *et al.*, 1989; McCarthy & Lawson, 1990; Morris *et al.*, 2005), it has demonstrated that CGRP<sup>+</sup>SP<sup>-</sup> neurons are a very prominent population of neurons. CGRP expressing neurons can be subdivided both based on their expression of SP and a number of different anatomical and

neurochemical features summarised in Table 4.2. There were two subpopulations of  $\text{CGRP}^+\text{SP}^+$  neurons: small unmyelinated C-fibre neurons that lacked NF200 and GAL expression, and medium myelinated  $\text{A}\delta$ -fibre neurons that expressed NF200 and GAL. We also determined that the overlooked  $\text{CGRP}^+\text{SP}^-$  neurons were a very prominent population of neurons that express NF200. There were a number of subpopulations of  $\text{CGRP}^+\text{SP}^-$  neurons: medium myelinated  $\text{A}\delta$ -fibre neurons that expressed TRPV1 and medium-large sized myelinated  $\text{A}\delta/\text{A}\beta$ -fibre neurons that lacked TRPV1.

The smaller  $\text{CGRP}^+\text{SP}^-\text{TRPV1}^+$  neurons were similar to the myelinated  $\text{A}\delta$ -fibre  $\text{CGRP}^+\text{SP}^+$  neurons. They both had similar central projections to lamina I/II of the spinal dorsal horn. It is not clear whether  $\text{CGRP}^+\text{SP}^-\text{TRPV1}^+$  neurons can be classified as peptidergic nociceptors. Without SP, CGRP most likely enhances nociceptive input to dorsal horn neurons (Biella *et al.*, 1991; Seybold *et al.*, 2003; Sun *et al.*, 2004; Bird *et al.*, 2006). These  $\text{CGRP}^+\text{SP}^-$  neurons did not appear utilise glutamate or galanin as a neurotransmitter, but did express VIP, which may be able to replace SP in certain conditions. Hence,  $\text{CGRP}^+\text{SP}^-$  neurons may just simply enhance the excitability of dorsal horn neurons that are activated by convergent input. Hence, it is likely that these  $\text{CGRP}^+\text{SP}^-$  afferents of laminae I/II had a modulatory role in nociception and may contribute to the central sensitisation resulting in hyperalgesia.

The larger  $\text{CGRP}^+\text{SP}^-\text{TRPV1}^-$  neurons are most likely not peptidergic nociceptors. They are likely low threshold mechanoreceptors, however their lack of VGlut1 suggests that they are not classical low threshold mechanoreceptors. Hence it is likely that these larger  $\text{CGRP}^+\text{SP}^-\text{TRPV1}^-$  neurons are a neurochemically unique population of mechanoreceptors that most likely corresponding to  $\text{A}\beta$  or  $\text{A}\delta$  neurons. The larger myelinated  $\text{A}\alpha/\beta$ -fibre  $\text{CGRP}^+\text{SP}^-\text{TRPV1}^-$  neurons with central projections to laminae IV/V of the dorsal horn were functionally different from the central projections of  $\text{A}\delta$ -fibre  $\text{CGRP}^+\text{SP}^-\text{TRPV1}^+$  neurons in lamina I/II. These  $\text{A}\alpha/\beta$ -fibre  $\text{CGRP}^+\text{SP}^-\text{TRPV1}^-$  neurons were most likely non-nociceptive mechanoreceptors but may synapse on wide dynamic range neurons and could contribute to mechanical allodynia.

## Chapter 8: Discussion and Conclusions

Overall, this research has led to an improved understanding of the properties of a presumed nociceptor. While CGRP<sup>+</sup>SP<sup>-</sup> neurons are unlikely to be involved in acute nociception, their modulatory effects may contribute to the central sensitisation resulting in the hyperalgesia and mechanical allodynia associated with inflammatory and chronic pain states.

---

# Reference List

---

## Reference List

- Aanonsen, L.M., Kajander, K.C., Bennett, G.J., & Seybold, V.S. (1992) Autoradiographic analysis of 125I-substance P binding in rat spinal cord following chronic constriction injury of the sciatic nerve. *Brain Research*, **596**, 259–268.
- Abraham, K.E. & Brewer, K.L. (2001) Expression of c-fos mRNA is increased and related to dynorphin mRNA expression following excitotoxic spinal cord injury in the rat. *Neuroscience Letters*, **307**, 187–191.
- Access Economics Pty Ltd (2007) The high price of pain: the economic impact of persistent pain in Australia. MBF Foundation (now BUPA) in collaboration with University of Sydney Pain Management Research Institute.
- Al-Chaer, E.D., Lawand, N.B., Westlund, K.N., & Willis, W.D. (1996a) Pelvic Visceral Input Into the Nucleus Gracilis is Largely Mediated by the Postsynaptic Dorsal Colu Pathway.
- Al-Chaer, E.D., Lawand, N.B., Westlund, K.N., & Willis, W.D. (1996b) Visceral nociceptive input into the ventral posterolateral nucleus of the thalamus: a new function for the dorsal column pathway. *J. Neurophysiol*, **76**, 2661–2674.
- Alvarez, F.J., Villalba, R.M., Zerda, R., & Schneider, S.P. (2004) Vesicular glutamate transporters in the spinal cord, with special reference to sensory primary afferent synapses. *J. Comp. Neurol*, **472**, 257–280.
- Amara, S.G., Arriza, J.L., Leff, S.E., Swanson, L.W., Evans, R.M., & Rosenfeld, M.G. (1985) Expression in brain of a messenger RNA encoding a novel neuropeptide homologous to calcitonin gene-related peptide. *Science*, **229**, 1094–1097.
- Amara, S.G., Jonas, V., Rosenfeld, M.G., Ong, E.S., & Evans, R.M. (1982) Alternative RNA processing in calcitonin gene expression generates mRNAs encoding different polypeptide products. *Nature*, **298**, 240–244.
- Ambalavanar, R., Dessem, D., Moutanni, A., Yallampalli, C., Yallampalli, U., Gangula, P., & Bai, G. (2006) Muscle inflammation induces a rapid increase in calcitonin gene-related peptide (CGRP) mRNA that temporally relates to CGRP immunoreactivity and nociceptive behavior. *Neuroscience*, **143**, 875–884.
- Ambalavanar, R., Moritani, M., Moutanni, A., Gangula, P., Yallampalli, C., & Dessem, D. (2006) Deep tissue inflammation upregulates neuropeptides and evokes nociceptive behaviors which are modulated by a neuropeptide antagonist. *Pain*, **120**, 53–68.
- Andrew, D. & Craig, A.D. (2001) Spinothalamic lamina I neurons selectively sensitive to histamine: a central neural pathway for itch. *Nat. Neurosci*, **4**, 72–77.
- Andrew, D. & Craig, A.D. (2002a) Responses of spinothalamic lamina I neurons to maintained noxious mechanical stimulation in the cat. *J. Neurophysiol*.
- Andrew, D. & Craig, A.D. (2002b) Quantitative responses of spinothalamic lamina I neurones to graded mechanical stimulation in the cat. *The Journal of Physiology*, **545**, 913–931.
- Apkarian, A.V. & Hodge, C.J. (1989) Primate spinothalamic pathways: I. A quantitative study of the cells of origin of the spinothalamic pathway. *J. Comp. Neurol*, **288**, 447–473.
- Arvidsson, J. & Pfaller, K. (1990) Central projections of C4–C8 dorsal root ganglia in the rat studied by anterograde transport of WGA-HRP. *J. Comp. Neurol*, **292**, 349–362.
- Azkue, J.J., Mateos, J.M., Elezgarai, I., Benítez, R., Lázaro, E., Streit, P., & Grandes, P. (1998) Glutamate-like immunoreactivity in ascending spinofugal afferents to the rat periaqueductal grey. *Brain Research*, **790**, 74–81.
- Bae, J.Y., Kim, J.H., Cho, Y.S., Mah, W., & Bae, Y.C. (2014) Quantitative analysis

- of afferents expressing substance P, calcitonin gene-related peptide, isolectin B4, neurofilament 200, and Peripherin in the sensory root of the rat trigeminal ganglion. *J. Comp. Neurol.*, **523**, 126–138.
- Bai, L., Xu, H., Collins, J.F., & Ghishan, F.K. (2001) Molecular and Functional Analysis of a Novel Neuronal Vesicular Glutamate Transporter. *J. Biol. Chem.*, **276**, 36764–36769.
- Bandler, K.R. (2007) Emotional and Behavioral Significance of the Pain Signal and the Role of the Midbrain Periaqueductal Gray (PAG). In Basbaum, A.I. & Bushnell, M.C. (eds), *The Senses: a Comprehensive Reference - Volume 5: Pain*. Academic Press, pp. 627–634.
- Basbaum, A.I. & Fields, H.L. (1979) The origin of descending pathways in the dorsolateral funiculus of the spinal cord of the cat and rat: further studies on the anatomy of pain modulation. *J. Comp. Neurol.*
- Basbaum, A.I. & Fields, H.L. (1984) Endogenous pain control systems: brainstem spinal pathways and endorphin circuitry. *Annu. Rev. Neurosci.*, **7**, 309–338.
- Basbaum, A.I. & Woolf, C.J. (1999) Pain. *Curr. Biol.*, **9**, R429–R431.
- Basbaum, A.I., Bautista, D.M., Scherrer, G., & Julius, D. (2009) Cellular and Molecular Mechanisms of Pain. *Cell*, **139**, 267–284.
- Bear, M.F., Connors, B.W., & Paradiso, M.A. (2011) *Neuroscience: Exploring the Brain*. Lippincott Williams and Wilkins.
- Beitel, R.E. & Dubner, R. (1976) Response of unmyelinated (C) polymodal nociceptors to thermal stimuli applied to monkey's face. *J. Neurophysiol.*, **39**, 1160–1175.
- Beitz, A.J. (1982) The nuclei of origin of brain stem enkephalin and substance P projections to the rodent nucleus raphe magnus. *NSC*, **7**, 2753–2768.
- Bellocchio, E.E., Hu, H., Pohorille, A., Chan, J., Pickel, V.M., & Edwards, R.H. (1998) The localization of the brain-specific inorganic phosphate transporter suggests a specific presynaptic role in glutamatergic transmission. *J. Neurosci.*, **18**, 8648–8659.
- Belmonte, C. & Viana, F. (2008) Molecular and cellular limits to somatosensory specificity. *Molecular Pain*, **4**, 14.
- Bennett, A.D., Chastain, K.M., & Hulsebosch, C.E. (2000) Alleviation of mechanical and thermal allodynia by CGRP<sub>8-37</sub> in a rodent model of chronic central pain. *Pain*.
- Bennett, G.J., Seltzer, Z., Lu, G.W., Nishikawa, N., & Dubner, R. (1983) The cells of origin of the dorsal column postsynaptic projection in the lumbosacral enlargements of cats and monkeys. *Somatosens Res*, **1**, 131–149.
- Bernard, J.F. & Besson, J.M. (1990) The spino (trigemino) pontoamygdaloid pathway: electrophysiological evidence for an involvement in pain processes. *J. Neurophysiol.*
- Bernard, J.F., Huang, G.F., & Besson, J.M. (1992) Nucleus centralis of the amygdala and the globus pallidus ventralis: electrophysiological evidence for an involvement in pain processes. *J. Neurophysiol.*, **68**, 551–569.
- Bernard, J.F., Peschanski, M., & Besson, J.M. (1989) A possible spino (trigemino)-ponto-amygdaloid pathway for pain. *Neuroscience Letters*, **100**, 83–88.
- Berthoud, H.R. & Powley, T.L. (1992) Vagal afferent innervation of the rat fundic stomach: morphological characterization of the gastric tension receptor. *J. Comp. Neurol.*, **319**, 261–276.
- Biella, G., Panara, C., Pecile, A., & Sotgiu, M.L. (1991) Facilitatory role of calcitonin gene-related peptide (CGRP) on excitation induced by substance P (SP) and noxious stimuli in rat spinal dorsal horn neurons. An iontophoretic

- study in vivo. *Brain Research*, **559**, 352–356.
- Bird, G.C., Han, J.S., Fu, Y., Adwanikar, H., Willis, W.D., & Neugebauer, V. (2006) Pain-related synaptic plasticity in spinal dorsal horn neurons: role of CGRP. *Molecular Pain*, **2**, 31.
- Black, J.A., Liu, S., Tanaka, M., Cummins, T.R., & Waxman, S.G. (2004) Changes in the expression of tetrodotoxin-sensitive sodium channels within dorsal root ganglia neurons in inflammatory pain. *Pain*, **108**, 237–247.
- Blyth, F.M., March, L.M., Brnabic, A.J., Jorm, L.R., Williamson, M., & Cousins, M.J. (2001) Chronic pain in Australia: a prevalence study. *Pain*, **89**, 127–134.
- Boucher, T.J. & McMahon, S.B. (2001) Neurotrophic factors and neuropathic pain. *Current Opinion in Pharmacology*, **1**, 66–72.
- Bowsher, D. (1957) Termination of the central pain pathway in man: the conscious appreciation of pain. *Brain*, **80**, 606–622.
- Bradbury, E.J., Burnstock, G., & McMahon, S.B. (1998) The Expression of P2X3 Purinoreceptors in Sensory Neurons: Effects of Axotomy and Glial-Derived Neurotrophic Factor. *Molecular and Cellular ...*, **12**, 256–268.
- Brain, S.D. & Grant, A.D. (2004) Vascular Actions of Calcitonin Gene-Related Peptide and Adrenomedullin. *Physiological Reviews*, **84**, 903–934.
- Brain, S.D. & Williams, T.J. (1985) Inflammatory oedema induced by synergism between calcitonin gene-related peptide (CGRP) and mediators of increased vascular permeability. *British Journal of Pharmacology*, **86**, 855–860.
- Bráz, J.M. & Basbaum, A.I. (2010) Differential ATF3 expression in dorsal root ganglion neurons reveals the profile of primary afferents engaged by diverse noxious chemical stimuli. *Pain*, **150**, 290–301.
- Breivik, H., Collett, B., Ventafridda, V., Cohen, R., & Gallacher, D. (2012) Survey of chronic pain in Europe: Prevalence, impact on daily life, and treatment. *European Journal of Pain*, **10**, 287–287.
- Brookes, S.J.H., Spencer, N.J., Costa, M., & Zagorodnyuk, V.P. (2013) Extrinsic primary afferent signalling in the gut. *Nature Reviews Gastroenterology & Hepatology*, 1–11.
- Brooks, J. & Tracey, I. (2005) REVIEW: from nociception to pain perception: imaging the spinal and supraspinal pathways. *Journal of Anatomy*.
- Brown, A.G. & Franz, D.N. (1969) Responses of spinocervical tract neurones to natural stimulation of identified cutaneous receptors. *Exp Brain Res*, **7**, 231–249.
- Brumovsky, P., Watanabe, M., & Hökfelt, T. (2007) Expression of the vesicular glutamate transporters-1 and -2 in adult mouse dorsal root ganglia and spinal cord and their regulation by nerve injury. *Neuroscience*, **147**, 469–490.
- Brumovsky, P.R., Robinson, D.R., La, J.-H., Seroogy, K.B., Lundgren, K.H., Albers, K.M., Kiyatkin, M.E., Seal, R.P., Edwards, R.H., Watanabe, M., Hökfelt, T., & Gebhart, G.F. (2011) Expression of vesicular glutamate transporters type 1 and 2 in sensory and autonomic neurons innervating the mouse colorectum. *J. Comp. Neurol*, **519**, 3346–3366.
- Burgess, P.R. & Perl, E.R. (1967) Myelinated afferent fibres responding specifically to noxious stimulation of the skin. *The Journal of Physiology*, **190**, 541–562.
- Burstein, R., Cliffer, K.D., & Giesler, G.J.J. (1990) Cells of origin of the spinothalamic tract in the rat. *J. Comp. Neurol*, **291**, 329–344.
- Burstein, R., Dado, R.J., Cliffer, K.D., & Giesler, G.J. (1991) Physiological characterization of spinothalamic tract neurons in the lumbar enlargement of rats. *J. Neurophysiol*, **66**, 261–284.
- Cameron, A.A., Khan, I.A., Westlund, K.N., & Willis, W.D. (1995) The efferent projections of the periaqueductal gray in the rat: a *Phaseolus vulgaris*-

- leucoagglutinin study. II. Descending projections. *J. Comp. Neurol*, **351**, 585–601.
- Cameron, A.A., Khan, I.A., Westlund, K.N., Cliffer, K.D., & Willis, W.D. (1995) The efferent projections of the periaqueductal gray in the rat: a Phaseolus vulgaris-leucoagglutinin study. I. Ascending projections. *J. Comp. Neurol*, **351**, 568–584.
- Cardenas, C.G., Del Mar, L.P., Cooper, B.Y., & Scroggs, R.S. (1997) 5HT<sub>4</sub> receptors couple positively to tetrodotoxin-insensitive sodium channels in a subpopulation of capsaicin-sensitive rat sensory neurons. *J. Neurosci*, **17**, 7181–7189.
- Carlton, S.M., McNeill, D.L., Chung, K., & Coggeshall, R.E. (1988) Organization of calcitonin gene-related peptide-immunoreactive terminals in the primate dorsal horn. *J. Comp. Neurol*, **276**, 527–536.
- Caterina, M.J., Leffler, A., Malmberg, A.B., Martin, W.J., Trafton, J., Petersen-Zeitz, K.R., Koltzenburg, M., Basbaum, A.I., & Julius, D. (2000) Impaired nociception and pain sensation in mice lacking the capsaicin receptor. *Science*, **288**, 306–313.
- Caterina, M.J., Rosen, T.A., Tominaga, M., Brake, A.J., & Julius, D. (1999) A capsaicin-receptor homologue with a high threshold for noxious heat. *Nature*, **398**, 436–441.
- Caterina, M.J., Schumacher, M.A., Tominaga, M., Rosen, T.A., Levine, J.D., & Julius, D. (1997) The capsaicin receptor: a heat-activated ion channel in the pain pathway. *Nature*, **389**, 816–824.
- Cavanaugh, D.J., Chesler, A.T., Bráz, J.M., Shah, N.M., Julius, D., & Basbaum, A.I. (2011) Restriction of Transient Receptor Potential Vanilloid-1 to the Peptidergic Subset of Primary Afferent Neurons Follows Its Developmental Downregulation in Nonpeptidergic Neurons. *Journal of Neuroscience*, **31**, 10119–10127.
- Cavanaugh, D.J., Lee, H., Lo, L., Shields, S.D., Zylka, M.J., Basbaum, A.I., & Anderson, D.J. (2009) Distinct subsets of unmyelinated primary sensory fibers mediate behavioral responses to noxious thermal and mechanical stimuli. *Proc. Natl. Acad. Sci. U.S.A.*, **106**, 9075–9080.
- Cervero, F. (2007) Pain Theories. In Basbaum, A.I. & Bushnell, M.C. (eds), *The Senses: a Comprehensive Reference - Volume 5: Pain*. Academic Press, pp. 5–10.
- Cervero, F. & Laird, J.M. (1991) One Pain or Many Pains? *Physiology*.
- Cervero, F., Handwerker, H.O., & Laird, J.M. (1988) Prolonged noxious mechanical stimulation of the rat's tail: responses and encoding properties of dorsal horn neurones. *The Journal of Physiology*, **404**, 419–436.
- Cervero, F., Iggo, A., & Molony, V. (1977) Responses of spinocervical tract neurones to noxious stimulation of the skin. *The Journal of Physiology*, **267**, 537–558.
- Chao, M.V. (2003) Neurotrophins and their receptors: A convergence point for many signalling pathways. *Nat. Rev. Neurosci*, **4**, 299–309.
- Cho, W.G. & Valtschanoff, J.G. (2008) Vanilloid receptor TRPV1-positive sensory afferents in the mouse ankle and knee joints. *Brain Research*, **1219**, 59–65.
- Christensen, B.N. & Perl, E.R. (1970) Spinal neurons specifically excited by noxious or thermal stimuli: marginal zone of the dorsal horn. *J. Neurophysiol*, **33**, 293–307.
- Christensen, M.D. & Hulsebosch, C.E. (1997) Chronic central pain after spinal cord injury. *J Neurotrauma*, **14**, 517–537.
- Chuang, H.H., Prescott, E.D., Kong, H., Shields, S., Jordt, S.E., Basbaum, A.I., Chao, M.V., & Julius, D. (2001) Bradykinin and nerve growth factor release the

- capsaicin receptor from PtdIns(4,5)P<sub>2</sub>-mediated inhibition. *Nature*, **411**, 957–962.
- Chung, K., Lee, W.T., & Carlton, S.M. (1988) The effects of dorsal rhizotomy and spinal cord isolation on calcitonin gene-related peptide-labeled terminals in the rat lumbar dorsal horn. *Neuroscience Letters*, **90**, 27–32.
- Chyczewski, M., Wojtkiewicz, J., Bossowska, A., Jałyński, M., Brzeski, W., Kowalski, I.M., & Majewski, M. (2006) Sources of porcine longissimus dorsi muscle (LDM) innervation as revealed by retrograde neuronal tract-tracing. *Folia Histochem. Cytobiol*, **44**, 189–194.
- Ciruela, A., Dixon, A.K., Bramwell, S., Gonzalez, M.I., Pinnock, R.D., & Lee, K. (2003) Identification of MEK1 as a novel target for the treatment of neuropathic pain. *British Journal of Pharmacology*, **138**, 751–756.
- Clark, F.M. & Proudfit, H.K. (1991) The projection of locus coeruleus neurons to the spinal cord in the rat determined by anterograde tracing combined with immunocytochemistry. *Brain Research*, **538**, 231–245.
- Clarke, J.N., Anderson, R.L., Haberberger, R.V., & Gibbins, I.L. (2011) Non-peptidergic small diameter primary afferents expressing VGlut2 project to lamina I of mouse spinal dorsal horn. *Molecular Pain*, **7**, 95.
- Coderre, T.J. (2007) Spinal Cord Mechanisms of Hyperalgesia and Allodynia. In Basbaum, A.I. & Bushnell, M.C. (eds), *The Senses: a Comprehensive Reference - Volume 5: Pain*. Academic Press, pp. 339–380.
- Coderre, T.J., Katz, J., Vaccarino, A.L., & Melzack, R. (1993) Contribution of central neuroplasticity to pathological pain: review of clinical and experimental evidence. *Pain*, **52**, 259–285.
- Commons, K.G. & Valentino, R.J. (2002) Cellular basis for the effects of substance P in the periaqueductal gray and dorsal raphe nucleus. *J. Comp. Neurol*, **447**, 82–97.
- Conrath, M., Taquet, H., Pohl, M., & Carayon, A. (1989) Immunocytochemical evidence for calcitonin gene-related peptide-like neurons in the dorsal horn and lateral spinal nucleus of the rat cervical spinal cord. *J. Chem. Neuroanat*, **2**, 335–347.
- Cridland, R.A. & Henry, J.L. (1988) Effects of intrathecal administration of neuropeptides on a spinal nociceptive reflex in the rat: VIP, galanin, CGRP, TRH, somatostatin and angiotensin II. *NEUROPEPTIDES*, **11**, 23–32.
- Crown, E.D., Ye, Z., Johnson, K.M., Xu, G.Y., McAdoo, D.J., Westlund, K.N., & Hulsebosch, C.E. (2005) Upregulation of the phosphorylated form of CREB in spinothalamic tract cells following spinal cord injury: Relation to central neuropathic pain. *Neuroscience Letters*, **384**, 139–144.
- Dai, Y., Fukuoka, T., Wang, H., Yamanaka, H., Obata, K., Tokunaga, A., & Noguchi, K. (2004) Contribution of sensitized P2X receptors in inflamed tissue to the mechanical hypersensitivity revealed by phosphorylated ERK in DRG neurons. *Pain*, **108**, 258–266.
- Darian-Smith, I., Johnson, K.O., LaMotte, C., Shigenaga, Y., Kenins, P., & Champness, P. (1979) Warm fibers innervating palmar and digital skin of the monkey: responses to thermal stimuli. *J. Neurophysiol*, **42**, 1297–1315.
- Davis, J.B., Gray, J., Gunthorpe, M.J., Hatcher, J.P., Davey, P.T., Overend, P., Harries, M.H., Latcham, J., Clapham, C., Atkinson, K., Hughes, S.A., Rance, K., Grau, E., Harper, A.J., Pugh, P.L., Rogers, D.C., Bingham, S., Randall, A., & Sheardown, S.A. (2000) Vanilloid receptor-1 is essential for inflammatory thermal hyperalgesia. *Nature*, **405**, 183–187.
- De Biasi, S. & Rustioni, A. (1990) Ultrastructural immunocytochemical localization

- of excitatory amino acids in the somatosensory system. *J. Histochem. Cytochem.*, **38**, 1745–1754.
- De Koninck, Y. & Henry, J.L. (1991) Substance P-mediated slow excitatory postsynaptic potential elicited in dorsal horn neurons in vivo by noxious stimulation. *Proc. Natl. Acad. Sci. U.S.A.*, **88**, 11344–11348.
- Debono, D.J., Hoeksema, L.J., & Hobbs, R.D. (2013) Caring for patients with chronic pain: pearls and pitfalls. *J Am Osteopath Assoc*, **113**, 620–627.
- Dhaka, A., Earley, T.J., Watson, J., & Patapoutian, A. (2008) Visualizing Cold Spots: TRPM8-Expressing Sensory Neurons and Their Projections. *Journal of Neuroscience*, **28**, 566–575.
- Ding, Y., Cesare, P., Drew, L., & Nikitaki, D. (2000) ATP, P2X receptors and pain pathways. *Journal of the autonomic ...*, **81**, 289–294.
- Djoughri, L. & Lawson, S.N. (2001) Differences in the size of the somatic action potential overshoot between nociceptive and non-nociceptive dorsal root ganglion neurones in the guinea-pig. *NSC*, **108**, 479–491.
- Djoughri, L. & Lawson, S.N. (2004) A $\beta$ -fiber nociceptive primary afferent neurons: a review of incidence and properties in relation to other afferent A-fiber neurons in mammals. *Brain Research Reviews*, **46**, 131–145.
- Djoughri, L., Bleazard, L., & Lawson, S.N. (1998) Association of somatic action potential shape with sensory receptive properties in guinea-pig dorsal root ganglion neurones. *The Journal of Physiology*, **513 ( Pt 3)**, 857–872.
- Doughty, S.E., Atkinson, M.E., & Shehab, S.A. (1991) A quantitative study of neuropeptide immunoreactive cell bodies of primary afferent sensory neurons following rat sciatic nerve peripheral axotomy. *Regul. Pept*, **35**, 59–72.
- Draxler, P., Honsek, S.D., Forsthuber, L., Hadschieff, V., & Sandkühler, J. (2014) VGlut3+ Primary Afferents Play Distinct Roles in Mechanical and Cold Hypersensitivity Depending on Pain Etiology. *J. Neurosci*, **34**, 12015–12028.
- Dubin, A.E. & Patapoutian, A. (2010) Nociceptors: the sensors of the pain pathway. *J. Clin. Invest*, **120**, 3760–3772.
- Dunn, P.M., Zhong, Y., & Burnstock, G. (2001) P2X receptors in peripheral neurons. *Progress in Neurobiology*, **65**, 107–134.
- Ebersberger, A., Charbel Issa, P., Vanegas, H., & Schaible, H.G. (2000) Differential effects of calcitonin gene-related peptide and calcitonin gene-related peptide 8-37 upon responses to N-methyl-D-aspartate or (R, S)-alpha-amino-3-hydroxy-5-methylisoxazole-4-propionate in spinal nociceptive neurons with knee joint input in the rat. *NSC*, **99**, 171–178.
- England, S., Bevan, S., & Docherty, R.J. (1996) PGE<sub>2</sub> modulates the tetrodotoxin-resistant sodium current in neonatal rat dorsal root ganglion neurones via the cyclic AMP-protein kinase A cascade. *The Journal of Physiology*, **495 ( Pt 2)**, 429–440.
- Euler, von, U.S. & Gaddum, J.H. (1931) An unidentified depressor substance in certain tissue extracts. *The Journal of Physiology*, 74–87.
- Fang, L., Wu, J., Zhang, X., Lin, Q., & Willis, W.D. (2005) Calcium/calmodulin dependent protein kinase II regulates the phosphorylation of cyclic AMP-responsive element-binding protein of spinal cord in rats following noxious stimulation. *Neuroscience Letters*, **374**, 1–4.
- Fernihough, J., Gentry, C., Bevan, S., & Winter, J. (2005) Regulation of calcitonin gene-related peptide and TRPV1 in a rat model of osteoarthritis. *Neuroscience Letters*, **388**, 75–80.
- Fields, H.L. & Heinricher, M.M. (1985) Anatomy and physiology of a nociceptive modulatory system. *Philos Trans R Soc Lond B Biol Sci*, **308**, 361–374.

- Finnerup, N.B., Sindrup, S.H., & Jensen, T.S. (2010) The evidence for pharmacological treatment of neuropathic pain. *Pain*, **150**, 573–581.
- Fitzgerald, M. & Lynn, B. (1977) The sensitization of high threshold mechanoreceptors with myelinated axons by repeated heating. *The Journal of Physiology*, **265**, 549–563.
- Flores, C.M., Leong, A.S., & Dussor, G.O. (2001) Capsaicin-evoked CGRP release from rat buccal mucosa: development of a model system for studying trigeminal mechanisms of neurogenic inflammation. *European Journal of ...*
- Floyd, K. & Morrison, J.F. (1974) Splanchnic mechanoreceptors in the dog. *Q J Exp Physiol Cogn Med Sci*, **59**, 361–366.
- Franco-Cereceda, A., Henke, H., Lundberg, J.M., Petermann, J.B., Hökfelt, T., & Fischer, J.A. (1987) Calcitonin gene-related peptide (CGRP) in capsaicin-sensitive substance P-immunoreactive sensory neurons in animals and man: distribution and release by capsaicin. *Peptides*, **8**, 399–410.
- Fried, G., Franck, J., Brodin, E., Born, W., Fischer, J.A., Hiort, W., & Hökfelt, T. (1989) Evidence for differential storage of calcitonin gene-related peptide, substance P and serotonin in synaptosomal vesicles of rat spinal cord. *Brain Research*, **499**, 315–324.
- Fujii, Y., Ozaki, N., Taguchi, T., Mizumura, K., Furukawa, K., & Sugiura, Y. (2008) TRP channels and ASICs mediate mechanical hyperalgesia in models of inflammatory muscle pain and delayed onset muscle soreness. *Pain*, **140**, 292–304.
- Fundin, B.T., Arvidsson, J., Aldskogius, H., Johansson, O., Rice, S.N., & Rice, F.L. (1997) Comprehensive immunofluorescence and lectin binding analysis of intervibrissal fur innervation in the mystacial pad of the rat. *J. Comp. Neurol*, **385**, 185–206.
- Galan, A., Lopez-Garcia, J.A., Cervero, F., & Laird, J.M.A. (2002) Activation of spinal extracellular signaling-regulated kinase-1 and -2 by intraplantar carrageenan in rodents. *Neuroscience Letters*, **322**, 37–40.
- Gamse, R. & Saria, A. (1985) Potentiation of tachykinin-induced plasma protein extravasation by calcitonin gene-related peptide. *Eur. J. Pharmacol*, **114**, 61–66.
- Gamse, R. & Saria, A. (1986) Nociceptive behavior after intrathecal injections of substance P, neurokinin A and calcitonin gene-related peptide in mice. *Neuroscience Letters*, **70**, 143–147.
- Gao, Y.-J. & Ji, R.-R. (2009) c-Fos or pERK, Which is a Better Marker for Neuronal Activation and Central Sensitization After Noxious Stimulation and Tissue Injury? *TOPAINJ*, **2**, 11–17.
- Gardell, L.R., Vanderah, T.W., Gardell, S.E., Wang, R., Ossipov, M.H., Lai, J., & Porreca, F. (2003) Enhanced evoked excitatory transmitter release in experimental neuropathy requires descending facilitation. *Journal of Neuroscience*, **23**, 8370–8379.
- Garry, M.G., Miller, K.E., & Seybold, V.S. (1989) Lumbar dorsal root ganglia of the cat: a quantitative study of peptide immunoreactivity and cell size. *J. Comp. Neurol*, **284**, 36–47.
- Gebhart, G.F. (2004) Descending modulation of pain. *Neuroscience & Biobehavioral Reviews*, **27**, 729–737.
- Gebhart, G.F. & Bielefeldt, K. (2007) Visceral Pain. In Basbaum, A.I. & Bushnell, M.C. (eds), *The Senses: a Comprehensive Reference - Volume 5: Pain*. Academic Press, pp. 543–569.
- Gibbins, I.L., Furness, J.B., & Costa, M. (1987) Pathway-specific patterns of the co-existence of substance P, calcitonin gene-related peptide, cholecystokinin and

- dynorphin in neurons of the dorsal root ganglia of the guinea-pig. *Cell Tissue Res*, **248**, 417–437.
- Gibbins, I.L., Furness, J.B., Costa, M., MacIntyre, I., Hillyard, C.J., & Girgis, S. (1985) Co-localization of calcitonin gene-related peptide-like immunoreactivity with substance P in cutaneous, vascular and visceral sensory neurons of guinea pigs. *Neuroscience Letters*, **57**, 125–130.
- Gibbins, I.L., Jobling, P., Teo, E.H., Matthew, S.E., & Morris, J.L. (2003) Heterogeneous expression of SNAP-25 and synaptic vesicle proteins by central and peripheral inputs to sympathetic neurons. *J. Comp. Neurol*, **459**, 25–43.
- Gibbins, I.L., Wattchow, D., & Coventry, B. (1987) Two immunohistochemically identified populations of calcitonin gene-related peptide (CGRP)-immunoreactive axons in human skin. *Brain Research*, **414**, 143–148.
- Gibson, S.J., Polak, J.M., Anand, P., Blank, M.A., Morrison, J.F., Kelly, J.S., & Bloom, S.R. (1984) The distribution and origin of VIP in the spinal cord of six mammalian species. **5**, 201–207.
- Gibson, S.J., Polak, J.M., Bloom, S.R., & Wall, P.D. (1981) The distribution of nine peptides in rat spinal cord with special emphasis on the substantia gelatinosa and on the area around the central canal (lamina X). *J. Comp. Neurol*, **201**, 65–79.
- Gibson, S.J., Polak, J.M., Bloom, S.R., Sabate, I.M., Mulderry, P.M., Ghatei, M.A., McGregor, G.P., Morrison, J.F., Kelly, J.S., & Evans, R.M. (1984) Calcitonin gene-related peptide immunoreactivity in the spinal cord of man and of eight other species. *J. Neurosci*, **4**, 3101–3111.
- Gibson, S.J., Polak, J.M., Katagiri, T., Su, H., Weller, R.O., Brownell, D.B., Holland, S., Hughes, J.T., Kikuyama, S., & Ball, J. (1988) A comparison of the distributions of eight peptides in spinal cord from normal controls and cases of motor neurone disease with special reference to Onuf's nucleus. *Brain Research*, **474**, 255–278.
- Gillan, M. (2012) Distribution of sensory neurons containing calcitonin gene-related peptide without substance P in skeletal muscle of mice, B.Sci(Hons) thesis, Flinders University, Adelaide.
- Gold, M.S. & Caterina, M.J. (2007) Molecular Biology of the Nociceptor/Transduction. In Basbaum, A.I. & Bushnell, M.C. (eds), *The Senses: a Comprehensive Reference - Volume 5: Pain*. Academic Press, pp. 43–73.
- Gold, M.S., Reichling, D.B., Shuster, M.J., & Levine, J.D. (1996) Hyperalgesic agents increase a tetrodotoxin-resistant Na<sup>+</sup> current in nociceptors. *Proc. Natl. Acad. Sci. U.S.A.*, **93**, 1108–1112.
- Goldstein, M.E., House, S.B., & Gainer, H. (1991) NF-L and peripherin immunoreactivities define distinct classes of rat sensory ganglion cells. *J. Neurosci Res*, **30**, 92–104.
- Guinard, D., Usson, Y., Guillermet, C., & Saxod, R. (1998) Merkel complexes of human digital skin: three-dimensional imaging with confocal laser microscopy and double immunofluorescence. *J. Comp. Neurol*, **398**, 98–104.
- Guo, A., Vulchanova, L., Wang, J., Li, X., & Elde, R.P. (1999) Immunocytochemical localization of the vanilloid receptor 1 (VR1): relationship to neuropeptides, the P2X3 purinoceptor and IB4 binding sites. *Eur J Neurosci*, **11**, 946–958.
- Güler, A.D., Lee, H., Iida, T., Shimizu, I., Tominaga, M., & Caterina, M. (2002) Heat-evoked activation of the ion channel, TRPV4. *Journal of Neuroscience*, **22**, 6408–6414.
- Hains, B.C. (2004) Altered Sodium Channel Expression in Second-Order Spinal Sensory Neurons Contributes to Pain after Peripheral Nerve Injury. *J. Neurosci*, **24**, 4832–4839.

- Hains, B.C., Klein, J.P., Saab, C.Y., Craner, M.J., Black, J.A., & Waxman, S.G. (2003) Upregulation of Sodium Channel Nav1.3 and Functional Involvement in Neuronal Hyperexcitability Associated with Central Neuropathic Pain after Spinal Cord Injury. *J. Neurosci*, **23**, 8881–8892.
- Hammond, D.L. & Ruda, M.A. (1989) Developmental alterations in thermal nociceptive threshold and the distribution of immunoreactive calcitonin gene-related peptide and substance P after neonatal administration of capsaicin in the rat. *Neuroscience Letters*, **97**, 57–62.
- Hanesch, U. & Schaible, H.G. (1995) Effects of ankle joint inflammation on the proportion of calcitonin gene-related peptide (CGRP)-immunopositive perikarya in dorsal root ganglia. *Prog Brain Res*, **104**, 339–347.
- Harmann, P.A., Chung, K., Briner, R.P., Westlund, K.N., & Carlton, S.M. (1988) Calcitonin gene-related peptide (CGRP) in the human spinal cord: a light and electron microscopic analysis. *J. Comp. Neurol*, **269**, 371–380.
- Hathway, G. & Fitzgerald, M. (2007) The Development of Nociceptive Systems. In Basbaum, A.I. & Bushnell, M.C. (eds), *The Senses: a Comprehensive Reference - Volume 5: Pain*. Academic Press, pp. 133–145.
- Heinricher, M.M. (2004) Neural Basis for the Hyperalgesic Action of Cholecystokinin in the Rostral Ventromedial Medulla. *J. Neurophysiol*, **92**, 1982–1989.
- Herzog, E., Gilchrist, J., Gras, C., Muzerelle, A., Ravassard, P., Giros, B., Gaspar, P., & Mestikawy, El, S. (2004) Localization of VGLUT3, the vesicular glutamate transporter type 3, in the rat brain. *Neuroscience*, **123**, 983–1002.
- Hicks, G.A., Coldwell, J.R., Schindler, M., Ward, P.A.B., Jenkins, D., Lynn, P.A., Humphrey, P.P.A., & Blackshaw, L.A. (2002) Excitation of rat colonic afferent fibres by 5-HT(3) receptors. *The Journal of Physiology*, **544**, 861–869.
- Hildebrand, C., Fried, K., Tuisku, F., & Johansson, C.S. (1995) Teeth and tooth nerves. *Progress in Neurobiology*, **45**, 165–222.
- Hillman, P. & Wall, P.D. (1969) Inhibitory and excitatory factors influencing the receptive fields of lamina 5 spinal cord cells. *Exp Brain Res*, **9**, 284–306.
- Hoheisel, U. & Mense, S. (1987) Observations on the morphology of axons and somata of slowly conducting dorsal root ganglion cells in the cat. *Brain Research*, **423**, 269–278.
- Hoheisel, U., Mense, S., & Scherertzke, R. (1994) Calcitonin gene-related peptide-immunoreactivity in functionally identified primary afferent neurones in the rat. *Anat. Embryol*, **189**, 41–49.
- Hoheisel, U., Unger, T., & Mense, S. (2005) Excitatory and modulatory effects of inflammatory cytokines and neurotrophins on mechanosensitive group IV muscle afferents in the rat. *Pain*, **114**, 168–176.
- Holden, J.E. & Naleway, E. (2001) Microinjection of carbachol in the lateral hypothalamus produces opposing actions on nociception mediated by alpha(1)- and alpha(2)-adrenoceptors. *Brain Research*, **911**, 27–36.
- Holden, J.E., Schwartz, E.J., & Proudfit, H.K. (1999) Microinjection of morphine in the A7 catecholamine cell group produces opposing effects on nociception that are mediated by alpha1- and alpha2-adrenoceptors. *NSC*, **91**, 979–990.
- Holden, J.E., Van Poppel, A.Y., & Thomas, S. (2002) Antinociception from lateral hypothalamic stimulation may be mediated by NK(1) receptors in the A7 catecholamine cell group in rat. *Brain Research*, **953**, 195–204.
- Holmgren, S., Fritsche, R., Karila, P., Gibbins, I., Axelsson, M., Franklin, C., Grigg, G., & Nilsson, S. (1994) Neuropeptides in the Australian lungfish *Neoceratodus forsteri*: effects in vivo and presence in autonomic nerves. *Am. J. Physiol*, **266**,

- R1568–R1577.
- Holzer, P. (1998) Neurogenic vasodilatation and plasma leakage in the skin. *General Pharmacology: The Vascular System*.
- Honore, P., Wismer, C.T., Mikusa, J., Zhu, C.Z., Zhong, C., Gauvin, D.M., Gomtsyan, A., Kouhen, El, R., Lee, C.-H., Marsh, K., Sullivan, J.P., Faltynek, C.R., & Jarvis, M.F. (2005) A-425619 [1-isoquinolin-5-yl-3-(4-trifluoromethylbenzyl)-urea], a novel transient receptor potential type V1 receptor antagonist, relieves pathophysiological pain associated with inflammation and tissue injury in rats. *J. Pharmacol. Exp. Ther.*, **314**, 410–421.
- Hökfelt, T., Johansson, O., Ljungdahl, A., Lundberg, J.M., & Schultzberg, M. (1980) Peptidergic neurones. *Nature*, **284**, 515–521.
- Hökfelt, T., Wiesenfeld-Hallin, Z., Villar, M.J., & Melander, T. (1987) Increase of galanin-like immunoreactivity in rat dorsal root ganglion cells after peripheral axotomy. *Neuroscience Letters*, **83**, 217–220.
- Hökfelt, T., Zhang, X., Verge, V., Villar, M.J., Elde, R.P., Bartfai, T., Xu, X.-J., & Wiesenfeld-Hallin, Z. (1993) Coexistence and interaction of neuropeptides with substance P in primary sensory neurons, with special reference to galanin. *Regul. Pept.*, **46**, 76–80.
- Hu, H.-Z., Gu, Q., Wang, C., Colton, C.K., Tang, J., Kinoshita-Kawada, M., Lee, L.-Y., Wood, J.D., & Zhu, M.X. (2004) 2-aminoethoxydiphenyl borate is a common activator of TRPV1, TRPV2, and TRPV3. *J. Biol. Chem.*, **279**, 35741–35748.
- Hua, X.-Y., Salgado, K.F., Gu, G., Fitzsimmons, B., Kondo, I., Bartfai, T., & Yaksh, T.L. (2005) Mechanisms of antinociception of spinal galanin: how does galanin inhibit spinal sensitization? *NEUROPEPTIDES*, **39**, 211–216.
- Hunt, S.P., Pini, A., & Evan, G. (1987) Induction of c-fos-like protein in spinal cord neurons following sensory stimulation. *Nature*, **328**, 632–634.
- Hunter, J.C., Fontana, D.J., Hedley, L.R., Jasper, J.R., Lewis, R., Link, R.E., Secchi, R., Sutton, J., & Eglén, R.M. (1997) Assessment of the role of alpha2-adrenoceptor subtypes in the antinociceptive, sedative and hypothermic action of dexmedetomidine in transgenic mice. *British Journal of Pharmacology*, **122**, 1339–1344.
- Hylden, J., Hayashi, D.R., & Dubner, R. (1986) Physiology and morphology of the lamina I spinomesencephalic projection. *Journal of ...*
- Iggo, A. (1955) Tension receptors in the stomach and the urinary bladder. *The Journal of Physiology*, **128**, 593–607.
- Immke, D.C. & McCleskey, E.W. (2001) Lactate enhances the acid-sensing Na<sup>+</sup> channel on ischemia-sensing neurons. *Nat. Neurosci.*, **4**, 869–870.
- Ishida-Yamamoto, A., Senba, E., & Tohyama, M. (1988) Calcitonin gene-related peptide- and substance P-immunoreactive nerve fibers in Meissner's corpuscles of rats: an immunohistochemical analysis. *Brain Research*, **453**, 362–366.
- Issberner, U., Reeh, P.W., & Steen, K.H. (1996) Pain due to tissue acidosis: a mechanism for inflammatory and ischemic myalgia? *Neuroscience Letters*, **208**, 191–194.
- Jang, J. (2004) Involvement of peripherally released substance P and calcitonin gene-related peptide in mediating mechanical hyperalgesia in a traumatic neuropathy model of the rat. *Neuroscience Letters*, **360**, 129–132.
- Jankowski, M.P., Rau, K.K., Ekmann, K.M., Anderson, C.E., & Koerber, H.R. (2013) Comprehensive phenotyping of group III and IV muscle afferents in mouse. *J. Neurophysiol.*, **109**, 2374–2381.
- Jessell, T., Tsunoo, A., Kanazawa, I., & Otsuka, M. (1979) Substance P: depletion in

- the dorsal horn of rat spinal cord after section of the peripheral processes of primary sensory neurons. *Brain Research*, **168**, 247–259.
- Ji, R.-R. & Rupp, F. (1997) Phosphorylation of transcription factor CREB in rat spinal cord after formalin-induced hyperalgesia: relationship to c-fos induction. *J. Neurosci*, **17**, 1776–1785.
- Ji, R.-R. & Woolf, C.J. (2001) Neuronal Plasticity and Signal Transduction in Nociceptive Neurons: Implications for the Initiation and Maintenance of Pathological Pain. *Neurobiology of Disease*, **8**, 1–10.
- Ji, R.-R., Baba, H., Brenner, G.J., & Woolf, C.J. (1999) Nociceptive-specific activation of ERK in spinal neurons contributes to pain hypersensitivity. *Nat. Neurosci*, **2**, 1114–1119.
- Ji, R.-R., Befort, K., Brenner, G.J., & Woolf, C.J. (2002) ERK MAP kinase activation in superficial spinal cord neurons induces prodynorphin and NK-1 upregulation and contributes to persistent inflammatory pain hypersensitivity. *Journal of Neuroscience*, **22**, 478–485.
- Ji, R.-R., Samad, T.A., Jin, S.-X., Schmoll, R., & Woolf, C.J. (2002) p38 MAPK activation by NGF in primary sensory neurons after inflammation increases TRPV1 levels and maintains heat hyperalgesia. *Neuron*, **36**, 57–68.
- Jobling, P. & Gibbins, I.L. (1999) Electrophysiological and morphological diversity of mouse sympathetic neurons. *J. Neurophysiol*, **82**, 2747–2764.
- Jones, R.C.W., Xu, L., & Gebhart, G.F. (2005) The mechanosensitivity of mouse colon afferent fibers and their sensitization by inflammatory mediators require transient receptor potential vanilloid 1 and acid-sensing ion channel 3. *Journal of Neuroscience*, **25**, 10981–10989.
- Jones, S.L. (1991) Descending noradrenergic influences on pain. *Prog Brain Res*, **88**, 381–394.
- Ju, G., Hökfelt, T., Brodin, E., Fahrenkrug, J., Fischer, J.A., Frey, P., Elde, R.P., & Brown, J.C. (1987) Primary sensory neurons of the rat showing calcitonin gene-related peptide immunoreactivity and their relation to substance P-, somatostatin-, galanin-, vasoactive intestinal polypeptide- and cholecystokinin-immunoreactive ganglion cells. *Cell Tissue Res*, **247**, 417–431.
- Julius, D. & Basbaum, A.I. (2001) Molecular mechanisms of nociception. *Nature*, **413**, 203–210.
- Kamogawa, H. & Bennett, G.J. (1986) Dorsal column postsynaptic neurons in the cat are excited by myelinated nociceptors. *Brain Research*, **364**, 386–390.
- Kangrga, I. & Randic, M. (1990) Tachykinins and calcitonin gene-related peptide enhance release of endogenous glutamate and aspartate from the rat spinal dorsal horn slice. *J. Neurosci*, **10**, 2026–2038.
- Karim, F., Wang, C.C., & Gereau, R.W., IV (2001) Metabotropic glutamate receptor subtypes 1 and 5 are activators of extracellular signal-regulated kinase signaling required for inflammatory pain in mice. *Journal of Neuroscience*, **21**, 3771–3779.
- Katter, J.T., Burstein, R., & Giesler, G.J.J. (1991) The cells of origin of the spinothalamic tract in cats. *J. Comp. Neurol*, **303**, 101–112.
- Kaufman, M.P. & Rybicki, K.J. (1987) Discharge properties of group III and IV muscle afferents: their responses to mechanical and metabolic stimuli. *Circ. Res*, **61**, I60–I65.
- Kaufman, M.P., Longhurst, J.C., Rybicki, K.J., Wallach, J.H., & Mitchell, J.H. (1983) Effects of static muscular contraction on impulse activity of groups III and IV afferents in cats. *J Appl Physiol Respir Environ Exerc Physiol*, **55**, 105–112.

## Reference List

- Kawamura, M., Kuraishi, Y., Minami, M., & Satoh, M. (1989) Antinociceptive effect of intrathecally administered antiserum against calcitonin gene-related peptide on thermal and mechanical noxious stimuli in experimental hyperalgesic rats. *Brain Research*, **497**, 199–203.
- Kawasaki, Y., Kohno, T., & Ji, R.-R. (2006) Different effects of opioid and cannabinoid receptor agonists on C-fiber-induced extracellular signal-regulated kinase activation in dorsal horn neurons in normal and spinal nerve-ligated rats. *J. Pharmacol. Exp. Ther*, **316**, 601–607.
- Kawasaki, Y., Kohno, T., Zhuang, Z.-Y., Brenner, G.J., Wang, H., Van Der Meer, C., Befort, K., Woolf, C.J., & Ji, R.-R. (2004) Ionotropic and metabotropic receptors, protein kinase A, protein kinase C, and Src contribute to C-fiber-induced ERK activation and cAMP response element-binding protein phosphorylation in dorsal horn neurons, leading to central sensitization. *Journal of Neuroscience*, **24**, 8310–8321.
- Keeble, J., Russell, F., Curtis, B., Starr, A., Pintér, E., & Brain, S.D. (2005) Involvement of transient receptor potential vanilloid 1 in the vascular and hyperalgesic components of joint inflammation. *Arthritis Rheum*, **52**, 3248–3256.
- Kestell, G. (2009) Characterisation of sensory neurons containing calcitonin gene-related peptide without substance P in the cervical spinal cord and paw skin of mice.
- Kevetter, G.A. & Willis, W.D. (1982) Spinothalamic cells in the rat lumbar cord with collaterals to the medullary reticular formation. *Brain Research*, **238**, 181–185.
- Koetzner, L. (2004) Nonopioid Actions of Intrathecal Dynorphin Evoke Spinal Excitatory Amino Acid and Prostaglandin E2 Release Mediated by Cyclooxygenase-1 and -2. *J. Neurosci*, **24**, 1451–1458.
- Kovelowski, C.J., Ossipov, M.H., Sun, H., Lai, J., Malan, T.P., & Porreca, F. (2000) Supraspinal cholecystokinin may drive tonic descending facilitation mechanisms to maintain neuropathic pain in the rat. *Pain*, **87**, 265–273.
- Kow, L.M. & Pfaff, D.W. (1988) Neuromodulatory actions of peptides. *Annu. Rev. Pharmacol. Toxicol*, **28**, 163–188.
- Kruger, L., Perl, E.R., & Sedivec, M.J. (1981) Fine structure of myelinated mechanical nociceptor endings in cat hairy skin. *J. Comp. Neurol*, **198**, 137–154.
- Kruger, L., Silverman, J.D., Mantyh, P.W., Sternini, C., & Brecha, N.C. (1989) Peripheral patterns of calcitonin-gene-related peptide general somatic sensory innervation: cutaneous and deep terminations. *J. Comp. Neurol*, **280**, 291–302.
- Kuraishi, Y., Kawamura, M., Yamaguchi, T., Houtani, T., Kawabata, S., Futaki, S., Fujii, N., & Satoh, M. (1991) Intrathecal injections of galanin and its antiserum affect nociceptive response of rat to mechanical, but not thermal, stimuli. *Pain*, **44**, 321–324.
- Kuwasako, K., Cao, Y.-N., Nagoshi, Y., Kitamura, K., & Eto, T. (2004) Adrenomedullin receptors: pharmacological features and possible pathophysiological roles. *Peptides*, **25**, 2003–2012.
- Lai, J., Ossipov, M.H., Vanderah, T.W., Malan, T.P., & Porreca, F. (2001) Neuropathic pain: the paradox of dynorphin. *Mol. Interv*, **1**, 160–167.
- Lawson, S.N. & Waddell, P.J. (1991) Soma neurofilament immunoreactivity is related to cell size and fibre conduction velocity in rat primary sensory neurons. *The Journal of Physiology*, **435**, 41–63.
- Lawson, S.N., Crepps, B.A., & Perl, E.R. (1997) Relationship of substance P to afferent characteristics of dorsal root ganglion neurones in guinea-pig. *The Journal of Physiology*, **505 ( Pt 1)**, 177–191.

- Lawson, S.N., Crepps, B.A., & Perl, E.R. (2002) Calcitonin gene-related peptide immunoreactivity and afferent receptive properties of dorsal root ganglion neurones in guinea-pigs. *The Journal of Physiology*, **540**, 989–1002.
- Lawson, S.N., Harper, A.A., Harper, E.I., Garson, J.A., & Anderton, B.H. (1984) A monoclonal antibody against neurofilament protein specifically labels a subpopulation of rat sensory neurones. *J. Comp. Neurol*, **228**, 263–272.
- Lawson, S.N., McCarthy, P.W., & Prabhakar, E. (1996) Electrophysiological properties of neurones with CGRP-like immunoreactivity in rat dorsal root ganglia. *J. Comp. Neurol*, **365**, 355–366.
- Le Bars, D. & Cadden, S.W. (2007) What is a Wide-Dynamic-Range Cell? In Basbaum, A.I. & Bushnell, M.C. (eds), *The Senses: a Comprehensive Reference - Volume 5: Pain*. Academic Press, pp. 331–338.
- Le Greves, P., Nyberg, F., Terenius, L., & Hökfelt, T. (1985) Calcitonin gene-related peptide is a potent inhibitor of substance P degradation. *Eur. J. Pharmacol*, **115**, 309–311.
- Lee, H. (2005) Altered Thermal Selection Behavior in Mice Lacking Transient Receptor Potential Vanilloid 4. *Journal of Neuroscience*, **25**, 1304–1310.
- Lee, S.E. & Kim, J.-H. (2007) Involvement of substance P and calcitonin gene-related peptide in development and maintenance of neuropathic pain from spinal nerve injury model of rat. *Neuroscience Research*, **58**, 245–249.
- Levine, J.D. & Alessandri-Haber, N. (2007) TRP channels: Targets for the relief of pain. *Biochimica et Biophysica Acta (BBA) - Molecular Basis of Disease*, **1772**, 989–1003.
- Lewinter, R.D., Scherrer, G., & Basbaum, A.I. (2008) Dense transient receptor potential cation channel, vanilloid family, type 2 (TRPV2) immunoreactivity defines a subset of motoneurons in the dorsal lateral nucleus of the spinal cord, the nucleus ambiguus and the trigeminal motor nucleus in rat. *Neuroscience*, **151**, 164–173.
- Lewinter, R.D., Skinner, K., Julius, D., & Basbaum, A.I. (2004) Immunoreactive TRPV-2 (VRL-1), a capsaicin receptor homolog, in the spinal cord of the rat. *J. Comp. Neurol*, **470**, 400–408.
- Li, Y., Dorsi, M.J., Meyer, R.A., & Belzberg, A.J. (2000) Mechanical hyperalgesia after an L5 spinal nerve lesion in the rat is not dependent on input from injured nerve fibers. *Pain*, **85**, 493–502.
- Liedtke, W., Tobin, D.M., Bargmann, C.I., & Friedman, J.M. (2003) Mammalian TRPV4 (VR-OAC) directs behavioral responses to osmotic and mechanical stimuli in *Caenorhabditis elegans*. *Proc. Natl. Acad. Sci. U.S.A.*, **100 Suppl 2**, 14531–14536.
- Light, A.R. (1992) *Pain and Headache, Volume 12 - the Initial Processing of Pain and Its Descending Control: Spinal and Trigeminal Systems*. Karger, Chapel Hill, NC.
- Light, A.R. & Durkovic, R.G. (1984) Features of laminar and somatotopic organization of lumbar spinal cord units receiving cutaneous inputs from hindlimb receptive fields. *J. Neurophysiol*, **52**, 449–458.
- Light, A.R. & Perl, E.R. (1979) Spinal termination of functionally identified primary afferent neurons with slowly conducting myelinated fibers. *J. Comp. Neurol*, **186**, 133–150.
- Light, A.R. & Willcockson, H.H. (1999) Spinal laminae I-II neurons in rat recorded in vivo in whole cell, tight seal configuration: properties and opioid responses. *J. Neurophysiol*, **82**, 3316–3326.
- Light, A.R., Huguen, R.W., Zhang, J., Rainier, J., Liu, Z., & Lee, J. (2008) Dorsal

- Root Ganglion Neurons Innervating Skeletal Muscle Respond to Physiological Combinations of Protons, ATP, and Lactate Mediated by ASIC, P2X, and TRPV1. *J. Neurophysiol*, **100**, 1184–1201.
- Lima, D. (2007) Ascending Pathways: Anatomy and Physiology. In Bushnell, M.C. & Basbaum, A.I. (eds), *The Senses: a Comprehensive Reference - Volume 5: Pain*. Academic Press, pp. 477–526.
- Lindsay, R.M. & Harmar, A.J. (1989) Nerve growth factor regulates expression of neuropeptide genes in adult sensory neurons. *Nature*, **337**, 362–364.
- Liu, C.N., Raber, P., Ziv-Sefer, S., & Devor, M. (2001) Hyperexcitability in sensory neurons of rats selected for high versus low neuropathic pain phenotype. *NSC*, **105**, 265–275.
- Liu, X.H. & Morris, R. (1999) Vasoactive intestinal polypeptide produces depolarization and facilitation of C-fibre evoked synaptic responses in superficial dorsal horn neurones (laminae I-IV) of the rat lumbar spinal cord in vitro. *Neuroscience Letters*, **276**, 1–4.
- Lonze, B.E. & Ginty, D.D. (2002) Function and regulation of CREB family transcription factors in the nervous system. *Neuron*, **35**, 605–623.
- Lovick, T.A. (1993) Integrated activity of cardiovascular and pain regulatory systems: role in adaptive behavioural responses. *Progress in Neurobiology*, **40**, 631–644.
- Löken, L.S., Wessberg, J., Morrison, I., McGlone, F., & Olausson, H. (2009) Coding of pleasant touch by unmyelinated afferents in humans. *Nat. Neurosci*, **12**, 547–548.
- Luebke, A.E., Dahl, G.P., Roos, B.A., & Dickerson, I.M. (1996) Identification of a protein that confers calcitonin gene-related peptide responsiveness to oocytes by using a cystic fibrosis transmembrane conductance regulator assay. *Proc. Natl. Acad. Sci. U.S.A.*, **93**, 3455–3460.
- Lundberg, J.M., Franco-Cereceda, A., Hua, X.-Y., Hökfelt, T., & Fischer, J.A. (1985) Co-existence of substance P and calcitonin gene-related peptide-like immunoreactivities in sensory nerves in relation to cardiovascular and bronchoconstrictor effects of capsaicin. *Eur. J. Pharmacol*, **108**, 315–319.
- Lynn, B. & Carpenter, S.E. (1982) Primary afferent units from the hairy skin of the rat hind limb. *Brain Research*, **238**, 29–43.
- Ma, W. & Bisby, M.A. (1997) Differential expression of galanin immunoreactivities in the primary sensory neurons following partial and complete sciatic nerve injuries. *NSC*, **79**, 1183–1195.
- Ma, W. & Bisby, M.A. (1998) Increase of calcitonin gene-related peptide immunoreactivity in the axonal fibers of the gracile nuclei of adult and aged rats after complete and partial sciatic nerve injuries. *Exp. Neurol*, **152**, 137–149.
- Ma, W. & Quirion, R. (2001) Increased phosphorylation of cyclic AMP response element-binding protein (CREB) in the superficial dorsal horn neurons following partial sciatic nerve ligation. *Pain*, **93**, 295–301.
- Ma, W. & Quirion, R. (2002) Partial sciatic nerve ligation induces increase in the phosphorylation of extracellular signal-regulated kinase (ERK) and c-Jun N-terminal kinase (JNK) in astrocytes in the lumbar spinal dorsal horn and the gracile nucleus. *Pain*, **99**, 175–184.
- Ma, W. & Quirion, R. (2006) Increased calcitonin gene-related peptide in neuroma and invading macrophages is involved in the up-regulation of interleukin-6 and thermal hyperalgesia in a rat model of mononeuropathy. *Journal of Neurochemistry*, **98**, 180–192.
- Ma, W., Chabot, J.-G., Schorscher-Petcu, A., Hong, Y., Wang, Z., & Quirion, R.

- (2009) CGRP and Adrenomedullin as Pain-Related Peptides. In Hay, D.L. & Dickerson, I.M. (eds), *The Calcitonin Gene-Related Peptide Family: Form, Function and Future Perspectives*. Springer Netherlands, Dordrecht, pp. 151–171.
- Ma, W., Chabot, J.G., Powell, K.J., Jhamandas, K., Dickerson, I.M., & Quirion, R. (2003) Localization and modulation of calcitonin gene-related peptide-receptor component protein-immunoreactive cells in the rat central and peripheral nervous systems. *Neuroscience*, **120**, 677–694.
- Ma, W., Ramer, M.S., & Bisby, M.A. (1999) Increased calcitonin gene-related peptide immunoreactivity in gracile nucleus after partial sciatic nerve injury: age-dependent and originating from spared sensory neurons. *Exp. Neurol*, **159**, 459–473.
- Ma, W., Ribeiro-da-Silva, A., Noel, G., Julien, J.P., & Cuello, A.C. (1995) Ectopic substance P and calcitonin gene-related peptide immunoreactive fibres in the spinal cord of transgenic mice over-expressing nerve growth factor. *Eur J Neurosci*, **7**, 2021–2035.
- Malin, S.A., Christianson, J.A., Bielefeldt, K., & Davis, B.M. (2009) TPRV1 expression defines functionally distinct pelvic colon afferents. *Journal of Neuroscience*, **29**, 743–752.
- Mantyh, P.W. (1997) Inhibition of Hyperalgesia by Ablation of Lamina I Spinal Neurons Expressing the Substance P Receptor. *Science*, **278**, 275–279.
- Marshall, G.E., Shehab, S.A., Spike, R.C., & Todd, A.J. (1996) Neurokinin-1 receptors on lumbar spinothalamic neurons in the rat. *NSC*, **72**, 255–263.
- Mason, R.T., Peterfreund, R.A., Sawchenko, P.E., Corrigan, A.Z., Rivier, J.E., & Vale, W.W. (1984) Release of the predicted calcitonin gene-related peptide from cultured rat trigeminal ganglion cells. *Nature*, **308**, 653–655.
- Matsuyama, T., Wanaka, A., Yoneda, S., Kimura, K., Kamada, T., Girgis, S., MacIntyre, I., Emson, P.C., & Tohyama, M. (1986) Two distinct calcitonin gene-related peptide-containing peripheral nervous systems: distribution and quantitative differences between the iris and cerebral artery with special reference to substance P. *Brain Research*, **373**, 205–212.
- McCarthy, P.W. & Lawson, S.N. (1989) Cell type and conduction velocity of rat primary sensory neurons with substance P-like immunoreactivity. *Neuroscience*, **28**, 745–753.
- McCarthy, P.W. & Lawson, S.N. (1990) Cell type and conduction velocity of rat primary sensory neurons with calcitonin gene-related peptide-like immunoreactivity. *Neuroscience*, **34**, 623–632.
- McCleskey, E.W. & Gold, M.S. (1999) Ion channels of nociception. *Annu. Rev. Physiol*, **61**, 835–856.
- McCoy, E.S., Taylor-Blake, B., & Zylka, M.J. (2012) CGRP $\alpha$ -Expressing Sensory Neurons Respond to Stimuli that Evoke Sensations of Pain and Itch. *PLoS ONE*, **7**, e36355.
- McGregor, G.P., Gibson, S.J., Sabate, I.M., Blank, M.A., Christofides, N.D., Wall, P.D., Polak, J.M., & Bloom, S.R. (1984) Effect of peripheral nerve section and nerve crush on spinal cord neuropeptides in the rat; increased VIP and PHI in the dorsal horn. *NSC*, **13**, 207–216.
- McKemy, D.D., Neuhauser, W.M., & Julius, D. (2002) Identification of a cold receptor reveals a general role for TRP channels in thermosensation. *Nature*, **416**, 52–58.
- McLatchie, L.M., Fraser, N.J., Main, M.J., Wise, A., Brown, J., Thompson, N., Solari, R., Lee, M.G., & Foord, S.M. (1998) RAMPs regulate the transport and

- ligand specificity of the calcitonin-receptor-like receptor. *Nature*, **393**, 333–339.
- McNamara, C.R., Mandel-Brehm, J., Bautista, D.M., Siemens, J., Deranian, K.L., Zhao, M., Hayward, N.J., Chong, J.A., Julius, D., Moran, M.M., & Fanger, C.M. (2007) TRPA1 mediates formalin-induced pain. *Proc. Natl. Acad. Sci. U.S.A.*, **104**, 13525–13530.
- McNeill, D.L., Carlton, S.M., & Hulsebosch, C.E. (1991) Intrasprouting of calcitonin gene-related peptide containing primary afferents after deafferentation in the rat. *Exp. Neurol*, **114**, 321–329.
- Mendell, L.M. & Wall, P.D. (1965) Responses of single dorsal cord cells to peripheral cutaneous unmyelinated fibres. *Nature*, **206**, 97–99.
- Menétrey, D., Chaouch, A., Binder, D., & Besson, J.M. (1982) The origin of the spinomesencephalic tract in the rat: an anatomical study using the retrograde transport of horseradish peroxidase. *J. Comp. Neurol*, **206**, 193–207.
- Menétrey, D., Giesler, G.J.J., & Besson, J.M. (1977) An analysis of response properties of spinal cord dorsal horn neurones to nonnoxious and noxious stimuli in the spinal rat. *Exp Brain Res*, **27**, 15–33.
- Mense, S. (2007) Anatomy of Nociceptors. In Basbaum, A.I. & Bushnell, M.C. (eds), *The Senses: a Comprehensive Reference - Volume 5: Pain*. Academic Press, pp. 11–41.
- Mense, S. (2008) Muscle pain: mechanisms and clinical significance. *Dtsch Arztebl Int*, **105**, 214–219.
- Mense, S. (2009) Algesic agents exciting muscle nociceptors. *Exp Brain Res*, **196**, 89–100.
- Mense, S. & Meyer, H. (1985) Different types of slowly conducting afferent units in cat skeletal muscle and tendon. *The Journal of Physiology*, **363**, 403–417.
- Merighi, A., Polak, J.M., Gibson, S.J., Gulbenkian, S., Valentino, K.L., & Peirone, S.M. (1988) Ultrastructural studies on calcitonin gene-related peptide-, tachykinins- and somatostatin-immunoreactive neurones in rat dorsal root ganglia: evidence for the colocalization of different peptides in single secretory granules. *Cell Tissue Res*, **254**, 101–109.
- Merskey, H. & Bogduk, N. (1994) *Classification of Chronic Pain*, Second Edition. edn. IASP Press, Seattle.
- Meyer, R.A. & Campbell, J.N. (1981) Myelinated nociceptive afferents account for the hyperalgesia that follows a burn to the hand. *Science*, **213**, 1527–1529.
- Michael, G.J. & Priestley, J.V. (1999) Differential expression of the mRNA for the vanilloid receptor subtype 1 in cells of the adult rat dorsal root and nodose ganglia and its downregulation by axotomy. *J. Neurosci*, **19**, 1844–1854.
- Micó, J.A., Ardid, D., Berrocoso, E., & Eschaliér, A. (2006) Antidepressants and pain. *Trends Pharmacol. Sci*, **27**, 348–354.
- Miki, K., Fukuoka, T., Tokunaga, A., & Noguchi, K. (1998) Calcitonin gene-related peptide increase in the rat spinal dorsal horn and dorsal column nucleus following peripheral nerve injury: up-regulation in a subpopulation of primary afferent sensory neurons. *NSC*, **82**, 1243–1252.
- Miletic, G. & Miletic, V. (2002) Increases in the concentration of brain derived neurotrophic factor in the lumbar spinal dorsal horn are associated with pain behavior following chronic constriction injury in rats. *Neuroscience Letters*, **319**, 137–140.
- Miletic, G., Hanson, E.N., Savagian, C.A., & Miletic, V. (2004) Protein kinase A contributes to sciatic ligation-associated early activation of cyclic AMP response element binding protein in the rat spinal dorsal horn. *Neuroscience Letters*, **360**, 149–152.

- Miletic, V. & Tan, H. (1988) Iontophoretic application of calcitonin gene-related peptide produces a slow and prolonged excitation of neurons in the cat lumbar dorsal horn. *Brain Research*, **446**, 169–172.
- Millan, M.J. (2002) Descending control of pain. *Progress in Neurobiology*.
- Millard, C.L. & Woolf, C.J. (1988) Sensory innervation of the hairs of the rat hindlimb: a light microscopic analysis. *J. Comp. Neurol*, **277**, 183–194.
- Miranda, A., Nordstrom, E., Mannem, A., Smith, C., Banerjee, B., & Sengupta, J.N. (2007) The role of transient receptor potential vanilloid 1 in mechanical and chemical visceral hyperalgesia following experimental colitis. *Neuroscience*, **148**, 1021–1032.
- Miyabe, T. & Miletic, V. (2005) Multiple kinase pathways mediate the early sciatic ligation-associated activation of CREB in the rat spinal dorsal horn. *Neuroscience Letters*, **381**, 80–85.
- Molander, C., Xu, Q., & Grant, G. (1984) The cytoarchitectonic organization of the spinal cord in the rat. I. The lower thoracic and lumbosacral cord. *J. Comp. Neurol*, **230**, 133–141.
- Molander, C., Xu, Q., Rivero-Melian, C., & Grant, G. (1989) Cytoarchitectonic organization of the spinal cord in the rat: II. The cervical and upper thoracic cord. *J. Comp. Neurol*, **289**, 375–385.
- Moqrich, A., Hwang, S.W., Earley, T.J., Petrus, M.J., Murray, A.N., Spencer, K.S.R., Andahazy, M., Story, G.M., & Patapoutian, A. (2005) Impaired thermosensation in mice lacking TRPV3, a heat and camphor sensor in the skin. *Science*, **307**, 1468–1472.
- Morris, J.L., Gibbins, I.L., & Holmgren, S. (1992) Galanin is more common than NPY in vascular sympathetic neurons of the brush-tailed possum. *Regul. Pept*, **37**, 101–109.
- Morris, J.L., König, P., Shimizu, T., Jobling, P., & Gibbins, I.L. (2005) Most peptide-containing sensory neurons lack proteins for exocytotic release and vesicular transport of glutamate. *J. Comp. Neurol*, **483**, 1–16.
- Morton, C.R. & Hutchison, W.D. (1989) Release of sensory neuropeptides in the spinal cord: studies with calcitonin gene-related peptide and galanin. *NSC*, **31**, 807–815.
- Morton, C.R. & Hutchison, W.D. (1990) Morphine does not reduce the intraspinal release of calcitonin gene-related peptide in the cat. *Neuroscience Letters*, **117**, 319–324.
- Mulderry, P.K., Ghatei, M.A., Spokes, R.A., Jones, P.M., Pierson, A.M., Hamid, Q.A., Kanse, S., Amara, S.G., Burrin, J.M., & Legon, S. (1988) Differential expression of alpha-CGRP and beta-CGRP by primary sensory neurons and enteric autonomic neurons of the rat. *NSC*, **25**, 195–205.
- Munger, B.L. (1982) Multiple afferent innervation of primate facial hairs--Henry Head and Max von Frey revisited. *Brain Research*, **257**, 1–43.
- Murphy, S.M., Matthew, S.E., Rodgers, H.F., Liturei, D.T., & Gibbins, I.L. (1998) Synaptic organisation of neuropeptide-containing preganglionic boutons in lumbar sympathetic ganglia of guinea pigs. *J. Comp. Neurol*, **398**, 551–567.
- Nahin, R.L. & Byers, M.R. (1994) Adjuvant-induced inflammation of rat paw is associated with altered calcitonin gene-related peptide immunoreactivity within cell bodies and peripheral endings of primary afferent neurons. *J. Comp. Neurol*, **349**, 475–485.
- National Health and Medical Research Council (2013) Australian code for the care and use of animals for scientific purposes. National Health and Medical Research Council, Canberra.

## Reference List

- Neubert, M.J., Kincaid, W., & Heinricher, M.M. (2004) Nociceptive facilitating neurons in the rostral ventromedial medulla. *Pain*, **110**, 158–165.
- Neumann, S., Doubell, T.P., Leslie, T., & Woolf, C.J. (1996) Inflammatory pain hypersensitivity mediated by phenotypic switch in myelinated primary sensory neurons. *Nature*, **384**, 360–364.
- Nichols, M.L. (1999) Transmission of Chronic Nociception by Spinal Neurons Expressing the Substance P Receptor. *Science*, **286**, 1558–1561.
- Noguchi, K., Senba, E., Morita, Y., Sato, M., & Tohyama, M. (1990) Alpha-CGRP and beta-CGRP mRNAs are differentially regulated in the rat spinal cord and dorsal root ganglion. *Brain Res. Mol. Brain Res*, **7**, 299–304.
- Nordin, M. (1990) Low-threshold mechanoreceptive and nociceptive units with unmyelinated (C) fibres in the human supraorbital nerve. *The Journal of Physiology*, **426**, 229–240.
- Nyberg, G. & Blomqvist, A. (1985) The somatotopic organization of forelimb cutaneous nerves in the brachial dorsal horn: an anatomical study in the cat. *J. Comp. Neurol*, **242**, 28–39.
- Obata, K. (2004) Role of Mitogen-Activated Protein Kinase Activation in Injured and Intact Primary Afferent Neurons for Mechanical and Heat Hypersensitivity after Spinal Nerve Ligation. *J. Neurosci*, **24**, 10211–10222.
- Obata, K., Yamanaka, H., Dai, Y., Mizushima, T., Fukuoka, T., Tokunaga, A., & Noguchi, K. (2004) Differential activation of MAPK in injured and uninjured DRG neurons following chronic constriction injury of the sciatic nerve in rats. *Eur J Neurosci*, **20**, 2881–2895.
- Obata, K., Yamanaka, H., Dai, Y., Tachibana, T., Fukuoka, T., Tokunaga, A., Yoshikawa, H., & Noguchi, K. (2003) Differential activation of extracellular signal-regulated protein kinase in primary afferent neurons regulates brain-derived neurotrophic factor expression after peripheral inflammation and nerve injury. *Journal of Neuroscience*, **23**, 4117–4126.
- Ogata, N. & Tatebayashi, H. (1993) Kinetic analysis of two types of Na<sup>+</sup> channels in rat dorsal root ganglia. *The Journal of Physiology*, **466**, 9–37.
- Oku, R., Satoh, M., Fujii, N., Otaka, A., Yajima, H., & Takagi, H. (1987) Calcitonin gene-related peptide promotes mechanical nociception by potentiating release of substance P from the spinal dorsal horn in rats. *Brain Research*, **403**, 350–354.
- Oliveira, A.L.R., Hydling, F., Olsson, E., Shi, T., Edwards, R.H., Fujiyama, F., Kaneko, T., H kfelt, T., Cullheim, S., & Meister, B.R. (2003) Cellular localization of three vesicular glutamate transporter mRNAs and proteins in rat spinal cord and dorsal root ganglia. *Synapse*, **50**, 117–129.
- Ospina, M. & Harstall, C. (2003) *How Prevalent Is Chronic Pain*. IASP.
- Ossipov, M.H. & Porreca, F. (2007) Neuropathic Pain: Basic Mechanisms (Animal). In Basbaum, A.I. & Bushnell, M.C. (eds), *The Senses: a Comprehensive Reference - Volume 5: Pain*. Academic Press, pp. 833–855.
- Ossipov, M.H., Zhang, E.-T., Carvajal, C., Gardell, L., Quirion, R., Dumont, Y., Lai, J., & Porreca, F. (2002) Selective mediation of nerve injury-induced tactile hypersensitivity by neuropeptide Y. *Journal of Neuroscience*, **22**, 9858–9867.
- Page, A.J. & Blackshaw, L.A. (1998) An in vitro study of the properties of vagal afferent fibres innervating the ferret oesophagus and stomach. *The Journal of Physiology*, **512 ( Pt 3)**, 907–916.
- Paik, S.K., Lee, D.S., Kim, J.Y., Bae, J.Y., Cho, Y.S., Ahn, D.K., Yoshida, A., & Bae, Y.C. (2010) Quantitative ultrastructural analysis of the neurofilament 200-positive axons in the rat dental pulp. *J Endod*, **36**, 1638–1642.
- Paintal, A.S. (1957) Responses from mucosal mechanoreceptors in the small

- intestine of the cat. *The Journal of Physiology*, **139**, 353–368.
- Pannese, E. (1994) Shape and size of neurons. In *Neurocytology Fine Structure of Neurons, Nerve Processes, and Neuroglial Cells*. New York, pp. 11–14.
- Parameswaran, N., Disa, J., Spielman, W.S., Brooks, D.P., Nambi, P., & Aiyar, N. (2000) Activation of multiple mitogen-activated protein kinases by recombinant calcitonin gene-related peptide receptor. *Eur. J. Pharmacol*, **389**, 125–130.
- Paré, M., Elde, R.P., Mazurkiewicz, J.E., Smith, A.M., & Rice, F.L. (2001) The Meissner corpuscle revised: a multiafferented mechanoreceptor with nociceptor immunochemical properties. **21**, 7236–7246.
- Paré, M., Smith, A.M., & Rice, F.L. (2002) Distribution and terminal arborizations of cutaneous mechanoreceptors in the glabrous finger pads of the monkey. *J. Comp. Neurol*, **445**, 347–359.
- Patapoutian, A., Tate, S., & Woolf, C.J. (2009) Transient receptor potential channels: targeting pain at the source. *Nat Rev Drug Discov*, **8**, 55–68.
- Peier, A.M., Moqrich, A., Hergarden, A.C., Reeve, A.J., Andersson, D.A., Story, G.M., Earley, T.J., Dragoni, I., McIntyre, P., Bevan, S., & Patapoutian, A. (2002) A TRP channel that senses cold stimuli and menthol. *Cell*, **108**, 705–715.
- Peier, A.M., Reeve, A.J., Andersson, D.A., Moqrich, A., Earley, T.J., Hergarden, A.C., Story, G.M., Colley, S., Hogenesch, J.B., McIntyre, P., Bevan, S., & Patapoutian, A. (2002) A heat-sensitive TRP channel expressed in keratinocytes. *Science*, **296**, 2046–2049.
- Peng, Y.B., Ringkamp, M., Meyer, R.A., & Campbell, J.N. (2003) Fatigue and paradoxical enhancement of heat response in C-fiber nociceptors from cross-modal excitation. *Journal of Neuroscience*, **23**, 4766–4774.
- Perry, M.J. & Lawson, S.N. (1993) Neurofilament in feline primary afferent neurones: a quantitative immunocytochemical study. *Brain Research*, **607**, 307–313.
- Persson, S., Boulland, J.-L., Aspling, M., Larsson, M., Fremeau, R.T., Edwards, R.H., Storm-Mathisen, J., Chaudhry, F.A., & Broman, J. (2006) Distribution of vesicular glutamate transporters 1 and 2 in the rat spinal cord, with a note on the spinocervical tract. *J. Comp. Neurol*, **497**, 683–701.
- Pierce, L.M., Rankin, M.R., Foster, R.T., Dolber, P.C., Coates, K.W., Kuehl, T.J., & Thor, K.B. (2006) Distribution and immunohistochemical characterization of primary afferent neurons innervating the levator ani muscle of the female squirrel monkey. *American Journal of Obstetrics and Gynecology*, **195**, 987–996.
- Plenderleith, M.B., Haller, C.J., & Snow, P.J. (1990) Peptide coexistence in axon terminals within the superficial dorsal horn of the rat spinal cord. *Synapse*, **6**, 344–350.
- Pomeranz, B., Wall, P.D., & Weber, W.V. (1968) Cord cells responding to fine myelinated afferents from viscera, muscle and skin. *The Journal of Physiology*, **199**, 511.
- Poyner, D.R., Sexton, P.M., Marshall, I., Smith, D.M., Quirion, R., Born, W., Muff, R., Fischer, J.A., & Foord, S.M. (2002) International Union of Pharmacology. XXXII. The mammalian calcitonin gene-related peptides, adrenomedullin, amylin, and calcitonin receptors. *Pharmacological Reviews*, **54**, 233–246.
- Presley, R.W., Menétrey, D., Levine, J.D., & Basbaum, A.I. (1990) Systemic morphine suppresses noxious stimulus-evoked Fos protein-like immunoreactivity in the rat spinal cord. *J. Neurosci*, **10**, 323–335.
- Price, D.D. & Mayer, D.J. (1974) Physiological laminar organization of the dorsal horn of *M. mulatta*. *Brain Research*, **79**, 321–325.

- Price, J. (1985) An immunohistochemical and quantitative examination of dorsal root ganglion neuronal subpopulations. *J. Neurosci*, **5**, 2051–2059.
- Price, M.P., McIlwrath, S.L., Xie, J., Cheng, C., Qiao, J., Tarr, D.E., Sluka, K.A., Brennan, T.J., Lewin, G.R., & Welsh, M.J. (2001) The DRASIC cation channel contributes to the detection of cutaneous touch and acid stimuli in mice. *Neuron*, **32**, 1071–1083.
- Priestley, J.V. (2009) Neuropeptides: Sensory Systems. In Squire, L.R. (ed), *Encyclopedia of Neuroscience*. Academic Press, Oxford, pp. 935–943.
- Ralston, H.J. (1979) The fine structure of laminae I, II and III of the macaque spinal cord. *J. Comp. Neurol*, **184**, 619–641.
- Ramon, Y. & Cajal, S. (1909) *Histologie Du Systeme Nerveux De L'homme Et Des Vertebres*. Maloine.
- Ranson, S.W. (1913) The course within the spinal cord of the non-medullated fibers of the dorsal roots: A study of Lissauer's tract in the cat. *J. Comp. Neurol*.
- Ranson, S.W. (1914) The tract of Lissauer and the substantia gelatinosa Rolandi. *American Journal of Anatomy*.
- Ravnefjord, A., Brusberg, M., Kang, D., Bauer, U., Larsson, H., Lindström, E., & Martinez, V. (2009) Involvement of the transient receptor potential vanilloid 1 (TRPV1) in the development of acute visceral hyperalgesia during colorectal distension in rats. *Eur. J. Pharmacol*, **611**, 85–91.
- Reeh, P.W., Bayer, J., Kocher, L., & Handwerker, H.O. (1987) Sensitization of nociceptive cutaneous nerve fibers from the rat's tail by noxious mechanical stimulation. *Exp Brain Res*, **65**, 505–512.
- Reinert, A., Kaske, A., & Mense, S. (1998) Inflammation-induced increase in the density of neuropeptide-immunoreactive nerve endings in rat skeletal muscle. *Exp Brain Res*, **121**, 174–180.
- Ren, K. & Dubner, R. (2007) Descending Control Mechanisms. In Basbaum, A.I. & Bushnell, M.C. (eds), *The Senses: a Comprehensive Reference - Volume 5: Pain*. Academic Press, Oxford, pp. 724–764.
- Rexed, B. (1954) A cytoarchitectonic atlas of the spinal cord in the cat. *J. Comp. Neurol*, **100**, 297–379.
- Ribeiro-da-Silva, A. & De Koninck, Y. (2007) Morphological and Neurochemical Organization of the Spinal Dorsal Horn. In Basbaum, A.I. & Bushnell, M.C. (eds), *The Senses: a Comprehensive Reference - Volume 5: Pain*. Academic Press, pp. 279–310.
- Rice, F.L. & Albrecht, P.J. (2007) Cutaneous Mechanisms of Tactile Perception: Morphological and Chemical Organization of the Innervation to the Skin. In Kaas, J.H. & Gardner, E.P. (eds), *The Senses: a Comprehensive Reference - Volume 6: Somatosensation*. Academic Press, pp. 1–31.
- Rice, F.L. & Rasmusson, D.D. (2000) Innervation of the digit on the forepaw of the raccoon. *J. Comp. Neurol*, **417**, 467–490.
- Rice, F.L., Fundin, B.T., & Arvidsson, J. (1997) Comprehensive immunofluorescence and lectin binding analysis of vibrissal follicle sinus complex innervation in the mystacial pad of the rat. *Journal of ...*
- Ringkamp, M. & Meyer, R.A. (2007) Physiology of Nociceptors. In Basbaum, A.I. & Bushnell, M.C. (eds), *The Senses: a Comprehensive Reference - Volume 5: Pain*. Academic Press, pp. 97–114.
- Ritter, A.M. & Mendell, L.M. (1992) Somal membrane properties of physiologically identified sensory neurons in the rat: effects of nerve growth factor. *J. Neurophysiol*, **68**, 2033–2041.
- Rittner, H., Machelska, H., & Stein, C. (2007) Immune System, Pain and Analgesia.

- In Basbaum, A.I. & Bushnell, M.C. (eds), *The Senses: a Comprehensive Reference - Volume 5: Pain*. Academic Press, pp. 407–427.
- Rock, K.L. & Kono, H. (2008) The Inflammatory Response to Cell Death. *Annu. Rev. Pathol. Mech. Dis*, **3**, 99–126.
- Rosenfeld, M.G., Mermod, J.J., Amara, S.G., Swanson, L.W., Sawchenko, P.E., Rivier, J., Vale, W.W., & Evans, R.M. (1983) Production of a novel neuropeptide encoded by the calcitonin gene via tissue-specific RNA processing. *Nature*, **304**, 129–135.
- Ruscheweyh, R., Forsthuber, L., Schoffnegger, D., & Sandkühler, J. (2007) Modification of classical neurochemical markers in identified primary afferent neurons with A $\beta$ -, A $\delta$ -, and C-fibers after chronic constriction injury in mice. *J. Comp. Neurol*, **502**, 325–336.
- Russo, A.F., Nelson, C., Roos, B.A., & Rosenfeld, M.G. (1988) Differential regulation of the coexpressed calcitonin/alpha-CGRP and beta-CGRP neuroendocrine genes. *J. Biol. Chem*, **263**, 5–8.
- Rustioni, A., Hayes, N.L., & O'Neill, S. (1979) Dorsal column nuclei and ascending spinal afferents in macaques. *Brain*, **102**, 95–125.
- Ryu, P.D., Gerber, G., Murase, K., & Randic, M. (1988) Actions of calcitonin gene-related peptide on rat spinal dorsal horn neurons. *Brain Research*, **441**, 357–361.
- Salter, M.W. & Henry, J.L. (1991) Responses of functionally identified neurones in the dorsal horn of the cat spinal cord to substance P, neurokinin A and physalaemin. *NSC*, **43**, 601–610.
- Sammons, M.J., Raval, P., Davey, P.T., Rogers, D., Parsons, A.A., & Bingham, S. (2000) Carrageenan-induced thermal hyperalgesia in the mouse: role of nerve growth factor and the mitogen-activated protein kinase pathway. *Brain Research*, **876**, 48–54.
- Seal, R.P., Wang, X., Guan, Y., Raja, S.N., Woodbury, C.J., Basbaum, A.I., & Edwards, R.H. (2009) Injury-induced mechanical hypersensitivity requires C-low threshold mechanoreceptors. *Nature*, **462**, 651–655.
- Seybold, V.S. (2009) The role of peptides in central sensitization. *Sensory Nerves*, 451–491.
- Seybold, V.S., Galeazza, M.T., Garry, M.G., & Hargreaves, K.M. (1995) Plasticity of calcitonin gene related peptide neurotransmission in the spinal cord during peripheral inflammation. *Can J Physiol Pharmacol*, **73**, 1007–1014.
- Seybold, V.S., McCarson, K.E., Mermelstein, P.G., Groth, R.D., & Abrahams, L.G. (2003) Calcitonin gene-related peptide regulates expression of neurokinin 1 receptors by rat spinal neurons. *J. Neurosci*, **23**, 1816–1824.
- Shehab, S.A. & Atkinson, M.E. (1986) Vasoactive intestinal polypeptide (VIP) increases in the spinal cord after peripheral axotomy of the sciatic nerve originate from primary afferent neurons. *Brain Research*, **372**, 37–44.
- Sheng, M. & Greenberg, M.E. (1990) The regulation and function of c-fos and other immediate early genes in the nervous system. *Neuron*, **4**, 477–485.
- Siddall, P.J., Xu, C.L., Floyd, N., & Keay, K.A. (1999) C-fos expression in the spinal cord of rats exhibiting allodynia following contusive spinal cord injury. *Brain Research*, **851**, 281–286.
- Skirboll, L., Hökfelt, T., Dockray, G., Rehfeld, J., Brownstein, M., & Cuello, A.C. (1983) Evidence for periaqueductal cholecystinin-substance P neurons projecting to the spinal cord. *J. Neurosci*, **3**, 1151–1157.
- Skofitsch, G. & Jacobowitz, D.M. (1985) Calcitonin gene-related peptide coexists with substance P in capsaicin sensitive neurons and sensory ganglia of the rat. *Peptides*, **6**, 747–754.

- Snider, W.D. & McMahon, S.B. (1998) Tackling pain at the source: new ideas about nociceptors. *Neuron*, **20**, 629–632.
- Song, X.-S., Cao, J.-L., Xu, Y.-B., He, J.-H., Zhang, L.-C., & Zeng, Y.-M. (2005) Activation of ERK/CREB pathway in spinal cord contributes to chronic constrictive injury-induced neuropathic pain in rats. *Acta Pharmacologica Sinica*, **26**, 789–798.
- Souslova, V., Cesare, P., Ding, Y., Akopian, A.N., & Stanfa, L. (2000) Warm-coding deficits and aberrant inflammatory pain in mice lacking P2X<sub>3</sub> receptors. *Nature*, **407**, 1015–1017.
- Staton, P.C., Wilson, A.W., Bountra, C., Chessell, I.P., & Day, N.C. (2012) Changes in dorsal root ganglion CGRP expression in a chronic inflammatory model of the rat knee joint: Differential modulation by rofecoxib and paracetamol. *European Journal of Pain*, **11**, 283–289.
- Steen, K.H., Issberner, U., & Reeh, P.W. (1995) Pain due to experimental acidosis in human skin: evidence for non-adapting nociceptor excitation. *Neuroscience Letters*, **199**, 29–32.
- Steiner, T.J. & Turner, L.M. (1972) Cytoarchitecture of the rat spinal cord. *The Journal of Physiology*, **222**, 123P–125P.
- Story, G.M., Peier, A.M., Reeve, A.J., Eid, S.R., Mosbacher, J., Hricik, T.R., Earley, T.J., Hergarden, A.C., Andersson, D.A., Hwang, S.W., McIntyre, P., Jegla, T., Bevan, S., & Patapoutian, A. (2003) ANKTM1, a TRP-like channel expressed in nociceptive neurons, is activated by cold temperatures. *Cell*, **112**, 819–829.
- Sugimoto, T., Takemura, M., & Wakisaka, S. (1988) Cell size analysis of primary neurons innervating the cornea and tooth pulp of the rat. *Pain*, **32**, 375–381.
- Sugiura, Y., Terui, N., & Hosoya, Y. (1989) Difference in distribution of central terminals between visceral and somatic unmyelinated (C) primary afferent fibers. *J. Neurophysiol*, **62**, 834–840.
- Sun, H., Ren, K., Zhong, C.M., Ossipov, M.H., Malan, T.P., Lai, J., & Porreca, F. (2001) Nerve injury-induced tactile allodynia is mediated via ascending spinal dorsal column projections. *Pain*, **90**, 105–111.
- Sun, Q., Tu, H., Xing, G.-G., Han, J.-S., & Wan, Y. (2005) Ectopic discharges from injured nerve fibers are highly correlated with tactile allodynia only in early, but not late, stage in rats with spinal nerve ligation. *Exp. Neurol*, **191**, 128–136.
- Sun, R.-Q., Lawand, N.B., & Willis, W.D. (2003) The role of calcitonin gene-related peptide (CGRP) in the generation and maintenance of mechanical allodynia and hyperalgesia in rats after intradermal injection of capsaicin. *Pain*, **104**, 201–208.
- Sun, R.-Q., Lawand, N.B., Lin, Q., & Willis, W.D. (2004) Role of Calcitonin Gene-Related Peptide in the Sensitization of Dorsal Horn Neurons to Mechanical Stimulation After Intradermal Injection of Capsaicin. *J. Neurophysiol*, **92**, 320–326.
- Suzuki, M., Mizuno, A., Kodaira, K., & Imai, M. (2003) Impaired pressure sensation in mice lacking TRPV4. *J. Biol. Chem*, **278**, 22664–22668.
- Suzuki, R., Morcuende, S., Webber, M., Hunt, S.P., & Dickenson, A.H. (2002) Superficial NK1-expressing neurons control spinal excitability through activation of descending pathways. *Nat. Neurosci*, **5**, 1319–1326.
- Szallasi, A., Cortright, D.N., Blum, C.A., & Eid, S.R. (2007) The vanilloid receptor TRPV1: 10 years from channel cloning to antagonist proof-of-concept. *Nat Rev Drug Discov*, **6**, 357–372.
- Szallasi, A., Nilsson, S., Farkas-Szallasi, T., Blumberg, P.M., Hökfelt, T., & Lundberg, J.M. (1995) Vanilloid (capsaicin) receptors in the rat: distribution in the brain, regional differences in the spinal cord, axonal transport to the

- periphery, and depletion by systemic vanilloid treatment. *Brain Research*, **703**, 175–183.
- Szolcsányi, J. (1996) Capsaicin-sensitive sensory nerve terminals with local and systemic efferent functions: facts and scopes of an unorthodox neuroregulatory mechanism. *Prog Brain Res*, **113**, 343–359.
- Takamori, S., Rhee, J.S., Rosenmund, C., & Jahn, R. (2000) Identification of a vesicular glutamate transporter that defines a glutamatergic phenotype in neurons. *Nature*, **407**, 189–194.
- Takamori, S., Rhee, J.S., Rosenmund, C., & Jahn, R. (2001) Identification of differentiation-associated brain-specific phosphate transporter as a second vesicular glutamate transporter (VGLUT2). *Journal of Neuroscience*, **21**, RC182.
- Tam Tam, S., Bastian, I., Zhou, X.F., Vander Hoek, M., Michael, M.Z., Gibbins, I.L., & Haberberger, R.V. (2011) MicroRNA-143 expression in dorsal root ganglion neurons. *Cell Tissue Res*, **346**, 163–173.
- Tamatani, M., Senba, E., & Tohyama, M. (1989) Calcitonin gene-related peptide- and substance P-containing primary afferent fibers in the dorsal column of the rat. *Brain Research*, **495**, 122–130.
- Tassicker, B.C., Hennig, G.W., Costa, M., & Brookes, S.J.H. (1999) Rapid anterograde and retrograde tracing from mesenteric nerve trunks to the guinea-pig small intestine in vitro. *Cell Tissue Res*, **295**, 437–452.
- Thomas, P.M., Nasonkin, I., Zhang, H., Gagel, R.F., & Cote, G.J. (2001) Structure of the mouse calcitonin/calcitonin gene-related peptide alpha and beta genes. *DNA Seq*, **12**, 131–135.
- Tie-Jun, S.S., Xu, Z., & Hökfelt, T. (2001) The expression of calcitonin gene-related peptide in dorsal horn neurons of the mouse lumbar spinal cord. *Neuroreport*, **12**, 739–743.
- Todaka, H. (2004) Warm Temperature-sensitive Transient Receptor Potential Vanilloid 4 (TRPV4) Plays an Essential Role in Thermal Hyperalgesia. *Journal of Biological Chemistry*, **279**, 35133–35138.
- Todd, A.J., Hughes, D.I., Polgár, E., Nagy, G.G., Mackie, M., Ottersen, O.P., & Maxwell, D.J. (2003) The expression of vesicular glutamate transporters VGLUT1 and VGLUT2 in neurochemically defined axonal populations in the rat spinal cord with emphasis on the dorsal horn. *Eur J Neurosci*, **17**, 13–27.
- Todd, A.J., McGill, M.M., & Shehab, S.A. (2000) Neurokinin 1 receptor expression by neurons in laminae I, III and IV of the rat spinal dorsal horn that project to the brainstem. *Eur J Neurosci*, **12**, 689–700.
- Todd, A.J., Puskár, Z., Spike, R.C., Hughes, C., Watt, C., & Forrest, L. (2002) Projection neurons in lamina I of rat spinal cord with the neurokinin 1 receptor are selectively innervated by substance p-containing afferents and respond to noxious stimulation. *Journal of Neuroscience*, **22**, 4103–4113.
- Tominaga, M. & Caterina, M.J. (2004) Thermosensation and pain. *J. Neurobiol*, **61**, 3–12.
- Tominaga, M., Caterina, M.J., Malmberg, A.B., Rosen, T.A., Gilbert, H., Skinner, K., Raumann, B.E., Basbaum, A.I., & Julius, D. (1998) The cloned capsaicin receptor integrates multiple pain-producing stimuli. *Neuron*, **21**, 531–543.
- Torebjork, H.E., LaMotte, R.H., & Robinson, C.J. (1984) Peripheral neural correlates of magnitude of cutaneous pain and hyperalgesia: simultaneous recordings in humans of sensory judgments of pain and evoked .... *J. Neurophysiol*.
- Traub, R.J., Solodkin, A., & Ruda, M.A. (1989) Calcitonin gene-related peptide immunoreactivity in the cat lumbosacral spinal cord and the effects of multiple

- dorsal rhizotomies. *J. Comp. Neurol*, **287**, 225–237.
- Treede, R.D., Jensen, T.S., Campbell, J.N., Cruccu, G., Dostrovsky, J.O., Griffin, J.W., Hansson, P., Hughes, R., Nurmikko, T., & Serra, J. (2008) Neuropathic pain: redefinition and a grading system for clinical and research purposes. In Presented at the Neurology, pp. 1630–1635.
- Treede, R.D., Meyer, R.A., & Campbell, J.N. (1998) Myelinated mechanically insensitive afferents from monkey hairy skin: heat-response properties. *J. Neurophysiol*, **80**, 1082–1093.
- Tschopp, F.A., Henke, H., Petermann, J.B., Tobler, P.H., Janzer, R., Hökfelt, T., Lundberg, J.M., Cuello, C., & Fischer, J.A. (1985) Calcitonin gene-related peptide and its binding sites in the human central nervous system and pituitary. *Proc. Natl. Acad. Sci. U.S.A.*, **82**, 248–252.
- Tsuda, M., Ueno, S., & Inoue, K. (1999) Evidence for the involvement of spinal endogenous ATP and P2X receptors in nociceptive responses caused by formalin and capsaicin in mice. *British Journal of Pharmacology*, **128**, 1497–1504.
- Turk, D.C. & Okifuji, A. (2001) Pain terms and taxonomies of pain. In Loeser, J.D., Butler, S.H., Chapman, C.R., & Turk, D.C. (eds), *Bonica's Management of Pain*, 3rd edn. Lippincott Williams & Wilkins, Philadelphia, pp. 17–25.
- Ueno, S., Tsuda, M., Iwanaga, T., & Inoue, K. (1999) Cell type-specific ATP-activated responses in rat dorsal root ganglion neurons. *British Journal of Pharmacology*, **126**, 429–436.
- van Rossum, D., Hanisch, U.K., & Quirion, R. (1997) Neuroanatomical localization, pharmacological characterization and functions of CGRP, related peptides and their receptors. *Neuroscience & Biobehavioral Reviews*, **21**, 649–678.
- Verge, V.M., Richardson, P.M., Wiesenfeld-Hallin, Z., & Hökfelt, T. (1995) Differential influence of nerve growth factor on neuropeptide expression in vivo: a novel role in peptide suppression in adult sensory neurons. *J. Neurosci*, **15**, 2081–2096.
- Vilimas, P.I., Yuan, S.Y., Haberberger, R.V., & Gibbins, I.L. (2011) Sensory Innervation of the External Genital Tract of Female Guinea Pigs and Mice. *The Journal of Sexual Medicine*, **8**, 1985–1995.
- Villar, M.J., Wiesenfeld-Hallin, Z., Xu, X.-J., Theodorsson, E., Emson, P.C., & Hökfelt, T. (1991) Further studies on galanin-, substance P-, and CGRP-like immunoreactivities in primary sensory neurons and spinal cord: effects of dorsal rhizotomies and sciatic nerve lesions. *Exp. Neurol*, **112**, 29–39.
- Vogt-Eisele, A.K., Weber, K., Sherkheli, M.A., Vielhaber, G., Panten, J., Gisselmann, G., & Hatt, H. (2009) Monoterpenoid agonists of TRPV3. *British Journal of Pharmacology*, **151**, 530–540.
- Wagman, I.H. & Price, D.D. (1969) Responses of dorsal horn cells of *M. mulatta* to cutaneous and sural nerve A and C fiber stimuli. *J. Neurophysiol*, **32**, 803–817.
- Waldeyer, W. (1889) *Das Gorilla-Rückenmark*. Akademie der Wissenschaften.
- Wang, J., Kawamata, M., & Namiki, A. (2005) Changes in properties of spinal dorsal horn neurons and their sensitivity to morphine after spinal cord injury in the rat. *Anesthesiology*, **102**, 152–164.
- Waxman, S.G., Kocsis, J.D., & Black, J.A. (1994) Type III sodium channel mRNA is expressed in embryonic but not adult spinal sensory neurons, and is reexpressed following axotomy. *J. Neurophysiol*, **72**, 466–470.
- Wiesenfeld-Hallin, Z., Hökfelt, T., Lundberg, J.M., Forssmann, W.G., Reinecke, M., Tschopp, F.A., & Fischer, J.A. (1984) Immunoreactive calcitonin gene-related peptide and substance P coexist in sensory neurons to the spinal cord and interact in spinal behavioral responses of the rat. *Neuroscience Letters*, **52**, 199–204.

- Wiesenfeld-Hallin, Z., Xu, X.-J., Håkanson, R., Feng, D.M., & Folkers, K. (1990) Plasticity of the peptidergic mediation of spinal reflex facilitation after peripheral nerve section in the rat. *Neuroscience Letters*, **116**, 293–298.
- Wiesenfeld-Hallin, Z., Xu, X.-J., Villar, M.J., & Hökfelt, T. (1990) Intrathecal galanin potentiates the spinal analgesic effect of morphine: electrophysiological and behavioural studies. *Neuroscience Letters*, **109**, 217–221.
- Williams, S., Evan, G.I., & Hunt, S.P. (1990) Changing patterns of c-fos induction in spinal neurons following thermal cutaneous stimulation in the rat. *NSC*, **36**, 73–81.
- Willis, W.D., Jr (2007) Physiological Characteristics of Second-Order Somatosensory Circuits in Spinal Cord and Brainstem. In Kaas, J.H. & Gardner, E.P. (eds), *The Senses: a Comprehensive Reference - Volume 6: Somatosensation*. pp. 1–30.
- Willis, W.D., Jr & Coggeshall, R.E. (1991) *Sensory Mechanisms of the Spinal Cord*, 2nd edn. Springer Science, New York, N.Y.
- Willis, W.D., Kenshalo, D.R.J., & Leonard, R.B. (1979) The cells of origin of the primate spinothalamic tract. *J. Comp. Neurol*, **188**, 543–573.
- Willis, W.D., Zhang, X., Honda, C.N., & Giesler, G.J. (2001) Projections from the marginal zone and deep dorsal horn to the ventrobasal nuclei of the primate thalamus. *Pain*, **92**, 267–276.
- Wood, J.N. (2007) Sodium Channels. In Basbaum, A.I. & Bushnell, M.C. (eds), *The Senses: a Comprehensive Reference - Volume 5: Pain*. Academic Press, pp. 89–95.
- Woolf, C. & Wiesenfeld-Hallin, Z. (1986) Substance P and calcitonin gene-related peptide synergistically modulate the gain of the nociceptive flexor withdrawal reflex in the rat. *Neuroscience Letters*, **66**, 226–230.
- Woolf, C.J. & Ma, Q. (2007) Nociceptors—Noxious Stimulus Detectors. *Neuron*, **55**, 353–364.
- Woolf, C.J., Thompson, S.W., & King, A.E. (1988) Prolonged primary afferent induced alterations in dorsal horn neurones, an intracellular analysis in vivo and in vitro. *J Physiol (Paris)*, **83**, 255–266.
- Wu, J., Fang, L., Lin, Q., & Willis, W.D. (2002) The role of nitric oxide in the phosphorylation of cyclic adenosine monophosphate—responsive element-binding protein in the spinal cord after intradermal injection of capsaicin. *The Journal of Pain*, **3**, 190–198.
- Xu, H., Delling, M., Jun, J.C., & Clapham, D.E. (2006) Oregon, thyme and clove-derived flavors and skin sensitizers activate specific TRP channels. *Nat. Neurosci*, **9**, 628–635.
- Xu, X.-J., Wiesenfeld-Hallin, Z., Villar, M.J., Fahrenkrug, J., & Hökfelt, T. (1990) On the Role of Galanin, Substance P and Other Neuropeptides in Primary Sensory Neurons of the Rat: Studies on Spinal Reflex Excitability and Peripheral Axotomy. *Eur J Neurosci*, **2**, 733–743.
- Yakovlev, A.G. & Faden, A.I. (1994) Sequential expression of c-fos protooncogene, TNF-alpha, and dynorphin genes in spinal cord following experimental traumatic injury. *Mol Chem Neuropathol*, **23**, 179–190.
- Yanagisawa, M., Yagi, N., Otsuka, M., Yanaihara, C., & Yanaihara, N. (1986) Inhibitory effects of galanin on the isolated spinal cord of the newborn rat. *Neuroscience Letters*, **70**, 278–282.
- Yeziarski, R.P. & Park, S.H. (1993) The mechanosensitivity of spinal sensory neurons following intraspinal injections of quisqualic acid in the rat. *Neuroscience Letters*, **157**, 115–119.

## Reference List

- Yu, C.-G. & Yeziarski, R.P. (2005) Activation of the ERK1/2 signaling cascade by excitotoxic spinal cord injury. *Molecular Brain Research*, **138**, 244–255.
- Yu, L.C., Hansson, P., & Lundeberg, T. (1996) The calcitonin gene-related peptide antagonist CGRP8-37 increases the latency to withdrawal responses bilaterally in rats with unilateral experimental mononeuropathy, an effect reversed by naloxone. *NSC*, **71**, 523–531.
- Yu, L.C., Hansson, P., Brodda-Jansen, G., Theodorsson, E., & Lundeberg, T. (1996) Intrathecal CGRP8-37-induced bilateral increase in hindpaw withdrawal latency in rats with unilateral inflammation. *British Journal of Pharmacology*, **117**, 43–50.
- Yu, S., Udem, B.J., & Kollarik, M. (2005) Vagal afferent nerves with nociceptive properties in guinea-pig oesophagus. *The Journal of Physiology*, **563**, 831–842.
- Yu, X.H., da Silva, A.R., & De Koninck, Y. (2005) Morphology and neurokinin 1 receptor expression of spinothalamic lamina I neurons in the rat spinal cord. *J. Comp. Neurol*, **491**, 56–68.
- Yu, Y., Lundeberg, T., & Yu, L.-C. (2002) Role of calcitonin gene-related peptide and its antagonist on the evoked discharge frequency of wide dynamic range neurons in the dorsal horn of the spinal cord in rats. *Regul. Pept*, **103**, 23–27.
- Zagorodnyuk, V.P. & Brookes, S.J.H. (2000) Transduction Sites of Vagal Mechanoreceptors in the Guinea Pig Esophagus. *J. Neurosci*, **20**, 6249–6255.
- Zagorodnyuk, V.P., Kyloh, M., Nicholas, S., Peiris, H., Brookes, S.J., Chen, B.N., & Spencer, N.J. (2011) Loss of visceral pain following colorectal distension in an endothelin-3 deficient mouse model of Hirschsprung's disease. *The Journal of Physiology*, **589**, 1691–1706.
- Zhang, H., Xie, W., & Xie, Y. (2005) Spinal cord injury triggers sensitization of wide dynamic range dorsal horn neurons in segments rostral to the injury **1055**, 103–110.
- Zoli, M., Jansson, A., Syková, E., Agnati, L.F., & Fuxe, K. (1999) Volume transmission in the CNS and its relevance for neuropsychopharmacology. *Trends Pharmacol. Sci*, **20**, 142–150.